

UNIVERSAL  
LIBRARY

**OU\_164031**

UNIVERSAL  
LIBRARY





OUP—880—5-8-74—10,000.

**OSMANIA UNIVERSITY LIBRARY**

94291

Call No.

541.3443

Accession No.

Author

B 89A

vol. I.

Title

This book should be returned on or before the date last marked below.



THE ADSORPTION OF  
GASES AND VAPORS



# THE ADSORPTION OF GASES AND VAPORS

Volume I

Physical Adsorption

By

STEPHEN BRUNAUER

Chemist, Bureau of Plant Industry  
United States Department of Agriculture

OXFORD UNIVERSITY PRESS  
LONDON: HUMPHREY MILFORD

Copyright, 1943, by Princeton University Press

*Manufactured in the United States of America*

## PREFACE

The subject of adsorption can be treated in various ways, two of which seem to be somewhat more direct than the others. One may sift the data of the hundreds of investigators who contributed to the field and try to find out what they reveal about the adsorptive properties of charcoal, silica gel, metals, oxides and other important adsorbents. The other way is to focus attention on the phenomenon of adsorption itself, and to inquire what certain experiments performed on charcoal or silica gel teach about the nature of the adsorption process. The first approach is more immediately practical, the second more fundamentally scientific. The present book follows the second method; it attempts to treat adsorption as a science, a branch of physical chemistry. Had I started the writing of this book a year later, I would doubtless have adopted the more practical approach because of its more direct relation to the needs of the war industry, but on the day of Pearl Harbor the greater part of this book was already written. As it is, it may prove to be useful in the training of scientists and technicians in colleges. Besides, a good practical chemist knows how to put science to use, and so perhaps this book will also find its way eventually into the stream of the industrial production of our nation.

The subject matter of adsorption can be divided into two parts: physical and chemical adsorption. Aside from a short general part, this book deals only with physical adsorption. I hope that some day I may write the second volume of this work about chemical adsorption, but that must wait until the end of the war. *Inter arma silent musae*. The writing of such a book is a long and time consuming process incompatible with present urgent work connected with the war. There is not much point in writing science, unless we make the world first safe for science.

It is with great pleasure that I express my gratitude in the first place to Dr. H. S. Taylor of Princeton University, who suggested the writing of this book, who read all the chapters in manuscript form, and without whose constant interest and encouragement this book would probably not have been written. In the second place I wish to express my appreciation to Dr. S. B. Hendricks of the Bureau of Plant Industry for his very helpful interest in the book and for reading

and criticizing some of the chapters. My obligation to Dr. V. R. Deitz of the National Bureau of Standards is twofold: he read all of the chapters and criticized them, and he permitted me to use his excellent card index on adsorption. My thanks are due also to Mrs. Constance Sherry, who made all the drawings for the figures of the book, to Dr. R. W. Hummer and Mrs. Lee Garby for reading the entire manuscript, and to Drs. S. Glasstone, R. A. Beebe, L. H. Cohan, L. F. Gleysteen and Mr. E. J. R. Prosen for reading individual chapters. Finally, I should like to record my grateful appreciation to the Chief of the Bureau of Plant Industry for his permission to write this book and for generously allowing me to use all the facilities of the Bureau, and to the Director of the Geophysical Laboratory of the Carnegie Institution of Washington for permitting me to use the library of the Laboratory.

May I also be permitted to make acknowledgment to four other scientists who, while not contributing directly to the writing of this book, yet made indirect contributions of inestimable value: to Dr. J. C. W. Frazer of Johns Hopkins University, who first made me interested in the field of adsorption, to Dr. P. H. Emmett of Johns Hopkins University, Dr. Edward Teller of George Washington University and Dr. W. Edwards Deming of the Census Bureau, my friends and former collaborators, together with whom in quieter days we learned something of the phenomenon of adsorption.

STEPHEN BRUNAUER

*Washington, August 24, 1942*



# CONTENTS

	PAGE
PREFACE.....	V
PART I	
GENERAL DISCUSSION	
CHAPTER I      Introduction.....	3
CHAPTER II     The Data of Adsorption.....	7
CHAPTER III    Experimental Methods.....	29
PART II	
PHYSICAL ADSORPTION	
CHAPTER IV     The Adsorption Isotherm I.....	53
CHAPTER V      The Adsorption Isotherm II.....	95
CHAPTER VI     The Adsorption Isotherm III.....	140
CHAPTER VII    The Heat of Adsorption I.....	180
CHAPTER VIII   The Heat of Adsorption II.....	218
CHAPTER IX     The Surface of the Adsorbent I.....	271
CHAPTER X      The Surface of the Adsorbent II.....	317
CHAPTER XI     The Pore Structure of the Adsorbent.....	365
CHAPTER XII    The Adsorbate.....	419
CHAPTER XIII   The Kinetics of Physical Adsorption.....	448
CHAPTER XIV    Mixed Adsorption.....	474
INDEX.....	499



Part One  
**GENERAL DISCUSSION**



## CHAPTER I

### INTRODUCTION

When a gas or vapor is brought in contact with an evacuated solid a part of it is taken up by the solid.<sup>1</sup> If this occurs at constant volume, the pressure drops; if at constant pressure, the volume decreases. The molecules that disappear from the gas phase either enter the *inside* of the solid, or remain on the *outside*, attached to its surface. The former phenomenon is called *absorption*, the latter *adsorption*.<sup>2</sup> Often the two occur simultaneously; the total uptake of the gas is then designated by the term *sorption*.<sup>3</sup> To study adsorption, one must carry out the experiments at temperatures, pressures, and concentrations at which either the absorption of the gas is negligible, or the two processes can be separated from each other with a fair degree of accuracy.

The solid that takes up the gas or vapor is called the *adsorbent*, the gas or vapor attached to the surface of the solid is called the *adsorbate*.<sup>4</sup> It is not always easy to tell whether the gas is inside the adsorbent, or attached to its outside. Most adsorbents are highly porous bodies with tremendously large internal surfaces. The external surface, even that visible under the best microscope, constitutes only a small fraction of the large total surface. However, as long as the gas does not penetrate into the field of force that exists between the atoms, ions, or molecules inside the solid, it is considered

<sup>1</sup> The phenomenon of adsorption was discovered more than a century and a half ago. The uptake of gases by charcoal was first described by C. W. Scheele in 1773 and by the Abbé F. Fontana in 1777. T. Lowitz in 1785 discovered that charcoal took the coloring matter out of solutions. The first systematic investigations were carried out by T. de Saussure when he measured the adsorption of a variety of gases on several adsorbents. Aside from mentioning the names of these early pathfinders no attempt will be made here to go into the history of adsorption. In the course of the discussion of the experimental and theoretical aspects of adsorption the work of most of the important contributors will be taken up.

<sup>2</sup> Originally the term *absorption* was used to designate both phenomena. The word *adsorption* as here defined was first introduced by H. Kayser at the suggestion of E. du Bois-Reymond in 1881.

<sup>3</sup> The term was introduced by J. W. McBain in 1909.

<sup>4</sup> Even though the term *adsorbate* is somewhat incorrect linguistically, its use has become general in the literature of adsorption, and it will be used as defined here throughout this book.

to be on the outside, even if it is adsorbed on the internal surface of the adsorbent.

If the gas enters the inside of a solid two things may happen: either the gas merely dissolves in it, forming a solid solution, or it reacts with the solid and forms a compound. If the gas remains attached to the surface of the solid, again two things may happen: there is either a weak interaction between solid and gas, similar to condensation, or a strong interaction, similar to chemical reactions. The former is called *physical adsorption*, the latter *chemical adsorption*, or *chemisorption*. The term *van der Waals adsorption* is often used as a synonym for the former and the term *activated adsorption* as a synonym for the latter. The name van der Waals adsorption implies that the same forces that are active in condensation, i.e., the van der Waals forces, are also active in physical adsorption. The name activated adsorption<sup>5</sup> implies that this type of adsorption requires activation energies, just as chemical reactions do.<sup>6</sup> Other names that are occasionally used for physical adsorption are low temperature adsorption, secondary adsorption, and capillary condensation; other synonyms for chemisorption are high temperature adsorption and primary adsorption.<sup>7</sup>

The phenomenon of physical adsorption is the subject of the present volume; chemisorption will be discussed in a forthcoming volume. The process of absorption will be taken up only to the extent to which it introduces complications into the study of adsorption. The large and important field of adsorption from solutions is also outside the scope of the present work.

### THE INTERFACE SOLID—GAS

The seat of adsorption is the place where the solid and gas come in contact with each other, i.e., the surface of the adsorbent. The atoms or molecules constituting the solid are held together by different

<sup>5</sup> The term was introduced by H. S. Taylor in 1931.

<sup>6</sup> In many cases chemical adsorption<sup>7</sup> takes place so rapidly even at liquid air temperatures that no activation energies can be measured.

<sup>7</sup> The names high and low temperature adsorption are often misleading: carbon monoxide is chemisorbed on catalytic iron at  $-183^{\circ}\text{C}$ ., while the physical adsorption of iodine on silica gel has been studied up to  $200^{\circ}\text{C}$ . The names primary and secondary adsorption imply that the gas is attached to the surface by primary and secondary valence forces. The name capillary condensation implies that capillary forces are responsible for physical adsorption. Since these implications are only occasionally true, but not always, it is preferable to use the names physical adsorption and chemisorption.

forces: electrostatic or Coulomb forces, exchange or homopolar valence forces, van der Waals forces, etc. In most solids several of these are operative, with one or the other predominating: in ionic crystals the electrostatic forces are the most important, in atomic lattices the homopolar binding forces. Whatever the nature of the forces an atom located inside the body of the solid is subjected to equal forces in all directions, whereas an atom in the plane of the surface is subjected to unbalanced forces, the inward pull being greater than the outward forces. This results in a tendency to decrease the surface; a solid has surface tension, just like a liquid.<sup>8</sup> Any process that tends to decrease the free surface energy (the product of the surface tension and the surface area) occurs spontaneously. An atom or a molecule of the gas adsorbed by the solid saturates some of the unbalanced forces of the surface, thereby decreasing the surface tension. Thus all adsorption phenomena (physical or chemical) are spontaneous and result in a *decrease of the free energy* of the system.

The adsorbed particles are either held rigidly to the surface, or they can move over the surface freely in two dimensions. Since prior to adsorption the gas molecules moved freely in three dimensions, the adsorption process is accompanied by a decrease in entropy. The change in the heat content of the system is  $\Delta H = \Delta F + T\Delta S$ ,<sup>9</sup> and since both  $\Delta F$  and  $\Delta S$  are negative,  $\Delta H$  must also be negative. This means that *all adsorption processes are exothermic*, a result found invariably, whether the measurements are made by direct or indirect methods. The decrease in the heat content of the system is called the *heat of adsorption*. In van der Waals adsorption it is of the same order of magnitude as the heats of condensation of gases, in chemisorption as the heats of chemical reactions. The heat of the van der Waals adsorption of nitrogen on an iron catalyst is about 2-3000 calories per mole; the heat of liquefaction of nitrogen gas is 1360 calories per mole. The heat of chemisorption of nitrogen on the same surface is an order of magnitude larger: 35,000 calories per mole. Evidence is strong that in the first case nitrogen is adsorbed in the molecular form; in the second case it dissociates into atoms. The surface iron atoms and the nitrogen atoms mutually saturate each other's free valence forces, consequently only one chemisorbed layer can form on the surface of the adsorbent. In van der Waals adsorp-

<sup>8</sup> As a matter of fact, the surface tensions of solids are much greater than those of liquids. Thus the surface tension of benzene at 20° C. is 28.8 dyne/cm., that of water is 72.75 dyne/cm., while that of barium sulfate is 310 dyne/cm.

<sup>9</sup> G. N. Lewis and M. Randall, *Thermodynamics*, New York 1923, p. 162.

tion, however, the nitrogen molecules adsorbed on the iron surface are still able to adsorb a second layer of nitrogen molecules, these in turn a third layer, and so on. When the surface can take up only one layer of adsorbed gas the adsorption is called *unimolecular*; <sup>10</sup> when more than one layer, it is called *multimolecular*.

### APPLICATIONS

The most important applications of gas-solid adsorption fall into three groups:

1. *Purification of gases.* Examples: the purification of carbon dioxide coming from fermenting vats to make it usable for carbonated water, the purification of hydrogen before catalytic hydrogenation, of ammonia before catalytic oxidation, the refining of helium, the drying of air and other gases, the purification of air in submarines, the deodorizing of refrigerating rooms. Closely allied to these is the use of adsorbents for protection in the gas masks of the soldier, the miner, the fireman.

2. *Separation and recovery of gases.* Examples: the separation of the rare gases, the extraction of gasoline from natural gas, the recovery of benzene and light oil from illuminating gas, the recovery of acetone, alcohol, and butanol from the waste gases of fermenting vats, the recovery of volatile solvent vapors in dry cleaning, in the manufacture of artificial silk, celluloid, rubber.

3. *Catalysis.* Adsorption plays a vital role in heterogeneous catalysis. The gases are adsorbed on the surface of the catalyst, react there, and finally the products desorb from the surface.<sup>11</sup>

<sup>10</sup> I. Langmuir used the term *monomolecular*. However, since it is a term of mixed Greek and Latin derivation, the use of *unimolecular* is preferable.

<sup>11</sup> Further applications are found in N. K. Chaney, A. B. Ray, and A. St. John, *Ind. Eng. Chem.*, 15, 1244 (1923).



## CHAPTER II

### THE DATA OF ADSORPTION

When a gas or vapor is admitted to a thoroughly evacuated adsorbent its molecules distribute themselves between the gas phase and the adsorbed phase. The disappearance of the molecules from the gas phase occurs with great rapidity in some cases, in others at a measurable rate. After a while the process stops and a state of stable equilibrium is reached. The amount of gas adsorbed per gram of adsorbent at equilibrium is a function of the temperature, the pressure, and the nature of the adsorbent and the adsorbate.

#### RATE OF ADSORPTION

The adsorption of gases and vapors is often very fast. Granular Darco G (an activated carbon adsorbent) adsorbs 300 times its own volume of nitrogen at  $-183^{\circ}\text{C}$ . in less than a minute.<sup>1</sup> Freundlich<sup>2</sup> determined photographically the rate of adsorption of carbon dioxide by charcoal and found that equilibrium was established in less than 20 seconds. A good adsorbent of war gases must have not only large adsorptive capacity, but also a great speed of action. Lamb, Wilson, and Chaney<sup>3</sup> found that a gas mask charcoal removed from air containing 7000 parts of chloropicrin per million all but 0.01% of the poison gas in 0.03 seconds.

In physical adsorption equilibrium is often established so quickly that the rate can not be measured. However, this is not always the case; the fast initial adsorption is frequently followed by a slow sorption process. The nature of the slow process varies; occasionally it can be traced to chemisorption, or to actual chemical reaction. Shah<sup>4</sup> found that in the adsorption of oxygen by charcoal at  $0^{\circ}\text{C}$ . most of the adsorbed gas was recovered as oxygen by evacuation at the same temperature. Some of the gas, however, came off only at higher temperatures, and not as oxygen but as carbon dioxide and carbon monoxide. Thus, although most of the oxygen was held by van der

<sup>1</sup> Unpublished results by P. H. Emmett and the author.

<sup>2</sup> H. Freundlich, *Colloid and Capillary Chemistry*, p. 108.

<sup>3</sup> A. B. Lamb, R. E. Wilson, and N. K. Chaney, *J. Ind. Eng. Chem.*, 11, 420 (1919).

<sup>4</sup> M. S. Shah, *J. Chem. Soc.*, 1929, 2670.

Waals adsorption, some of the oxygen was bound so strongly to the surface carbon atoms that on evacuation at higher temperatures these were removed from the surface along with the oxygen.

McBain<sup>5</sup> demonstrated that the uptake of hydrogen by coconut charcoal at liquid air temperature consisted of two processes, one taking place very rapidly, the other—which he believed to be solution of hydrogen in the atomic form—much more slowly. He transferred the charcoal saturated with hydrogen into a vacuum, and found that the adsorbed hydrogen came off quickly, the dissolved hydrogen slowly. He then increased the pressure of hydrogen in the gas phase to a value lower than that necessary to establish equilibrium with the solution process. At first there was a quick lowering in the pressure due to increased physical adsorption, but then a slow increase in pressure followed due to the fact that some of the hydrogen was still coming out of the solution. While it is possible that McBain's atomic hydrogen was dissolved in the charcoal, it seems more likely that the slow process was actually activated adsorption rather than solution.

There are other instances in which the slow process must definitely be ascribed to physical effects. It was found, for example, that a sample of air-dried soil (Barnes soil, No. 10308) took several hours to equilibrate with nitrogen at  $-183^{\circ}\text{C}$ ., although 95% or more of the adsorption took place in the first minute.<sup>1</sup> Certainly at this low temperature one would not expect any of the constituents of the soil to react with nitrogen or to chemisorb it, nor would one expect any appreciable solubility of nitrogen in the soil. Probably the slow process in this case is due to the penetration of nitrogen molecules into some of the exceedingly fine pores of the adsorbent. In other cases the blocking of the adsorption by molecules already adsorbed slows down the rate; e.g., Harned<sup>6</sup> found that in the adsorption of chloropicrin by charcoal adsorbed air acted as inhibitor. In still other cases foreign molecules in the gas phase slow down the adsorption by blocking diffusion of the gas to be adsorbed into narrow capillaries. Patrick and Cohan<sup>7</sup> found that 1.0 mm. pressure of air, oxygen, or nitrogen slowed down the adsorption of water by silica gel (at  $25^{\circ}\text{C}$ . and 4.6 mm. pressure of water) considerably. In general, it seems safe to conclude that in van der Waals adsorption the gas molecules are adsorbed as rapidly as they can reach the surface. The slow effects are either due to chemisorption, chemical reaction, solution, or

<sup>5</sup> J. W. McBain, *Phil. Mag.*, 18, 1916 (1909).

<sup>6</sup> H. S. Harned, *J. Am. Chem. Soc.*, 42, 372 (1920).

<sup>7</sup> W. A. Patrick and L. H. Cohan, *J. Phys. Chem.*, 41, 437 (1937).

to the inability of the molecules to get in contact with the surface of the adsorbent.

Chemical adsorption also may be instantaneous, or it may proceed at a measurable rate.<sup>8</sup> Thus at  $-183^{\circ}\text{C}$ . almost every iron atom on the surface of an iron synthetic ammonia catalyst chemisorbs a molecule of carbon monoxide with such speed that the rate can not be measured.<sup>9</sup> Roberts<sup>10</sup> found that hydrogen is chemisorbed very rapidly at liquid air temperature by a clean tungsten wire, each atom of

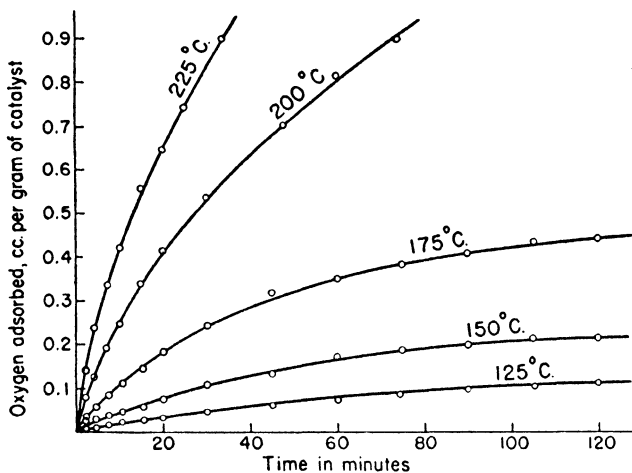


Fig. 1.—The rate of adsorption of oxygen on a cobalt chromite catalyst.

the surface adsorbing one hydrogen atom. On the other hand Taylor and Williamson<sup>11</sup> found that the rate of adsorption of hydrogen on a manganous oxide catalyst was not too fast to be measured even at  $305^{\circ}\text{C}$ .

In Fig. 1 rate curves are shown for the adsorption of oxygen by a cobalt chromite catalyst, obtained by Frazer and Heard.<sup>12</sup> The rate of adsorption increases with temperature; a result invariably found in

<sup>8</sup> In some papers the term *chemisorption* is used to designate instantaneous chemical adsorption, and the term *activated adsorption* is reserved for chemical adsorptions whose rates can be measured.

<sup>9</sup> P. H. Emmett and S. Brunauer, *J. Am. Chem. Soc.*, **59**, 310 (1937).

<sup>10</sup> J. K. Roberts, *Proc. Roy. Soc.*, **A152**, 445 (1935).

<sup>11</sup> H. S. Taylor and A. J. Williamson, *J. Am. Chem. Soc.*, **53**, 813 (1931).

<sup>12</sup> J. C. W. Frazer and L. Heard, *J. Phys. Chem.*, **42**, 855 (1938).

experiments on adsorption rates. In Fig. 2 some of the rate curves cross each other. These curves represent the adsorption of hydrogen by a zinc oxide catalyst, obtained by Taylor and Sickman.<sup>13</sup> The reason for the crossing is that the amount adsorbed when equilibrium is reached decreases with temperature. The 306° C. curve crosses the 218° and 184° C. curves because the initial rate is higher but the final amount adsorbed is less than that at the lower temperatures.

Taylor<sup>14</sup> was the first to point out that the rate of chemisorption increases exponentially with the temperature, just like the rates of

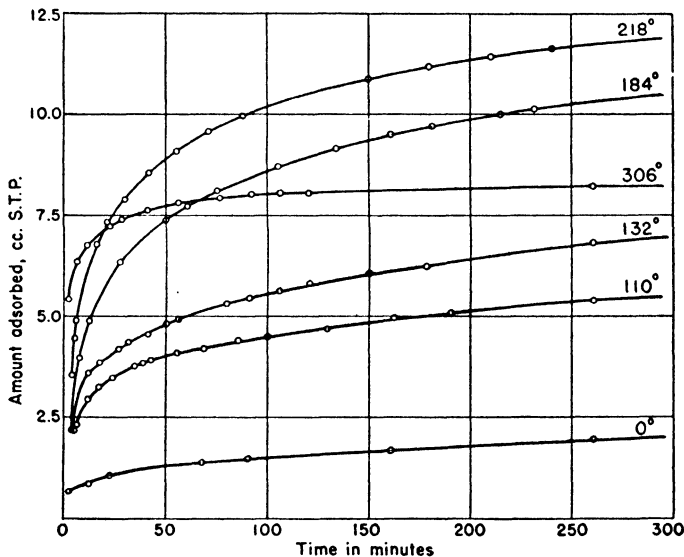


FIG. 2.—The rate of adsorption of hydrogen on a zinc oxide catalyst.

chemical reactions, and he showed that the energy of activation can be calculated from the temperature coefficient of the rate. Because this type of adsorption possesses an energy of activation, he named it *activated adsorption*. There is some opposition even today to accepting the concept of activated adsorption. The energies of activation obtained by adsorption rate measurements have been ascribed by various investigators to solution, diffusion, migration, or reaction on the surface, rather than to the chemisorption process itself. In spite

<sup>13</sup> H. S. Taylor and D. V. Sickman, *J. Am. Chem. Soc.*, 54, 602 (1932).

<sup>14</sup> H. S. Taylor, *J. Am. Chem. Soc.*, 53, 578 (1931).

of the opposition, the concept of activated adsorption is entirely reasonable. Since the surface of an adsorbent has unsaturated valence forces, the chemisorption process has a certain degree of similarity to a reaction between an atom (or a free radical) and a molecule in the gas phase. That such reactions often, though not always, require energies of activation, was established experimentally by Polanyi and his collaborators<sup>15</sup> and theoretically by Eyring and Polanyi.<sup>16</sup> The activation energies measured for adsorption processes are of the same order of magnitude as the activation energies in reactions between free radicals and saturated molecules.

The determination of the rate of activated adsorption may be complicated by the simultaneous occurrence of chemical reaction or solution (absorption processes). Only under conditions where the rates of these other processes are very slow or negligible can one measure the rate of activated adsorption. A further complication may come about if the chemisorbed particles have a certain degree of mobility over the surface. If the motion of the particle requires an activation energy, the process is called *activated migration*. The energy of activation of the migration process may sometimes be mistaken for the energy of activation of the adsorption process. These problems will be considered in detail in Volume II.

### ADSORPTION EQUILIBRIUM

The amount of gas or vapor adsorbed when equilibrium is established at a given temperature and pressure is a function of the nature of the adsorbent and adsorbate. This includes on the one hand the physical structure of the adsorbent (the extent of its surface, the sizes, shapes, and distribution of pores) and its chemical constitution, and on the other, the physical and chemical properties of the adsorbed gas molecules. The earliest correlation of adsorption with certain physical properties of the adsorbed gases was made in 1814 by de Saussure<sup>17</sup> who found that the most easily condensible gases are adsorbed in the largest quantities by a given adsorbent. Since that time numerous such comparisons have been made, one of which is reproduced in Table I. The data were obtained by W. Hene.<sup>18</sup> A

<sup>15</sup> H. v. Hartel and M. Polanyi, *Z. phys. Chem.*, **B11**, 97 (1930); H. v. Hartel, N. Meer, and M. Polanyi, *Z. phys. Chem.*, **B19**, 139 (1932).

<sup>16</sup> H. Eyring and M. Polanyi, *Z. phys. Chem.*, **B12**, 279 (1931); H. Eyring, *J. Am. Chem. Soc.*, **53**, 2537 (1931).

<sup>17</sup> T. de Saussure, *Gilbert's Ann. der Physik*, **47**, 113 (1814); *Ann. Phil.*, **6**, 241, 331 (1815).

<sup>18</sup> W. Hene, Dissertation, University of Hamburg, 1927.

comparison of the volumes of the different gases adsorbed by a given weight of adsorbent at a constant temperature and pressure reveals that the adsorption increases as the boiling point of the gas increases. Although the order is not entirely the same, the parallelism is obvious. Similarly, the adsorption increases with increasing critical tempera-

TABLE I  
 ADSORPTION OF GASES BY CHARCOAL  
 1 g. of adsorbent, temperature 15° C.

Gas	Volume Adsorbed	Boiling Point	Critical Temperature
COCl <sub>2</sub>	440 cc.	-8° C	183° C
SO <sub>2</sub>	380	-10	137
CH <sub>3</sub> Cl	277	-24	143
NH <sub>3</sub>	181	-33	132
H <sub>2</sub> S	99	-62	100
HCl	72	-83	52
N <sub>2</sub> O	54	-90	37
C <sub>2</sub> H <sub>2</sub>	49	-84	36
CO <sub>2</sub>	48	-78	31
CH <sub>4</sub>	16	-164	-87
CO	9	-190	-140
O <sub>2</sub>	8	-182	-118
N <sub>2</sub>	8	-195	-146
H <sub>2</sub>	5	-252	-241

ture. This is a corollary of the other relationship since the boiling point is approximately two-thirds of the critical temperature on the absolute temperature scale.

Arrhenius<sup>19</sup> pointed out a parallelism of the same sort between the volumes of different gases adsorbed by charcoal and their van der Waals constants, *a*. Schmidt<sup>20</sup> found a relation between the heats of vaporization of gases and their adsorption. All of these relations connect certain condensation properties of gases with their van der Waals adsorption.

Naturally one would not expect and can not find any relation between condensation properties of gases and their chemical adsorption. Chemisorption is *specific*, it is based on chemical forces between the atoms, ions, or molecules of the surface and the gas. Thus at -183° C. almost every atom of the surface of an iron catalyst chemisorbs a carbon monoxide molecule, but there is no chemisorption of nitrogen or hydrogen. At 100° C. the surface is covered with chemisorbed hydrogen, but the chemisorption of nitrogen is still inappre-

<sup>19</sup> S. Arrhenius, *Theories of Solutions*, p. 68.

<sup>20</sup> O. Schmidt, *Z. phys. Chem.*, 133, 263 (1928).

cial. At 450° C. the surface is about half covered with nitrogen, the chemisorption of hydrogen is small, and the chemisorption of carbon monoxide is zero.<sup>21</sup>

For a given gas and unit weight of a given adsorbent the amount of gas adsorbed at equilibrium is a function of the final pressure and temperature only

$$(1) \quad a = f(p, T)$$

where  $a$  is the amount adsorbed per gram of adsorbent,  $p$  is the equilibrium pressure, and  $T$  is the absolute temperature. When true equilibrium is present it does not matter whether one has started with a higher or a lower pressure than the final value; as long as the final pressure is the same the amount of gas adsorbed is the same. This is also true with respect to the temperature. Usually either the pressure or the temperature alone is varied, while the other is kept constant. When the pressure of the gas is varied and the temperature is kept constant, the plot of the amount adsorbed against the pressure is called the *adsorption isotherm*, and the isotherm equation is

$$(2) \quad a = f(p) \quad T = \text{constant}$$

This is the most frequently determined experimental relation in the field of adsorption. The explicit form of the function will be discussed later. When the temperature is varied and the pressure is kept constant one obtains the *adsorption isobar*

$$(3) \quad a = f(T) \quad p = \text{constant}$$

A third method of expressing the results of adsorption is by means of the *adsorption isostere*, i.e., the variation of the equilibrium pressure with respect to the temperature for a definite amount of gas adsorbed

$$(4) \quad p = f(T) \quad a = \text{constant}$$

The amount adsorbed is usually expressed as the volume of gas at 0° C. and 760 mm. pressure (S.T.P.) taken up per gram of adsorbent, or as the weight of gas adsorbed per gram of adsorbent. The number of moles or number of molecules adsorbed per gram of adsorbent is also used. Occasionally, concentration units are used instead of pressure, such as the molar density of the adsorbate in the gas phase.

Another line of attack in the study of adsorption equilibrium is to determine the energy changes involved. The heat given out in the adsorption process can be measured either by direct calorimetric means,

<sup>21</sup> S. Brunauer and P. H. Emmett, *J. Am. Chem. Soc.*, **62**, 1732 (1940).

or it can be evaluated with the help of certain thermodynamic formulas from the adsorption isotherms, isobars, or isosteres. The heat of adsorption is most frequently expressed as calories (or kilocalories) evolved per mole of gas adsorbed.

### THE ADSORPTION ISOTHERM

At constant temperature the adsorption of a gas or vapor increases with increasing pressure. In Fig. 3 adsorption isotherms of ammonia on charcoal are shown, obtained by plotting the experimental data of

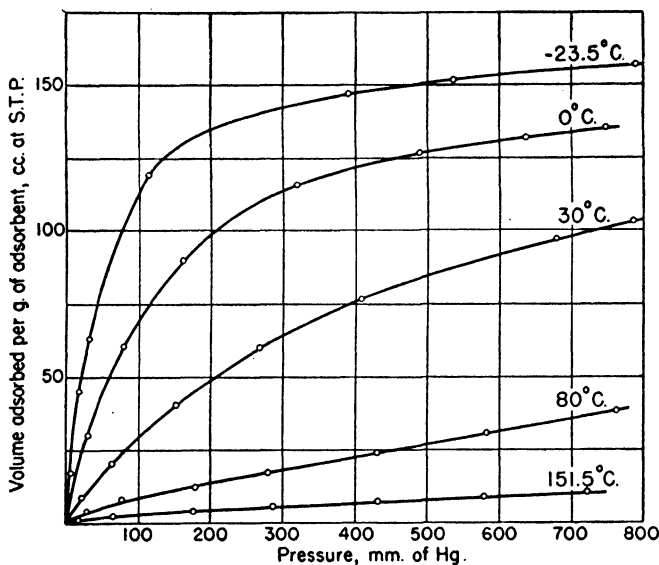


FIG. 3.—Adsorption isotherms of ammonia on charcoal.

Titoff.<sup>22</sup> These isotherms are among the earliest ones obtained in the field. They represent pure physical adsorption, even at the highest temperatures.

Since the adsorption process is always exothermic, the amount adsorbed at equilibrium must always decrease with increasing temperature according to the principle of Le Chatelier. Figure 3 shows that this is actually the case: the lower the temperature the greater the adsorption. At small adsorptions the volume increases linearly with pressure.

<sup>22</sup> A. Titoff, *Z. phys. Chem.*, 74, 641 (1910).



The 151.5° C. isotherm is a straight line up to almost atmospheric pressure, obeying Henry's law,

$$(5) \quad v = kp$$

where  $v$  is the volume adsorbed and  $p$  is the pressure. At somewhat higher adsorptions for equal increments of  $p$  the increments of  $v$  become smaller and smaller. The volume adsorbed becomes proportional to a power of the gas pressure smaller than unity

$$(6) \quad v = k'p^{1/n}$$

where  $n > 1$ . This equation is generally referred to as the *Freundlich isotherm* equation, although Freundlich was not its originator.<sup>23</sup> At

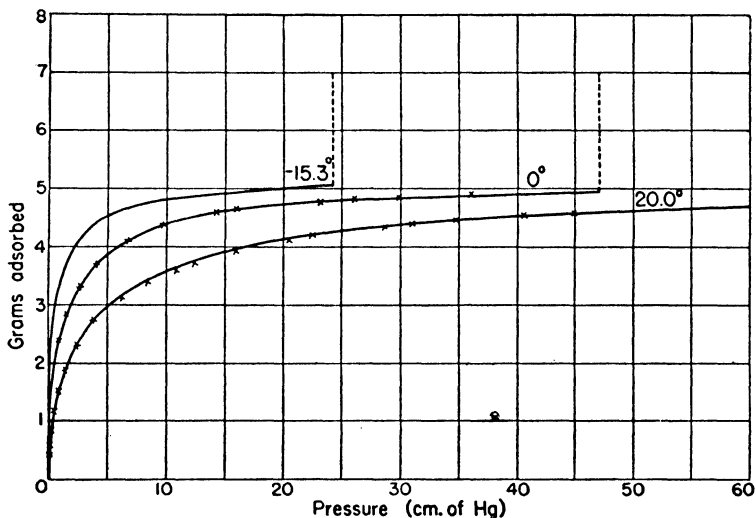


FIG. 4.—Adsorption isotherms of ethyl chloride on charcoal.

still higher adsorptions  $v$  increases only slightly with  $p$ , as the upper portion of the  $-23.5^{\circ}$  C. isotherm shows. The approach to saturation is seen even more clearly in Fig. 4. The curves represent isotherms of ethyl chloride on charcoal, obtained by Goldmann and Polanyi.<sup>24</sup> At the highest pressures the adsorption hardly increases at all with pressure. The last two points of the  $-15.3^{\circ}$  C. isotherm show less than

<sup>23</sup> J. W. McBain, *The Sorption of Gases and Vapours by Solids*, London, 1932, p. 5.

<sup>24</sup> F. Goldmann and M. Polanyi, *Z. phys. Chem.*, 132, 321 (1928).

1% increase in adsorption for a 17% increase in pressure. The adsorption in this region is approximately independent of the pressure, i.e.,

$$(7) \quad v = k''$$

We shall refer to isotherms having such shapes as Langmuir isotherms, since the adsorption mechanism postulated by Langmuir leads to isotherms of this type (Chapter IV).

The isotherms of Fig. 4 also represent van der Waals adsorption. Even though in most texts on physical chemistry the type of adsorption

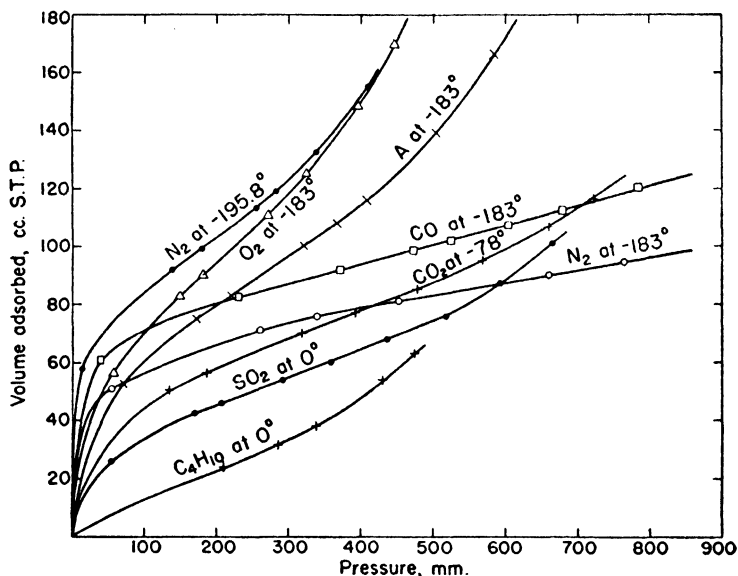


Fig. 5.—Adsorption isotherms of different gases on silica gel.

isotherm shown in Figs. 3 and 4 is the only one included, actually in van der Waals adsorption it is not the most frequently encountered isotherm type. Brunauer and Emmett<sup>25</sup> determined the adsorption isotherms of a number of gases on 30 different substances, including unpromoted and promoted iron catalysts, copper catalysts, supported nickel and nickel oxide catalysts, pumice, glaucosil, silica gel, chromic oxide gel, crystalline chromic oxide, potassium chloride, anhydrous copper sulfate, copper sulfate pentahydrate, soil samples, soil colloids, dry powdered bacteria, activated charcoal, and Darco (an activated

<sup>25</sup> S. Brunauer and P. H. Emmett, *J. Am. Chem. Soc.*, 59, 2682 (1937).

carbon). They obtained the isotherm type shown in Fig. 4 in one case only, on charcoal; for the 29 other adsorbents they obtained the type of isotherm shown in Fig. 5. The curves represent adsorption isotherms of seven gases on silica gel. This isotherm type is called S-shaped or sigmoid isotherm. It consists of a low pressure region concave to the pressure axis, a high pressure region convex to the pressure axis, and an intermediate linear portion, the length and slope of which depends on the adsorbent, the adsorbate, and the temperature. In two of the curves of Fig. 5 (nitrogen and carbon monoxide at  $-183^{\circ}\text{C}.$ ) the upper convex region sets in only at pressures higher

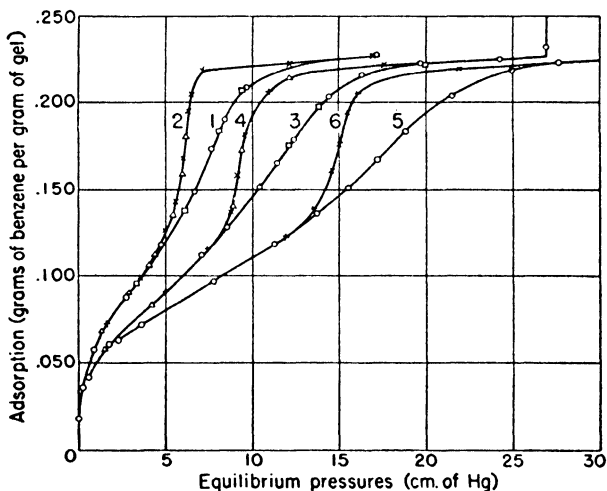


FIG. 6.—Adsorption isotherms of benzene on ferric oxide gel. Curves 1 and 2 at  $40^{\circ}$ , curves 3 and 4 at  $50^{\circ}$ , curves 5 and 6 at  $60^{\circ}\text{C}.$  oo Adsorption, xx Desorption, □□ Second adsorption, △△ Second desorption.

than 800 mm., consequently these isotherms show only the low pressure concave and the intermediate linear portion.

Another frequently found type of van der Waals adsorption isotherm is shown in Fig. 6. The isotherms represent the adsorption of benzene by ferric oxide gel obtained by Lambert and Clark.<sup>28</sup> In these curves the low pressure region is concave to the pressure axis, the intermediate region is convex, and the high pressure region is again concave. The lower parts of the curves are similar to the S-shaped isotherms of Fig. 5; the upper parts are like the upper portions of the

<sup>28</sup> B. Lambert and A. M. Clark, *Proc. Roy. Soc.*, A122, 497 (1929).

isotherms of Fig. 4, a large increase in pressure producing only a slight increase in adsorption. The curves also illustrate a phenomenon often encountered in van der Waals adsorption, the hysteresis with respect to pressure. Curves 1, 3, and 5 represent the adsorption equilibria reached when the pressure of the gas is increased over the adsorbent; curves 2, 4, and 6 give the equilibria obtained by decreasing the pressure. The curves show that the same equilibria are reached from

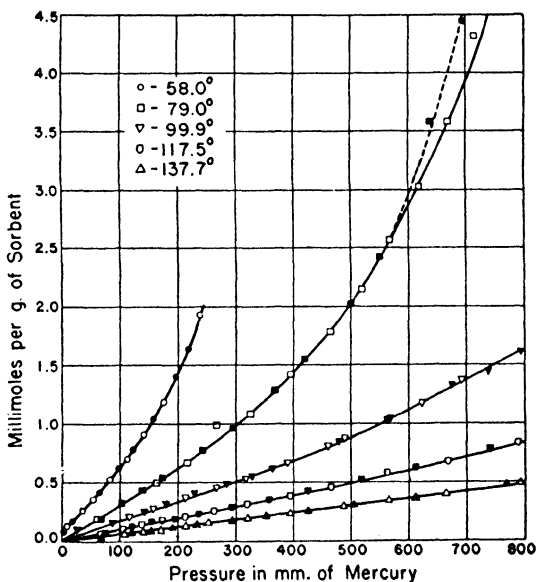


FIG. 7.—Adsorption isotherms of bromine on silica gel. The solid points represent desorption readings.

the adsorption and desorption sides only in the lower pressure region. At higher pressures the desorption curves correspond to larger adsorptions than the adsorption curves.

The isotherm types shown in Figs. 4, 5, and 6 are similar to each other in the low pressure region; they are all concave with respect to the pressure axis. There are two other physical adsorption isotherm types which start out to be convex with respect to the pressure axis. One of these types is illustrated in Fig. 7. The curves represent the adsorption of bromine by silica gel obtained by Reyerson and Cam-

eron.<sup>27</sup> The solid points indicate desorption readings. Evidence of hysteresis is found only at the highest adsorptions measured (79° C.).

Figure 8 shows an isotherm of the adsorption of water vapor by charcoal, plotted from the experimental data of Coolidge.<sup>28</sup> The isotherm has a low pressure region convex to the pressure axis and a high pressure concave region. It is a combination of the type shown in Fig. 7 (lower region) and that shown in Fig. 6 (upper region). The curves of Figs. 4-8 represent the five different isotherm types

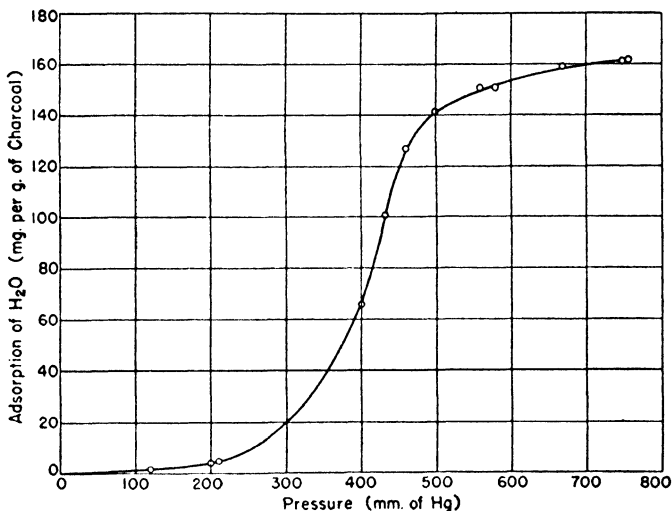


FIG. 8.—Adsorption isotherm of water vapor on coconut charcoal at 100° C.

found in the literature of van der Waals adsorption. It will be seen later that the first type (Fig. 4) represents unimolecular, the four others (Figs. 5-8) multimolecular adsorption. Their interpretation is discussed in Chapter VI.

The situation is much simpler in chemical adsorption. Only one type of isotherm has been found, similar in shape to the isotherms of Figs. 3 and 4. Fig. 9 shows adsorption isotherms of nitrogen on two different iron catalysts obtained by Emmett and Brunauer.<sup>29</sup> The isotherms are concave toward the pressure axis throughout the entire

<sup>27</sup> L. H. Reyerson and A. E. Cameron, *J. Phys. Chem.*, **39**, 181 (1935).

<sup>28</sup> A. S. Coolidge, *J. Am. Chem. Soc.*, **49**, 708 (1927).

<sup>29</sup> P. H. Emmett and S. Brunauer, *J. Am. Chem. Soc.*, **56**, 35 (1934).

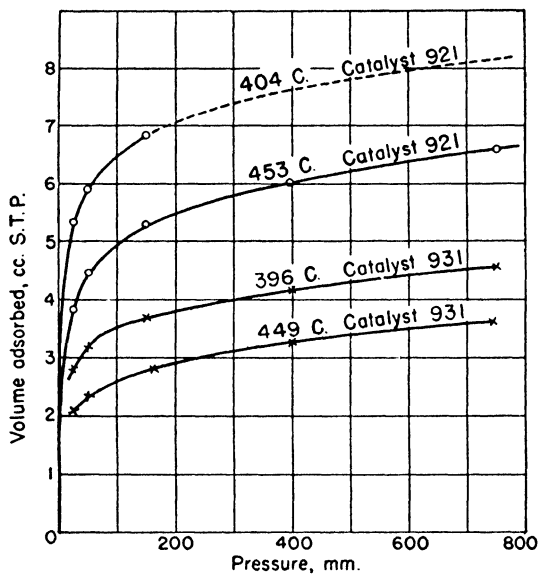


Fig. 9.—Chemisorption isotherms of nitrogen on two promoted iron catalysts.

pressure range investigated. The amount adsorbed decreases with temperature just as in van der Waals adsorption. Figure 10 shows the adsorption of hydrogen by tungsten at 200° C. on three differently

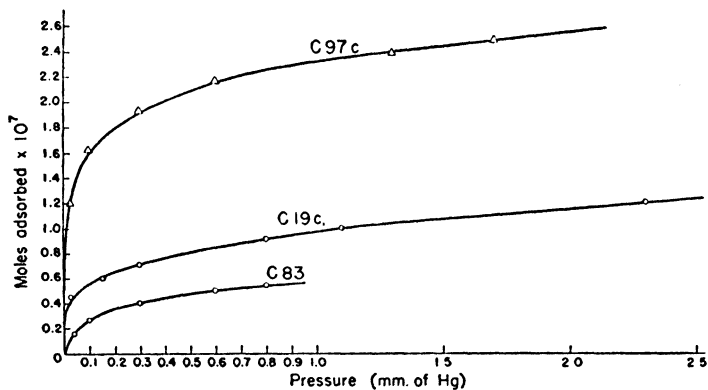


Fig. 10.—Chemisorption isotherms of hydrogen on three different tungsten powders at 200° C.

prepared tungsten powders, obtained by Frankenburger and Hodler.<sup>20</sup> The isotherms of Figs. 9 and 10 represent adsorption in a unimolecular layer.

### THE ADSORPTION ISOBAR

The isobar is a plot of the amount of gas or vapor adsorbed against temperature at constant pressure. When true equilibrium is reached, whether in van der Waals adsorption or in chemisorption, the volume adsorbed decreases with temperature. One obtains curves of the type shown in Fig. 11. These are isobars of the adsorption of am-

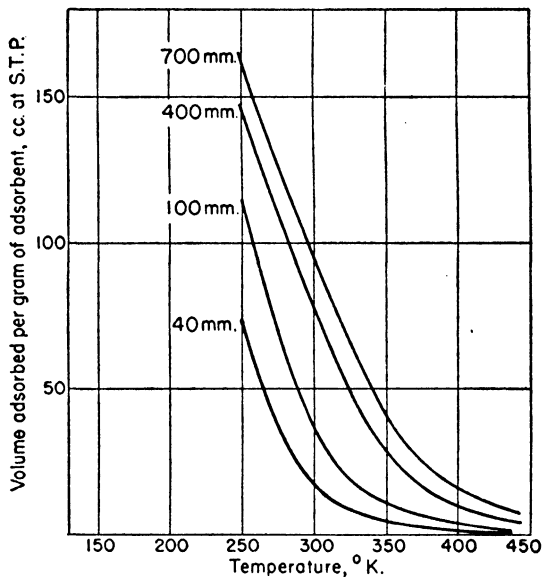


FIG. 11.—Adsorption isobars of ammonia on charcoal.

monia on charcoal, plotted from the data of Titoff.<sup>22</sup> It should be noted that these are the same experimental data that were plotted in the form of isotherms in Fig. 3. The experimental points are completely reversible with respect to temperature.

If a gas can be adsorbed in two forms, i.e., in the form of van der Waals adsorption at low temperatures and in the chemisorbed form at higher temperatures, one finds that the adsorption first decreases with increasing temperature, due to decreasing van der Waals adsorp-

<sup>20</sup> W. Frankenburger and A. Hodler, *Trans. Far. Soc.*, **28**, 229 (1932).

tion, then begins to increase when the chemisorption becomes appreciable. Langmuir<sup>31</sup> was the first to notice this phenomenon. He measured the adsorption of carbon monoxide on a clean platinum surface at liquid air temperature. When he removed the liquid air bath he found that the adsorption first decreased, then increased again.

Benton and White<sup>32</sup> found that the adsorption isobar of a gas that can be attached to the surface of the adsorbent in two different forms shows two descending portions with an ascending portion between them, as illustrated in Fig. 12. The curves are isobars of the

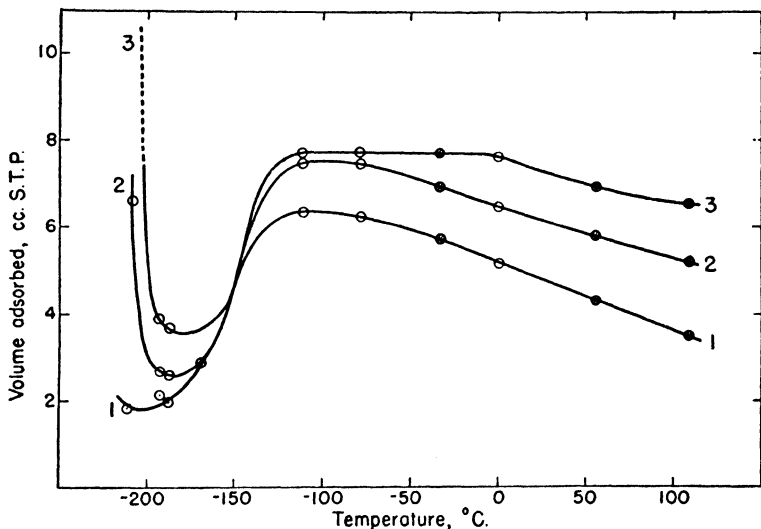


Fig. 12.—Adsorption isobars of hydrogen on nickel. Curve 1 at 2.5 cm., curve 2 at 20 cm., curve 3 at 60 cm. pressure.

adsorption of hydrogen by nickel. The low temperature descending portion corresponds to physical adsorption, the high temperature descending portion to chemical adsorption. In these regions the adsorption is reversible with respect to temperature, and the points represent true equilibria. In the ascending region the adsorption is composite, both physical and chemical adsorption are present, and the adsorption is not reversible with respect to temperature (pseudo-equilibrium). Thus if the temperature is lowered from  $-110^{\circ}\text{C}.$  the adsorption does

<sup>31</sup> I. Langmuir, *J. Am. Chem. Soc.*, **40**, 1361 (1918).

<sup>32</sup> A. F. Benton and T. A. White, *J. Am. Chem. Soc.*, **52**, 2325 (1930).



not decrease, as would be expected if the ascending region represented true equilibria. On the contrary, it increases. The interpretation of these results will be discussed in Volume II.

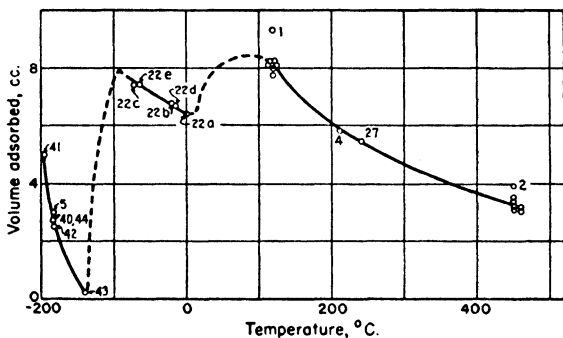


FIG. 13.—Adsorption isobar of hydrogen on iron at 760 mm. pressure.

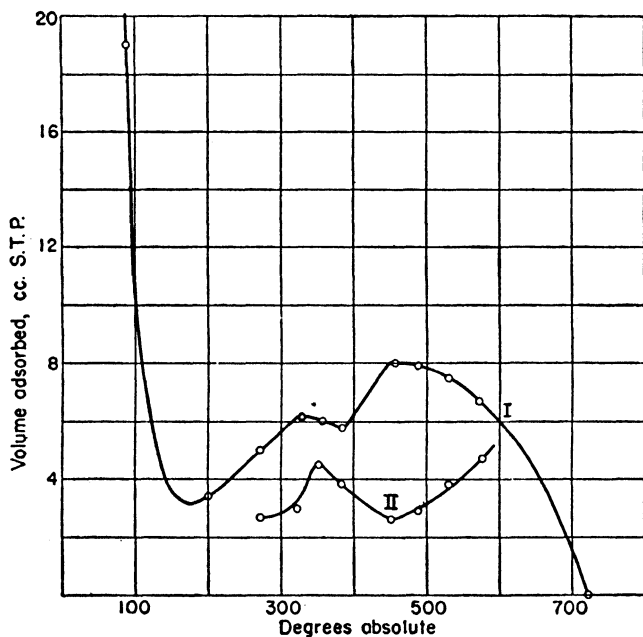


FIG. 14.—Adsorption isobar of hydrogen on zinc oxide at 760 mm. pressure.  
Curve I after 1000 minutes, curve II after 5 minutes.

Figure 13 shows a 760 mm. isobar of the adsorption of hydrogen by an iron catalyst, obtained by Emmett and Harkness.<sup>33</sup> The curve shows three descending portions, the lowest temperature region representing van der Waals adsorption, the two high temperature regions two different types of activated adsorption. It will be seen later that the two activated adsorptions probably correspond to two different chemical bindings between hydrogen atoms and the iron atoms of the surface. Similar isobars were found by Taylor and Strother<sup>34</sup> for the adsorption of hydrogen by zinc oxide, shown in Fig. 14. The points of curve I represent adsorption after 1000 minutes, those of curve II after 5 minutes. The two high temperature descending portions of curve I correspond to two different activated adsorptions. A comparison of curves I and II reveals that the rates of the two activated adsorptions are quite different.

#### THE ADSORPTION ISOSTERE

A plot of the variation of the equilibrium pressure with temperature corresponding to a constant amount of gas adsorbed is called an isostere. In Fig. 15 the data of Titoff<sup>22</sup> for the adsorption of ammonia by charcoal are replotted in the form of isosteres. Figures 3, 11, and 15 represent the same experimental data plotted in the forms of isotherms, isobars, and isosteres. Actually, the experiments were performed by measuring the adsorption at different pressures, keeping the temperature constant; the isotherm is, therefore, the plot related most closely to experiment. It is also the plot most frequently used to express the data in physical adsorption; isobars and isosteres are seldom used.

The isosteres resemble the vapor pressure curves of liquids. For a given volume of gas adsorbed the pressure increases at first slowly then rapidly with temperature. Thus the curves are convex with respect to the temperature axis.

There is more than a mere superficial resemblance between vapor pressure curves and adsorption isosteres. On the vapor pressure curve every point represents a pressure and temperature at which the liquid and its vapor are in equilibrium with each other; on the adsorption isostere every point represents a pressure and temperature at which the adsorbent-adsorbate complex is in equilibrium with the vapor or gas. For equilibrium systems the Clapeyron-Clausius equation permits the evaluation of the heat change involved in the transi-

<sup>33</sup> P. H. Emmett and R. W. Harkness, *J. Am. Chem. Soc.*, **57**, 1631 (1935).

<sup>34</sup> H. S. Taylor and C. O. Strother, *J. Am. Chem. Soc.*, **56**, 586 (1934).

tion from one phase to the other,

$$(8) \quad \frac{d \ln p}{d(1/T)} = - \frac{q}{R}$$

where  $q$  is the change in the heat content of the system accompanying the phase change and  $R$  is the gas constant.

If the logarithm of the vapor pressure of the liquid is plotted against the reciprocal of the absolute temperature, a straight line is obtained,

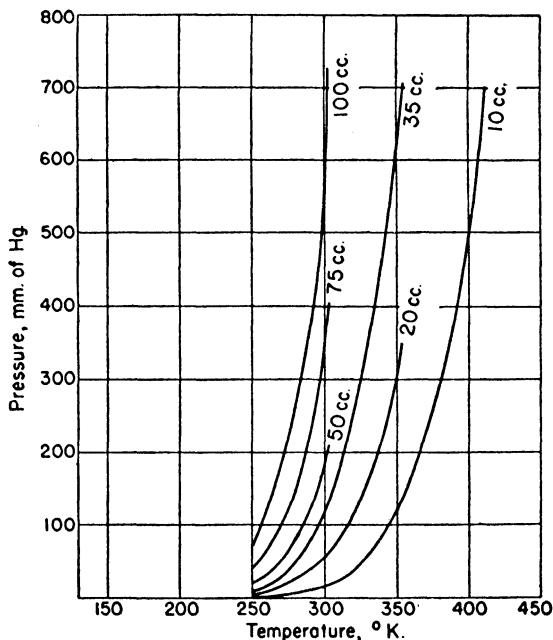


FIG. 15.—Adsorption isotherms of ammonia on charcoal.

the slope of which gives the heat of vaporization. In a similar manner plots of  $\ln p$  against  $1/T$  obtained from adsorption isotherms give the heats of adsorption. Figure 16 shows such plots obtained from the isotherms of Fig. 15. The slopes of the straight lines give the heats of adsorption. As the figure shows, the lines are not entirely parallel; the heats of adsorption are not quite the same for the different quantities of ammonia adsorbed on the surface of the charcoal.

## HEAT OF ADSORPTION

Figure 16 shows that the heat of adsorption of ammonia on charcoal is the greatest for the first quantities of gas adsorbed, and decreases as more and more adsorption takes place. Ordinarily the *differential heats of adsorption*,  $q_d$ , obtained from isosteres by means of equation (8), decrease with increasing amounts of gas adsorbed. However, this is not always true; occasionally  $q_d$  remains constant, or even in-

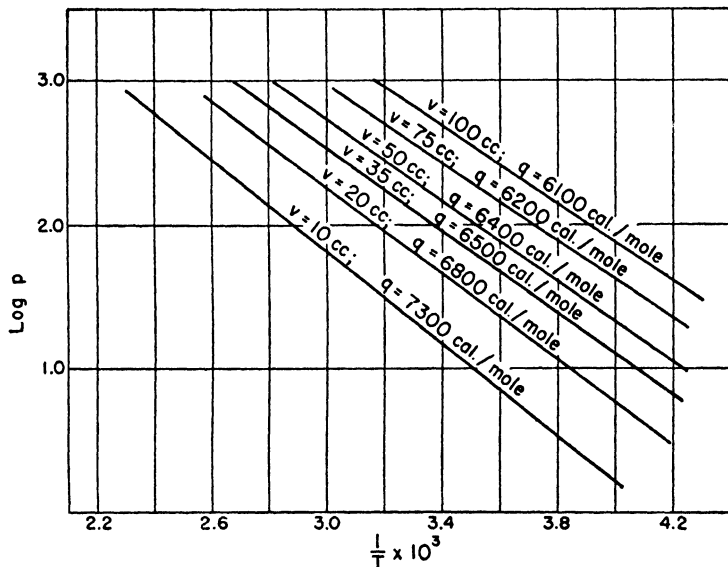


FIG. 16.—The isosteric heats of adsorption of ammonia on charcoal.

creases with increasing adsorption. Examples of all three cases are known in both physical and chemical adsorption.

The variation in  $q_d$  is due either to interaction between the adsorbed particles, or to the non-uniformity of the surface of the adsorbent. When the quantity of gas admitted is insufficient to cover the entire surface, at first the most active part of the surface adsorbs the gas, and the heat of adsorption is the largest. Subsequently, the less active portions of the surface also become covered, with the development of smaller heats of adsorption. The variation in the heats of adsorption over the surface is one of the many examples cited by Taylor<sup>35</sup> to prove the heterogeneity of the surfaces of catalysts.

<sup>35</sup> H. S. Taylor, *J. Phys. Chem.*, 30, 145 (1926); *Proc. Roy. Soc., A* 108, 105 (1925).

The heat of adsorption can also be determined by direct calorimetric measurements. If a quantity of gas is admitted to the evacuated adsorbent, the heat evolved is called the *integral heat of adsorption*; it is the average heat of adsorption for that part of the surface which is covered with adsorbed gas when equilibrium is established. If one admits sufficiently small quantities of gas at a time, and measures the heat evolved calorimetrically, one can approximate the differential heats of adsorption for the mean of the volumes adsorbed before and after the measurement. The relations between calorimetric and isosteric heats of adsorption, and between differential and integral heats of adsorption are discussed in Chapter VIII.

#### COMPARISON BETWEEN PHYSICAL ADSORPTION AND CHEMISORPTION

The differences between physical adsorption and chemisorption may be briefly summarized in six points.

1. The most fundamental difference between the two adsorptions lies in the *forces* involved; the forces between adsorbent and adsorbate in van der Waals adsorption are similar to those active in condensation phenomena, and the forces in chemisorption are similar to those active in chemical reactions.

2. The different forces of interaction between surface and gas manifest themselves in a difference in the *strength of binding* between adsorbent and adsorbate. The *heat of adsorption* in van der Waals adsorption is of the same order of magnitude as the heats of condensation of gases, in chemisorption as the heats of chemical reactions.

3. A second manifestation of the difference between the forces of interaction is found in the *specificity* of chemisorption and the non-specificity of van der Waals adsorption.<sup>36</sup> At sufficiently low temperatures van der Waals adsorption takes place between any surface and any gas, but chemisorption depends on chemical affinity between the particular adsorbent and adsorbate.

4. In van der Waals adsorption the *rate of adsorption* is rapid; the gas molecules are adsorbed as rapidly as they can reach the surface. In chemisorption an *energy of activation* must be supplied to the system before the adsorbent-adsorbate complex can form.<sup>37</sup>

<sup>36</sup> The more precise meaning of the term "specificity" is discussed in Chapter X. It is shown there that a certain degree of specificity exists even in physical adsorption.

<sup>37</sup> The energy of activation in many cases is so small that the chemisorption proceeds at a rapid rate even at low temperatures.

5. The *adsorption isotherm* in chemisorption always indicates unimolecular adsorption, in van der Waals adsorption it is either unimolecular or multimolecular.

6. The *adsorption isobar* of gases that can be adsorbed in two different forms on the same adsorbent shows two regions in which the adsorption decreases with temperature, one corresponding to physical, the other to chemical adsorption. Some isobars show three descending regions, indicating two different activated adsorptions, besides the physical adsorption.

From the foregoing it is clear that the two adsorptions are very different from each other; as different as ordinary condensation and chemical reaction. Essentially, van der Waals adsorption may be called surface condensation, chemisorption surface reaction. Since the forces involved are different, the fundamental laws that deal with the mechanisms of the two adsorptions are different. On the other hand, there are laws that deal with equilibrium states only, without involving the specification of any sort of mechanism. These are valid for both adsorptions. Thus the thermodynamic law expressed in the Clapeyron-Clausius equation (8) can be used to calculate  $q$  for both physical and chemical adsorption. Similarly, the Freundlich equation (6) that merely describes the shape of the isotherm without implying any mechanism may be applicable to both adsorptions.

Under conditions in which the two adsorptions occur simultaneously, they are usually separated on the basis of the difference in their *reversibility* with respect to temperature and pressure. The removal of chemisorbed gas from the surface is usually difficult, while physical adsorption is readily reversible. Evacuating the system, preferably combined with a slight raising of the temperature, can ordinarily remove the physical adsorption completely and leave the chemisorption unaffected. Chemical methods also are occasionally useful. The amount of chemisorbed nitrogen on an iron catalyst, for example, can be determined by reducing the surface with hydrogen and titrating the ammonia formed.<sup>29</sup>

## CHAPTER III

### EXPERIMENTAL METHODS

In all adsorption measurements the first step is to obtain the surface of the adsorbent in the highest possible state of purity, i.e., to free it as completely as possible from gases already adsorbed before the beginning of the experiment. In general we may divide all adsorption measurements into two groups: (1) determination of the amount adsorbed, and (2) determination of the heat given out in the adsorption process. Since these measurements require different types of apparatus, they will be discussed separately.

In the study of adsorption rates and adsorption equilibria one always determines the quantity of gas or vapor adsorbed. In rate measurements the amount adsorbed is a function of time, in equilibrium measurements it is a function of the pressure or temperature. The determination may be direct or indirect. It is direct when either the volume or the weight of the adsorbed material is measured, indirect when the measurement is made on some other physical property of the adsorbed phase that has a known functional relation to the amount adsorbed.

#### PURIFICATION OF THE SURFACE OF THE ADSORBENT

If the surface of the adsorbent holds only gas adsorbed in the van der Waals form, the purification is quite simple. Since the forces of binding between adsorbent and adsorbate are weak, evacuating the system with a mercury diffusion pump until a good vacuum (about  $10^{-4}$  mm.) is obtained usually suffices to remove the adsorbed gas. Heating the adsorbent slightly helps to speed up the procedure.

In most adsorption measurements the investigator has to contend with the problem of removing chemisorbed gas. Adsorbents exposed to air often hold chemisorbed oxygen, water, or carbon dioxide on their surfaces. Metallic adsorbents reduced from the oxides and oxides reduced from higher oxides always hold some chemisorbed hydrogen. The removal of these gases is difficult, requiring long continued evacuation at high temperatures. Often it is impossible to get rid of them completely without permanently injuring the surface of the adsorbent.

- When a porous adsorbent is heated to a high temperature part of its adsorptive capacity is destroyed. This process is called *sintering*.

(The mechanism of sintering is discussed in Chapter X.) The temperature at which sintering sets in is different for different adsorbents. Copper, reduced from the oxide, sinters strongly around 200° C.; iron barely begins to sinter at 350° C. and strongly sinters only around 450° C. Coconut charcoal begins to sinter above 1100° C. To remove the chemisorbed gas *completely* some adsorbents must be evacuated at temperatures that are likely to produce sintering. In order to avoid this the investigator must often be satisfied with removing most of the gas, without a complete cleaning of the surface. The procedure of evacuating a copper catalyst for 2 hours at 200° C.,<sup>1</sup> or an iron catalyst for 1 hour at 450° C.,<sup>2</sup> while sufficient to remove most of the chemisorbed hydrogen, is probably not long enough to remove all of it.<sup>3</sup>

In addition to evacuation chemical means are often helpful in removing chemisorbed gas. Thus part of the nitrogen chemisorbed on an iron catalyst comes off very slowly by pumping at 450° C. To get all of the nitrogen off the surface by evacuation one would have to use higher temperatures, and that would result in strong sintering. Instead, one can reduce the surface with hydrogen at 450° C., and the nitrogen comes off readily in the form of ammonia.<sup>2</sup> After the reduction most of the chemisorbed hydrogen can be pumped off at 450° C.

One of the most effective methods of purifying the surface prior to van der Waals adsorption is to adsorb and pump off repeatedly the vapor whose adsorption is to be studied afterwards.<sup>4</sup> A variant of this method is to pour the liquid adsorbate over the adsorbent.<sup>5</sup> Occasionally, however, such treatment injures the adsorbent (Chapter X).

The effect of chemisorbed gases on the adsorption of gases and vapors is discussed in detail in later chapters. Briefly, the inhibiting effect is strong in adsorption rate measurements and in equilibrium measurements where chemisorptions are involved, but less strong in van der Waals adsorption. At small adsorptions, i.e., when the

<sup>1</sup> A. F. Benton and T. A. White, *J. Am. Chem. Soc.*, 54, 1373 (1932).

<sup>2</sup> P. H. Emmett and S. Brunauer, *J. Am. Chem. Soc.*, 56, 35 (1934).

<sup>3</sup> J. K. Roberts (*Proc. Roy. Soc.*, A152, 445, 1935) believes that the surface of such adsorbents is always covered with a layer of chemisorbed hydrogen, no matter how long the evacuation is continued. However, chemisorption experiments on iron catalysts indicate that at most only a small fraction of the surface is covered with hydrogen. These experiments will be discussed in Volume II.

<sup>4</sup> H. S. Harned, *J. Am. Chem. Soc.*, 42, 372 (1920).

<sup>5</sup> M. T. Isselstein, *Physikal. Zeitsch.*, 29, 873 (1928).



molecules are adsorbed on the most active part of the surface, there is a definite inhibiting effect even on van der Waals adsorption,<sup>6</sup> but at higher adsorptions the effect is negligible.<sup>7</sup>

From the foregoing it is clear that one can not set up hard and fast rules for the optimum conditions of evacuation of adsorbents. The investigator himself has to choose his conditions, often by trial and error. The temperature can not be too high, otherwise the adsorbent sinters; and it can not be too low, otherwise too much chemisorbed gas remains on the surface. Often the disturbing effect of impurities is so great that one has to risk a small amount of sintering. In such cases frequent check runs are made to determine the condition of the surface, and the results are corrected to some arbitrarily chosen condition of the surface, used as a state of reference.

There are some adsorbents which do not sinter and can be made completely free of gas. Metallic wires and filaments (platinum, tungsten, etc.) are non-porous, have almost plane surfaces, and can be heated to very high temperatures without appreciably altering the surface.<sup>8</sup> Due to the fact that one deals here with very small surfaces, the adsorption can be measured only at very low pressures (about  $10^{-4}$  mm.). This is because at higher pressures the adsorption is small compared to the total amount of gas in the apparatus and the experimental error is correspondingly large. On such adsorbents van der Waals adsorption can not be studied, partly because it is small at low pressures, partly because the walls of the container and the rest of the apparatus would adsorb much more gas than the filament itself. The method is suitable, however, for the study of certain chemisorptions because these are specific, and because often a large fraction of the surface is covered at very low pressures.

Besides the impurities incidental to preparing the adsorbent, one also has to contend with impurities that may get to the surface from the other parts of the apparatus. The most troublesome among these is stopcock grease vapor. To avoid it, investigators often use apparatus containing no stopcocks, only mercury cut-off valves. Coolidge<sup>9</sup> showed that under the conditions ordinarily prevailing in an adsorption apparatus the adsorption of mercury vapor by charcoal is negligible. In very accurate work one may use a low temperature (dry ice or liquid air) trap to catch the mercury vapor.

<sup>6</sup> J. Howard, *Trans. Far. Soc.*, **30**, 278 (1934).

<sup>7</sup> S. Brunauer and P. H. Emmett, *J. Am. Chem. Soc.*, **62**, 1732 (1940).

<sup>8</sup> I. Langmuir, *J. Am. Chem. Soc.*, **40**, 1361 (1918); J. K. Roberts, *Proc. Roy. Soc.*, **A152**, 445 (1935).

<sup>9</sup> A. S. Coolidge, *J. Am. Chem. Soc.*, **49**, 1949 (1927).

## DETERMINATION OF THE AMOUNT OF GAS ADSORBED

## A. The Volumetric Method

The oldest and probably still most widely used method for determining the amount of gas adsorbed is to measure the volume taken up. The method can be illustrated in its simplest form with the apparatus of Pease<sup>10</sup> shown in Fig. 17.<sup>11</sup> Its essential parts are

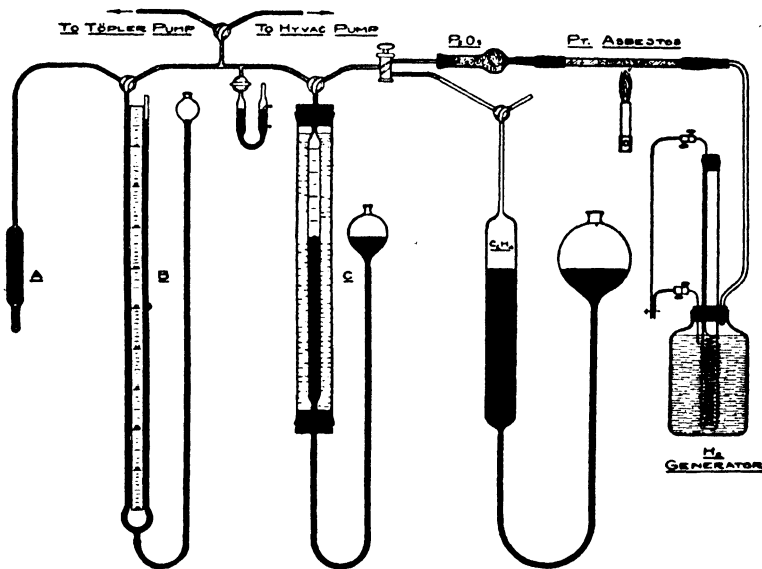


FIG. 17.—The adsorption apparatus of Pease.

bulb *A*, containing the adsorbent, mercury manometer *B*, gas buret *C*, and a system for evacuating the adsorbent, not shown in the figure. During evacuation bulb *A* is surrounded by a furnace; during the adsorption experiment it is immersed in a constant temperature bath. Prior to adsorption the volume and pressure of the gas are measured. The stopcock that leads to the evacuated adsorbent is then opened. After equilibrium is established the volume and pressure of the gas are again measured. Part of the gas that left buret *C* is adsorbed, and part of it fills up the evacuated space surrounding the adsorbent

<sup>10</sup> R. N. Pease, *J. Am. Chem. Soc.*, 45, 1196 (1923).

<sup>11</sup> The apparatus of Pease is essentially the same as the earlier ones of I. F. Homfray (*Z. Physik. Chem.*, 74, 150, 1910), A. Titoff (*Z. Physik. Chem.*, 74, 642, 1910), and L. B. Richardson (*J. Am. Chem. Soc.*, 39, 1829, 1917).

(including the pore space within the adsorbent itself). In order to know the volume adsorbed one must know the volume of this "dead space." It is measured by using a gas that is not adsorbed, helium being the most suitable. Sometimes other gases, like argon, nitrogen, etc., are used at temperatures at which their adsorption is likely to be negligible.

The accuracy of the adsorption measurements depends on the accuracy of the dead space determination. This in turn depends on the extent to which the calibrating gas is adsorbed. The adsorption of helium by charcoal was measured by Miss Homfray.<sup>12</sup> She found that it amounted to 1.82 cc. per gram of charcoal at  $-190^{\circ}\text{C}$ . and 704 mm. pressure. Taylor and Howard<sup>13</sup> found that the adsorption of helium on chromic oxide gel was 0.27 cc. per gram at  $-191^{\circ}\text{C}$ . and 760 mm. pressure. This corresponds to about 0.5% covering of the surface of the gel. At  $-78^{\circ}\text{C}$ . the adsorption of helium is barely measurable on either of these adsorbents; at  $0^{\circ}\text{C}$ . the adsorption is zero. It seems, therefore, that if the dead space is measured with helium around  $0^{\circ}\text{C}$ . no error will be introduced due to its adsorption. Since in most adsorption apparatus part of the dead space is at room temperature and part of it in a constant temperature bath, one must determine the dead space at least at two different temperatures to obtain the volumes of the two parts separately. Not only too low but also too high temperatures must be avoided, because at higher temperatures some error may be introduced by the solubility of helium in glass.<sup>14</sup>

After the dead space has been determined by means of helium, the volume of gas adsorbed can be calculated from the equation

$$(1) \quad v = v_t - v_r - v_h(1 + \alpha)$$

where  $v_t$  is the total volume of the gas in buret  $C$  before adsorption,  $v_r$  is the volume of gas remaining in the buret after adsorption,  $v_h$  is the volume of helium necessary to fill the dead space at the equilibrium pressure and temperature, and  $\alpha$  is a correction factor that takes account of the deviation of the gas in the dead space from the ideal gas laws. At the boiling point and atmospheric pressure  $\alpha$  may amount to as much as 10%.

An adsorption apparatus of somewhat greater complexity is shown in Fig. 18. This apparatus was used by Coolidge<sup>15</sup> for the study of

<sup>12</sup> I. F. Homfray, *Z. Phys. Chem.*, **74**, 129 (1910).

<sup>13</sup> H. S. Taylor and J. Howard, *J. Am. Chem. Soc.*, **56**, 2259 (1934).

<sup>14</sup> Unpublished results of A. F. Benton.

<sup>15</sup> A. S. Coolidge, *J. Am. Chem. Soc.*, **46**, 596 (1924).

the adsorption of vapors by charcoal. One of the main features is that it contains no stopcocks;<sup>16</sup> mercury cut-off valves are used instead (5, 6, 11, 24). The mercury is raised and lowered by means of pressure and vacuum applied to reservoirs 27. The apparatus consists of four parts. Part A contains the loading devices. Bulb 1 holds air-free water, bulb 2 air-free benzene, both confined by mercury in the capillary tubes and in the bulbs above them. The other liquids

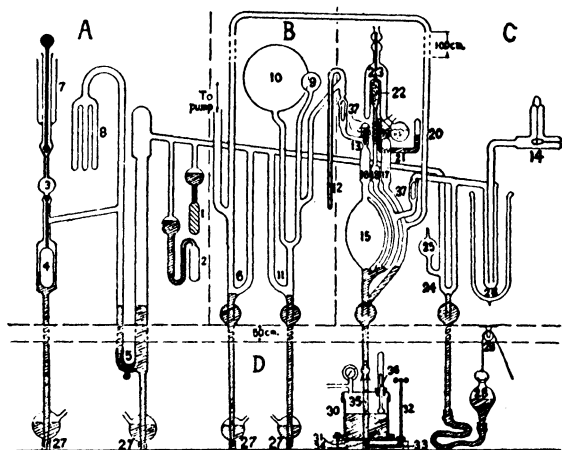


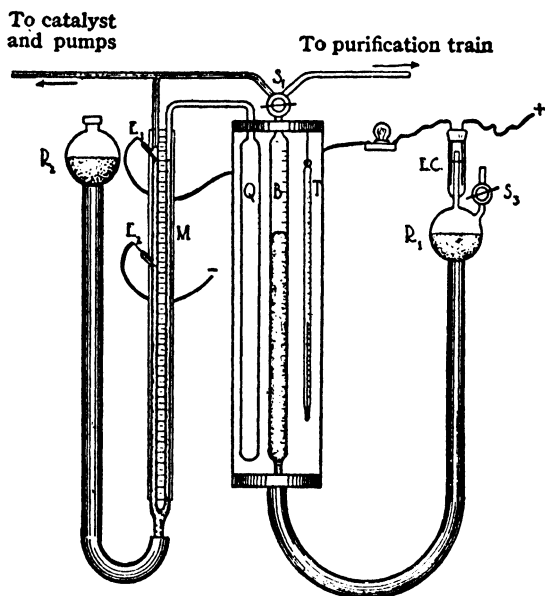
Fig. 18.—The adsorption apparatus of Coolidge.

are introduced into the apparatus through the air-lock 3, provided with two mercury sealed glass valves. Part B contains the vapor measuring devices. The volumes of flasks 9 and 10 are known, their temperature is fixed by surrounding them with a water bath, and the pressure is measured in Part C. The volume of the water used as adsorbate is measured as a liquid in the capillary buret 12. Part C contains the pressure measuring devices. These are a quartz fiber manometer 14, to measure pressures from  $10^{-4}$  mm. to 0.05 mm., a modified McLeod gage 15 for pressures from 0.02 to 1 mm., and two manometric arrangements for higher pressures. One of these is made up of arms 17 and 18, to read pressures from 1 to 100 mm. by means of a micrometer microscope; the other is between 20 and 21 to read pressures above 100 mm. by means of a meter scale. Part D contains the devices for raising and lowering mercury. The charcoal is con-

<sup>16</sup> A neat and simple apparatus without stopcocks was used by F. Goldmann and M. Polanyi (*Z. Physik. Chem.*, 132, 329, 1928).

tained in cell 22, made of pyrex glass like the rest of the apparatus when the evacuation is carried out at temperatures lower than  $550^{\circ}\text{C}.$ , and replaced by a porcelain cell when higher temperatures are used. To provide for the constant temperature of the adsorption experiments, the cell is surrounded with jacket 23, containing a suitable boiling liquid.

The experimental arrangements of Pease and Coolidge measure the adsorption at constant volume. Sometimes, particularly in rate



Constant pressure control system.

Fig. 19.—The constant pressure adsorption apparatus of Taylor and Strother.

measurements, it is desired to determine the adsorption at constant pressure. An arrangement of this type is illustrated with the apparatus of Taylor and Strother<sup>17</sup> shown in Fig. 19. The pressure control is made by raising the level of mercury in the reservoir  $R_2$  to a height at which the contact between the meniscus of the mercury in manometer  $M$  and the tungsten electrode  $E_1$  is just broken. As the gas is adsorbed, the pressure decreases, and the mercury makes

<sup>17</sup> H. S. Taylor and C. O. Strother, *J. Am. Chem. Soc.*, 56, 586 (1934).

contact with  $E_1$ . This closes an electric circuit which sends current through the electrolytic cell  $E.C.$  The gas generated exerts a pressure on the surface of the mercury reservoir  $R_1$ , forcing the mercury into the buret  $B$ . This builds up the pressure inside, which results in breaking the contact between  $E_1$  and the meniscus. The stopcock  $S_2$  serves to release the pressure at the completion of the experiment.<sup>18</sup>

In the methods described so far the adsorption is determined in a static system. Dynamic methods find widespread application in practical research, such as the testing of gas masks. A measured concentration of the toxic gas in air is passed through the adsorbent at a certain rate, and the exit gas mixture is analyzed at definite intervals. The time is noted at which the toxic gas begins to appear in the exit mixture, and the decrease in the efficiency of the adsorbent with time is followed.<sup>19</sup>

A dynamic method was used by Markham and Benton<sup>20</sup> to investigate the adsorption of gas mixtures. Their apparatus is shown in Fig. 20. The gases are mixed in reservoirs 1 and 2, passed through drying tubes  $X$  and  $Y$ , thence either through bulb  $B$  that contains the adsorbent, or directly to buret  $A$  for measurement and analysis. The manometer  $M$  measures the pressure in bulb  $B$ . The adsorption run consists in passing the gas mixture over the adsorbent for a sufficiently long time to reach equilibrium, meanwhile maintaining a constant pressure of 760 mm. by regulating the head of concentrated sulfuric acid in  $N$ . After equilibrium is established the gas is removed from  $B$  by means of the Töpler pump  $T$ , measured in gas buret  $A$ , and then analyzed. From the total volume of gas withdrawn from the bulb and from its analysis one obtains the total volume of each component separately (the sum of the gas adsorbed and in the dead space). The volume of each component in the dead space is obtained from the determination of the total dead space by means of helium and from the analysis of the original gas mixture which is passed over

<sup>18</sup> Constant pressure adsorption apparatus was also used by P. V. McKinney (*J. Phys. Chem.*, **37**, 382, 1933) and by P. H. Emmett and S. Brunauer (*J. Am. Chem. Soc.*, **56**, 36, 1934). A more sensitive manostat was constructed by T. Soller, S. Goldwasser and R. A. Beebe (*J. Am. Chem. Soc.*, **58**, 1704, 1936).

<sup>19</sup> The efficiency of an adsorbent in gas mask testing is defined as  
Percent efficiency

$$= \frac{\text{Concentration of toxic gas in entering mixture} - \text{Concentration in exit gas}}{\text{Concentration in entering mixture}}$$

× 100

A dynamic apparatus for gas mask testing is described by A. C. Fieldner, G. G. Oberfell, M. C. Teague and J. N. Lawrence, *J. Ind. Eng. Chem.*, **11**, 519 (1919).

<sup>20</sup> E. C. Markham and A. F. Benton, *J. Am. Chem. Soc.*, **53**, 497 (1931).

the adsorbent. The difference between the two gives the volume of each component adsorbed.<sup>21</sup>

### B. The Gravimetric Method

The second direct method for determining the amount of gas or vapor adsorbed is to measure the increase in the weight of the adsorbent. The success of this method is largely due to a sorption

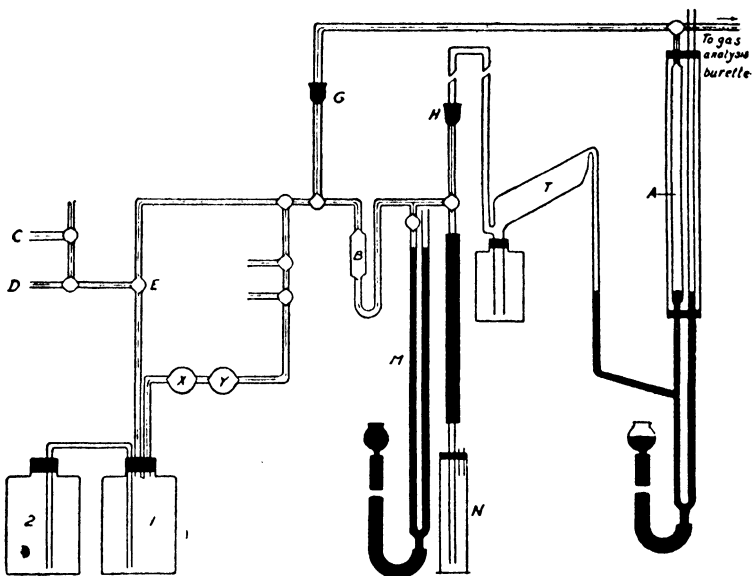


FIG. 20.—The dynamic adsorption apparatus of Markham and Benton.

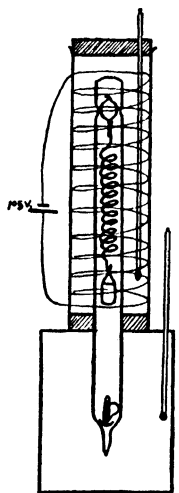
balance developed by McBain and Bakr<sup>22</sup> and shown in Fig. 21. The essential part of it is a helical spring made of fused silica. The spring ends in two hooks. The upper hook is attached to a glass sphere, the lower hook holds the bucket that contains the adsorbent.

<sup>21</sup> A volumetric apparatus for the study of the adsorption of gas mixtures was used also by A. Magnus and A. Krauss (*Z. Physik. Chem.*, A158, 183, 1932). Instead of the continuous flow method of Markham and Benton they used a circulatory system. A volumetric apparatus and a dynamic method was also used by A. R. Ubbelohde and A. Egerton (*Proc. Roy. Soc.*, A134, 512, 1931) in their determinations of the rates at which desorption equilibria are established in the charcoal-hydrogen system.

<sup>22</sup> J. W. McBain and A. M. Bakr, *J. Am. Chem. Soc.*, 48, 690 (1926).

The balance is built into a glass tube that is completely sealed off before the beginning of the adsorption determinations.

The first step in the experiments is to calibrate the spring balance. This is done by determining its length under no load, and the extensions due to the weight of the bucket, to an additional 0.1 g., to 0.2 g., etc. The calibration is carried out at all temperatures that are later used in the experiments. Next the liquid whose vapor is to be



The  
sorption balance in  
superposed adjust-  
able thermostats.

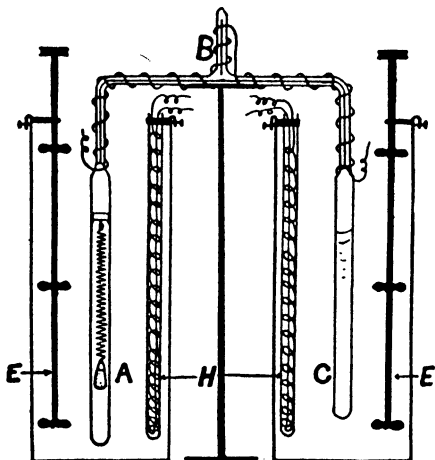
FIG. 21.—The quartz fiber sorption balance of McBain and Bakr.

adsorbed is distilled in a vacuum into a thin walled glass bulb which is then sealed. A small iron bar encased in glass is attached to the bulb, and the bulb and bar are placed at the bottom of the glass container of the balance. The bucket is filled with the adsorbent, the spring with the bucket attached is placed in the container tube, and the upper end of the tube is sealed. The lower narrow end of it is then connected to a vacuum system, and the tube is thoroughly evacuated while the upper part is heated with an electric furnace as shown in Fig. 21. When the evacuation is complete, the bottom of the tube is sealed off. The lower part of the tube is then placed in a freezing mixture and the bulb containing the adsorbent is broken by



raising the iron bar with an electromagnet and dropping it. The pressure in the system is varied by placing the lower part in a thermostat and varying its temperature. As long as some of the liquid is present, the pressure will be equal to its vapor pressure. The temperature of the adsorption is fixed by placing the upper part of the tube in another thermostat.

The McBain-Bakr sorption balance is a very handy instrument for determining the adsorption of vapors, particularly at high pressures.<sup>23</sup> Fig. 22 shows the apparatus in which Morris and Maass<sup>24</sup> determined



*Diagrammatic sketch of  
high pressure sorption apparatus.*

Fig. 22.—The high pressure adsorption apparatus of Morris and Maass.

the adsorption of propylene by alumina up to the critical pressure (46 atm.) with the help of the sorption balance. The bomb ABC is made of special pyrex bomb tubing of 12 mm. bore and 2–3 mm. wall thickness. The alumina adsorbent is contained in a perforated aluminum basket suspended on the quartz spiral in arm A; the propylene is contained in arm C. The two arms are connected by capillary tubing B which is heat-lagged to prevent the condensation

<sup>23</sup> J. W. McBain and G. T. Britton were the first to use the sorption balance in the study of the adsorption of vapors at high pressures (*J. Am. Chem. Soc.*, 52, 2198, 1930).

<sup>24</sup> H. E. Morris and O. Maass, *Can. J. Res.*, 9, 240 (1933).

of propylene. Each arm is placed in a separate thermostat, the temperature of *A* determining the temperature, the temperature of *C* determining the pressure of the adsorption experiment. Since considerable danger is involved in investigating high pressure phenomena in glass apparatus, the entire apparatus is placed in a wooden case, strapped with band iron. The observations are made through two windows of shatter-proof glass. The extension of the quartz spiral is determined by means of a cathetometer, placed four feet from the apparatus and protected by a sheet of heavy plate glass.

The main source of error in the determination of the weight of adsorbed material is in the buoyancy correction. The adsorption is usually calculated by the equation

$$(2) \quad W = w + d_m v_a - w_0$$

where *W* is the weight of the adsorbed material, *w* is the apparent weight of the adsorbent plus the adsorbate, *w*<sub>0</sub> is the weight of the adsorbent in vacuo, *d*<sub>*m*</sub> is the density of the surrounding vapor, and *v*<sub>*a*</sub> is the true volume of the adsorbent. As long as the experiments are carried out at low pressures the buoyancy correction is small, but at high pressures where *d*<sub>*m*</sub> is large the correction is quite large. Thus McBain and Britton<sup>23</sup> used a buoyancy correction in the adsorption of nitrous oxide by charcoal at 13.9° C. and 42.8 atm. pressure that was equal to 36% of the total weight adsorbed, and Morris and Maass<sup>24</sup> used a correction in the adsorption of propylene by alumina at 90.2° C. and 39.4 atm. pressure that amounted to 45%. Under such conditions it is of great importance to know the true volume of the adsorbent, *v*<sub>*a*</sub>. This is equal to *w*<sub>0</sub>/*d*<sub>*a*</sub> where *d*<sub>*a*</sub> is the true density of the adsorbent. The determination of the true density of a porous body is not a simple matter. Coolidge and Fornwalt<sup>25</sup> determined the density of coconut charcoal by displacement in several liquids. They found the values of 0.629 in mercury, 2.06 in benzene and 2.12 in ether. Obviously, mercury can not penetrate into all of the pores of the charcoal where benzene and ether can penetrate, and doubtless there are fine pores into which even ether can not penetrate. Densities determined by means of helium come probably the closest to the true density of the adsorbents (Chapter XI).

Coolidge<sup>26</sup> pointed out that the amount of gas or vapor adsorbed at high pressures depends on the definition of the dead space. According to the classical definition the amount adsorbed is the excess

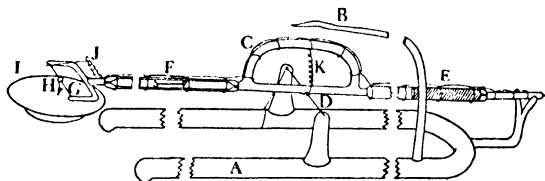
<sup>23</sup> A. S. Coolidge and H. J. Fornwalt, *J. Am. Chem. Soc.*, 56, 561 (1934).

<sup>26</sup> A. S. Coolidge, *J. Am. Chem. Soc.*, 56, 554 (1934).

material present in the pores of the adsorbent over the amount that would be present in the pore space if the vapor had its normal density at the temperature and pressure of the experiment. With this definition the amount adsorbed is calculated by means of equation (2). Another possible definition is to make the amount adsorbed equal to all the material contained in the pore volume, on the assumption that all matter in the pores is under the influence of adsorption forces. If this definition is adopted, one has to consider in the buoyancy correction not merely the volume of the adsorbent, but also the volume of the adsorbed phase. The weight adsorbed then becomes

$$(3) \quad W' = w + d_m v_a + d_m v_s - w_0$$

where  $v_s$  is the volume of the adsorbed phase. At lower pressures  $d_m v_s$  is negligible, but at high pressures it is large. Thus in the adsorption of carbon dioxide by charcoal at 25° C. and 7.2 atm. pressure



The adsorption of water vapor on silica surfaces.

FIG. 23.—The beam type microbalance of Barrett, Birnie and Cohen.

the weight adsorbed on the basis of the first (classical) definition was 0.361 g. per g., on the basis of the second definition 0.371 g. per g., a difference of less than 3%. On the other hand in the adsorption of nitrous oxide by charcoal at 0° C. and 54.4 atm. pressure the weight adsorbed on the basis of the first definition was 0.085 g. per g., on the basis of the second it was 0.852 g. per g., a ten fold difference.<sup>25</sup>

Although most investigators who determine gravimetrically the amount adsorbed use the spring balance of McBain and Bakr, some use the beam type balance.<sup>27</sup> The two important advantages of the beam type microbalance are its greater sensitivity and the almost complete elimination of buoyancy effects.

Figure 23 shows a microbalance designed by Barrett, Birnie and Cohen<sup>28</sup> for the study of the adsorption of water vapor on silica sur-

<sup>27</sup> A very sensitive quartz beam microbalance was used by J. W. McBain and H. G. Tanner (*Proc. Roy. Soc., A125*, 579, 1929) for measuring the adsorbed films on platinum.

<sup>28</sup> H. M. Barrett, A. W. Birnie and M. Cohen, *J. Am. Chem. Soc.*, **62**, 2839 (1940).

faces. It consists of a long, hollow glass beam supported at its center by a fine tungsten torsion filament to which it is sealed at *D*. On one end of the beam is a platinum basket *I*, that contains the adsorbent, on the other end is a pointer made of a short tungsten wire. The increase in the weight of the adsorbent causes a movement of the pointer which is read by a microscope. The balance is calibrated by means of an iron rider *F*, that is placed inside the hollow arm. It is moved by a solenoid and the motion is observed through another microscope. The pointer half of the beam contains also a platinum compensating weight *E*. The balance rests in a waterjacketed glass tube, thermostated within  $0.01^\circ$ . To eliminate electrostatic charges on the balance and to ground the basket, the beam is wound with fine platinum wire.

At the outset the fused silica counterweight is placed in the basket and the rider is moved by the solenoid until the beam swings freely. When the balance comes to equilibrium the position of the pointer is noted. The rider is then moved a short distance and the positions of the rider and the pointer are again observed with the two microscopes. From the weight of the rider and the distance of the basket from the center one can calculate the change in load corresponding to a given pointer movement. After the balance is calibrated for the entire range of pointer readings, the silica counterweight is replaced by an equal weight of silica powder that is used as adsorbent. The apparatus is evacuated, and the rider is adjusted until the pointer swings freely. Water vapor is then admitted and the new pointer position is read after pressure equilibrium is established. The sensitivity of this balance is  $10^{-7}$  g., whereas the sensitivity of the spring balance is only of the order of  $10^{-4}$  g.<sup>29</sup>

Gravimetric methods can be used not only in static adsorption apparatus but also in dynamic systems. Williams<sup>30</sup> passed a stream of air saturated with benzene over U tubes containing silica gel, and followed the course of the adsorption by weighing the tubes at frequent intervals. The "dynamic retentivity" method of Burrage<sup>31</sup> consists in saturating the adsorbent with the vapor at a definite temperature

<sup>29</sup> J. Giesen used a sensitive microbalance for adsorption measurements as early as 1903 (*Ann. der Physik* (4), 10, 838, 1903). Besides the spring type and the beam type balance mention should be made of the torsion balance of R. Seliger (*Physikal. Z.*, 22, 563, 1921) and of the floating balance of H. H. Chambers and A. King (*J. Chem. Soc.*, 1939, 139).

<sup>30</sup> E. C. Williams, *J. Soc. Chem. Ind.*, 43, 97T (1924).

<sup>31</sup> L. J. Burrage, *J. Phys. Chem.*, 34, 2202 (1930); 37, 33 (1933).

and pressure, then passing dry air through the system at a known rate, noting the decrease in the weight of the adsorbent.<sup>32</sup>

### C. Indirect Methods

Some investigators have determined other physical properties of the adsorbed gas than its volume or weight. The use of such indirect methods has in some cases thrown interesting light on the mechanism of adsorption processes. Two of these methods will be briefly discussed here: an optical method,<sup>33</sup> and the method of the accommodation coefficients.<sup>34</sup>

An optical method<sup>35</sup> for the study of the adsorbed layer was recently revived by Frazer<sup>36</sup> at the suggestion of Herzfeld. It consists of shining light, plane polarized at 45° to the angle of incidence, at the boundary layer between solid and gas, and analyzing the reflected beam. If the boundary between solid and gas were perfectly sharp, the reflected beam would be plane polarized. Actually this never happens. The light is always more or less elliptically polarized. This is partly caused by roughnesses and vibrations in the surface, but is due predominantly to the presence of an adsorbed layer of gas at the interface. The ellipticity of the reflected beam is measured either by a Babinet compensator or by a photometric determination of the ratio of the two axes of the ellipse. There is a functional relation, derived by Drude,<sup>37</sup> between the ellipticity and the thickness of the transition layer (adsorbed phase), which contains the wave length of the light used, and the dielectric constants of the solid, the adsorbed layer and the gas.<sup>38</sup> By assuming a reasonable value for the dielectric

<sup>32</sup> A. G. Foster (*Trans. Far. Soc.*, 32, 1559, 1936) compared the dynamic reactivity method with static adsorption methods, and found that the former is entirely unreliable for certain systems, and at best it gives only approximately correct results.

<sup>33</sup> A different optical method, based on changes in interference colors caused by changes in the adsorbed film, was used by Mrs. M. B. Coelingh (*Kolloid Z.*, 87, 251, 1939). See Chapter XI.

<sup>34</sup> Several other indirect methods are discussed in later chapters.

<sup>35</sup> This method was first used by Lord Rayleigh, *Phil. Mag.* (6), 23, 431 (1903).

<sup>36</sup> J. H. Frazer, *Phys. Rev.* (2), 33, 97 (1929); 34, 644 (1929).

<sup>37</sup> P. Drude, *Lehrbuch der Optik*, p. 272.

<sup>38</sup> The relation is

$$\rho = \frac{\pi}{\lambda} \frac{(\epsilon_1 + \epsilon_2)^{1/2}}{\epsilon_1 - \epsilon_2} \int_0^d \frac{(\epsilon - \epsilon_1)(\epsilon - \epsilon_2)}{\epsilon} dz$$

where  $\rho$  is the ellipticity (the ratio of minor to major axis);  $\epsilon_1$ ,  $\epsilon_2$  and  $\epsilon$  are the dielectric constants of the gas, solid, and the adsorbed phase, respectively;  $\lambda$  is the wave length of the light used, and  $z$  is the position in the adsorbed layer measured

constant of the adsorbed phase, the thickness of the layer can be calculated.

The study of the accommodation coefficients in the heat interchange between gases and solid surfaces brought out much important information about adsorption phenomena. When a gas molecule strikes a hot surface it may be adsorbed, or it may rebound, the collision resulting in an interchange of energy. If the temperature of the gas is  $T_1$  before and  $T_2$  after the collision, and the temperature of the surface is  $T'_2$ , the accommodation coefficient is defined as

$$(4) \quad a = (T_2 - T_1)/(T'_2 - T_1)$$

The accommodation coefficient is a measure of the efficiency of the heat interchange. Its value depends strongly on the purity of the solid surface, as was shown by Roberts.<sup>39</sup> A pure tungsten surface, for example, has an accommodation coefficient with neon of about 0.07, but the value rises to 0.6 when the surface is covered with some impurity. Thus the accommodation coefficient can be used as an indicator of the degree of covering of the surface. Miss Blodgett and Langmuir<sup>40</sup> proved by this method that hydrogen has two activated adsorptions on tungsten.

#### DETERMINATION OF THE HEAT OF ADSORPTION

In the direct determination of the heat of adsorption both isothermal and adiabatic calorimeters have been applied. In the isothermal calorimeter the heat is allowed to escape from the system and is utilized to produce a phase change such as, for example, the melting of ice. The system remains at a constant temperature, and the heat developed is calculated from the amount of ice melted. In the adiabatic calorimeter the heat is kept in the system, and the amount evolved is calculated from the temperature rise.

Favre<sup>41</sup> was the first to measure heats of adsorption quantitatively, using the isothermal method with mercury as the calorimeter substance. Dewar<sup>42</sup> determined the heats of adsorption of gases on charcoal at  $-185^\circ\text{C}$ . with the help of a liquid air calorimeter. The most widely used calorimeter of the isothermal type is the ice calorim-

from the surface. The integration is carried out over the entire adsorbed layer ( $d$  is the thickness of the adsorbed layer).

<sup>39</sup> J. K. Roberts, *Proc. Roy. Soc.*, A129, 146 (1930); 135, 192 (1932); 142, 518 (1933).

<sup>40</sup> K. B. Blodgett and I. Langmuir, *Phys. Rev.*, 40, 78 (1932).

<sup>41</sup> P. A. Favre, *Ann. Chim. Phys.*, (5), 1, 209 (1874).

<sup>42</sup> J. Dewar, *Proc. Roy. Soc.*, 74, 124 (1904).

eter,<sup>43</sup> a modern variant of which is shown in Fig. 24. This apparatus was used by Marshall and Bramston-Cook<sup>44</sup> for measuring the heat of adsorption of oxygen on charcoal. The parts of the apparatus on the right serve to determine the amount of gas adsorbed, the calorimeter itself is on the left. Quartz tube *D* contains the charcoal, which is thoroughly outgassed prior to the experiment. Tube *D* is placed in the calorimeter tube, which is connected at *A* through capillary tubing

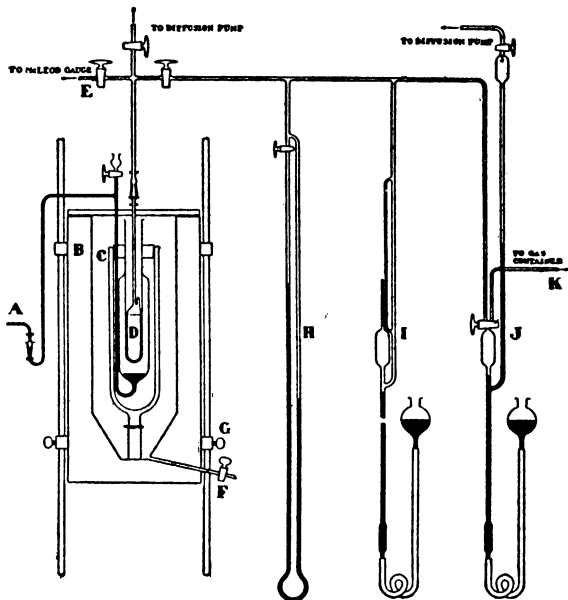


FIG. 24.—The ice calorimeter of Marshall and Bramston-Cook.

with a fixed capillary of calibrated bore. The calorimeter tube contains the ice mantle, and the rest of it is filled with mercury. The capillary tubing is also filled with mercury. As the heat of adsorption melts the ice, the volume contraction causes a movement of the mercury in the calibrated capillary. From the observed contraction the

<sup>43</sup> Ice calorimeters were used by A. Titoff (*Z. Phys. Chem.*, 74, 641, 1910), by A. B. Lamb and A. S. Coolidge (*J. Am. Chem. Soc.*, 42, 1147, 1920) and by F.G. Keyes and M. J. Marshall (*J. Am. Chem. Soc.*, 49, 160, 1927). The above described apparatus of Marshall and Bramston-Cook is a modification of the arrangement of Keyes and Marshall.

<sup>44</sup> M. J. Marshall and H. E. Bramston-Cook, *J. Am. Chem. Soc.*, 51, 2019 (1929).

quantity of ice melted is calculated, which in turn gives the amount of heat developed.

The rest of the calorimeter arrangement serves as heat insulator. The calorimeter tube proper is placed in a silvered Dewar flask provided with a large stopper, through which the neck of the calorimeter passes. The space *C* is filled with cracked ice and distilled water. As the ice melts more is added, and an equal quantity of water is removed at *F*.

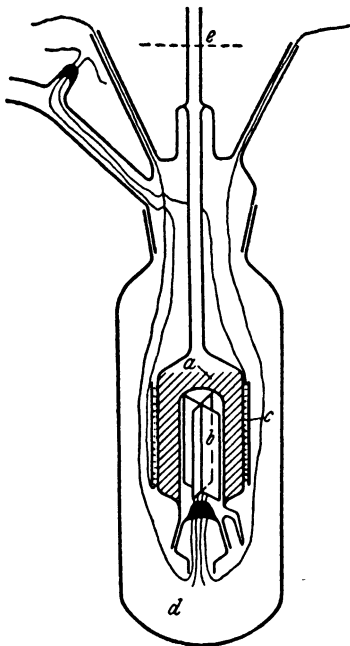


FIG. 25.—The adiabatic calorimeter of Taylor, Kistiakowsky and Florsdorf.

The outer vessel has double walls, the space *B* being packed to the top with wool waste. It is covered with a 1/2 inch thick piece of felt to prevent too rapid melting of the ice in *C*.

Besides liquid air, mercury, and ice, other substances were also used in isothermal calorimeters. Gregg<sup>45</sup> used phenol, melting at 40° C., and Sachse<sup>46</sup> used diphenyl ether, melting at 26.55° C.

<sup>45</sup> S. J. Gregg, *J. Chem. Soc.*, 1927, 1494.

<sup>46</sup> H. Sachse, *Z. Phys. Chem.*, A143, 94 (1929).



In recent years adiabatic calorimeters have found more favor with investigators of the heats of adsorption.<sup>47</sup> Perhaps the most important reason is that they do not restrict the adsorption to one particular temperature. A calorimeter of this type is shown in Fig. 25. It was used by Taylor, Kistiakowsky and Flosdorf.<sup>48</sup> In the center of the calorimeter is a very sensitive platinum resistance thermometer *b*, wound in the form of a cross on thin mica. The adsorbent *a* is in the ring-shaped space surrounding the thermometer. The calorimeter tube proper is wound on the outside with a platinum heating coil *c*, used for electrical calibration. It is protected outward by a layer of mica. The tube is placed in a large vacuum flask *d*, filled with ice to the height shown by the dotted line in the figure. The flask is placed in the ice thermostat *f*. The calorimeter is connected at *e* to the vacuum system and the gas inlet.

The great drawback of an adiabatic calorimeter of the sort described above is that the temperature rise of the thermometer is strongly dependent on the thermal conductivity of the adsorbent and the gas. Since porous adsorbents are very poor conductors and since gases at low pressures are also slow in conducting heat, erroneous values are likely to be obtained for the heats of adsorption at low pressures. This situation was pointed out by Bull, Hall and Garner,<sup>49</sup> and analyzed more thoroughly by Schwab and Brennecke.<sup>50</sup> The anomalous initial heats of adsorption obtained by some investigators will be discussed in Volume II.

A construction that attempts to eliminate difficulties arising from temperature gradients within the system is shown in Fig. 26, the calorimeter of Bull, Hall and Garner.<sup>49</sup> The silica reaction vessel is double-walled, and through the tubes *PP* as well as through the stoppers *OO* water is circulated at constant temperature. By changing the temperature of the circulating water immediately after the adsorption has started, the calorimeter could be made almost completely adiabatic. The reaction vessel and the furnace *F* is surrounded by an air thermostat to eliminate temperature gradients throughout the system. The activated carbon adsorbent is held in the platinum gauze vessel *A*. The platinum-platinum-rhodium thermocouple

<sup>47</sup> Adiabatic calorimeters were used by R. A. Beebe and H. S. Taylor (*J. Am. Chem. Soc.*, 46, 44, 1924), by E. A. Blench and W. E. Garner (*J. Chem. Soc.*, 125, 1291, 1924), and by A. Magnus and M. Braner (*Z. anorg. Chem.*, 151, 141, 1926).

<sup>48</sup> H. S. Taylor, G. B. Kistiakowsky and E. W. Flosdorf, *J. Am. Chem. Soc.*, 49, 2200 (1927).

<sup>49</sup> H. I. Bull, M. H. Hall and W. E. Garner, *J. Chem. Soc.*, 1931, 837.

<sup>50</sup> G. M. Schwab and W. Brennecke, *Z. Phys. Chem.*, B16, 19 (1932).

wires entering at *MM* had to be immersed at least to a depth of 3.5 cm. in the carbon adsorbent, otherwise erroneous results were obtained. Since the experiments indicated that in the first admissions adsorption occurred only on the outer layers of the carbon, the platinum gauze vessel was later replaced by another container. This was made of a cylindrical tube of platinum foil closed at each end, with a gauze tube

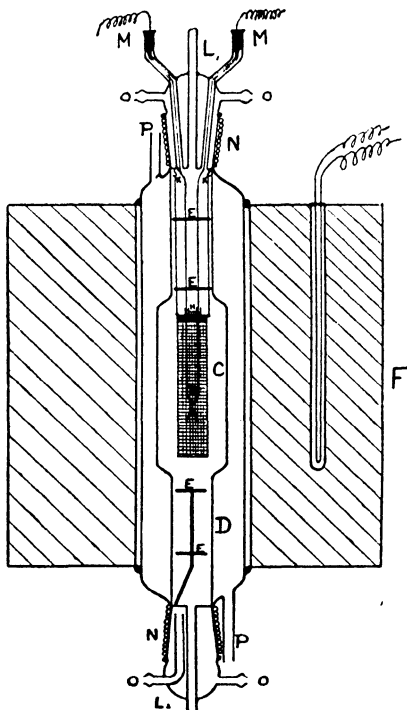


FIG. 26.—The calorimeter of Bull, Hall and Garner.

along its axis. Two small holes were made at one end to admit the adsorbent and the thermocouple. The adsorbent was placed in the annular space between the gauze tube and the cylinder.

In Garner's arrangement the gas is admitted to the space between the calorimeter proper and the silica reaction vessel. Since the gas is on the outside of the radiating surface, considerable loss of heat takes place, except at very low pressures. In Taylor's arrangement gas is admitted to the inside of the radiating surface and the glass vessel is surrounded by high vacuum. As a result, Garner's calori-

meter works satisfactorily at low pressures, Taylor's at higher pressures.<sup>51</sup> In subsequent work Garner and Veal<sup>52</sup> constructed calorimeters based on Taylor's model that worked well for the integral heats of adsorption of both slow and rapid adsorption processes and for the differential heats of adsorption of slow processes.<sup>53</sup>

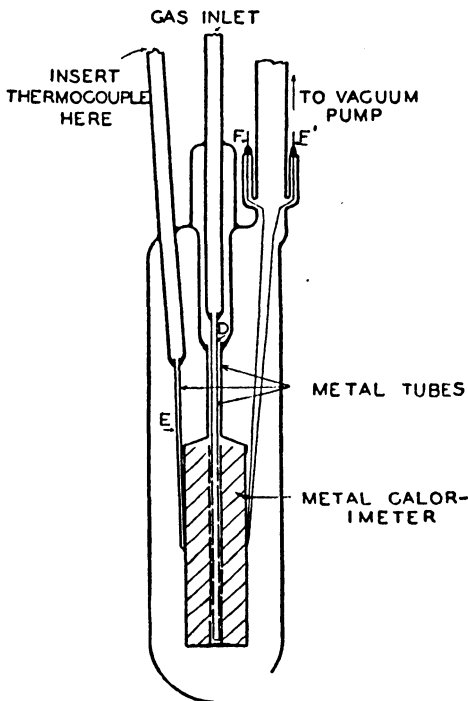


Fig. 27.—The calorimeter of Beebe and Orfield.

The adiabatic calorimeter was further developed by Beebe and his collaborators.<sup>54</sup> The latest arrangement is shown in Fig. 27. It was

<sup>51</sup> In the calorimeter used by A. F. H. Ward the gas is admitted to the inside of the radiating surface, as in Taylor's, but the calorimeter is surrounded by air instead of vacuum (*Proc. Roy. Soc.*, A133, 506, 1931).

<sup>52</sup> W. E. Garner and F. J. Veal, *J. Chem. Soc.*, 1935, 1436.

<sup>53</sup> We may mention also the calorimeter of E. B. Maxted and C. H. Moon. In order to prevent too rapid loss of heat from the thermocouple at higher pressures, they placed it in a thin sheath made of pyrex glass (*Trans. Far. Soc.*, 32, 1375, 1936).

<sup>54</sup> R. A. Beebe and E. L. Wildner, *J. Am. Chem. Soc.*, 56, 642 (1934); R. A. Beebe, G. W. Low, Jr. and S. Goldwasser, *J. Am. Chem. Soc.*, 58, 2196 (1936).

used by Beebe and Orfield<sup>55</sup> to determine heats of adsorption at  $-183^{\circ}\text{C}$ . The temperature is measured by a single junction copper-constantan thermocouple and a sensitive galvanometer, the time-temperature curves being recorded photographically. The thermocouple is led in either by inserting it into the metal tube *E* which is soldered to the calorimeter cylinder, or through the tungsten bridge wires *F* and *F'*, in which case the thermocouple itself is soldered to the cylinder. The calorimeter is made of silver. The space between the silver cylinder and the outer pyrex tube can be highly evacuated even when there is residual pressure of gas over the adsorbent. Thus the loss of heat from the calorimeter to the surroundings is slight. After each differential heat determination is completed, a little helium is admitted to the outer space to bring back rapidly the temperature of the calorimeter to that of the surrounding bath. The calorimeter's inner metal tube *D*, made of platinum, is perforated with many small holes to bring a large part of the adsorbent into simultaneous contact with the incoming gas. This serves to minimize the creation of temperature gradients and hot spots within the adsorbent. To insure further rapid heat distribution there are six vertical vanes of perforated copper foil placed inside the silver cylinder, and fine copper shot is intermixed with the granules of the adsorbent. This type of calorimeter works very well up to pressures of a few millimeters.<sup>56</sup>

An extremely simple adiabatic calorimeter was used by Roberts.<sup>3</sup> He determined the amount of gas adsorbed on a tungsten wire and at the same time used the wire itself as a calorimeter. As the gas was adsorbed, heat was given out and the temperature of the wire rose. From the measured change in the resistance of the wire its temperature change was obtained, and since the mass and the specific heat of the wire were known, Roberts was able to calculate the heat evolved.

<sup>55</sup> R. A. Beebe and H. M. Orfield, *J. Am. Chem. Soc.*, 59, 1627 (1937).

<sup>56</sup> Satisfactory calorimeters were developed also by Magnus and his collaborators (A. Magnus and W. Kälberer, *Z. anorg. Chem.*, 164, 347, 1927; A. Magnus and H. Giebenhain, *Z. Phys. Chem.*, A143, 265, 1929).

Part Two

**PHYSICAL ADSORPTION**



## CHAPTER IV

### THE ADSORPTION ISOTHERM I

In Chapter II it was shown that the data of adsorption equilibrium can be plotted in the form of isotherms, isobars and isosteres. A theory that gives a *complete* account of the adsorption isotherm accounts for the isobar and isostere as well, since a series of adsorption isotherms can always be replotted in the form of a series of isobars or isosteres. This was done for Titoff's data<sup>1</sup> on the adsorption of ammonia by charcoal in Figs. 3, 11 and 15. It was also shown in Chapter II that the differential heats of adsorption can be calculated from the adsorp-

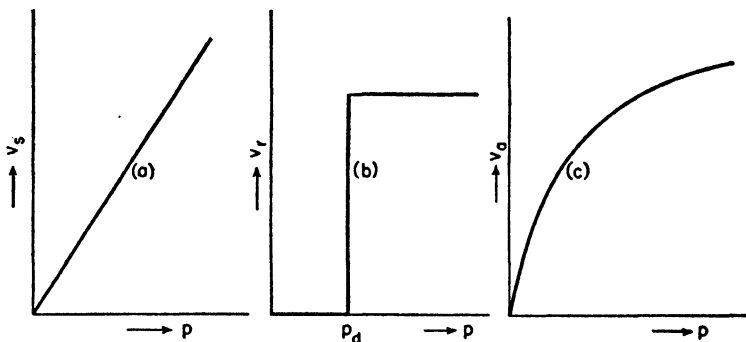


FIG. 28.—Isotherms of solution, chemical reaction and adsorption.

tion isotherms by means of the Clapeyron-Clausius equation. Thus the theory of the adsorption isotherm is actually the theory of adsorption equilibrium. No information can be obtained from the isotherm about the rate of adsorption; the kinetics of adsorption constitutes a separate study. The rate of physical adsorption is discussed in Chapter XIII.

In Fig. 28 the shape of the simplest adsorption isotherm is compared with the shapes of what one may call the "absorption isotherms." Curves (a) and (b) represent the variation with pressure of the volume of gas taken up by the solid when the gas enters the inside of the solid.

<sup>1</sup> A. Titoff *Z. phys. Chem.*, 74, 641 (1910).

Curve (a) represents solution of the gas in the solid, the pressure dependence of the volume dissolved obeying Henry's law

$$(1) \quad v_s = k_s p$$

Curve (b) shows the "isotherm" of a chemical reaction between solid and gas. At first no gas is taken up until the pressure reaches  $p_d$ , the dissociation pressure of the solid. When that pressure is reached all the gas is taken up, and the pressure remains constant until the reaction is complete. After that no more gas is taken up with increasing pressure. This behavior can be expressed by the equations

$$(2) \quad v_r = 0 \quad \text{when } p < p_d,$$

$$(3) \quad v_r = k_r \quad \text{when } p > p_d$$

Finally, curve (c) gives a simple type of van der Waals adsorption isotherm.

It was pointed out in Chapter II that in the low pressure region the volume adsorbed varies with the first power of the pressure

$$(4) \quad v_a = k_1 p$$

Thus the dependence is similar to that given in equation (1) for solution. Many isotherms at high pressures show a region in which the volume adsorbed is independent of the pressure

$$(5) \quad v_a = k_2$$

The volume adsorbed in this case is proportional to the zero power of the pressure, just as it is in equation (3) for chemical reaction. In the intermediate pressure range the adsorption varies with a power of the pressure that is smaller than 1 but greater than 0

$$(6) \quad v_a = k p^{1/n}$$

where  $n > 1$ . This is the Freundlich adsorption isotherm equation.

### THE FREUNDLICH EQUATION

The Freundlich equation is an empirical equation. When it is obeyed it gives a concise analytical expression for the experimental facts, rather than a clear cut picture of the mechanism of adsorption. It is the oldest isotherm equation (often referred to as the "classical" equation), and is still widely used by investigators, particularly in industrial practice.

In the last three decades numerous attempts have been made to give a theoretical meaning to the equation. Some of the more recent ones achieved a partial success, but even now the picture is far from



being entirely clear. Since these attempts at interpretation are based on the Langmuir equation, they are taken up after the discussion of that equation.

If we take the logarithm of equation (6) we obtain

$$(7) \quad \log v = \log k + \frac{1}{n} \log p$$

This is a linear equation, suitable for testing the validity of the formula. If a plot of  $\log v$  against  $\log p$  gives a straight line, the adsorption data obey the Freundlich equation. The slope of the straight line then gives  $1/n$ , the intercept gives  $\log k$ .

Figure 29(a) shows adsorption isotherms of carbon monoxide on coconut charcoal obtained by Miss Homfray.<sup>2</sup> In Fig. 29(b)  $\log v$  is plotted against  $\log p$ . For the pressure and temperature range investigated, quite satisfactory straight lines are obtained, showing that

TABLE II  
ADSORPTION CONSTANTS OF GASES ON COCONUT CHARCOAL  
1 g. of adsorbent, temperature 0° C.

Gas	$k$	$\frac{1}{n}$	Boiling Point
N <sub>2</sub>	0.26	0.87	-195
CO	0.56	0.76	-192
A	0.22	0.88	-186
CH <sub>4</sub>	2.69	0.56	-160
C <sub>2</sub> H <sub>4</sub>	23.7	0.23	-102.5
CO <sub>2</sub>	8.25	0.53	-78

the data obey the Freundlich equation. The slopes of the lines, i.e., the values of  $1/n$ , increase with increasing temperature. The values of  $1/n$  for the five isotherms are 0.38, 0.56, 0.76, 0.82 and 0.84 at -78.3, -33.6, 0, 20 and 46.2° C., respectively. Thus with increasing temperature  $1/n$  approaches the limiting value of unity. This corresponds to the fact that for small adsorptions equation (4), Henry's law, is obeyed. The intercepts of the lines give  $\log k$ . The values of  $k$  for the five isotherms are 12.0, 2.5, 0.56, 0.29 and 0.15, taken in the same order as above. When  $p = 1$ ,  $k = v$ ; i.e.,  $k$  is the volume adsorbed at unit pressure. The rapid decrease in  $k$  with increasing temperature is a measure of the decrease in adsorption with increasing temperature when the pressure is unity.

Table II shows the adsorption constants of several gases on coconut charcoal at 0° C. They were evaluated by Freundlich<sup>3</sup> from the

<sup>2</sup> I. F. Homfray, *Z. phys. Chem.*, 74, 129 (1910).

<sup>3</sup> H. Freundlich, *Colloid and Capillary Chemistry*, London, 1926, p. 120.

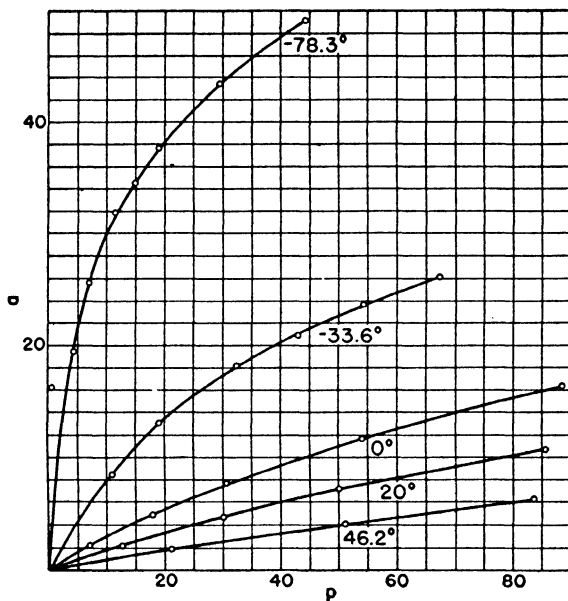


FIG. 29a.—Adsorption isotherms of carbon monoxide on charcoal. Amount adsorbed in cc. S.T.P., pressure in cm. of Hg.

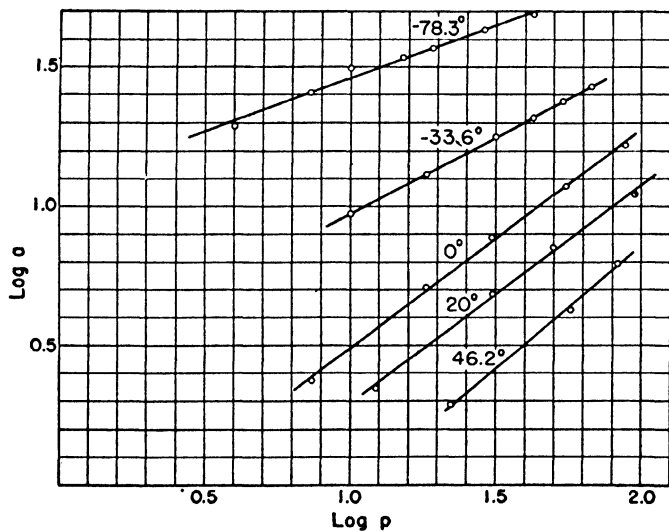


FIG. 29b.—The isotherms of Fig. 29a plotted according to the Freundlich equation.

adsorption data of Miss Homfray.<sup>2</sup> A comparison of the constants with the boiling points of the gases shows that on the whole  $k$  increases and  $1/n$  decreases with increasing boiling point of the gas, but the correlation is very poor.

In Fig. 30 Titoff's data<sup>1</sup> for the adsorption of ammonia by charcoal are plotted according to the Freundlich equation. (The same data

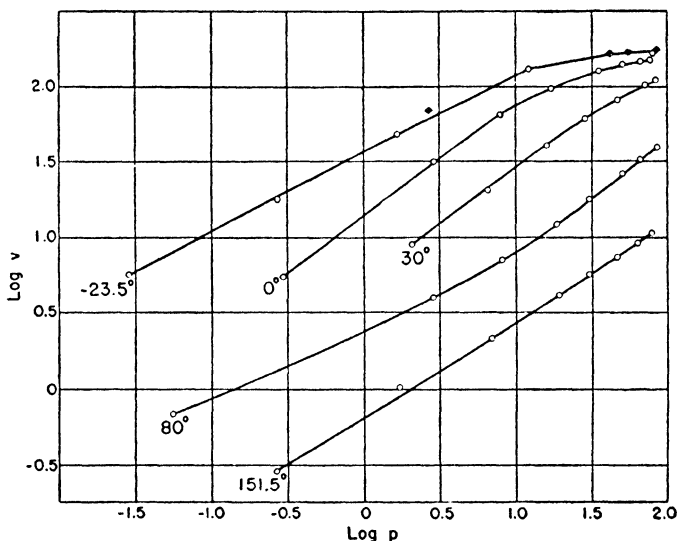


FIG. 30.—The isotherms of Fig. 3 plotted according to the Freundlich equation.

were plotted in the form of isotherms, isobars and isosteres in Figs. 3, 11 and 15.) The agreement is very poor, particularly at high pressures and low temperatures.

In general, a large number of the experimental results in the field of van der Waals adsorption (and even in chemisorption) can be expressed by means of the Freundlich equation in the middle pressure range. A still larger number can not be expressed satisfactorily.<sup>4</sup> Where the equation is obeyed, it can be used as an interpolation formula. An example of this is found in the work of Peters and Weil,<sup>5</sup>

<sup>4</sup> A large number of empirical modifications of the Freundlich equation have been proposed to fit better the experimental data. As examples we may cite K. Peters (*Z. phys. Chem.*, A180, 79, 1937) and W. Rogers and M. Sclar (*J. Phys. Chem.*, 36, 2284, 1932).

<sup>5</sup> K. Peters and K. Weil, *Z. phys. Chem.*, A148, 1 (1930):

who studied the adsorption of argon, krypton and xenon on charcoal. They determined experimentally six adsorption isotherms: three for xenon, two for krypton and one for argon. These are given in Fig. 31. They plotted  $\log v$  against  $\log p$ , and from the slopes and intercepts of the straight lines evaluated the constants  $k$  and  $1/n$ . Table III gives

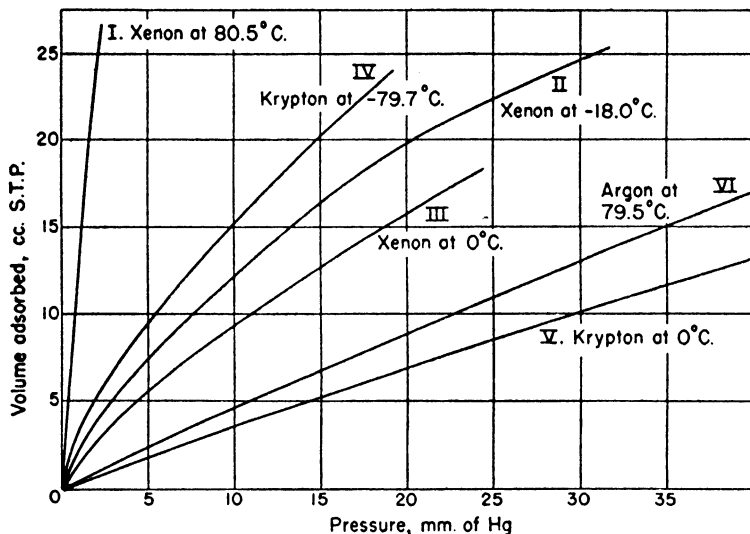


Fig. 31.—Adsorption isotherms of argon, krypton and xenon on charcoal.

the values of these constants. Those in parentheses were obtained by interpolation and extrapolation. For example,  $k$  for krypton at 255° K was obtained from the ratio

$$(8) \quad \frac{k_{\text{Xe}, 193} - k_{\text{Xe}, 255}}{k_{\text{Kr}, 193} - (k_{\text{Kr}, 255})} = \frac{k_{\text{Xe}, 255} - k_{\text{Xe}, 273}}{(k_{\text{Kr}, 255}) - k_{\text{Kr}, 273}}$$

Thus from the three known  $k$  values for xenon and the two known  $k$  values for krypton the unknown  $k_{\text{Kr}, 255}$  could be calculated. Having obtained in this manner three isotherms for each of the three gases, they were able to plot quite accurately by interpolation any number of isotherms between  $-80$  and  $0^\circ \text{C}$ . Figure 32 gives for the entire temperature range the  $\log v$  vs.  $\log p$  plots for the three gases.

Peters and Weil suggested that the data represented in Fig. 32 could be utilized for the quantitative separation of the three gases by

means of desorption from charcoal. They thought that with the help of these data one could calculate the pressure, temperature, and the amount of adsorbent necessary to produce any given separation for any specified gas mixture. This belief was based on the assumption

TABLE III  
ADSORPTION CONSTANTS OF RARE GASES ON CHARCOAL  
1 g. of adsorbent

Gas	$T = 193^{\circ} \text{ K.}$		$T = 255.2^{\circ} \text{ K.}$		$T = 273.2^{\circ} \text{ K.}$	
	$k$	$\frac{1}{n}$	$k$	$\frac{1}{n}$	$k$	$\frac{1}{n}$
Argon	0.500	0.950	(0.0764)	(1.0)	(0.0581)	(1.0)
Krypton	2.927	0.711	(0.497)	(0.885)	0.340	1.0
Xenon	15.99	0.574	2.458	0.692	1.583	0.77

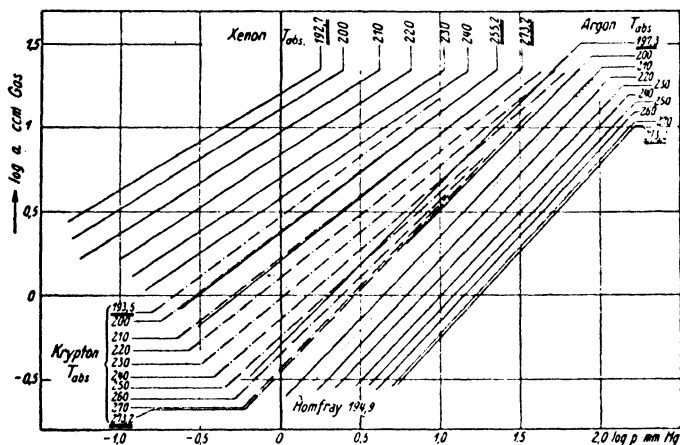


FIG. 32.—Adsorption isotherms of argon, krypton and xenon on charcoal plotted according to the Freundlich equation.

that the gases do not influence each other's adsorption. It will be shown in Chapter XIV, in the discussion of mixed adsorption, that this assumption is incorrect. The method of fractionation by means of desorption is, indeed, applicable to the separation of rare gases, but no exact quantitative conclusions can be drawn from the data of Peters and Weil.

## THE LANGMUIR EQUATION

Until the year 1914 there existed no satisfactory theoretical treatment of the surface adsorption of gases and vapors. In 1915 two entirely independent theories were proposed, by Polanyi and by Langmuir. Their approach was different: Langmuir believed that adsorption was a chemical process and that the adsorbed layer was unimolecular, Polanyi believed that adsorption was a physical process and that the adsorbed phase was many layers thick. Both treatments were successful in many instances, and both have their limitations. The Polanyi theory applies to van der Waals adsorption only, the Langmuir theory applies within limits to both chemical and physical adsorption.

The Langmuir equation is perhaps the most important single equation in the field of adsorption. Although there are at present isotherm equations that fit experimental data which do not obey the Langmuir equation, and others that fit the data over a wider range, in most cases the starting point in their derivations is the Langmuir equation. Because of the central position of the Langmuir equation in the theory of adsorption we shall discuss here three of its derivations: the original kinetic derivation of Langmuir, the thermodynamic derivation of Volmer, and the statistical derivation of Fowler.

*A. The Kinetic Derivation*

When the molecules of a gas or vapor collide with the surface of a solid, the collision may be either elastic or inelastic. In some cases, very infrequently, the molecule may be elastically reflected from the surface without any energy exchange taking place. Ordinarily, however, the collision is inelastic, and the molecule stays in contact with the surface for a certain length of time. After a while it leaves the surface and returns to the gas phase. According to Langmuir<sup>6</sup> this time lag is responsible for the phenomenon of adsorption.

It happens sometimes, especially at high temperatures, that the time of sojourn of a molecule on the surface is so short that thermal equilibrium is not reached. For example, Roberts<sup>7</sup> found accommodation coefficients<sup>8</sup> much smaller than unity for the collision of helium and neon with a clean tungsten surface. In other cases the time lag

<sup>6</sup> I. Langmuir, *J. Am. Chem. Soc.*, 40, 1361 (1918).

<sup>7</sup> J. K. Roberts, *Proc. Roy. Soc.*, A129, 146 (1930); 135, 192 (1932); 142, 518 (1933).

<sup>8</sup> See Chapter II, equation (4).

may be long, particularly in chemisorption which involves a strong binding of the molecule to the surface.

When the rate at which molecules strike the surface is  $\mu$  and the rate at which they evaporate is  $\nu$ , the net rate of adsorption is

$$(9) \quad \frac{ds}{dt} = \alpha\mu - \nu$$

where  $s$  is the surface concentration (the number of gas molecules adsorbed per sq. cm. surface), and  $\alpha$  is the condensation coefficient (the ratio of the number of molecules that condense on the surface to the total number of molecules that strike the surface). Because elastic collisions are infrequent the value of  $\alpha$  is always close to unity.

At equilibrium  $\frac{ds}{dt} = 0$ , and

$$(10) \quad \alpha\mu = \nu$$

which is the most general form of the isotherm equation. The value of  $\mu$  for a unit surface is obtained from the kinetic theory of gases <sup>9</sup>

$$(11) \quad \mu = \frac{p}{(2\pi mkT)^{1/2}}$$

where  $m$  is the mass of a molecule and  $k$  is Boltzmann's constant. The value of  $\nu$  is dependent on the strength of binding between the solid and the adsorbed molecule. If  $q$  is the heat given out when a molecule is adsorbed, then only those molecules will be able to desorb that acquire an energy quantity equal to or greater than  $q$ . The rate of evaporation will then be

$$(12) \quad \nu = k_0 e^{-q/kT}$$

If one divides  $\nu$  by  $s$ , i.e., the number of molecules that evaporate from unit surface per second by the total number of molecules adsorbed on a unit surface, one obtains the average probability per second for the evaporation of a molecule. The reciprocal of this is the average life of an adsorbed molecule on the surface

$$(13) \quad \tau = s/\nu$$

The forces active in adsorption have a short range of action. The valence forces decrease exponentially with the distance between an adsorbed molecule and an atom of the surface, the van der Waals

<sup>9</sup> See, for example, K. F. Herzfeld, "Kinetische Theorie der Wärme," Leipzig, 1925, p. 29.

forces decrease with the seventh power of the distance. It is quite unlikely therefore that a surface saturated with a complete layer of adsorbed molecules would be able to attract and adsorb a second layer of molecules. On the other hand, if the forces of interaction between the already adsorbed molecules and the molecules in the gas phase are sufficiently strong, a second adsorbed layer may form. Let  $q_1$  and  $q_2$  be the heats of adsorption in the first and second layers. Since the rate of evaporation varies exponentially with  $q$ , a relatively small change in  $q$  causes a great change in  $\nu$ .

Langmuir<sup>10</sup> in later papers discussed the two cases  $q_1 < q_2$  and  $q_1 > q_2$ . When the forces between the molecules of the adsorbate are greater than the forces between the adsorbent and the adsorbate, i.e., when  $q_2 > q_1$ , there is a tendency on the part of the adsorbed molecules to form clusters in the first layer, and on top of these clusters a second, third, and even higher layers may form before the adsorption in the first layer is complete. When molecules of iodine, cadmium or mercury condense on a glass surface at not too low temperatures, discrete crystals of the condensed substance form, indicating that the forces of interaction between iodine and iodine are greater than those between iodine and glass. Langmuir believed that when  $q_2 > q_1$ , one always obtains discontinuous condensed films rather than true van der Waals adsorption. As a matter of fact, it will be shown in Chapter VI that this situation leads to continuous adsorption isotherms that are convex toward the pressure axis at low pressures, the types shown in Figs. 7 and 8.<sup>11</sup>

When  $q_1 > q_2$ , one obtains the more usual types of isotherms, which are concave toward the pressure axis at low pressures (shown in Figs. 3-6). As the pressure is raised the surface becomes covered with a unimolecular adsorbed layer. Langmuir<sup>10</sup> thought that after the completion of the first layer a considerable increase in pressure would be necessary to form the second layer. However, ordinarily one does not get such discontinuous isotherms. In chemisorption  $q_1$  is so much greater than  $q_2$  that a second layer does not form at all, and only unimolecular adsorption occurs. In van der Waals adsorption  $q_1$  is only slightly greater than  $q_2$ , and the second layer begins to form before the first layer is complete.<sup>12</sup>

<sup>10</sup> I. Langmuir, *J. Am. Chem. Soc.*, **54**, 2798 (1932); Nobel Lecture, 1932.

<sup>11</sup> S. Brunauer, L. S. Deming, W. E. Deming and E. Teller, *J. Am. Chem. Soc.*, **62**, 1723 (1940).

<sup>12</sup> S. Brunauer, P. H. Emmett and E. Teller, *J. Am. Chem. Soc.*, **60**, 309 (1938).



We may proceed now, following Langmuir, to derive the explicit form of the isotherm equation (10). The quantities  $\alpha$ ,  $\mu$ , and  $\nu$  are functions of  $p$ ,  $T$ , and  $s$ . Instead of the surface concentration one may use the fraction of the surface covered

$$(14) \quad \theta = s/s_1$$

where  $s_1$  is the surface concentration when a complete unimolecular layer has been formed.

Langmuir introduced two assumptions in the derivation of his equation. The first is that the probability of evaporation of a molecule from the surface is the same whether the neighboring positions on the surface are occupied by other molecules or not. This is equivalent to assuming that the forces of interaction between the adsorbed molecules themselves are negligible. It is expressed by the equation

$$(15) \quad \nu = \nu_1 \theta$$

where  $\nu_1$  is the rate of evaporation from a completely covered surface. Equation (15) also implies a uniform heat of adsorption over the entire surface.

Langmuir's second simplifying assumption is that every molecule coming from the gas phase that strikes a molecule already adsorbed on the surface is elastically reflected, and only those molecules condense that strike the bare surface. This is expressed by

$$(16) \quad \alpha\mu = \alpha_0(1 - \theta)\mu$$

where  $\alpha_0$  is the condensation coefficient on the bare surface, and  $1 - \theta$  is the fraction of the surface that is bare. This assumption is equivalent to the postulation of unimolecular adsorption. The value of  $\alpha_0$  is always close to unity.

Substituting equations (15) and (16) into (10) and solving for  $\theta$  one obtains the Langmuir isotherm equation

$$(17) \quad \theta = \frac{\frac{\alpha_0}{\nu_1} \mu}{1 + \frac{\alpha_0}{\nu_1} \mu}$$

One may write this equation in the form

$$(18) \quad \theta = \frac{bp}{1 + bp}$$

where  $b$ , the adsorption coefficient, is a function of the temperature only. Its value can be obtained from (15), (16), (11), and (12)

$$(19) \quad b = \frac{\alpha_0 e^{q/kT}}{k_0(2\pi mkT)^{1/2}}$$

If we call  $v$  the volume adsorbed at pressure  $p$ , and  $v_m$  the volume adsorbed when the surface is covered with a complete unimolecular layer, then

$$(20) \quad \theta = v/v_m$$

and substituting into equation (18) we obtain

$$(21) \quad v = \frac{v_m b p}{1 + b p}$$

In spite of the fact that the two simplifying assumptions embodied in equations (15) and (16) considerably limit the scope of the Langmuir equation (21), still it has found application in a large number of instances. Some examples will be given later.

### B. The Thermodynamic Derivation

Volmer<sup>13</sup> showed that an isotherm equation of the same form as Langmuir's can be derived from thermodynamic considerations. When a gas is in equilibrium with an adsorbed layer, the work involved in the isothermal transfer of an infinitesimal amount of gas from the gas phase to the adsorbed phase is zero. The transfer involves compression of the gas and expansion of the adsorbed layer. The change in free energy is

$$(22) \quad dF_{\text{gas}} - dF_{\text{ads}} = 0$$

In order that this change may be expressed in terms of  $p$ ,  $v$ , and  $T$ , one must know the equation of state of the gas in both phases. Volmer assumed that in the gas phase the perfect gas law is obeyed

$$(23) \quad pv = RT$$

It was pointed out in Chapter II that physical adsorption resembles surface condensation. It may be assumed, therefore, that the adsorbed layer behaves like a two-dimensional imperfect gas or possibly like a two-dimensional liquid. Volmer used an equation of state similar to the van der Waals equation for imperfect gases

$$(24) \quad \varphi(\Omega - \beta) = RT$$

<sup>13</sup> M. Volmer, *Z. phys. Chem.*, 115, 253 (1925).

where  $\varphi$  is the pressure of the two-dimensional gas,  $\Omega$  is the surface covered by one mole of the adsorbate, and  $\beta$  is a surface correction factor, analogous to the volume correction factor  $b$  in the van der Waals equation.<sup>14</sup> The surface pressure  $\varphi$  is analogous to the three-dimensional gas pressure. It is the force acting on a unit length of the boundary line of the surface, tending to expand the adsorbate and to increase the surface. This "spreading force" is opposed to the surface tension and is given by

$$(25) \quad \varphi = \sigma_0 - \sigma$$

where  $\sigma_0$  is the surface tension of the pure surface and  $\sigma$  is that of the surface containing the adsorbate. The reciprocal of  $\Omega$  is  $s$ , the surface concentration, the number of moles of gas adsorbed per sq. cm. surface. The constant  $\beta$  corresponds to that part of the surface which is not available for the motion of the adsorbed molecules. According to kinetic theory it is twice the surface occupied by a mole of gas.

The explicit form of equation (22) is given by<sup>15</sup>

$$(26) \quad vdp - \Omega d\varphi = 0$$

From equation (23) one obtains

$$(27) \quad dp = - \frac{RTdv}{v^2}$$

and from equation (24)

$$(28) \quad d\varphi = - \frac{RTd\Omega}{(\Omega - \beta)^2}$$

Substituting equations (27) and (28) into (26), one gets

$$(29) \quad \frac{\Omega d\Omega}{(\Omega - \beta)^2} = \frac{dv}{v}$$

If one assumes that  $2\Omega\beta \gg \beta^2$ , one can write

$$(30) \quad \frac{d\Omega}{(\Omega - 2\beta)} = \frac{dv}{v}$$

This restricts the validity of Volmer's considerations to adsorptions not too close to saturation of the surface. Integrating (30) and

<sup>14</sup> The introduction of another correction factor, analogous to the van der Waals constant  $a$ , will be discussed later.

<sup>15</sup> See G. N. Lewis and M. Randall, *Thermodynamics*, New York, 1923, equation (10) on p. 162 and equation (17) on p. 247.

removing logarithms, one obtains

$$(31) \quad \Omega - 2\beta = k'v$$

where  $k'$  is the integration constant. Substituting  $\Omega = 1/s$ , and  $v = RT/p$

$$(32) \quad \frac{1}{s} = \frac{k'RT}{p} + 2\beta$$

and finally

$$(33) \quad s = \frac{\frac{1}{k'RT} p}{1 + \frac{2\beta}{k'RT} p}$$

Since the volume of gas adsorbed by the entire surface is  $As$ , where  $A$  is the surface area of the adsorbent, equations (21) and (33) give a formally similar dependence of the volume adsorbed on pressure. The constant  $b$  of equation (21) may be identified with  $2\beta/k'RT$  of equation (33), and  $v_m$  with  $A/2\beta$ . The latter implies that at complete covering of the surface the area occupied by each molecule is equal to four times the cross-sectional area of the molecule in the gas phase. However, in view of the fact that the assumptions and implications entering the kinetic and thermodynamic derivations are somewhat different, it seems to be of dubious value to identify Langmuir's  $v_m$  with Volmer's  $A/2\beta$ .

### C. The Statistical Derivation

The complete statistical derivation of the Langmuir equation, given by Fowler,<sup>16</sup> will not be reproduced here.<sup>17</sup> Fowler emphasizes the fact that the original kinetic derivation is apt to obscure the essentially thermodynamic character of the equation and may lead to the erroneous belief that the form of the equation depends on the mechanism of condensation and evaporation of the adsorbed molecules. As a matter of fact, it depends only on the entire set of states, adsorbed and gaseous, that are accessible to the molecules at equilibrium. The statistical derivation is based on three assumptions: (1) the

<sup>16</sup> R. H. Fowler, *Proc. Cambridge Phil. Soc.*, 31, 260 (1935).

<sup>17</sup> Statistical derivations of the Langmuir equation were also made by S. C. Kar (*Physik. Z.*, 26, 615, 1925), by S. C. Kar and A. Ganguli (*Physik. Z.*, 30, 918, 1929), by T. Sexl (*Z. Physik*, 48, 607, 1928), by M. Temkin (*Acta Physiochim. U. R. S. S.*, 1, 36, 1934), and others. Recently W. Band (*J. Chem. Phys.*, 8, 178, 1940) derived statistically the isotherm equation for a mobile unimolecular layer adsorbed on the surface of a liquid.

molecules of the gas are adsorbed without dissociation to definite points of attachment on the surface of the adsorbent; (2) each point of attachment can accommodate one and only one adsorbed molecule; and (3) the energies of the states of any adsorbed molecule are independent of the presence or absence of any other adsorbed molecules on neighboring points of attachment. These assumptions are similar to those of Langmuir. The first assumption, although not stated, is implied in the kinetic derivation. When dissociation occurs, the form of the Langmuir equation is different from equation (21). (It will be given in Volume II.) The second assumption corresponds to Langmuir's assumption of unimolecularity, embodied in equation (16). The third corresponds to the assumption of no interaction between adsorbed molecules, expressed in equation (15).

On the basis of the three assumptions, using the Fermi-Dirac statistics, Fowler derived the equation

$$(34) \quad \theta = \frac{b(T) \cdot p}{1 + b(T) \cdot p}$$

where  $b(T)$  is a function of the temperature alone. Its explicit form is given by

$$(35) \quad b(T) = \frac{h^3}{(2\pi m)^{3/2} (kT)^{5/2}} \frac{f_a(T)}{f_g(T)} e^{q/kT}$$

where  $h$  is Planck's constant,  $f_a(T)$  is the partition function of the adsorbed states attached to a specified surface atom,  $f_g(T)$  is the partition function for the rotations and vibrations of the free gas molecule, and  $q$  is the energy required to transfer the molecule from the lowest adsorbed state to the lowest gaseous state. Since the assumptions of Fowler are similar to Langmuir's, the adsorption coefficient  $b$  must have approximately the same meaning in both derivations. A comparison of (19) and (35) shows that this is actually true.

Equations (34) and (35) were also derived on the basis of the theory of absolute reaction rates by Laidler, Glasstone and Eyring.<sup>18</sup>

#### APPLICATIONS OF THE LANGMUIR EQUATION

In this chapter only a few applications of the Langmuir equation to physical adsorption are discussed. We have seen that the Freundlich equation can not describe an isotherm completely from the lowest to the highest pressure region. When it is applicable, it can be used only in the middle pressure range. In contrast to this, the Langmuir

<sup>18</sup> K. J. Laidler, S. Glasstone and H. Eyring, *J. Chem. Phys.*, 8, 659 (1940).

equation is capable of fitting experimental data from zero pressure to saturation. The equation is

$$(21) \quad v = \frac{v_m b p}{1 + b p}$$

At low pressures, or more correctly at small adsorptions,  $b p$  can be neglected in comparison with 1 in the denominator and the equation reduces to

$$(36) \quad v = v_m b p$$

The adsorption varies linearly with pressure, as in equation (4). In the high pressure or high adsorption region, we may neglect 1 in comparison with  $b p$  in the denominator, and the equation becomes

$$(37) \quad v = v_m$$

The adsorption is independent of the pressure as in equation (5). In the intermediate region the complete equation (21) must be used.

#### A. Small Adsorptions

It was pointed out in Chapter II that at small adsorptions the variation of the amount adsorbed is approximately linear with pressure. In Figs. 3 and 29(a) the isotherms at the highest temperatures are almost linear up to atmospheric pressure. In Fig. 31 the krypton isotherm at 0° C. is exactly linear up to 52 mm. pressure. Further examples are shown in Fig. 33, giving some adsorption isotherms of argon on silica gel obtained by Kälberer and Mark.<sup>19</sup> In the temperature range between -22 and 60° C. the isotherms are accurately linear from 0.1 to 2 mm. pressure. The adsorptions measured correspond only to a small fraction of one per cent of the surface covered. The isotherms remain linear up to atmospheric pressure.

In contrast, the isotherms shown in Fig. 34 are not linear even at low pressures. They represent isotherms of carbon dioxide on silica gel samples at 0° C. obtained by Kälberer and Schuster.<sup>20</sup> The curvature at low pressures can be understood if we consider that equation (36) gives a linear dependence on pressure of the amount adsorbed only if  $b$  is really constant over the range of adsorption investigated. An inspection of equation (35) shows that this is true only if  $q$ , the heat of adsorption, is independent of the amount of gas adsorbed. However, there are two factors that may cause a variation in  $q$ . In

<sup>19</sup> W. Kälberer and H. Mark, *Z. phys. Chem.*, A139, 151 (1928).

<sup>20</sup> W. Kälberer and C. Schuster, *Z. phys. Chem.*, A141, 270 (1929).

the first place interaction between the adsorbed molecules may increase or decrease the heat of adsorption, depending on whether the molecules attract or repel each other. This cause probably does not

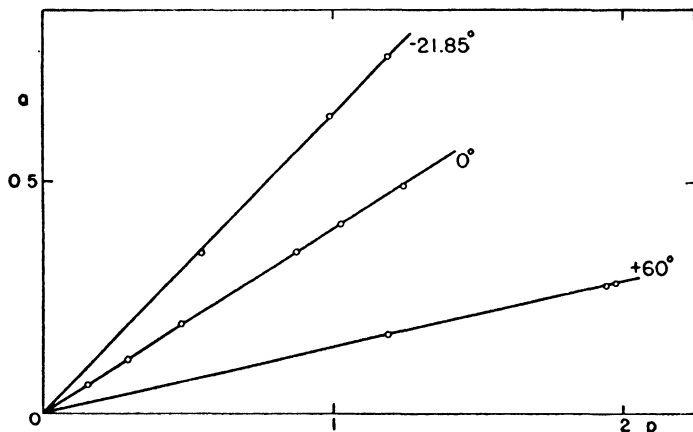


FIG. 33.—Adsorption isotherms of argon on silica gel at low pressures. Amount adsorbed in cc. S.T.P., pressure in mm.

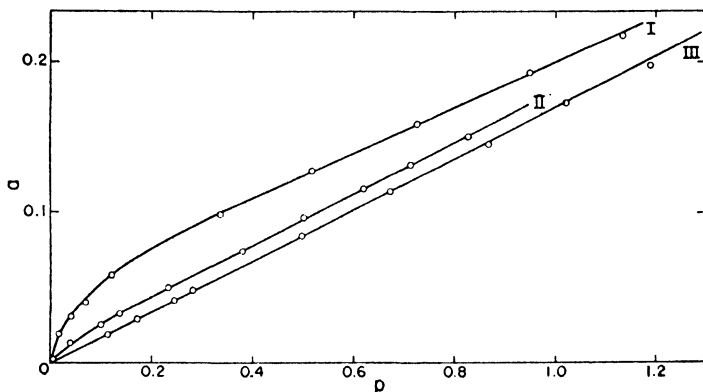


FIG. 34.—Adsorption isotherms of carbon dioxide on three different silica gels at 0° C. and low pressures. Amount adsorbed in cc. S.T.P., pressure in mm.

operate in the isotherms of Fig. 34, since only a small fraction of the surface is covered. The molecules are adsorbed at such great distances from each other that they can not interact.<sup>21</sup> In the second

<sup>21</sup> It will be shown in Chapter XIV that this is not always true.

place a variation in  $q$  may be caused by the non-uniformity of the surface, i.e., if the molecules are adsorbed on points of the surface that exhibit various degrees of unsaturation. The variation of  $q$  over the surface will be discussed in detail in Chapter VIII.

The curvatures of the isotherms of Fig. 34 probably indicate a variation in  $q$  over the different points of the surface. Since adsorption always takes place first on the points that have the highest  $q$  values, the effect of the variation of  $q$  due to surface inhomogeneity is

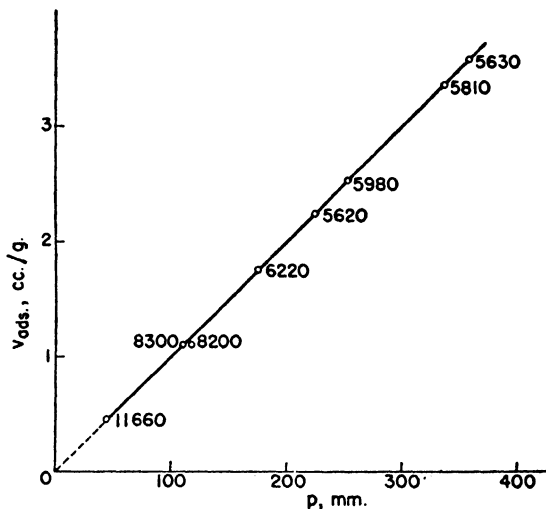


Fig. 35.—Adsorption isotherm of carbon dioxide on silica gel at 75° C.

always to produce a curve concave toward the pressure axis, as are the curves of Fig. 34. However, there is another effect that may produce a curvature in the opposite direction. According to equation (35) a variation in  $b$  can be produced also by a variation in  $f_a(T)$ , the partition function of the adsorbed states. This function may vary in the same sense as the  $q$  factor, or it may vary in the opposite sense. In the latter case, if  $f_a(T)$  increases more rapidly than  $e^{q/kT}$  decreases with increasing adsorption, the curve will be convex toward the pressure axis.

Occasionally the decrease in  $e^{q/kT}$  is just compensated by an increase in  $f_a(T)$  in such manner that a straight line isotherm is produced. This is illustrated in Fig. 35, representing the adsorption of carbon dioxide by silica gel at 75° C., obtained by Kälberer and Schuster.<sup>20</sup>



The numbers along the isotherm indicate the calorimetrically determined differential heats of adsorption, corresponding to the particular amounts of gas adsorbed. The isotherm has a slight curvature near the origin, due to the very high initial heats of adsorption. However, from a pressure of 40 mm. to 360 mm. the isotherm is linear, even though the heat of adsorption decreases from 11,660 calories per mole to less than half of this value. On the basis of the Langmuir theory this can be explained only if we assume a compensation by the factor  $f_a(T)$ .

Adsorption isotherms determined at very low pressures likewise sometimes exhibit a straight line dependence and sometimes do not. Thus Chaplin<sup>22</sup> found that the adsorption of nitrogen by charcoal at 25° C. between the pressure limits  $2 \times 10^{-4}$  and  $1.3 \times 10^{-2}$  mm. was a linear function of the pressure. On the other hand, Polanyi and Welke<sup>23</sup> determined three adsorption isotherms of sulfur dioxide on charcoal at pressures between  $5 \times 10^{-5}$  and  $1.6 \times 10^{-3}$ ,  $1 \times 10^{-4}$  and  $6 \times 10^{-3}$ , and  $7 \times 10^{-4}$  and  $2.8 \times 10^{-1}$  mm. All three isotherms were non-linear.<sup>24</sup>

### B. Intermediate Adsorptions

Proceeding now to the middle pressure range, we can transform equation (21) into a linear form by rearranging terms

$$(38) \quad \frac{p}{v} = \frac{1}{v_m b} + \frac{p}{v_m}$$

The equation in this form is suitable for testing the experimental data. The first test is whether a plot of  $p/v$  against  $p$  gives a straight line. It must be emphasized, however, that obtaining a satisfactory straight line is a necessary but not a sufficient condition for the applicability of Langmuir's theory to the data in question. From the slope and intercept of the straight line the constants  $v_m$  and  $b$  can be evaluated. These are neither arbitrary nor empirical constants<sup>25</sup> but well defined physical quantities, as we have seen in the derivations of the equation. If the values obtained from the straight line plot are wholly unreason-

<sup>22</sup> R. Chaplin, *Phil. Mag.*, (7) 2, 1198 (1926).

<sup>23</sup> M. Polanyi and K. Welke, *Z. phys. Chem.*, A132, 371 (1928).

<sup>24</sup> J. L. Shereshefsky and C. E. Weir (*J. Am. Chem. Soc.*, 58, 2022, 1936) obtained some curious shaped isotherms for the adsorption of oxygen and nitrogen on glass at liquid air temperatures and at very low pressures. These will be discussed in Chapter XII.

<sup>25</sup> J. W. McBain in "The Sorption of Gases and Vapours by Solids" treats the Langmuir constants on pages 477 and 487 as arbitrary or empirical constants.

able, one must conclude that Langmuir's theory, at least in its simplest form expressed in equation (21), does not fit the data. Furthermore, it should be noted that both  $v_m$  and  $b$  are functions of the temperature,  $v_m$  changing slightly,  $b$  strongly with temperature. From the explicit form of  $b$ , expressed in equation (35), its approximate value can be calculated at some other temperature; the slight change in  $v_m$  with temperature can also be approximately estimated, as will be seen later. Using these new values of  $v_m$  and  $b$ , the entire isotherm can be calcu-

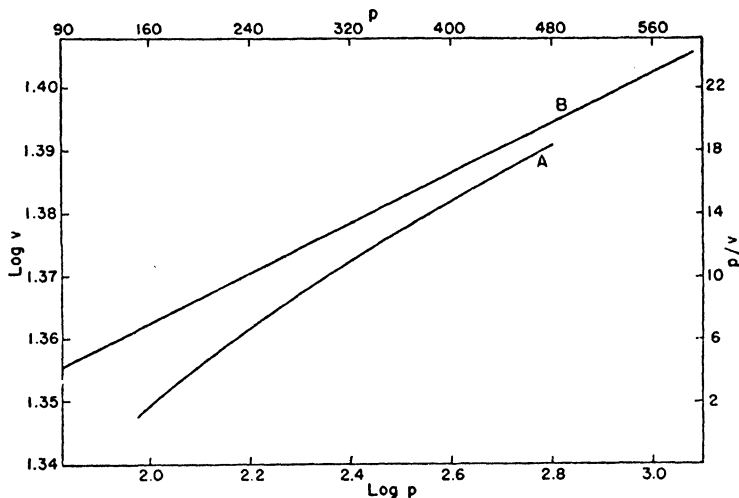


FIG. 36.—An adsorption isotherm of ammonia on chabazite at 0° C. plotted according to the Freundlich equation (A) and the Langmuir equation (B). Volume adsorbed in cc. S.T.P., pressure in mm.

lated at some other temperature. If the experimental isotherm at this new temperature is in complete disagreement with the calculated one, again we must conclude that equation (21) is not applicable, even if a straight line was obtained when the data were plotted according to equation (38).

Figure 36 gives an adsorption isotherm of ammonia on chabazite at 0° C. obtained by Evans.<sup>26</sup> Curve A gives the plot according to the Freundlich equation, i.e.,  $\log v$  against  $\log p$ , and Curve B according to the Langmuir equation, i.e.,  $p/v$  against  $p$ . The data do not obey the Freundlich equation, but they obey the Langmuir equation.

<sup>26</sup> M. G. EVANS, *J. Chem. Soc.*, 1931, 1556.

Evans at the same time measured the differential heats of adsorption by means of an ice calorimeter, and found them to be constant within the range of adsorption investigated. Thus the adsorbent-adsorbate system studied by him was ideal for the test of the Langmuir equation.

Figure 37 illustrates the application of Langmuir's equation to the adsorption of methane and nitrogen on mica at  $90^{\circ}\text{K}$ ., obtained by

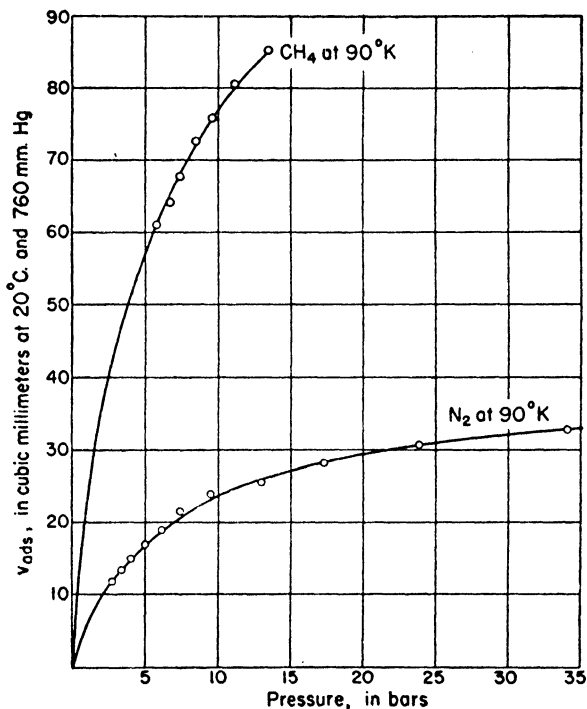


FIG. 37.—Adsorption isotherms of methane and nitrogen on mica.

Langmuir.<sup>6</sup> The experimental data were first plotted according to equation (38), and from the straight lines the constants  $v_m$  and  $b$  were evaluated. Their values were the following:  $b = 0.168$ ,  $v_m = 123$  for methane, and  $b = 0.156$  and  $v_m = 38.9$  for nitrogen. Using these constants and equation (21) one obtains the isotherms represented by the two curves of Fig. 37. The circles give the experimental points of Langmuir. The agreement between the calculated and the experimental curves is quite satisfactory. (Actually it is not quite so good

for all of Langmuir's isotherms as in these two cases.) Nevertheless, even though each of the isotherms can be fitted by equation (21), the constants used in calculating the two curves are inconsistent with each other. Since  $v_m$  is the volume of gas necessary to cover the *entire* surface with a unimolecular adsorbed layer, and since the nitrogen and methane molecules are roughly equal in size, the values of  $v_m$  for the two isotherms should have been approximately equal. As a matter of fact, the value of  $v_m$  used for methane is more than three times as large as the value for nitrogen. One must conclude, therefore, that Langmuir's theory in its simple form does not explain satisfactorily these experimental data.

It is very likely that the discrepancy is due to the inhomogeneity of the adsorbing surface resulting in a variation of the heat of adsorption over the surface. For a composite surface Langmuir proposed the equation

$$(39) \quad v = \frac{v_1 b_1 p}{1 + b_1 p} + \frac{v_2 b_2 p}{1 + b_2 p} + \cdots \frac{v_n b_n p}{1 + b_n p} + \cdots$$

where  $v_1 + v_2 + \cdots v_n + \cdots = v_m$ , and the constants  $b_1, b_2, \cdots b_n, \cdots$  depend on  $q_1, q_2 \cdots q_n \cdots$ , the heats of adsorption on the different surface elements. Due to the large number of constants equation (39) can not be tested quantitatively, but qualitatively it can account for the inconsistent  $v_m$  values of the two isotherms of Fig. 37. The adsorptions of methane and nitrogen correspond only to a part of the surface covered, and they probably take place on different surface elements with different Langmuir constants  $v_i, b_i$ , and  $v_j, b_j$ .

Langmuir assumed that the packing of the molecules in the adsorbed layer is the same as their packing in the liquid state. Knowing the geometrical surface of the mica or glass used, he calculated the volume of gas necessary to cover it with a unimolecular layer. A comparison of this with the  $v_m$  values obtained from the adsorption isotherms of nitrogen, methane, argon, oxygen, carbon monoxide and carbon dioxide on mica and glass showed that he always dealt with adsorption in less than a unimolecular layer. The  $v_m$  values ranged from 3 to 86% of the calculated volume for a complete layer. Since there is good reason to believe that the true surface of mica or glass is larger than the geometrical surface,<sup>27</sup> actually even smaller fractions of the surface were involved in the adsorptions studied by Langmuir. His experiments were carried out at very low pressures, the highest pressure being 0.13 mm. Had he gone to somewhat higher pressures,

<sup>27</sup> See Chapter IX.

he would have obtained a more complete covering of the surface, and at still higher pressures multimolecular adsorption.<sup>28</sup>

Zeise<sup>29</sup> applied the Langmuir equation to the adsorption data of Miss Homfray,<sup>2</sup> Titoff,<sup>1</sup> and Richardson,<sup>30</sup> who measured the adsorption of a number of gases on charcoal. On the whole, he obtained quite satisfactory agreement between theory and experiment, but he

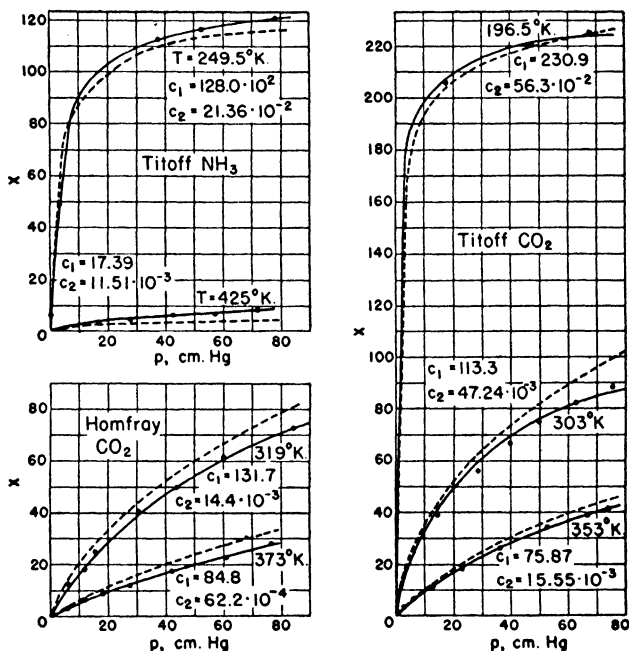


FIG. 38.—The testing of the Langmuir equation and the potential theory by Zeise. The continuous curves represent the isotherms calculated on the basis of the Langmuir equation, the broken curves were calculated on the basis of the potential theory. Amount adsorbed in milligrams per gram of adsorbent.

calculated each isotherm separately and independently from the others. Some of his curves are shown in Fig. 38, representing isotherms obtained by Titoff for the adsorption of ammonia and carbon dioxide and by Miss Homfray for the adsorption of carbon dioxide by charcoal. The continuous curves are the isotherms calculated on the basis of

<sup>28</sup> See Chapter VI.

<sup>29</sup> H. Zeise, *Z. phys. Chem.*, **A136**, 385 (1928); **A138**, 289 (1928).

<sup>30</sup> L. B. Richardson, *J. Am. Chem. Soc.*, **39**, 1829 (1917).

Langmuir's theory, the dotted curves represent isotherms calculated on the basis of Polanyi's theory (Chapter V). Although the fit between the experimental data and Langmuir's equation is satisfactory, again the same difficulty is encountered as in the previously discussed isotherms of Langmuir. In that case the  $v_m$  values obtained for different gases on the same adsorbent were inconsistent with each other. In the isotherms of Fig. 38 the  $v_m$  values of the same gas on the same adsorbent but at different temperatures are inconsistent. Thus for ammonia on charcoal  $v_m$  (the constant  $c_1$  in the figure) changes from 128 at 249.5° K. to 17.4 at 424.5° K., a 7.4-fold change. Richardson's data (not shown in the figure) indicate a 4.4-fold change in the  $v_m$  value of carbon dioxide on charcoal in the temperature range of 209–418° K. Although, as we shall see later,  $v_m$  changes slightly with the temperature, it is hard to account for such large changes. Furthermore, as Polanyi<sup>31</sup> pointed out, the other constant  $b$  ( $c_2$  in the figure), does not depend exponentially on the temperature, as the Langmuir theory demands.

Another example of the same sort is found in the experiments of Markham and Benton<sup>32</sup> who investigated the adsorption of oxygen, carbon monoxide and carbon dioxide on silica. If both sides of equation (38) are divided by  $p$  one obtains

$$(40) \quad \frac{1}{v} = \frac{1}{v_m b} \cdot \frac{1}{p} + \frac{1}{v_m}$$

Figure 39 shows that the plots of  $1/v$  against  $1/p$  give very good straight lines. In such a plot the value of  $v_m$  is given by the reciprocal of the intercept, and the isotherms of the three gases have roughly equal intercepts, as the figure shows. The actual values of  $v_m$  are 397 cc for oxygen at 0° C., 322.6 cc for carbon monoxide at 0° C., and 426.4 cc for carbon dioxide at 100° C. However, three other isotherms, not shown in the figure gave widely different  $v_m$  values, that for carbon monoxide at 100° C. being as low as 60.2 cc. Because of this discrepancy Markham and Benton concluded that the equation must be regarded as empirical, in spite of the excellent straight lines obtained.

The explanation advanced to account for the inconsistencies in the  $v_m$  values of Langmuir's experiments can also account for the discrepancies in the  $v_m$  values of Markham and Benton, and of Zeise. The adsorption of different gases at the same temperature, or of the same gas at different temperatures, does not necessarily take place on

<sup>31</sup> M. Polanyi, *Z. phys. Chem.*, **A138**, 459 (1928).

<sup>32</sup> E. C. Markham and A. F. Benton, *J. Am. Chem. Soc.*, **53**, 497 (1931).

the same part of the surface. The fraction of the surface on which the adsorption takes place may be sufficiently homogeneous to give a satisfactory fit with Langmuir's equation (21), but the  $v_m$  value calculated is not the volume of the gas necessary to cover the entire surface with a unimolecular layer. It is only the volume of gas necessary to cover this homogeneous fraction with a unimolecular layer, the  $v_1$

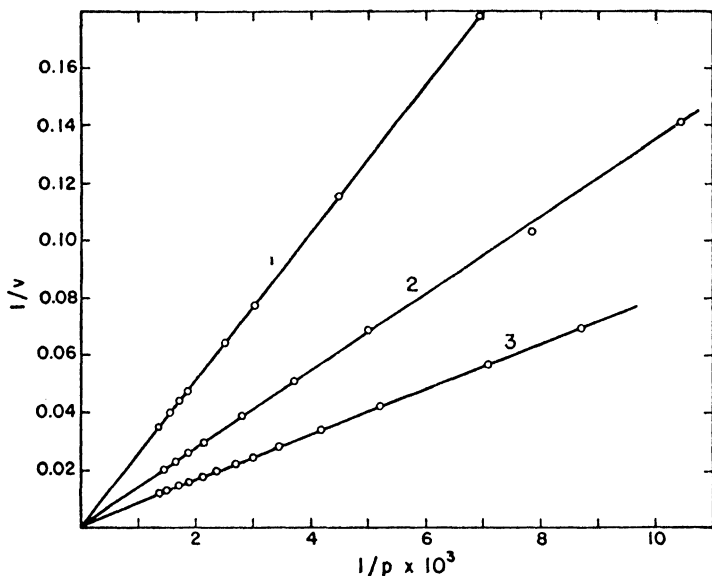


FIG. 39.—Variation of  $1/v$  with  $1/p$  for the adsorption of oxygen at 0° C. (curve 1), carbon monoxide at 0° C. (curve 2) and carbon dioxide at 100° C. (curve 3). Volume adsorbed in cc. S.T.P., pressure in mm.

of equation (39). When one deals with different gases, or with the same gas at different temperatures, this manifests itself in inconsistent  $v_m$  values. Naturally, at the same time one obtains inconsistent  $b$  values as well.

If the above explanation is correct, it should lead to two consequences that can be tested readily by experiment. In the first place, if the adsorption is carried to higher pressures where a larger part of the surface is covered, the inhomogeneity should show up. A plot according to equation (38) should deviate from the straight line, indicating that the surface is composite, and that equation (39) should be used instead of equation (21). There are many such examples in the

literature of adsorption, usually designated by the investigator with the statement that "the Langmuir equation does not apply." In Fig. 40 the data of Reyerson and Wishart<sup>33</sup> for the adsorption of chlorine by silica gel are plotted according to equation (38). Obviously, none of the isotherms gives a straight line, showing that equation (21) is not obeyed. However, with some imagination one may subdivide each of the isotherms into a number of straight line

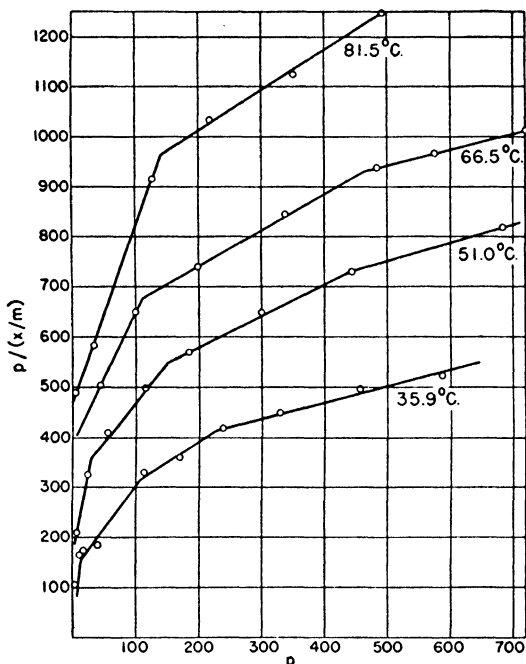


FIG. 40.—Adsorption isotherms of chlorine on silica gel plotted according to the Langmuir equation. Amount adsorbed in millimoles per gram of adsorbent, pressure in mm.

portions, each portion corresponding to adsorption on a fraction of the surface that has roughly the same heat of adsorption. Of course, one could just as well have drawn smooth continuous curves through each of the isotherms, implying a continuous rather than a discrete distribution of  $q$  over the surface. On a crystalline surface one would expect a relatively small number of different surface types, correspond-

<sup>33</sup> L. H. Reyerson and A. W. Wishart, *J. Phys. Chem.*, 41, 943 (1937).



ing to the different developed crystal faces. This would give rise to a discontinuous distribution of  $q$  values. On an amorphous adsorbent there may possibly be such a large number of adsorbing centers of differing heats of adsorption that a plot according to equation (38) would give a continuous curve rather than the type of curve shown in Fig. 40.

The second consequence of the proposed explanation is that if the adsorption is carried out under such conditions that the *entire* surface of the adsorbent is known to be covered, then one should get  $v_m$  values that are consistent with each other when obtained from isotherms of different gases, or of the same gas at different temperatures. One can be sure of a complete saturation of the surface only if one carries the adsorption measurements to the highest pressure attainable at any temperature, i.e., to the saturation pressure of the vapor.

### C. Large Adsorptions

Brunauer and Emmett<sup>34</sup> determined the adsorption isotherms of several gases on charcoal at or near their boiling points. Their plots of  $p/v$  against  $p$  are given in Fig. 41. The experimental points lie on good straight lines, except at low pressures, where the points fall below the straight lines. This indicates larger adsorptions at low pressures, due to the higher heats of adsorption on the more active parts of the surface. The values of  $v_m$  calculated from the straight lines are given in Table IV. The surface area of the charcoal, given

TABLE IV  
VALUES OF  $v_m$  FOR ADSORPTION ISOTHERMS ON CHARCOAL

Gas	Temperature °C	Curve in Fig. 49	$V_m$ cc. at S.T.P./g.	Surface Area sq.m./g.
N <sub>2</sub>	-195.8	4	181.5	795
N <sub>2</sub>	-183	1	173.0	795
A	-195.8		215.5	804
A	-183	5	215.5	839
O <sub>2</sub>	-183	6	234.6	894
CO	-183	3	179.5	820
CO <sub>2</sub>	-78	2	185.5	853

in the last column, was calculated from the  $v_m$  values by assuming close packing of the adsorbed molecules on the surface. The diameters of the molecules were taken from the densities of the liquids at the corresponding temperatures. If the surface area of the charcoal used in these experiments is taken as 845 sq. m./g., the *maximum* devia-

<sup>34</sup> S. Brunauer and P. H. Emmett, *J. Am. Chem. Soc.*, 59, 2682 (1937).

tion from this value is less than 6%. It is true that a butane isotherm at 0° C. gave a surface area which is about 25% smaller than the average obtained from the five gases of Table IV, but it should be remembered that when molecules greatly differing in size and shape are compared, our lack of knowledge of their true packing on the surface is more likely to show up. It is also probable that there are pores in the charcoal into which the larger butane molecules can not penetrate, and so the surface available for butane adsorption is actually smaller.

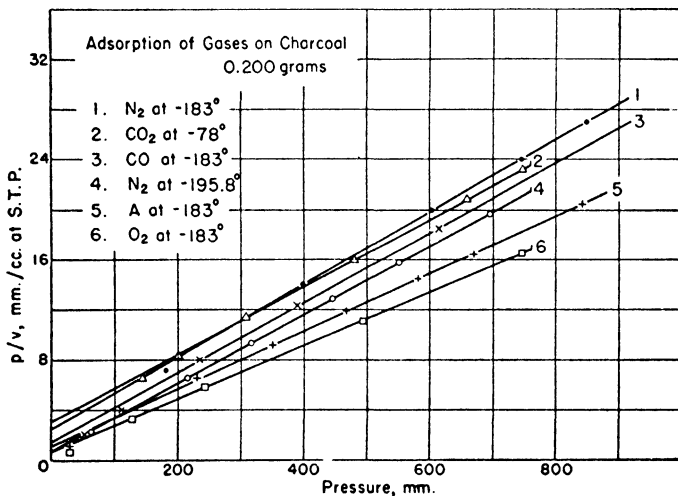


FIG. 41.—Adsorption isotherms of different gases on charcoal, plotted according to the Langmuir equation.

Table IV shows not merely that five different gases (nitrogen, argon, oxygen, carbon monoxide, and carbon dioxide) give consistent  $v_m$  values, but also that the  $v_m$  values of the same gas at two different temperatures (at 77.3 and 90.1° K.) show striking agreement. The surface area values of the charcoal calculated from the two nitrogen isotherms are the same, and those obtained from the two argon isotherms differ only by 2% from the average.

A brief inspection of Fig. 5 in Chapter II reveals that the adsorption values obtained by Goldmann and Polanyi<sup>35</sup> for a charcoal surface saturated by ethyl chloride are consistent with each other in terms of the Langmuir theory. The difference between the saturation adsorptions at -15.3° and 20.0° C. is only a few per cent.

<sup>35</sup> F. Goldmann and M. Polanyi, *Z. phys. Chem.*, A132, 321 (1928).

If the adsorption measurements are carried out near the critical temperature, or at higher temperatures, one must use high pressures to approach complete covering of the surface. Fig. 42 shows the experimental data of McBain and Britton<sup>36</sup> for the adsorption of nitrous oxide by steam activated sugar charcoal, plotted according to the straight line equation (38). The adsorbed amount was determined

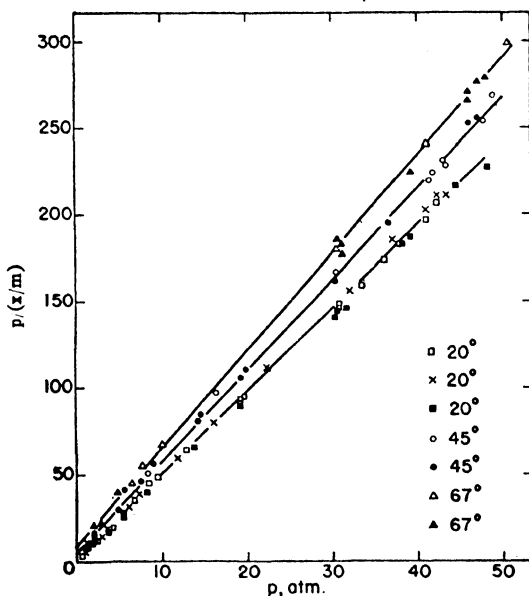


FIG. 42.—Adsorption isotherms of nitrous oxide on charcoal at high pressures plotted according to the Langmuir equation. Amount adsorbed in grams per gram of adsorbent.

by the gravimetric method, and the experiments were carried up to 50 atm. pressure. The ordinate in the figure is  $p/(x/m)$ , where  $x$  is the weight of the adsorbed gas, and  $m$  is the weight of the adsorbent. As the figure shows, satisfactory straight lines were obtained. The slopes of the lines are slightly different, that of the 20° C. isotherm being the smallest, that of the 67° C. isotherm the largest. Since  $v_m$  is given by the reciprocal of the slope, this means that  $v_m$  at 20° C. is about 20% larger than at 67° C. The explanation of this is probably that the packing of the molecules on the surface in physical ad-

<sup>36</sup> J. W. McBain and G. T. Britton, *J. Am. Chem. Soc.*, 52, 2198 (1930).

sorption is similar to the packing in the liquid state. McBain compares the surface of the adsorbent at saturation to a vessel full of liquid. If one raises the temperature, the liquid expands and overflows from the vessel; thus less liquid is contained in the full vessel at higher temperatures. Similarly  $v_m$ , which is proportional to the number of molecules held by the surface at saturation, is smaller at higher temperatures due to the liquid-like expansion of the adsorbed layer.<sup>37</sup> While this explanation is very plausible, it can probably not account for such large changes in  $v_m$  as are indicated in Fig. 38.<sup>38</sup>

Summarizing, we may state that when the adsorption takes place in a unimolecular layer (or part of a layer), the data can often be fitted satisfactorily by means of the simple Langmuir equation (21).<sup>39</sup> This usually happens when one deals with a relatively homogeneous surface, or surface element. When the heat of adsorption varies strongly over the surface, equation (21) is not obeyed. In such cases the data can be qualitatively interpreted in terms of the more general equation (39). Neither equation (21) nor (39) can account for adsorption in multimolecular layers.

The application of Langmuir's theory to mixed adsorption is discussed in Chapter XIV, and the application to chemisorption in Volume II.

#### THE DERIVATION OF THE FREUNDLICH EQUATION<sup>40</sup>

Zeldowitch<sup>41</sup> showed that the Freundlich equation can be derived from the Langmuir equation by assuming a certain type of distribution of the heats of adsorption over the surface.

For a heterogeneous surface the Langmuir equation (39) can be written in the form

$$(41) \quad v = \sum_i \frac{a_i p}{p + b_i}$$

<sup>37</sup> The liquid-like expansion of the adsorbed layer was measured by Goldmann and Polanyi (Chapter V).

<sup>38</sup> A. Antropoff (*Z. Elektrochem.*, 39, 616, 1933; 42, 544, 1936) determined the adsorption isotherms of nitrogen and argon on charcoal up to 200 atm. pressure, and found that they obey the Langmuir equation.

<sup>39</sup> Some investigators use empirical modifications of the Langmuir equation to obtain better fit with experiment. See, for example, H. Bradley (*Trans. Far. Soc.*, 51, 1652, 1935).

<sup>40</sup> Earlier derivations of the Freundlich equation were based on the Gibbs adsorption equation with certain added empirical assumptions. See, for example, H. Freundlich, *Colloid and Capillary Chemistry*, London, 1926, p. 113 and E. K. Rideal, *Surface Chemistry*, Cambridge, 1931, p. 184.

<sup>41</sup> J. Zeldowitch, *Acta Physiochim. U. R. S. S.*, 1, 961 (1934).

where the parameters  $b$  depend on the properties of the elementary spaces of the surface on which the adsorption is taking place, and the parameters  $a$  depend on their number. The most important factor on which  $b$  depends is the heat of adsorption. If this varies continuously over the surface, the summation in equation (41) can be replaced by the integration

$$(42) \quad v = \int_0^{\infty} \frac{pa(b)db}{p + b}$$

The distribution function  $a(b)$  is unknown. However, if one assumes arbitrarily that it has the form

$$(43) \quad a(b) = Ab^{1/n-1}$$

then integration of equation (42) under certain conditions gives the Freundlich equation

$$(44) \quad v = kp^{1/n}$$

Since in the derivation the form of  $a(b)$  was empirically so chosen as to give the Freundlich equation, the treatment of Zeldowitsh must be regarded as inconclusive. It would receive a firmer foundation if it could be shown independently that the distribution of the heat of adsorption over the surface is correctly represented by equation (43) when the Freundlich equation is obeyed.

Zeldowitsh also deduced expressions for the temperature variation of the two constants  $k$  and  $1/n$ . Up to a certain temperature  $T_F$  this is given by

$$(44) \quad 1/n = T/T_F; \quad \log k = a_1T + a_2$$

and above  $T_F$  by

$$(45) \quad 1/n = 1; \quad \log k = b_1 + b_2/T$$

where  $a_1$ ,  $a_2$ ,  $b_1$ , and  $b_2$  are constants. These relations are approximately obeyed in the isotherms of Urry,<sup>42</sup> obtained for the adsorption of oxygen by silica gel between 90 and 273° K., and in the isotherms of Miss Homfray,<sup>2</sup> obtained for the adsorption of carbon monoxide by charcoal between 200 and 300° K.

Baly<sup>43</sup> showed that the Freundlich equation can also be obtained by assuming that the adsorption is multimolecular, and that each adsorbed layer obeys a separate Langmuir equation with different

<sup>42</sup> W. D. Urry, *J. Phys. Chem.*, **36**, 1831 (1932).

<sup>43</sup> E. C. C. Baly, *Proc. Roy. Soc.*, **A160**, 465 (1937).

constants. If each consecutive adsorbed layer has a smaller heat of adsorption than the next lower lying layer, and if the difference between the heats of adsorption of the first and second layer is large, but between any other two consecutive layers is small, a plot of  $\log v$  against  $\log p$  gives a curve which is linear in the middle pressure range.

### THE WILLIAMS-HENRY EQUATION

In 1918 Williams<sup>44</sup> deduced two equations, one for the adsorption isotherm and one for the adsorption isostere, and applied them with success in a number of cases. In 1922 Henry<sup>45</sup> deduced two equations of identical form by an entirely different line of reasoning and made further applications of the equations. The derivation of Williams is largely thermodynamic with certain assumptions relative to the nature of the forces of interaction between adsorbent and adsorbate. Since the kinetic derivation is simpler, it will be reproduced here instead of the more laborious derivation of Williams.

The starting point in the derivation is the Langmuir equation (21); consequently the assumptions that went into the derivation of that equation also form the basis of the Williams-Henry equation. Equation (21) can be rearranged in the form

$$(46) \quad v = v_m b p \left( 1 - \frac{v}{v_m} \right)$$

In the statistical derivation of the Langmuir equation the second assumption was that each adsorbed molecule is held by one point of attachment to the surface. If a molecule is held by more than one point of attachment, the equation takes the form

$$(47) \quad v = v_m b p \left( 1 - \frac{v}{v_m} \right)^n$$

where  $n$  is the number of vacant adjacent points of attachment required for the condensation of a molecule. The exponent  $n$  appears in equation (47) because the chance of a molecule to find one vacant spot on the surface is  $1 - \theta$ , while the chance to find  $n$  adjacent vacant spots is  $(1 - \theta)^n$ .

Taking the logarithm of equation (47) and transposing terms, one obtains

$$(48) \quad \ln \frac{v}{p} = \ln v_m b + n \ln \left( 1 - \frac{v}{v_m} \right)$$

<sup>44</sup> A. M. Williams, *Proc. Roy. Soc. Edinburgh*, 38, 23 (1918); 39, 48 (1919); *Proc. Roy. Soc.*, A96, 287, 298 (1919).

<sup>45</sup> D. C. Henry, *Phil. Mag.*, (6), 44, 689 (1938).

An expansion of the last term into a series gives

$$(49) \quad \ln \left( 1 - \frac{v}{v_m} \right) = - \left[ \left( \frac{v}{v_m} \right) + \frac{1}{2} \left( \frac{v}{v_m} \right)^2 + \frac{1}{3} \left( \frac{v}{v_m} \right)^3 + \dots \right]$$

Substituting (49) into (48) and neglecting all terms of the series but the first, we get

$$(50) \quad \ln \frac{v}{p} = \ln v_m b - \frac{n}{v_m} v$$

This is the Williams-Henry isotherm equation. The higher terms of the series can be neglected only for small values of  $v/v_m$ ; therefore the equation can be safely applied only up to about 30% covering of the surface. When  $v/v_m = 0.3$ , the neglected terms amount to about 20%.

Recently Wilkins<sup>46</sup> derived by thermodynamic and statistical reasoning the equation

$$(51) \quad \ln \frac{v}{p} = \ln v_m b - \frac{B}{v_m} v - \frac{C}{v_m^2} v^2 - \dots$$

This equation is identical in form with the Williams-Henry equation, except that one more term of the series given in equation (49) is included. The constants  $B$  and  $C$  are similar in type to virial coefficients.

In deriving the adsorption isostere we may start again with equation (47). In this case  $v = \text{constant}$ , and the functional relation between  $p$  and  $T$  is sought. Henry assumed that  $v_m$  and  $n$  are independent of the temperature, which is not entirely correct. However, since in comparison with  $b$  they vary only slightly with temperature, he did not introduce a great error by writing

$$(52) \quad p = C_1/b$$

where  $C_1$  is independent of the temperature. Henry further assumed that the temperature dependence of  $b$  is of the form

$$(53) \quad b = \frac{C_2}{T} e^{q/RT}$$

Inspection of equation (35) shows that the variation of  $b$  with temperature has a considerably more complicated form than that given in equation (53). One gets the type of dependence given in (53) only if it is assumed that the molecules in the adsorbed phase behave like a two-dimensional ideal gas. Wilkins<sup>46</sup> showed that the isotherm in

<sup>46</sup> F. J. Wilkins, *Proc. Roy. Soc., A164*, 496 (1938).

such a case is given by

$$(54) \quad v = p \frac{v_m}{RT} \frac{W_2}{W_1} e^{q/RT}$$

where  $W_1$  and  $W_2$  are the statistical weights of the internal energies of the molecules in the gas phase and in the adsorbed phase. Since equation (54) is equivalent to equation (36), i.e.,  $v = v_m b p$ , the temperature dependence of  $b$  is of the form given in (53). This assumption

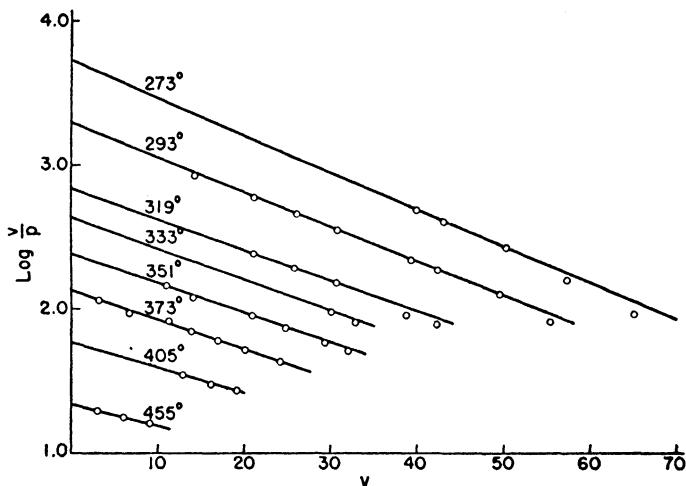


FIG. 43.—Adsorption isotherms of ethylene on charcoal plotted according to the Williams-Henry equation.

naturally restricts the validity of the isostere equation to small adsorptions. Substituting (53) into (52), one gets

$$(55) \quad p = C_3 T e^{-q/RT}$$

Taking logarithms and transposing, one obtains the Williams-Henry isostere equation

$$(56) \quad \ln \frac{p}{T} = \ln C_3 - \frac{q}{RT}$$

Returning now to the isotherm equation (50), we can see that it is of a linear form, and its validity can be tested by plotting  $\log v/p$  against  $v$ . Fig. 43 represents the adsorption isotherms of Miss Homfray<sup>2</sup> for ethylene on charcoal plotted by Williams<sup>44</sup> according to equation (50). On the whole, quite satisfactory straight lines are



obtained. The experimental points at higher adsorptions deviate from the straight lines, as would be expected on the basis of the foregoing discussion. Williams calculated from his theory the specific surface areas of the charcoals used by Miss Homfray<sup>2</sup> and Titoff,<sup>1</sup> obtaining the values of 130 sq. m./g. for the former and 800 sq. m./g. for the latter. From an adsorption isotherm of argon at  $-190^{\circ}\text{C}$ . obtained by Miss Homfray and an isotherm of carbon dioxide at

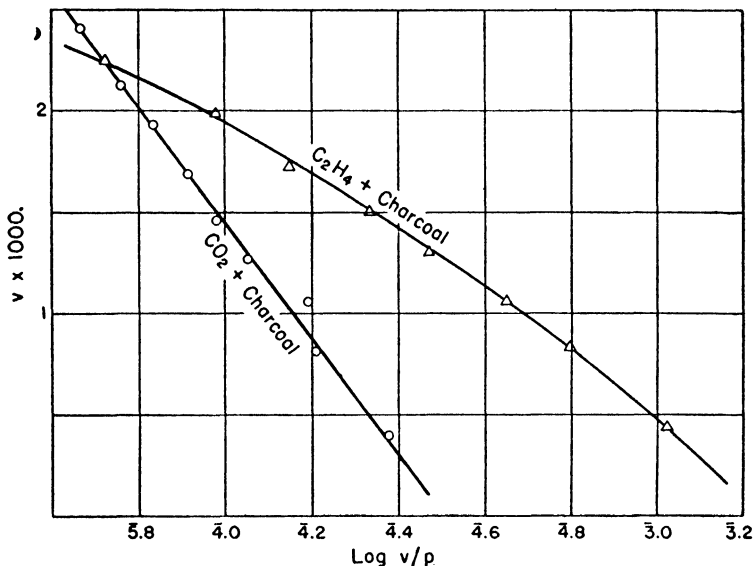


FIG. 44.—Adsorption isotherms of ethylene and carbon dioxide on charcoal at  $0^{\circ}\text{C}$ . plotted according to the Williams-Henry equation. Amount adsorbed in moles of gas per gram of adsorbent, pressure in cm. of Hg.

—  $76.5^{\circ}\text{C}$ . obtained by Titoff one can estimate that the charcoal of the former had a surface area of about 420 sq. m./g. and of the latter 550 sq. m./g. Williams' calculation of the surface area of Titoff's charcoal was mostly guesswork, but the data of Miss Homfray allowed fairly accurate calculation on the basis of his theory. The fact that Williams obtained a surface area that corresponds only to one third of the probable value indicates that his equation encounters the same difficulty as the Langmuir equation (21)—from which it was indeed derived above. Both equations assume uniform heat of adsorption over the surface, and both are obeyed if a part of the surface has

roughly the same  $q$  values. However, the  $v_m$  values calculated by either equation do not correspond to saturation of the entire surface, but only to saturation of that part of the surface over which  $q$  is approximately uniform. Both equations can also be obeyed even if  $q$  varies over the surface, provided the variation of  $q$  is compensated by an opposite variation of  $f_a(T)$  in equation (35), so as to keep  $b$  approximately constant.

Another example of the application of the Williams-Henry isotherm equation is shown in Fig. 44. The curves represent an isotherm of carbon dioxide and one of ethylene on charcoal at 0° C. obtained by

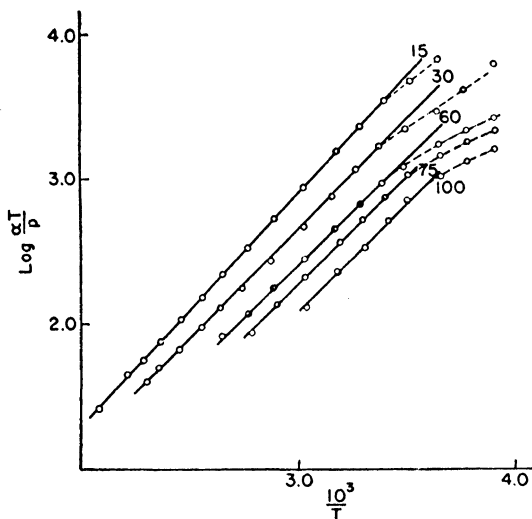


FIG. 45.—Adsorption isosteres of ammonia on charcoal plotted according to the Williams-Henry equation.

Gregg.<sup>47</sup> Carbon dioxide, acetylene, nitrous oxide, carbon monoxide, and nitrogen gave good straight lines; ethylene, sulfur dioxide, and ammonia did not give straight lines. Gregg concluded that although at 0° C. the gases that are far removed from their boiling points give fairly satisfactory straight lines, this is insufficient evidence for the validity of the fundamental assumptions of either Williams or Henry.

The isostere equation (56) is also linear. It can be tested by plotting  $\log p/T$  against  $1/T$ . Fig. 45 represents adsorption isosteres of ammonia on charcoal, calculated by Williams from the experimental

<sup>47</sup> S. J. Gregg, *J. Chem. Soc.*, 1927, 1494.

data of Richardson.<sup>30</sup> The ordinate used in the figure is  $\log \frac{\alpha T}{p}$ . The volume adsorbed,  $\alpha$ , is constant for each isostere, its inclusion therefore does not change the shape of the curve, it only shifts the curve upward by a constant amount. If one multiplies equation (56) by  $-1$ , and adds to both sides  $\ln \alpha$ , one obtains

$$(57) \quad \ln \frac{\alpha T}{p} = \ln \frac{\alpha}{C_3} + \frac{q}{RT}$$

The curves of the figure indicate a systematic deviation from the straight line at low temperatures (the dotted portion of the isosteres). The deviation is more marked for larger values of  $\alpha$ .

Wilkins<sup>46</sup> pointed out that if one uses equation (51) the shape of the isotherm depends on the sign of  $B$ , the second virial coefficient. If  $B$  is negative, the net intermolecular force in the adsorbed layer is repulsive, and the isotherm is concave toward the pressure axis. If  $B$  is positive, the net intermolecular force is attractive, and the adsorption isotherm becomes convex to the pressure axis. Neither Wilkins, nor anybody else has so far attempted to test the validity of the Williams-Henry equation for isotherms of the type shown in Figs. 7 and 8.<sup>48</sup>

### THE EQUATION OF MAGNUS

The Langmuir equation and the Williams-Henry equation both deal with adsorption in a unimolecular layer. Another theoretical treatment of unimolecular adsorption was proposed by Magnus<sup>49</sup> in 1929 and was tested experimentally, mostly by himself and his collaborators.

When Langmuir derived his equation, he believed that the forces between surface and gas are chemical in nature. Nevertheless, since the law of forces does not enter into his equation it is applicable to physical adsorption as well as to chemisorption. Magnus assumed that the forces of interaction between surface and gas are electrostatic. He further assumed that the adsorbed molecules on the surface behave like a two-dimensional imperfect gas, obeying an equation of state analogous to the van der Waals equation. These two assumptions restrict the applicability of his theory to physical adsorption.

<sup>48</sup> By a novel and ingenious but not very rigorous argument A. Gorbatschew (*Z. phys. Chem.*, 117, 129, 1925) deduced the equations of Langmuir, Williams, and Freundlich, as well as several other adsorption equations not discussed in the present book.

<sup>49</sup> A. Magnus, *Z. phys. Chem.*, A142, 401 (1929).

In the thermodynamic derivation of the Langmuir equation Volmer<sup>18</sup> used an equation of state for the adsorbed phase that contained a term analogous to the van der Waals constant  $b$

$$(24) \quad \varphi(\Omega - \beta) = RT$$

Magnus adopts an equation of state that is completely analogous to the three-dimensional van der Waals equation

$$(58) \quad \left( \varphi - \frac{\alpha}{\Omega^2} \right) (\Omega - \beta) = RT$$

As in Volmer's derivation,  $\varphi$  is the pressure of the two-dimensional gas. Magnus sets this equal to  $gp$ , where  $p$  is the pressure in the gas phase and  $g$  is a constant.  $\Omega$  and  $\beta$  also have the same meaning as in Volmer's derivation:  $\Omega = A/v$ , where  $A$  is the surface area of the adsorbent and  $v$  is the number of moles of gas adsorbed;  $\beta$  is analogous to the van der Waals constant  $b$ . The new constant  $\alpha$  is analogous to the van der Waals constant  $a$ , except that it has a different sign. The positive sign of  $a$  corresponds to attraction between the molecules in the gas phase, the negative sign of  $\alpha$  corresponds to repulsion between the adsorbed molecules.<sup>50</sup>

Magnus believes that physical adsorption on electrically conducting surfaces is due to the electrostatic image forces of Lord Kelvin. If the molecule has a permanent dipole, it is attracted by the surface just as if the surface were an imaginary plane half way between the dipole and its mirror image with the poles reversed. (See Fig. 81 in Chapter VII.) If the gas molecule is non-polar, it becomes polarized when it reaches the field of force of the surface. This induced dipole is then attracted to the surface. Since the adsorbed dipoles are lined up by the surface all similarly oriented and parallel to each other, the adsorbate molecules repel each other. Hence the negative sign of  $\alpha$  in equation (58). Magnus found from his experimental data that the correction term  $\alpha/\Omega^2$  actually always has a negative sign, and he regarded this as the strongest argument in support of his theory.<sup>51</sup>

As we have seen before, Volmer derived from equation (24) the two-constant Langmuir equation. The addition of the constant  $\alpha$

<sup>50</sup> At about the same time and independently from Magnus, N. Semenov (Z. phys. Chem., B7, 471, 1930) proposed an adsorption equation identical with equation (58), except that  $\alpha$  has a positive sign. Semenov assumed that the forces of interaction between the adsorbed molecules are attractive.

<sup>51</sup> The electrostatic interpretation of the adsorption forces is discussed in detail in Chapter VII.

results in the three-constant isotherm equation of Magnus. Substituting the values given above for  $\varphi$  and  $\Omega$  into equation (58) and rearranging terms, we obtain

$$(59) \quad v = \frac{k_1 k_2 p - k_3 v^2}{1 + k_1 p - \frac{k_3}{k_2} v^2}$$

where  $k_1 = g\beta/RT$ ,  $k_2 = A/\beta$ , and  $k_3 = \alpha/ART$ . The equation is written in a form similar to Langmuir's; it differs only by the terms containing  $v^2$ . Obviously, if  $\alpha = 0$ , then  $k_3 = 0$ , and the equation becomes identical with Volmer's formulation of the Langmuir equation.

At small adsorptions the equation reduces to Henry's law, as does Langmuir's

$$(60) \quad v = k_1 k_2 p = \frac{gA}{RT} p$$

or rearranging

$$(61) \quad \left(\frac{p}{v}\right)_0 = \frac{RT}{gA}$$

The ratio of the pressure to the amount adsorbed should be constant in the low pressure region. As a matter of fact, Magnus found that such a constant relationship was seldom obtained in the region of the smallest adsorption. Usually he found curves of the type shown in Fig. 34, in which a curved portion at the lowest pressures is followed by a linear portion at somewhat higher pressures. His interpretation was the same as that of Kälberer and Schuster<sup>20</sup> for the curves of Fig. 34. The adsorption at the lowest pressures occurs on the most active part of the surface with the highest heats of adsorption, and  $q$  is not even approximately constant in this region.

At higher pressures the complete equation (59) must be used. For the purpose of testing it can be put in the form

$$(62) \quad p = v \left(\frac{p}{v}\right)_0 \left( \frac{1}{1 - \frac{\beta}{A} v} + \frac{\alpha}{ART} v \right)$$

The constant  $(p/v)_0$  is calculated from the adsorption data at low pressures, and the two other constants are obtained by the method of trial and error.

Since the theory applies only to conductors, its use is limited to charcoal and the metals. The adsorption of carbon dioxide on charcoal<sup>52</sup> obeys the equation, the adsorption of chlorine on silica

<sup>52</sup> A. Magnus and H. Kratz, *Z. anorg. Chem.*, 184, 241 (1929).

gel<sup>53</sup> and the adsorption of ethylene on silica gel and alumina<sup>54</sup> do not obey it. The isotherms on silica gel and alumina are different from the charcoal isotherms, they do not flatten out at higher pressures. When equation (62) is tried, imaginary values are often obtained for  $\beta$ . This might possibly be considered as being in line with Magnus' theory, but the isotherms on metals do not obey the equation either. The experimental data for the adsorption of carbon dioxide and ethylene by gold powder, and ethylene by pyrophoric iron<sup>55</sup> do not agree with the theory. The data for iron deviate more strongly from the equation than the data obtained for gold. Magnus ascribed the deviations to activated adsorption on the metals. He pointed to the fact that the highest heat of adsorption obtained for ethylene on charcoal was about 7500 cal./mole, whereas the same gas on gold and on iron gave maximum heats of adsorption of 9500, and 11,700 cal./mole, respectively. It will be seen later, however, that a difference of this order of magnitude is not sufficiently great to ascribe it with certainty to activated adsorption.

The Magnus equation apparently works fairly satisfactorily for charcoal, but not for metals and silica gel, or alumina. It was pointed out in Chapter II that Brunauer and Emmett<sup>34</sup> obtained similar isotherms for metals and silica gel (the type shown in Fig. 5), but the isotherms for their charcoal were entirely different from those of any other substance investigated by them (the type shown in Fig. 4). The charcoal isotherms indicated unimolecular adsorption even up to the vapor pressure of the liquid, the others all indicated multimolecular adsorption. This may possibly be the reason why Magnus obtained agreement with his theory only on charcoal. Even though at the temperatures and pressures he used the first adsorbed layer was not complete yet, it is possible that the disagreement for all adsorbents except charcoal was caused by the fact that a second layer began to form before the first was completed.<sup>56</sup>

Figure 46 illustrates the application of the equation of Magnus to his data for the adsorption of carbon dioxide by charcoal.<sup>49</sup> The continuous curves were calculated by means of equation (62), the circles represent the experimental points. The agreement is quite

<sup>53</sup> A. Magnus and A. Müller *Z. phys. Chem.*, **A148**, 241 (1930).

<sup>54</sup> A. Magnus and H. Windeck, *Z. phys. Chem.*, **A153** 113 (1931).

<sup>55</sup> A. Magnus and R. Klar, *Z. phys. Chem.*, **A161**, 241 (1932).

<sup>56</sup> It is assumed in the above explanation that the charcoal and silica gel used by Magnus and his collaborators were similar to those used by Brunauer and Emmett. It will be seen later that isotherms obtained for some charcoals indicate multimolecular adsorption, and that some silica gels exhibit unimolecular adsorption.

satisfactory, except for the 373° K. isotherm. It is possible that the constant  $(p/v)_0$ , evaluated from the low pressure region of this isotherm, was somewhat too small, due to incomplete temperature equilibration. If a slightly higher value is used, one obtains the dotted curve that fits the isotherm quite well. Magnus found that the data do not obey the Langmuir equation.

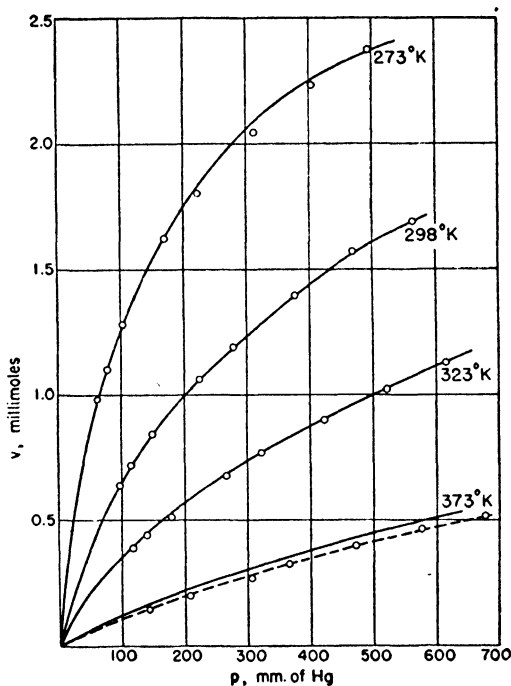


FIG. 46.—Adsorption isotherms of carbon dioxide on charcoal calculated on the basis of the Magnus equation.

The constants were evaluated separately for each isotherm, but they have about the right temperature dependence. The value of  $\beta$  should be only slightly dependent on temperature; therefore Magnus used the same value for the four isotherms. The value of  $\alpha$  should vary approximately linearly according to the theory, and Magnus actually found a linear variation. The third constant,  $(p/v)_0$ , was evaluated from the low pressure region of each isotherm; it was chosen arbitrarily only for the dotted 373° K. isotherm.

A great drawback of Magnus' theory is its very limited applicability. He found that not even all of the charcoal data obeyed his equation.<sup>54</sup> In contrast to Langmuir's theory, the theory of Magnus makes certain deductions about the variation of the heat of adsorption with the pressure and with temperature. These are discussed in Chapter VIII. The application of the theory to mixed adsorption is discussed in Chapter XIV.



## CHAPTER V

### THE ADSORPTION ISOTHERM II

In Chapter IV we discussed the derivations of the isotherm equations of Langmuir, Williams and Henry, and Magnus. In all three derivations it is assumed that adsorption is unimolecular and, as we have seen, each equation has had a certain degree of success in accounting for the experimental facts. In the present chapter two other theories of van der Waals adsorption are discussed: the potential theory and the capillary condensation theory. These two theories approach the problem of adsorption from very different angles, but they have a common feature; they consider adsorption multimolecular, i.e., more than one layer in thickness. At present there is no unanimous agreement among investigators on the existence of multimolecular adsorption, especially on plane surfaces. The experiments that were performed to test directly the thickness of the adsorbed layer are discussed in Chapter X. In the present chapter the multimolecular nature of physical adsorption is treated only as an assumption entering into the theories, to be tested by the success or failure of the theory in accounting for the experimental facts.

The potential theory<sup>1</sup> in its original form as advanced by Polanyi in 1914 assumed that adsorption was due to long range attractive forces extending out from the surface of the adsorbent. This, however, did not enter into the quantitative formulation of the theory, and so it was easy to modify the picture later to accord more nearly with the modern concepts of the nature of molecular forces. In 1928 Goldmann and Polanyi<sup>2</sup> pointed out that the potential theory is applicable to unimolecular adsorption also, but on the basis of their own experimental data and the data of Coolidge<sup>3</sup> they concluded that the adsorbed layer was more than one molecular diameter thick.

The capillary condensation theory attributes adsorption to condensation of the gas in the capillaries of the adsorbent.<sup>4,5</sup> It has long been known that a liquid that wets the wall of a capillary has a lower

<sup>1</sup> M. Polanyi, *Verh. deut. physik. Ges.*, 15, 55 (1916).

<sup>2</sup> F. Goldmann and M. Polanyi, *Z. phys. Chem.*, A132, 313 (1928).

<sup>3</sup> A. S. Coolidge, *J. Am. Chem. Soc.*, 48, 1795 (1926).

<sup>4</sup> R. Zsigmondy, *Z. anorg. Chem.*, 71, 356 (1911).

<sup>5</sup> J. McGavack, Jr. and W. A. Patrick, *J. Am. Chem. Soc.*, 42, 946 (1920).

vapor pressure in the capillary than in the normal bulk phase. This behavior was extrapolated to capillaries of molecular dimensions by Zsigmondy<sup>4</sup> in 1911. He assumed that in such very small capillaries condensation can take place at pressures considerably lower than the normal vapor pressure. The capillaries of the smallest radii fill at the lowest pressures. As the pressure is increased, always larger capillaries fill, until finally at the saturation pressure all the pores of the adsorbent fill with liquid.

Multimolecular adsorption and capillary condensation are necessarily always preceded by unimolecular adsorption. A complete theory must be applicable to the entire range of adsorption. The capillary condensation theory can not handle unimolecular adsorption; consequently it can account for only a part of the adsorption isotherm. The potential theory can handle both unimolecular and multimolecular adsorption. Although it was originally built on the concept of thick adsorbed layers, paradoxically it gives the most satisfactory quantitative treatment that exists at present for unimolecular adsorption on surfaces that possess strongly varying heats of adsorption. However, the theory gives no analytical formulation for the adsorption isotherm, and the sole criterion of its validity is the accuracy with which it accounts for the temperature dependence of the adsorption isotherm.

### THE POTENTIAL THEORY

The picture on which Polanyi built his theory originated with de Saussure<sup>6</sup> as far back as 1814. According to this view, the adsorbent exerts a strong attractive force upon the gas in its vicinity, this attraction giving rise to adsorption. The forces of attraction reaching out from the surface are so great that many adsorbed layers can form on the surface. These layers are under compression, partly because of the attractive force of the surface, partly because each layer is compressed by all the layers adsorbed on top of it. The compression is the greatest on the first adsorbed layer, less on the second, and so on until the density decreases to that of the surrounding gas. Thus the structure of the adsorbed phase according to the "compressed film" theory is similar to that of the atmosphere surrounding the earth.

Eucken<sup>7</sup> was the first to conceive of the force of adsorption as an intermolecular potential gradient, but the correct quantitative formu-

<sup>6</sup> T. de Saussure, *Gilbert's Ann. der Physik*, 47, 113 (1814).

<sup>7</sup> A. Eucken, *Verh. deut. physik. Ges.*, 16, 345 (1914).

lation of the theory is due to Polanyi.<sup>8,1</sup> He defined the adsorption potential at a point near the adsorbent as the work done by the adsorption forces in bringing a molecule from the gas phase to that point. This work is conceived of as a work of compression and mathematically its value is given by the so-called hydrostatic equation<sup>9</sup>

$$(1) \quad \epsilon_i = \int_{\delta_x}^{\delta_i} V dp$$

Here  $\epsilon_i$  is the adsorption potential at a point where the density of the adsorbed substance is  $\delta_i$ ,  $\delta_x$  is the density in the gas phase, and  $V = M/\delta$ , where  $M$  is the molecular weight of the adsorbate. To

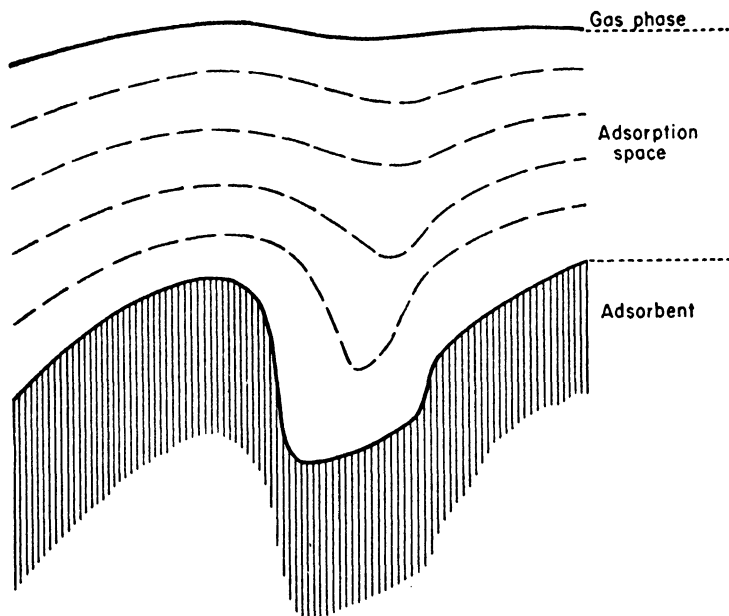


FIG. 47.—Cross-section of the adsorbed phase according to the potential theory.

evaluate this integral, one must be able to express the molar volume  $V$ , or the density  $\delta$ , as a function of the pressure both in the gas phase and in the adsorbed phase. The equation of state of the adsorbed gas is unknown, but Polanyi assumed that the gas obeys the

<sup>8</sup> M. Polanyi, *Verh. deut. physik. Ges.*, 16, 1012 (1914).

<sup>9</sup> Derivations are given in references 1 and 8. See also G. N. Lewis and M. Randall, *Thermodynamics*, New York, 1923, p. 162, equation (10).

same equation of state in the adsorbed phase as in the gas phase. The assumption was based on the similarity between van der Waals adsorption and condensation. The notable success of the theory indicates that this assumption is adequately fulfilled.

Figure 47 gives a cross-section of the adsorbed phase as it is pictured by the potential theory. The shaded region represents the cross-section of the adsorbent, the full line is the boundary surface between the gas phase and the adsorbed phase, and the dotted lines

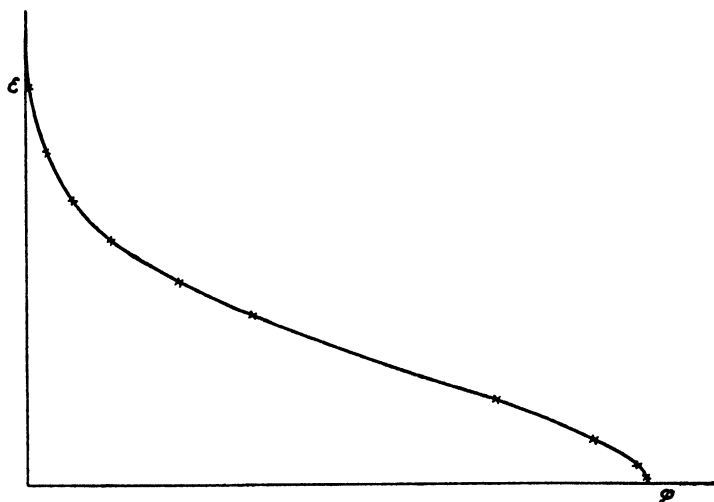


FIG. 48.—Characteristic curve of carbon dioxide on charcoal.

are equipotential surfaces. The potential along the surface of the adsorbent is  $\epsilon_0$ , the potentials along the consecutive potential surfaces are  $\epsilon_1, \epsilon_2 \dots \epsilon_i, \dots$  etc. It is assumed that the adsorption potential is similar to the gravitation potential, i.e., along the  $i$ -th surface its value is always  $\epsilon_i$ , regardless of the number and kind of molecules that are located between the  $i$ -th surface and either the adsorbent or the gas phase. This assumption received complete justification later in London's<sup>10</sup> quantum-mechanical theory of van der Waals forces, to be discussed in Chapter VII.

Each of the potential surfaces together with the surface of the adsorbent encloses a volume. These volumes are  $\varphi_1, \varphi_2, \dots \varphi_i, \dots$  etc. The volume enclosed by the adsorbent surface and the boundary

<sup>10</sup> F. London, *Z. phys. Chem.*, B11, 222 (1931).

surface between the gas phase and the adsorbed phase is  $\varphi_{\max}$ , the volume of the entire adsorption space. The potential along the outermost surface is zero. At the surface of the adsorbent, where  $\varphi = 0$ , the potential has its maximum value,  $\epsilon_0$ . Between these two limits the shape of the curve  $\epsilon = f(\varphi)$  is shown in Fig. 48. The curve was calculated by Polanyi<sup>1</sup> from Titoff's data<sup>11</sup> for the adsorption of carbon dioxide by charcoal.

The potential theory assumes that the adsorption potential does not change with the temperature

$$(2) \quad \frac{d\epsilon_i}{dT} = 0$$

from which it follows that

$$(3) \quad \frac{d\varphi_i}{dT} = 0$$

This means that the curve representing the potential distribution in the adsorption space, i.e.,  $\epsilon = f(\varphi)$ , is the same for all temperatures. For this reason the curve is called the *characteristic curve*.

Since  $\epsilon$  and  $\varphi$  can be expressed in principle as functions of the pressure, the temperature and the amount of gas adsorbed, the equation  $\epsilon = f(\varphi)$  can be regarded as equivalent to an isotherm equation. The potential theory, however, does not attempt to deduce this equation from more fundamental kinetic or thermodynamic considerations. Since a large number of variables enter into the equation (such as the size and shape of the surface and the capillaries of the adsorbent, and the nature of the interaction between adsorbent and adsorbate), Polanyi reasoned that the simplest way to attack the problem was to evaluate the potential distribution (the characteristic curve) from one experimentally determined isotherm, and then to calculate all the other isotherms from this curve.

It was shown in Chapter IV that the Langmuir equation can be tested by three criteria: (1) whether the experimental data fit the equation, (2) whether the constants of the equation, representing independently measurable physical quantities, have reasonable values, and (3) whether the equation reproduces correctly the temperature dependence of the adsorption. Since the potential theory offers no isotherm equation, the sole criterion by which its validity can be judged is this last one, namely, whether one can calculate from one isotherm all the others at different temperatures with a fair degree of accuracy.

<sup>11</sup> A. Titoff, *Z. phys. Chem.*, 74, 641 (1910).

The variation of the density within the adsorption space is illustrated by the curves shown in Fig. 49, taken from Lowry and Olmstead.<sup>12</sup> The adsorbed gas contained in the elementary volumes  $\varphi_1, \varphi_2, \dots \varphi_i \dots$  has different densities  $\delta_1, \delta_2, \dots \delta_i \dots$ . The maximum density is reached at the surface of the adsorbent, the minimum in the immediate vicinity of the gas phase. The latter,  $\delta_x$ , is equal to

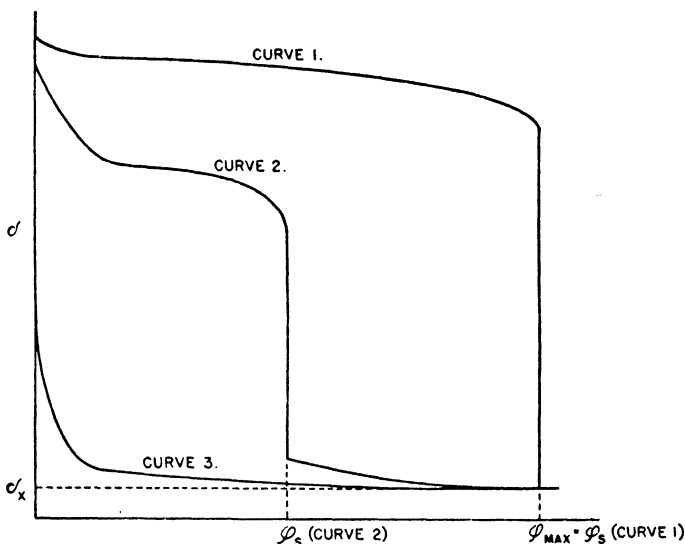


FIG. 49.—Variation of the density within the adsorbed phase according to the potential theory.

the density of the gas. Below the critical temperature in a part of the adsorption space the density is equal to or greater than the density of the liquid; the volume of this part of the adsorption region is  $\varphi_s$ . The shape of the curves  $\delta = f(\varphi)$  is strongly dependent on temperature and pressure. Curve 1 in Fig. 48 illustrates the situation far below the critical temperature and at a pressure near saturation. In this case practically the entire adsorption volume is filled with liquid, so that  $\varphi_s = \varphi_{\max}$ . At the other extreme is Curve 3, representing the density distribution far above the critical temperature. Here the density of the adsorbed layer is nowhere as high as that of the liquid. Curve 2 shows an intermediate situation where part of the adsorbate is in the liquid state, and part of it is in the gaseous state. Even

<sup>12</sup> H. H. Lowry and P. S. Olmstead, *J. Phys. Chem.*, **31**, 1601 (1927).

though  $\varphi_s$  here is less than half of  $\varphi_{\max}$ , by far the greater part of the adsorbed substance lies in  $\varphi_s$  because the density is much greater there.

The weight of gas adsorbed can be obtained by integrating  $(\delta - \delta_z)d\varphi$  between the limits 0 and  $\varphi_{\max}$

$$(4) \quad x = \int_0^{\varphi_{\max}} \delta d\varphi - \delta_z \varphi_{\max}$$

The correction term  $\delta_z \varphi_{\max}$  is usually negligible, except at very high pressures (where  $\delta_z$  becomes large) and at high temperatures (where  $\delta$  becomes small). In order to carry out the integration  $\delta$  must be known as a function of  $\varphi$ . As will be seen later, this function is obtained with the help of the characteristic curve and the equation of state of the gas.

#### APPLICATIONS OF THE POTENTIAL THEORY

The testing of the theory consists of two steps: the calculation of the characteristic curve from an experimental isotherm, and the calculation of other isotherms from the characteristic curve. The isotherm used for obtaining the characteristic curve must cover the potential distribution in the entire adsorption space. Since the places of low potential fill only at low temperatures, an isotherm below the critical temperature must be used for the calculation. On the other hand, the temperature of the isotherm can not be too low, otherwise a large portion of the adsorption space fills at very low pressures, and the potential distribution in the region of high potentials can not be evaluated accurately. If such an ideal isotherm is not available in practice, the characteristic curve must be calculated from two or more isotherms.

The first calculations were made by Polanyi,<sup>1</sup> but the method was considerably improved by Berenyi.<sup>13,14</sup> Both distinguished three different methods of calculation: (1) for isotherms taken sufficiently far below the critical temperature that practically all of the adsorbed gas is in the liquid form; (2) for isotherms below but near to the critical temperature, where besides liquid there is also compressed gas in the adsorption space in an amount that is not negligible; and (3) for isotherms above the critical temperature, where there is only compressed gas in the adsorption space. The three curves of Fig. 49 correspond to these three different density distributions.

<sup>13</sup> L. Berenyi, *Z. phys. Chem.*, 94, 628 (1920).

<sup>14</sup> L. Berenyi, *Z. phys. Chem.*, 105, 55 (1923).

The calculation of the characteristic curve from an isotherm considerably below the critical temperature is the simplest. In the first approximation the potential is calculated on the basis of two assumptions: (1) the vapor in the gas phase obeys the ideal gas laws; (2) the liquid in the adsorbed phase is incompressible. Thus  $\epsilon_i$  is merely the work of compressing an ideal gas isothermally from  $p_z$ , the pressure existing in the gas phase, to  $p_0$ , the vapor pressure of the liquid. In this case equation (1) takes the form

$$(5) \quad \epsilon_i = \int_{p_z}^{p_0} \frac{RT}{p} dp = RT \ln \frac{p_0}{p_z}$$

It should be noted that the work of creating a liquid surface is neglected in this expression. Although this work is not negligible in comparison with  $\epsilon_i$ , the error introduced into the calculation is not very great.

Since the liquid is assumed to be incompressible, the value of  $\varphi_i$  corresponding to  $\epsilon_i$  is given simply by the equation

$$(6) \quad \varphi_i = \frac{x}{\delta_T}$$

where  $x$  is the weight of the adsorbed vapor, and  $\delta_T$  is the density of the liquid at temperature  $T$ . To each pair of values of  $x$  and  $p_z$ , i.e., to each point on the adsorption isotherm, there corresponds a pair of values of  $\varphi_i$  and  $\epsilon_i$ , i.e., a point on the characteristic curve.

The second approximation consists in applying a correction to  $\varphi_i$  for the compressibility of the adsorbed liquid and to  $\epsilon_i$  for the deviation of the vapor from the ideal gas laws. Berenyi<sup>14</sup> did this in a simple empirical manner. If the adsorbed liquid were incompressible and would not expand with temperature, one would have

$$(7) \quad \varphi_i = \frac{x}{\delta_B}$$

where  $\delta_B$  is the density of the normal liquid at its boiling point. To take care of the variation of  $\delta$  with pressure and temperature two corrections are needed. The compressibility correction is the more difficult one to make, because one must assume arbitrarily a certain potential distribution in the adsorption space and a certain value for  $\epsilon_0$ , the adsorption potential along the adsorbent surface. Using the value of  $\epsilon_0 = 6000$  cal. and assuming a linear decrease of  $\epsilon$  with  $\varphi$ , Berenyi calculated from Amagat's measurements on ether the compressibility corrections  $f_c$ , given in Table V(a). The first column gives the ratio of the temperature of the isotherm to the boiling point  $T_B$ ,



the other columns give the factors by which  $\delta_T$  must be multiplied to obtain the average density of the adsorbed layer when the pressure in the gas phase is  $p_x$ .

TABLE V  
CORRECTIONS OF  $\delta_B$   
(a) Compressibility Correction,  $f_c$

$T/T_B$	$p_x = 0.1$	1	10	100	1000 mm. of Hg
0.6	1.01	1.02	1.03	—	—
0.8	1.01	1.02	1.03	1.04	—
1.0	1.01	1.03	1.05	1.07	1.09
1.2	1.01	1.04	1.07	1.10	1.12
1.4	1.01	1.05	1.09	1.13	1.16

(b) Temperature Expansion Correction,  $f_T$

$T/T_B$	$f_T$
0.6	1.16
0.8	1.10
1.0	1.00
1.2	0.89
1.4	0.74

(c) Total Correction,  $f$

$T/T_B$	$p_x = 0.1$	1	10	100	1000 mm. of Hg
0.6	1.17	1.18	1.19	—	—
0.8	1.11	1.12	1.13	1.14	—
1.0	1.01	1.03	1.05	1.07	1.09
1.2	0.90	0.93	0.96	0.99	1.01
1.4	0.75	0.79	0.83	0.87	0.90

If the value of  $\delta_T$  is not available and only  $\delta_B$  is known, the corrections for the temperature expansion of the adsorbed layer can be obtained from Table V(b). Berenyi calculated these by averaging the temperature expansion of 12 different liquids. He found that the expansion of none of the liquids deviated by more than 2-3% from the factors given. To obtain  $\delta_T$  one must multiply  $\delta_B$  by  $f_T$ . Finally, the total correction factor  $f$  is given by Table V(c). The corrected value of  $\varphi_i$  is therefore

$$(8) \quad \varphi_i = \frac{x}{f_c \delta_T} = \frac{x}{f \delta_B}$$

Due to the similarity of the temperature expansion and compressibility relations of liquids at corresponding temperatures these factors are applicable to all liquids, and the error will not amount to more than a few per cent.

The correction of  $\epsilon_i$  that takes care of the deviation of the vapor from the ideal gas laws is quite insignificant up to the neighborhood of the critical temperature. Berenyi put it in the form

$$(9) \quad \epsilon_i = RT \ln \frac{p_0}{p_x} + \eta$$

and even at  $T/T_B = 1.4$  the value of  $\eta$  is hardly more than 100 cal. This is only a few percent of  $\epsilon_i$ . Berenyi gives for  $\eta$  at  $T/T_B = 1.0$ , 1.2 and 1.4 the values 0, 46 and 137 cal., respectively.

Figure 50 gives the characteristic  $\epsilon - \varphi$  curve for the adsorption of sulfur dioxide by silica gel, calculated by Berenyi<sup>14</sup> from the

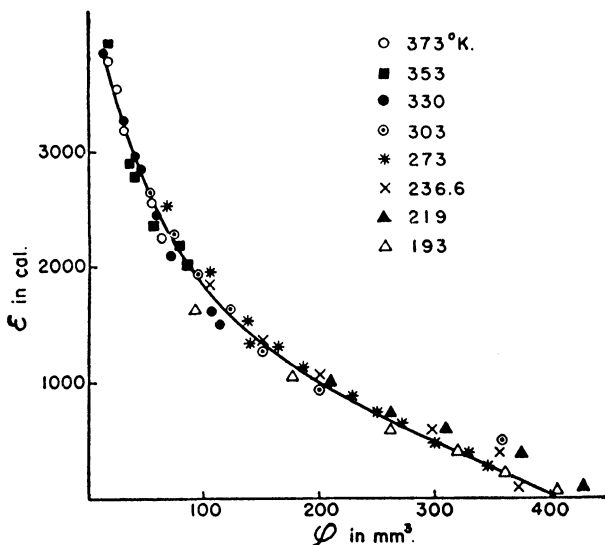


Fig. 50.—Characteristic curve of sulfur dioxide on silica gel.

experimental results of McGavack and Patrick.<sup>5</sup> All the eight isotherms from 193 to 373° K fall on a single curve, as demanded by the theory. From this curve Berenyi recalculated the individual isotherms, and the results are shown in Fig. 51. The curves give the calculated isotherms, the circles the experimental points. The agreement is quite satisfactory.

The calculation of the characteristic curve from an isotherm above the critical temperature is somewhat more complicated than the above described method. Berenyi suggests<sup>13</sup> that one should first calculate

a tentative  $\epsilon - \varphi$  curve from the isotherm on the basis of the empirical relations

$$(10) \quad \varphi_i = \frac{22400xb}{M}$$

$$(11) \quad \epsilon_i = RT \ln \frac{0.14T}{p_x b}$$

where  $M$  is the molecular weight and  $b$  is the van der Waals constant  $b$ . According to van der Waals the density of a gas at infinite compression

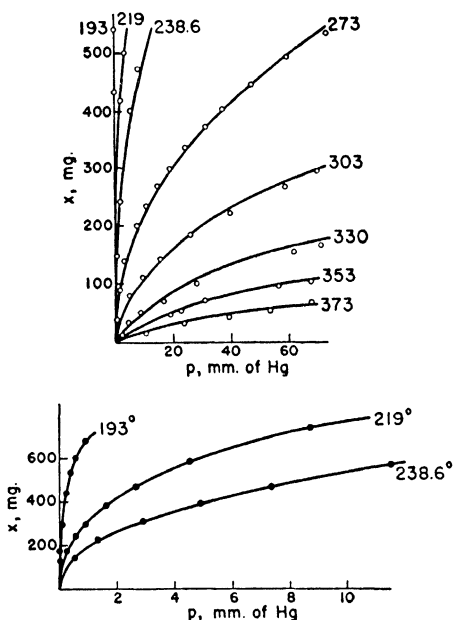


FIG. 51.—Adsorption isotherms of sulfur dioxide on silica gel calculated from the characteristic curve of Fig. 50.

is  $M/22400b$ , thus the  $\varphi_i$  calculated from equation (10) is a minimum value. The characteristic curve obtained from equations (10) and (11) usually serves as a good zeroth approximation.

The correction of the tentative  $\epsilon - \varphi$  curve involves two preliminary calculations. In the first place one must evaluate the potential as a function of the density in the adsorbed phase, i.e., the function

$\epsilon = g(\delta)$ . This function is obtained from the equation

$$(12) \quad \epsilon_i = \int_{V_i}^{V_i} V dp$$

where  $V_i = RT/p_i$  (assuming that the vapor obeys the ideal gas laws), and  $V_i = M/\delta_i$ . If the compressibility data of the gas are available up to high pressures, the molar volume can be plotted against the pressure and the curve integrated graphically. If accurate experimental data are not available, the equation of state of the gas can be used and the integration can be performed analytically. Using the van der Waals equation to express  $V$  as a function of  $p$  and integrating equation (12) one obtains

$$(13) \quad \epsilon_i = 4.57T \log \frac{0.2785T}{p_i(V_i - b)} - \frac{1083a}{V_i} + \frac{1.985T}{\frac{V_i}{b} - 1}$$

where  $a$  and  $b$  are the van der Waals constants of the gas and  $V_i = M/22400\delta_i$ . In this equation the parameters  $p_i$  and  $T$  are regarded as constants, and  $\epsilon_i$  as a function of  $V_i$  (or  $\delta_i$ ). To each point of the adsorption isotherm there corresponds a curve calculated on the basis of equation (13).

The second preliminary step is to calculate the density distribution in the adsorption space, i.e., the function  $\delta = h(\varphi)$ . This is done by eliminating  $\epsilon$  from the two functions  $\epsilon = f(\varphi)$  and  $\epsilon = g(\delta)$ . This means simply that one takes from one curve the value of  $\varphi_i$  and from the other curve the value of  $\delta_i$  that corresponds to the same  $\epsilon_i$ , and plots  $\delta_i$  against  $\varphi_i$ . Since there is only one  $\epsilon - \varphi$  curve but as many  $\epsilon - \delta$  curves as there are points on the adsorption isotherm, there will be also as many  $\delta - \varphi$  curves as there are points on the isotherm. To each pressure there corresponds a different density distribution in the adsorption space.

From the  $\delta - \varphi$  curve  $x$  can be obtained by graphical integration, since we have seen that

$$(14) \quad x = \int_0^{\varphi_{\max}} \delta d\varphi$$

The term  $\delta_x \varphi_{\max}$  is negligible in equation (4), as was pointed out in the previous section.

To correct the tentative  $\epsilon - \varphi$  curve, the calculated values of  $x$  must be obtained for a number of different equilibrium pressures. First one sets  $p_x = p_1$ , and calculates the  $\epsilon - \delta$  curve as described

above. Taking this curve and the tentative  $\epsilon - \varphi$  curve, one obtains the  $\delta - \varphi$  curve by eliminating  $\epsilon$  from the two curves. By graphical integration of the  $\delta - \varphi$  curve one then gets  $x_1$ , the calculated value of  $x$  corresponding to pressure  $p_1$ . Next one takes another point of the isotherm and by similar calculations obtains  $x_2$ , corresponding to  $p_2$ . The corrected values of  $\varphi$  are given by the equation

$$(15) \quad \varphi_{\text{corr.}} = \varphi_{\text{tent.}} \frac{x_{\text{obs.}}}{x_{\text{calc.}}}$$

With the corrected values of  $\varphi$  one plots the new  $\epsilon - \varphi$  curve, which may be called the first approximation. The whole process is then repeated, using the new  $\epsilon - \varphi$  curve. Berenyi found that the con-

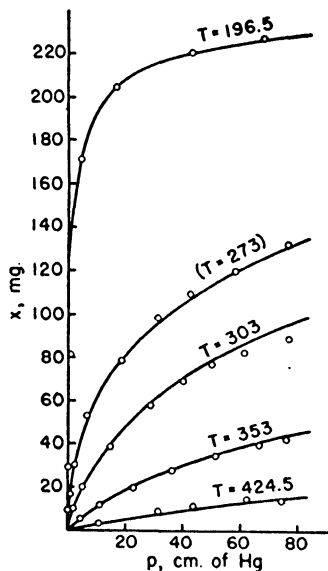


FIG. 52.—Adsorption isotherms of carbon dioxide on charcoal calculated from the 273° K. isotherm on the basis of the potential theory.

vergence is so rapid that one never needs more than two approximations to obtain the final characteristic curve.

The calculation of the characteristic curve from an isotherm taken in the intermediate temperature range is also described by Polanyi<sup>1</sup> and by Berenyi.<sup>13</sup> The method is relatively simple, and it need not be discussed here. It is also unnecessary to go into the calculation of the

individual isotherms from the final characteristic curve because it consists merely in reversing the order of the steps in the above described methods of calculation.

Figure 52 shows Titoff's <sup>11</sup> isotherms for the adsorption of carbon dioxide by charcoal, calculated by Berenyi <sup>13</sup> on the basis of the potential theory. The characteristic curve was calculated from the 273° K. isotherm *alone*, and all isotherms were calculated from this curve. This is a more rigorous test of the theory than obtaining the characteristic curve from *all* of the isotherms and recalculating the

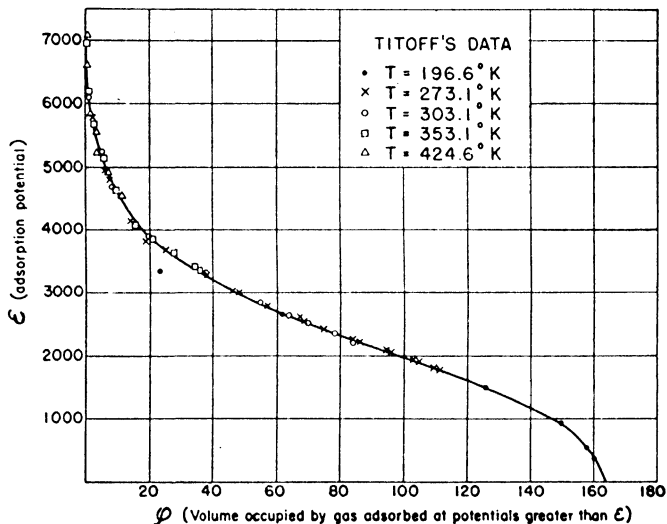


Fig. 53.—Characteristic curve of carbon dioxide on charcoal (Titoff's data).

individual isotherms, as was done in Figs. 50 and 51. The theory withstands even this more exacting test, as Fig. 52 shows. In a wide temperature range, from 196.5 to 424.5° K., i.e., from about 110 degrees below to 120 degrees above the critical temperature of the gas, all isotherms can be obtained from one taken somewhat below the critical temperature. The data of Miss Homfray <sup>15</sup> and Richardson <sup>16</sup> for the adsorption of carbon dioxide on charcoal do not give quite as good agreement, but the deviations are probably not greater than the experimental error.

<sup>15</sup> I. F. Homfray, *Z. phys. Chem.*, 74, 129 (1910).

<sup>16</sup> L. B. Richardson, *J. Am. Chem. Soc.*, 39, 1828 (1917).

The method of calculation of the characteristic curve was further improved by Lowry and Olmstead.<sup>12</sup> They examined all experimental data obtained for the adsorption of carbon dioxide on charcoal by the different investigators. Their main improvement over Berenyi's method was the use of the equation of state of van Laar, instead of van der Waals, in the regions where actual experimental data for the compressibility of carbon dioxide were not available. The characteristic curve obtained from Titoff's data is shown in Fig. 53. The average deviation of the experimental points from the calculated curve is 4.53%, as compared to Berenyi's 7.16%. However, Berenyi used

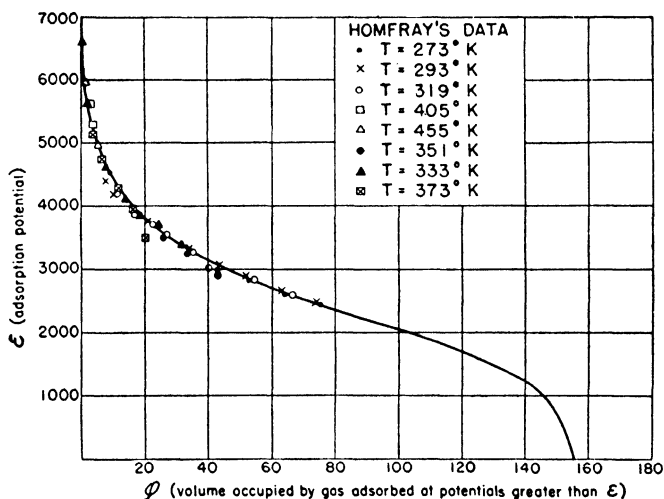


FIG. 54.—Characteristic curve of carbon dioxide on charcoal (Miss Homfray's data).

only one isotherm in calculating the characteristic curve, therefore only part of the improvement can be ascribed to the method of Lowry and Olmstead.

Figure 54 gives their characteristic curve for the data of Miss Homfray. The average deviation here is 5.85% against Berenyi's 12.47%, a considerable improvement. The characteristic curves obtained from Titoff's and Miss Homfray's experiments show a striking similarity to each other as well as to the curves calculated by Lowry and Olmstead from the data of Richardson,<sup>16</sup> Chappuis,<sup>17</sup> and Lowry and Morgan.<sup>18</sup> There are relatively small differences in the

<sup>17</sup> P. Chappuis, *Wied. Ann.*, 12, 161 (1881).

<sup>18</sup> H. H. Lowry and S. O. Morgan, *J. Phys. Chem.*, 29, 1105 (1925).

maximum potential  $\epsilon_0$  and in the volume of the adsorption space  $\varphi_{\max}$ . The course of the curves between the intercepts on the two axes is also very similar.

The work of Polanyi, Berenyi, and Lowry and Olmstead proves conclusively that with the help of the theory one can calculate from one experimental isotherm all others at different temperatures. Polanyi<sup>19</sup> also investigated, together with Berenyi, the relation between the characteristic curves of different gases obtained on the same adsorbent. They found empirically the following relation between the maximum adsorption potential  $\epsilon_0$  and the van der Waals constant  $a$  of the gas

$$(16) \quad \epsilon_0 = k\sqrt{a}$$

Table VI shows that this equation holds quite well for all gases investigated, except hydrogen. In 1890 Prince Galitzine<sup>20</sup> and later

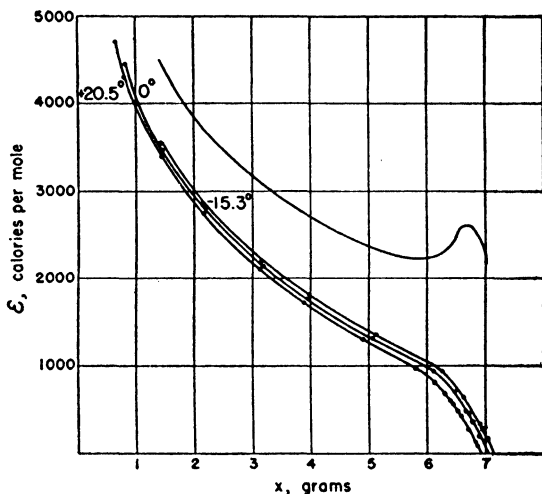


FIG. 55.—Affinity curves of carbon disulfide on charcoal. The top curve is the "heat" curve (discussed later), the three lower curves are the affinity curves.

Berthelot<sup>21</sup> proposed the rule that the attraction potential between two different molecules at a fixed distance is proportional to the expression  $\sqrt{a_1 a_2}$ , where  $a_1$  and  $a_2$  are the van der Waals  $a$  constants

<sup>19</sup> M. Polanyi *Z. Electrochem.*, **26**, 370 (1920).

<sup>20</sup> Prince B. Galitzine, *Wied. Ann.*, **41**, 770 (1890).

<sup>21</sup> D. Berthelot, *Compt. rend.*, **126**, 1856 (1898).



of the two molecules. Applied to adsorption this rule must result in equation (16), since one of the two substances—the charcoal adsorbent—is always the same. The equation illustrates clearly the non-specific nature of van der Waals adsorption. The adsorption poten-

TABLE VI  
THE RELATION BETWEEN  $\epsilon_0$  AND  $a$ .  
Charcoal used as adsorbent

Adsorbed Gas	$\epsilon_0$ in Calories	$10^3 \sqrt{a}$	$\epsilon_0/10^3 \sqrt{a}$
C <sub>2</sub> H <sub>4</sub>	7100	94.1	75
CO <sub>2</sub>	6100	84.7	72
CH <sub>4</sub>	5230	60.8	86
CO	4840	53.0	91
O <sub>2</sub>	4450	51.9	86
N <sub>2</sub>	4320	51.8	83
A	4100	51.0	80
H <sub>2</sub>	about 3000	20.6	150

tial is a product to which the surface contributes the same share regardless of what the gas is, and the gas contributes the same share regardless of what the surface is.<sup>22</sup>

If the adsorption potential is plotted against the amount of gas adsorbed at constant temperature, one gets the "affinity curve." Figure 55 represents the affinity curves of Goldmann and Polanyi,<sup>2</sup> obtained for the adsorption of carbon disulfide by charcoal. The abscissa is  $x$ , the weight of gas adsorbed at  $p_x$ ; the ordinate is the adsorption potential  $\epsilon_i$ , calculated from equation (5)

$$(5) \quad \epsilon_i = RT \ln \frac{p_0}{p_x}$$

The data were determined sufficiently far below the critical temperature to use this simple expression. The affinity curves resemble closely in shape the characteristic  $\epsilon - \varphi$  curve, but there is only one  $\epsilon - \varphi$  curve for all isotherms, whereas there is one  $\epsilon - x$  curve for each isotherm. The reason for this is that to a definite value of  $\epsilon_i$  there corresponds a constant volume in the adsorption space  $\varphi_i$ , independent of the temperature, but the quantity of adsorbate contained in this constant volume is different at different temperatures, due to the liquid-like temperature expansion of the adsorbed sub-

<sup>22</sup> This is not always true. Specificity in physical adsorption is discussed in Chapter X.

stance.<sup>23</sup> According to the potential theory

$$(17) \quad \left( \frac{x_1}{x_2} \right)_{\epsilon=\text{const.}} = \left( \frac{\delta_1}{\delta_2} \right)_{\epsilon=\text{const.}}$$

At constant potential the ratio of the amounts adsorbed at two different temperatures is equal to the ratio of the densities of the adsorbed substance at the two temperatures. Since at constant potential the density decreases with increasing temperature, the adsorption will also decrease with increasing temperature. Figure 55 shows that the affinity curves are almost parallel to each other, those at lower temperatures having the larger adsorption for constant  $\epsilon$ . The specific temperature expansion coefficient of the adsorption layer,  $\alpha$ , can be calculated for any value of  $\epsilon$  from the affinity curves, since

$$(18) \quad \alpha = - \frac{1}{\delta} \left( \frac{\partial \delta}{\partial T} \right)_{\epsilon} = - \frac{1}{x} \left( \frac{\partial x}{\partial T} \right)_{\epsilon}$$

The maximum value of  $x$  at temperature  $T$  is attained when  $p_x = p_0$  and  $\epsilon = 0$ . This value,  $x_b$ , is the amount adsorbed when the entire adsorption space is filled with the liquid adsorbate. (The density distribution then corresponds to that shown in Curve 1, Fig. 49.) As a matter of fact,  $x_b$  is also the amount adsorbed when the adsorbent is directly immersed in the liquid. The value of the specific temperature expansion coefficient for  $\epsilon = 0$  is obtained from equation (18)

$$(19) \quad \alpha_b = \frac{x_{b1} - x_{b2}}{(T_2 - T_1)x_{b2}}$$

where  $x_{b1}$  and  $x_{b2}$  are the values of  $x_b$  at temperatures  $T_1$  and  $T_2$ . If one determines the apparent density of charcoal by immersion in the liquid adsorbate at two different temperatures, one can obtain  $\alpha_b$  by an independent experimental method.<sup>24</sup> This was done by Goldmann and Polanyi<sup>2</sup> for four different liquids, and in three of the four cases they obtained very good agreement between the experimental value of  $\alpha_b$  and the value calculated from the affinity curves by means of equation (19). A comparison of  $\alpha_b$  with  $\alpha_l$ , the temperature expansion coefficient of the normal liquid, showed that the former was about 20%

<sup>23</sup> The concept of the thermal expansion of the adsorbed phase was adopted by J. W. McBain to explain the variation of  $v_m$  with temperature, discussed in Chapter IV.

<sup>24</sup> Earlier W. D. Harkins and D. T. Ewing (*J. Am. Chem. Soc.*, 43, 1787, 1921) used the method of determining the apparent density of charcoal by immersion in different liquids to prove that the adsorbed layer is under very high compression (Chapter XI).

smaller than the latter. Since the adsorbed substance according to the potential theory is similar to a highly compressed liquid,  $\alpha_b$  should actually be smaller than  $\alpha_l$ .

The average compression in the adsorbed layer can be calculated from the hydrostatic equation (12). The potential is

$$(20) \quad \epsilon_i = \int_{V_i}^{V_z} V dp = \int_{V_i}^{V_z} p dV - p_z V_z + p_i V_i$$

with  $V_z = RT/p_z$  and  $V_i = M/\delta_i$ . As a rough approximation one may neglect the first two terms on the right side of the equation, and

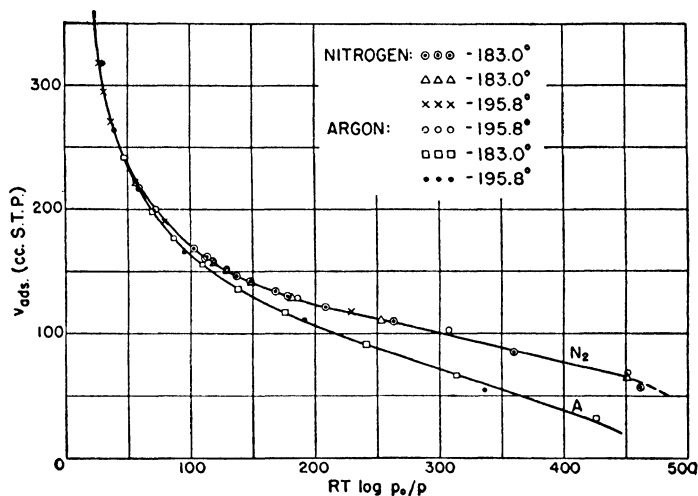


FIG. 56.—Affinity curves of nitrogen and argon on a singly promoted iron catalyst.

substitute  $\delta_l$ , the density of the liquid, for  $\delta_i$ . The mean adsorption potential is then given by

$$(21) \quad \bar{\epsilon}_i = \bar{p}_i \frac{M}{\delta_l}$$

If  $\bar{\epsilon}_i$  is taken as 3000 cal.,  $\bar{p}_i$  must be of the order of 1000 atm. The temperature expansion of a liquid under a compression of 1000 atm. should be about 40% smaller than that of the liquid at atmospheric pressure. As we have seen,  $\alpha_b$  was found to be only 20% smaller than  $\alpha_l$ .

Figure 56 shows affinity curves obtained by Emmett and Brunauer<sup>25</sup> for the adsorption of nitrogen and argon on an aluminum oxide

<sup>25</sup> P. H. Emmett and S. Brunauer, *J. Am. Chem. Soc.*, 57, 2732 (1935).

promoted iron catalyst. The nitrogen curve was calculated from four isotherms (two at 77.3 and two at 90.1° K.), the argon curve from two isotherms (one at 77.3 and one at 90.1° K.). It is to be noted that for each gas the affinity curves at the two temperatures coincide. This is in spite of the fact that the density of liquid nitrogen changes by 7.6% between the two temperatures, and that argon in the bulk phase is liquid at the higher and solid at the lower temperature. (The affinity curves coincide for other unpromoted and promoted iron catalysts, too.) Thus apparently in this case the temperature expansion of the adsorbed phase is negligibly small. The isotherms from which the affinity curves were calculated are shown in Fig. 71, Chapter VI. They are S-shaped isotherms, whereas all previous potential theory calculations were made on Langmuir-type isotherms.

The potential theory has also been applied to adsorption at high pressures. It follows from the theory that if the adsorption measurements are carried to sufficiently high pressures, the amount adsorbed must at some point begin to decrease with increasing pressure. Equation (4) shows that if the gas is subjected to so great compression that its density becomes equal to the density of the adsorbate, the amount adsorbed will become zero. Since at lower pressures the adsorption increases with pressure, and at very high pressures it decreases to zero, it must have a maximum at some intermediate pressure. Antropoff<sup>26</sup> investigated the adsorption of argon and nitrogen on charcoal up to 200 atm. pressure, and Coolidge and Fornwalt<sup>27</sup> measured the adsorption of carbon dioxide, nitrous oxide and silicon tetrafluoride on charcoal up to 100 atm. pressure. The adsorption isotherms exhibited maxima in both sets of investigations.

According to the ordinary definition of adsorption the amount adsorbed is the *excess* material present in the pores of the adsorbent over the amount that would be present if the gas or vapor had its normal density at the temperature and pressure of the experiment. It follows from this definition, without regard to any theory of adsorption, that at infinite pressure the amount adsorbed must be zero. The adsorption isotherm therefore must pass through a maximum. The potential theory, however, does not merely predict the maximum, it enables one to calculate the course of the entire isotherm quantitatively, if the equation of state of the gas is known. Coolidge and Fornwalt made such calculations for the adsorption of carbon monoxide

<sup>26</sup> A. Antropoff, *Z. Elektrochem.*, 42, 544 (1936).

<sup>27</sup> A. S. Coolidge and H. J. Fornwalt, *J. Am. Chem. Soc.*, 56, 561 (1934).

on charcoal up to 100 atm. pressure and found quite satisfactory agreement between the potential theory and their experimental results.

### CRITICISM AND MODIFICATION OF THE POTENTIAL THEORY

In 1930 McBain and Britton<sup>28</sup> published an "experimental disproof" of the potential theory. Since the fallacy of this disproof has not been pointed out as yet, it seems desirable to discuss the subject in some detail.

The first step in the argument of McBain and Britton is to point out that according to the potential theory the adsorption of nitrogen should *decrease* when the pressure is raised from 1 to 60 atm. at constant temperature. The second step is to prove experimentally that the adsorption actually increases very strongly. There is no question about the correctness of their experimental results; the fallacy is in their theoretical reasoning. The potential theory, far from predicting a decrease in the adsorption, predicts an increase of the order of magnitude found by them.

The reasoning of McBain and Britton is briefly as follows. Assume first that the average extra compression within the adsorption space over that of the surrounding gas is 1000 atm. If the surrounding gas is at 1 atm. pressure, the gas in the adsorption space is under a compression of 1001 atm. If nitrogen is the adsorbed gas and the temperature is 16° C., the density at 1001 atm. is 0.5861 g./cc. Since the density at 1 atm. is 0.00118, the increase in density due to adsorption is 0.5849. If the surrounding gas is at 60 atm. pressure, the adsorbate is under a compression of 1060 atm., and the density at this pressure is 0.5995. However, the density of the gas at 60 atm. pressure is 0.07163, therefore the increase in density due to adsorption is only 0.5279. They conclude from this that on raising the pressure from 1 to 60 atm. the adsorption should decrease from 0.5849 to 0.5279. If the average compression in the adsorbed layer is assumed to be 100 atm., or even lower, the same reasoning would still lead to the conclusion that the adsorption should decrease with pressure.

The error of the above argument lies in the belief that  $\bar{p}_i$ , the average compression in the adsorption space, can be obtained simply as the sum of two terms:  $p_z$ , the external pressure, and  $\bar{p}$ , the pressure due to the adsorbent, assumed to be *independent* of  $p_z$ . This assumption not only does not follow from the potential theory, but is entirely contradictory to its concepts. The value of  $\bar{p}$  according to the theory

<sup>28</sup> J. W. McBain and G. T. Britton, *J. Am. Chem. Soc.*, **52**, 2198 (1930).

is not the same when  $p_z = 1$  and  $p_z = 60$  atm. The density distribution in the adsorption space,  $\delta = h(\varphi)$ , depends very strongly on  $p_z$ . If one wishes to test the theory, one must calculate the density distribution according to its postulates and not according to the erroneous short-cut proposed by McBain and Britton.

A very rough calculation shows that McBain and Britton's experimental results are in agreement with the potential theory. According to equation (13) the potential  $\epsilon_i$  that corresponds to any specified value of  $\delta_i$ , the density in the adsorption space, is  $RT \ln 60$  calories higher at 1 atm. than at 60 atm. pressure. Since  $T = 289^\circ \text{K.}$ , this is equal to a difference of 2350 calories. An inspection of the  $\epsilon - \varphi$  curve of Berenyi<sup>13</sup> calculated from Titoff's data<sup>11</sup> for the adsorption of nitrogen by charcoal shows that the value of  $\varphi_i$  corresponding to the same  $\delta_i$  at the two pressures is at least three times as large at 60 atm. as at 1 atm. Thus the adsorption should be *at least* three times as large at 60 atm. pressure. As a matter of fact, McBain and Britton found a 2.5 to 7.2 fold increase in adsorption on four different charcoal samples.

In 1928 Zeise<sup>29</sup> compared Polanyi's theory with Langmuir's, using the data of Miss Homfray,<sup>15</sup> Titoff,<sup>11</sup> and Richardson.<sup>16</sup> He came to the conclusion that the data are better fitted by the Langmuir equation. Some of his curves were shown in Fig. 38. The full curves represent the calculations based on the Langmuir equation, the dotted curves on the potential theory. The weak points in Zeise's calculations relative to Langmuir's theory were discussed in Chapter IV. It may be added now that Zeise's comparisons were unfair for three reasons: (1) he calculated all of the Langmuir isotherms individually, whereas all of the Polanyi isotherms were calculated from one isotherm; (2) he used Berenyi's<sup>13</sup> calculations instead of the more accurate results of Lowry and Olmstead;<sup>12</sup> and (3) he did not use all of Berenyi's data, only the poorest ones.

In 1928 Polanyi, in collaboration with Goldmann,<sup>2</sup> modified the picture underlying the potential theory to bring it into accord with the ideas of modern physics. The quantum mechanical theory of atomic and molecular interactions does not recognize the existence of long range forces reaching far out from the surface of the adsorbent and attracting many layers of adsorbed molecules. However, it was pointed out by Goldmann and Polanyi that the old picture is not an indispensable part of the theory, and that one can substitute in its place the picture of unimolecular adsorption without altering in any

<sup>29</sup> H. Zeise *Z. phys. Chem.*, *A136*, 385 (1928); *A138*, 289 (1928).

manner the quantitative aspects of the theory. According to the unimolecular picture the adsorbate behaves like a two-dimensional liquid that covers the surface in the form of little "islands." Instead of the three-dimensional distribution of the adsorption potential perpendicular to the surface one substitutes a two dimensional distribution over the surface. The place of equipotential surfaces is taken by lines of equal potential. With increasing pressure the places of lower potential become covered with the adsorbate, i.e., the islands of liquid grow in size, new islands form, and some of them flow together. Finally the whole surface becomes covered with adsorbed liquid when the vapor pressure is reached. The temperature expansion of the adsorbed layer in this case becomes two-dimensional and follows the picture given in the treatment of the temperature dependence of  $v_m$  in Chapter IV.

To find out whether their adsorption data indicated unimolecular or multimolecular adsorption, Goldmann and Polanyi reasoned in the following manner. If the volume of the adsorption space is constant, at saturation the charcoal should hold the same volume of liquid, regardless of the nature of the adsorbate, i.e.,

$$(22) \quad \frac{x_b}{\delta_l} = \text{const.}$$

where  $x_b$  is the weight of vapor adsorbed at the saturation pressure and  $\delta_l$  is the density of the liquid.<sup>30</sup> On the other hand, if at the saturation pressure only one layer is adsorbed, then the surface area calculated from the saturation adsorption of different vapors should be the same. The number of moles of vapor adsorbed is  $x_b/M$ ; the surface area covered by a mole of adsorbate is proportional to  $(M/\delta_l)^{2/3}$ , if one assumes that the molecules are spherical; it follows therefore that for unimolecular adsorption

$$(23) \quad \frac{x_b}{M} \left( \frac{M}{\delta_l} \right)^{2/3} = \text{const.}$$

Table VII shows that equation (22) is better fulfilled than (23). Goldmann and Polanyi concluded therefore that the adsorption of vapors on their charcoal was not unimolecular. Nevertheless, they have pointed out that as little as 20% excess over the unimolecular adsorption is sufficient to account for the constancy of the last column

<sup>30</sup> This implies that the adsorbent is a perfectly rigid body, unaffected by the presence of the adsorbate. It will be seen in Chapter XI that this is not entirely true.

of the table and for the less satisfactory agreement of the fourth column. An excess of 40 to 50% would account for the results comfortably.

In spite of the excellent constancy of  $x/\delta_i$  obtained by Goldmann and Polanyi for their four adsorbates, it is not certain that the adsorption of vapors on their charcoal was more than one molecular layer thick. In the first place, in calculating the volume of the adsorption space the density of the adsorbed phase  $\delta_i$  should have been

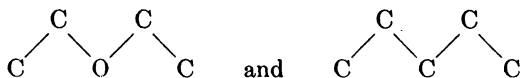
TABLE VII  
ADSORPTION AT SATURATION ON 10 G. OF CHARCOAL AT 0° C.

Substance	$X_b$ in grams	$\frac{X_b}{M}$	$\frac{X_b}{M} \left( \frac{M}{\delta_i} \right)^{1/3}$	$\frac{X_b}{\delta_i}$
<i>Data of Goldmann and Polanyi</i>				
Ethyl chloride	4.98	0.0773	1.32	5.40
Ethyl ether	3.96	0.0534	1.16	5.38
<i>n</i> -Pentane	3.46	0.0480	1.12	5.38
Carbon disulfide	7.02	0.0923	1.40	5.42
<i>Data of Coolidge</i>				
Ethyl ether	3.62	0.0488	1.06	4.90
Carbon disulfide	5.81	0.0764	1.16	4.50
Ethyl formate	4.30	0.0580	1.06	4.54
Methyl acetate	4.70	0.0634	1.16	4.90
Chloroform	6.74	0.0564	1.04	4.42
Carbon tetrachloride	7.10	0.0461	0.96	4.35
Methyl alcohol	3.65	0.1139	1.32	4.50
Water	4.24	0.2358	1.62	4.24

used instead of  $\delta_i$ . Partly because of the high compression in the adsorption space and partly because the temperature expansion of the adsorbed layer is different from that of the normal liquid,  $\delta_i$  is different from  $\delta_l$ . Even though the compressibilities and temperature expansion coefficients of the four liquids differ only slightly, using the  $\delta_i$  values instead of  $\delta_l$  would have made the agreement in the last column less striking. More important than this is the fact that the fourth column does not represent a correct estimate of the surface of the charcoal. Such elongated molecules as pentane and ether can not be assumed to be spherical, since there are good reasons to believe that orientation is not negligible in van der Waals adsorption. It is more probable that a pentane molecule will lie flat on a charcoal surface than that the chain will be perpendicular to the surface. It should be



noted that ethyl ether and *n*-pentane, having almost identical structures



also give almost identical surface values (1.16 and 1.12). The two other molecules, somewhat similar to each other in shape, also show good agreement between their surface values (1.32 and 1.40). The disagreement between the two pairs can be understood, because if the molecules lie flat on the surface, the spherical surface area assignment will be only slightly too small for the two shorter molecules, but much too small for the two longer ones.

The isotherms of Goldmann and Polanyi are very similar to the charcoal isotherms of Brunauer and Emmett.<sup>31</sup> Both sets of data obey the Langmuir equation. This was shown for the latter in Fig. 41 and will be shown for the former in Fig. 74. The Langmuir equation implies unimolecular adsorption. The surface area values calculated for the charcoal of Brunauer and Emmett from the isotherms of five different vapors showed a maximum deviation from the average of less than 6% (Table IV). The  $x_b/\delta_i$  values of Coolidge<sup>3</sup> show a maximum deviation of more than 7% (Table VII). McBain, Lucas, and Chapman<sup>32</sup> found that the volume of liquid adsorbed at saturation on charcoal was 11.7% greater for acetic acid than for toluene at 120° C. It seems difficult therefore to come to a definite conclusion on the basis of such comparison as is offered in Table VII.

Summarizing, we may state that Polanyi's theory is eminently successful in accounting for the temperature dependence of physical adsorption. The calculations of Berenyi and of Lowry and Olmstead prove definitely that the adsorbed substance behaves very much like a compressed gas, and at lower temperatures like a liquid. The deviations of the experimental data from the theory are partly due to experimental error, although slight systematic deviations were also found. This is understandable, since one would not expect the adsorbed gas to obey *exactly* the three dimensional equation of state. It is indeed surprising how far-reaching the agreement actually is.

The potential theory applies to both unimolecular and multimolecular adsorption. It is the only theory of physical adsorption that can handle quantitatively adsorption on a strongly heterogeneous

<sup>31</sup> S. Brunauer and P. H. Emmett, *J. Am. Chem. Soc.*, **59**, 2682 (1937).

<sup>32</sup> J. W. McBain, H. S. Lucas, and P. F. Chapman, *J. Am. Chem. Soc.*, **52**, 2678 (1930).

surface. Since the theory does not attempt to formulate an isotherm equation, the scope of information obtainable from it is limited. One can not determine with its help the extent of the surface of the adsorbent or the pore size distribution; indeed, one can not even tell whether the adsorption is unimolecular or multimolecular. It does give information, however, about the distribution of the heat of adsorption over the surface. This will be discussed in Chapter VIII.

### THE CAPILLARY CONDENSATION THEORY

In 1911 Zsigmondy,<sup>4</sup> while examining the pore structure of silica gel under the ultramicroscope, came to the conclusion that the gel contained much finer capillaries than had been supposed by previous investigators. Since silica gel was known to take up large quantities of water, the idea occurred to him to correlate the adsorption of water with the capillary properties of the gel. It was long known that if a capillary is immersed in a liquid that wets its walls, the liquid rises in the capillary and forms a meniscus which is concave toward the vapor phase. The vapor pressure over the meniscus is lower than the normal vapor pressure of the liquid by an amount equal to the pressure exerted by the column of liquid in the capillary. The vapor pressure lowering over a cylindrical capillary is given by the Kelvin equation <sup>33</sup>

$$(24) \quad \ln p_0 - \ln p = \frac{2\sigma V}{rRt}$$

where  $p$  is the equilibrium pressure over the meniscus in the capillary,  $p_0$  is the normal vapor pressure,  $\sigma$  is the surface tension and  $V$  is the molar volume of the liquid at temperature  $T$ , and  $r$  is the radius of the capillary. The smaller the radius, the greater the vapor pressure lowering according to equation (24). Zsigmondy concluded therefore that in capillaries as small in diameter as one finds in silica gel liquid would condense at pressures far below the normal vapor pressure. This was the first formulation of the capillary condensation theory.

To-day, 30 years later, practically all investigators of adsorption phenomena agree that capillary condensation plays some role in van der Waals adsorption. There is, however, considerable difference of opinion as to how great a role is to be assigned to it. Zsigmondy himself distinguished between direct adsorption on the walls of the capillaries and capillary condensation. Patrick <sup>5</sup> on the other hand was of the opinion for a while that all physical adsorption was due to capillary condensation. Later he admitted the existence of unimolecular

<sup>33</sup> W. Thomson, *Phil. Mag.*, (4), 42, 448 (1871).

adsorption, but attributed all further adsorption to capillary condensation. Most investigators believe now that capillary condensation becomes important only when the adsorbents have capillaries at least several molecular diameters in width, and only at pressures not very far removed from the saturation pressure.

The capillary condensation theory went through two separate lines of development. Patrick, believing that the use of the Kelvin equation (24) down to pore diameters of molecular magnitude was unjustified, adopted in its place an empirical equation, and with his collaborators tested its validity for the adsorption of a variety of gases on silica gel. The other school followed Zsigmondy in using the Kelvin equation as the fundamental equation of the theory, and investigated the extent to which adsorption phenomena can be explained with its help. These two developments will now be discussed in turn.

### A. The Empirical Approach of Patrick

The starting point of the derivation is the Freundlich equation

$$(25) \quad v_g = k' p^{1/n}$$

where  $v_g$  is the volume of gas adsorbed, and  $k'$  and  $1/n$  are empirical constants. According to McGavack and Patrick <sup>6</sup> if one deals with capillary condensation, the basis of comparison should not be the volume of gas adsorbed at pressure  $p$ , but the volume of liquid condensed in the capillaries at the relative pressure  $p/p_0$ . They propose therefore to rewrite equation (25) in the form

$$(26) \quad v_l = k'' (p/p_0)^{1/n}$$

This equation can be tested by plotting  $\log v_l$  against  $\log (p/p_0)$ . McGavack and Patrick plotted their adsorption isotherms, obtained for sulfur dioxide on silica gel from  $-80$  to  $100^\circ \text{C.}$ , according to the logarithmic form of equation (26), and obtained good straight lines, as is seen in Fig. 57. (The adsorption isotherms were shown in Fig. 51.) At the same relative pressure more liquid is adsorbed at lower temperatures, but the isotherms converge in such manner that at  $p = p_0$  the same volume of liquid is taken up at all temperatures. At the saturation pressure all capillaries of the adsorbent are filled with liquid. From the constancy of the total pore volume it follows that the maximum value of  $v_l$  should be the same at all temperatures. It was shown before that the potential theory also demands the constancy of  $v_l = x/\delta_l$  at the saturation pressure at different temperatures.

The next step was to account for the divergence of the curves of Fig. 57 at lower values of  $p/p_0$ . McGavack and Patrick assumed that at any particular value of  $p/p_0$ , not merely at the saturation pressure, the volume of the liquid adsorbed is the same at all temperatures. They explained the divergence by postulating that the density of the adsorbed liquid is markedly different from the density of the normal liquid at the lower pressures. This is due to the fact that the

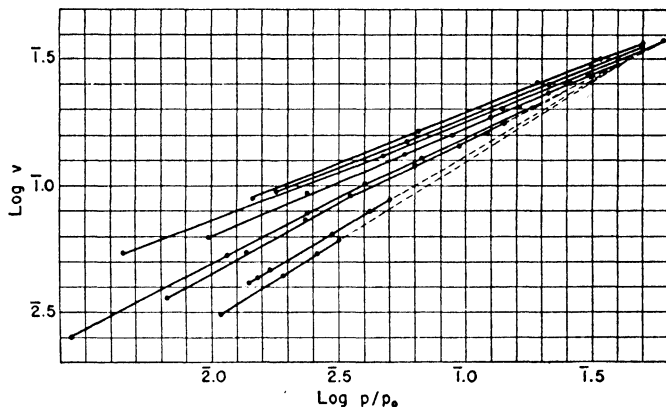


FIG. 57.—Adsorption isotherms of sulfur dioxide on silica gel plotted according to equation (26).

liquid in a capillary is under a large *negative* hydrostatic pressure, which can be calculated from the Gibbs equation<sup>34</sup>

$$(27) \quad \frac{dp}{dP} = \frac{V_l}{V_g}$$

where  $dp$  is the change in the vapor pressure,  $dP$  the change in the hydrostatic pressure, and  $V_l$  and  $V_g$  are the molar volumes of the condensed phase and the gas phase, respectively. Thus according to this view—in contrast with the potential theory—the adsorbed liquid is under tension and not under compression. Using equation (27) they calculated that at 30° C. sulfur dioxide condensed in the capillaries of silica gel at 9.55 mm. external pressure is under a negative hydrostatic pressure of 530 atm., and that at 706 mm. external pressure the negative hydrostatic pressure is 420 atm.

<sup>34</sup> See, for example, G. N. Lewis and M. Randall, *Thermodynamics*, New York, 1923, p. 183.

If in equation (26) one uses the corrected volume of the condensed phase instead of the volume of the normal liquid, then according to McGavack and Patrick all the isotherms of Fig. 57 should coincide. Since they had no direct experimental data to correct the volume for the effect of the negative hydrostatic pressure, they made the correction empirically. It was known that the greater the surface tension of a liquid is, the smaller is its compressibility. They tried therefore to

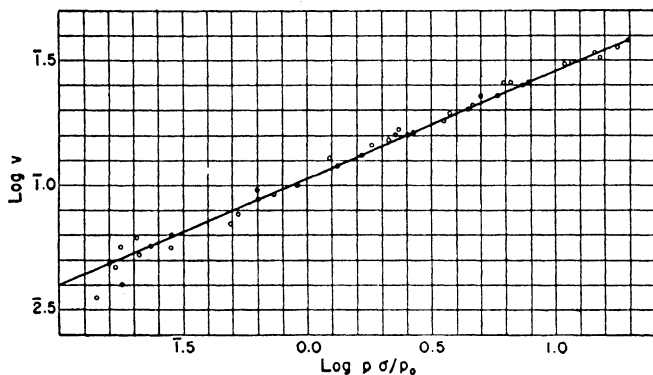


FIG. 58.—Adsorption isotherms of sulfur dioxide on silica gel plotted according to the Patrick equation.

correct for the volume change by dividing  $v_l$  with a fractional power of the surface tension

$$(28) \quad v_l = v_a \sigma^{1/m}$$

where  $v_a$  is the volume of the adsorbed phase and  $1/m$  is an empirical constant. Not knowing the value of  $m$  they set it arbitrarily equal to  $n$  in equation (26). Such a procedure obviously can not be justified theoretically, but it is justified empirically—if it works. The complete equation is then

$$(29) \quad v_l = k(p\sigma/p_0)^{1/n}$$

Plotting  $\log v_l$  against  $\log (p\sigma/p_0)$  they found that the isotherms of Fig. 57 actually did coincide, as shown in Fig. 58. They concluded that this confirmed their assumption that the volume occupied by the adsorbed phase was the same at the same values of  $p/p_0$ , regardless of the temperature.

Coolidge<sup>3</sup> pointed out that such a conclusion is untenable since it contradicts the Kelvin equation (24). The relative pressure  $p/p_0$

depends not merely on the capillary radius  $r$ , but also on  $\sigma$ ,  $V$ , and  $T$ , all functions of the temperature. Even if one denies the validity of the Kelvin equation for the relation between  $p/p_0$  and  $r$  for very small capillaries, there is no reason to suppose that  $\sigma$ ,  $V$ , and  $T$  cease to be involved in the correct unknown theoretical relationship, and therefore cease to confer a temperature coefficient upon the relative pressure. While this is true, it may be pointed out that both the Kelvin equation and Patrick's view can be correct at the same time if

$$(30) \quad \sigma V = cT$$

where  $c$  is a constant. Although such a relation was never found to hold for normal liquids, if  $\sigma$  and  $V$  are very different in small capillaries than in the bulk phase perhaps such temperature dependence is not entirely impossible. Coolidge also pointed out that the device of correcting for distension by dividing the calculated volumes of liquid by a fractional power of  $\sigma$  is illogical, because the distension can not be the same fraction of the volume at all pressures. At saturation there should be no distension, since as McGavack and Patrick themselves have pointed out the volume of liquid taken up at saturation is the same at all temperatures. This is true only if correction is not applied; the suggested correction naturally destroys the agreement.

Perhaps the most important test of an empirical equation is not its logical consistency, but its success or failure in application. After the adsorption of sulfur dioxide <sup>5</sup> Patrick and his collaborators investigated the adsorption of ammonia <sup>35</sup> and butane <sup>36</sup> on silica gel, and obtained good straight lines according to equation (29). However, Gregg <sup>37</sup> pointed out that if one substitutes into that equation  $1/T$  in place of  $\sigma$ , entirely empirically, one obtains almost as good agreement for the adsorption of sulfur dioxide, and quite as good agreement for the adsorption of ammonia and butane.

According to Patrick's view not only isotherms obtained for the same gas at different temperatures but also isotherms of different gases on the same adsorbent should fall on the same curve when plotted according to equation (29). The adsorption of carbon tetrachloride, ethyl alcohol and water vapor on silica gel <sup>38</sup> gave curves that did not coincide, nor were they good straight lines, with the exception of the carbon tetrachloride curve. Similarly the adsorption

<sup>35</sup> L. Y. Davidheiser and W. A. Patrick, *J. Am. Chem. Soc.*, **44**, 1 (1922).

<sup>36</sup> W. A. Patrick and J. S. Long, *J. Phys. Chem.*, **29**, 336 (1925).

<sup>37</sup> S. J. Gregg, *J. Phys. Chem.*, **32**, 616 (1928).

<sup>38</sup> W. A. Patrick and L. H. Opdycke *J. Phys. Chem.*, **29**, 601 (1925).

of carbon dioxide and nitrous oxide on silica gel<sup>39</sup> gave curves that did not coincide. In each case Patrick found an explanation for the disagreement with his equation, but Gregg<sup>37</sup> pointed out that in both sets of experiments the curves came quite close together by using  $1/T$  in place of Patrick's  $\sigma$ .

Reyerson and Cameron<sup>40</sup> used the Patrick equation to fit their data obtained for the adsorption of bromine on silica gel. The results

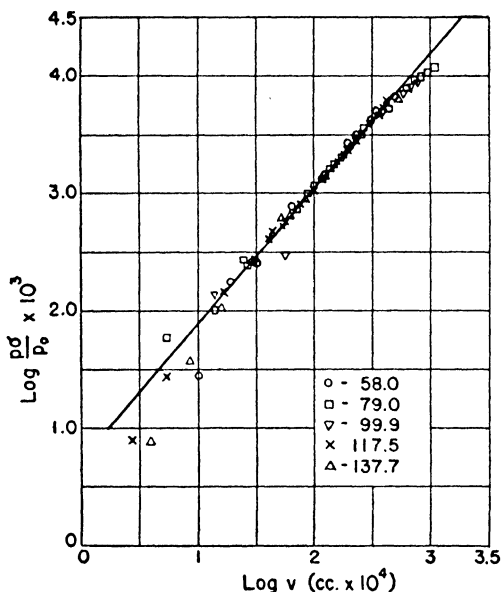


FIG. 59.—Adsorption isotherms of bromine on silica gel plotted according to the Patrick equation.

are shown in Fig. 59. The experimental points deviate from the straight line at high and low adsorptions. (The adsorption isotherms were shown in Fig. 7.) The same data plotted according to the Freundlich equation and the Langmuir equation gave no agreement at all. The adsorption isotherms obtained for iodine on silica gel showed less good agreement with the Patrick equation than the bromine data.

<sup>39</sup> W. A. Patrick, W. C. Preston and A. E. Owens, *J. Phys. Chem.*, **29**, 421 (1925).

<sup>40</sup> L. H. Reyerson and A. E. Cameron, *J. Phys. Chem.*, **39** 181 (1935).

The conclusion from the above considerations is that the Patrick equation should be regarded as an empirical equation, which it really is. Since neither the Freundlich equation from which it was derived, nor the insertion of the other terms ( $p_0$  and  $\sigma$  raised to a fractional power) follows directly from any consistently developed theory of capillary condensation, one can not conclude that if the data obey the Patrick equation, the theory of capillary condensation is confirmed. The criterion of the validity of any empirical equation is its success in fitting the experimental data. When the Patrick equation is valid, it is a useful tool as an interpolation formula.

### *B. The Theoretical Approach*

It is possible that the extrapolation of the Kelvin equation to capillaries of molecular dimensions is not entirely justified, yet in the absence of a better theoretical expression it is the only valid means of testing the theory of capillary condensation. However, in testing the equation one immediately encounters the difficulty of not knowing what values of  $\sigma$  and  $V$  should be used in equation (24). There are reasons to believe that the surface tension and the molar volume of the condensed phase in the extremely narrow pores of the adsorbent are different from those of the normal liquid in the bulk phase.

We have seen that according to the potential theory the adsorbed liquid is under a very great compression. This was confirmed by the experiments of Harkins and Ewing,<sup>24</sup> Goldmann and Polanyi,<sup>2</sup> and others. According to Patrick's view the adsorbed liquid is under tension, it is therefore less dense than the ordinary liquid.<sup>41</sup> Regardless of which view is correct, one should not substitute into equation (24) simply the normal value of  $V$ . Nevertheless if one does that, the error introduced is not great, since liquids are only slightly compressible. On the other hand the surface tension may undergo large changes in the narrowest capillaries, and the use of the normal value may introduce serious errors. Shereshefsky<sup>42</sup> found that the vapor pressure lowering of water and toluene in capillaries of  $2\mu$  radius was 8-9 times as large as the value calculated from the Kelvin equation. He concluded from this that in capillaries of this size  $\sigma$  must be much greater than its normal value. However, Cohan and Meyer<sup>43</sup> measured directly  $\sigma$  and  $V$  for water and toluene in capillaries of  $2\mu$  radius and found that the values were the same as in the bulk phase. (They

<sup>41</sup> This subject is further discussed in Chapter XI.

<sup>42</sup> J. L. Shereshefsky, *J. Am. Chem. Soc.*, **50**, 2966 (1928).

<sup>43</sup> L. H. Cohan and G. E. Meyer, *J. Am. Chem. Soc.*, **62**, 2715 (1940).



determined the product  $\sigma V$  by measuring the rise of the liquids in the capillaries, then measured  $\sigma$  separately by determining the pressure necessary to prevent any capillary rise.) Of course, these experiments do not exclude the possibility that in capillaries having much smaller radii than  $2\mu$  there may be a change in  $\sigma$  and  $V$ .

Kubelka<sup>44, 45</sup> in his approach to the theory of capillary condensation accepts the validity of the Kelvin equation for the capillaries of the adsorbent, but rejects the use of the normal values of  $\sigma$  and  $V$  in his calculations. If the adsorbate wets the walls of the adsorbent incompletely, the Kelvin equation takes the form

$$(31) \quad RT \ln \frac{p_0}{p} = \frac{2\sigma V \cos \theta}{r}$$

where  $\theta$  is the angle of wetting. (For complete wetting  $\theta = 0^\circ$  and equation (31) reduces to equation (24).) Kubelka suggests that since the correct value of  $\sigma V$  is not known, one can replace it by an empirical constant, and rewrite equation (31) solving for  $r$

$$(32) \quad r = \frac{B \cos \theta}{-\ln \frac{p}{p_0}}$$

Here  $B$  is assumed to have a constant value for any particular temperature. With the help of this semi-empirical equation Kubelka attempts to prove that the adsorption of vapors on charcoal can be explained by the theory of capillary condensation. The proof involves a comparison of the isotherms of different vapors on the same adsorbent and at the same temperature. If the Kelvin equation is valid, one can write it for two different vapors as

$$(33) \quad r_1 = -\frac{2\sigma_1 V_1 \cos \theta_1}{RT \ln \frac{p_1}{p_{01}}} \quad \text{and} \quad r_2 = -\frac{2\sigma_2 V_2 \cos \theta_2}{RT \ln \frac{p_2}{p_{02}}}$$

If one compares equal volumes of the liquid adsorbed, then  $r_1 = r_2$ , and one gets

$$(34) \quad \ln \frac{p_1}{p_{01}} = \frac{\sigma_1 V_1 \cos \theta_1}{\sigma_2 V_2 \cos \theta_2} \ln \frac{p_2}{p_{02}}$$

If one plots from the two isotherms the values of the relative pressure that correspond to the same volume of liquid adsorbed against each

<sup>44</sup> P. Kubelka, *Z. Elektrochem.*, **37**, 637 (1931).

<sup>45</sup> P. Kubelka, *Kolloid Zeitschr.*, **55**, 129 (1931); **58**, 189 (1932).

other, one should obtain according to equation (34) a straight line, passing through the origin. This is called the curve of "equivalent pressures." The slope of the straight line can be calculated if the values of  $\sigma$ ,  $V$  and  $\cos \theta$  are known. If these values are not known, one can use equation (32) instead of (31) and obtain

$$(35) \quad \ln \frac{p_1}{p_{01}} = \frac{B_1 \cos \theta_1}{B_2 \cos \theta_2} \ln \frac{p_2}{p_{02}}$$

This is also a straight line passing through the origin. Its slope can not be calculated from known physical constants, but Kubelka

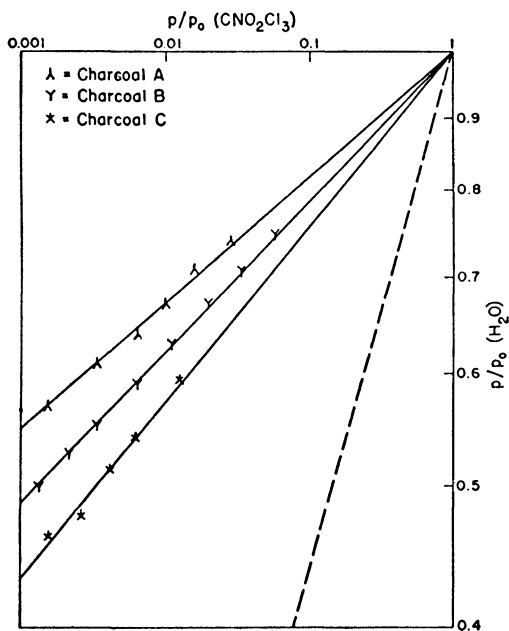


FIG. 60.—Equivalent pressure curves of chloropicrin and water on three different charcoals.

concluded that if such a plot of equivalent pressures does give a straight line, it is a sufficient proof of the correctness of the capillary condensation theory.

Figure 60 gives Kubelka's curves for the equivalent pressures of chloropicrin and water on three different kinds of charcoal. According to Kubelka, if both liquids would wet the charcoal completely, the

equivalent pressure curves of the three charcoals would coincide. This is because according to the capillary condensation theory the adsorbent is entirely inert, and its sole function is to supply a set of capillaries of various sizes. On the other hand, if one of the liquids does not wet the charcoal completely, the angle of wetting may be different for the different kinds of charcoal. Water does not wet charcoal completely, therefore one obtains the three different curves shown in Fig. 60. Organic liquids wet the charcoal completely, and Kubelka found that the equivalent pressure curves of benzene and

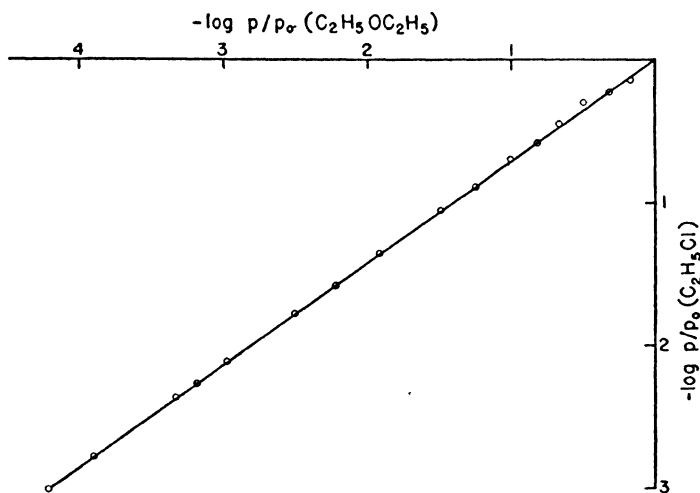


FIG. 61.—Equivalent pressure curve of ether and ethyl chloride on charcoal.

chloropicrin, benzene and ether, and chloropicrin and ether actually did coincide for the different charcoals. The three curves of Fig. 60 are fairly good straight lines, passing through the origin. The dotted line was calculated on the basis of equation (34), setting  $\cos \theta_1 = \cos \theta_2 = 1$ .

Lindau<sup>46</sup> analyzed Kubelka's arguments and showed their weak points. If the surface tension of the liquid in capillaries of small radii is different from that of the bulk liquid, then  $B$  in equation (32) can not be a constant but must be a function of the capillary radius.<sup>47</sup>

<sup>46</sup> G. Lindau, *Kolloid Zeitschr.*, 60, 253 (1932).

<sup>47</sup> J. W. McBain pointed out that the assumption that  $\sigma$  is different in small capillaries implies that the walls of the capillary are not inert but exert forces upon the liquid. This in turn means that one does not deal with pure capillary condensation but with a combination of adsorption and capillary condensation. (*Sorption of Gases and Vapours by Solids*, London, 1932, p. 434.)

At low values of  $p/p_0$  the capillaries of smallest radii fill with liquid, and the deviation from the normal value of  $\sigma$  may be quite large. At high values of  $p/p_0$  the largest capillaries fill, and the value of  $\sigma$  may be only slightly different from that of the bulk phase. Thus the curve of equivalent pressures according to equation (35) can not be a straight line. Yet all the experimental data of Goldmann and Polanyi<sup>2</sup> and of Coolidge<sup>48</sup> give equivalent pressure curves that are excellent straight lines from the lowest pressures to the highest pressures measured. Figure 61 shows the curve calculated by Lindau from the

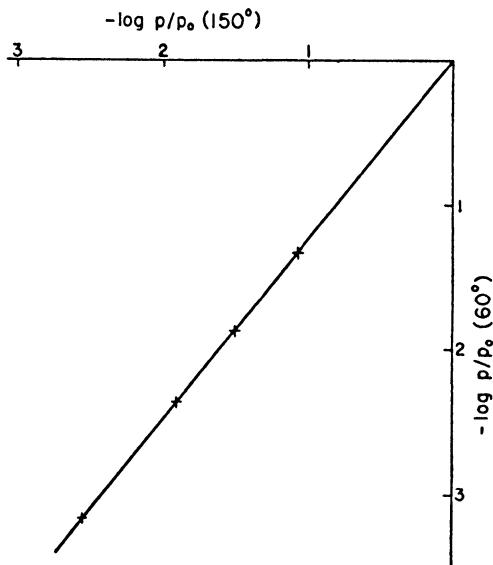


FIG. 62.—Equivalent pressure curve of carbon disulfide on charcoal at 60 and 150° C.

data of Goldmann and Polanyi for the adsorption of ether and ethyl chloride by charcoal. There is not the slightest indication of the deviation from the straight line demanded by Kubelka's theory.

Two other consequences of Kubelka's theory are in direct contradiction with the experimental facts. If  $\sigma = f(r)$ , then the equivalent pressure curve of one vapor at two different temperatures can not be a straight line. Actually all available data give good straight lines. An example of this is given in Fig. 62, representing the equivalent pressure curve of carbon disulfide on charcoal at 60 and at 150° C.

<sup>48</sup> A. S. Coolidge *J. Am. Chem. Soc.*, 46, 596 (1924).

The calculation was made by Lindau on the basis of Coolidge's data.<sup>45</sup> Furthermore, if  $\sigma$  depends on the capillary radii the equivalent pressure curves of two vapors obtained for different charcoals can not coincide, since different charcoals have different distributions of capillaries. Kubelka found, however, that the equivalent pressure curves of organic vapors do coincide for different charcoals, as was mentioned before. It is clear therefore that Kubelka's semi-empirical proof of the applicability of the capillary condensation theory to the adsorption of vapors by charcoal is incorrect.

If one discards the concept of the variation of  $\sigma$  with the capillary radius and returns to the original Kelvin equation, then it follows that the equivalent pressure curves should indeed be straight lines through the entire range of adsorption. In this case, however, the slope can be calculated from equation (34). In Fig. 60 the dotted line shows that the calculated slope is incorrect. In other cases Kubelka found sometimes better, sometimes even poorer agreement.

Polanyi<sup>49</sup> pointed out that the potential theory also demands that the equivalent pressure curves be straight lines passing through the origin. Lindau<sup>46</sup> developed this idea further and showed that calculations based on the potential theory give the correct slopes. If one compares the adsorption of two different vapors at the same temperature, taking equal volumes of liquid adsorbed, the corresponding potentials have a constant ratio to each other. For  $\varphi = 0$ , it follows from equation (16) that

$$(36) \quad \frac{\epsilon_{01}}{\epsilon_{02}} = \sqrt{\frac{a_1}{a_2}}$$

where  $\epsilon_{01}$  and  $\epsilon_{02}$  are the maximum potentials, and  $a_1$  and  $a_2$  are the van der Waals constants of the two vapors. Assuming that this relation is approximately valid for other values of the potential too, one obtains

$$(37) \quad RT \ln \frac{p_1}{p_{01}} = \sqrt{\frac{a_1}{a_2}} RT \ln \frac{p_2}{p_{02}}$$

Thus the slopes of the equivalent curves on the basis of the potential theory are simply equal to  $\sqrt{a_1/a_2}$ . Lindau found that the calculated slopes were in fair agreement with the observed ones.

The potential theory has not been developed satisfactorily for the calculation of the adsorption of one gas from that of another gas, but as we have seen, it accounts excellently for the temperature

<sup>49</sup> M. Polanyi, *Trans. Far. Soc.*, **28**, 316 (1932).

dependence of the adsorption isotherm. It is of greater interest therefore to compare the slopes of equivalent pressure curves of the same gas at different temperatures calculated on the basis of the capillary condensation theory and the potential theory. Taking equal volumes of the liquid adsorbed at two different temperatures, the Kelvin equation states that  $r_1 = r_2$ , and assuming complete wetting one can write

$$(38) \quad r_1 = -\frac{2\sigma_1 V_1}{RT_1 \ln \frac{p_1}{p_{01}}} \quad \text{and} \quad r_2 = -\frac{2\sigma_2 V_2}{RT_2 \ln \frac{p_2}{p_{02}}}$$

The equivalent pressure equation is

$$(39) \quad \ln \frac{p_1}{p_{01}} = \frac{\sigma_1 V_1 T_2}{\sigma_2 V_2 T_1} \ln \frac{p_2}{p_{02}}$$

On the other hand the potential theory states that for equal volumes of liquid adsorbed  $\varphi_1 = \varphi_2$ , from which it follows that

$$(40) \quad -RT_1 \ln \frac{p_1}{p_{01}} = -RT_2 \ln \frac{p_2}{p_{02}}$$

The equation of the equivalent pressure curve is

$$(41) \quad \ln \frac{p_1}{p_{01}} = \frac{T_2}{T_1} \ln \frac{p_2}{p_{02}}$$

A comparison of equations (39) and (41) shows that both theories demand straight lines passing through the origin, but the slope according to the Kelvin equation is  $\sigma_1 V_1 T_2 / \sigma_2 V_2 T_1$ , whereas according to the potential theory it is simply  $T_2 / T_1$ . Some of the results of Lindau's calculations are shown in Table VIII. The agreement with

TABLE VIII  
SLOPES OF THE EQUIVALENT PRESSURE CURVES

Vapor	Temperatures ° C.	Kelvin Equation	Potential Theory	Observed Slope	Investi- gator
Carbon disulfide	0, 60	1.54	1.22	1.22	C. <sup>1</sup>
Carbon disulfide	60, 150	2.17	1.27	1.26	C.
Carbon disulfide	0, 20.5	1.15	1.08	1.09	G.a.P. <sup>2</sup>
Ethyl ether	0, 20.5	1.19	1.08	1.09	G.a.P.
Benzene	0, 60	1.50	1.22	1.22	C.
Benzene	60, 150	1.94	1.27	1.24	C.
Pentane	0, 20.5	0.83	0.93	0.91	G.a.P.
Ethyl chloride	0, 20	1.19	1.07	1.06	G.a.P.

<sup>1</sup> Coolidge, *J. Am. Chem. Soc.*, 46, 596 (1924).

<sup>2</sup> Goldmann and Polanyi, *Z. phys. Chem.*, A152, 313 (1928).

the potential theory and the disagreement with the capillary condensation theory are particularly striking for the results of Coolidge.<sup>48</sup>

Lindau noticed that close to saturation the slopes of the equivalent pressure curves begin to deviate from the potential theory value and approach the Kelvin equation value. Table IX illustrates this for

TABLE IX  
SLOPE OF THE EQUIVALENT PRESSURE CURVE OF ETHYL CHLORIDE ON CHARCOAL  
Temperatures = 0 and 20° C.  
Slope according to potential theory = 1.07  
Slope according to capillary condensation theory = 1.19

Volume adsorbed cc./10 g. of charcoal	Observed slope
5.10	1.23
5.09	1.16
5.02	1.11
4.99	1.04
4.48	1.05
4.24	1.06
4.09	1.06
3.58	1.06
3.04	1.06
2.62	1.08
1.65	1.06
1.33	1.08
0.77	1.06
0.55	1.06

the adsorption of ethyl chloride by charcoal, determined by Goldmann and Polanyi.<sup>2</sup> The table shows the values of the observed slope for different volumes of the liquid adsorbed. It should be noted that the first significant deviation from the potential theory occurs at 5.02 cc. of liquid adsorbed, while the adsorption at saturation is 5.40 cc. Thus one can ascribe at most only 7% of the total adsorption at saturation to capillary condensation. In the adsorption of carbon disulfide by charcoal no significant deviation from the Polanyi slope occurs even at 5.02 cc. adsorbed, so that in this case even less of the adsorption can be attributed to capillary condensation.

In view of the lack of success of the semi-empirical method of Kubelka, the only completely logical method of attack is to assume not merely the validity of the Kelvin equation, but also the applicability of the normal values of  $\sigma$  and  $V$  in the calculations. This enables one to investigate the extent to which adsorption phenomena

can be explained on the basis of the theory of capillary condensation. It becomes clear at once that adsorption at low pressures can not be due to capillary condensation, because to condense liquids at low values of  $p/p_0$  capillaries would be required the radii of which are smaller than the diameter of a molecule. Coolidge<sup>3</sup> pointed out that in his experiments on the adsorption of benzene by charcoal at 0° C. when the amount of liquid adsorbed is 0.2 cc., or about 50% of the saturation adsorption, the calculated value of  $r$  is 2.89Å. Since the smallest dimension of a benzene molecule is 3.7Å, obviously one can not deal here with capillary condensation. Similarly, when McGavack and Patrick<sup>5</sup> had 0.1 cc. of liquid sulfur dioxide adsorbed by silica gel at 0° C., which is about 24% of the maximum adsorption, the calculated value of  $r$  was 3.16Å, again smaller than the diameter of an SO<sub>2</sub> molecule. Furthermore, even if one assumes that condensation can occur in capillaries as small as these, and calculates from the known adsorption of a certain substance at one temperature the value of  $p/p_0$  at which the same volume of liquid is adsorbed at another temperature, or the same volume of another liquid is adsorbed at the same temperature, one arrives at results that are wholly erroneous. The calculations of Coolidge<sup>3</sup> based on his own experiments<sup>48</sup> are shown in Table X. They were made on the basis of the adsorption of 0.2 cc.

TABLE X

THE INAPPLICABILITY OF THE KELVIN EQUATION AT LOW PRESSURES

Volume of liquid adsorbed = 0.2 cc. at 0° C.

Radius of capillary = 2.89Å

Substance	Temperature °C.	Log $p/p$ Calculated	Log $p/p$ Observed
Benzene	99	1.82	2.74
Benzene	150	1.19	2.44
Carbon disulfide	0	2.65	2.60
Ethyl ether	0	2.51	4.00
Water	0	1.80	0.26

of liquid benzene at 0° C. The calculated value of the pressure for the adsorption of 0.2 cc. of liquid ether is too high by a factor of 31, for 0.2 cc. of water it is too low by a factor of 35.

It follows from the above considerations that capillary condensation can play a role only at higher relative pressures. Schuchowitzki,<sup>50</sup> on the basis of some ideas advanced by Polanyi,<sup>49</sup> subdivided the adsorption isotherm into four regions. He assumed that in physical

<sup>50</sup> A. A. Schuchowitzki, *Kolloid Zeitschr.*, 66, 139 (1934).



adsorption the forces were due to two potentials, and wrote

$$(42) \quad \chi = \epsilon + \pi$$

where  $\chi$  is the total potential,  $\epsilon$  is the Polanyi potential, i.e., that caused by the interaction between the adsorbent and the adsorbate, and  $\pi$  is the Kelvin potential, i.e., that caused by the concavity of the meniscus in the capillary. In the lowest pressure region  $\chi < \epsilon$ , because part of  $\epsilon$  is used up in creating a liquid surface.<sup>51</sup> After the first adsorbed layer is complete one reaches the second region where  $\chi = \epsilon$ ; here the potential theory is applicable and capillary condensation is not yet appreciable. In the third region  $\chi > \epsilon$ ; this is the intermediate region where the full equation (42) must be used. Finally, in the fourth region  $\chi = \pi$ ; here  $\epsilon$  becomes negligible and the theory of capillary condensation becomes valid.

Schuchowitzki attempted to investigate the third region quantitatively. He reasoned that if both adsorption and capillary condensation take place simultaneously, the Kelvin potential takes the form

$$(43) \quad \pi = RT \ln \frac{p_0}{p} = \frac{2\sigma V}{r - h}$$

where  $h$  is the thickness of the adsorbed layer. The adsorption potential can be expressed on the basis of London's quantum mechanical treatment<sup>10</sup> as

$$(44) \quad \epsilon = \frac{c}{r^3}$$

where  $c$  is a constant.<sup>52</sup> If one assumes that the two potentials are simply additive, one can obtain  $\chi$  as the sum of  $\pi$  and  $\epsilon$  from equations (43) and (44). The equivalent pressure curve of a vapor at two different temperatures will then be

$$(45) \quad Q = \frac{\ln \frac{p_{01}}{p_1}}{\ln \frac{p_{02}}{p_2}} = \frac{\frac{2\sigma_1 V_1}{r_1 - h_1} + \frac{c}{r_1^3}}{\frac{2\sigma_2 V_2}{r_2 - h_2} + \frac{c}{r_2^3}} \cdot \frac{T_2}{T_1}$$

For an adsorbent with very fine pores, such as charcoal, Schuchowitzki sets  $r_1 = r_2$  and  $h_1 = h_2$ . The slope of the curve is thus given by the expression

$$(46) \quad Q = \frac{2\sigma_1 V_1 r^3 + c(r - h)}{2\sigma_2 V_2 r^3 + c(r - h)} \cdot \frac{T_2}{T_1}$$

<sup>51</sup> It was pointed out before that the potential theory neglects the energy necessary to create a liquid surface.

<sup>52</sup> The London equation is discussed in detail in Chapter VII.

Table XI gives an example of how the calculated values of  $Q$  compare with the observed ones. The calculations are based on the data of Coolidge<sup>48</sup> for the adsorption of methyl alcohol by charcoal at 0 and 50° C. The agreement is not very striking, since all the values of  $Q$  calculated from equation (46) must necessarily fall within the narrow range between 1.18, the potential theory value of the slope, and 1.34, the capillary condensation theory value. Nevertheless, Schuchowitzki's approach is worth further testing as well as

TABLE XI  
CALCULATIONS OF  $Q$   
Methyl alcohol on charcoal (Coolidge) at 0 and 50° C.  
Slope according to potential theory = 1.18  
Slope according to Kelvin equation = 1.34

Volume Adsorbed cc./100 g. of Charcoal	$Q$ Observed	$Q$ Calculated
35.3	1.31	1.26
26.4	1.25	1.245
17.6	1.23	1.24
8.82	1.21	1.23
5.29	1.18	1.21

further improvement along theoretical lines. It is unfortunate that he chose charcoal to test the theory instead of an adsorbent with wider pores, such as silica gel. Schuchowitzki is incorrect in attributing the deviations of the observed  $Q$  values from the potential theory slope to capillary condensation. On the basis of Table XI one would be led to believe that capillary condensation begins at very small adsorptions. Actually, even if one calculates the value of  $r$  at the *largest* adsorption measured by Coolidge, one obtains only the low value of 6.8Å. Since the molecular diameter of methyl alcohol is 4.4Å, it is doubtful whether one can speak here about capillary condensation in the entire adsorption range. Perhaps deviation from the potential theory should rather be attributed to the fact that the potential can not be calculated through the entire pressure and temperature range by means of the simple equation (5).

A striking characteristic of capillary condensation is the appearance of hysteresis loops in the adsorption isotherms. Such isotherms were shown in Fig. 6, representing the adsorption of benzene on ferric oxide gel, measured by Lambert and Clark.<sup>53</sup> For the same volume of vapor adsorbed the equilibrium pressure of the adsorption side is

<sup>53</sup> B. Lambert and A. M. Clark, *Proc. Roy. Soc., A122*, 497 (1929).

higher than that of the desorption side. The various theories accounting for hysteresis are discussed in Chapter XI. Every reasonable explanation advanced so far is based on the assumption that hysteresis is due to capillary condensation. Foster<sup>54</sup> and Cohan<sup>55</sup> attribute reversible hysteresis to a delay in the formation of the meniscus in the capillary. It follows from this that the adsorption branch of the hysteresis loop is due to multimolecular adsorption and capillary condensation, while the desorption branch represents capillary condensation only.

That this view is essentially correct was shown by Foster,<sup>54</sup> using a simple and convincing argument. To compare equal volumes of liquid adsorbed at different temperatures one can put the Kelvin equation in the form

$$(47) \quad \pi = RT \ln \frac{p_0}{p} = K \frac{\sigma}{\delta}$$

In place of  $V$  one can write  $M/\delta$ , where  $M$  is the molecular weight and  $\delta$  is the density of the liquid, and in place of  $2M/r$  one can write the constant  $K$ , since  $r = \text{constant}$  for equal volumes of the liquid adsorbed. There are two things to be noted about equation (47). In the first place  $\pi$ , the potential of capillary condensation, is temperature dependent, since both  $\sigma$  and  $\delta$  are functions of the temperature. In contrast to this, the adsorption potential  $\epsilon$  is independent of temperature. In the second place the product  $\pi\delta/\sigma$  is constant according to equation (47). To check whether these two consequences of the capillary condensation theory are fulfilled, Foster made calculations

TABLE XII  
HYSTERESIS AND THE KELVIN EQUATION  
Benzene on Ferric Oxide Gel (Lambert and Clark)

Temperature °C.	$\pi$ calories/mole	$\sigma/\delta$	$\pi\delta/\sigma$
40	670	29.68	22.57
50	645	28.52	22.62
60	616	27.31	22.55

on the isotherms of Lambert and Clark,<sup>53</sup> shown in Fig. 6, both for the adsorption and desorption side of the hysteresis loop. The results of his calculations for 0.22 cc. of liquid benzene adsorbed per gram of ferric oxide gel, for the *desorption* side, are shown in Table XII. The

<sup>54</sup> A. G. Foster, *Trans. Far. Soc.*, 28, 645 (1932).

<sup>55</sup> L. H. Cohan, *J. Am. Chem. Soc.*, 60, 433 (1938).

potential is temperature dependent, as is demanded by the capillary condensation theory, and the product  $\pi\delta/\sigma$  is constant within one half of one per cent. This striking agreement leaves little doubt about the correctness of the view that the descending portion of the hysteresis loop is due to capillary condensation. The potential of the ascending portion shows negligible temperature dependence, conforming to the Polanyi theory and indicating multimolecular adsorption.

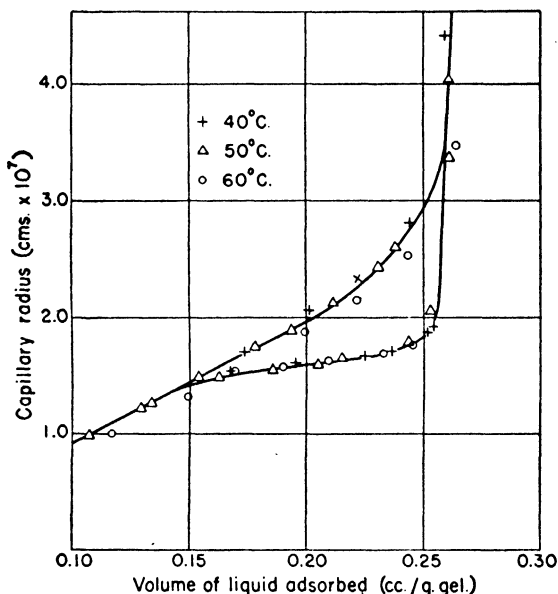


FIG. 63.—Adsorption isotherms of benzene on ferric oxide gel plotted according to the Kelvin equation.

Foster shows the effect of temperature on the equilibrium in the hysteresis area by plotting the capillary radius against the volume of liquid adsorbed. Such a plot for the adsorption of benzene by ferric oxide gel is given in Fig. 63. The plot represents the same three isotherms that were shown in Fig. 6. Instead of the volume or weight of the vapor adsorbed the volume of the liquid adsorbed is used as one of the coordinates, and instead of the pressure, or the relative pressure, the capillary radius calculated from the Kelvin equation is used as the other. The figure shows that the three desorption isotherms fall on the same curve, while the three adsorption isotherms

do not, showing that the former obey, the latter do not obey the Kelvin equation. That multimolecular adsorption precedes capillary condensation is clear from the fact that the hysteresis region begins at a radius of  $14\text{\AA}$ , while the diameter of a benzene molecule is  $6.6\text{\AA}$  at  $50^\circ\text{C}$ . (calculated from the liquid density on the assumption that the molecules are spheres).<sup>56</sup>

Summarizing, we may state briefly that capillary condensation can not account for adsorption at low pressures, but at higher pressures it probably plays an important role for all adsorbents except those that have exceedingly fine pores.

<sup>56</sup> The phenomenon of hysteresis is discussed in detail in Chapter XI.

## CHAPTER VI

### THE ADSORPTION ISOTHERM III

In Chapter IV we discussed the theories of unimolecular adsorption and in Chapter V two of the theories of multimolecular adsorption. The present chapter deals with two more recently proposed theories, both based on the assumption that physical adsorption is more than one molecular layer thick. The first of these is the polarization theory, proposed by de Boer and Zwikker <sup>1</sup> in 1929 and derived again in a slightly different form by Bradley <sup>2</sup> in 1936. It explains the adsorption of non-polar molecules on ionic adsorbents by assuming that the uppermost layer of the adsorbent induces dipoles in the first layer of adsorbed molecules, which in turn induce dipoles in the next layer, and so on until several layers are built up. The second theory was propounded in two papers; one by Brunauer, Emmett and Teller <sup>3</sup> in 1938, the other by Brunauer, Deming, Deming and Teller <sup>4</sup> in 1940. It is based on the assumption that the same forces that produce condensation are also chiefly responsible for the binding energy of multimolecular adsorption. For want of a better name this theory will be referred to in this book as the theory of multimolecular adsorption. Even though the potential theory, the capillary condensation theory and the polarization theory also deal with multimolecular adsorption, each of these theories is known by its own name, so that no confusion will be created by calling the fourth theory the theory of multimolecular adsorption.

According to both the polarization theory and the multimolecular adsorption theory the forces involved in adsorption are short range forces. While the potential theory (in its older multimolecular version) assumed that the forces of adsorption reach far out from the surface, the theories discussed in the present chapter assume that only the first adsorbed layer is attracted strongly by the surface. The second layer is adsorbed essentially not by the surface, but by the first adsorbed layer, and the adsorption thus propagates from layer

<sup>1</sup> J. H. de Boer and C. Zwikker, *Z. phys. Chem.*, **B3**, 407 (1929).

<sup>2</sup> R. S. Bradley, *J. Chem. Soc.*, 1936, 1467.

<sup>3</sup> S. Brunauer, P. H. Emmett and E. Teller, *J. Am. Chem. Soc.*, **60**, 309 (1938).

<sup>4</sup> S. Brunauer, L. S. Deming, W. E. Deming and E. Teller, *J. Am. Chem. Soc.*, **62**, 1723 (1940).

to layer. The two theories differ from each other with respect to the type of forces that are assumed to produce the adsorption. According to the polarization theory adsorption is due to induced dipoles, according to the multimolecular adsorption theory it is due to the totality of forces usually designated as van der Waals forces, among which the most important are the dispersion forces of London.<sup>5</sup> These forces are discussed in detail in Chapter VII.

### THE POLARIZATION THEORY

Below the critical temperature the adsorption isotherms of gases on most adsorbents consist of two regions: at low pressures the isotherms are concave, at high pressure convex toward the pressure axis. (Examples of these so-called S-shaped isotherms were shown in Fig. 5.) The higher pressure convex region has been attributed by many investigators to capillary condensation, but nobody has so far derived an isotherm equation on the basis of the capillary condensation theory that describes an S-shaped curve. The polarization theory was the first to give a quantitative account of the S-shaped isotherm.

According to de Boer and Zwikker<sup>1</sup> the induced dipole in the  $i$ -th layer polarizes the  $(i + 1)$ st layer, giving rise to induced dipole moments and binding energies that decrease exponentially with the number of layers. Let  $\mu_i$  be the dipole moment of an adsorbed molecule in the  $i$ -th layer. The value of  $\mu_i$  for all layers, except the first and the last, satisfies the equation

$$(1) \quad \mu_i = k(\mu_{i-1} + \mu_{i+1})$$

where  $k$  is a constant. Let us assume that

$$(2) \quad \mu_i = c_1 C^i$$

where  $c_1$  and  $C$  are constants. Substituting into equation (1) we obtain

$$(3) \quad c_1 C^i = k c_1 (C^{i-1} + C^{i+1})$$

If we divide both sides by  $c_1 C^{i-1}$  we obtain a quadratic equation in  $C$ , the solution of which is

$$(4) \quad C = 1 \frac{-\sqrt{1-4k^2}}{2k}$$

Thus equation (2) is a solution of (1), with the value of  $C$  given by (4). The induced dipole moment according to equation (2) decreases

<sup>5</sup> F. London, *Z. phys. Chem.*, B11, 222 (1931).

exponentially with the number of layers. The measure of this decrease is  $C$  since

$$(5) \quad C = \mu_i / \mu_{i-1}$$

The binding energy is proportional to the square of the dipole moment, consequently

$$(6) \quad \varphi_i = c_2 C^{2i}$$

where  $\varphi_i$  is the binding energy of the  $i$ -th layer, and  $c_2$  is a constant. The equilibrium pressure of the  $n$ -th layer (the top layer),  $p_n$ , according to Boltzmann's law varies exponentially with the binding energy of that layer. If the only binding energy is that due to polarization, the pressure is given by

$$(7) \quad p_n = c_3 e^{-\varphi_n/RT}$$

where  $c_3$  is a constant. It follows therefore that

$$(8) \quad \ln \frac{p_n}{c_3} = - \frac{c_2}{RT} C^{2n}$$

This is identical with the equation of de Boer and Zwicker

$$(9) \quad \ln \frac{p_n}{K_3 p_0} = K_2 K_1^n$$

if  $c_3$  is replaced by  $K_3 p_0$ ,  $-c_2/RT$  by  $K_2$ , and  $C^2$  by  $K_1$ . To get the customary form of isotherm equation one can substitute  $n = v/v_m$ , where  $v$  is the volume of gas adsorbed at the pressure  $p_n$ , and  $v_m$  is the volume of gas adsorbed in a complete unimolecular layer.

If  $n$  (or  $v$ ) is plotted against  $p_n$  according to equation (9), one obtains an S-shaped isotherm. This is illustrated in Fig. 64, representing the adsorption of argon on partly hydrated zinc oxide, obtained by Hüttig and Juza.<sup>6</sup> The abscissa is  $p/p_0$ , the ordinate is the number of moles of argon adsorbed per mole of adsorbent. The curve was calculated by de Boer and Zwicker; the circles give the experimental points. The value of the constant  $K_3$  was found by trial and error to be 1.1045. Obviously, the dotted portion of the isotherm representing the region where  $p_n > p_0$  is virtual, since adsorption can not be measured beyond  $p_0$ .

de Boer and Zwicker found empirically that the value of  $K_3$  is often close to unity. Bradley,<sup>2</sup> using a somewhat different derivation and neglecting certain terms, arrived at an equation similar to (9),

<sup>6</sup> G. F. Hüttig and R. Juza, *Z. anorg. und allgem. Chem.*, 177, 313 (1928).



with  $K_3 = 1$ . Starting with this two-constant equation and taking logarithms one obtains

$$(10) \quad \log \log \frac{p}{p_0} = \log \frac{K_2}{2.303} + \frac{v}{v_m} \log K_1$$

According to equation (10) a plot of  $\log \log (p/p_0)$  against  $v$  should give a straight line. This is illustrated in Fig. 65, showing the adsorption of argon on dehydrated copper sulfate and aluminum sulfate, obtained by Bradley. The experimental results were first plotted according to

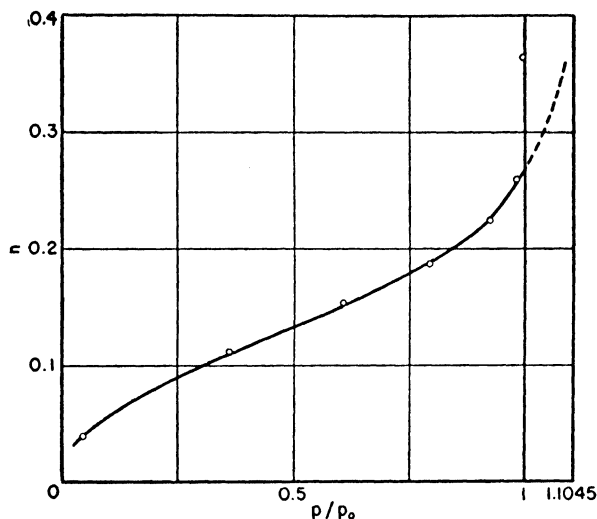


FIG. 64.—Adsorption isotherm of argon on zinc oxide at 86.7° K. calculated according to the polarization theory.

equation (10) and, as Fig. 65(a) shows, fairly good straight lines were obtained. The constants were then evaluated from the straight line plots and the isotherms were calculated. In Fig. 65(b) the curves represent the calculated isotherms, the circles the experimental points.

We have seen in Chapters IV and V that the correctness of a theory is by no means proven if its isotherm equation fits satisfactorily certain experimental data. In spite of the good agreement between equations (9) and (10) and the experimental data, shown in Figs. 64 and 65, it is not difficult to prove that the polarization theory can not account for the multimolecular adsorption of argon. The reason is that the polarization of the second layer of adsorbed gas by the first

layer is already much too small to constitute the major portion of the binding energy between the two adsorbed layers.

In order to get the value of  $C$ , the ratio of the strengths of the induced dipole moments in two consecutive layers, one must know the extent of the surface of the adsorbent. We have seen that  $C = K_1^{1/2}$ , and the slope of the straight line according to equation (10) is  $(\log K_1)/v_m$ . Bradley<sup>2</sup> measured the sizes of the adsorbent particles microscopically, calculated the surface, and obtained a value for  $v_m$  by assuming that the packing of the argon molecules on the surface was the same as in the liquid state. Knowing  $v_m$  he was able to calculate  $K_1$  and  $C$ .

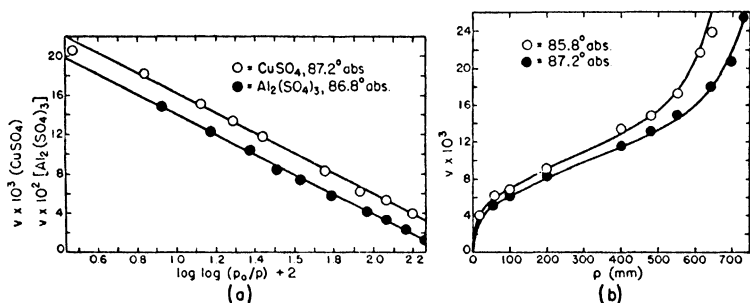


Fig. 65.—Adsorption isotherms of argon on copper sulfate and aluminum sulfate plotted according to the polarization theory.

The value of  $C$  thus obtained was 0.99 for the adsorption of argon on aluminum sulfate, and almost as large for copper sulfate. Such large values of  $C$  would of course lead to thick films of 100 or more adsorbed layers. Bradley believed that even at half the saturation pressure more than 30 layers of argon were adsorbed on either adsorbent. He found further that no thick film formation occurs on potassium chloride. He attributed this to the small polarizing power of the alkali metals and to the approximate equality of the ionic radii of potassium and chlorine.

Emmett and Brunauer<sup>7</sup> pointed out that the estimate of surface made by Bradley on the basis of microscopic examination must have been erroneous, since such examination reveals only the external surface of the particles. There was good reason to suspect that the crystals of copper sulfate and aluminum sulfate, obtained by dehydration of the hydrates, are highly porous with large internal surfaces. They estimated that the surface value obtained by Bradley was too

<sup>7</sup> P. H. Emmett and S. Brunauer, *J. Am. Chem. Soc.*, **59**, 1553 (1937).

small by a factor of 20. This was confirmed by Brunauer and Emmett<sup>8</sup> when they determined the adsorption isotherms of argon on copper sulfate pentahydrate, on anhydrous copper sulfate and on potassium chloride. These isotherms are shown in Fig. 66. It should be noted in the first place that potassium chloride gives an S-shaped isotherm, just like copper sulfate, indicating multimolecular adsorption.

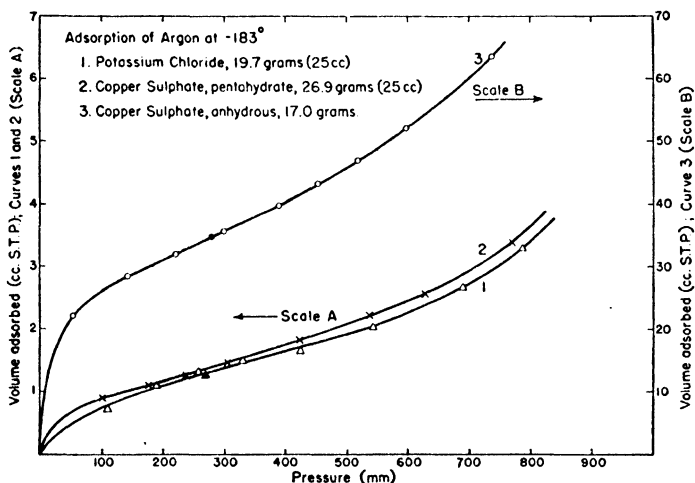


FIG. 66.—Adsorption isotherms of argon on some ionic adsorbents.

In the second place, when copper sulfate is dehydrated the specific adsorptive capacity increases 39 fold. (Calculated on the basis of a mole of copper sulfate the increase is 25 fold.) It seems therefore that the dehydrated copper sulfate of Bradley was highly porous, with an internal surface about 20 times as large as the microscopically determined geometric surface. Bradley observed no thick film formation on potassium chloride, because his experimental method was not sensitive enough to detect a few adsorbed argon layers when the adsorbent had no internal surface and the total surface was merely the small external surface.

Although it is clear that Bradley's surface estimate was erroneous, and that he therefore obtained wrong values for the constants  $K_1$  and  $C$ , this in itself is no refutation of the polarization theory. It means merely that at saturation the number of adsorbed layers was not 100

<sup>8</sup> S. Brunauer and P. H. Emmett, *J. Am. Chem. Soc.*, 59, 2682 (1937).

or more but about 4 or 5. The next question is whether the polarization theory can account for the building up of as many as 4 or 5 adsorbed layers. It will be shown now that even a second adsorbed layer can not build up by the propagation of induced dipoles.

The estimating of  $C$  can be carried out in the following manner.<sup>3</sup> The field of a dipole  $\mu_1$  at a distance  $r$  is proportional to  $\mu_1/r^3$ , and the dipole  $\mu_2$  induced in a molecule of polarizability  $\alpha$  at that distance is proportional to  $\mu_1\alpha/r^3$ . The ratio  $\mu_2/\mu_1$ , i.e., the constant  $C$ , is therefore proportional to the dimensionless number  $\alpha/r^3$ , and the ratio of the binding energies in two successive layers, i.e., the constant  $K_1$ , is proportional to  $\alpha^2/r^6$ .

The polarizability of a gas molecule  $\alpha$  is given by the equation

$$(11) \quad 2\pi\alpha = (n - 1)V_g/N$$

where  $n$  is the index of refraction extrapolated to infinite wave length,  $V_g$  is the molar volume of the gas, and  $N$  is Avogadro's number.

First it may be assumed that the separation of the argon atoms in the adsorbed state is about the same as in the solid state. For a face centered cubic lattice, such as that of solid argon, the distance  $r$  between the nearest neighbors is given by the equation

$$(12) \quad r^3 = \sqrt{2}V_s/N$$

where  $V_s$  is the molar volume of the solid. From (11) and (12) it follows that

$$(13) \quad \frac{\alpha}{r^3} = \frac{n - 1}{2^{3/2}\pi} \frac{V_g}{V_s}$$

For argon gas at 0° C. and 760 mm. pressure,  $n - 1 = 278 \times 10^{-6}$ , and by using the density of solid argon at 40° K. one obtains

$$(14) \quad \alpha/r^3 = 0.029$$

If one assumes that the separation of argon atoms in the adsorbed state is the same as in the liquid state,  $\alpha/r^3$  becomes even smaller.

The ratio of induced dipole moments in two successive layers is given by

$$(15) \quad \mu_i/\mu_{i-1} = C = d.\alpha/r^3$$

where  $d$  is a constant dependent upon the geometrical structure of the adsorbed layers and the relative orientation of the dipoles. If the adsorbed argon atoms build up in a close packing of spheres, and the dipoles in one layer are all oriented in the same direction and perpen-

dicular to the surface, then the value calculated for  $d$  is  $-0.35$ . The minus sign signifies that the dipoles in successive layers point alternately toward the surface and away from the surface. From (14) and (15) we obtain  $C = -0.01$ , as contrasted to Bradley's value of  $0.99$ . Since  $K_1 = C^2$ , its value is about  $1 \times 10^{-4}$ . Hence the binding energy that can be attributed to polarization is negligibly small even in the second layer.

If in the calculation we assume a type of orientation of the dipoles different from that given above, the value of  $d$  will be different. Nevertheless, it seems certain that for gases for which  $\alpha/r^3$  is as small as it is for argon the portion of the binding energy due to polarization forces operating between the adsorbed layers must be very small. For molecules of larger polarizability the case will be more favorable.

TABLE XIII  
ADSORPTION OF WATER BY COPPER OXIDE AT 25° C.

$p_0 = 23.83$  mm.  
 $\log (p_0/p) = 4.898 \times 0.8902^a + 0.0762$

$p$ mm. of Hg	$a_{\text{obs}}$ mg. per g.	$a_{\text{calc}}$ mg. per g.
0.25	9	8.1
2.6	14	14.7
5.1	19	18.2
10.1	25	24.2
12.9	27	27.7
17.0	36	35.5
18.7	45	44.3
19.7	56	56.7

de Boer<sup>9</sup> chose iodine for his experiments because of its large polarizability. However, even here  $\alpha/r^3$  is only  $0.1$ , and so it is unlikely that the energy of polarization constitutes an appreciable portion of the binding energy of the second layer.

If the adsorbed gas consists of molecules with large permanent dipoles, it is possible that many layers can build up by the mechanism of de Boer and Zwikker. For this case Bradley<sup>10</sup> derived the three-constant equation

$$(16) \quad \log (p_0/p) = K_1 K_2^a + K_3$$

where  $a$  is the weight of the adsorbed gas. Table XIII shows Bradley's calculations, based on the experimental data of Bray and Draper,<sup>11</sup>

<sup>9</sup> J. H. de Boer, *Z. phys. Chem.*, **B13**, 134 (1931); **B14**, 149 (1931); **B17**, 161 (1932).

<sup>10</sup> R. S. Bradley, *J. Chem. Soc.*, 1936, 1799.

<sup>11</sup> W. C. Bray and H. D. Draper, *Proc. Nat. Acad. Sci.*, **12**, 297 (1926).

for the adsorption of water on copper oxide. Although the agreement is quite satisfactory, it can not be considered a sufficient proof of the validity of the polarization theory for the adsorption of molecules with large permanent dipoles. Judgment must be reserved until the theory is more thoroughly tested. It should be remembered that the agreement of equations (9) and (10) with the experimental data was also quite good, and yet in view of the considerations advanced above these equations must be regarded at present as merely empirical relationships.<sup>12</sup>

Palmer and Clark<sup>13</sup> investigated the adsorption of various organic vapors on vitreous silica powder, and noted that if the logarithm of the Polanyi potential is plotted against the amount adsorbed, in many cases very good straight lines were obtained. The Polanyi potential is given by

$$(17) \quad \epsilon = RT \ln (p_0/p)$$

consequently a straight line plot of  $\log \epsilon$  against  $v$  is formally identical with equation (10). Acetonitrile, methyl acetate, chloroform, acetone and benzene gave good straight lines, methyl and ethyl alcohol gave curved lines. Particularly striking were the results for acetone and benzene obtained by Palmer<sup>14</sup> and shown in Fig. 67. The plot of  $\log \log (p_0/p)$  against  $v$  is linear from 5% to 95% of the saturation pressure. Interestingly, the deviation from the straight line close to saturation is not in the direction of increased adsorption—such an effect could be explained by capillary condensation—but in the direction of decreased adsorption. Palmer explained the decrease by assuming that some of the particles of the adsorbent have sharp acute angles and that the adsorbed film surrounding them has a strong curvature. This gives rise to a Kelvin effect which is just the opposite of capillary condensation. The smaller the radius of curvature of the particle, the greater is the *increase* in the vapor pressure of the adsorbate, resulting in a smaller adsorption than expected. Although this explanation is reasonable, it should be remembered that we do not know what gives rise to the linearity of the curves of Fig. 67. It becomes therefore a matter of speculation what causes the deviation from linearity.

<sup>12</sup> The straight line relationship between  $\log \log (p_0/p)$  and the amount adsorbed was first discovered empirically by S. Lenher and I. R. McHaffie (*J. Phys. Chem.*, **31**, 719, 1927).

<sup>13</sup> W. G. Palmer and R. E. D. Clark, *Proc. Roy. Soc.*, **A149**, 360 (1935).

<sup>14</sup> W. G. Palmer, *Proc. Roy. Soc.*, **A160**, 254 (1937).

Concluding, we may repeat that various investigators have found that plots of  $\log \log (p_0/p)$  against the amount adsorbed give good straight lines for some of their adsorption data. In other cases the three constant-equations (9) and (16) proved to be useful. Although

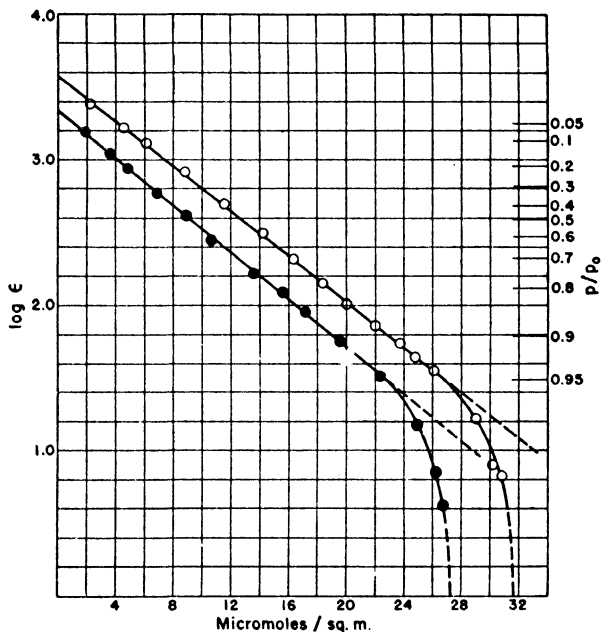


FIG. 67.—Adsorption isotherms of acetone and benzene on vitreous silica plotted according to Palmer's equation.

these equations found interpretation on the basis of the polarization theory, in view of the difficulties discussed in this section it is best to regard them at present only as useful empirical relationships.

### THE MULTIMOLECULAR ADSORPTION THEORY

In Chapter II we discussed the five isotherm types that can be found in the literature of van der Waals adsorption and illustrated them with the examples shown in Figs. 3–8. In Fig. 68 these isotherm types are shown together. They are imaginary, not real isotherms. Type I is the Langmuir adsorption isotherm, Type II is the S-shaped or sigmoid isotherm; no names have been attached to the other three types. Types II and III are closely related to Types IV and V, but

the two former indicate adsorption that increases indefinitely as the vapor pressure  $p_0$  is approached, whereas the two latter suggest that the maximum adsorption is attained, or almost attained, at some pressure lower than the vapor pressure of the gas.

The Type I isotherm represents unimolecular adsorption. The most successful interpretation of isotherms of this type has been given by Langmuir (Chapter IV). The Type II isotherm has been generally

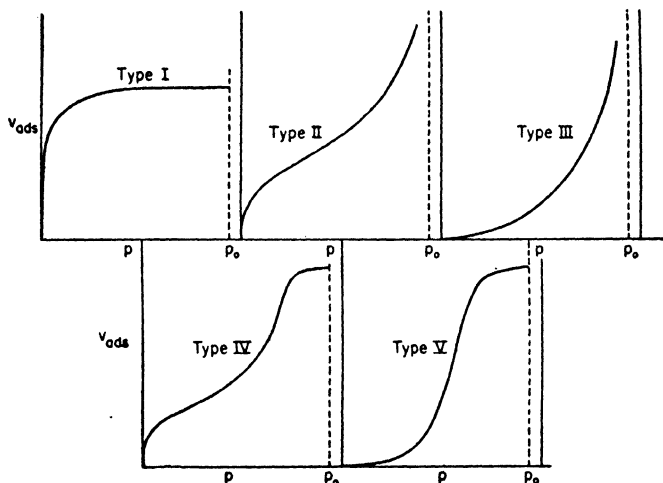


FIG. 68.—The five isotherm types in physical adsorption.

attributed to multimolecular adsorption. The potential theory and the capillary condensation theory both deal with multimolecular adsorption, but neither accounts for the shape of the isotherm. Only the polarization theory gives an analytical expression that describes the shape of the Type II isotherm, but the fundamental assumption on which the theory has been built is untenable. Furthermore, although the five isotherm types represent closely related phenomena, no one has attempted to derive an equation that would include even any two of them as special cases. The multimolecular adsorption theory is the first attempt to give a unified theory of physical adsorption. Its most general equation <sup>4</sup> includes all five isotherm types as special cases and describes the shape of each isotherm type through the entire range of adsorption, from zero pressure to saturation pressure. This includes the region of unimolecular adsorption, multimolecular



adsorption and capillary condensation, in contrast to the separate treatments accorded to these three regions by the previously discussed theories.

### A. Adsorption Without Capillary Condensation

The fundamental assumption of the theory of multimolecular adsorption is that the same forces that are active in condensation are also producing the phenomenon of van der Waals adsorption. On this assumption one can derive an isotherm equation by a method that is a generalization of Langmuir's treatment of unimolecular adsorption.

Let  $s_0, s_1, s_2 \dots s_i, \dots$  represent the surface area that is covered by 0, 1, 2,  $\dots i, \dots$  layers of adsorbed molecules. Since at equilibrium  $s_0$  must remain constant, the rate of condensation on the bare surface must be equal to the rate of evaporation from the first layer, or

$$(18) \quad a_1 p s_0 = b_1 s_1 e^{-E_1/RT}$$

where  $p$  is the pressure,  $E_1$  is the heat of adsorption in the first layer, and  $a_1$  and  $b_1$  are constants. This is essentially Langmuir's equation for unimolecular adsorption. As we have seen in Chapter IV it involves the assumption that  $a_1, b_1$  and  $E_1$  are independent of the number of adsorbed molecules already present in the first layer.

At equilibrium  $s_1$  also must remain constant. From the principle of microscopic reversibility it follows therefore that

$$(19) \quad a_2 p s_1 = b_2 s_2 e^{-E_2/RT}$$

or the rate of condensation on top of the first layer is equal to the rate of evaporation from the second layer. In equation (19)  $E_2$  is the heat of adsorption in the second layer, and  $a_2$  and  $b_2$  are constants. Extending the same argument to  $s_2, s_3$ , etc., we obtain <sup>15</sup>

$$(20) \quad \begin{array}{rcl} a_3 p s_2 & = & b_3 s_3 e^{-E_3/RT} \\ & \cdot & \cdot \\ & \cdot & \cdot \\ & \cdot & \cdot \\ a_i p s_{i-1} & = & b_i s_i e^{-E_i/RT} \end{array}$$

<sup>15</sup> E. C. C. Baly (*Proc. Roy. Soc., A160*, 465, 1937) also started out to develop a multilayer adsorption theory by generalizing Langmuir's treatment of unimolecular adsorption. However, since he did not make the simplifying assumptions embodied in equations (24) and (25), he was unable to perform the summation indicated in equation (23), and had to proceed empirically. Thus the similarity between Baly's treatment and the treatment discussed above ceases beyond the first step.

The total surface of the adsorbent is given by

$$(21) \quad A = \sum_{i=0}^{\infty} s_i$$

and the total volume adsorbed is

$$(22) \quad v = v_0 \sum_{i=0}^{\infty} i s_i$$

where  $v_0$  is the volume adsorbed on one square centimeter of the adsorbent surface when it is covered with a complete unimolecular layer. It follows that

$$(23) \quad \frac{v}{Av_0} = \frac{v}{v_m} = \frac{\sum_{i=0}^{\infty} i s_i}{\sum_{i=0}^{\infty} s_i}$$

where  $v_m$  is the volume of gas adsorbed when the entire adsorbent surface is covered with a complete unimolecular layer.

The summation indicated in equation (23) can be carried out, if we make the simplifying assumptions that

$$(24) \quad E_2 = E_3 = \dots E_i = E_L$$

where  $E_L$  is the heat of liquefaction, and

$$(25) \quad \frac{b_2}{a_2} = \frac{b_3}{a_3} = \dots \frac{b_i}{a_i} = g$$

where  $g$  is an appropriate constant. This is equivalent to assuming that the evaporation-condensation properties of the molecules in the second and higher adsorbed layers are the same as those of the liquid state. This assumption seems reasonable, since the adsorbate molecules in the first layer are in contact with the adsorbent, but in the second layer they are in contact with other adsorbate molecules only. Since the van der Waals forces have a very short range of action, the effect of the adsorbent is probably quite small already in the second layer. It is probable therefore that the structure of the second layer is quite similar to that of the liquid.

We can express now  $s_1, s_2, s_3, \dots s_i \dots$  in terms of  $s_0$ .

$$(26) \quad s_1 = y s_0, \quad \text{where} \quad y = (a_1/b_1) p e^{E_1/RT}$$

$$(27) \quad s_2 = x s_1, \quad \text{where} \quad x = (p/g) e^{E_L/RT}$$

$$(28) \quad s_3 = x s_2 = x^2 s_1$$

$$(29) \quad s_i = x s_{i-1} = x^{i-1} s_1 = y x^{i-1} s_0 = c x^i s_0,$$

where

$$(30) \quad c = y/x = (a_1 g/b_1) e^{(E_1 - E_L)/RT}$$

Substituting into equation (23) we obtain

$$(31) \quad \frac{v}{v_m} = \frac{cs_0 \sum_{i=1}^{\infty} ix^i}{s_0 \{1 + c \sum_{i=1}^{\infty} x^i\}}$$

The summation represented in the denominator is merely the sum of an infinite geometric progression

$$(32) \quad \sum_{i=1}^{\infty} x^i = \frac{x}{1-x}$$

About the summation in the numerator we may note that

$$(33) \quad \sum_{i=1}^{\infty} ix^i = x \frac{d}{dx} \sum_{i=1}^{\infty} x^i = \frac{x}{(1-x)^2}$$

Substituting (32) and (33) into (31), we obtain

$$(34) \quad \frac{v}{v_m} = \frac{cx}{(1-x)(1-x+cx)}$$

If the adsorption takes place on a free surface, then at  $p_0$ , the saturation pressure of the gas, an infinite number of layers can build up on the adsorbent. To make  $v = \infty$  when  $p = p_0$ ,  $x$  must be equal to unity in equation (34). From (27) it follows that

$$(35) \quad (p_0/g)e^{EL/RT} = 1$$

and

$$(36) \quad x = p/p_0$$

Substituting into equation (34) we obtain the isotherm equation

$$(37) \quad v = \frac{v_m c p}{(p_0 - p) \{1 + (c - 1)(p/p_0)\}}$$

For the purpose of testing equation (37) can be put in the form

$$(38) \quad \frac{p}{v(p_0 - p)} = \frac{1}{v_m c} + \frac{c - 1}{v_m c} \frac{p}{p_0}$$

Equation (38) is the isotherm equation of the multimolecular adsorption theory for adsorption taking place on a free surface. It is a linear equation, i.e., the plot of the function  $p/v(p_0 - p)$  against  $p/p_0$  gives a straight line, if the theory is obeyed. The intercept of the straight line is  $1/v_m c$ , the slope is  $(c - 1)/v_m c$ . Thus one can obtain the two constants  $v_m$  and  $c$  from the experimental data.

It may be worth reemphasizing that the correctness of the theory is not proven if a plot of the data according to equation (38) gives a straight line. It is also necessary that the evaluated constants should have reasonable values. The surface constant  $v_m$  can be determined experimentally, as discussed in Chapter IX. The constant  $c$  is given by equations (30) and (25)

$$(39) \quad c = \frac{a_1 b_2}{b_1 a_2} e^{(E_1 - E_L)/RT}$$

From the nature of the constants  $a_1$ ,  $b_1$ ,  $a_2$  and  $b_2$  it follows that  $a_1 b_2 / b_1 a_2$  will not differ much from unity. We may write therefore as an approximation that

$$(40) \quad c = e^{(E_1 - E_L)/RT}$$

Thus from the constant  $c$  one can obtain  $E_1$ , the average heat of adsorption in the first layer. This is a quantity that can be independently determined by direct and indirect methods, as we have seen in Chapter II.

If the adsorption does not take place on a free surface but in a limited space, then at saturation not an infinite but only a finite number of layers can build up on the surface of the adsorbent. Let us imagine, for example, that the adsorption occurs in a capillary consisting of two plane parallel walls. If the maximum number of layers that can be adsorbed on each wall of the capillary is  $n$ , then the summation of the two series in equation (31) is to be carried to  $n$  terms only, and not to infinity. One obtains in place of equation (38)

$$(41) \quad v = \frac{v_m c x}{1 - x} \frac{1 - (n + 1)x^n + nx^{n+1}}{1 + (c - 1)x - cx^{n+1}}$$

where  $x = p/p_0$ , as before, and  $v_m$  and  $c$  also have the same meanings as before. It is not impossible that other factors than capillaries can limit the maximum number of layers that can be adsorbed. In such event equation (41) may still remain valid.

Equation (41) has two important limiting cases. If  $n = 1$ , it reduces to the equation

$$(42) \quad v = \frac{v_m \frac{c}{p_0} p}{1 + \frac{c}{p_0} p}$$

A comparison with equation (21) of Chapter IV reveals that this is Langmuir's equation with the constant  $b$  having the value  $c/p_0$ .

The other limit is when  $n = \infty$ , i.e., when the adsorption takes place on a free surface. In this case equation (41) reduces to (38). It should also be noted that when  $x$  is small and  $n$  is at least as large as 4 or 5, equation (38) becomes a very good approximation to (41). To use equation (41) one should therefore plot the experimental data in the low pressure region according to the linear equation (38), evaluate  $v_m$  and  $c$  from the slope and intercept of the straight line, then using these values in equation (41) solve for the best average value of  $n$ . The application of equations (38), (41) and (42) is discussed in the next section.

Since in the derivation of equation (41) the forces of capillary condensation were neglected, the equation can be regarded only as a more or less rough approximation in the higher pressure region. The equation that considers capillary condensation will be derived later. Equation (41) includes as special cases the isotherm types designated as I, II and III in Fig. 68. If  $n = 1$ , it reduces to (42), and we obtain a Type I isotherm. If  $n > 1$ , we obtain either Type II or Type III isotherms, depending on the value of the constant  $c$ . If the attractive forces between adsorbent and adsorbed gas are greater than the attractive forces between the molecules of the adsorbate in the liquid state, i.e., if  $E_1 > E_L$  in equation (40), we obtain S-shaped Type II isotherms. If on the other hand the forces between adsorbent and adsorbate are small, i.e., if  $E_1 < E_L$ , we obtain Type III isotherms.

The formation of multimolecular layers on an adsorbent below the saturation pressure is analogous in many respects to the formation of multimolecular clusters in a non-ideal gas. There is, however, an important difference. In the gas the number of multimolecular clusters is negligible compared to the number of single molecules (except in the vicinity of the critical point), whereas on a surface multimolecular layers form far below the saturation pressure. This difference can be explained on the basis of surface tension considerations. In the gas the large free surface energy of small clusters makes their formation improbable. In adsorption, however, the "liquid" surface is practically complete after the first layer has been adsorbed, so that during the formation of successive layers hardly any surface tension has to be overcome.

## B. Applications

### 1. Type II Isotherms

Two applications of the straight line equation (38) are shown in Figs. 69 and 70. Figure 69 represents the adsorption of nitrogen at

90.1° K. on a variety of adsorbents <sup>7,8</sup> and Fig. 70 the adsorption of different gases on silica gel.<sup>8</sup> The curves are typical S-shaped isotherms. Those obtained for silica gel were given in Fig. 5. Between relative pressures of 0.05 and 0.35 the plots give very good straight lines.

The values of the constants  $v_m$  and  $E_1 - E_L$ , obtained from the slopes and intercepts of Fig. 69, are given in Table XIV. The table

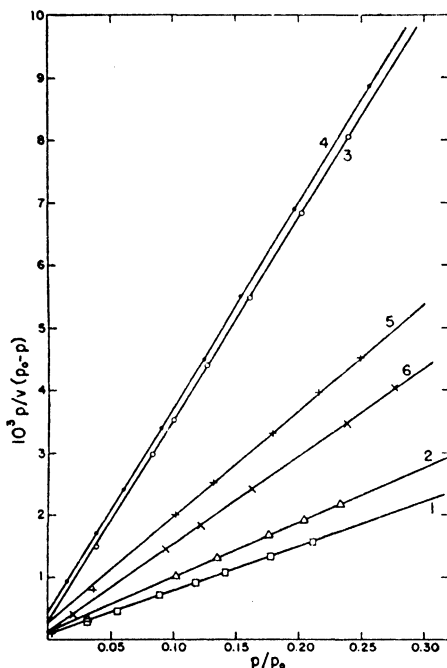


FIG. 69.—Adsorption isotherms of nitrogen on six different adsorbents at 90.1° K. plotted according to the straight line equation (38) of the theory of multimolecular adsorption.

gives also the constants for six other isotherms not shown in Fig. 69. A comparison of columns 3 and 4 shows that the agreement between the experimental and theoretical  $v_m$  values is very satisfactory for all twelve isotherms. (The experimental determination of  $v_m$  is discussed in Chapter IX.) The two seldom differ from each other by as much as 10%. The heat of adsorption in the first layer,  $E_1$ , can be obtained from the last column. Since  $E_L$  is 1330 calories for nitrogen,  $E_1$  is

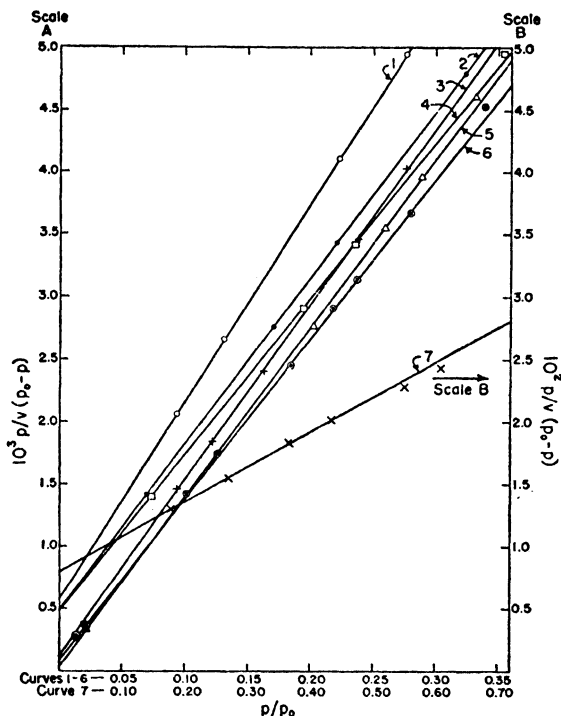


Fig. 70.—Adsorption isotherms of six different gases on silica gel plotted according to the straight line equation of the theory of multimolecular adsorptions.

TABLE XIV

VALUES OF CONSTANTS FOR THE ADSORPTION OF NITROGEN AT 90.1° K.

Substance	Curve in Fig. 69	$\tau_m$ (theoretical) cc. per g.	$\tau_m$ (experimental) cc. per g.	$E_1 - E_L$ cal. per mole
Unpromoted Fe catalyst 973I	1	0.13	0.12	794
Unpromoted Fe catalyst 973II		0.29	0.27	774
Fe-Al <sub>2</sub> O <sub>3</sub> catalyst 954		2.86	2.78	894
Fe-Al <sub>2</sub> O <sub>3</sub> catalyst 424	2	2.23	2.09	774
Fe-Al <sub>2</sub> O <sub>3</sub> -K <sub>2</sub> O catalyst 931		0.81	0.76	911
Fe-Al <sub>2</sub> O <sub>3</sub> -K <sub>2</sub> O catalyst 958	3	0.56	0.55	854
Fe-K <sub>2</sub> O catalyst 930		0.14	0.12	772
Fused Cu catalyst	4	0.05	0.05	776
Commercial Cu catalyst		0.09	0.10	834
Cr <sub>2</sub> O <sub>3</sub> gel	5	53.3	50.5	738
Cr <sub>2</sub> O <sub>3</sub> glowed		6.09	6.14	835
Silica gel		116.2	127.0	794

about 2200 calories. This value is of the right order of magnitude for the heat of the physical adsorption of nitrogen. We may thus conclude that the constants obtained from the straight line plots are reasonable and give considerable support to the theory.

It is interesting to note from the last column of Table XIV that the value of  $E_1 - E_L$  changes very little from adsorbent to adsorbent. It is  $840 \pm 70$  calories for the 12 adsorbents of the table. At first this result seems rather surprising. However, it is clear from Figs. 69 and 70 that for  $p/p_0$  values smaller than 0.05 the experimental points do not fall on the straight line, indicating that equation (38) breaks down for adsorption on the most active part of the surface. As we have seen in Chapter IV the reason for this is that the Langmuir

TABLE XV  
VALUES OF CONSTANTS FOR THE ADSORPTION OF GASES ON SILICA GEL

Gas	Temp. ° C.	Curve in Fig. 70	$V_m$ , calc. cc. S.T.P./g.	$V_m$ , exp. cc. S.T.P./g.	Surface, calc. sq. m./g.	$E_1 - E_L$ cal./mole
N <sub>2</sub>	-195.8	6	127.9	135.3	560	719
N <sub>2</sub>	-183	3	116.2	127.0	534	794
A	-183	2	119.3	122.0	464	594
O <sub>2</sub>	-183	4	125.1	132.0	477	586
CO	-183	5	121.2	132.0	550	973
CO <sub>2</sub>	- 78	1	99.0	102.3	455	1335
C <sub>4</sub> H <sub>10</sub>	0	7	58.2	28.1*	387	930

\* The reason for the very low experimental butane value is discussed in Chapter IX.

equation is valid only if the heat of adsorption is at least approximately uniform over the surface, or part of the surface. The value of  $E_1$ , as obtained from the linear plot of the multimolecular adsorption theory, must be regarded therefore as the average heat of adsorption on the *less active* part of the adsorbing surface.<sup>16</sup>

Table XV gives the constants calculated from the straight lines of Fig. 70, representing the adsorption of six different gases on silica gel. From the calculated constants  $v_m$  we can obtain the absolute

<sup>16</sup> W. D. Harkins and G. E. Boyd (*J. Am. Chem. Soc.*, 64, 1195, 1942) determined experimentally the heat of emersion of a crystalline powder out of a liquid. They compared this energy quantity with  $E_1 - E_L$  and found considerable disagreement between the two sets of values, the experimental values being always larger. However, as the investigators realized, the comparison can be made only on the basis of assumptions that oversimplify the problem. The most important reason for the disagreement is that the experimental heat of emersion is dependent on the heat of adsorption over the *entire* surface, whereas  $E_1$  is the heat of adsorption over the *less active* part of the surface.



surface of the adsorbent if we know the packing of the adsorbed molecules on the surface. If we assume that the molecules have the same packing as in the liquid state we obtain the surface area values given in column 6. The five gases, nitrogen, oxygen, argon, carbon monoxide and carbon dioxide give a surface area of 500 square meters per gram of silica gel, with a maximum deviation of about 10%. However, the surface obtained from the butane isotherm is more than 20% too low. This again illustrates the point discussed in Chapter V that the assignment of a spherical shape to elongated molecules leads to too low surface area values. Furthermore, silica gel has some fine pores into which the larger butane molecules can not penetrate. The last column gives the  $E_1 - E_L$  values for the seven isotherms, showing that different gases on the same adsorbent have different heats of adsorption.

At relative pressures greater than 0.35 to 0.50 the plot of the experimental data according to equation (38) deviates with increasing pressure more and more strongly from the straight line. The points deviate in the direction of too small adsorption at a given value of  $p/p_0$  to conform to equation (38). It becomes therefore necessary to use the three-constant equation (41). One first evaluates  $v_m$  and  $c$  by plotting the data according to (38) up to  $p/p_0 = 0.35$  and then, using these values in equation (41), one obtains by the method of trial and error the value of  $n$  that gives the best agreement with the experimental points. Figure 71 illustrates this. It represents the adsorption isotherm of nitrogen at 77.3° K. on an aluminum oxide promoted iron catalyst.<sup>7</sup> After the constants  $v_m$  and  $c$  were obtained from a straight line plot, four isotherms were calculated using the  $n$  values of 5, 6, 7 and  $\infty$ . It should be noted that up to  $p/p_0 = 0.35$  the four isotherms are identical and begin to diverge only at higher relative pressures. Up to about  $x = 0.58$  the value of  $n = 5$  gives a good fit, but at higher relative pressures higher  $n$  values give a better fit ( $n = 7$  at  $x = 0.72$ ). If one takes an average value of  $n = 6$ , the theoretical curve will be in error to the extent of + 5% at  $x = 0.58$ , and - 7% at  $x = 0.72$ . This means that the iron catalyst has pores of considerably varying diameters. On the other hand an adsorption isotherm of oxygen at 90.1° K. on the activated carbon adsorbent Darco G<sup>8</sup> could be fitted by a value of  $n = 2.2$  from  $x = 0.02$  to 0.93, and no experimental point was off the curve as much as 4%, indicating a rather uniform pore size in this adsorbent.

In some cases it was found that the deviation of the experimental points from the straight line plots at higher  $x$  values is in the opposite

direction from the one discussed above, i.e., in the direction indicating too large rather than too small adsorption. This is exemplified by Curve 7 in Fig. 70, representing the adsorption of butane on silica gel. One would expect such deviation if the heat of adsorption in the second layer were still appreciably greater than the heat of lique-

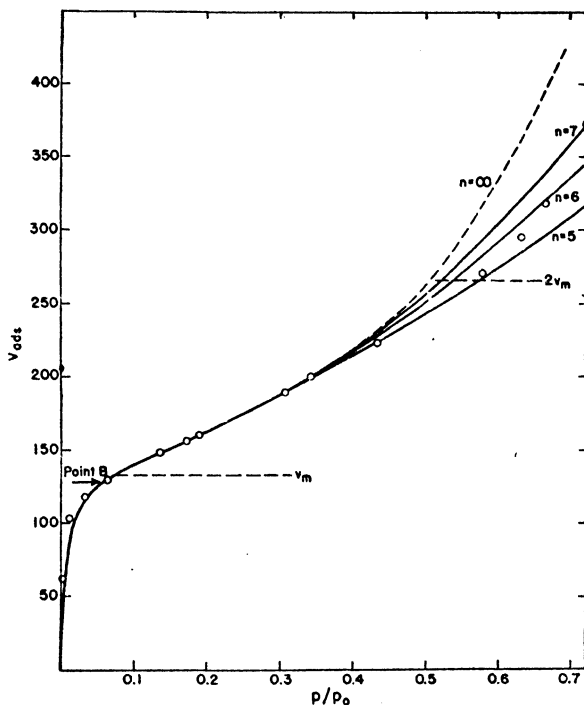


FIG. 71.—Adsorption isotherm of nitrogen on a singly promoted iron catalyst at 77.3° K. plotted according to equation (41) of the theory of multimolecular adsorption.

faction, rather than equal to it, as was assumed in the derivation of equations (38) and (41).

So far we have discussed the testing of equations (38) and (41) from two standpoints: (1) with respect to their ability to fit the experimental data, (2) as to the agreement of the constants evaluated from the curves with independently determined experimental quantities. However, no theory can be considered satisfactory unless it

accounts correctly for the temperature dependence of the adsorption isotherm.

In order to be able to calculate from one isotherm another at a different temperature, one must examine how  $c$ ,  $v_m$  and  $n$  change with temperature. The dependence of  $c$  is exponential, since it is approximately equal to  $e^{(E_1-E_L)/RT}$ ; and it can be assumed that  $E_1 - E_L$  changes only slightly with temperature. The variation of  $v_m$  is due to the thermal expansion of the adsorbed layer with increasing temperature, as we discussed in Chapters IV and V. As a first approximation we may assume that  $v_m$  changes with temperature as  $d_L^{2/3}$ , where  $d_L$  is the density of the liquefied gas. For the same reason  $n$  should vary approximately as  $d_L^{1/3}$ , which is of course a very small variation. It was found empirically that for not too great changes in temperature the variation of  $n$  is actually negligible. With these assumptions the adsorption isotherms of nitrogen and argon obtained on an aluminum oxide promoted iron catalyst at 77.3° K. were calculated from the

TABLE XVI

VALUES OF CONSTANTS FOR THE ADSORPTION OF SULFUR DIOXIDE ON SILICA GEL  
(McGavack and Patrick)

Temp. ° C.	$v_m$ cc./g.	$d_L$ g./cc.	$E_1 - E_L$ cal./mole	$E_L$ cal./mole	$E_1$ cal./mole
40	91.6	1.327	1789	4940	6730
30	96.6	1.356	1750	5190	6940
0	105.8	1.435	1705	5840	7540
-34.4	118.6	1.522	1587		
-54	129.2	1.573	1458		
-80	131.0	1.642	1364		

$n = 3.5$  for all six isotherms.

90.1° K. isotherms. Figure 72 shows the results. The agreement between the calculated curves and the experimental points<sup>7</sup> appears to be quite satisfactory.

Unfortunately, one can not always safely assume that  $v_m$  changes with temperature as  $d_L^{2/3}$ . The change in  $v_m$  may sometimes be considerably greater, and sometimes less. An example of the former is afforded by the isotherms of McGavack and Patrick<sup>17</sup> for the adsorption of sulfur dioxide by silica gel at temperatures between -80 and 40° C. (The isotherms were shown in Fig. 51.) In Table XVI, column 2, the  $v_m$  values are listed for the six isotherms. The value of  $v_m$  at -80° C. is 1.43 times as large as at 40° C., whereas it

<sup>17</sup> J. McGavack, Jr. and W. A. Patrick, *J. Am. Chem. Soc.*, **42**, 946 (1920).

should be only 1.15 times as large if  $v_m$  would vary as  $d_L^{2/3}$ . It should be also noted that in these isotherms  $E_1 - E_L$  decreases markedly with decreasing temperature.<sup>18</sup>

The experimental data of Bradley<sup>2</sup> for the adsorption of argon on anhydrous copper sulfate, shown in Fig. 65(b), as well as the data of Brunauer and Emmett<sup>8</sup> for the same system, shown in Fig. 66, can be represented satisfactorily by equation (41).  $E_1 - E_L$  was found

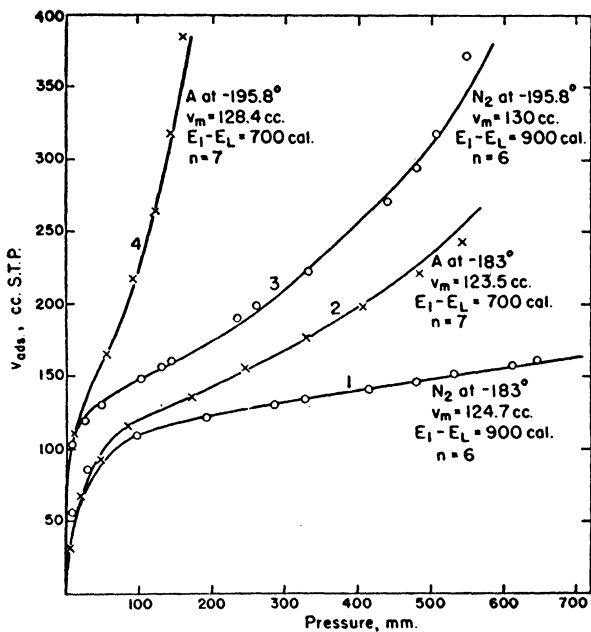


Fig. 72.—Adsorption isotherms of nitrogen and argon on iron plotted according to equation (41) of the theory of multimolecular adsorption.

to be 750 cal. for Bradley's isotherms, 780 cal. for the isotherm of Brunauer and Emmett, and  $n$  was about 5 in each case. The surfaces of the two samples were somewhat different,  $v_m$  for Bradley's isotherms was  $6.4 \times 10^{-3}$  moles of argon per mole of copper sulfate, for the isotherm of Brunauer and Emmett it was  $10.8 \times 10^{-3}$  moles per mole. Thus Bradley's microscopic measurement of the surface was in error by a factor of 18.5.

<sup>18</sup> The temperature dependence of the heat of adsorption is discussed in Chapter VIII.

## 2. Type III Isotherms

If  $c \leq 1$ , or  $E_1 \leq E_L$ , equations (38) and (41) describe Type III isotherms. Some isotherms of this type have been shown in Fig. 7, representing the adsorption of bromine on silica gel, obtained by Reyerson and Cameron.<sup>19</sup> Brunauer and Emmett<sup>7</sup> measured the adsorption of seven different gases on two samples of silica gel sent to them by Reyerson. In fitting their adsorption data with equation (41) Brunauer, Emmett and Teller<sup>8</sup> found that silica gel has rather large sized capillaries,  $n$  being about 9. Because of this large value one does not make a serious mistake if one sets  $n = \infty$ , and uses the simpler two-constant equation (38) to fit the data of Reyerson and Cameron. Another simplification suggested itself with respect to the constant  $c$ . Reyerson and Cameron calculated from the Clapeyron-Clausius equation (Chapter II, equation 8) that the differential heat of adsorption of bromine on silica gel was 7700 calories per mole. This value, however, is the heat of adsorption for the first part of the unimolecular layer covered, and so  $E_1$ , the average heat of adsorption for the entire first layer, may possibly be smaller than this. The heat of liquefaction of bromine is 7200 calories per mole, therefore Brunauer, Deming, Deming and Teller<sup>4</sup> assumed as a first approximation that  $E_1 = E_L$ , or  $c = 1$ . If this is true, it follows from equation (38) that  $v = v_m$  when  $p = 0.5 p_0$ , and thus the constant  $v_m$  can be obtained from one of the isotherms. The 79° C. isotherm gives the value  $v_m = 3.62$  millimoles of bromine per gram of silica gel, as indicated in Fig. 73. If one calculates the area covered by a bromine molecule on the surface from the density of liquid bromine, one obtains for the specific surface of silica gel the value of 470 sq. m./g. This is in excellent agreement with the value of 500 sq. m./g., obtained from the Type II isotherms of nitrogen, argon, oxygen, carbon monoxide and carbon dioxide, discussed in the previous section. The fact that different gases give different isotherm types on the same adsorbent, and yet the surface area evaluated from the Type II and Type III isotherms is the same, is one of the most striking confirmations of the theory of multimolecular adsorption.

Having obtained the constants  $c = 1$  and  $v_m = 3.62$  millimoles of bromine per gram of silica gel at 79° C., one can proceed to calculate the isotherms by equation (38). The values of  $c$  and  $v_m$  for the three other isotherms were calculated by the method described in the previous section. Figure 73 shows the results. The four curves give

<sup>19</sup> L. H. Reyerson and A. E. Cameron, *J. Phys. Chem.*, **39**, 181 (1935).

the calculated isotherms; the circles, squares and triangles the experimental points of Reyerson and Cameron. (The empty circles, etc., represent adsorption points, the full circles desorption points.) Clearly, the equation not only describes the shapes of the curves but also gives the correct temperature dependence of Type III isotherms, since  $c$  and  $v_m$  were obtained from only one isotherm.

Reyerson and Cameron have also determined the adsorption of iodine on silica gel. Their results are striking because of the very

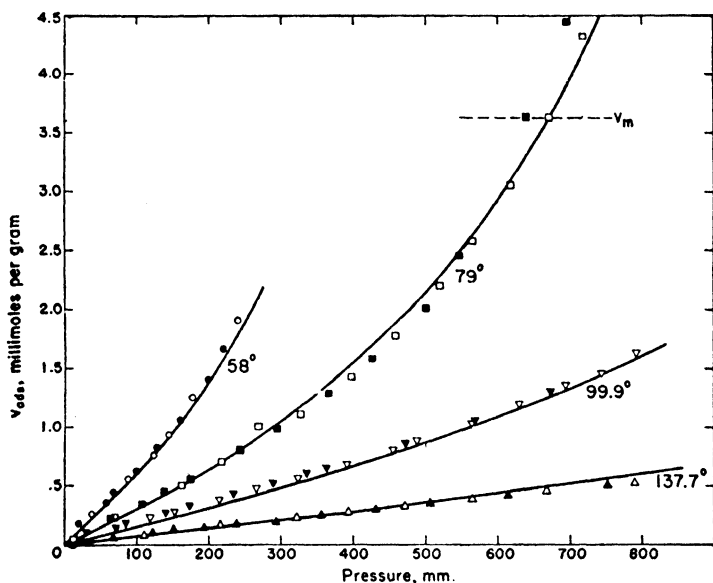


Fig. 73.—Adsorption isotherms of bromine on silica gel plotted according to equation (38) of the theory of multimolecular adsorption.

small adsorption values obtained. In fitting their data we may again assume that  $n = \infty$ , and therefore equation (38) applies. Using the surface area obtained from the bromine isotherms, and assuming that the packing of the iodine molecules on the surface is the same as in the liquid state, we calculate that  $v_m = 2.93$  millimoles of iodine per gram of silica gel. We have seen that for bromine at  $p = 0.5 p_0$  the amount adsorbed was just sufficient to cover the surface of the entire silica gel with a unimolecular layer. Not so with iodine: the  $178.4^\circ \text{C}$ . isotherm shows an adsorption of  $0.12$  millimoles per gram at  $p = 0.5 p_0$

(330 mm.), which is only one twenty-fourth of the amount necessary to cover the surface with a complete adsorbed layer. This indicates that the forces of adsorption are considerably weaker than the forces existing between iodine molecules in the liquid state. A value of  $E_L - E_1 = 3500$  calories gives a good fit for the  $178.4^\circ$  C. isotherm, as Fig. 74 shows. One can then proceed to calculate the values of

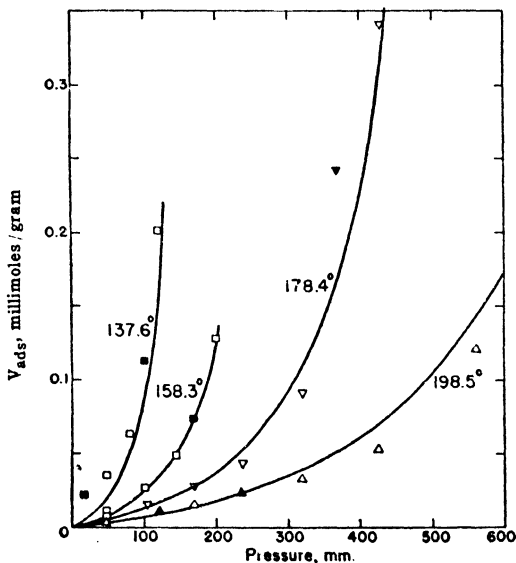


FIG. 74.—Adsorption isotherms of iodine on silica gel plotted according to equation (38) of the theory of multimolecular adsorption.

$v_m$  and  $c$  at the other temperatures and obtain the three other isotherms shown in the figure.

Since we have found that  $E_1 = E_L$  for bromine on silica gel, and  $E_1 < E_L$  for iodine, we might suspect that  $E_1 > E_L$  for chlorine. This means that instead of Type III isotherms we should expect the more customary Type II isotherms. The experiments of Reyerson and Wishart<sup>20</sup> have shown that this is actually the case. Since they worked with small  $p/p_0$  values (their experiments extend only up to  $p/p_0 = 0.096$ ), their isotherms represent the lower region of Type II curves, the region that is concave toward the pressure axis. These

<sup>20</sup> L. H. Reyerson and A. W. Wishart, *J. Phys. Chem.*, 41, 943 (1937).

isotherms were discussed from the point of view of Langmuir's theory in Chapter IV (See Fig. 40).<sup>21</sup>

If  $E_1 \ll E_L$ , then no appreciable adsorption takes place until the pressure reaches a value close to  $p_0$ , the saturation pressure. Such curiously shaped isotherms were obtained by McHaffie and Lenher,<sup>22</sup> who found that no measurable adsorption of water on glass took place until  $p/p_0$  became greater than 0.7. Even more exaggerated results were obtained by Frazer, Patrick and Smith,<sup>23</sup> who found that within their experimental error of a few molecular layers practically no adsorption of toluene took place on virgin glass up to quite close to the saturation pressure. In terms of the multimolecular adsorption theory these papers give examples of adsorption phenomena in which the forces of adhesion (e.g., between glass and toluene) are considerably smaller than the forces of cohesion (between toluene and toluene).<sup>24</sup>

### 3. Type I Isotherms

In physical adsorption very few adsorbents give Type I isotherms. Only certain charcoals and chabasite<sup>25</sup> were found to give isotherms of this type. The curves are characterized by continually decreasing slopes, becoming practically zero in the neighborhood of the saturation pressure. Such isotherms can be fitted by equation (42) which, as we have seen, is a limiting case of equation (41), with  $n = 1$ . According to the multimolecular adsorption theory this means that some charcoals and chabasite have exceedingly narrow pores, probably not more than two molecular diameters in width.

Equation (42) can be put in the linear form

$$(43) \quad p/v = p_0/cv_m + p/v_m$$

This is a special form of the Langmuir equation and can be tested by plotting  $p/v$  against  $p$ . An example of this was given in Fig. 41, Chapter IV, in which the adsorption isotherms of five different gases on charcoal were plotted according to equation (43). Very good straight lines were obtained and, as Table IV showed, the values of the

<sup>21</sup> Recently L. H. Reyerson and C. Bemmells (*J. Phys. Chem.*, **46**, 31, 1942) extended the isotherms of chlorine on silica gel to higher relative pressures, and found that the results agreed well with the theory of multimolecular adsorption.

<sup>22</sup> I. R. McHaffie and S. Lenher, *J. Chem. Soc.*, **127**, 1559 (1925).

<sup>23</sup> J. C. W. Frazer, W. A. Patrick and H. E. Smith, *J. Phys. Chem.*, **31**, 897 (1927).

<sup>24</sup> These important experiments are discussed in detail in Chapter X.

<sup>25</sup> Unpublished results of P. H. Emmett.



constant  $v_m$  obtained from the six different isotherms were entirely consistent with each other.

Since the variation of  $c$ ,  $v_m$  and  $p_0$  with the temperature is known, or can be evaluated, equation (43) can be used to calculate from one isotherm others at different temperatures. As an illustration, Fig. 75 shows the isotherms of Goldmann and Polanyi<sup>26</sup> for ethyl chloride on charcoal, calculated on the basis of equation (43). The 0° C. isotherm was plotted according to equation (43), and the constants  $c$  and  $v_m$

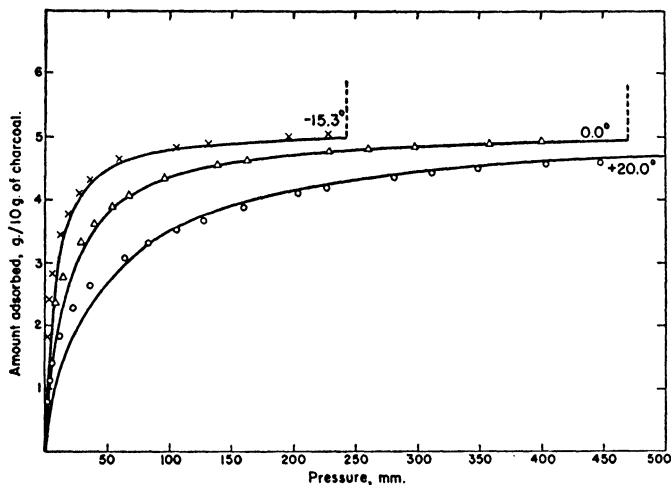


Fig. 75.—Adsorption isotherms of ethyl chloride on charcoal plotted according to the Langmuir equation (43).

were evaluated. Taking  $v_m$  the same at  $-15$  and  $20^\circ$  C. as at  $0^\circ$  C., and assuming that  $c$  is given by  $e^{(E_1 - E_L)/RT}$ , the isotherms at  $-15.3$  and  $20.0^\circ$  C. were calculated. In Fig. 75 the curves represent the calculated isotherms, the points are experimental. It is seen that equation (43) is applicable only to that portion of the isotherm which corresponds to  $p/p_0$  values greater than 0.1. In the higher pressure region (from  $p/p_0 = 0.1$  to 0.95) the calculated isotherms agree fairly well with the observed points.

Keesom and Schmidt<sup>27</sup> measured the adsorption of helium and neon at temperatures close to their boiling points. In spite of the

<sup>26</sup> F. Goldmann and M. Polanyi, *Z. phys. Chem.*, **132**, 321 (1928).

<sup>27</sup> W. H. Keesom and G. Schmidt, *Proc. Acad. Sci. Amsterdam*, **36**, 825 (1933); **36**, 832 (1933).

fact that the adsorption took place on a glass surface, and not on an adsorbent with narrow capillaries like charcoal or chabasite, a unimolecular adsorbed layer was not exceeded even close to the saturation pressure. This may possibly be explained by assuming that the heat of adsorption in the second layer was considerably smaller than the heat of liquefaction. At these very low temperatures, not far from the absolute zero, the glass may hold the adsorbed helium or neon atoms rigidly in such configurations that the binding energy of the second layer is much smaller than  $E'_L$ .

### C. Adsorption with Capillary Condensation

Equation (41) includes the first three isotherm types as special cases, but not the last two types. The shapes of Type IV and V isotherms suggest that a complete or almost complete filling of the pores and capillaries of the adsorbent occurs at a pressure lower than the vapor pressure of the gas. This lowering of the vapor pressure indicates that as the pressure of the gas is increased some additional forces appear that make the heat of adsorption, or the energy of binding, in some higher layer to be greater than  $E_L$ , the heat of liquefaction of the gas. This can be easily understood, since the *last adsorbed layer in a capillary is attracted on both sides*, and so its heat of evaporation must be greater than that of the other layers.<sup>28</sup> We shall denote this *additional* energy of evaporation by  $Q$ . The rate of evaporation of the adsorbed gas from the last layer then will not be proportional to  $e^{-E_L/RT}$ , but to  $e^{-(E_L+Q)/RT}$ . When the last layer is adsorbed not only is the heat of liquefaction liberated, but in addition twice the surface energy is set free, since two surfaces disappear. Thus if the last adsorbed layer fits in exactly and without strain,  $Q$  is equal to  $2\sigma S$ , where  $\sigma$  is the surface tension, and  $S$  is the surface area covered by one mole of the liquefied gas spread out into a unimolecular layer. The value of  $S$  will naturally depend on the assumed type of packing. If the fit of the last layer is not exact,  $Q$  will be smaller.

The derivation of the adsorption isotherm equation is similar to the derivation of equation (41). Let  $s_0, s_1, s_2, \dots, s_i, \dots$  represent the surface area that is covered by 0, 1, 2,  $\dots, i, \dots$  layers of adsorbed molecules. When equilibrium is established the principle of microscopic reversibility demands that all of the following evaporation-

<sup>28</sup> Of course, the heat of adsorption of the first layer also is usually greater than that of the other layers.

condensation equilibria be true :

$$\begin{aligned}
 (44) \quad & a p s_0 = b s_1 e^{-E_1/RT} \\
 & a p s_1 = b s_2 e^{-E_L/RT} \\
 & a p s_2 = b s_3 e^{-E_L/RT} \\
 & \cdot \quad \cdot \\
 & \cdot \quad \cdot \\
 & \cdot \quad \cdot \\
 & a p s_{n-2} = b s_{n-1} e^{-E_L/RT} \\
 & a p s_{n-1} = b s_n e^{-(E_L+Q)/RT}
 \end{aligned}$$

The approximations used are the same as in the derivation of equations (38) and (41). It should be noted that  $E_L$  is not the heat of adsorption of an isolated molecule of the  $i$ -th layer condensing on top of the  $(i - 1)$ -st layer, but rather the average energy liberated in the building up of the  $i$ -th layer. Thus the average interaction of the molecules in the  $i$ -th layer is roughly taken into account.

We again suppose that the adsorption takes place in a capillary consisting of two plane parallel walls. We assume that the maximum number of layers that can fit into this capillary is  $2n - 1$ . The total volume of gas adsorbed is obtained by summing up the volume of gas adsorbed on each surface element of *one wall* of the capillary and multiplying the result by two. The only exception is the volume adsorbed on the surface element  $s_n$ , which appears only once, since it is common to both walls of the capillary. The summation is carried out in a manner similar to that used in the derivation of equation (41). One obtains the equation

$$(45) \quad v = \frac{v_m c x}{1 - x} \frac{1 + (\frac{1}{2}ng - n)x^{n-1} - (ng - n + 1)x^n + \frac{1}{2}ngx^{n+1}}{1 + (c - 1)x + (\frac{1}{2}cg - c)x^n - \frac{1}{2}cgx^{n+1}}$$

where  $g = e^{Q/RT}$ , and all other terms have the same meaning as in equation (41). If the maximum number of layers that can fit into the capillary is  $2n$ , i.e., an even number, the equation will be slightly different

$$(46) \quad v = \frac{v_m c x}{1 - x} \frac{1 + (\frac{1}{2}ng - \frac{1}{2}n)x^{n-1} - (ng + 1)x^n + (\frac{1}{2}ng + \frac{1}{2}n)x^{n+1}}{1 + (c - 1)x + (\frac{1}{2}cg - \frac{1}{2}c)x^n - (\frac{1}{2}cg + \frac{1}{2}c)x^{n+1}}$$

Equations (45) and (46) describe Type IV and V isotherms, depending on the value of  $c$ ; for  $c > 1$  one obtains Type IV, for  $c < 1$  Type V isotherms. If the capillary forces are very small, i.e., if  $Q = 0$ , or  $g = 1$ , equation (46) reduces to (41). This describes Type II and III isotherms, depending on the value of  $c$ , as we have seen before.

Finally, when  $n = 1$ , we obtain Type I isotherms. Thus equation (46) includes all the five different isotherm types as special cases, and the same is true of (45).

In the derivation of equations (45) and (46) it was assumed that whatever happens on one wall of the capillary, the same happens on a corresponding spot of the opposite wall, so that the layers building up on the two walls of the capillary always meet *in the middle*. This may be a fairly good approximation, but actually it must be true that when one layer is adsorbed on a surface element of one of the walls, there is a certain probability that on a corresponding surface element of the opposite wall there are zero, one, two, three, or more layers adsorbed. Consequently the last adsorbed layer may form not only in the middle of the capillary, but in any other part. A derivation that takes care of this situation was given by Brunauer, Deming, Deming and Teller.<sup>4</sup> The equation obtained by them is

$$(47) \quad v = v_m \left\{ \frac{x}{1-x} + \frac{2(c-1)x + 2(c-1)^2x^2 + (\bar{n}c^2 + \bar{n}h - 2\bar{n}c - \bar{n}^2c^2)x^{\bar{n}}}{2[1 + 2(c-1)x + (c-1)^2x^2 + (c^2 + h - 2c - \bar{n}c^2)x^{\bar{n}}]} \right. \\ \left. + \frac{(2c + \bar{n}^2c^2 + 2\bar{n}c - 2c^2 - \bar{n}c^2 - 2h - 2\bar{n}h)x^{\bar{n}+1} + (\bar{n}h + 2h)x^{\bar{n}+2}}{(\bar{n}c^2 + 2c - 2c^2 - 2h)x^{\bar{n}+1} + hx^{\bar{n}+2}} \right\}$$

where  $\bar{n}$  is the maximum number of layers that can fit into the capillary, and  $h = (\bar{n}c^2 - c^2 + 2c)g$ . All other terms have the same meaning as in equation (45). In the derivation of equation (47) it was assumed that the  $\bar{n}$  layers do not fill the capillary exactly. In that case there are  $\bar{n} + 1$  different ways of leaving a gap when  $\bar{n}$  layers are adsorbed. If the  $\bar{n}$  layers fill the capillary exactly, the statistical weight of  $\bar{n}$  adsorbed layers will be 1. The derivation then leads to an equation identical in form with (47), but with  $h = c^2g$ .

Since equations (45), (46), and (47) represent an attempt to include capillary condensation in the theory of multimolecular adsorption, it is of some interest to compare the two theories with each other. We may take the idealized case of an adsorbent consisting of capillaries bounded by two plane parallel walls, all capillaries having the width  $D$ . Then the equilibrium pressure in the capillaries will be given by the Kelvin equation

$$(48) \quad p_k = p_0 e^{-2\sigma V/DRT}$$

where  $p_0$ ,  $\sigma$  and  $V$  are the vapor pressure, surface tension and molar volume of the liquefied gas at temperature  $T$ . Below  $p_k$  the capillaries are empty, except for an adsorbed monolayer, while above  $p_k$  the capillaries are completely full. According to the theory of multi-

molecular adsorption, on the other hand, adsorption begins below  $p_k$ , and the capillaries are not completely filled even above  $p_k$ . The reason for this difference is that the multimolecular adsorption theory takes account of the fluctuations by considering in detail empty, partly full and full capillaries, while in the capillary condensation theory only the probabilities of empty and full capillaries are compared. It is assumed in the latter theory that the state of greater probability is always realized, even when detailed calculation shows

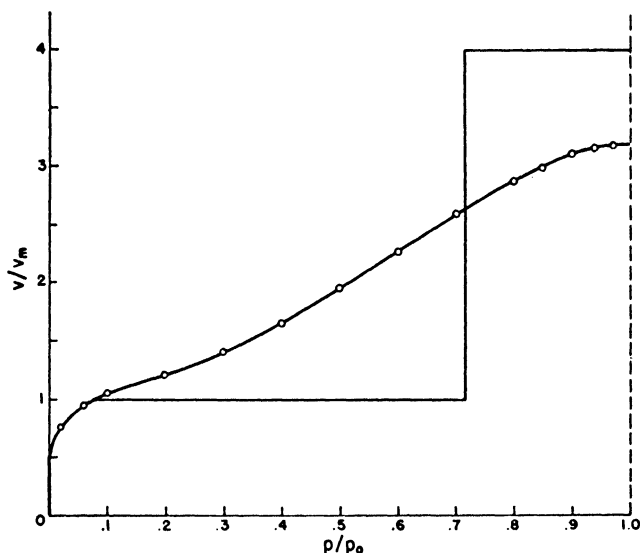


FIG. 76.—Comparison between the theory of multimolecular adsorption and the capillary condensation theory.

that the probability of partially full capillaries is much greater. Experimentally the sharp rise in adsorption demanded by the capillary condensation theory has never been found. This is explained by a continuously varying distribution of capillary radii. The multimolecular adsorption theory deduces smooth isotherms even when the capillary size in the adsorbent is uniform.

In Fig. 76 Curve 1 shows an isotherm calculated on the basis of the multimolecular adsorption theory, and Curve 2 an isotherm based on the capillary condensation theory. The constants of the curves are those of nitrogen at 76° K.,  $c$  is taken to be 150, and  $\bar{n}$  is 8. It is assumed that 8 layers of adsorbed nitrogen would fill the capillaries

exactly, without leaving any gap. This means in the first place that in the calculation equation (47) was used with  $h = c^2g$ ; in the second place that  $Q$  is exactly  $2\sigma S$ , as discussed before. On the basis of cubic close packing  $S = 3^{1/2}N^{1/3}V^{2/3}/2^{2/3}$ , where  $N$  is Avogadro's number.

As the curves show, capillary condensation equilibrium corresponds to a pressure at which the walls of the capillary are covered with a unimolecular adsorbed layer and the rest of the capillary is roughly half full. Thus for  $\bar{n} = 8$  capillary condensation would occur at a pressure at which  $v/v_m$  is about 2.5. A further peculiarity of the multimolecular adsorption curve is that the limiting value of  $v/v_m$  at the saturation pressure is not  $\bar{n}/2$ , which would correspond to a completely full capillary, but less. Actually the value of  $\bar{n}/2$  is closely approached only if the value of  $g$  is high and that of  $\bar{n}$  is low. For sufficiently high values of  $\bar{n}$  only  $\bar{n}/3$  layers will be adsorbed near saturation.<sup>4</sup> That large capillaries do not fill completely even near  $p_0$  is probably due to the crude manner in which the multimolecular adsorption theory calculates the fluctuations. It seems likely that one would get completely full capillaries at  $p_0$  if the interaction of each molecule with its neighbors were taken into account in detail. For smaller capillaries, with not too small  $g$  values, the multimolecular adsorption theory predicts that the capillaries are practically full at  $p_0$ , and so the above difficulty does not arise.

#### *D. Applications to Type IV and V Isotherms*

An inspection of equation (47) shows that for small values of  $x$ , or  $p/p_0$ , the  $\bar{n}$ -th and higher powers of  $x$  can be neglected, and the equation reduces to (38). From a straight line plot one can evaluate the constants  $v_m$  and  $c$ . An approximate value of  $\bar{n}$  can be obtained from the largest adsorption measured in the neighborhood of the saturation pressure, since  $v/v_m \sim \bar{n}/2$  if the capillaries are completely filled. Knowing the three other constants,  $h$  can be obtained from adsorption points at large  $p/p_0$  values. Further improvements in the four constants can be made by the method of trial and error.<sup>29</sup> Figure 77 illustrates an application of equation (47). The isotherms represent the adsorption of benzene on ferric oxide gel at 40, 50, and 60° C., obtained by Lambert and Clark.<sup>30</sup> (The same isotherms were shown in Fig. 6.) Using the constants  $v_m = 0.081$  g. of benzene per g. of gel,  $c = 27$  ( $E_1 - E_L = 2190$  cal.),  $h = 47,400$  ( $Q = 1690$  cal.), and

<sup>29</sup> For further suggestions see reference 4.

<sup>30</sup> B. Lambert and A. M. Clark, *Proc. Roy. Soc.*, A122, 497 (1929).

$\bar{n} = 6$ , the curve in the middle of the figure (the 50° C. isotherm) was obtained. Then using the same values of  $v_m$ ,  $\bar{n}$ ,  $E_1 - E_L$ , and  $Q$  the 40 and 60° C. isotherms were calculated. As the figure shows the temperature dependence is satisfactorily reproduced. That one can not expect a perfect fit from equation (47) becomes clear if we consider the following facts:

(1) In the derivation of the equation it was assumed that the capillaries of the adsorbent are uniform in size, whereas actually most

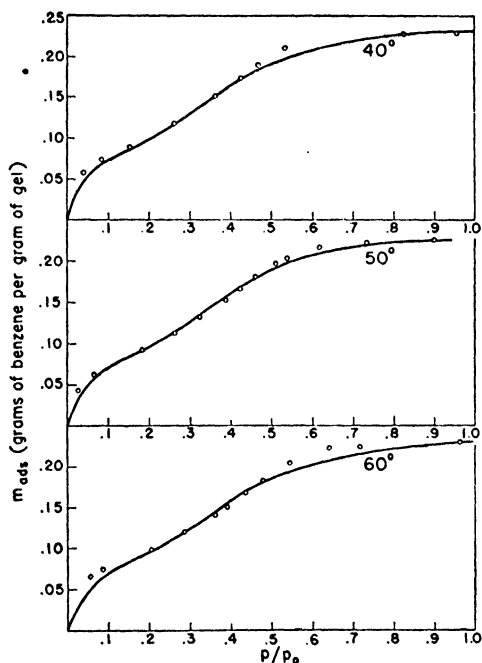


FIG. 77.—Adsorption isotherms of benzene on ferric oxide gel plotted according to equation (47) of the theory of multimolecular adsorption.

adsorbents have capillaries of differing sizes. Thus in the idealized case for which equation (47) was derived one obtains an expression for an imaginary *average* sized capillary.

(2) It was assumed that the walls of the capillary are parallel, whereas actually the walls may often be convergent (V-shaped pores). To take care of this factor one would need a fifth constant, the angle  $\theta$ , which would make the equation extremely complicated.

(3) It was assumed that the adsorption takes place in capillaries open on the sides. If one deals with completely enclosed capillaries, the amount adsorbed in each consecutive layer will be less and less, and the maximum adsorption that can occur in each layer will not have the constant value  $v_m$ , but will be a function of  $\bar{n}$ .

Equations (45), (46) and (47) can be used to clear up some apparent discrepancies between surface area values obtained from adsorption isotherms of different gases for the same adsorbent. Some investigators have reported Type I and II isotherms for the same adsorbent with different gases. These isotherms at first sight seem incompatible with each other in terms of the theory of multimolecular adsorption. Thus Schlüter<sup>31</sup> found that carbon disulfide on powdered glass and silver gave S-shaped isotherms, but pentane on the same two adsorbents gave Langmuir type isotherms.<sup>32</sup> An inspection of the curves for powdered glass indicates that the surface of the adsorbent evaluated by means of pentane is about four times as large as that obtained from the carbon disulfide adsorption, while  $n$  seems to be 1 for pentane, but at least 6 for carbon disulfide. Since Schlüter measured the adsorption isotherms on two different samples of the same adsorbent, he ought to have gotten approximately equal surface area values and also  $n$  values that are compatible with each other. Similar results were obtained by Pidgeon,<sup>33</sup> who found that benzene gave a Type I isotherm on active silica, while water and ethyl alcohol gave Type II isotherms on the same adsorbent.

Figure 78 suggests a reconciliation of this apparent discrepancy. It represents six isotherms of two imaginary gases  $A$  and  $B$ , on the same adsorbent. For the sake of simplicity the isotherms were calculated by means of equation (45). Gas  $A$  consists of smaller molecules than gas  $B$ , so that when the capillaries are completely full they can hold one and a half times as many molecules of  $A$  as of  $B$  ( $n = 6$  and  $4$ , respectively). It is assumed that the forces of adsorption in the first layer are about the same for both gases (i.e., the  $c$  values are about equal), but that the additional adsorption forces appearing in the last layer are very different, rather small for  $A$ , but quite strong for  $B$  ( $g = 5$  to  $45$  for the former,  $200$  to  $1000$  for the latter). Superficial inspection of the three isotherms of gas  $B$  would suggest that they are

<sup>31</sup> H. Schlüter, *Z. phys. Chem.*, **A153**, 68 (1931).

<sup>32</sup> However, P. H. Emmett was unable to reproduce Schlüter's experiments. He obtained S-shaped isotherms for both carbon disulfide and pentane on powdered glass and silver (Unpublished results).

<sup>33</sup> L. M. Pidgeon, *Can. J. Research*, **12**, 41 (1935).



Type I isotherms, indicating that at saturation only one layer is adsorbed. If one would calculate the surface area of the adsorbent from these pseudo-Langmuir type isotherms and compare it with the surface area value obtained from the Type II isotherms of gas *A*, one would find that *B* gives four times as large a surface value as *A* does. At the same time the *n* value for *A* would come out to be 6, while the apparent *n* value for *B* is 1. Actually the explanation is that the

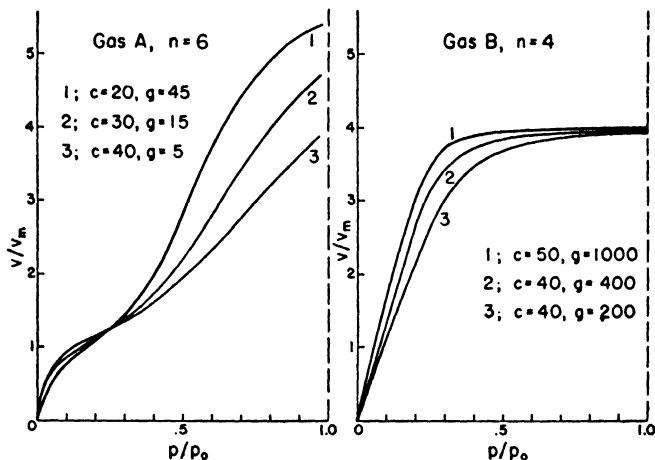


FIG. 78.—Adsorption isotherms calculated on the basis of equation (45) of the theory of multimolecular adsorption.

isotherms of gas *B* are not Type I but Type IV isotherms, which appear to be Langmuir type because of the large values of the constant *g*. The three isotherms of gas *A* also illustrate how a Type IV isotherm changes gradually into a Type II isotherm as the values of *g* get smaller.

A different explanation from that given above is needed to reconcile the results of Coolidge<sup>34</sup> with the multimolecular adsorption theory. Figure 79 shows an isotherm of carbon disulfide obtained by him on a sample of coconut charcoal, and an isotherm of water vapor obtained on another sample of the same charcoal. The constants evaluated from the isotherms should therefore be consistent with each other. The water vapor curve appears to be a Type V isotherm, and indeed we can fit it satisfactorily with the help of equation (45) if we make the value of *n* about 9. On the other hand the shape of the carbon

<sup>34</sup> A. S. Coolidge, *J. Am. Chem. Soc.*, 46, 596 (1924).

disulfide isotherm is of the Langmuir type, indicating unimolecular adsorption. Calculating the surface of the charcoal from the two different isotherms, one finds an approximately five fold discrepancy.

To resolve the difficulty we may suggest two alternative explanations. It is possible that the structure of charcoal is not entirely rigid, and that both its surface and its pore diameter are functions of the adsorbate molecules. We may suppose, for example, that charcoal

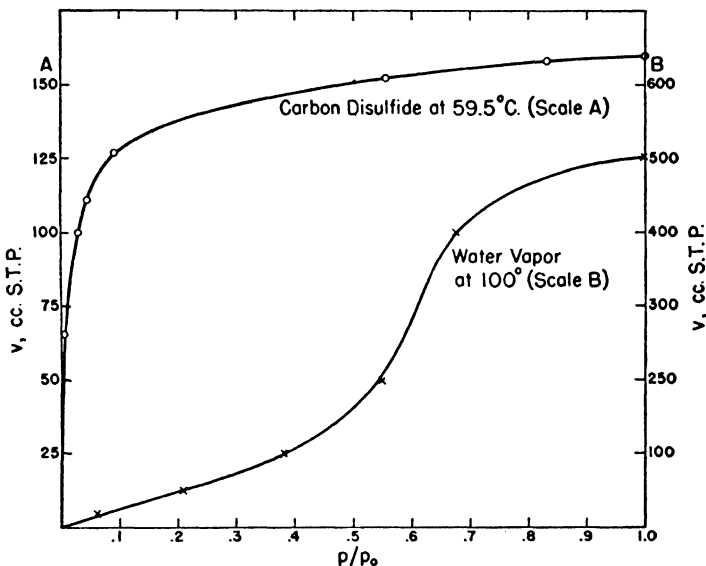


FIG. 79.—Adsorption isotherms of carbon disulfide and water on charcoal.

consists of a layer-like structure, similar to graphite. The force of interaction between the carbon atoms of the adsorbent and the carbon disulfide molecules may be sufficiently strong to permit the latter to penetrate between the layers with comparative ease. On the other hand the interaction between charcoal and water is weak (charcoal being a strongly hydrophobic substance), which makes it difficult for water to penetrate between the carbon layers. At low pressures there is very little penetration; but as some water molecules succeed in penetrating with increasing pressure it becomes easier for other molecules to penetrate, owing to the large dipole attraction between the water molecules themselves. This hypothesis accounts for the most

important characteristics of the two isotherms, namely, (1) that  $E_1 - E_L$  is positive for carbon disulfide and negative for water, (2) that the carbon disulfide isotherm represents unimolecular adsorption with a large surface, and (3) that the water isotherm represents multimolecular adsorption with a smaller surface.

The second explanation is based on the assumption that both isotherms represent unimolecular adsorption. The carbon disulfide curve is just a customary Langmuir type isotherm. The shape of the water isotherm indicates that at low relative pressures very little adsorption takes place because of the small force of interaction between the surface carbon atoms and the water molecules. However, as soon as some adsorption has taken place the large dipole attraction between the water molecules allows further adsorption to proceed more easily. Thus eventually a sharp rise in adsorption occurs, until the capillary is filled. If this second explanation is correct, the water vapor curve does not represent multimolecular adsorption, and one is not justified in using equations (45), (46), or (47) to fit it.

Whether the adsorption of water on charcoal represents unimolecular or multimolecular adsorption, the shape of the isotherm according to the theory of multimolecular adsorption is due to two factors: (1) at lower pressures the isotherm is convex toward the pressure axis because  $E_1$  is smaller than  $E_L$ ; (2) at higher pressures filling of the capillaries cuts off further adsorption.<sup>35</sup> The first of these assumptions is independently confirmed by measurements of the heats of adsorption. Coolidge<sup>36</sup> determined the isosteric heats of adsorption of water on charcoal, and Keyes and Marshall<sup>37</sup> measured the heats of adsorption by the direct calorimetric method. In both instances the value of  $E_1$  was found to be slightly lower than  $E_L$ .

#### CRITICISM OF THE MULTIMOLECULAR ADSORPTION THEORY

The multimolecular adsorption theory is the first attempt to arrive at a unified theory of physical adsorption. It describes the entire course of an adsorption isotherm, including unimolecular adsorption, multimolecular adsorption and capillary condensation, whereas previous theories have dealt only with one or another of these adsorption regions. At the same time it supplies an isotherm equation that

<sup>35</sup> According to the second explanation the capillaries are very narrow, less than three molecular diameters in width.

<sup>36</sup> A. S. Coolidge, *J. Am. Chem. Soc.*, **49**, 708 (1927).

<sup>37</sup> F. G. Keyes and M. J. Marshall, *J. Am. Chem. Soc.*, **49**, 156 (1927).

can describe all the five different isotherm types, whereas previous equations have dealt only with one type of isotherm at a time, and no equations have been offered at all for three of the five isotherm types.

The theory has several limitations. At low pressures it reduces to the Langmuir equation, consequently all the criticism that has been levelled against the Langmuir theory can be directed equally well against the multimolecular adsorption theory in the low pressure region of the adsorption isotherm. The most active parts of the surfaces of most adsorbents are strongly heterogeneous, with strongly varying heats of adsorption, therefore the Langmuir equation is not obeyed. For most adsorbents the theory breaks down in the region from zero pressure to  $p/p_0 = 0.05$ , and for some adsorbents to as high as 0.10. It may be restated that in this region the only theory that can deal successfully with physical adsorption is the potential theory.

The multimolecular adsorption theory is at its best in the middle adsorption region, i.e., in the region preceding and following the building up of a unimolecular layer. There are several reasons for this. In the first place the less active parts of the surfaces of most adsorbents are roughly homogeneous, therefore an average value of  $E_1$  can be used without introducing a serious error. In the second place the heterogeneity of the surface does not show up any more in the second adsorbed layer, and so  $E_L$  becomes a very good approximation to the heat of adsorption in that layer. Finally, since most adsorbents have capillaries that are at least several molecular diameters wide, the difficulties due to capillary condensation do not yet begin to appear in this region. Thus the two-constant equation (38) is obeyed very closely for many adsorbents to at least  $p/p_0 = 0.35$ , and sometimes to 0.50. This fact enables one to evaluate accurately the surface area of the adsorbent. The method is further discussed in Chapter IX.

At high adsorptions the theory leads to an incomplete filling of the capillaries for larger sized capillaries. This is probably due to the crudeness of the method of calculating the fluctuations. Another difficulty is that the theory calculates the adsorption for an average sized capillary. If the adsorbent has a uniform capillary size, or at least if the variation from the average is not too great, the theory can give a good fit for the isotherm; but if the variation is great, only a rough description can be obtained. If one is interested in the distribution of the capillaries of the adsorbent, one can get a rough approximation by using the capillary condensation theory. The great simplicity of handling the Kelvin equation instead of equations (45) or (47) is obvious.

The multimolecular adsorption theory is not applicable above the critical temperature because the simplifications introduced in equations (24), (25), (35) and (36) can not be made. Since the forces of condensation are responsible for multimolecular adsorption, it seems likely that above the critical temperature only unimolecular adsorption exists. The question of the existence of multimolecular adsorption above the critical temperature is discussed in Chapter XII.

## CHAPTER VII

### THE HEAT OF ADSORPTION I

According to the theory of multimolecular adsorption<sup>1,2</sup> physical adsorption is characterized by the four constants appearing in the isotherm equation. Two of these constants,  $v_m$  and  $n$ , may be designated as *size constants*, one depending on the size of the total adsorbing surface, the other on the average width of the pores. These sizes are not measured in absolute units but in terms of the dimensions of the adsorbed molecules. The constant  $v_m$  depends on the number of molecules required to cover the entire surface with a unimolecular adsorbed layer; thus the surface area of the adsorbent is measured in terms of the cross-sectional area of the adsorbed molecule. The constant  $n$  is equal to the maximum number of adsorbed layers that can fit in a capillary; therefore the pore width is measured in terms of the thickness of the adsorbed molecule perpendicular to the surface. The other two constants,  $c$  and  $g$ , may be designated as *energy constants*, since they are dependent upon the heats of adsorption of the successive layers.

The heat of adsorption in the first layer, which determines the value of  $c$ , results from interaction between the adsorbent and the adsorbate; the heats of adsorption of all other layers result from interaction between the adsorbate molecules themselves. It has been assumed in the derivation of the theory of multimolecular adsorption that the heat of adsorption in each layer, except the first and the last, is equal to the heat of liquefaction of the adsorbed gas. The constant  $c$  depends on the difference between the heat of adsorption of the first layer and the heat of liquefaction, and the constant  $g$  on the difference between the heat of adsorption of the last layer and the heat of liquefaction. The energy difference  $E_1 - E_L$  can be positive or negative, because the interaction between adsorbent and adsorbate can be either stronger or weaker than the interaction between the adsorbate molecules themselves. The heat of adsorption in the last layer, however, is always greater than the heat of liquefaction, since in addition to the interaction energy between the adsorbate molecules

<sup>1</sup> S. Brunauer, P. H. Emmett and E. Teller, *J. Am. Chem. Soc.*, **60**, 309 (1938).

<sup>2</sup> S. Brunauer, L. S. Deming, W. E. Deming and E. Teller, *J. Am. Chem. Soc.*, **62**, 1723 (1940).

the system further loses energy by the disappearance of free liquid surfaces. The upper limit of this additional energy loss  $Q$  is  $2\sigma S$ , where  $\sigma$  is the surface tension and  $S$  is the surface area covered by a mole of the adsorbate spread out into a unimolecular layer. Ordinarily, however,  $Q$  will be smaller than  $2\sigma S$ , because the adsorbed layers may not fit exactly in the capillary. Thus the relation between the width of the capillary and the thickness of the adsorbed molecules influences the energy quantity  $Q$ , and consequently the value of the constant  $g$ .

In the present and subsequent chapters we shall take up individually the factors that determine van der Waals adsorption: the heat of adsorption, the surface of the adsorbent, and the pore structure of the adsorbent. Chapters VII and VIII deal with the heat of adsorption. In Chapter VII the fundamental physical theories of van der Waals forces are presented, with particular emphasis on their application to the calculation of heats of adsorption. In Chapter VIII we discuss the experimental results on the heats of adsorption which further reveal the nature of physical adsorption.

### THE PHYSICAL NATURE OF VAN DER WAALS FORCES <sup>3</sup>

The equation of state of van der Waals for imperfect gases can be put in the form

$$(1) \quad p = \frac{RT}{v - b} - \frac{a}{v^2}$$

The observed pressure can be considered as the difference between two terms: the dynamic pressure and the attractive pressure.

The equation of state of a perfect gas is

$$(2) \quad p = RT/v$$

By definition there are no forces between the molecules of a perfect gas. A comparison of equations (1) and (2) shows that the van der Waals equation implies both attractive and repulsive forces between the molecules of an imperfect gas.

The constant  $b$  in the dynamic pressure term is a measure of the repulsion between the molecules. The nature of the repulsive forces can be easily understood in terms of our physical picture of the mole-

<sup>3</sup> For further study of the problem we may suggest the following treatments: J. C. Slater, *Introduction to Chemical Physics*, New York, 1939, p. 352. O. K. Rice, *Electronic Structure and Chemical Binding*, New York, 1940, p. 354. E. A. Moelwyn-Hughes, *Physical Chemistry*, Cambridge, 1940, p. 363. F. London, *Trans. Far. Soc.*, 33, 8 (1937).

cule. We now visualize the molecule as consisting of a positive nucleus, surrounded by an external electron cloud. Let us consider for simplicity a monatomic molecule: a rare gas atom. This has a spherically symmetrical charge distribution, i.e., the positive nucleus is at the center of the sphere, and the electrons form a spherical shell of negative electricity on the outside. If two such atoms are not in actual contact there will be neither attraction nor repulsion between them, since according to a theorem in electrostatics a spherically symmetrical charge distribution has an external field just equal to that which it would have if all of its charges were placed at the center. Thus a rare gas atom has no external field. However, the situation becomes different if the two atoms collide in the gas phase and there is an interpenetration of the electron clouds. In this case the electrons no longer shield the nuclear charges completely and the positive nuclei begin to repel each other. The greater the interpenetration, i.e., the closer the nuclei approach each other, the stronger will be the repulsion. Thus the repulsion between neutral molecules can be explained by the electrostatic Coulomb forces that exist between the constituent parts (electrons and nuclei) of the molecules.

Equation (1) shows that the external pressure is smaller than the dynamic pressure by the amount  $a/v^2$ . This implies attractive forces between the molecules, and the van der Waals constant  $a$  gives a measure of these attractive or cohesive forces. It is not immediately obvious what gives rise to attractive forces between uncharged molecules at great distances; it is not surprising therefore that the problem of van der Waals attraction was not attacked successfully until recent years. The electrostatic origin of the forces was long suspected, since gravitational or magnetic forces are too small to account for the observed cohesion. As a matter of fact we know now that there are three electrostatic effects that jointly account for the attractive van der Waals forces: the orientation effect of Keesom, the induction effect of Debye, and the dispersion effect of London.

Many of the uncharged molecules have dipole moments, and it was suggested by Keesom <sup>4</sup> in 1912 that the interaction between these dipole moments is responsible for the van der Waals attraction. If the center of gravity of the positive charges does not coincide with the center of gravity of the negative charges, the molecule is said to possess a permanent dipole moment. Ammonia, water, alcohol and phenol are typical examples of dipole molecules. The dipole moment

<sup>4</sup> W. H. Keesom, *Physik. Z.*, 22, 129, 643 (1921).



is defined as the product of the charge and the distance between the centers of gravity of the positive and negative charges

$$(3) \quad \mu = ex$$

When two molecules having dipole moments  $\mu_1$  and  $\mu_2$  approach each other, the interaction between the dipoles will manifest itself in two ways. In the first place the dipoles exert forces upon each other, attraction or repulsion, depending upon their relative orientations. If the unlike charges are closer to each other than the like charges, the net effect will be attraction, otherwise repulsion. In the second place each dipole is acted upon by a torque in the field of the other. These torques tend to orient the dipoles parallel to each other, the positive end of one being closer to the negative end of the other.

Since molecules in the gas phase have rotational degrees of freedom, in the case of dipole molecules we deal with rotating dipoles. If the dipoles rotated uniformly in all directions, the net force would be zero, because the force changes sign when the dipole is reversed. However, the rotation is not uniform, because the torques tend to keep the dipoles in parallel positions. Each particular position of the two dipoles corresponds to a certain mutual potential energy. Due to the Maxwell-Boltzmann distribution law the orientations having lower potential energies will be statistically favored, and the dipoles will be oriented in the position of minimum potential energy more often than in any other position. Thus on the average the attraction will preponderate over the repulsion. Averaging over all positions, Keesom found for the interaction energy,

$$(4) \quad U_0 = -\frac{2}{3} \frac{\mu_1^2 \mu_2^2}{r^6} \frac{1}{kT}$$

where  $U_0$  is the potential energy due to the orientation effect,  $r$  is the distance between the centers of the two dipoles, and  $k$  is Boltzmann's constant. Keesom attributed van der Waals attraction to this orientation effect.

In 1920 Debye<sup>5</sup> pointed out that the orientation effect alone can not account for van der Waals cohesion. According to equation (4) the attraction potential diminishes linearly with the absolute temperature, but the experimentally obtained van der Waals cohesion corrections indicate no such rapid decrease with temperature. He concluded therefore that there must be an additional interaction energy term which is independent of temperature.

<sup>5</sup> P. Debye, *Physik. Z.*, 21, 178 (1920).

Keesom considered the molecules as rigid dipoles, i.e., he assumed that the charge distribution of a molecule does not change under the influence of another molecule in its vicinity. Actually, however, the charge distribution of a molecule is disturbed by the presence of another charged body: the molecule is said to become polarized. This is an example of the phenomenon of induction. It is a long known fact that when an electric charge is brought near to a conductor it induces a charge of opposite sign on the neighboring side of the conductor and a charge of the same sign on the far side of the conductor. In a similar manner the positive end of a dipole distorts the electric charge in a nearby molecule, producing a negative charge on the neighboring side and a positive charge on the opposite side; in other words, a dipole is induced in the other molecule. The interaction between the inducing dipole and induced dipole gives rise always to attraction. This is the Debye induction effect.

The induced dipole moment is proportional to the external field that produces it

$$(5) \quad \mu = \alpha E$$

where  $E$  is the field strength, and the proportionality constant  $\alpha$  is called the polarizability. The interaction energy due to induction between a molecule having dipole moment  $\mu_1$  and another molecule having polarizability  $\alpha_2$  is

$$(6) \quad U_I = - \frac{\alpha_2 \mu_1^2}{r^6}$$

If the other molecule has a dipole moment  $\mu_2$ , the interaction energy due to mutual induction is

$$(7) \quad U_I = - \frac{\alpha_1 \mu_2^2 + \alpha_2 \mu_1^2}{r^6}$$

If both molecules are of the same kind this reduces to

$$(8) \quad U_I = - \frac{2\alpha\mu^2}{r^6}$$

Debye believed that the sum of  $U_0$  and  $U_I$  gives the van der Waals energy of attraction between dipole molecules. The interaction potential varies inversely as the sixth power of the distance between the molecules in both equations (4) and (8). Since the force is given by

$$(9) \quad F = - \frac{dU}{dr}$$

the van der Waals attraction forces vary inversely as the seventh power of the distance between the molecules. Since  $U_I$  is independent of the temperature, part of the interaction energy does not vanish with increasing temperature. This is in accordance with the experimental facts. Nevertheless, it is obvious that the orientation and induction effects can at best account only for the van der Waals attraction between molecules possessing permanent dipoles. But many molecules, such as hydrogen, helium, argon, nitrogen, methane, etc., do not have permanent dipoles. To explain the van der Waals

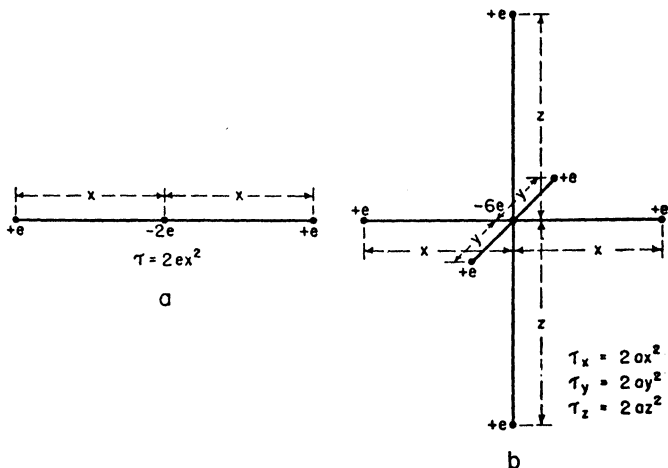


FIG. 80.—The quadrupole moment. (a) Rigid rod-shaped quadrupole. (b) Three-dimensional quadrupole.

attraction between two such molecules Debye and Falckenhagen<sup>6</sup> assumed the existence of quadrupole moments. They suggested that the quadrupole moment in one molecule induces a dipole moment in the other, and the interaction between permanent quadrupole and induced dipole gives rise to van der Waals attraction.

The simplest example of a quadrupole is shown in Fig. 80(a), taken from Hückel.<sup>7</sup> This consists of two similar dipoles laid end to end in such manner that either the two positive or the two negative charges coincide in the center. Such an arrangement has no dipole moment since the centers of gravity of the positive and negative

<sup>6</sup> H. Falckenhagen, *Physik. Z.*, 22, 302 (1921).

<sup>7</sup> E. Hückel, *Adsorption und Kapillarkondensation*, Leipzig, 1928, p. 94.

charges coincide. The quadrupole moment is defined as

$$(10) \quad \tau = 2ex^2$$

where  $e$  is the charge and  $x$  is the distance between the positive and negative charge. The most general example of a quadrupole is shown in Fig. 80(b). The three components of the quadrupole moment are

$$(11) \quad \tau_x = 2ex^2, \quad \tau_y = 2ey^2, \quad \tau_z = 2ez^2.$$

These components are called the electrical moments of inertia of the molecule.

When two similar quadrupole molecules induce dipoles into each other, the mutual interaction energy is

$$(12) \quad U_q' = -\frac{3}{2} \frac{\alpha \tau^2}{r^8}$$

where  $\alpha$  is the polarizability of the molecules. The interaction potential in this case varies inversely as the eighth power of the distance between the molecules. Except at small distances, the quadrupole-dipole interaction must therefore be negligible.

Dipole moments can be determined by physical measurements that do not depend on the previously discussed theories, but quadrupole moments can not be measured experimentally. Their existence was inferred solely from the fact that attractive van der Waals forces existed between molecules having no permanent dipoles, and their magnitude was calculated from the van der Waals corrections. The advent of quantum mechanics, however, threw new light on this subject. It turned out that the charge distribution in the rare gas atoms has exact spherical symmetry; these atoms therefore can not have either permanent dipoles, or quadrupoles, or any other multipoles. Molecules like hydrogen and nitrogen do possess quadrupoles, but the quadrupole calculated for hydrogen from quantum mechanics can account for only 1/100 part of the van der Waals attraction that exists between hydrogen molecules. It appeared therefore that there must exist another effect that gives rise to attraction between molecules having no permanent electric moments of any sort. This effect, discovered by London<sup>8</sup> in 1930, is called the dispersion effect.

For the sake of simplicity let us consider an argon atom as an example of a non-polar molecule. Such an atom does have a dipole moment at any instant. There are 18 electrons moving around the central nucleus in various directions, and it is very unlikely that at

<sup>8</sup> F. London, *Z. phys. Chem.*, B11, 222 (1930).

any instant the electrons should be so arranged as to give exactly zero dipole moment. An extreme example of this is a hydrogen atom, which can never have zero dipole moment since the electron is always on one side of the nucleus or on the other side. The instantaneous dipole moment of an argon atom will be relatively small, since some of the electrons will be on one side of the nucleus and some on the other side. The dipole moment will be constantly fluctuating in magnitude and in direction. Since the orientation in one direction is just as probable as in the opposite direction, the average dipole moment will be zero.

Ordinarily, in the experimental determination of the dipole moment of a molecule one actually measures the average dipole moment. When an argon atom is placed in an electric field, the orientation of the atom is so much slower than the velocity of the electronic motion that one measures the time average of the instantaneous dipole moments, which is zero. Thus the argon atom is said to possess no permanent dipole moment. There are, however, two phenomena in which the fluctuating dipole is of very great importance. In the first place, the oscillating dipole moment is connected with the radiation of light; in the second place, it is responsible for the van der Waals attraction between molecules. Thus these two processes are related to each other, and London derived an equation by means of quantum mechanics that shows the dependence of the van der Waals attraction between two atoms upon the probabilities of various optical transitions which the atoms can make. Because of the connection with the phenomenon of the dispersion of light, these attractive forces are called dispersion forces.

The fluctuating dipole moment in the argon atom creates a fluctuating electric field around the atom, which produces displacements of the charge in a near-by atom. The displacements will be in phase with the fluctuations. The force exerted by the fluctuating field on the displaced charge will not average to zero, because there is a tendency on the part of the fluctuating dipole and the induced dipole to move in phase with each other. There will result a net attraction given by

$$(13) \quad U_D = -\frac{3}{2} \frac{\alpha \overline{\mu^2}}{r^6}$$

where  $U_D$  is the dispersion energy,  $\alpha$  is the polarizability and  $\overline{\mu^2}$  is the mean square dipole moment. This will be different from zero even when the mean dipole moment is zero.

For the purpose of our discussion it is not necessary to reproduce the complete equation that London derived for the dispersion potential. Instead of this rather complicated expression London used with considerable success the approximation formula

$$(14) \quad U_D = -\frac{3}{4} \frac{h\nu_0\alpha^2}{r^6}$$

where  $h\nu_0$  is a characteristic energy term that can be evaluated from the experimentally determined optical dispersion formula of the gas. The approximation amounts to the substitution of one electrical oscillator in place of all the oscillators that make up the atom. Such a substitution was found permissible for some simple molecules, such as the rare gas atoms, hydrogen, nitrogen, methane, etc.

TABLE XVII  
THE DISPERSION OF LIGHT BY NEON GAS AT 273.1° K. AND 1 ATM.

$(c/\nu = \lambda) \times 10^4$ cm. in vacuum	$(n - 1) \times 10^4$	
	Observed	Calculated
5462.23	6725.0	6724.5
4917.40	6737.2	6736.7
4359.54	6754.0	6754.3
4078.98	6766.2	6766.2
4047.68	6767.5	6767.6
3907.56	6774.4	6774.6
3664.10	6789.1	6788.8
3342.42	6812.9	6812.9
3132.59	6832.4	6832.7
3022.37	6844.7	6844.9
2968.13	6851.6	6851.3
2894.44	6861.2	6860.9

The evaluation of the main frequency  $\nu_0$  from the dispersion formula will now be illustrated by an example. The simplified Drude-Voigt dispersion formula, called the Sellmeier equation, gives the relation between the index of refraction  $n$  and the frequency of light  $\nu$

$$(15) \quad n - 1 = \frac{k}{\nu_0^2 - \nu^2}$$

where  $\nu_0$  is the frequency of the electrical oscillator responsible for the refraction, and  $k$  is a constant at a given temperature and pressure of the gas. Equation (15) can often reproduce the experimental facts with great accuracy, as shown in Table XVII. The data were obtained by Cuthbertson and Cuthbertson<sup>9</sup> for the dispersion of light by neon

<sup>9</sup> C. Cuthbertson and M. Cuthbertson, *Proc. Roy. Soc., A135*, 40 (1932).

gas at 273.1° K. and 1 atm. pressure. Using the values  $\nu_0^2 = 3.9160 \times 10^{31} \text{ sec.}^{-2}$  and  $k = 2.61303 \times 10^{27} \text{ sec.}^{-2}$ , they calculated the values for  $n - 1$  shown in the last column. Clearly, therefore, the assumption of a single electrical oscillator of frequency  $\nu_0$  is sufficient to reproduce the dispersion curve of neon. The same is true for the other rare gases.

The  $\nu_0$  of equation (15) is the same as the  $\nu_0$  of the van der Waals potential in equation (14). London<sup>10</sup> noticed that for all gases whose dispersion formulas were expressible by means of equation (15) the energy term  $h\nu_0$  was roughly equal to the ionization potential. This is shown in Table XVIII, columns 2 and 3. Column 2 gives the

TABLE XVIII  
DISPERSION EFFECT BETWEEN SIMPLE MOLECULES

Gas	$h\nu_I$ Electron Volts	$h\nu_0$ Electron Volts	$\alpha \cdot 10^{24}$ cm. <sup>3</sup>	$C \cdot 10^{18}$ Electron Volts.cm. <sup>3</sup>
He	24.5	25.5	0.20	0.77
Ne	21.5	25.7	0.39	2.93
A	15.4	17.5	1.63	34.7
Kr	13.3	14.7	2.46	69
Xe	11.5	12.2	4.00	146
H <sub>2</sub>	16.4		0.81	8.3
N <sub>2</sub>	17.0	17.2	1.74	38.6
O <sub>2</sub>	13.0	14.7	1.57	27.2
CO	14.3		1.99	42.4
CH <sub>4</sub>	14.5		2.58	73
CO <sub>2</sub>		15.45	2.86	94.7
Cl <sub>2</sub>	18.2		4.60	288
HCl	13.7		2.63	71
HBr	13.3		3.58	128
HI	12.7		5.4	278
Na		2.1	29.7	960

ionization energy  $h\nu_I$ , and column 3 gives the value of  $h\nu_0$  evaluated from the dispersion formula (15). London suggested therefore that, at least to a first approximation, one can use the ionization potential in place of  $h\nu_0$  even for molecules whose dispersion formulas have not been determined.

We can put equation (14) in the form

$$(16) \quad U_D = -\frac{C}{r^6}$$

with the value of  $C$  given by

$$(17) \quad C = \frac{3}{4} h\nu_0 \alpha^2$$

<sup>10</sup> F. London, *Trans. Far. Soc.*, **33**, 8 (1937).

In Table XVIII, column 4 gives the polarizabilities of the molecules and column 5 the values of the dispersion energy constant  $C$ . It is interesting to note that the value of this constant shows a thousand fold variation from helium to sodium.

For molecules possessing permanent dipole moments the van der Waals energy of attraction is obtained by summing up the orientation, induction, and dispersion potentials,  $U_0$ ,  $U_I$  and  $U_D$ , given by equations (4), (8) and (14), respectively.

$$(18) \quad U = -\frac{1}{r^6} \left( \frac{2}{3} \frac{\mu^4}{kT} + 2\mu^2\alpha + \frac{3}{4} h\nu_0\alpha^2 \right)$$

It is instructive to compare the relative importance of the three effects for some simple dipole molecules. In Table XIX, taken from

TABLE XIX  
ORIENTATION, INDUCTION AND DISPERSION ENERGIES

Gas	$\mu \cdot 10^{18}$	$\alpha \cdot 10^{24}$	$\frac{h\nu_0}{\text{Electron Volts}}$	$U_0$ erg cm. <sup>6</sup>	$U_I$ erg cm. <sup>6</sup>	$U_D$ erg cm. <sup>6</sup>
CO	0.12	1.99	14.3	0.0034	0.057	67.5
HI	0.38	5.4	12	0.35	1.68	382
HBr	0.78	3.58	13.3	6.2	4.05	176
HCl	1.03	2.63	13.7	18.6	5.4	105
NH <sub>3</sub>	1.5	2.21	16	84	10	93
H <sub>2</sub> O	1.84	1.48	18	190	10	47

London,<sup>10</sup> the energy values are shown for six molecules. In columns 2, 3 and 4 the dipole moments, polarizabilities and characteristic energies are tabulated for the six gases. In columns 5, 6 and 7 the orientation, induction, and dispersion energies are given, calculated by means of equation (18). The induction effect is always small, it amounts at most to 5% of the total van der Waals attraction. The orientation effect is negligibly small for molecules having small dipole moments, such as CO and HI, and it is much smaller than the dispersion effect even for molecules having as large dipole moments as HCl. Only for molecules having very large dipole moments, such as NH<sub>3</sub> and H<sub>2</sub>O, does the orientation effect become equal to or greater than the dispersion effect, and the latter is never negligible.

According to equation (18) for molecules without permanent dipoles the van der Waals potential is given solely by the dispersion effect, since  $\mu = 0$ . However, this is not entirely true; equation (14) does not represent the van der Waals potential completely for all distances even for rare gas atoms. At small values of  $r$  two other



effects must be considered: an additional attraction term and the energy of repulsion.

The attraction energy term expressed in equation (16) arises from the fluctuating dipoles that even a non-polar molecule possesses, as we have seen. However, besides these fluctuating dipoles a molecule also possesses fluctuating quadrupoles. These induce dipoles in a neighboring molecule, and the mutual interaction energy between fluctuating quadrupole and induced dipole is given by

$$(19) \quad U_q = -\frac{D}{r^3}$$

where  $D$  is a constant. Equation (19) is analogous to equation (12), which represents the interaction potential between a permanent quadrupole and an induced dipole moment. Margenau<sup>11</sup> calculated the fluctuating quadrupole-induced dipole interaction for hydrogen and helium atoms, and found that for small distances it was not negligible in comparison with the fluctuating dipole-induced dipole interaction. For two helium atoms at the equilibrium distance of 2.9 Å the quadrupole-dipole interaction amounts to 26% of the dipole-dipole interaction.

In the complete van der Waals attraction potential of non-polar molecules there are even higher interaction terms than that given in equation (19). The next higher term is the fluctuating quadrupole-induced quadrupole interaction which varies inversely as  $r^{10}$ . This term, however, appears to be always negligible. Margenau calculated that for two helium atoms at the equilibrium distance the quadrupole-quadrupole term amounts to only 3% of the dipole-dipole term.

The second energy term which is of great importance for small distances is the van der Waals repulsion energy. At the beginning of this section it was pointed out that if two molecules come sufficiently near to each other, they repel each other.

Originally the repulsion potential was expressed in the form of an inverse power function, just like the attraction terms

$$(20) \quad U_r' = \frac{B'}{r^n}$$

where  $B'$  and  $n$  are constants. Lennard-Jones<sup>12</sup> determined the value of  $n$  from the virial coefficients of gases and found that  $n = 12$  gives the best results, although even as low values of  $n$  as 9 and 10 could

<sup>11</sup> H. Margenau, *Phys. Rev.*, **38**, 747 (1931).

<sup>12</sup> J. E. Lennard-Jones, *Proc. Phys. Soc.*, **43**, 471 (1931).

fit the experimental data with suitable adjustment of the constant  $B'$ . Quantum mechanics, however, revealed that the repulsion potential is more correctly represented by an exponential law

$$(21) \quad U_r = B_r e^{-r/\rho_0}$$

where  $B_r$  and  $\rho_0$  are constants that can be evaluated from experiment.

The van der Waals interaction energy between two non-polar molecules is given by the sum of  $U_r$ ,  $U_D$  and  $U_q$ . On the basis of equations (21), (16) and (19) this can be written as

$$(22) \quad U = B_r e^{-r/\rho_0} - \frac{C}{r^6} - \frac{D}{r^8}$$

The first and third terms on the right hand side decrease much more rapidly with  $r$  than the second term; they are important therefore only for small distances. Furthermore, the repulsion energy is positive, the quadrupole-dipole term is negative, and so the two terms partially balance each other. In some calculations therefore one does not commit a serious error by neglecting them in comparison with the second term. We shall now discuss two tests of London's theory, in which it is assumed that the first and third terms of equation (22) are negligible and the van der Waals interaction is ascribed solely to the dipole-dipole term.

The first of these tests is the calculation of the van der Waals constant  $a$  from the dispersion effect. The van der Waals constants  $a$  and  $b$  are related to the dispersion energy constant  $C$  by the equation

$$(23) \quad a = \frac{4\pi^2 N_A^3 C}{9b}$$

where  $N_A$  is Avogadro's number. London<sup>10</sup> calculated  $C$  by means of equation (17), then using the experimental value of  $b$  calculated  $a$  by means of equation (23). The results are given in Table XX. A comparison of columns 3 and 4 shows a very good agreement between the theoretical and experimental values of  $a$ . Since the experimental values of  $a$  may be in error to the extent of about 30%, and since neglecting the two terms in equation (22) may introduce an error of about the same order of magnitude in the calculated values of  $a$ , the agreement between the absolute values must be considered fortuitous. On the other hand the agreement between the relative values through a 150 fold variation of  $a$  can not be ascribed to chance; one must conclude therefore that these calculations confirm London's theory.

The second test of the theory is the calculation of the heats of sublimation of molecular crystal lattices from the dispersion effect. In this calculation one must take into account the forces exerted on one molecule by all of its neighbors. London<sup>8</sup> proved that the dispersion forces are additive, i.e., the force (or potential) between two molecules is independent of the presence of other molecules in the

TABLE XX  
CALCULATION OF THE VAN DER WAALS CONSTANT  $a$  AND OF THE  
HEAT OF SUBLIMATION

Gas	$b(\text{exp.})$ cm. <sup>3</sup>	$a \times 10^{-4} (\text{calc.})$ atm. cm. <sup>3</sup> g. <sup>-2</sup>	$a \times 10^{-4} (\text{exp.})$ atm. cm. <sup>3</sup> g. <sup>-2</sup>	$L_s(\text{calc.})$ kcal./mole	$L_s(\text{exp.})$ kcal./mole
He	24	4.8	3.5	0.47	0.59
Ne	17	26	21	1.92	2.03
A	32.3	163	135	3.17	2.80
Kr	39.8	253	240		
Xe	51.5	430	410		
H <sub>2</sub>	26.5	46	24.5		
N <sub>2</sub>	39.6	147	135	1.64	1.86
O <sub>2</sub>	31.9	135	136	1.69	2.06
CO	38.6	166	144	1.86	2.09
CH <sub>4</sub>	42.7	256	224	2.42	2.70
CO <sub>2</sub>	42.8	334	361		
Cl <sub>2</sub>	54.8	680	632	7.18	7.43
HCl	40.1	283	366	3.94	5.05
HBr	44.2	510	442	4.45	5.52
HI				6.65	6.21

immediate vicinity. Since in a close-packed crystal a molecule has 12 nearest neighbors, the potential of a molecule in the lattice should be roughly equal to 12 times the mutual dispersion potential of two molecules given in equation (14). However, to calculate the heat of sublimation by taking 12 times the mutual potential and multiplying it by Avogadro's number would be to commit the error of counting each molecule twice. The total energy therefore is six times the interaction energy of a pair of molecules. This, however, takes into account only the interaction of immediate neighbors. Actually the more distant molecules also make some contribution to the attractive energy, so that the total energy is 7.38 times the mutual interaction energy of a pair of molecules. The distance of approach of the molecules in the lattice is obtained from the density of the crystal.

For the latent heat of sublimation London<sup>10</sup> gives the formula

$$(24) \quad L = 3.04 \times 10^{62} \frac{C\delta^2}{M^2} \text{ cal./mole}$$

where  $\delta$  is the density,  $M$  is the molecular weight, and  $C$  is the dispersion energy constant, calculated by means of equation (17). In order to avoid complications due to thermal motions, London corrected the experimental values of  $L$  and  $\delta$  to  $0^\circ$  K. The results are shown in the last two columns of Table XX. The agreement between theory and experiment is again quite satisfactory. Particularly interesting is the hydrogen halide series. In spite of the fact that the dipole moment decreases strongly from hydrogen chloride to hydrogen iodide (Table XIX, column 2), the heat of sublimation increases, showing that the major portion of the van der Waals energy can not be due to the permanent dipoles these molecules possess.

Shortly after the appearance of London's treatment the problem of inter-molecular forces between non-polar molecules was attacked by Slater and Kirkwood<sup>13</sup> on the basis of an entirely different quantum mechanical approach. Using a variational method to determine the perturbation energy, they obtained for the mutual potential of two similar molecules

$$(25) \quad U_s = -\frac{3}{4} \frac{eh}{r^6} \left( \frac{N_e \alpha^3}{m} \right)^{1/2}$$

where  $e$  and  $m$  are the charge and mass of the electron,  $\alpha$  is the polarizability, and  $N_e$  is the number of electrons in the outermost shell.

The relation between equation (25) and London's equation (14) can be better judged if one puts the latter in the form

$$(26) \quad U_D = -\frac{3}{4} \frac{eh}{r^6} \left( \frac{f \alpha^3}{m} \right)^{1/2}$$

where  $f$  is given by

$$(27) \quad f = m \alpha v_0^2 / e^2$$

The term  $f$  gives the effective number of dispersion electrons. It is usually referred to as the " $f$  value" of the dispersion curve. A comparison of equations (25) and (26) shows that  $f$  in London's equation is replaced by  $N_e$  in the equation of Slater and Kirkwood. Since  $N_e$  is usually greater than  $f$ , the dispersion energy  $U_s$  is usually greater than  $U_D$ .

Although London's treatment has the greater generality, Slater and Kirkwood achieved striking success in their calculation of the intermolecular forces between helium atoms. Their treatment is well adapted also for the fundamental calculation of polarizabilities. For the polarizability of helium they obtained the value of  $0.210 \times 10^{-24}$

<sup>13</sup> J. C. Slater and J. G. Kirkwood, *Phys. Rev.*, **37**, 682 (1931).

cc., which agrees very well with the experimental value of  $0.205 \times 10^{-24}$  cc. For the mutual interaction potential of two helium atoms they deduced the equation

$$(28) \quad U_{H_2} = \left\{ 7.7e^{-2.43r/a_0} - \frac{0.68}{(r/a_0)^6} \right\} \cdot 10^{-10} \text{ ergs}$$

where  $a_0$  is the radius of the Bohr orbit of hydrogen. Kirkwood and Keyes,<sup>14</sup> using this intermolecular potential, calculated the second virial coefficient of helium at different temperatures and obtained excellent agreement with experiment. They also calculated various other physical properties of helium with the help of the theoretical second virial coefficient. One example of these calculations is shown

TABLE XXI  
HELIUM PRESSURES CALCULATED FROM THE THEORETICAL VIRIAL

Temperature °C.	$v$ Liters/Mole	$p$ (obs.) atm.	$p$ (calc.) atm.
200	2.000	19.52	19.51
	0.400	99.82	99.60
100	2.000	15.40	15.39
	0.333	95.11	94.96
0	2.000	11.27	11.27
	0.250	94.12	93.97
-100	2.000	7.15	7.15
	0.200	75.66	75.45

in Table XXI. The pressure of helium was calculated at several temperatures and volumes by means of the expansion

$$(29) \quad p = (RT/v)(1 + B/v + 4B^2/3v^2)$$

where  $B$  is the theoretical second virial coefficient. It will be seen that the agreement between theory and experiment is very satisfactory.

It is an interesting fact that van der Waals forces play an important role even in the building of ionic crystal lattices. Born and Mayer<sup>15</sup> calculated that van der Waals forces contribute about 1 to 5% of the total lattice energy of the alkali halides. This seems to be a relatively small amount, and yet Mayer<sup>16</sup> showed that this small contribution is sufficient to explain the transition from the NaCl-like crystal structure to the CsCl-like structure. Seventeen of the twenty alkali halides

<sup>14</sup> J. G. Kirkwood and F. G. Keyes, *Phys. Rev.*, **37**, 832 (1931).

<sup>15</sup> M. Born and J. E. Mayer, *Z. Physik*, **75**, 1 (1932).

<sup>16</sup> J. E. Mayer, *J. Chem. Phys.*, **1**, 270 (1933).

crystallize in the NaCl-type lattice, and three crystallize in the CsCl-type lattice. Because of the large van der Waals attraction between the heavy  $\text{Cs}^+$  ion on the one hand, and the  $\text{Cl}^-$ ,  $\text{Br}^-$  and  $\text{I}^-$  ions on the other, CsCl, CsBr and CsI form crystal lattices in which the ions of the same kind have smaller distances from each other than in the NaCl-type lattice. Even CsF and RbI crystallize in the NaCl-type structure, and the transition to the denser form comes at CsCl, just as the theory demands.

### FUNDAMENTAL THEORY OF THE HEAT OF ADSORPTION

The development of the theory of the heat of van der Waals adsorption followed closely the development of the theory of van der Waals forces. Although de Saussure<sup>17</sup> had shown already in 1814 that the most readily condensable gases are adsorbed in the largest amounts by a variety of adsorbents, it was another hundred years before Eucken<sup>18</sup> first attempted to prove quantitatively that "the force of adsorption, at least in the case of the so-called physical adsorption, is essentially the same as the ordinary physical molecular attraction."

Eucken assumed that the attraction potential between a surface and a gas molecule can be expressed by an inverse power law

$$(30) \quad \varphi = -\frac{a_1}{r^m}$$

where  $r$  is the distance between the surface and the gas molecule and  $a_1$  and  $m$  are constants.<sup>19</sup> The concentration of the adsorbate at a distance  $r$  from the surface can be obtained from the Maxwell-Boltzmann distribution law

$$(31) \quad c_r = c_g e^{-\varphi/kT}$$

where  $c_r$  and  $c_g$  are the concentrations of the gas at a distance  $r$  from the surface and in the gas phase, respectively. The amount adsorbed

<sup>17</sup> T. de Saussure, *Gilbert's Ann. der Physik.*, 47, 113 (1814).

<sup>18</sup> A. Eucken, *Verh. d. deutschen phys. Ges.*, 16, 345 (1914); *Z. Elektrochem.*, 28, 6 (1922).

<sup>19</sup> The relation between the adsorption potential  $\varphi$  and the Polanyi potential  $\epsilon$  is given by

$$\varphi = \epsilon + E_L$$

where  $E_L$  is the heat of condensation of the gas. The adsorption potential differs from the heat of adsorption by the heat of compression, which is often negligible. In the present chapter the terms adsorption potential and heat of adsorption are used interchangeably. The relations between these energy terms and others are discussed in detail in Chapter VIII.

is given by

$$(32) \quad v = A \int_{r_0}^{\infty} (c_r - c_g) dr = A c_g \int_{r_0}^{\infty} (e^{a_1/r^m k T} - 1) dr$$

where  $v$  is the number of moles of gas adsorbed,  $A$  is the surface area of the adsorbent, and  $r_0$  is the distance of closest approach to the surface. Eucken assumed that  $r_0$  is equal to the radius of the adsorbed molecule. For  $\varphi \gg kT$  the integration gives

$$(33) \quad \frac{v}{c_g} = \frac{A r_0 e^{C_0/T}}{\frac{m C_0}{T} - b(m)}$$

with

$$(34) \quad C_0 = \frac{a_1}{r^m k}$$

Since  $a_1/r^m$  has the dimension of energy and  $k$ , the Boltzmann constant, that of energy per degree,  $C_0$  has the dimension of temperature.  $RC_0$  is the amount of work necessary to take one mole of the adsorbed gas from the surface to infinite distance. The term  $b(m)$  in equation (33) is a function of  $m$  usually negligible in comparison with  $mC_0/T$ . Neglecting this term, and introducing the pressure of the gas in place of the concentration, i.e.,  $p = c_g RT$ , we obtain

$$(35) \quad \frac{v}{p} = \frac{A r_0}{R C_0 m} e^{C_0/T}$$

At constant temperature all the terms on the right hand side of equation (35) are constant. Thus Eucken's equation applies only to the linear beginning portion of the adsorption isotherm. Eucken did not attempt to derive the law of force for the attraction from fundamental physical considerations; he merely evaluated  $m$ , the exponent of  $r$  in equation (30), from the adsorption isotherm itself. He succeeded in fitting the adsorption data of Miss Homfray<sup>20</sup> for nitrogen on charcoal by using the constants  $m = 4$ ,  $C_0 = 2200$ , and  $\log A r_0 = -0.805$ .

Eucken also considered the repulsion energy by using the equation

$$(36) \quad \varphi = -\frac{a_1}{r^m} + \frac{a_2}{r^n}$$

Although there are two constants in the repulsion energy term,  $a_2$  can be eliminated by the condition that at the equilibrium distance  $r_0$

<sup>20</sup> I. F. Homfray, *Z. phys. Chem.*, 74, 129 (1910).

the forces of attraction and repulsion just balance each other

$$(37) \quad \left( \frac{d\varphi}{dr} \right)_{r=r_0} = 0$$

The adsorption potential of a molecule in the equilibrium position then becomes

$$(38) \quad kC_0 = \frac{a_1}{r^m} \left( 1 - \frac{m}{n} \right)$$

Using the constants  $m = 4$ ,  $n = 6$ ,  $C_0 = 1980$ , and  $\log Ar_0 = -2.31$ , Eucken obtained a slightly better fit for the data of Miss Homfray than he did with the three-constant equation (35). However, the fact that he did not know the surface of Miss Homfray's charcoal and therefore had to select empirically a value for  $Ar_0$  greatly diminishes the value of the quantitative aspects of his considerations.

Lorenz and Landé<sup>21</sup> were the first to attempt to evaluate the heat of adsorption from fundamental physical considerations. Following Keesom's idea that the van der Waals attraction between molecules possessing permanent dipoles is due to the interaction of these dipoles<sup>4</sup> (orientation effect), Lorenz and Landé calculated the order of magnitude of the heat of adsorption between a dipole molecule and a conducting and completely polarizable surface.

Lord Kelvin showed that the force of attraction between a dipole and an electrically conducting surface can be obtained by substituting in the place of the surface a mirror image of the dipole in the surface with the poles reversed, and calculating the force between the dipole and its mirror image. Figure 81, taken from Magnus,<sup>22</sup> illustrates the method. The circle represents the cross section of a water molecule, imagined as a sphere; the point in the center represents the oxygen ion, and the two points on the circumference the two hydrogen ions. The center of gravity of the positive charge lies midway between the two hydrogen ions, the center of gravity of the negative charge coincides with the center of the oxygen ion. The distance between the two centers of gravity is  $x$ , and the dipole moment is  $ex$ , where  $e$  is the charge. The distance between the middle points of the dipole and its mirror image is  $2r$ , and the angle between the dipole axis and the line connecting the middle points is  $\beta$ . If  $r \gg x$ , the interaction potential is given by

$$(39) \quad \varphi_{rd} = - \frac{\mu^2}{(2r)^3} (1 + \cos^2 \beta)$$

<sup>21</sup> R. Lorenz and A. Landé, *Z. anorg. Chem.*, **125**, 47 (1922).

<sup>22</sup> A. Magnus, *Z. phys. Chem.*, **A142**, 401 (1922).



where  $\mu$  is the dipole moment of the molecule. (The subscript *rd* signifies rigid dipole.)

The amount of gas adsorbed can be obtained again with the help of the Maxwell-Boltzmann distribution law, expressed in equation (31), but the value of  $\varphi$  is now given by equation (39). The integration

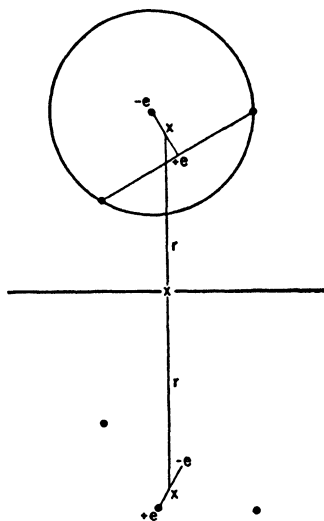


FIG. 81.—The interaction between a dipole molecule and a conducting surface by means of the electrostatic image force of Kelvin.

must be carried out over all the values of  $\cos \beta$ . If it is assumed that  $\varphi_{rd} \gg kT$ , one obtains

$$(40) \quad \frac{v}{p} = \frac{Ar_0}{6RC_0} \frac{e^{C_0/T}}{C_0/T}$$

with

$$(41) \quad C_0 = \frac{\mu^2}{4r_0^3k}$$

Since all terms on the right hand side of equation (40) are constant at constant temperature, the equation can be valid only for the linear beginning portion of the adsorption isotherm.

A comparison of equations (34) and (41) shows that Lorenz and Landé obtained a physical interpretation for  $a_1$  and  $m$ , which appeared as empirical constants in Eucken's treatment. For the interaction of a permanent dipole with a conducting surface  $a_1 = \mu^2/4$ , and  $m = 3$ .

It will be seen later that the interaction energy between a gas molecule and a surface is inversely proportional to the third power of the distance between molecule and surface not only for the orientation effect here discussed, but also for the induction and dispersion effects.

Lorenz and Landé estimated the order of magnitude of  $C_0$  by setting

$$(42) \quad \begin{aligned} \mu &\approx 10^{-18}, & r_0 &\approx 10^{-8}, & k &= 1.37 \times 10^{-16} \\ C_0 &\approx \frac{10^{-36}}{4 \times 10^{-24} \times 1.37 \times 10^{-16}} \approx 2000^\circ \end{aligned}$$

Since the heat of adsorption is  $RC_0$ , it is approximately equal to 4000 calories per mole. This has the right order of magnitude for the heats of physical adsorption. However, the assumed value of  $1\text{\AA}$  for  $r_0$  is really much too small. If one makes  $r_0 = 2\text{\AA}$ , the value of  $\varphi$  decreases 8 fold, giving a value of only 500 calories. It seems therefore that although  $\varphi_{rd}$  may be an important constituent of the heat of adsorption for dipole molecules, it is insufficient to account alone for the entire heat of adsorption.

Jaquet<sup>23</sup> went a step farther in the calculation of the heats of adsorption by considering the induction effect along with the orientation effect. If one regards a molecule not as a rigid dipole but as a polarizable dipole, the interaction potential between it and its mirror image is given by

$$(43) \quad \varphi_{pd} = -\frac{\mu^2}{(2r)^3} \left( \frac{2}{1-2\eta} \cos^2 \beta + \frac{1}{1-\eta} \sin^2 \beta \right)$$

with

$$(44) \quad \eta = \frac{\alpha}{(2r)^3}$$

Here  $\alpha$  is the polarizability of the molecule, and  $\mu$ ,  $r$ , and  $\beta$  have the same meaning as in equation (39). When  $\alpha = 0$ , equation (43) reduces to equation (39).

At very low temperatures the dipoles are all oriented, i.e.,  $\beta = 0$ . Equation (43) then takes on the simplified form

$$(45) \quad \varphi_{pd} = -\frac{\mu^2}{(2r)^3} \frac{2}{1-2\eta}$$

Jaquet showed that in the temperature range in which equation (45) is valid the adsorption potential of a polarizable dipole is 33% greater than that of a rigid dipole. In other words, the induction effect amounts to one third of the orientation effect.

<sup>23</sup> E. Jaquet, *Fortschritte Chem., Phys., phys. Chem., Series B*, 18, H7 (1925).

At high temperatures all values of  $\beta$  become equally probable, and the mean potential is given by

$$(46) \quad \bar{\varphi}_{pd} = -\frac{\mu}{(2r)^3} \frac{2}{3} \left( \frac{1}{1-2\eta} + \frac{1}{1-\eta} \right)$$

Since the expression for the adsorption potential contains the dipole moment of the gas molecule, one can calculate the magnitude of the dipole from the experimentally determined heat of adsorption, provided all other factors are known. Jaquet performed this calculation for three dipole gases: ammonia, sulfur dioxide and water. His results are shown in Table XXII. The values of  $\varphi$ , given in column 2, were calculated from the adsorption isotherms of Titoff<sup>24</sup> for ammonia on charcoal, of McGavack and Patrick<sup>25</sup> for sulfur dioxide on

TABLE XXII  
CALCULATION OF DIPOLE MOMENTS FROM HEATS OF ADSORPTION

Gas	$\varphi$ ergs $\times 10^{13}$	$\mu_{\text{max.}}$ e.s.u. $\times 10^{18}$	$\mu_{\text{min.}}$ e.s.u. $\times 10^{18}$	$\mu_{\text{obs.}}$ e.s.u. $\times 10^{18}$
NH <sub>3</sub>	3.5	1.58	1.36	1.49
SO <sub>2</sub>	3.8	1.79	1.55	1.61
H <sub>2</sub> O	8.55	1.98	1.72	1.84

silica gel, and of Gustaver<sup>26</sup> for superheated steam on charcoal. The dipole moments were calculated both on the assumption that the dipole is completely rigid (the orientation effect alone), and on the assumption that the dipole is completely polarizable (orientation and induction effect). The former assumption gives a minimum value for the dipole moment, the latter a maximum value. The experimental dipole moments were taken from Smyth.<sup>27</sup> A comparison of the last three columns of Table XXII shows that for all three gases the observed dipole moment falls between the calculated upper and lower limits.

Jaquet also calculated the interaction energy between a quadrupole molecule and a conducting surface. For a rigid rod-shaped quadrupole, the type shown in Fig. 80a), the adsorption potential is given by

$$(47) \quad \varphi_{rq} = -\frac{9}{4} \frac{\tau^2}{(2r)^5} \left( 1 + \frac{2}{3} \cos^2 \beta + \cos^4 \beta \right)$$

<sup>24</sup> A. Titoff, *Z. phys. Chem.*, **74**, 641 (1910).

<sup>25</sup> J. McGavack and W. A. Patrick, *J. Am. Chem. Soc.*, **42**, 946 (1920).

<sup>26</sup> B. Gustaver, *Kolloidchem. Beihefte*, **15**, 259 (1921).

<sup>27</sup> C. P. Smyth, *Dielectric Constant and Molecular Structure*, New York, 1931, p. 192.

where  $\tau$ , the quadrupole moment, is equal to  $2ex^2$ , and  $\beta$  is the angle between the quadrupole axis and the normal to the surface.

To obtain the amount of gas adsorbed one can use again the Maxwell-Boltzmann law, with  $\varphi$  given by equation (47). Integrating over all values of  $\cos \beta$ , we get

$$(48) \quad \frac{v}{p} = \frac{Ar_0}{24.5RC_0} \frac{e^{C_0/T}}{C_0/T}$$

with

$$(49) \quad C_0 = \frac{\tau^2}{5.47r_0^3k}$$

At high temperatures it may be assumed that all values of  $\beta$  are equally probable. One obtains then the mean interaction potential from equation (47)

$$(50) \quad \bar{\varphi}_{rq} = -\frac{16}{5} \frac{\tau^2}{(2r_0)^5}$$

For the mean potential of a polarizable rod-shaped quadrupole Jaquet derived the equation

$$(51) \quad \bar{\varphi}_{pq} = -\frac{16}{5} \frac{\tau_k^2}{(2r_0)^5} + 3\alpha \frac{\Sigma \tau^2}{(2r_0)^8}$$

where  $\alpha$  is the polarizability and

$$(52) \quad \tau_k^2 = \tau_x^2 + \tau_y^2 + \tau_z^2 - \tau_x\tau_y - \tau_y\tau_z - \tau_z\tau_x$$

$$(53) \quad \Sigma \tau^2 = \tau_x^2 + \tau_y^2 + \tau_z^2$$

The definitions of the three electric moments of inertia,  $\tau_x$ ,  $\tau_y$  and  $\tau_z$ , were given in equation (11).

Jaquet calculated the quadrupole moments of a number of molecules from their heats of adsorption by means of equation (51). He first evaluated  $\tau_k$  from the equation of state of the gas according to the method of Debye,<sup>5</sup> then substituting the known values of  $r_0$ ,  $\alpha$  and  $\tau_k$  into equation (51) obtained the mean quadrupole moment  $\bar{\tau}$  from the experimental value of  $\bar{\varphi}_{pq}$ . The quadrupole moments thus obtained were of the right order of magnitude. It should be remembered, however, that the quadrupole moments are not independently measurable physical constants like the dipole moments, consequently their calculation from heats of adsorption is not as significant as the calculation of the dipole moments, discussed before.

The treatments of Lorenz and Landé<sup>20</sup> and Jaquet<sup>22</sup> deal with the interaction between polar molecules and conducting surfaces. Iliin<sup>28</sup>

<sup>28</sup> B. Iliin, *Phil. Mag.*, (6), 48, 193 (1924), 50, 1144 (1925); *Z. Physik*, 33, 435 (1925).

was the first to attempt the derivation of the interaction between non-polar molecules and surfaces containing electric charges. He assumed that the charges in the surface induce a dipole moment in the non-polar molecule, and that the attraction between this induced dipole and the surface charges gives rise to adsorption.

According to Iliin the strength of the electric field surrounding the adsorbent is given by

$$(54) \quad E = \frac{E_0}{\epsilon}$$

where  $E_0$  is the field strength in vacuum and  $\epsilon$  is the dielectric constant of the gas. For the variation of  $E_0$  with the distance from the adsorbent he assumed the inverse power law

$$(55) \quad E_0 = \frac{e_1}{r^\nu}$$

where  $e_1$  is a constant dependent on the charge distribution of the adsorbent and  $\nu$  is another constant. The dipole induced in a molecule at a point where the field strength is  $E$  is given by

$$(56) \quad \mu = \alpha \frac{E_0}{\epsilon} = \frac{E_0}{4\pi n} \frac{\epsilon - 1}{\epsilon}$$

where  $\alpha$  is the polarizability of the gas molecule, and  $n$  is the number of gas molecules per cc. The substitution

$$(57) \quad \alpha = \frac{\epsilon - 1}{4\pi n}$$

is permissible only for molecules possessing no permanent dipole moments. The force acting on an induced dipole is

$$(58) \quad F = \frac{e_1^2 \nu}{4\pi n r^{2\nu+1}} \frac{\epsilon - 1}{\epsilon}$$

The adsorption potential is the force times the distance through which it acts, i.e.,  $F \Delta r$ . The amount adsorbed is calculated with the help of the Maxwell-Boltzmann law according to Eucken's method, given in equations (31) and (32). The result is

$$(59) \quad \frac{v}{p} = \frac{A r_0}{\varphi_0} (e^{\varphi_0/kT} - 1)$$

with

$$(60) \quad \varphi_0 = F_0 r_0 = \frac{e_1^2 \nu}{4\pi n r_0^{2\nu}} \frac{\epsilon - 1}{\epsilon}$$

Iliin showed that by substituting equation (60) into equation (59) one obtains the relationship

$$(61) \quad \log \left( v \frac{\epsilon - 1}{\epsilon} \right) = C_1 + C_2 \frac{\epsilon - 1}{\epsilon}$$

where  $C_1$  and  $C_2$  are constants at constant temperature and pressure. Thus a plot of  $\log \left( v \frac{\epsilon - 1}{\epsilon} \right)$  against  $\frac{\epsilon - 1}{\epsilon}$  should give a straight line for different gases adsorbed on the same adsorbent. Using the data of Miss Homfray<sup>20</sup> and Titoff<sup>24</sup> for the adsorption of different gases on charcoal, Iliin actually did obtain a straight line relationship. However, Hückel<sup>29</sup> pointed out that this test is so insensitive that it can by no means be regarded as a decisive confirmation of Iliin's theory.

It was shown in Table XIX that for most molecules the dispersion energy is the largest constituent of the van der Waals attraction potential. Only for molecules having very large dipole moments does the orientation energy exceed the dispersion energy. It would be expected therefore that in the van der Waals adsorption of non-polar gases by non-ionic adsorbents the dispersion forces would play a decisive role. As a matter of fact, even for molecules with fairly large dipole moments, such as HCl, the orientation effect can constitute only a small part of the heat of adsorption. Using equation (41), a rough calculation shows that the orientation potential amounts to only 10% of the heat of adsorption of HCl on charcoal. Although the dispersion effect is undoubtedly important even in the adsorption of the strongest dipole molecules, it probably does not constitute the dominant portion of the heats of adsorption. This is evidenced by the fact that Jaquet successfully calculated the approximate magnitudes of the dipole moments of  $\text{NH}_3$ ,  $\text{SO}_2$  and  $\text{H}_2\text{O}$  from their heats of adsorption on the basis of the orientation and induction effects only, as was shown in Table XXII.

The dispersion effect was introduced in the calculation of the heats of adsorption by London.<sup>8</sup> He objected to attributing van der Waals adsorption to attraction between permanent dipoles in the gas molecules and electric charges in the surface, on the ground that such a picture would necessitate a change in the sign of the force of interaction every time a molecule moved from one point of the surface to a neighboring point. This would greatly hinder the motion of the molecule over the surface, contradicting the generally held view that in

<sup>29</sup> E. Hückel, *Adsorption und Kapillarkondensation*, Leipzig, 1928, p. 135.

physical adsorption the molecules possess free mobility over the surface. An evidence of free motion was given in the discussion of the potential theory in Chapter V, namely, that the equation of state of the gas is obeyed even in the adsorbed phase. Another evidence was supplied by Volmer and Adhikari<sup>30</sup> who proved experimentally the mobility of adsorbed molecules, as will be discussed in Chapter XIII. These facts point to the importance of the dispersion forces in adsorption, since these forces are always attractive and do not change sign as the molecule moves over the surface.

The dispersion potential between a molecule of the gas and an atom or a molecule of the adsorbent can be written according to equation (16)

$$(62) \quad \varphi = -\frac{C}{r^6}$$

The interaction between a gas molecule and the entire surface of the adsorbent can be very simply calculated if one assumes that the distances between the atoms of the adsorbent are small compared with the distances between the gas molecule and the adsorbent atoms. In this case the summation over the atoms of the adsorbent can be replaced by an integration. For the mutual dispersion energy of an infinitely large surface and an isolated gas molecule London obtained

$$(63) \quad \varphi_D = -\int \frac{C}{r^6} N dv = -\frac{N\pi C}{6r^3}$$

where  $N$  is the number of adsorbent atoms per cc., and  $dv$  is the volume element. Due to the integration over the three dimensions of the adsorbent, the exponent of  $r$  in the denominator is decreased by 3. Thus the adsorption potential for the orientation, induction, and dispersion effects is inversely proportional to the third power of the distance between molecule and surface according to equations (39), (43) and (63)

The value of the dispersion constant  $C$  for two molecules of the same kind was given in equation (17). For two dissimilar molecules its value is

$$(64) \quad C = \frac{3}{2} \alpha \alpha' \frac{JJ'}{J + J'}$$

where  $\alpha$  and  $\alpha'$  are the polarizabilities and  $J$  and  $J'$  are the characteristic energies of the two molecules ( $J = h\nu_0$  and  $J' = h\nu_0'$ ). Equation

<sup>30</sup> M. Volmer and G. Adhikari, *Z. phys. Chem.*, 119, 46 (1926).

(64) is applicable to the case of adsorption also;  $\alpha$  and  $J$  are then the polarizability and characteristic energy of the adsorbate, and  $\alpha'$  and  $J'$  are those of the adsorbent.—Substituting equation (64) into equation (63), we obtain

$$(65) \quad \varphi_D = - \frac{N\pi}{4} \frac{\alpha\alpha'}{r^3} \frac{JJ'}{J + J'}$$

An exact evaluation of the adsorption potential from equation (65) is not possible because some of the experimental data are missing. Particularly the value of  $J'$  for the adsorbent is unknown, and as a matter of fact in this case the substitution of one characteristic vibration in place of all the different vibrations that the adsorbent can execute is not permissible. Nevertheless, to show at least the order of magnitude of  $\varphi_D$ , London calculated the heats of adsorption of a number of gases on charcoal, using the ionization potential of carbon for  $J'$ , and calculating  $\alpha'$  from the atomic refraction of carbon. The value of  $N$  was obtained by assuming that the true density of charcoal was the same as that of graphite. The distance  $r$  between a carbon atom of the surface and an adsorbate molecule was assumed to be made up of two parts

$$(66) \quad r = \frac{d_1}{2} + \frac{d_2}{2}$$

For  $d_1/2$  London took half the distance between layers of graphite, i.e., 1.67Å, and he calculated the values of  $d_2/2$  from the van der Waals constants  $b$  of the adsorbed gases. The values of  $\varphi_D$  thus calculated seemed to be in fair agreement with the experimental heats of adsorption. However, de Boer and Custers<sup>31</sup> pointed out that London committed a numerical error that made his calculated values ten times as large as they should have been. To explain the great discrepancy that resulted they suggested that the adsorption of gases on charcoal occurs in pockets, tubes and cavities of various shapes, where the heats of adsorption are considerably larger than on plane surfaces.

While the explanation of de Boer and Custers may be entirely correct, another possible cause of the discrepancy may be suggested here. First of all, as de Boer and Custers pointed out, the use of integration in place of summation over the atoms of the adsorbent in equation (63) is not justified when  $r$  is as small as 3.0–3.4Å, the values used in London's calculations. Summation would give about twice as large  $\varphi_D$  values as integration. The value of  $\varphi_D$  for the

<sup>31</sup> J. H. de Boer and J. F. H. Custers, *Z. phys. Chem.*, B25, 225 (1934).



adsorption of nitrogen by charcoal is about 600 calories per mole when calculated on the basis of equation (65); using summation in place of integration would lead to about 1200 calories per mole. In the second place it should be remembered that the isotherms obtained on most charcoals indicate that the adsorption occurs in very narrow capillaries. If charcoal consists of graphite-like layers and the nitrogen molecules are adsorbed between the layers, the adsorbate molecules are in contact with two layers of carbon atoms instead of one, therefore  $\varphi_D$  is twice as large as on a free plane surface. This would make the calculated heat of adsorption about 2400 calories per mole, as compared to the experimental value of about 3200 calories per mole. Considering the approximations involved in the theory and the uncertainties in the assumed values of  $J'$ ,  $\alpha'$ ,  $N$ , and  $r^3$ , one can not expect more than an agreement in the order of magnitude between calculated and experimental values.

Lenel<sup>32</sup> calculated the heats of adsorption of argon, krypton, and carbon dioxide on ionic crystals. The attraction potential between a rare gas atom and an ionic crystal consists of two main parts: the dispersion effect and the so-called influence effect. The latter is due to the fact that the charged ions of the lattice induce a dipole moment in the rare gas atom, which results in an attraction between the ions and the induced dipole.

The more important of the two energy terms is the dispersion potential. Lenel assumed that the rare gas atom sits on the surface in such position that it is in contact with the largest possible number of ions, then he calculated the dispersion energy between the atom and each neighboring ion of the lattice according to London's equation (65). He took the polarizabilities and characteristic energies of the ions from Mayer.<sup>16</sup> The characteristic energies here are not simply the ionization potentials of the free ions. The ionization potential measures only the work necessary to remove an electron from a closed shell, but when an electron is removed from the surface of an ionic crystal one must add to this the work expended against the Coulomb forces in removing the free electron from the surrounding ions. Mayer evaluated the polarizabilities from the extrapolated indices of refraction of the ionic crystals by ascribing part of the polarizability of the crystal to the positive and part to the negative ion. Lenel, following London, divided the distance  $r$  into two parts, assumed  $d_1/2$  to be equal to the Goldschmidt radius of the ion and calculated  $d_2/2$ , the

<sup>32</sup> F. V. Lenel, *Z. phys. Chem.*, **B23**, 379 (1933).

radius of the rare gas atom, from the lattice distance of the solidified gas.

In calculating the ion-induced dipole interaction (influence effect) one can not use the mean polarizability of the rare gas atom, because the field of the ionic lattice is very inhomogeneous. Practically the entire effect depends on that part of the electron shell of the atom which is in the immediate vicinity of the ions. The expression for the interaction energy was derived by Teller, and it is given by

$$(68) \quad \varphi_I = \int \frac{(P - P_0)^2 \rho}{J} dv$$

where  $P_0$  is the potential at the center of the rare gas atom,  $P$  is the potential and  $\rho$  is the electron density in the volume element  $dv$ , and  $J$  is the characteristic energy of the adsorbed atom. It was pointed out in the previous section that for rare gases  $J$  can be set equal to the ionization potential. The potential distribution in the vicinity of the surface of an ionic lattice was calculated according to the method of Born,<sup>33</sup> and the electron density in the different parts of the rare gas atom was calculated according to the method of Fermi.<sup>34</sup> The influence energy was obtained by subdividing that part of the electron shell of the rare gas atom which is nearest to an ion of the surface into sixteen volume elements, calculating  $P$  and  $\rho$  separately for each element, forming the product  $(P - P_0)^2 \rho \cdot \Delta v$  for each, summing up the products, and dividing by  $J$ . Figure 82 illustrates the calculation of the influence energy between an argon atom and a potassium ion. The intersecting circles represent surfaces of equal potential and surfaces of equal electron density. Outside of the sixteen volume elements the rest of the argon atom contributes very little to the influence effect.

Since the equilibrium position of the influence forces is different from that of the dispersion forces, a correction must be applied to the calculated influence energy. The potential minimum for the dispersion forces is at the point where the rare gas atom is in contact with the largest possible number of lattice ions, but the potential minimum for the influence forces is at the point where the atom is exactly above a positive ion, as shown in Fig. 82. The correction applied to the influence energy at the point where the dispersion potential has its minimum amounts to about 10–20%.

<sup>33</sup> M. Born, *Atomtheorie des festen Zustandes*, Leipzig, 1923, p. 722.

<sup>34</sup> E. Fermi, *Quantentheorie und Chemie*, Leipzig Lectures, 1928, p. 95.

A comparison of the calculated heats of adsorption with the experimental values is given in Table XXIII. Columns 3 and 4 reveal that the dispersion energy is from two to four times as large as the influence energy. The experimental heats of adsorption were measured by Lenel himself, using the indirect method discussed in

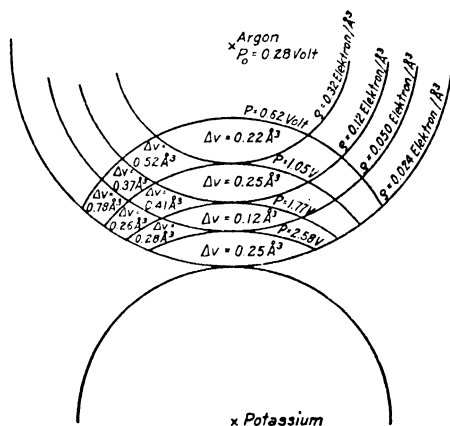


FIG. 82.—The influence force (ion-induced dipole interaction) between a potassium ion and an argon atom.

Chapters II and VIII. The agreement between theory and experiment is quite satisfactory. Lenel did not make an allowance for the repulsion energy. He argued that the repulsion term in equation (22) is probably small compared with the dipole-dipole term, and furthermore that it is roughly balanced by the quadrupole-dipole term, which is also neglected. In justification of Lenel's point of view we may

TABLE XXIII  
HEATS OF ADSORPTION ON IONIC CRYSTALS  
All energy values are given in calories

Gas and Adsorbent	Experimental Heat of Adsorption	$\varphi_D$	$\varphi_I$	$\varphi_E$	Theoretical Heat of Adsorption
A on KCl	2080	1500	370	—	1870
A on KI	2520	1420	680	—	2100
A on LiF	1770	1230	540	—	1770
Kr on KCl	2620	1930	550	—	2480
CO <sub>2</sub> on KCl	6350	2900	740	(2700)	(6340)
CO <sub>2</sub> on KI	7450	3300	1140	3250	7690

recall that London successfully calculated the van der Waals constants  $a$  and the heats of sublimation of molecular crystals by using the dipole-dipole term alone and neglecting the two other terms.

In the calculation of the heats of adsorption of carbon dioxide on ionic crystals there is a third term in the attraction potential, due to the fact that carbon dioxide possesses a large permanent quadrupole moment. The attraction between the ions and the quadrupole gives rise to the electrostatic potential  $\varphi_E$ . Lenel calculated the magnitude of the quadrupole moment from the heat of adsorption of carbon dioxide on potassium chloride, then using this value calculated  $\varphi_E$  for the interaction of carbon dioxide with potassium iodide. The theoretical heat of adsorption, i.e., the sum of  $\varphi_D$ ,  $\varphi_I$  and  $\varphi_E$ , is 7690 calories, as compared to the experimental value of 7450 calories (Table XXIII).

London's treatment of the interaction between a non-polar molecule and a surface is applicable only to adsorbents that are non-conductors, such as ionic crystals. The interaction between a metal and a non-polar molecule was first treated by Lennard-Jones.<sup>35</sup> He assumed that the metal was a completely polarizable body and calculated the interaction between the conducting surface and the fluctuating dipole of the gas molecule by the method of electrical images. The treatment was half-classical, half quantum mechanical. He treated the metal classically by assuming that the effect of the metal on the molecule was the same as that of the classical image potential acting on the electrons and nuclei of the molecule. On the other hand he regarded the molecule as a quantum mechanical system, with the image potential acting on it as a perturbation. The expression derived by him was <sup>36</sup>

$$(68) \quad \varphi_{DL} = - \frac{e^2 \overline{x^2}}{12r^3}$$

where  $e^2 \overline{x^2}$  is the mean square dipole moment (same as  $\overline{\mu^2}$  in equation 13), and  $r$  is the distance between the molecule and the atoms of the metal surface. Here again the attraction potential varies as the inverse third power of  $r$ .

The quantity  $\overline{x^2}$  can be calculated when the electron distribution in the molecule is known. It can also be obtained from the magnetic

<sup>35</sup> J. E. Lennard-Jones, *Trans. Far. Soc.*, 28, 333 (1932).

<sup>36</sup> Actually Lennard-Jones had 6 in the denominator instead of 12, a numerical error that made his calculated heats of adsorption twice as large as they should have been.

susceptibility of the gas. The interaction potential then becomes

$$(69) \quad \varphi_{DL} = \frac{mc^2\chi}{2N_A r^3}$$

where  $m$  is the mass of the electron,  $c$  is the velocity of light,  $\chi$  is the magnetic susceptibility of the gas, and  $N_A$  is Avogadro's number. The distance of closest approach of copper atoms in the metal is  $2.54\text{\AA}$ , that of argon atoms in the solid is  $3.84\text{\AA}$ . Lennard-Jones assumed that in the adsorption of argon by copper the distance  $r$  is the average of these two distances, i.e.,  $3.2\text{\AA}$ . Using this distance, the value of  $\varphi_{DL}$  is 5000 calories per mole. Allowing 40% for the repulsion potential, the heat of adsorption becomes 3000 calories, which is of the right order of magnitude.

Bardeen<sup>37</sup> improved the calculation of Lennard-Jones by treating the metal as well as the molecule quantum-mechanically. He obtained for the interaction energy

$$(70) \quad \varphi_{DB} = - \frac{e^2 \bar{x}^2}{12r^3} \frac{C_B e^2 / 2r_s h\nu_0}{1 + C_B e^2 / 2r_s h\nu_0}$$

where  $C_B$  is a numerical constant (approximately equal to 2.5),  $r_s$  is the radius of a sphere containing one metal electron, and  $h\nu_0$  is the characteristic energy of the gas (approximately equal to its ionization potential). For ordinary electron densities in the metal and with  $h\nu_0$  equal to about one Rydberg unit (13.5 electron volts) the factor  $C_B e^2 / 2r_s h\nu_0$  is about equal to unity. Thus  $\varphi_{DB}$ , the dispersion potential according to Bardeen, is still proportional to  $1/r^3$ , but it is only half as large as  $\varphi_{DL}$ , the image value of Lennard-Jones. The discrepancy is due to the fact that Lennard-Jones neglected a term in the kinetic energy of the metal-molecule system.

Margenau and Pollard<sup>38</sup> calculated the adsorption potential between molecule and metallic surface by using a somewhat different picture. They subdivided the metal into small elements and considered the interaction between the dipole field of a small element and a molecule. The interaction of a half infinite metal body with the molecule was then obtained by adding the contributions of the small elements. The resulting equation is

$$(71) \quad \varphi_{DM} = \varphi_1 + \varphi_2 = - \left[ \frac{e^2 \hbar}{m} \alpha_m(\nu_0) \frac{f}{\nu_0} + \frac{C_B e^2}{2r_s} \alpha_s(0) \right] / 8r^3$$

<sup>37</sup> J. Bardeen, *Phys. Rev.*, **58**, 727 (1940).

<sup>38</sup> H. Margenau and W. G. Pollard, *Phys. Rev.*, **60**, 128 (1941).

where  $\alpha_m(\nu_0)$  is the polarizability of the metal for the frequency  $\nu_0$ ,  $f$  is the  $f$  value of the dispersion formula of the gas (defined in equation 27),  $\alpha_g(0)$  is the static polarizability of the gas, and  $\nu_0$ ,  $C_B$  and  $r_s$  were defined in connection with equation (70). The polarizability of the metal for frequency  $\nu_0$  is given by

$$(72) \quad \alpha_m(\nu_0) = -\rho e^2 / 4\pi^2 m \nu_0^2$$

where  $\rho$  is the number of electrons per unit volume of the metal. The value of  $f$  when the dispersion formula contains only one frequency is

$$(73) \quad f = m\alpha_g(0)\nu_0^2/e^2$$

Since  $\alpha_m(\nu_0)$  is negative for the resonance frequencies of the molecule, the energy term  $\varphi_1$  is positive, giving rise to repulsion. The

TABLE XXIV  
DISPERSION POTENTIALS FOR GAS-METAL SYSTEMS  
All energy values are given in electron volts

Metal	Gas	$\varphi_1$	$-\varphi_2$	$-\varphi_{DM}$	$-\varphi_{DB}$	$-\varphi_{DL}$
Na	He	0.02	0.23	0.21	0.16	0.61
	A	0.20	1.80	1.60	1.19	3.54
	H <sub>2</sub>	0.12	0.89	0.77	0.53	1.40
	N <sub>2</sub>	0.24	1.92	1.68	1.42	3.95
Ag	He	0.04	0.30	0.26	0.20	0.61
	A	0.47	2.37	1.90	1.42	3.54
	H <sub>2</sub>	0.28	1.18	0.90	0.62	1.40
	N <sub>2</sub>	0.55	2.53	1.98	1.78	3.95
Pt	He	0.05	0.31	0.27	0.20	0.61
	A	0.53	2.49	1.96	1.46	3.54
	H <sub>2</sub>	0.32	1.23	0.92	0.64	1.40
	N <sub>2</sub>	0.62	2.65	2.03	1.72	3.95
Cu	He	0.06	0.34	0.28	0.21	0.61
	A	0.67	2.69	2.02	1.52	3.54
	H <sub>2</sub>	0.41	1.34	0.93	0.67	1.40
	N <sub>2</sub>	0.80	2.88	2.08	1.80	3.95
Zn, Cd, Hg rough average	He	0.08	0.38	0.30	0.23	0.61
	A	0.95	3.02	2.07	1.63	3.54
	H <sub>2</sub>	0.58	1.50	0.92	0.71	1.40
	N <sub>2</sub>	1.13	3.23	2.10	1.92	3.95

values of  $\varphi_{DM}$ , the dispersion potential according to Margenau and Pollard, as well as the values of its two constituent parts  $\varphi_1$  and  $\varphi_2$  are given in Table XXIV for a number of gas-metal systems. The values were calculated for  $r = 1\text{\AA}$ . To obtain the adsorption po-

tential one must therefore divide the values of the table by  $r^3$ . Thus for the adsorption of argon by copper  $\varphi_{DM}$  is 2.02 electron volts or 46,500 calories, and this is to be divided by  $3.2^3$ . This gives a heat of adsorption of 1420 calories per mole, a value much too small. Of course, it is possible that the nuclei of argon and copper come somewhat closer to each other than the  $3.2\text{\AA}$  assumed by Lennard-Jones,<sup>35</sup> in which case the calculated heat of adsorption would be larger than 1420 calories.

The last two columns of Table XXIV give the values of  $\varphi$  according to Bardeen and Lennard-Jones, calculated by means of equations (70) and (68). Bardeen's values are somewhat smaller than those of Margenau and Pollard, but the two are in fairly good agreement. The image potential, however, is considerably larger than the two others. Since the treatment of Lennard-Jones assumed that the metals are completely polarizable,  $\varphi_{DL}$  in the last column of the table is the same for the interaction of any particular gas with all metals. The heats of adsorption, however, will be different for the different metals, because  $r^3$  will be different. (The value of  $r$  depends upon the density of the metal.)

Lennard-Jones, Bardeen, and Margenau and Pollard obtained dispersion potentials that decrease as the third power of the distance between molecule and surface. It was pointed out by Prosen, Sachs, and Teller<sup>39</sup> that these three treatments are valid only for large values of  $r$ , and that for small distances the potential is proportional to  $1/r$  if a free electron gas is assumed in the metal, and to  $1/r^2$  if a degenerate Fermi gas is assumed. The treatment of Prosen, Sachs and Teller was based on the perturbation theory, which is applicable only if the molecule is so far from the surface that the wave functions of the molecule and metal electrons do not overlap appreciably. On the other hand, the Coulomb interaction between the electrons of the metal was neglected in the calculations, which is permissible only for small values of  $r$ . The treatment therefore is probably valid only for the first adsorbed layer on the surface of the metal.

For a free electron gas in the metal Prosen and Sachs<sup>40</sup> give the equation

$$(74) \quad \varphi_{DP} = - \frac{\pi \alpha e^2 \rho}{2r}$$

where  $\alpha$  is the polarizability of the gas, and  $\rho$  is the number of free electrons per unit volume of the metal. This formula should hold

<sup>39</sup> E. J. R. Prosen, R. G. Sachs and E. Teller, *Phys. Rev.*, 57, 1066 (1940).

<sup>40</sup> E. J. R. Prosen and R. G. Sachs, To be published in *Phys. Rev.*

for low electron densities, i.e., for semi-conductors and possibly for metals at high temperatures. When the Fermi degeneracy of the electron gas is taken into consideration the potential becomes

$$(75) \quad \varphi_{DS} = - \frac{\alpha e^2 k_m^2}{8\pi^2} \frac{\ln 2k_m r}{r^2}$$

where  $k_m$  is connected with the electron density  $\rho$  by the equation

$$(76) \quad k_m^3 = 3\pi^2 \rho$$

A calculation of  $\varphi_{DS}$  for the adsorption of argon by copper on the basis of equation (75) gives a value of 2750 calories per mole, if we again assume that  $r = 3.2\text{\AA}$ . This value is quite close to the experimental heat of adsorption.

Graphite as an adsorbent forms a transition between a metallic and a covalent surface. Barrer<sup>41</sup> believes that although graphite is a good conductor, imperfections in the crystals lead to a weakening of the metallic interlaminar binding, and chemisorbed hydrogen and oxygen also tend to make the surface more covalent. He calculated therefore the heats of adsorption of hydrogen, argon and nitrogen on graphite in two different ways: by assuming first a covalent and then a metallic structure for the adsorbent.

For the calculation of the heat of adsorption on a covalent surface Barrer used the equation

$$(77) \quad \varphi_{\text{cov.}} = - C \sum \left( \frac{1}{r^6} - \frac{1}{2} \frac{r_0^6}{r^{12}} \right)$$

where  $r_0$  is the equilibrium distance from the surface. This equation differs from London's equation (63) in two respects. In the first place, instead of integrating Barrer used the more accurate summation process. The summation was carried out to the nearest 100 carbon atoms, beyond which the attractive potential became negligible. In the second place the repulsion term was also taken into consideration.

For the calculation of the dispersion energy constant  $C$  Barrer used two formulas. First he used London's equation (64), but instead of the numerical factor  $3/2$  he adopted  $9/4$ , suggested by Born and Mayer;<sup>15</sup> then he calculated  $C$  by Kirkwood's formula<sup>42</sup>

$$(78) \quad C = 6mc^2 \frac{\alpha_1 \alpha_2}{\frac{\alpha_1}{\chi_1} + \frac{\alpha_2}{\chi_2}}$$

<sup>41</sup> R. M. Barrer, *Proc. Roy. Soc., A161*, 476 (1937).

<sup>42</sup> J. G. Kirkwood, *Phys. Z.*, **33**, 57 (1932).



where  $m$  is the mass of the electron,  $c$  is the velocity of light,  $\alpha_1$  and  $\alpha_2$  are the polarizabilities and  $\chi_1$  and  $\chi_2$  are the diamagnetic susceptibilities of the adsorbent and the adsorbate.

In the calculation of the van der Waals attraction by a metallic surface Barrer used the image force equation (68) of Lennard-Jones,<sup>35</sup> and allowed 40% for the repulsion energy. The results of all of his calculations are summarized in Table XXV. The experimental heats of adsorption, given in the last column, were determined by Barrer himself. He found that the heats of adsorption decreased with increasing amounts of gas adsorbed. He assumed that the initial high values were due to adsorption in crevices, and attributed the final low values to adsorption on plane surfaces. These are the values listed in the last column.

TABLE XXV  
HEATS OF ADSORPTION ON GRAPHITE

Substance	$\alpha \cdot 10^{24}$	$\chi \cdot 10^{30}$	$J$ kcal.	$\varphi$ (in calories)			$\Delta H - RT$ Experimental
				London	Kirk- wood	Lennard- Jones	
Carbon	0.937	10.54	259				
Hydrogen	0.775	4.20	377	780	670	487	900
Argon	1.65	27.8	396	1690	2520	3180	2200
Nitrogen	1.75	18.3	402	1810	2240	1990	2300

$$r_0 = 3.7\text{\AA}$$

Barrer concluded that Kirkwood's formula gave the best agreement with experiment. It should not be forgotten, however, that the assumption of  $3.7\text{\AA}$  for  $r_0$  may be too high, making the calculated values of  $\varphi$  too low, and that neglecting the quadrupole-dipole term also makes  $\varphi$  too low. It is possible that a more accurate calculation would give a better agreement with London's formula. At any rate the above calculations are too inaccurate to enable one to decide definitely which of the three methods gives the best fit with experiment.

So far the most elaborate calculation of the heat of van der Waals adsorption was carried out by Orr<sup>43</sup> for the systems argon-potassium chloride and argon-caesium iodide. His treatment differs from that of Lenel<sup>32</sup> in several respects. In the first place he calculated the dispersion energy not by London's equation (64), but by Kirkwood's equation (78), since Barrer<sup>41</sup> found that the latter agrees better with experiment. In the second place Orr calculated the ion-induced

<sup>43</sup> W. J. C. Orr, *Trans. Far. Soc.*, **35**, 1247 (1939).

dipole interaction, or influence energy, by a method different from that of Lenel. Finally, he included the repulsive potential in the treatment. In contrast with Barrer, who assumed that the repulsion varied as  $r^{-12}$ , Orr used the quantum mechanically more correct exponential dependence on  $r$ . Like Barrer, Orr also used summation instead of integration to obtain the heat of adsorption. It is interesting to note that while the dispersion energy was summed over the nearest 250 ions, and the influence energy over the nearest 88–96 ions, the repulsion energy had to be summed over only the nearest 16 ions, showing how much shorter the range of the repulsion forces is. The quadrupole interaction was neglected by Orr also. The calculated heat of adsorption for argon on potassium chloride was 1593 calories per mole for the argon atom located above the center of the lattice cell of the (100) plane, 1314 calories per mole for the argon located above the mid-point of the lattice edge, 1423 calories per mole for the argon directly above the  $K^+$  ion, and 1233 calories for the atom directly above the  $Cl^-$  ion. The experimentally determined value<sup>44</sup> was 2100 calories per mole, or about 500 calories higher than the highest theoretical value. A similar discrepancy of about 500 calories was also obtained between the experimental and theoretical heats of adsorption of argon on cesium iodide. Orr ascribed the higher experimental values to adsorption in the cracks of the crystal. He also calculated the variation of the heat of adsorption with the fraction of the surface covered. These calculations are discussed in Chapter VIII.

In conclusion we may summarize now the main points of this chapter. The van der Waals interaction between non-polar molecules has three important constituent parts: (1) the attraction between fluctuating dipole and induced dipole (dispersion effect), varying as  $r^{-6}$ ; (2) the attraction between fluctuating quadrupole and induced dipole, varying as  $r^{-8}$ ; and (3) the repulsion energy, decreasing exponentially with  $r$  (equation 22). At the usual equilibrium distances the first of the three terms is by far the most important. When the molecules possess permanent dipoles two other effects must be considered besides the ones mentioned: the mutual attraction between the permanent dipoles (orientation effect), varying as  $r^{-6}$  (equation 4); and the attraction between the permanent dipole and induced dipole (induction effect) varying also as  $r^{-6}$  (equation 8). If the molecules possess permanent quadrupoles, one must consider the attraction between permanent quadrupole and induced dipole, varying as  $r^{-8}$

<sup>44</sup> W. J. C. Orr, *Proc. Roy. Soc., A173*, 349 (1939).

(equation 12). The quadrupole-quadrupole interaction, varying as  $r^{-10}$ , is usually negligible.

The most important part of the interaction potential between a non-conducting surface and a non-polar molecule is the dispersion potential, varying as  $r^{-3}$  (equation 65). The interaction of the fluctuating quadrupole with the surface and the repulsion potential were not treated so far quantitatively. The potential between a conducting surface and a non-polar molecule also varies as  $r^{-3}$  (equations 60, 70 and 71), except that at small distances it varies as  $r^{-2} \ln r$  (equation 75). If the molecule possesses a permanent dipole the orientation and induction effects must also be considered; these also vary as  $r^{-3}$  (equation 43). Finally if the molecule possesses a permanent quadrupole the interaction potential varies as  $r^{-5}$  (equation 47).

It will be seen from the foregoing discussion that the problem of the fundamental nature of van der Waals forces has been successfully attacked by theoretical physics in the last two decades. Particularly great advances have been made in the last ten years by the application of quantum mechanics. Of course, the problem is far from being solved quantitatively as yet. For the simplest system that can be checked by experiment, i.e., the van der Waals interaction of two helium atoms, the calculations give quantitatively correct answers, but the calculations of the heats of sublimation and heats of adsorption are still only semi-quantitative. However, in view of the fact that great advances have been made in our understanding of the intermolecular forces in recent years, perhaps it is not too optimistic to expect that this progress will continue, and that the calculations of the heats of adsorption will come ever closer to the completely quantitative stage.

## CHAPTER VIII

### THE HEAT OF ADSORPTION II

In the previous chapter we discussed the fundamental physical theory of van der Waals forces and the application of the theory to the calculation of the heats of adsorption. In the present chapter we collect some of the experimental results in order to throw further light on the subject of physical adsorption. The results may be classified in two groups. The first group includes comparisons (a) between heats of van der Waals adsorption measured calorimetrically and calculated from isotherms, (b) between heats of van der Waals adsorption and other energy quantities, such as heats of chemisorption, liquefaction, compression and the adsorption potential, and (c) between heats of van der Waals adsorption of different gases on the same adsorbent and of the same gas on different adsorbents. The second group of results deals with the variation of the heat of van der Waals adsorption (a) with the amount of gas adsorbed and (b) with temperature.

#### CALORIMETRIC AND ISOSTERIC HEATS OF ADSORPTION

The experimental details of the direct calorimetric determination of the heats of adsorption have been discussed in Chapter III. The indirect method that utilizes adsorption isotherms for the calculation of the heats of adsorption has been briefly outlined in Chapter II. We shall now discuss the thermodynamic principles underlying the two methods and compare the experimental results obtained by them.

If we admit  $n$  moles of an ideal gas to a thoroughly evacuated adsorbent weighing 1 gram,  $a$  moles of gas will be adsorbed and a certain amount of heat will be liberated in the process. Let us assume first that no external work is done during the adsorption. If  $u_g$  is the energy of the gas per mole in the gas-phase and  $u_a$  is the energy of the gas per mole in the adsorbed phase, the loss of heat from the system due to adsorption is

$$(1) \quad q_i = nu_g - (n - a)u_g - au_a = a(u_g - u_a)$$

The quantity of heat  $q_i$  is called the integral heat of adsorption. If we increase the amount of gas adsorbed by  $da$ , an additional amount

of heat  $dq$  will be liberated. The differential coefficient  $(\partial q_i/\partial a)_T$  is called the differential heat of adsorption. Differentiating equation (1) with respect to  $a$  we obtain

$$(2) \quad q_d = u_g - u_a + a \left[ \frac{\partial(u_g - u_a)}{\partial a} \right]_T$$

where  $q_d$  is the differential heat of adsorption. For an ideal gas  $u_g$  is a function of the temperature only, consequently

$$(3) \quad q_d = u_g - u_a - a \left( \frac{\partial u_a}{\partial a} \right)_T$$

If the adsorption occurs isothermally and without change in the total number of molecules, then work is done in the process. This work is  $p dv$ , where  $dv$  is the volume of gas adsorbed. Since we deal with an ideal gas

$$(4) \quad p dv = da RT$$

therefore the work done per mole of gas adsorbed is  $RT$ . Hückel<sup>1</sup> defines the isothermal heat of adsorption as

$$(5) \quad q_{\text{isotherm}} = q_d + RT$$

When the heat of adsorption is determined calorimetrically, one measures a value that lies somewhere between  $q_d$  and  $q_{\text{isotherm}}$ . The adsorption does not occur without external work, but it is difficult to decide to what extent this work is transferred to the calorimeter as heat. However,  $RT$  usually does not amount to more than about 5–10% of the total heat of adsorption, which is not much greater than the experimental error in many of these measurements.

In Table XXVI, taken from Hückel,<sup>1</sup> some comparisons are given between differential and integral heats of adsorption. The data represent calorimetric measurements of the heats of adsorption of nitrogen and ammonia on charcoal, obtained by Titoff.<sup>2</sup> The first column gives the amounts of gas adsorbed, the second the differential heats of adsorption  $\Delta q/\Delta a$ , the third and fourth give the integral heats of adsorption in two different units, in calories per gram of adsorbent and in calories per mole of gas adsorbed. As the table shows, the integral heats are greater for some values of  $a$  and smaller for others, than the differential heats.

<sup>1</sup> E. Hückel, *Adsorption und Kapillarkondensation*, Leipzig, 1928, p. 22–35.

<sup>2</sup> A. Titoff, *Z. phys. Chem.*, 74, 641 (1910).

The indirect method of determining the differential heats of adsorption is based on certain thermodynamic principles which we shall now briefly discuss.

In an adsorbent-adsorbate system equilibrium is established when the isothermal transfer of a small quantity of gas from the adsorbed

TABLE XXVI  
DIFFERENTIAL AND INTEGRAL HEATS OF ADSORPTION

$a \times 10^3$ Moles/g. of Charcoal	$q_d$ Calories/Mole	Calories/g. $q_i$ of Charcoal	$q_i/a$ Calories/Mole
Nitrogen			
1.157	8350	0.097	8350
10.91	4650	0.509	4660
18.7	4075	0.865	4620
32.5	4720	1.52	4660
45.2	4550	2.09	4620
58.3	4770	2.72	4650
Ammonia			
24.2	11270	2.7	11270
134.6	8540	12.2	9030
269.5	8060	23.1	8550
403	7830	33.5	8300
516	7880	42.1	8140
568	8380	46.3	8150
591	8650	48.4	8180
606	8710	49.8	8200

phase to the gas phase brings about no change in the free energy of the system, i.e., when

$$(6) \quad \left( \frac{\partial F_g}{\partial n} \right)_T = \left( \frac{\partial F_a}{\partial a} \right)_T$$

$F_g$ , the free energy of the gas, is a function of  $n$  and  $T$ , and  $F_a$ , the free energy of the adsorbate, is a function of  $a$  and  $T$ . Let  $F_g$  and  $F_a$  be measured in calories per cc., and  $n$  and  $a$  be measured in moles per cc.

According to the second law of thermodynamics <sup>3</sup>

$$(7) \quad H_g = F_g - T \left( \frac{\partial F_g}{\partial T} \right)_n$$

$$H_a = F_a - T \left( \frac{\partial F_a}{\partial T} \right)_a$$

<sup>3</sup> See, for example, G. N. Lewis and M. Randall, *Thermodynamics*, New York, 1923, p. 162, equation (12).

where  $H_g$  and  $H_a$  are the heat contents of the gas in the gas phase and the adsorbed phase. Differentiating the first equation with respect to  $n$  and the second with respect to  $a$ , we obtain

$$(8) \quad \begin{aligned} \frac{\partial^2 F_g}{\partial n \partial T} &= \frac{1}{T} \frac{\partial F_g}{\partial n} - \frac{1}{T} \frac{\partial H_g}{\partial n} \\ \frac{\partial^2 F_a}{\partial a \partial T} &= \frac{1}{T} \frac{\partial F_a}{\partial a} - \frac{1}{T} \frac{\partial H_a}{\partial a} \end{aligned}$$

Subtracting the first equation from the second and considering equation (6) we get

$$(9) \quad \frac{\partial^2 F_a}{\partial a \partial T} - \frac{\partial^2 F_g}{\partial n \partial T} = \frac{1}{T} \left( \frac{\partial H_g}{\partial n} - \frac{\partial H_a}{\partial a} \right)$$

We introduce now the notation

$$(10) \quad \begin{aligned} nu_g &= H_g \\ au_a &= H_a \end{aligned}$$

where  $u_g$  and  $u_a$  are the heat contents of the gas per mole before and after adsorption. Substituting (10) into (9), and considering that for an ideal gas  $u_g$  is a function of the temperature only, i.e.,

$$(11) \quad \frac{\partial u_g}{\partial n} = 0$$

we obtain

$$(12) \quad \frac{\partial^2 F_a}{\partial a \partial T} - \frac{\partial^2 F_g}{\partial n \partial T} = \frac{1}{T} \left( u_g - u_a - a \frac{\partial u_a}{\partial a} \right) = \frac{q_d}{T}$$

Let us return now to the original equilibrium equation (6). Since  $F_g$  is a function of  $n$  and  $T$ , and  $F_a$  a function of  $a$  and  $T$ , the complete differential equation for the equilibrium is

$$(13) \quad \left( \frac{\partial^2 F_g}{\partial n^2} \right)_T dn + \frac{\partial^2 F_g}{\partial n \partial T} dT = \left( \frac{\partial^2 F_a}{\partial a^2} \right)_T da + \frac{\partial^2 F_a}{\partial a \partial T} dT$$

If we keep  $a$  constant, the first term on the right hand side becomes zero, and transposing terms we get

$$(14) \quad \left( \frac{\partial n}{\partial T} \right)_a = \left[ \frac{\partial^2 F_a}{\partial a \partial T} - \frac{\partial^2 F_g}{\partial n \partial T} \right] / \left( \frac{\partial^2 F_g}{\partial n^2} \right)_T$$

The free energy of a perfect gas can be expressed by the following equation

$$(15) \quad F_g = nc_v(T - T \ln T) + RTn \ln n + (H_0 - TS_0)n$$

where  $c_v$  is the specific heat per mole at constant volume,  $H_0$  is a constant heat content term and  $S_0$  is a constant entropy term. Partial differentiation with respect to  $n$  gives

$$(16) \quad \left( \frac{\partial F_g}{\partial n} \right)_T = c_v(T - T \ln T) + RT(1 + \ln n) + (H_0 - TS_0)$$

and differentiating again we obtain

$$(17) \quad \left( \frac{\partial^2 F_g}{\partial n^2} \right)_T = \frac{RT}{n}$$

We return now to equation (14). On the right hand side of the equation the numerator is given by equation (12) and the denominator by equation (17). Substituting, we get

$$(18) \quad \left( \frac{\partial n}{\partial T} \right)_a = q_d \frac{n}{RT^2}$$

The left hand side of the equation can be evaluated from the ideal gas law

$$(19) \quad p = nRT$$

Differentiating with respect to  $T$

$$(20) \quad \frac{dp}{dT} = \frac{dn}{dT} RT + nR$$

and rearranging

$$(21) \quad \frac{dn}{dT} = \frac{dp}{dT} \frac{1}{RT} - \frac{p}{RT^2}$$

Substituting equations (19) and (21) into equation (18) we finally obtain

$$(22) \quad RT^2 \left( \frac{\partial \ln p}{\partial T} \right)_a = q_d + RT$$

Hückel<sup>1</sup> called the energy term on the right hand side of equation (22) the isothermal heat of adsorption (equation 5). Since, however,  $q_d + RT$  always refers to a definite quantity of gas adsorbed at different temperatures and pressures, it is more correctly called the isosteric heat of adsorption. The integrated form of equation (22) for a small pressure and temperature range is

$$(23) \quad \frac{RT_1 T_2}{T_1 - T_2} \ln \frac{p_1}{p_2} = q_{\text{isosteric}}$$

Here  $p_1$  and  $p_2$  are the equilibrium pressures for the same amount of



gas adsorbed at temperatures  $T_1$  and  $T_2$ . The equation is analogous to the Clapeyron-Clausius equation, the differential heat of adsorption taking the place of the heat of condensation.

Equation (22) can also be put in the form

$$(24) \quad \left( \frac{\partial \ln p}{\partial (1/T)} \right)_a = - \frac{q_{\text{isosteric}}}{R}$$

For a small range of  $p$  and  $T$  the term  $q/R$  can be assumed to be approximately constant. A plot of  $\ln p$  against  $1/T$  for a constant amount of gas adsorbed should then be a straight line, the slope of which gives the isosteric heat of adsorption.

TABLE XXVII  
CALORIMETRIC AND ISOSTERIC HEATS OF ADSORPTION I

$a$ cc. at S.T.P.	$\frac{dq}{da}$ (Isosteric) Calories per cc.	$\frac{\Delta q}{\Delta a}$ (Calorimetric) Calories per cc.	Found at $a$ cc. at S.T.P.
CO <sub>2</sub> on Charcoal			
1.82	0.363	0.345	0 to 2.3
4.02	0.344	}	2.3 to 11.3
10.3	0.311		11.3 to 22.6
19.72	0.293	0.305	22.6 to 33.4
28.87	0.281	0.300	33.4 to 43.9
34.07	0.288	}	43.9 to 50.8
38.14	0.285		
41.4	0.290		
44.9	0.287	0.292	
CH <sub>3</sub> OH on Charcoal			
29.7	0.615	0.619	0 to 21.7
65.4	0.563	0.553	21.7 to 47.4
126.5	0.533	0.542	47.4 to 75.3
		0.524	75.3 to 127.4

According to the foregoing discussion the calorimetric heat of adsorption should be equal to the isosteric heat of adsorption within an uncertainty of  $RT$  calories per mole. This amounts to about 5–10% of the total heat of adsorption. Tables XXVII and XXVIII, taken from Kruyt and Modderman,<sup>4</sup> illustrate the type of agreement obtained between the calorimetric and isosteric heats of adsorption. In Table XXVII the differential heats of adsorption of carbon dioxide on charcoal were determined by Titoff;<sup>2</sup> the calorimetric values were

<sup>4</sup> H. R. Kruyt and J. G. Modderman, *Chem. Rev.*, 7, 259 (1930).

measured at 0° C., the isotherms were obtained at 0 and 30° C. The isosteric  $dq/da$  values for methyl alcohol on charcoal were calculated from the isotherms of Coolidge<sup>5</sup> measured at 0 and 33.3° C.; the calorimetric values were obtained by Lamb and Coolidge<sup>6</sup> at 0° C. The isosteric heats of adsorption, calculated by means of equation (23) and given in the second column, correspond to the amounts of gas adsorbed given in the first column. The third column gives the calorimetric heats of adsorption, and the fourth column the volumes of gas adsorbed before and after the determination of the heat evolved.

TABLE XXVIII  
CALORIMETRIC AND ISOSTERIC HEATS OF ADSORPTION II

$a$ cc. at S.T.P.	$dq/da$ (Isosteric) Calories per cc.	$\Delta q/\Delta a$ (Calorimetric) Calories per cc.	Found at $a$ cc. at S.T.P.
N <sub>2</sub> on Charcoal			
1.5	0.198	}	0 to 3
3.5	0.171		3 to 5.5
4.6	0.214		
5.6	0.200		5.5 to 7.7
8.1	0.203		7.7 to 13.5
H <sub>2</sub> O on Charcoal			
0.41	0.423	}	0 to 20.6
1.49	0.459		
4.21	0.465		
16.3	0.481		20.6 to 60.7
191	0.507		60.7 to 102.1
198	0.502	}	102.1 to 143.8
208	0.508		

All heat values are given in calories per cc. of gas adsorbed, to obtain them in the more customary unit of calories per mole one must multiply them by 22,400. In view of the experimental errors involved in both types of measurements the agreement can be considered very satisfactory.

The data of Table XXVIII represent the results of different investigators using different types of charcoals, and yet the agreement is surprisingly good. The nitrogen isotherms were determined by Miss Homfray<sup>7</sup> on coconut charcoal at 0 and 9.3° C., the calorimetric

<sup>5</sup> A. S. Coolidge, *J. Am. Chem. Soc.*, 48, 1795 (1926).

<sup>6</sup> A. B. Lamb and A. S. Coolidge, *J. Am. Chem. Soc.*, 42, 1146 (1920).

<sup>7</sup> I. F. Homfray, *Z. phys. Chem.*, 74, 196 (1910).

heats were measured by Gregg<sup>8</sup> on birchwood charcoal at 0° C. The water isotherms were obtained by Coolidge<sup>9</sup> on sugar charcoal at 0 and 20° C., the calorimetric values were measured by Keyes and Marshall<sup>10</sup> on French gas mask charcoal at 0° C. In the case of nitrogen the  $dq/da$  values may be regarded as approximately independent of  $a$  for the range of adsorption investigated, and the calorimetric and isosteric heats are equal within the experimental error. In the case of water the lack of agreement between the absolute values of the isosteric and calorimetric heats should not be attributed either to experimental error or to failure of the theory. There is no reason why the differential heats of adsorption of a vapor on different char-

TABLE XXIX  
CALORIMETRIC AND ISOSTERIC HEATS OF ADSORPTION III

Vapor	Heat of Adsorption (kcal./mole)	
	Isosteric	Calorimetric
CH <sub>3</sub> Cl	8.3 (1)	9.2 (3)
CH <sub>2</sub> Cl <sub>2</sub>	10.5 (1)	12.4 (3)
CHCl <sub>3</sub>	10.7 (1)	14.4 (3)
CCl <sub>4</sub>	8.9 (1)	15.5 (3)
C <sub>2</sub> H <sub>5</sub> Cl	10.6 (2)	12.2 (3)
n-C <sub>3</sub> H <sub>7</sub> Cl	12.3 (2)	14.6 (3)
iso-C <sub>3</sub> H <sub>7</sub> Cl	12.3 (2)	13.1 (3)
n-C <sub>4</sub> H <sub>9</sub> Cl	13.4 (2)	15.6 (3)
ter-C <sub>4</sub> H <sub>9</sub> Cl	11.6 (2)	13.6 (3)

The investigators were: (1) Pearce and Johnstone,<sup>11</sup> (2) Pearce and Taylor,<sup>12</sup> and (3) Pearce and Reed.<sup>13, 14</sup>

coals should be exactly equal. The striking fact about the data for water is that the course of the  $dq/da$  vs.  $a$  curves is very similar and very unusual: both the isosteric and calorimetric heats of adsorption start with small values at small adsorptions and increase to larger values at large adsorptions. This behavior will be further discussed later.

The agreement between calorimetric and isosteric heats of adsorption is not always as good as shown in Tables XXVII and XXVIII. Table XXIX gives a comparison between the calorimetric and isosteric heats of adsorption of a number of organic chlorides, determined by Pearce and his collaborators.<sup>11, 12, 13, 14</sup> The calorimetric values repre-

<sup>8</sup> S. J. Gregg, *J. Chem. Soc.*, 1927, 1494.

<sup>9</sup> A. S. Coolidge, *J. Am. Chem. Soc.*, 49, 708 (1927).

<sup>10</sup> F. G. Keyes and M. J. Marshall, *J. Am. Chem. Soc.*, 49, 156 (1927).

<sup>11</sup> J. N. Pearce and H. F. Johnstone, *J. Phys. Chem.*, 34, 1260 (1930).

<sup>12</sup> J. N. Pearce and A. L. Taylor, *J. Phys. Chem.*, 35, 1091 (1931).

<sup>13</sup> J. N. Pearce and G. H. Reed, *J. Phys. Chem.*, 35, 905 (1931).

<sup>14</sup> J. N. Pearce and G. H. Reed, *J. Phys. Chem.*, 39, 293 (1935).

sent the integral heats of adsorption for 1 mole of vapor adsorbed on 500 grams of charcoal (44.8 cc. per gram). The isosteric heats were calculated from plots of  $\ln p$  vs.  $1/T$  for constant amounts of vapor adsorbed, according to equation (24). Except for carbon tetrachloride the plots gave good straight lines with approximately equal slopes, indicating that the differential heats of adsorption do not change much with the amount of vapor adsorbed. This fact constitutes the justification for comparing the heat values of columns 2 and 3. It will be noted that the isosteric heats are consistently lower than the calorimetric heats.

McBain<sup>15</sup> called attention to the fact that since the amount of gas adsorbed at the saturation pressure  $p_0$  varies with the temperature, it is impossible to construct isosteres when  $a$  approaches  $a_0$ , the saturation value. On the basis of statistical mechanical arguments Wilkins<sup>16</sup> concluded that equation (22) should not be applied to equal amounts of gas adsorbed at different temperatures and pressures, but to equal fractions of the surface covered. If one constructs these  $\theta$  isosteres in place of the  $a$  isosteres of equation (22) or (24), one avoids the difficulty mentioned by McBain. Furthermore, according to Wilkins, the  $a$  isosteres lead to differential heats of adsorption that are too low, as evidenced by the results of Pearce and Taylor.<sup>12</sup> While Wilkins' arguments may be valid, it should not be forgotten that the integral heat of adsorption is greater than the differential heat, if the latter is a continuously decreasing function of  $a$ . The data of Pearce and Reed<sup>13,14</sup> show that this condition is definitely fulfilled, one would expect therefore their calorimetric integral heats to be larger than the isosteric differential heats of adsorption. Moreover, Tables XXVII and XXVIII show absolutely no evidence of the isosteric heats being lower than the calorimetric heats.

#### HEATS OF CHEMISORPTION AND PHYSICAL ADSORPTION

In the discussion of the determination of the calorimetric and isosteric heats of adsorption nothing was said that would restrict the validity of either method to van der Waals adsorption only. Both methods rest on thermodynamic principles, and the nature of the forces active in the adsorption process does not come into consideration. The heats of chemisorption therefore can also be determined calorimetrically or calculated from adsorption isotherms, and actually

<sup>15</sup> J. W. McBain, *The Sorption of Gases and Vapours by Solids*, London, 1932, p. 141.

<sup>16</sup> F. J. Wilkins, *Proc. Roy. Soc.*, A164, 496 (1938).

both methods, have been frequently employed. Chemisorption and physical adsorption of the same gas can occur on the same adsorbent at two different temperatures, or even at the same temperature, and the quantities of heat evolved usually differ so widely that the two adsorptions can be easily separated. The heats of chemisorption will be discussed in detail in Volume II; in the present section we shall only make comparisons between heats of chemisorption and van der Waals adsorption.

The four gases, argon, nitrogen, oxygen and carbon monoxide show tremendous differences in chemical reactivity, but their condensation characteristics are very similar. The boiling point of oxygen is  $-183^{\circ}\text{C}$ , of argon  $-186^{\circ}\text{C}$ , of carbon monoxide  $-190^{\circ}\text{C}$  and of nitrogen  $-195^{\circ}\text{C}$ . Three of the four molecules, argon, oxygen and nitrogen, have no dipole moments, carbon monoxide has a very small dipole moment. Since the polarizabilities, ionization energies and the diameters of the four molecules are roughly equal, we would expect on the basis of Chapter VII that their heats of van der Waals adsorption on the same adsorbent would also be nearly equal. As a matter of fact Dewar<sup>17</sup> measured experimentally the heats of adsorption of the four gases on charcoal by means of his liquid air calorimeter (Chapter III), and obtained the values of 3600 calories per mole for argon, 3700 for nitrogen, 3700 for oxygen and 3400 for carbon monoxide. Thus the heats of physical adsorption of the four gases on charcoal are approximately equal and are in the neighborhood of 3–4000 calories per mole.

Blench and Garner<sup>18</sup> determined the differential heats of adsorption of oxygen on norite, a vegetable charcoal, and found that for the first small quantities of oxygen adsorbed  $q_a$  has a value of 60,000 calories per mole at  $18^{\circ}\text{C}$ . With increasing temperature the initial  $q_a$  rises to 220,000 calories per mole at  $450^{\circ}\text{C}$ . At  $200^{\circ}\text{C}$ . the value of  $q_a$  for 0.224 cc. of oxygen adsorbed per gram of charcoal is 116,000 calories per mole, and above  $200^{\circ}\text{C}$ . the heat of adsorption is greater than the heat of formation of carbon dioxide. The oxygen adsorbed in this manner can not be recovered as such; it is removed by evacuation at high temperatures in the form of carbon monoxide and carbon dioxide. Garner and his collaborators used adiabatic calorimeters (Chapter III). Keyes and Marshall,<sup>19</sup> using the ice calorimeter, obtained 72,000 calories per mole for the initial heat of adsorption of oxygen on charcoal, and Marshall and Bramston-Cook,<sup>19</sup> also using the ice calorimeter,

<sup>17</sup> J. Dewar, *Proc. Roy. Soc.*, A74, 122 (1904).

<sup>18</sup> E. A. Blench and W. E. Garner, *J. Chem. Soc.*, 125, 1288 (1924).

<sup>19</sup> M. J. Marshall and H. E. Bramston-Cook, *J. Am. Chem. Soc.*, 51, 2019 (1929).

obtained a value of 89,600 calories per mole for the adsorption of 0.03 cc. of oxygen per gram of coconut charcoal. Some of these heat values are almost as large, others are larger than the heats of chemical reactions between carbon and oxygen. Unquestionably, therefore, the above investigators dealt with clear-cut examples of chemical adsorption.

The relation between the heats of chemisorption and van der Waals adsorption for the charcoal-oxygen system is illustrated in Fig. 83,

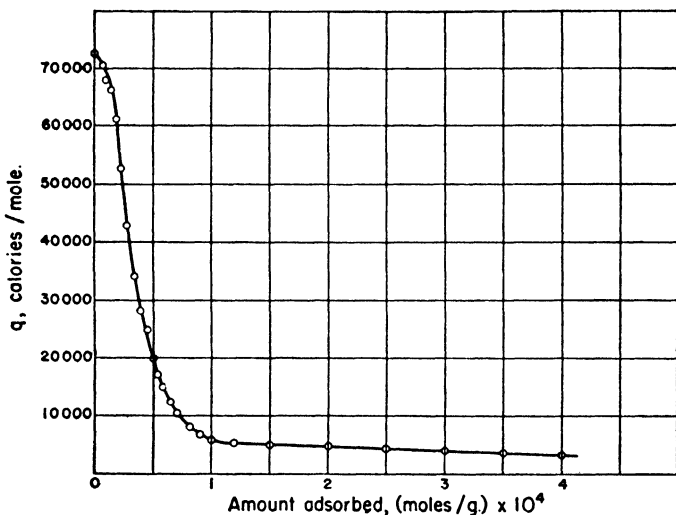


FIG. 83.—The calorimetric heats of adsorption of oxygen on charcoal.

taken from Keyes and Marshall.<sup>10</sup> The initial large differential heat of adsorption of 72,000 calories per mole drops very rapidly with increasing adsorption, and levels off around the value of 4000 calories per mole, which corresponds to the heat of van der Waals adsorption. This value is quite close to the 3700 calories per mole obtained by Dewar.<sup>17</sup>

As the foregoing results show, the heats of chemisorption of oxygen on charcoal are twenty to fifty times as large as the heats of van der Waals adsorption. There are other adsorbent-adsorbate systems which exhibit almost as large differences as the charcoal-oxygen system. Beebe and Stevens<sup>20</sup> obtained calorimetrically 120,000 calories per mole for the initial heat of adsorption of oxygen

<sup>20</sup> R. A. Beebe and N. P. Stevens, *J. Am. Chem. Soc.*, 62, 2134 (1940).

on a promoted iron catalyst at  $-183^{\circ}\text{C}$ . With increasing adsorption  $q_d$  decreased slowly to about 90,000 calories per mole, but at 0.9 cc. of oxygen adsorbed per gram of iron it dropped suddenly to 4000 calories per mole. Here the difference between the heats of chemisorption and van der Waals adsorption is about thirty fold. The heats evolved in the formation of the three iron oxides,  $\text{FeO}$ ,  $\text{Fe}_3\text{O}_4$  and  $\text{Fe}_2\text{O}_3$  are 128, 133 and 127 kcal. per mole of oxygen, respectively, which are about equal to the initial heat of adsorption of 120 kcal. per mole. As a matter of fact, it is somewhat questionable whether one should designate the uptake of oxygen by the iron catalyst chemisorption or actual chemical reaction, since the oxygen sorbed was sufficient to oxidize several of the top layers of the catalyst.

The heats of chemisorption and physical adsorption of carbon monoxide and nitrogen on the same type of promoted iron catalyst were also measured. In these cases the investigators dealt definitely with surface adsorption. Beebe and Stevens<sup>20</sup> determined calorimetrically the heats of adsorption of carbon monoxide on iron, and found for the initial heat of chemisorption 17 kcal./mole at  $-183^{\circ}\text{C}$  and 34 kcal./mole at  $0^{\circ}\text{C}$ . The heats of van der Waals adsorption ranged from 3.7 to 5 kcal./mole, depending on the amount of carbon monoxide adsorbed. The heat of chemisorption of nitrogen on iron was obtained by Emmett and Brunauer<sup>21</sup> from adsorption isotherms at 400 and  $450^{\circ}\text{C}$ .; it amounted to about 35 kcal./mole for 0.010 to 0.014 cc. of nitrogen adsorbed per gram of iron. The heats of van der Waals adsorption of nitrogen on iron, measured calorimetrically by Beebe and Stevens, ranged from 2.5 to 4.4 kcal./mole at  $-183^{\circ}\text{C}$ . Argon naturally has no chemisorption. For the heats of physical adsorption Beebe and Stevens obtained values between 2.5 and 3.0 kcal./mole at  $-183^{\circ}\text{C}$ ., depending on the amount adsorbed. Thus the heats of van der Waals adsorption of argon, nitrogen, oxygen and carbon monoxide on iron are roughly equal, and are in the neighborhood of 4 kcal./mole, just as on charcoal. As far as chemisorptions are concerned, however, the four gases show very great differences. Argon is not chemisorbed; oxygen, nitrogen and carbon monoxide are chemisorbed with heat evolutions that approximate the heats of formation of iron oxides, iron nitrides and iron carbonyl.

Another interesting comparison between heats of van der Waals adsorption and chemisorption is afforded by the calorimetric measurements of Beebe and Dowden<sup>22</sup> for the same four gases on chromic

<sup>21</sup> P. H. Emmett and S. Brunauer, *J. Am. Chem. Soc.*, **56**, 35 (1934).

<sup>22</sup> R. A. Beebe and D. A. Dowden, *J. Am. Chem. Soc.*, **60**, 2912 (1938).

oxide. The heats of van der Waals adsorption of argon, nitrogen, oxygen and carbon monoxide at  $-183^{\circ}\text{C}$ . ranged from 2.7 to 4.2, 2.7 to 4.6, 3.0 to 4.8 and 3.2 to 4.6 kcal./mole, respectively, depending on the amount of gas adsorbed. Among the four gases argon had no chemisorption, and oxygen had the largest heats of chemisorption, about 25 kcal./mole at  $-183^{\circ}$  and 50 kcal./mole at  $0^{\circ}\text{C}$ . The initial heat of chemisorption of carbon monoxide was about 12 kcal., that of nitrogen about 8 kcal./mole. The last two values are only two to three times as large as the heats of van der Waals adsorption, there is some doubt therefore whether these values actually represent heats of chemisorption. We have seen in Chapter VII that the heats of adsorption in narrow crevices and capillaries are larger than on plane surfaces, and in pockets, tubes and cells of the adsorbent they can attain values that are several times as large as the usual heats of adsorption.

Aside from such borderline cases as the adsorption of nitrogen by chromic oxide, the heats of van der Waals adsorption and chemisorption are ordinarily easily distinguishable. Further interesting examples are found in the heats of adsorption of hydrogen on a variety of metal and oxide catalysts. For the heat of physical adsorption of hydrogen on copper Benton<sup>23</sup> obtained 1000 calories per mole (isosteric); for the heat of chemisorption Beebe<sup>24</sup> measured values between 11,500 and 13,300 calories per mole, and Taylor and Kistiakowsky<sup>25</sup> obtained values as high as 20,000 calories per mole (calorimetric). For the heat of van der Waals adsorption of hydrogen on iron Benton<sup>23</sup> obtained 1600 calories per mole, Emmett and Harkness<sup>26</sup> 2000 calories per mole, and for the chemisorption of hydrogen on iron the latter investigators obtained about 8500 calories per mole (isosteric). Except for the measurements of Emmett and Harkness, the above heats of chemisorption and van der Waals adsorption were not determined on the same adsorbents. However, the heats of van der Waals adsorption of hydrogen are not likely to vary much on different samples of copper and iron.

For oxide catalysts the heats of chemisorption of hydrogen were found to be ten to twenty times as large as the heats of physical adsorption. For the heats of physical adsorption and chemisorption of hydrogen on ZnO Taylor and Sickman<sup>27</sup> obtained 1100 and 21,000

<sup>23</sup> A. F. Benton, *Trans. Far. Soc.*, **28**, 202 (1932).

<sup>24</sup> R. A. Beebe, *Trans. Far. Soc.*, **28**, 761 (1932).

<sup>25</sup> H. S. Taylor and G. B. Kistiakowsky, *Z. phys. Chem.*, **125**, 341 (1927).

<sup>26</sup> P. H. Emmett and R. W. Harkness, *J. Am. Chem. Soc.*, **57**, 1631 (1935).

<sup>27</sup> H. S. Taylor and D. V. Sickman, *J. Am. Chem. Soc.*, **54**, 602 (1932).



calories per mole, on a mixed  $\text{MnO-Cr}_2\text{O}_3$  catalyst Taylor and Williamson<sup>28</sup> obtained 2000 and 20,000 calories per mole, and on a mixed  $\text{ZnO-Mo}_2\text{O}_3$  catalyst Taylor and Ogden<sup>29</sup> obtained also 2000 and 20,000 calories per mole (isosteric). Calorimetrically Garner and Veal<sup>30</sup> measured heats of adsorption of 10,000 to 13,000 calories per mole for hydrogen on a mixed  $\text{ZnO-Cr}_2\text{O}_3$  catalyst at 18° C., and Beebe and Dowden<sup>22</sup> 3000 to 5000 calories per mole on  $\text{Cr}_2\text{O}_3$  at - 183° C. The values of Garner and Veal undoubtedly represent chemisorption, but the values of Beebe and Dowden are very likely due to simultaneous occurrence of chemisorption and physical adsorption.

### HEATS OF VAN DER WAALS ADSORPTION AND LIQUEFACTION

The heats of van der Waals adsorption are of the same order of magnitude as the heats of liquefaction of gases. Most theories of van der Waals adsorption ascribe liquid-like properties to the adsorbate: according to the potential theory the adsorbate at low temperatures behaves like a strongly compressed liquid, the capillary condensation theory assumes that the molecular volumes and the surface tensions of the adsorbate and the liquid are the same, and the theory of multimolecular adsorption assumes that adsorbate and liquid have the same evaporation-condensation characteristics. The forces active in physical adsorption are the same as those active in condensation, as we have seen in Chapter VII.<sup>31</sup>

<sup>28</sup> H. S. Taylor and A. T. Williamson, *J. Am. Chem. Soc.*, 53, 813 (1931).

<sup>29</sup> H. S. Taylor and G. Ogden, *Trans. Far. Soc.*, 30, 1178 (1934).

<sup>30</sup> W. E. Garner and F. J. Veal, *J. Chem. Soc.*, 1935, 1487.

<sup>31</sup> O. Schmidt (*Z. phys. Chem.*, 133, 263, 1928) assumes that the relation between the heats of adsorption of different gases on the same adsorbent and the heats of liquefaction of the same gases is given by the equation

$$(a) \quad q = k\sqrt{E_L}$$

This relationship is analogous to equation (16), Chapter V. If we substitute (a) into equation (35), Chapter VII, and take logarithms, we obtain

$$(b) \quad \log v = k_1\sqrt{E_L} - k_2$$

provided  $p$  and  $T$  are considered constants. If one plots the logarithms of the volumes of different gases adsorbed on the same adsorbent at a given temperature and pressure against the heats of liquefaction of the same gases, one ought to obtain a straight line according to equation (b). Since equation (35), Chapter VII, is valid only for the linear beginning portion of the adsorption isotherm, equation (b) should be valid only for small adsorptions. Schmidt proved that the straight line equation is obeyed fairly well in a large number of cases.

The heat of adsorption may be smaller or larger than the heat of liquefaction. It was pointed out by Brunauer, Deming, Deming and Teller<sup>32</sup> that the relative magnitude of the heat of adsorption  $E_1$  and the heat of liquefaction  $E_L$  plays an important role in determining the shape of the adsorption isotherm in the low pressure region. If  $E_1$  is greater than  $E_L$ , the isotherm at low pressures is concave to the pressure axis (i.e., Type I, II or IV isotherm); if  $E_1$  is smaller than  $E_L$ , the isotherm is convex to the pressure axis at low pressures (i.e., Type III or V isotherm). This was discussed in detail in Chapter VI.

Ordinarily the heats of adsorption are larger than the heats of liquefaction, but there are a few examples known where the reverse is true. Coolidge<sup>9</sup> found that the amounts of water vapor adsorbed by charcoal in the temperature range  $-30$  to  $+20^\circ\text{C}$ . were the same at equal values of the relative pressure,  $p/p_0$ . From this he concluded that  $E_1 - E_L$  is zero in that temperature range. At higher temperatures  $E_1 - E_L$  becomes negative. Table XXX gives comparisons

TABLE XXX  
HEATS OF ADSORPTION OF WATER BY CHARCOAL

Temperature °C.	$E_1$ Calories/Mole	$E_L$ Calories/Mole	$E_L - E_1$ Calories/Mole
-15	11,100		
0		10,740	
10	10,000	10,650	650
40	9,300	10,350	1050
80	8,300	9,940	1640
128	7,200	9,360	2160
187	5,200		

between the isosteric heats of adsorption  $E_1$ , calculated by Coolidge from his isotherms, and the heats of liquefaction of water vapor at the same temperatures, taken from the International Critical Tables.<sup>33</sup> At all temperatures above  $10^\circ\text{C}$ .  $E_L$  is greater than  $E_1$ , and the difference  $E_L - E_1$  increases with increasing temperature. According to the theory of multimolecular adsorption, therefore, water vapor on charcoal should give Type V isotherms, and as we have seen in Chapter VI this is actually the case.

The heat of adsorption of water on charcoal was calorimetrically determined by Keyes and Marshall.<sup>10</sup> In two series of experiments with the ice calorimeter they obtained 10,510 and 9460 calories per

<sup>32</sup> S. Brunauer, L. S. Deming, W. E. Deming and E. Teller, *J. Am. Chem. Soc.*, **62**, 1723 (1940).

<sup>33</sup> International Critical Tables, V, 138.

mole, the average being 10,000 calories per mole. The heat of liquefaction at 0° C. is 10,740 calories per mole.

A second example of  $E_L$  being greater than  $E_1$  was also found by Coolidge<sup>34</sup> in the adsorption of mercury vapor by charcoal. From the isostere corresponding to the adsorption of 1 mg. of mercury per gram of charcoal he calculated a heat of adsorption of 8900 calories per mole, which is much smaller than the heat of vaporization, 13,000 calories per mole. The adsorption was measured in the temperature range 100–480° C.

Langmuir<sup>35</sup> pointed out that the evaporation of cadmium, mercury and iodine from glass is very much faster than the evaporation of the same molecules from their own liquids. Since the rate of evaporation depends exponentially on the heat of vaporization, this implies that  $E_1$  for the adsorption of cadmium, mercury and iodine on glass is smaller than  $E_L$  for the corresponding vapor.

When the cohesive forces between molecules of the same species are very large, one would expect that  $E_L$  may be equal to or greater than  $E_1$ . Water and iodine may serve as examples. Water has a large permanent dipole moment giving rise to strong orientation forces, iodine has a large polarizability, producing strong dispersion forces. Direct evidence that  $E_L$  is greater than  $E_1$  for water on charcoal and iodine on glass was given above. Indirect evidence from the shape of the adsorption isotherms can be found in the experiments of McHaffie and Lenher<sup>36</sup> and Frazer, Patrick and Smith<sup>37</sup> for the system water vapor-glass, and of Patrick and Land<sup>38</sup> and Reyerson and Cameron<sup>39</sup> for the system iodine-silica gel.<sup>40</sup>

The great majority of adsorption experiments deal with systems for which the heat of adsorption is greater than the heat of liquefaction. The ratio of the heat of adsorption to the heat of liquefaction seems to be the greater, the lower the boiling point of the gas. Stout

<sup>34</sup> A. S. Coolidge, *J. Am. Chem. Soc.*, **49**, 1949 (1927).

<sup>35</sup> I. Langmuir, *J. Am. Chem. Soc.*, **54**, 2798 (1932).

<sup>36</sup> I. R. McHaffie and S. Lenher, *J. Chem. Soc.*, **127**, 1559 (1925).

<sup>37</sup> J. C. W. Frazer, W. A. Patrick and H. E. Smith, *J. Phys. Chem.*, **31**, 897 (1927).

<sup>38</sup> W. A. Patrick and W. E. Land, *J. Phys. Chem.*, **38**, 1201 (1934).

<sup>39</sup> L. H. Reyerson and A. E. Cameron, *J. Phys. Chem.*, **39**, 181 (1935).

<sup>40</sup> J. H. de Boer (*Z. phys. Chem.*, **B14**, 457, 1931) found that the heat of adsorption of iodine on barium chloride was 1700 calories smaller than the heat of sublimation of iodine. He made the comparison with the heat of sublimation, since at the temperature of his experiments the stable bulk phase was the solid and not the liquid.

and Giaque<sup>11</sup> calculated for the heat of adsorption of helium on  $\text{NiSO}_4 \cdot 7\text{H}_2\text{O}$  the value of 140 calories per mole at  $4.23^\circ \text{K}$ .; the heat of vaporization of helium is about 20 calories per mole. Dewar<sup>17</sup> obtained for the heat of adsorption of hydrogen on charcoal 1600 calories per mole at  $-185^\circ \text{C}$ .; the heats of adsorption of hydrogen on metals and oxides at liquid air temperatures are between 1000 and 2000 calories per mole, as we have seen in the previous section. The heat of vaporization of hydrogen is about 220 calories per mole. Thus for the two lowest boiling gases, helium and hydrogen, the heats of adsorption exceed the heats of liquefaction roughly seven fold.

TABLE XXXI  
HEATS OF ADSORPTION OF ORGANIC VAPORS BY CHARCOAL

Vapor	$n$	$m$	$q_m$ Calories/Mole	$E_L$ Calories/Mole
$\text{C}_2\text{H}_5\text{Cl}$	0.915	0.7385	12,000	6220
$\text{CS}_2$	0.9205	0.7525	12,500	6830
$\text{CH}_3\text{OH}$	0.938	0.742	13,100	9330
$\text{C}_2\text{H}_5\text{Br}$	0.900	0.900	13,900	6850
$\text{C}_2\text{H}_5\text{I}$	0.956	0.737	14,000	7810
$\text{CHCl}_3$	0.935	0.8285	14,500	8000
$\text{HCOOC}_2\text{H}_5$	0.9075	0.944	14,500	8380
$\text{C}_6\text{H}_6$	0.959	0.774	14,700	7810
$\text{C}_2\text{H}_5\text{OH}$	0.928	0.871	15,000	10,650
$\text{CCl}_4$	0.930	0.893	15,300	8000
$(\text{C}_2\text{H}_5)_2\text{O}$	0.9215	0.917	15,500	6900

Nitrogen, carbon monoxide, argon and oxygen constitute the next lowest boiling group of gases. The heats of adsorption of these gases at liquid air temperatures on charcoal, silica gel, metals and oxides are in the vicinity of 3-4000 calories per mole; their heats of liquefaction are approximately 1500 calories per mole. The ratio of the heat of adsorption to the heat of liquefaction is roughly 2.5.

Table XXXI represents the heats of adsorption of a number of organic vapors on charcoal at  $0^\circ \text{C}$ ., obtained calorimetrically by Lamb and Coolidge.<sup>6</sup> The heats of adsorption decrease slightly with increasing adsorption for all eleven vapors; the values given in the fourth column of the table correspond to the heats of adsorption in the middle region, where 1 mole of vapor is adsorbed by 500 grams of charcoal. The fifth column gives the heats of liquefaction of the vapors at  $0^\circ \text{C}$ . The ratio of  $q_m/E_L$  for this group of gases is between 1.5 and 2.

<sup>11</sup> J. W. Stout and W. F. Giaque, *J. Am. Chem. Soc.*, **60**, 393 (1938).

NET HEAT OF ADSORPTION, HEAT OF WETTING, HEAT OF  
COMPRESSION AND ADSORPTION POTENTIAL

The energy difference  $E_1 - E_L$  was called by Lamb and Coolidge<sup>8</sup> the net heat of adsorption. They found that if the net heat of adsorption is divided by the molar volume of the liquid adsorbed, an approximately constant value is obtained for all eleven vapors of Table XXXI. The net heat per cc. of liquid adsorbed is 87.7 calories, with an average error of 7.4%. Even Titoff's<sup>2</sup> values for carbon dioxide and ammonia on charcoal were found to be close to the average value. From this constancy Lamb and Coolidge concluded that the heat of adsorption was due to the attractive forces of the charcoal upon the liquids, and that for a given volume of liquid, i.e., for a given volume of the filled pore space, the heat liberated was nearly equal for all liquids investigated.

To obtain an estimate of the order of magnitude of the attractive forces Lamb and Coolidge compared the net heats of adsorption with the heats of compression of the liquids. The data for seven of the liquids were available from 20 to 80° C. up to 12,000 atm. pressure. By extrapolating Bridgman's<sup>42</sup> data, taking into consideration the changes in compressibilities and heats of compression at high pressures, they calculated that a pressure of about 37,000 atmospheres could account for the entire net heat of adsorption. The parallelism between the net heats of adsorption and the heats of compression is shown in Fig. 84. The strikingly similar course of the two curves led Lamb and Coolidge to the conclusion that the net heats of adsorption are merely heats of compression.

Interestingly, the negative net heats of adsorption of water on charcoal at 0° C., obtained by Coolidge<sup>9</sup> and by Keyes and Marshall,<sup>10</sup> fit very well in this idea of Lamb and Coolidge. As the temperature is raised from 0° C. the density of water increases, the heat of compression is therefore negative. However, the net heat of adsorption of water at higher temperatures is still negative, as was shown in Table XXX, whereas the heat of compression above 4° C. is positive.

In the discussion of the potential theory in Chapter V we cited evidence indicating that the adsorbed phase is under strong compression. Harkins and Ewing<sup>43</sup> determined the apparent specific gravity of charcoal by immersion in different liquids and obtained different values. The differences could be explained on the assumption that the adsorbed liquids in the pores of the charcoal were under a com-

<sup>8</sup> P. W. Bridgman, *Proc. Am. Acad.*, 49, 1 (1913).

<sup>43</sup> W. D. Harkins and D. T. Ewing, *J. Am. Chem. Soc.*, 43, 1787 (1921).

pression of about 12,000 atmospheres. Goldmann and Polanyi,<sup>44</sup> by performing similar experiments, came also to the conclusion that the adsorbed phase is under great compression. Further, it was found that although the volumes of liquid adsorbed by charcoal at saturation do not differ much, the greatest volume almost always belongs to the

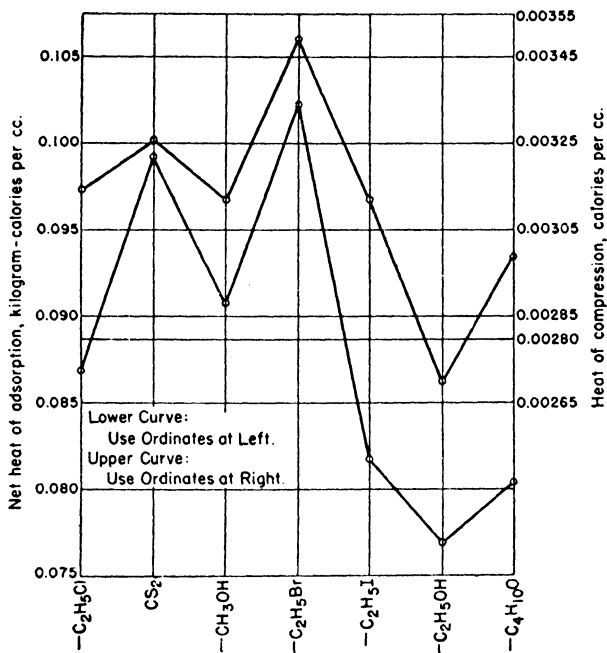


Fig. 84.—The parallelism between heats of compression and net heats of adsorption of seven vapors on charcoal.

liquid of greatest compressibility. Although these and other experiments tend to show that the adsorbed phase is under great compression,<sup>45</sup> nevertheless this does not mean that the entire net heat of adsorption is due to compression. Indeed, Coolidge<sup>9</sup> himself pointed out later that the net heat of adsorption is usually the greatest for the first quantities of gas adsorbed, which have nothing to compress.

Goldmann and Polanyi<sup>44</sup> showed that only a part of the net heat of adsorption is due to the heat of compression. We may recall from

<sup>44</sup> F. Goldmann and M. Polanyi, *Z. phys. Chem.*, 132, 321 (1928).

<sup>45</sup> The density of the adsorbed phase will be further discussed in Chapter XII.

Chapter V, equation (5), that the Polanyi adsorption potential for low temperatures is given by

$$(25) \quad \epsilon_x = RT \ln \frac{p_0}{p_x}$$

where  $p_x$  is the equilibrium pressure over the adsorbent when  $x$  grams of gas are adsorbed at temperature  $T$ . The Polanyi potential is the free energy of the isothermal transfer of an infinitesimal amount of adsorbate from the liquid phase to the adsorbed phase when the latter already contains  $x$  grams of gas adsorbed. If we call  $U_x$  the heat given out in the same process, then according to the second law of thermodynamics<sup>3</sup> we can write

$$(26) \quad U_x = \epsilon_x - T \left( \frac{\partial \epsilon_x}{\partial T} \right)_x$$

Goldmann and Polanyi called  $U_x$  the differential heat of wetting. That this is the same as the net heat of adsorption we can see by substituting equation (25) into (26)

$$(27) \quad U_x = RT^2 \left( \frac{\partial \ln p_x}{\partial T} \right)_x - RT^2 \frac{\partial \ln p_0}{\partial T}$$

The first term on the right hand side is the differential heat of adsorption, as a comparison with equation (22) reveals; the second term is the latent heat of vaporization according to the Clapeyron-Clausius equation.

On the basis of equation (26) the differential heat of wetting, or the net heat of adsorption, can be calculated for any value of  $x$  from the Polanyi potential and its variation with temperature. In Fig. 55, Chapter V, the affinity curves of Goldmann and Polanyi were given for carbon disulfide on charcoal. The curves represent the variation of  $\epsilon_x$  with  $x$ , and the value of  $(\partial \epsilon_x / \partial T)_x$  can be calculated from two neighboring curves. One can thus obtain the value of  $U_x$  for each value of  $x$ . The calculated heat curve is shown in Fig. 55 above the affinity curves.

The variation of  $\epsilon_x$  with  $T$  can be written as

$$(28) \quad \left( \frac{\partial \epsilon_x}{\partial T} \right)_x = - \left( \frac{\partial \epsilon_x}{\partial x} \right)_T \left( \frac{\partial x}{\partial T} \right)_{\epsilon_x}$$

From equations (26) and (28) it follows that

$$(29) \quad U_x - \epsilon_x = T \left( \frac{\partial \epsilon_x}{\partial x} \right)_T \left( \frac{\partial x}{\partial T} \right)_{\epsilon_x}$$

According to the potential theory the addition of more gas to the amount already adsorbed results in a compression of the adsorbed layer. The heat given out in the compression of a liquid is proportional to the pressure and to the thermal expansion of the liquid. The pressure in this case is equal to the decrease in the potential perpendicular to the surface  $\epsilon_x = \text{constant}$ , it is therefore proportional to  $-(\partial\epsilon_x/\partial x)_T$ . The thermal expansion is proportional to  $-(\partial x/\partial T)_{\epsilon_x}$ . Thus the term on the right hand side of equation (29) is the differential heat of compression. According to Goldmann and Polanyi, therefore, the heat of compression is not equal to the net heat of adsorption  $U_x$ , but to the difference between  $U_x$  and the adsorption potential  $\epsilon_x$ . Since  $\epsilon_x$  is a positive quantity the heat of compression is always smaller than  $U_x$ . The value of the differential latent heat of compression can be calculated from the curves of Fig. 55 for any value of  $x$ ; it is simply the difference between the ordinates of the heat curves and the affinity curves. The variation of  $U_x$  with  $x$  will be discussed later.

When 1 gram of an evacuated adsorbent is immersed in a liquid, the heat liberated is called the integral heat of wetting, or more generally simply the heat of wetting

$$(30) \quad U_i = \int_0^{x_b} U_x dx$$

where  $x_b$ , as defined in Chapter V, is the weight of gas adsorbed per gram of adsorbent at the saturation pressure  $p_0$ . From equations (27) and (30) it follows that

$$(31) \quad U_i = q_{im} - q_L$$

where  $q_{im}$  is the integral heat of adsorption from zero adsorption to the maximum adsorption of  $x_b$  grams, and  $q_L$  is the heat of evaporation of  $x_b$  grams of liquid. Patrick and Greider<sup>46</sup> proved experimentally the correctness of equation (31) for the heat of wetting of silica gel by water and by sulfur dioxide. They found that at 0° C. the mean weight of water adsorbed at saturation was 361.2 mg. per gram of silica gel, and the mean value of the integral heat of adsorption up to saturation was 236.2 calories per gram of gel. The heat of evaporation of 361.2 mg. of water is 215.6 calories at 0° C., giving at saturation a net heat of 20.6 calories per gram of gel. Patrick and Grimm<sup>47</sup> obtained experimentally a heat of wetting of 19.22 calories per gram of gel at 25° C. Good agreement was obtained also for sulfur dioxide

<sup>46</sup> W. A. Patrick and C. G. Greider, *J. Phys. Chem.*, **29**, 1031 (1925).

<sup>47</sup> W. A. Patrick and F. V. Grimm, *J. Am. Chem. Soc.*, **43**, 2144 (1921).



on silica gel; however, in that case the calculation involved an extrapolation of the adsorption isotherm to the saturation pressure by means of the Freundlich equation, which is entirely unjustified.

As we have seen at the beginning of this section, Lamb and Coolidge<sup>6</sup> found that the net heats of adsorption per unit volume of liquid adsorbed were about the same for all of their eleven vapors. Kruyt and Modderman<sup>4</sup> pointed out that if this finding were generally valid, it would follow that all liquids should have the same heat of wetting for the same adsorbent, since the volume of liquid adsorbed at saturation is nearly the same for different vapors adsorbed on the same adsorbent. This, however, is not the case. As Table XXXII

TABLE XXXII  
HEATS OF WETTING OF CHARCOAL AND SILICA GEL

Liquid	Heat of Wetting (Calories/Gram)			
	Charcoal (1)	Charcoal (2)	Charcoal (3)	Silica gel (3)
H <sub>2</sub> O	12.4		8.4	16.0
(C <sub>2</sub> H <sub>5</sub> ) <sub>2</sub> O	28.3			
C <sub>6</sub> H <sub>6</sub>	29.4	32.7	21.0	11.2
CS <sub>2</sub>	30.0	31.2	29.5	6.7
C <sub>2</sub> H <sub>5</sub> OH	28.4	23.3		
CH <sub>3</sub> OH	30.2			
C <sub>2</sub> H <sub>5</sub> Cl	32.8			
C <sub>6</sub> H <sub>5</sub> NO <sub>2</sub>			27.1	14.3
CCl <sub>4</sub>			20.0	6.3
Petroleum ether			23.8	4.3
CH <sub>3</sub> COCH <sub>3</sub>		28.6		

The investigators were: (1) Andress and Berl,<sup>48</sup> (2) Bartell and Fu,<sup>49</sup> and (3) Culbertson and Winter.<sup>50</sup>

shows, the heats of wetting of charcoal by organic liquids are not very different, although not equal, but the heats of wetting of silica gel by organic liquids are quite far apart.

The heats of wetting of charcoals by water are considerably smaller than the heats of wetting by organic liquids. McBain<sup>51</sup> pointed out that on the basis of the results of Coolidge<sup>9</sup> and Keyes and Marshall<sup>10</sup> one should expect negative heats of wetting for the water-charcoal system. This view is erroneous, and is based on a

<sup>48</sup> K. Andress and E. Berl, *Z. phys. Chem.*, **122**, 81 (1926).

<sup>49</sup> F. E. Bartell and Y. Fu, *J. Phys. Chem.*, **33**, 1758 (1929).

<sup>50</sup> J. L. Culbertson and L. L. Winter, *J. Am. Chem. Soc.*, **59**, 308 (1937).

<sup>51</sup> J. W. McBain, *The Sorption of Gases and Vapours by Solids*, London, 1932, p. 415.

lack of distinction between differential and integral heats of wetting. It is true that the differential heat of wetting ought to be negative at small adsorptions, but the experimentally measured integral heat of wetting need not be negative. In fact, if the interpretation of Coolidge's water-charcoal isotherms given in Chapter VI in terms of the theory of multimolecular adsorption is correct, then the heat of adsorption is smaller than  $E_L$  only at low pressures; at higher pressures it becomes equal to  $E_L$ , and at still higher pressures becomes greater than  $E_L$ . Thus one can account for the relatively small positive values of the heats of wetting.

While the heats of wetting of charcoal by organic liquids are larger than the heats of wetting by water, for silica gel the reverse is true. The reason for this is that  $\text{SiO}_2$  is built of ions, and the forces of interaction between these ions and the large dipole moments of the adsorbed water molecules exceed the dispersion forces that operate between  $\text{SiO}_2$  and the adsorbed organic molecules. Nitrobenzene has almost as large heat of wetting as water for silica gel, but nitrobenzene is not merely a large polarizable molecule, it also has a large dipole moment. Charcoal, on the other hand, is non-ionic, and so the dispersion forces between the large, polarizable organic molecules and the carbon surface outweigh the sum of the small dispersion and somewhat larger orientation forces that exist between water and the carbon surface. This is of course a very crude qualitative argument, but it is probably essentially correct.

#### HEATS OF ADSORPTION OF DIFFERENT GASES ON THE SAME ADSORBENT AND OF THE SAME GAS ON DIFFERENT ADSORBENTS

Although this subject has not been investigated thoroughly, there are a few simple rules that can be deduced on the basis of existing experimental data. The first is that the heat of adsorption increases as the boiling point of the gas increases. We have seen that helium, boiling at 4.2° K., has a heat of adsorption of about 140 calories per mole; hydrogen, boiling at 20.4° K., has a heat of adsorption of about 1500 calories per mole, and the four gases, argon, nitrogen, oxygen and carbon monoxide, boiling in the temperature range 77.3–90.1° K., have heats of adsorption of about 3–4000 calories per mole. We did not specify the adsorbents for these gases because the heats of adsorption seem to be roughly the same whether the adsorbent is charcoal, a metal, or an oxide.

For ammonia, carbon dioxide, and nitrous oxide Favre<sup>52</sup> obtained heats of adsorption of 7200, 7300 and 7400 calories per mole, respectively. For ethylene, acetylene, carbon dioxide and nitrous oxide Gregg<sup>8</sup> obtained values of 6600, 8100, 6900 and 7200 calories per mole, respectively. These heats of adsorption were obtained on charcoal. The boiling points of the five gases lie between 169 and 240° K. Finally, the vapors listed in Table XXXI have their boiling points between 300 and 350° K., and the heats of adsorption fall between 12,000 and 15,500 calories per mole.

Although in general the heats of adsorption increase with increasing boiling points of the gases, this rule is by no means rigorous. Thus

TABLE XXXIII  
HEATS OF ADSORPTION OF ORGANIC VAPORS BY CHARCOAL

Vapor	Heat of Adsorption ( $q_m$ ) kcal./mole	Investigators
CH <sub>3</sub> OH	13.1	Lamb and Coolidge <sup>6</sup>
C <sub>2</sub> H <sub>5</sub> OH	15.0	Lamb and Coolidge <sup>6</sup>
C <sub>3</sub> H <sub>7</sub> OH	16.4	Cameron <sup>53</sup>
C <sub>2</sub> H <sub>5</sub> Cl	12.0	Lamb and Coolidge <sup>6</sup>
C <sub>2</sub> H <sub>5</sub> Br	13.9	Lamb and Coolidge <sup>6</sup>
C <sub>2</sub> H <sub>5</sub> I	14.0	Lamb and Coolidge <sup>6</sup>
CH <sub>4</sub>	4.5	Whitehouse <sup>54</sup>
CH <sub>3</sub> Cl	9.2	Pearce and Reed <sup>13</sup>
CH <sub>2</sub> Cl <sub>2</sub>	12.4	Pearce and Reed <sup>13</sup>
CHCl <sub>3</sub>	14.4	Pearce and Reed <sup>13</sup>
CCl <sub>4</sub>	15.5	Pearce and Reed <sup>13</sup>
CH <sub>3</sub> Cl	9.2	Pearce and Reed <sup>14</sup>
C <sub>2</sub> H <sub>5</sub> Cl	12.2	Pearce and Reed <sup>14</sup>
n-C <sub>3</sub> H <sub>7</sub> Cl	14.6	Pearce and Reed <sup>14</sup>
iso-C <sub>3</sub> H <sub>7</sub> Cl	13.1	Pearce and Reed <sup>14</sup>
n-C <sub>4</sub> H <sub>9</sub> Cl	15.6	Pearce and Reed <sup>14</sup>
sec-C <sub>4</sub> H <sub>9</sub> Cl	14.4	Pearce and Reed <sup>14</sup>
ter-C <sub>4</sub> H <sub>9</sub> Cl	13.6	Pearce and Reed <sup>14</sup>

methyl alcohol boils at 337° K. and has a heat of adsorption of 13,100 calories per mole, while ether boils at 307° K., and yet its heat of adsorption is as high as 15,500 calories per mole. To understand the differences between the members of such a group as is represented in Table XXXI one must consider the detailed structures of the molecules, their sizes, polarizabilities, dipole moments, etc., as was discussed in Chapter VII.

Some other interesting rules can be deduced from Table XXXIII, representing the heats of adsorption of a number of organic vapors on

<sup>52</sup> P. A. Favre, *Ann. chim. phys.*, (5), 1, 209 (1874).

<sup>53</sup> H. K. Cameron, *Trans. Far. Soc.*, 26, 239 (1930).

<sup>54</sup> A. G. R. Whitehouse, *J. Soc. Chem. Ind.*, 45, 13T (1926).

charcoal. The second column of the table gives  $q_m$ , the integral heat of adsorption of 1 mole of vapor on 500 grams of charcoal. The value of  $q_m$  increases with increasing size of the molecule. The addition of successive  $\text{CH}_2$  groups causes smaller and smaller increase. Addition of the first  $\text{CH}_2$  group to  $\text{CH}_3\text{OH}$  increases  $q_m$  by 1.9 kcal., addition of a second  $\text{CH}_2$  group increases it only by 1.4 kcal. Similarly, addition of the first  $\text{CH}_2$  group to  $\text{CH}_3\text{Cl}$  causes an increase of 3.0 kcal., the second 2.4 kcal., and the third 1.0 kcal. Of course, these are all approximate values.

Replacement of the hydrogen atoms by chlorine atoms in  $\text{CH}_4$  causes an increase in the heat of adsorption. The first replacement results in the largest increase; each successive replacement produces a smaller increase. The first replacement raises  $q_m$  by 4.7 kcal., the second by 3.2, the third by 2.0, and the fourth by 1.1 kcal.

Replacement of hydrogen atoms by OH radicals causes a greater increase in  $q_m$  than replacement by Cl. Methyl, ethyl and propyl alcohol have larger heats of adsorption than the corresponding chlorides. This is true in spite of the fact that the chlorides have slightly larger dipole moments. Possibly the main factor accounting for the smaller heats of adsorption of the chlorides is their larger molecular radius, which makes the distances of the chloride molecules from the surface larger than the distances of the alcohol molecules. Since the heat of adsorption is inversely proportional to  $r^3$ , it should be inversely proportional to the molecular volume. The ratios of the molecular volumes of methyl chloride to methyl alcohol, ethyl chloride to ethyl alcohol, and propyl chloride to propyl alcohol are 1.37, 1.20 and 1.18, respectively; the ratios of the heats of adsorption of methyl alcohol to methyl chloride, ethyl alcohol to ethyl chloride, and propyl alcohol to propyl chloride are 1.42, 1.23 and 1.12, respectively. Notwithstanding this numerical parallelism, one should not put too much emphasis on such rough qualitative considerations. As we have seen in Chapter VII, the dispersion energies are proportional to the polarizabilities and characteristic energies of the molecules. These data are not available for the six molecules considered, but it seems that in this case the larger polarizabilities of the chloride molecules are compensated by smaller characteristic energies. The orientation energies are also determined here by the molecular volumes alone, since the dipole moments of the corresponding chlorides and alcohols are approximately equal.

Table XXXIII also shows that branched chain compounds have smaller heats of adsorption than straight chain compounds. Isopropyl

chloride has a smaller heat of adsorption than normal propyl chloride, secondary butyl chloride than normal butyl chloride, and tertiary butyl chloride than secondary butyl chloride. This is true again in spite of the fact that the branched chain compounds have slightly larger dipole moments. Probably here also the explanation has to do with the distances of the molecules from the surface. If the organic vapor molecules have a tendency to lie flat on the charcoal surface, the average distance of the branched chain molecule from the surface will be greater than that of the straight chain molecule, which results in a smaller interaction energy.<sup>55</sup>

The heats of adsorption of the ethyl halides, just like those of the hydrogen halides, increase with increasing atomic weight of the halogen, again in spite of the fact that the dipole moments decrease from the chloride to the iodide. Although these molecules have dipole moments between  $1.66$  and  $1.99 \times 10^{-18}$  e.s.u.,<sup>56</sup> the dispersion forces outweigh the orientation forces.

An exceptionally interesting comparison between heats of adsorption of different gases on the same adsorbent is afforded by the results of Reyerson and Cameron<sup>39</sup> and Reyerson and Wishart<sup>57</sup> for the adsorption of the halogens by silica gel. The heat of adsorption increases as we pass from chlorine to iodine, and yet the amount adsorbed at equal relative pressures decreases very strongly. This apparent paradox was solved by the theory of multimolecular adsorption, as we have seen in Chapter VI. The decisive factor for the shape of the isotherm in physical adsorption is not the absolute value of the heat of adsorption, but the difference between the heat of adsorption and the heat of liquefaction, i.e., the net heat of adsorption. The net heat is approximately zero for bromine, positive for chlorine and negative for iodine, thus accounting for the great differences in the amounts of gas adsorbed at equal relative pressures.

Passing now to comparisons between heats of adsorption of the same gas on different adsorbents, it is well to emphasize again the

<sup>55</sup> Further interesting comparisons between heats of adsorption of organic vapors on the same adsorbent can be found in the works of J. N. Pearce and J. F. Eversole (*J. Phys. Chem.*, **38**, 383, 1934), J. N. Pearce and A. C. Hanson (*Proc. Iowa Acad. Sci.*, **41**, 140, 1934), J. N. Pearce and P. E. Peters (*J. Phys. Chem.*, **42**, 229, 1938), and W. A. Felsing and C. T. Ashby (*J. Am. Chem. Soc.*, **56**, 2226, 1934). The first three papers give isosteric heats of adsorption of dichloro-hydrocarbons, ketones, esters and ethers on charcoal, the last gives integral  $q_m$  values for the adsorption of ammonia and the three methylamines on silica gel.

<sup>56</sup> C. P. Smyth, *Dielectric Constant and Molecular Structure*, New York, 1931, p. 193.

<sup>57</sup> L. H. Reyerson and A. W. Wishart, *J. Phys. Chem.*, **41**, 943 (1937).

striking lack of specificity in this respect. In Chapter VI attention was called to the fact that the  $E_1 - E_L$  values, evaluated from adsorption isotherms on the basis of the multimolecular adsorption theory, were very nearly the same for the same gas on a variety of different adsorbents. In Table XIV these values were listed for nitrogen on a dozen different substances, including unpromoted and promoted iron catalysts, copper, chromic oxide, and silica gel. The average of the net heat values was 840 calories per mole, and no individual value differed by as much as 9%.

In the present chapter we have already cited numerous examples showing that the heats of adsorption of a gas on different adsorbents are approximately equal. For the heat of adsorption of hydrogen on charcoal at  $-185^\circ\text{C}$ . Dewar<sup>17</sup> measured calorimetrically 1600 calories per mole, for hydrogen on iron Benton<sup>23</sup> obtained 1600 calories per mole from isotherms at  $-183$  and  $-195^\circ\text{C}$ . For hydrogen on different mixed oxide catalysts Taylor and his collaborators<sup>28,29</sup> found heats of adsorption of 2000 calories per mole, while Emmett and Harkness<sup>26</sup> obtained the same value for hydrogen on iron (isosteric heats). For nitrogen on iron and on chromic oxide Beebe and his collaborators<sup>20,22</sup> determined calorimetrically values decreasing with increasing amounts adsorbed from 4500 to 2600 calories per mole. In the same range fall the values of 3700 calories per mole, obtained by Dewar<sup>17</sup> for nitrogen on charcoal and 3000 calories per mole, obtained by Kälberer and Schuster<sup>58</sup> for nitrogen on silica gel.

For the heat of adsorption of carbon dioxide on silica gel Magnus<sup>59</sup> measured 7100 calories per mole and for carbon dioxide on charcoal 7800 calories per mole. For carbon dioxide on charcoal Gregg<sup>8</sup> obtained 7900 calories per mole. For ethylene on silica gel Kälberer and Schuster<sup>58</sup> obtained 7200 calories per mole, and for ethylene on charcoal Gregg<sup>8</sup> measured 8100 calories per mole. These values correspond to small amounts of gas adsorbed (roughly 3 cc. per gram) and to temperatures at or near to  $0^\circ\text{C}$ . In general, the heats of adsorption of non-polar gases on charcoal are slightly higher than on silica gel and most other adsorbents.

In view of the foregoing examples we can conclude that the heats of van der Waals adsorption of a gas on different adsorbents do not show very great differences.<sup>60</sup> Although the methods of calculation

<sup>58</sup> W. Kälberer and C. Schuster, *Z. phys. Chem.*, **A141**, 270 (1929).

<sup>59</sup> A. Magnus, *Z. phys. Chem.*, **A142**, 401 (1929).

<sup>60</sup> A notable exception is chabasite, which exhibits much higher heats of physical adsorption than other adsorbents. This point is further discussed in Chapter XI.

of the interaction energy between a given molecule and an ionic adsorbent on the one hand and the same molecule and a metallic conductor on the other are quite different, these different treatments lead to approximately the same heat values. Thus for the heat of adsorption of argon on potassium iodide calculation gives 2100 calories per mole, for argon on copper 2700, and for nitrogen on charcoal 2400 calories per mole (Chapter VII). Of course, all of these values are only rough approximations, and somewhat too low when compared with the experimental heats of adsorption.

In the next section we discuss the variation of the differential heats of adsorption with the amount of gas adsorbed. Usually the initial heats of adsorption are larger than the values obtained on later additions of gas. The differences between the initial values of  $q_d$  of a gas on different adsorbents are ordinarily much greater than the differences in consecutive values. If the heat of adsorption is calculated for a sufficiently large amount of gas adsorbed, the differences for different adsorbents tend to disappear. This fact is shown in Table XXXIV, taken from Kruyt and Modderman.<sup>4</sup> The integral

TABLE XXXIV  
HEATS OF ADSORPTION OF CARBON DIOXIDE ON DIFFERENT CHARCOALS

Type of Charcoal	Temperature of Outgassing, ° C.	$q_i$ Calories per cc.	Investigators
French Gasmask	900	0.313	Keyes and Marshall <sup>10</sup>
Wood charcoal	600	0.313	Magnus and Kälberer <sup>61</sup>
Various kinds	unknown	0.311	Favre <sup>62</sup>
Birchwood	400	0.311	Gregg <sup>8</sup>
Coconut charcoal	400	0.311	Titoff <sup>2</sup>
Wood Charcoal	100	0.308	Magnus and Kälberer <sup>61</sup>
Evonymus europaeus	unknown	0.304	Chappuis <sup>62</sup>

heats of adsorption of carbon dioxide on different charcoals were calculated for the entire pressure range from 0 to 760 mm. In spite of the great differences in the kind of charcoal used and in the previous treatment of the charcoal, the values of  $q_i$  are almost the same (approximately 7000 calories per mole). All values of the table are calorimetric.

<sup>61</sup> A. Magnus and W. Kälberer, *Z. anorg. allgem. Chem.*, 164, 345, 357 (1927).

<sup>62</sup> P. Chappuis, *Wied. Ann.*, 19, 21 (1883).

VARIATION OF THE HEAT OF ADSORPTION WITH THE  
AMOUNT OF GAS ADSORBED

In Chapter VII the heat of adsorption was calculated as the interaction energy between an isolated molecule and an ideal uniform adsorbing surface. We discussed the heat of adsorption of argon on copper or nitrogen on charcoal as if it were a constant quantity, characteristic of the adsorbent-adsorbate system, and did not consider so far its dependence on such factors as temperature, pressure, or the amount of gas adsorbed.

One of the fundamental assumptions in the derivation of the Langmuir equation is that the heat of adsorption does not vary with the amount of gas adsorbed. The same assumption is involved also in the derivation of the equation of Williams and Henry, as we have seen in Chapter IV. When the adsorption isotherms obey these equations, the investigator may possibly deal with an approximately uniform surface, or at least with a roughly homogeneous part of a surface.

An approximately constant heat of adsorption was found by Evans<sup>63</sup> for the adsorption of ammonia on chabasite at 0° C., discussed in Chapter IV. Other examples can be found in the data of Tables XXVII and XXVIII. The  $dq/da$  values of carbon dioxide on charcoal are roughly constant from 20 to 45 cc. adsorbed, the values for water on charcoal can be considered constant from 20 to 200 cc. adsorbed, and the values for nitrogen on charcoal are practically constant in the entire range of adsorption given in the table. In this last case probably less than 10% of the surface was covered with nitrogen.

Examples of constant heats of adsorption over the entire surface of an adsorbent, or even over a large part of the surface, are very rare. Ordinarily the differential heats of adsorption vary considerably with the amount of gas adsorbed, and often the variation is quite complex. Chappuis,<sup>62</sup> the first investigator of differential heats of adsorption, had already noticed this variation.

There are two factors that may cause variation in the differential heats of adsorption, one depending on the nature of the adsorbent, the other on the nature of the adsorbate. We have seen in Chapter VII that the heat of adsorption of an isolated molecule on a plane surface is different from that of a molecule located in the crevices, pockets, tubes, or cells of an adsorbent. Even on a plane surface the heat of adsorption may vary considerably because of differences in

<sup>63</sup> M. G. Evans, *J. Chem. Soc.*, 1931, 1556.



the packing of the surface atoms: a molecule adsorbed on a (100) crystal plane will have a different heat of adsorption from one adsorbed on a (111) plane. Furthermore, variation in the heats of adsorption may be produced by interaction between the adsorbed molecules themselves. If the adsorbed molecules have permanent dipoles the surface forces may line up these dipoles parallel and oriented in the same direction; in this case there will be repulsion between the molecules, diminishing the heat of adsorption. If the molecules are non-polar, the dispersion forces between them will lead to attraction, increasing the heat of adsorption. The attractive or repulsive forces increase as the surface becomes filled with adsorbed molecules, since the average distance between the molecules decreases.

Usually, though not always, the initial value of the differential heat of adsorption is also its maximum value, successive additions of gas causing a decrease in  $q_d$ . Sometimes the decrease is quite sharp, as is illustrated in Fig. 85, representing the isosteric  $q_d$  values obtained by Barrer<sup>64</sup> for hydrogen, argon, and nitrogen on graphite in the temperature range 71–288° K. Curve I for nitrogen shows that  $q_d$  decreases 1900 calories during the adsorption of the first 20 cc., but only 200 calories during the adsorption of the next 60 cc. Curves II represent the variation of  $q_d$  during the adsorption of the first few tenths of cc. of gas. For argon  $q_d$  drops 600 calories for the first 0.8 cc. adsorbed, but only about 150 calories for the last 60 cc. adsorbed.

The maximum value of the heat of adsorption in Barrer's curves appears when only a very small fraction of the surface is covered with the adsorbate. Since the average distance between the adsorbed molecules is too large to permit appreciable interaction, the cause of the maximum must be found in the structure of the adsorbent. One possibility is that the different densities of packing of the carbon atoms in the prismatic and in the basal surfaces of graphite cause the variation. In this case we would expect the large heat values to occur on the prismatic surfaces, since the prismatic area is small, and the large  $q_d$  values to occur only on a small part of the surface. However, calculation shows that the theoretical heat of adsorption is smaller on the prismatic surfaces than on the basal surfaces. Barrer attributes the initial large values to adsorption in the cracks of the adsorbent. As the angle of intersection between the two surfaces that form the crack becomes more acute a crack with two parallel sides is approximated. In such a crack the heat of adsorption would be twice as large as on a

<sup>64</sup> R. M. Barrer, *Proc. Roy. Soc., A161*, 476 (1937).

plane surface. The initial and final values of  $q_d$  are actually quite near to this 2 : 1 ratio: 4600 and 2500 calories per mole for nitrogen, 4100 and 2400 for argon, and 2000 and 1100 for hydrogen.

The initial decrease in the heat of adsorption is not always as sharp as in Barrer's curves. A more gradual decrease in  $q_d$  is illus-

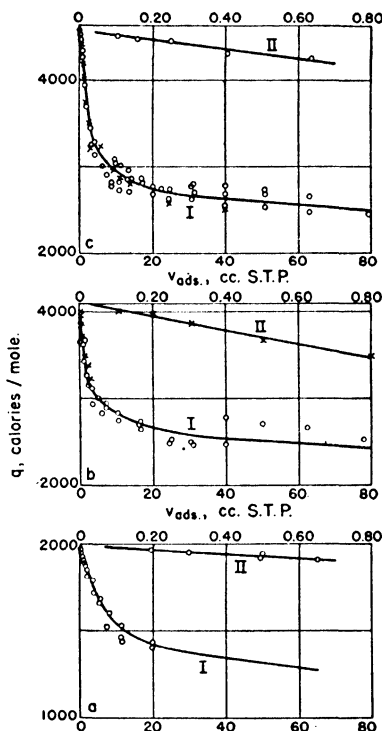


FIG. 85.—Isosteric differential heats of adsorption of (a) hydrogen, (b) argon and (c) nitrogen on graphite.

trated in Fig. 86, representing the isosteric heats of adsorption of hydrogen and deuterium on charcoal in the temperature range 17 to 90° K., obtained by Dingenen and Itterbeek.<sup>65</sup> There is a monotonous decrease in  $q_d$  for both gases from about 2000 calories per mole to values approaching the heats of liquefaction. (The height of the arrow represents the magnitude of the heat of liquefaction.) The

<sup>65</sup> W. van Dingenen and A. van Itterbeek, *Physica*, 6, 49 (1939).

heat of adsorption of deuterium is about 180 calories larger than that of hydrogen through the entire range of adsorption.

To describe the variation of the heat of adsorption with the amount of gas adsorbed, Lamb and Coolidge<sup>6</sup> suggested the empirical exponential formula

$$(32) \quad q = ma^n$$

where  $q$  is the total heat evolved when the amount of gas adsorbed is  $a$  cc. per gram (integral heat of adsorption), and  $m$  and  $n$  are constants.

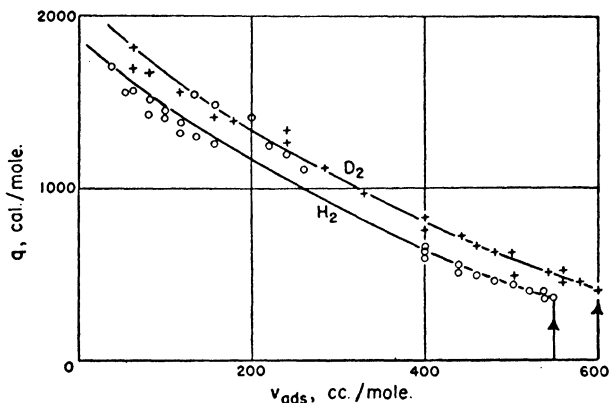


FIG. 86.—Heats of adsorption of hydrogen and deuterium on charcoal.

The values of these constants for the eleven vapors they investigated were given in Table XXXI.

Equation (32) can be put in the logarithmic form

$$(33) \quad \log q = \log m + n \log a$$

The plots of  $\log q$  against  $\log a$  often give very good straight lines, as shown in Fig. 87 for ethyl alcohol and carbon disulfide on charcoal. The slopes of the straight lines give the values of the constant  $n$ . For ethyl alcohol and carbon disulfide  $n$  is 0.928 and 0.9205, respectively, consequently the two lines are almost parallel. As a matter of fact, the  $n$  values of all eleven vapors are quite close to each other, as Column 2, Table XXXI shows. Furthermore, the value of  $n$  is near to unity in all cases, which means that the differential heats of adsorption decrease only slightly with the amount of vapor adsorbed.

This can be seen by differentiating  $q$  with respect to  $a$  in equation (32)

$$(34) \quad \frac{dq}{da} = \frac{mn}{a^{(1-n)}}$$

When the exponent  $1 - n$  becomes zero,  $dq/da$  becomes constant; i.e., the differential heats of adsorption become independent of the amount adsorbed. We can see from Table XXXI that the value of  $1 - n$  is very small for each of the eleven vapors. Lamb and Coolidge found

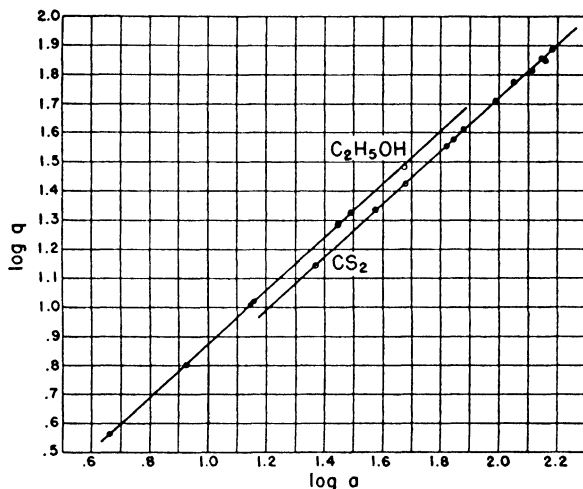


Fig. 87.—Heats of adsorption of alcohol and carbon disulfide on charcoal plotted according to the equation of Lamb and Coolidge.

some parallelism between  $1 - n$  and the boiling points of the liquids: the higher the boiling point, the smaller was the value of  $1 - n$ . Thus the variation of  $dq/da$  with  $a$  was the largest for the lowest boiling substances; for example,  $1 - n$  for ammonia calculated from the experiments of Chappuis<sup>62</sup> was 0.305, which is 3–4 times as large as the values obtained for the organic vapors of the table.

Other investigators also found that the Lamb-Coolidge equation (32) describes their results with reasonable accuracy. Patrick and Greider<sup>46</sup> found that for the adsorption of water vapor and sulfur dioxide by silica gel the values of  $n$  were 0.914 and 0.860, respectively. Sulfur dioxide boils at a higher temperature than ammonia, but at a lower temperature than the vapors of Table XXXI, and its  $n$  value also

falls between those of ammonia and the organic vapors. However, Gregg<sup>8</sup> found for ethane, ethylene, and acetylene on charcoal the  $n$  values 0.966, 0.945 and 0.925, respectively, in spite of the fact that these gases boil at considerably lower temperatures than ammonia.

Although equation (32) is useful in giving a concise description of experimental data, it reveals very little about the nature of the adsorption process itself. Another important objection to its use was voiced by Kruyt and Modderman,<sup>4</sup> who pointed out that when the curve showing the variation of  $dq/da$  with  $a$  has an extremum, the curve giving the variation of  $q$  with  $a$  should have a point of inflection which, however, can not be expressed by the exponential formula. The reason why the formula seems often satisfactory is shown in Fig. 88. Here curve II gives the variation of  $q$  with  $a$  for an imaginary

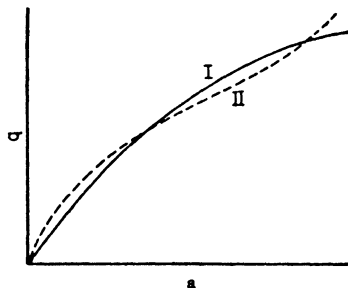


FIG. 88.—Variation of the integral heat of adsorption with the amount adsorbed.

gas as determined by experiment, and curve I represents the results by the exponential formula (32). The deviations of the real curve from the formula are distributed on both sides and may be attributed erroneously to experimental error. It is better therefore to give fully the variation of  $dq/da$  with  $a$ , as found by experiment.

The variation of the differential heats of adsorption with the amount adsorbed is not always as simple as in Figs. 85 and 86. The curves are often quite complicated, showing minima and maxima. An example of this is given in Fig. 89, taken from Kruyt and Modderman,<sup>4</sup> showing the variation of  $dq/da$  with  $a$  for ether on charcoal. Curve I gives the results of Keyes and Marshall<sup>10</sup> at 0° C., curve II those of Lamb and Coolidge<sup>6</sup> at 0° C., and curve III those of Pearce and McKinley<sup>66</sup> at 25° C.—all calorimetric data. Although these investigators worked with charcoals of different structures and ad-

<sup>66</sup> J. N. Pearce and L. McKinley, *J. Phys. Chem.*, **32**, 360 (1928).

sorbing capacities, the course of the curves seems to be surprisingly similar. All three curves show first a descending, then an approximately horizontal, and then again a descending portion; two of the curves then continue with an ascending portion. Thus there are minima in the curves representing the data of Lamb and Coolidge, and Pearce and McKinley, which can not be reproduced by the exponential formula (32).

The appearance of minima in the  $q_d$  vs.  $a$  curves is by no means infrequent. The data of Table XXVI show that Titoff<sup>2</sup> obtained

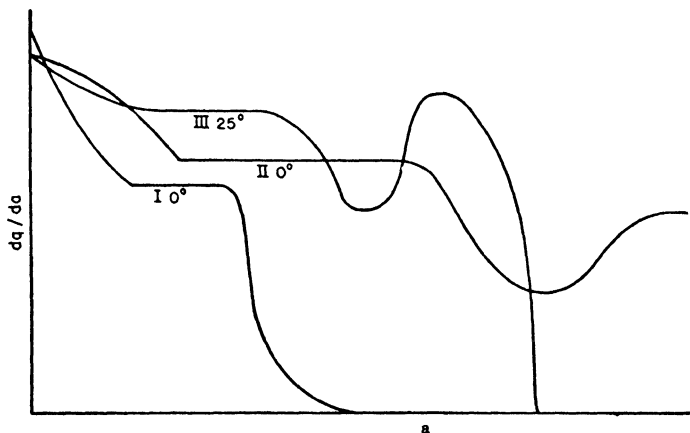


FIG. 89.—The differential heats of adsorption of ether on charcoal.

minima for both nitrogen and ammonia on charcoal. Chappuis<sup>62</sup> also found a minimum for ammonia on charcoal. Gregg<sup>8</sup> and Pearce and McKinley<sup>66</sup> obtained minima for several organic vapors on charcoal, and Williams<sup>67</sup> found two minima for sulfur dioxide on blood charcoal.

There are a number of different ways to account for the complex dependence of the heat of adsorption on the amount of gas adsorbed. According to the theory of multimolecular adsorption, discussed in Chapter VI, the  $q_d$  vs.  $a$  curve ought to show: (1) a descending portion having  $q_d$  values greater than  $E_1$ , corresponding to adsorption on the most active part of the surface; (2) an approximately horizontal portion with heat of adsorption  $E_1$ , corresponding to adsorption on the less active and roughly homogeneous part of the surface; (3) another

<sup>67</sup> A. M. Williams, *Proc. Roy. Soc. Edinburgh*, 37, 162 (1917).

descending portion due to the transition of  $q_d$  from  $E_1$  to  $E_L$ ; (4) another longer or shorter flat portion where the heat of adsorption is  $E_L$ ; and (5) an ascending portion due to liberation of the heat of capillary condensation  $Q$ . Thus the theory of multimolecular adsorption is able to explain a minimum in the region of large adsorptions, as for example in curves II and III of Fig. 89.

Polanyi and Welke<sup>68</sup> studied the adsorption of sulfur dioxide by charcoal at very low pressures and found that the heat of adsorption calculated from isotherms at 0 and 5° C. had a minimum in the region of very small adsorptions. As Fig. 90 shows, there is at first a very

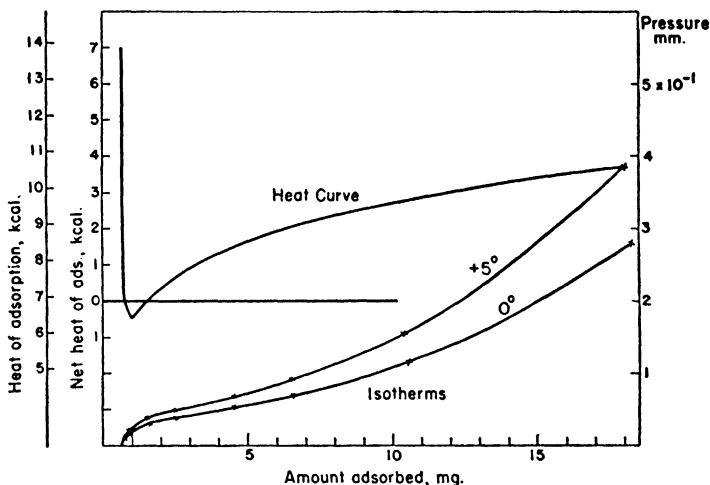


Fig. 90.—Heats of adsorption and adsorption isotherms of sulfur dioxide on charcoal.

sharp decrease in  $q_d$  with increasing adsorption, and a minimum is reached when about 1 mg. of  $\text{SO}_2$  is adsorbed. This corresponds to less than 1% of the charcoal surface covered with adsorbed gas. The value of  $q_d$  at its minimum is somewhat smaller than the heat of liquefaction of sulfur dioxide. Beyond the minimum  $q_d$  increases steadily, but the experiments were carried only up to 18.5 mg.  $\text{SO}_2$  adsorbed, which still corresponds to only a few percent of the surface covered. Polanyi and Welke suggest that the initial decrease in the heat of adsorption is caused by the heterogeneity of the surface, the large initial values of  $q_d$  being due to adsorption on the most active

<sup>68</sup> M. Polanyi and V. Welke, *Z. phys. Chem.*, **132**, 371 (1928).

points of the charcoal. When about 1 mg. of  $\text{SO}_2$  is adsorbed the adsorbate which at the lowest pressures behaves like a two-dimensional gas begins to condense to a two-dimensional liquid. The appearance of the heat of condensation causes the rise in  $q_d$ . This explanation would account for a minimum in the heat of adsorption curve at very small adsorptions.<sup>69</sup>

Roberts<sup>70</sup> showed that interaction between the adsorbed molecules can lead to a complex variation of  $q_d$  with  $a$  even if the adsorption takes place on a plane, uniform surface. He considered two cases: the adsorption of dipole molecules on the surface of a conductor, and the adsorption of non-polar molecules on the surface of an ionic crystal (the latter in collaboration with Orr<sup>71</sup>).

When an isolated molecule possessing a rigid permanent dipole moment is adsorbed on the surface of a conductor there is only one term in the interaction energy: the attraction between the dipole and its mirror image (Chapter VII). When the surface is completely covered by the adsorbate there is interaction not merely between the dipole and its mirror image, but also between the dipole and the mirror images of all of the other dipoles. If the adsorbed dipoles are all lined up parallel to each other and normal to the surface, the totality of the electric images can be considered as two infinite parallel sheets of charges of opposite sign. The combined effect of such an arrangement is smaller than that of a single image. The heat of adsorption will therefore decrease with increasing surface covering, due to this depolarizing effect. Furthermore, dipoles lined up parallel and oriented in the same direction repel each other, and this repulsion between neighboring adsorbed molecules further decreases the heat of adsorption.

It was shown in Chapter VII that all molecules are polarizable to some extent, and that the dispersion effect is not negligible even for the strongest dipole molecules. The dispersion forces between neighboring adsorbed molecules lead to attraction, and the greater the fraction of the surface covered, the greater is the attraction. Thus in contrast with the orientation effect the dispersion effect results in an increase in the heat of adsorption with the amount of gas adsorbed.

Roberts<sup>70</sup> carried out numerical calculations for two dipole gases, ammonia and sulfur dioxide. The results are shown in Fig. 91(a). Curves I give the variation of the heat of adsorption with  $\theta$ , the

<sup>69</sup> Phase transitions in the adsorbate are further discussed in Chapter XII.

<sup>70</sup> J. K. Roberts, *Trans. Far. Soc.*, **34**, 1342 (1938).

<sup>71</sup> J. K. Roberts and W. J. C. Orr, *Trans. Far. Soc.*, **34**, 1346 (1938).



fraction of the surface covered, caused by the dispersion forces alone; curves II represent the variation due to the orientation forces alone; and curves III give the combined effect. The full curves refer to sulfur dioxide, the broken curves to ammonia. Since the two effects do not differ greatly in magnitude and are opposite in sign, the varia-

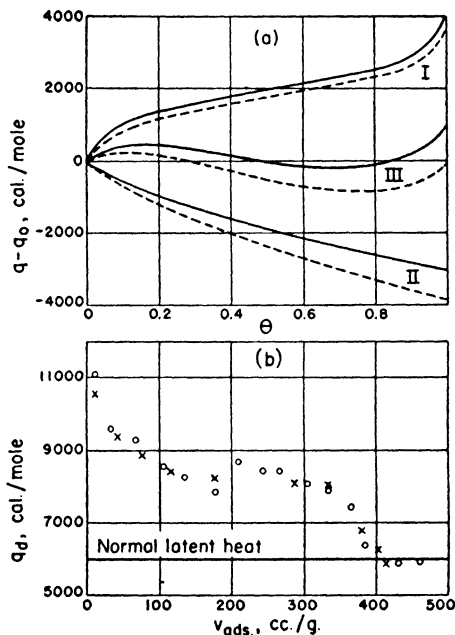


Fig. 91.—(a) The interaction energy between adsorbed molecules. (b) The heat of adsorption of sulfur dioxide on charcoal.

tion of  $q_d$  with  $\theta$  is necessarily small. The resultant curves for both gases have wavy shapes with maxima and minima.

For comparison Roberts plotted on the same scale in Fig. 91(b) the variation of  $q_d$  with  $a$  for sulfur dioxide on charcoal, obtained by Williams.<sup>67</sup> Like Polanyi and Welke<sup>68</sup> and Barrer,<sup>64</sup> Roberts also attributes the initial drop in the heat of adsorption to the heterogeneity of the charcoal surface, possibly to adsorption in the crevices or on other active parts of the surface. The approximately constant middle portion of the curve corresponds to adsorption on the plane surface, the wavy shape being caused by the superposition of the opposing

orientation and dispersion effects. In the vicinity of 300 cc. adsorbed  $q_d$  begins to decrease toward  $E_L$ , the normal latent heat of vaporization, because the second adsorbed layer begins to form. The blood charcoal used by Williams had wider pores than the charcoals of Polanyi. The adsorption isotherm of sulfur dioxide was S-shaped, with a strong upward bend in the curve around 400 cc. adsorbed. Around the same point  $q_d$  becomes equal to  $E_L$ , as shown in Fig. 91(b).

The calculations of Roberts and Orr<sup>71</sup> for the adsorption of the non-polar gas argon on the ionic lattice of cesium iodide led to similar

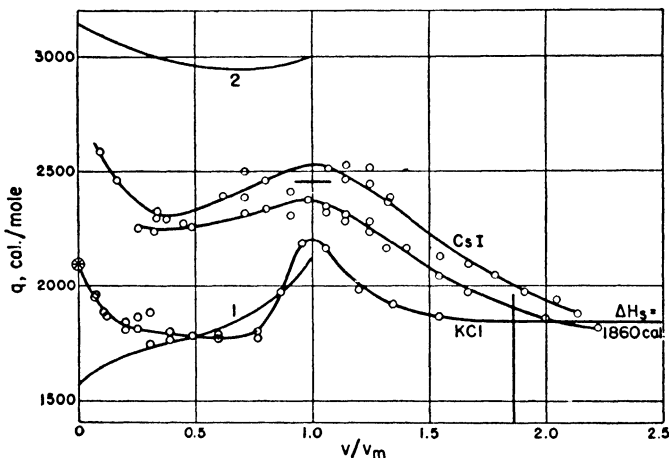


FIG. 92.—Heats of adsorption of argon on potassium chloride and cesium iodide.

results. Here the orientation effect is replaced by the influence effect, i.e., by the interaction between the ions of the surface and the dipoles induced in the argon atoms by these ions (Chapter VII). The repulsion between the induced dipoles causes a decrease in the heat of adsorption, which becomes greater with increasing surface covering. This effect, however, is overbalanced by the increase in the heat of adsorption due to dispersion forces between the adsorbed argon atoms. The net effect is a slight increase in  $q_d$  in the entire adsorption region from  $\theta = 0$  to  $\theta = 1$ .

Subsequently Orr<sup>72</sup> made more refined calculations on the variation of the heat of adsorption with the amount of gas adsorbed for the systems argon-potassium chloride and argon-cesium iodide. The results are shown in Fig. 92, in which curve 1 gives the calculated plot

<sup>72</sup> W. J. C. Orr, *Trans. Far. Soc.*, **35**, 1247 (1939).

of the heat of adsorption against  $\theta$ , the fraction of the surface covered, for potassium chloride, and curve 2 gives the same for cesium iodide. Due to van der Waals attraction between the adsorbed argon atoms the heat of adsorption on potassium chloride increases from 1593 to 2127 calories per mole between  $\theta = 0$  and  $\theta = 1$ . In contrast with this the heat of adsorption on cesium iodide at first decreases. The reason is that the (100) planes in CsI contain only like ions, either  $\text{Cs}^+$  or  $\text{I}^-$ . The layer of similar ions induces dipoles in the argon atoms, all oriented in the same direction. This results in repulsion between the adsorbed atoms and in a decrease of the heat of adsorption up to  $\theta = 0.6$ . For greater values of  $\theta$  the dispersion attraction outweighs the electrostatic repulsion and the heat of adsorption rises again.

Orr<sup>73</sup> measured experimentally the adsorption isotherms of argon on potassium chloride and cesium iodide and calculated the differential heats of adsorption by the Clapeyron-Clausius equation (23). The variation of  $q_d$  with  $\theta$  is also given in Fig. 92. It will be noted that the theoretical values check the experimental values for KCl from  $\theta = 0.5$  to  $\theta = 1.0$ . At smaller adsorptions the two curves diverge. Orr suggests that the initial large heat values are due to adsorption in the cracks and crevices of the crystal. The shapes of the experimental curves for CsI are similar to the theoretical curve 2, but there is a difference of 5–700 calories in the absolute values.

Orr also measured the isosteric heats of adsorption of oxygen and nitrogen on KCl and CsI. The curves obtained are similar to the argon curves. At  $\theta = 1$  there are fairly sharp maxima for all three gases on KCl, and rather flat maxima on CsI. Beyond the maximum the heat of adsorption decreases to the heat of liquefaction. In the case of argon at the temperatures of the measurements the bulk phase is the solid, and the heats of adsorption seem to decrease toward the heat of sublimation of solid argon, 1860 calories per mole. At  $\theta = 1.2$  the heat of adsorption differs from this value only by 150 calories, which is about equal to the experimental error.<sup>74</sup>

<sup>73</sup> W. J. C. Orr, *Proc. Roy. Soc., A173*, 349 (1939).

<sup>74</sup> A number of investigators derived isotherm equations based on the assumption that the heat of adsorption varies with the amount of gas adsorbed. Most of these equations were not subjected to experimental test; some were tested for chemisorption data. We may mention here as examples the works of R. H. Fowler (*Proc. Cambridge Phil. Soc.*, 32, 144, 1936), R. Peierls (*Proc. Cambridge Phil. Soc.*, 32, 471, 1936), J. S. Wang (*Proc. Roy. Soc., A161*, 127, 1937), J. K. Roberts (*Proc. Cambridge Phil. Soc.*, 34, 577, 1938), F. J. Wilkins (*Proc. Roy. Soc., A164*, 496, 1938), M. Temkin and V. Pyzhev (*Acta Physicochim. U.R.S.S.*, 12, 327, 1940), K. J. Laidler, S. Glasstone and H. Eyring (*J. Chem. Phys.*, 8, 659, 1940), A. R. Miller and J. K. Roberts (*Proc.*

Orr's adsorption isotherms for argon and oxygen on potassium chloride show an interesting feature: a point of inflection at adsorptions corresponding to about 30% surface covering. Theoretically one should always obtain such a point of inflection on the isotherm when the adsorbed molecules attract each other, but in practice the inflection may not be noticeable. Thus the flatter maxima in the cesium iodide curves of Fig. 92 are insufficient to lead to noticeable points of inflection in the isotherms.

Goldmann and Polanyi <sup>44</sup> investigated the variation of the net heat of adsorption, or differential heat of wetting, with the amount of gas

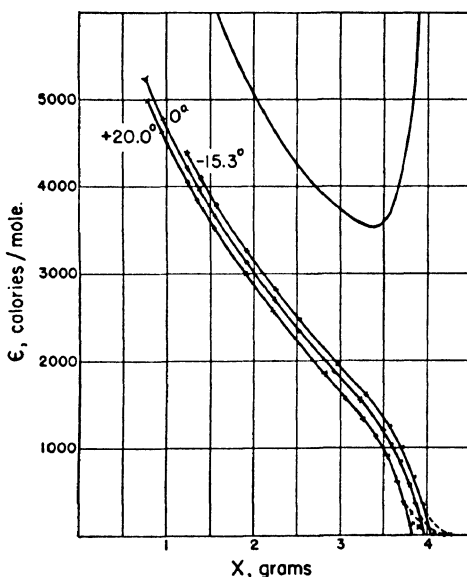


Fig. 93.—Heat curve and affinity curves of ether on charcoal.

adsorbed, and also the variation of the adsorption potential with the amount adsorbed. They called the former "heat curves" and the latter "affinity curves." An example of their results was given in Fig. 55, Chapter V; another example is shown in Fig. 93. The latter represents the heat curve and the affinity curves of ether on charcoal. The affinity curves were calculated from the adsorption isotherms

Cambridge Phil. Soc., 37, 82, 1941), and S. Brunauer, K. S. Love and R. G. Keenan (*J. Am. Chem. Soc.*, 64, 751, 1942). These papers will be discussed in Volume II.

according to the method of the potential theory described in Chapter V. The differential net heats of adsorption corresponding to the different amounts of gas adsorbed were neither obtained calorimetrically nor calculated from adsorption isotherms by means of the Clapeyron-Clausius equation, but were calculated from the affinity curves according to the equation

$$(35) \quad U_x = \epsilon_x + T \left( \frac{\partial \epsilon_x}{\partial x} \right)_T \left( \frac{\partial x}{\partial T} \right)_{\epsilon_x}$$

The term  $(\partial \epsilon_x / \partial x)_T$  is the slope of the affinity curve, and the term  $(\partial x / \partial T)_{\epsilon_x}$  is the distance between two neighboring affinity curves along the  $x$  direction.

The plot of  $\epsilon_x$  against  $x$  is always a monotonously decreasing curve, since adsorption always occurs on the part of the adsorbent that has the highest potential. On the other hand, the net heat of adsorption may decrease or increase with the amount adsorbed, as shown in Figs. 55 and 93. At about 85% of the saturation adsorption  $x_b$  the heat of adsorption has a minimum, then it begins to increase with increasing amounts adsorbed. The change in the direction of the heat curve is due to the fact that the affinity curves begin to bend sharply toward the  $x$ -axis. Since the affinity curves run approximately parallel with each other  $(\partial x / \partial T)_{\epsilon_x}$  is practically constant, and although  $\epsilon_x$  keeps on decreasing, this is overbalanced by the sudden increase in  $(\partial \epsilon_x / \partial x)_T$ , the slope of the affinity curve. This, of course, is a purely formal explanation of the minimum in the heat of adsorption. Goldmann and Polanyi gave no physical explanation, but it seems likely that the rise in the heat of adsorption at these large adsorptions is due to the appearance of the heat of capillary condensation.

The differential heat of compression,  $U_x - \epsilon_x$ , in Fig. 93 is approximately constant from 1.5 to 3.0 grams of ether adsorbed per 10 grams of charcoal, and is about 2000 calories per mole. There is an even longer approximately constant region in Fig. 55; from 2 to 6 grams of carbon disulfide adsorbed per 10 grams of charcoal the heat of compression is roughly 1000 calories per mole. On the other hand, Emmett and Brunauer<sup>75</sup> found that the affinity curves calculated from adsorption isotherms of argon on an  $\text{Al}_2\text{O}_3$  promoted iron catalyst, measured at 77.3 and 90.1° K., coincided, and the same was true for the affinity curves of nitrogen at the same two temperatures (Fig. 56, Chapter V). This means that  $(\partial x / \partial T)_{\epsilon_x}$  in equation (35) is zero, consequently the heat of compression is also zero.

<sup>75</sup> P. H. Emmett and S. Brunauer, *J. Am. Chem. Soc.*, 59, 2682 (1937).

Dixon<sup>76</sup> calculated the Polanyi potentials from adsorption isotherms of carbon dioxide on charcoal at 0° C., measured by Magnus and Kälberer,<sup>61</sup> and compared these with the heats of adsorption determined calorimetrically by the same investigators. For a charcoal sample outgassed at 600° C. the difference between the heat of adsorption and the Polanyi potential was approximately constant from 8.89 to 100.0 mg. of carbon dioxide adsorbed per gram of charcoal, and was about 3100 calories per mole. Since the heat of condensation is 2400 calories per mole, the difference of 700 calories per mole corresponds to the latent heat of compression.

Although the plot of the differential heat of adsorption against the amount of gas adsorbed in almost every case investigated begins with a descending portion, there are a few cases known where the curve begins with an ascending portion. Examples of this were shown in Table XXVIII; for the system water vapor-charcoal the  $dq/da$  values show an increase with increasing  $a$  at small adsorptions. This is true for both the calorimetric data of Keyes and Marshall<sup>10</sup> and the isosteric heats of adsorption of Coolidge.<sup>9</sup> These results can readily be explained on the basis of the theory of multimolecular adsorption. For adsorption processes that yield Type III and V isotherms the theory assumes that the heat of adsorption in the first layer is smaller than the heat of liquefaction. It will be recalled that Coolidge obtained Type V isotherms for water on charcoal. We would expect, therefore, the heat of adsorption to start with a value lower than  $E_L$  and to increase with increasing adsorption to  $E_L$ . As Table XXVIII shows, this is what actually happens; the first  $dq/da$  value of Coolidge is 9480 calories per mole, that of Keyes and Marshall 8530 calories per mole, while  $E_L$  is 10,740 calories per mole. At large adsorptions  $dq/da$  should rise to values greater than  $E_L$  due to appearance of the heat of capillary condensation, and actually Coolidge's values for 191 cc. or more water adsorbed are greater than  $E_L$ .<sup>77</sup>

Another example of an initial rise in the heat of van der Waals adsorption was obtained by Palmer,<sup>78</sup> who investigated the adsorption of benzene, acetone, and methyl alcohol on vitreous silica. He calculated  $U_x$  for his vapors from affinity curves using equation (35), and obtained  $q_d$  by adding the latent heat of vaporization. Since the

<sup>76</sup> J. K. Dixon, *J. Phys. Chem.*, **34**, 870 (1930).

<sup>77</sup> H. Cassel (*Z. Elektrochem.*, **37**, 642, 1931) finds that the differential heat of adsorption of alcohol on mercury starts with a value of 6.9 kcal./mole and rises with increasing adsorption to 10.6 kcal./mole. The heat of vaporization is 10.1 kcal./mole.

<sup>78</sup> W. G. Palmer, *Proc. Roy. Soc.*, **A168**, 190 (1938).

surface of his silica powder was known (Chapter IX), he plotted  $q_a$  against the fraction of the surface covered with adsorbed vapor. The curves are shown in Fig. 94. The  $q_a$  values for acetone and benzene give monotonously decreasing curves approaching the heat of condensation in the vicinity of  $\theta = 1$ . On the other hand methyl alcohol gives a curve with an initial ascending portion. Palmer attributed this

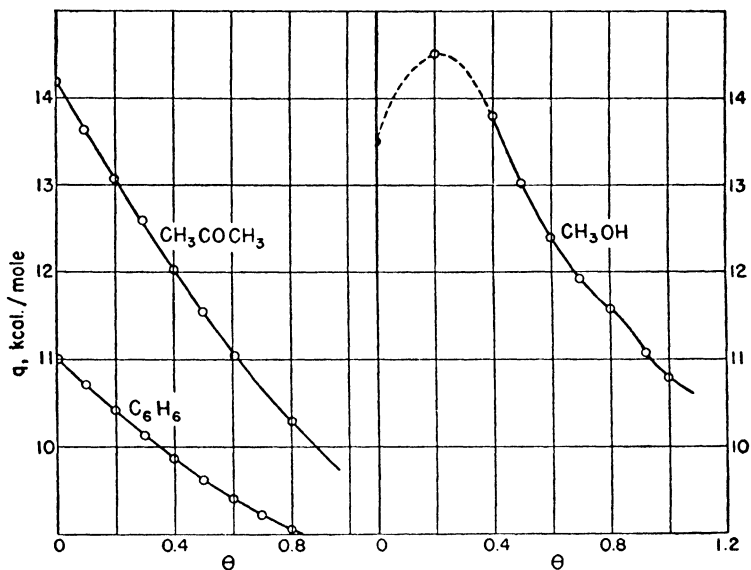


Fig. 94.—Heats of adsorption of three vapors on vitreous silica.

to the tendency of methyl alcohol to form associated molecules. The energy of attraction between the alcohol molecules adds on to the interaction energy between methyl alcohol and the silica surface, resulting in an increase of  $q_a$ . It is interesting to note that such initial ascending portions in the  $q_a$  vs.  $a$  curves were obtained for the two small highly polar molecules water and methyl alcohol, both characterized by a strong tendency toward association.

We may now summarize briefly the conclusions of this section. The often very complex shapes of the curves showing the variation of the differential heats of adsorption with the amount of gas adsorbed can be at least qualitatively explained by two factors. The first is the heterogeneity of the surface; atoms of the surface separated by different distances and arranged in different geometrical configurations

have different interaction energies with the same molecule; similarly, the heats of adsorption in crevices, pockets, tubes, and cells of the adsorbent are different from those on a plane surface. The second factor is the interaction between the adsorbed molecules; orientation forces lead to repulsion, dispersion forces to attraction. When the surface is covered with an adsorbed layer, the building up of the second layer causes a change in the heat of adsorption. Ordinarily there is a decrease, but occasionally one finds an increase in the heat of adsorption.

#### VARIATION OF THE HEAT OF ADSORPTION WITH TEMPERATURE

An examination of the equations of Chapter VII reveals that the interaction energy between a molecule and a surface does not contain the temperature explicitly. Since the terms entering the equations do not depend strongly on the temperature we would expect that the heat of adsorption, at least to the first approximation, would be independent of the temperature. Nevertheless, there are terms in the equations that may cause either an increase or a decrease in the heat of adsorption with increasing temperature. The most important is the  $r^3$  term that appears in the denominator. The equilibrium distance  $r$  between the molecule and the surface increases with increasing temperature due to thermal vibrations. This would therefore result in a decrease of the heat of adsorption with increasing temperature. On the other hand the length of the dipole or quadrupole moment of an adsorbed molecule may increase with increasing temperature, causing an increase in the heat of adsorption. As a matter of fact, examples can be found for all three cases: independence of the heat of adsorption from the temperature, decrease with increasing temperature, and increase with increasing temperature. Cases are also known in which the differential heats of adsorption plotted against the amounts of gas adsorbed for two different temperatures cross each other; in other words, the heat of adsorption decreases with increasing temperature for a certain range of surface covering and increases for another range.

Magnus<sup>59</sup> derived a theoretical equation for the temperature dependence of the interaction energy between a dipole or a quadrupole and a conducting surface. The equation is

$$(36) \quad C_0 = C_K - \frac{2}{3}mT$$

The term  $C_0$  is equal to  $q_0/R$ , where  $q_0$  is the approximately constant heat of adsorption in the beginning linear region of the adsorption isotherm, and  $R$  is the gas constant. The physical meaning of  $C_0$  for dipole and quadrupole molecules was given in Chapter VII,



equations (41) and (49).  $C_K$  is the value of  $C_0$  at  $0^\circ \text{K.}$ , and  $m$  is a constant depending on the type of electric moment the molecule possesses. According to Magnus  $m = 11$  for carbon dioxide; a plot of  $C_0$  against  $T$  therefore should give a straight line with a slope  $-7\frac{1}{3}$ . Table XXXV shows that this is approximately true for the heats of adsorption of carbon dioxide on charcoal and on silica gel. The last column gives the values of  $C_0$  calculated by means of equation (36); the values of the constants  $C_K$  and  $m$  are given in the table. It will be noted that  $\frac{2}{3}m = 8$  for silica gel and 9 for charcoal, not far from the theoretical value of  $7\frac{1}{3}$ . The decrease in the heat of adsorption for a 63 degree rise in temperature is 1170 calories per mole for silica gel

TABLE XXXV  
VARIATION OF HEATS OF ADSORPTION WITH TEMPERATURE

$T$ $^\circ \text{K.}$	$q/R$ Experimental	$q/R$ Calculated
CO <sub>2</sub> on Silica Gel; $C_K = 4180^\circ$ , $\frac{2}{3}m = 8$		
285.5	3557	3521
298	3439	3438
310.5	3323	3343
323	3230	3234
333.5	3107	3109
348	2971	2965
CO <sub>2</sub> on Charcoal; $C_K = 4590^\circ$ , $\frac{2}{3}m = 9$		
285.5	3907	3903
298	3804	3813
310.5	3686	3710
323	3595	3592
333.5	3449	3455
348	3283	3285

and 1250 calories per mole for charcoal. Kälberer and Schuster,<sup>58</sup> by extrapolating their isosteric heats of adsorption for carbon dioxide on silica gel to the linear region of the adsorption isotherm, obtained 7200 calories per mole at  $0^\circ$ , and 5370 calories per mole at  $75^\circ \text{C.}$ ; a decrease of 1830 calories per mole for a temperature increase of 75 degrees.

Another example of the heat of adsorption decreasing with increasing temperature was given in Table XXX. The isosteric heats of adsorption of water on charcoal, obtained by Coolidge,<sup>9</sup> decrease from 11,100 calories per mole at  $-15^\circ \text{C.}$  to 5200 calories per mole at  $187^\circ \text{C.}$ , a drop of 6000 calories for a 200 degree rise in temperature. The decrease in the heat of adsorption is greater than the decrease in the heat of liquefaction: between 10 and  $128^\circ \text{C.}$  the former drops 2800 calories, the latter only 1300 calories.

The isotheric heats of adsorption of sulfur dioxide on silica gel, calculated by Krulyt and Modderman<sup>4</sup> from the adsorption isotherms of McGavack and Patrick,<sup>79</sup> behave irregularly up to about 50 cc. of gas adsorbed per gram of gel. In this range of adsorption  $dq/da$  decreases with temperature for certain values of  $a$  and increases for other values. At larger adsorptions, however,  $dq/da$  shows a regular decrease with increasing temperature. Since the surface of the silica gel at complete covering adsorbs about 110 cc. of sulfur dioxide, the irregular behavior of the heat of adsorption occurs while the first and more active half of the surface is being covered by the adsorbate. One can calculate  $E_1$ , the heat of adsorption on the less active part of the silica gel surface, on the basis of the theory of multimolecular adsorption, and the calculated values show a decrease with increasing temperature, in agreement with the calculations of Krulyt and Modderman.<sup>4</sup> The values of  $E_1$ , calculated by Brunauer, Emmett and Teller<sup>80</sup> and shown in the last column of Table XVI, agree even in magnitude with the isosteric heats of adsorption. This is gratifying since the  $E_1$  values are obtained from individual isotherms, while the  $dq/da$  values are calculated from two isotherms. The methods of calculation are also entirely different.

The differential heats of adsorption of nitrogen, argon and hydrogen on graphite, obtained by Barrer<sup>64</sup> and shown in Fig. 85, are independent of the temperature. The nitrogen curves were calculated from seven isotherms between 79.5 and 273° K. Although the values are scattered, there seems to be no definite trend. Thus by taking the five isotherms at 89.0, 113.8, 131.2, 155.5 and 194.5° K. and calculating from neighboring pairs the values of  $dq/da$  for 8 cc. of nitrogen adsorbed Barrer obtained 2760, 3060, 3050 and 2820 calories per mole. The mean of the four values is 2920 calories per mole and the maximum deviation is 5%. A deviation of this magnitude in the 113.8–131.2° K. temperature range can be accounted for by a combined error of 0.4° in the two temperature readings.

The heats of adsorption of hydrogen and deuterium on charcoal, obtained by Dingenen and Itterbeek<sup>65</sup> and shown in Fig. 86, exhibit also no temperature dependence. The values for deuterium were calculated from eight isotherms between 17.5 and 90.1° K.

The integral heats of adsorption of organic vapors on charcoal are independent of the temperature, as the data collected in Table XXXVI clearly illustrate. The heats of adsorption given in the table are

<sup>79</sup> J. McGavack and W. A. Patrick, *J. Am. Chem. Soc.*, **42**, 946 (1920).

<sup>80</sup> S. Brunauer, P. H. Emmett and E. Teller, *J. Am. Chem. Soc.*, **60**, 309 (1938).

calorimetrically determined  $q_m$  values; i.e., they represent the integral heats of adsorption of one mole of gas on 500 grams of charcoal. For 15 different organic vapors the  $q_m$  values at 0, 20, 25 and 50° are equal within the experimental error, without any exception. Since the investigators, Lamb and Coolidge,<sup>6</sup> Pearce and McKinley,<sup>66</sup> Pearce

TABLE XXXVI  
INTEGRAL HEATS OF ADSORPTION OF ORGANIC VAPORS ON  
CHARCOAL AT DIFFERENT TEMPERATURES

Vapor	Integral Heat of Adsorption (kcal./mole)		
	0° C.	25° C.	50° C.
CH <sub>3</sub> OH	13.1 (1)	13.9 (2)	
C <sub>2</sub> H <sub>5</sub> OH	15.0 (1)	15.6 (4)	
CH <sub>3</sub> Cl		9.2 (3)	9.2 (3)
CH <sub>2</sub> Cl <sub>2</sub>		12.8 (3)	12.1 (3)
CHCl <sub>3</sub>	14.5 (1)	14.5 (2)	14.5 (3)
		14.3 (3)	
CCl <sub>4</sub>	15.3 (1)	15.4 (2)	15.4 (3)
		15.6 (3)	
		15.8 (4)	
C <sub>2</sub> H <sub>5</sub> Cl	12.0 (1)	11.6 (2)	12.2 (3)
n-C <sub>3</sub> H <sub>7</sub> Cl		15.0 (2)	14.6 (3)
iso-C <sub>3</sub> H <sub>7</sub> Cl		12.9 (3)	13.3 (3)
n-C <sub>4</sub> H <sub>9</sub> Cl		15.4 (3)	15.7 (3)
sec-C <sub>4</sub> H <sub>9</sub> Cl		14.5 (3)	14.4 (3)
ter-C <sub>4</sub> H <sub>9</sub> Cl		13.7 (3)	13.6 (3)
CS <sub>2</sub>	12.5 (1)	12.5 (2)	
(C <sub>2</sub> H <sub>5</sub> ) <sub>2</sub> O	15.5 (1)	15.8 (2)	
C <sub>6</sub> H <sub>6</sub>	14.7 (1)	15.7 (2)	
		14.4 (4)	

The investigators were: (1) Lamb and Coolidge,<sup>6</sup> (2) Pearce and McKinley,<sup>66</sup> (3) Pearce and Reed<sup>13,14</sup> and (4) Swietoslawski and Bartoszewicz.<sup>81</sup> The data of Swietoslawski and Bartoszewicz were obtained at 20° C.

and Reed<sup>13,14</sup> and Swietoslawski and Bartoszewicz<sup>81</sup> used calorimeters of different designs, both isothermal and adiabatic, the closeness of the agreement between their results is truly remarkable.

Figure 95 shows the effect of temperature on the heat of adsorption of helium on charcoal, obtained by Itterbeek and Dingenen.<sup>82</sup> They adopted the less customary method of plotting the heat of adsorption against the pressure, instead of the amount adsorbed. The heats of adsorption were calculated from eleven isotherms measured at liquid hydrogen temperatures, from 7.73 to 20.38° K. On such plots the heats of adsorption increase with increasing temperatures. However,

<sup>81</sup> W. Swietoslawski and E. Bartoszewicz, *Roczniki Chem.*, 11, 78 (1931).

<sup>82</sup> A. van Itterbeek and W. van Dingenen, *Physica*, 5, 529 (1938).

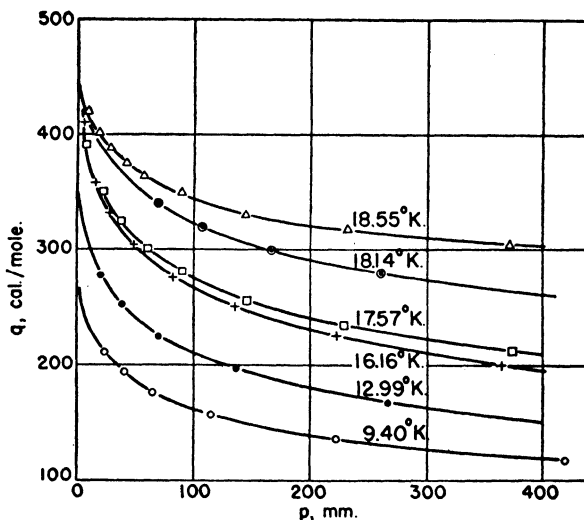


FIG. 95.—Heats of adsorption of helium on charcoal.

Itterbeek and Dingenen stated that the integral heats of adsorption for given amounts of helium adsorbed at different temperatures were independent of the temperature.

So far we have discussed cases in which the heats of adsorption decreased with increasing temperature or were independent of the

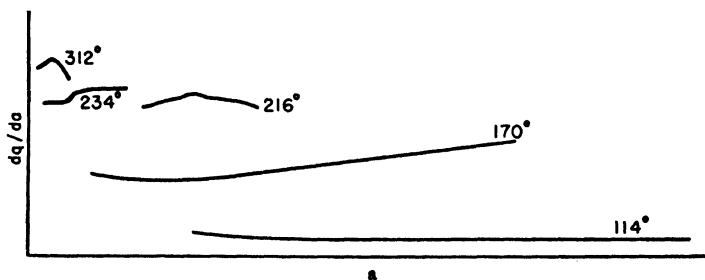


FIG. 96.—Differential heats of adsorption of argon on charcoal.

temperature. In Fig. 96, taken from Kruyt and Modderman,<sup>4</sup> an example is given of the heat of adsorption increasing with increasing temperature. The data represent the variation of the differential heats of adsorption with the amounts adsorbed at different tempera-

tures, calculated from Miss Homfray's <sup>7</sup> isotherms for argon on charcoal. The increase in  $dq/da$  with temperature is very large; much more than proportional to the temperature. For 15 cc. of argon adsorbed per gram of charcoal the calculated values of  $dq/da$  are 560, 1860 and 3610 calories per mole at 114, 170 and 215° K., respectively. Already the magnitudes of the first two values cast doubt upon their correctness. Actually these heats of adsorption have been calculated from isotherms very far apart; the first from isotherms at 83 and 145, the second from isotherms at 145 and 194.7° K. Since the first of the isotherms was measured near the boiling point of argon, the second slightly below its critical temperature, and the third about 40 degrees above the critical temperature, it is possible that the adsorbed gas was in different states of aggregation at the three different temperatures, and the use of the Clapeyron-Clausius equation was not justified. In a similar manner Kruijff and Modderman calculated from Titoff's <sup>2</sup> data for the adsorption of 0.4 cc. hydrogen per gram of charcoal  $dq/da$  values of 1725 and 3300 calories per mole at 233.5 and 313° K., respectively. These values are also unreasonable, and again both were obtained from isotherms 80 degrees apart. It should be remembered that equation (23) is obtained by integrating equation (22) with the assumption that  $q_a$  is independent of the temperature, which may be a good enough approximation for a small range of temperatures but can not be valid for an interval of 80 degrees.

A more clear-cut example of the heat of adsorption increasing with increasing temperature is shown in Fig. 97. The data represent the isosteric heats of adsorption of hydrogen on charcoal, obtained by Itterbeek and Dingenen.<sup>83</sup> In plotting these data no attempt was made to draw smooth curves through the experimental points, because it is difficult to tell whether the deviations from the smooth curves are due to experimental error, or to actually existing flat maxima and minima. The important fact is that the 69.4° K. curve indicates higher heats of adsorption through the entire range investigated than the 60.8° K. curve, and although the difference is not very great (only 70 to 200 calories), it seems to be real. Another interesting fact is that the 81.8° K. curve at smaller adsorptions indicates  $q_a$  values smaller than either of the other curves. Thus up to about 80 cc. of hydrogen adsorbed the heat of adsorption plotted against the temperature for any given constant amount adsorbed would exhibit a maximum.

An examination of the theoretical equations of Chapter VII reveals that there exist some factors that may possibly explain an in-

<sup>83</sup> A. van Itterbeek and W. van Dingenen, *Physica*, 4, 389 (1937).

crease in the heat of adsorption with increasing temperature. In the first place the heat of adsorption for polar molecules is proportional to the square of the dipole or quadrupole moment. There is some evidence<sup>84</sup> that the length of the dipole moment increases with temperature, and this would lead to an increased heat of adsorption. This explanation, of course, could not account for the results obtained for hydrogen, argon, or other non-polar gases. There is another factor,

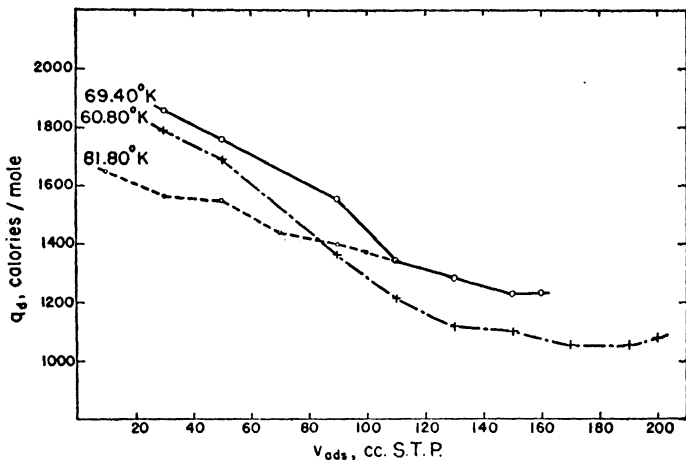


FIG. 97.—Heats of adsorption of hydrogen on charcoal.

however, that might explain a slight increase in the heat of adsorption with temperature for gases adsorbed on charcoal. Equation (74), Chapter VII, derived by Prosen and Sachs,<sup>85</sup> shows that the heat of adsorption of a molecule on a semi-conductor is proportional to the electron density. The electron density of semi-conductors increases with temperature, and since charcoal is a semi-conductor this would lead to an increase in the heat of adsorption of gases on charcoal.<sup>86</sup>

Crossing curves similar to those shown in Fig. 97 are by no means exceptional among the data of the heats of adsorption. Another example is given in Fig. 98, representing the differential heats of adsorption of ether on charcoal, calculated from the isotherms of Goldmann

<sup>84</sup> C. P. Smyth, *Dielectric Constant and Molecular Structure*, New York, 1931, pages 83 and 96.

<sup>85</sup> E. J. R. Prosen and R. G. Sachs. To be published in *Phys. Rev.*

<sup>86</sup> This suggestion was made by Professor K. F. Herzfeld of The Catholic University of America.

and Polanyi<sup>44</sup> by Kruyt and Modderman.<sup>4</sup> The shapes of the two curves are quite similar, each showing a very broad minimum, a very sharp maximum, and a final decrease of  $dq/da$  to the heat of liquefaction of ether. The two curves cross each other twice; through the largest part of the adsorption range the heat of adsorption is greater at the lower temperature, but there is an intermediate range where the reverse is true.

From the foregoing discussion we can draw the conclusion that the heat of adsorption is rather insensitive to temperature. In the theo-

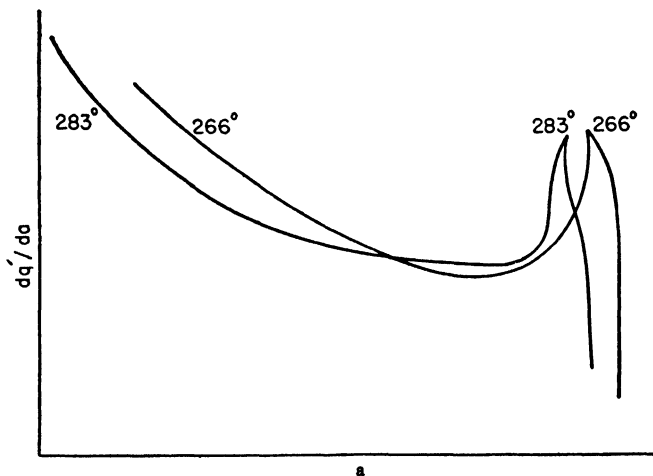


FIG. 98.—Heats of adsorption of ether on charcoal.

retical equations derived for the heat of adsorption of a molecule on a surface the temperature does not appear explicitly, but several of the terms depend on the temperature to some extent. Depending on the preponderance of one term over another the heat of adsorption may increase or decrease with increasing temperature, or again it may be practically independent of the temperature. The integral heats of adsorption, obtained calorimetrically for large quantities of gas adsorbed, show very little temperature dependence.

In the calculation of the isosteric heats of adsorption it should be remembered that the same amount of adsorbate at two different temperatures may not be in strictly comparable conditions. In the first place it is possible that the adsorbate at the lower temperature is in the form of a liquid, at the higher temperature in the form of a

compressed gas, or partly liquid, partly gas.<sup>87</sup> In the second place, even if there is no change in the state of aggregation, the same quantity of adsorbate may be adsorbed on two different parts of the surface at the two different temperatures. It may happen that at the higher temperature parts of the surface previously blocked become available for adsorption. For example, certain impurities adsorbed on the surface may be removed by the adsorbate, or new pores may open up because of thermal expansion of the adsorbent. Obviously, the greater the temperature difference, the greater is the possibility of not finding the adsorbate in strictly comparable states at the two temperatures. However, this possibility exists, although to a smaller extent, even if the heats of adsorption are calculated from isotherms that are not very far apart.

<sup>87</sup> See the discussion of the potential theory in Chapter V and the nature of the adsorbate in Chapter XII.



## CHAPTER IX

### THE SURFACE OF THE ADSORBENT I

According to the theory of multimolecular adsorption the physical adsorption of gases and vapors in the first layer is determined by two factors: the net heat of adsorption and the surface of the adsorbent. Occasionally a gas has very different interaction energies with different adsorbents; for example, the net heat of adsorption of water on ionic crystals is positive, whereas on charcoal it is negative. In such cases one obtains very different isotherm types, as was discussed in Chapter VI. Most gases, however, have positive net heats on all adsorbents, and the heats of adsorption of a given gas on different adsorbents are approximately equal, as we have seen in Chapters VII and VIII. This being the case, the factor of decisive importance in physical adsorption is not the nature of the adsorbent, but the extent of its surface area. In the present chapter we discuss the various methods that have been developed for the determination of the surface areas of adsorbents.

If the absolute surface area of a finely divided substance is to be determined, the most direct method is visual observation of the particles and actual measurement of their dimensions. For adsorbents, however, this can be done only in exceptional cases, namely, when the particles have smooth external surfaces and negligibly small internal surfaces. Ordinarily adsorbents are highly porous bodies possessing tremendously large internal surfaces and negligible external surfaces. Since the chemist works with molecules, he is interested in every part of the surface to which a molecule can penetrate, including the surfaces bounding the cracks, crevices, pores, capillaries and channels within the adsorbent. Thus for the chemist, and particularly for the investigator of adsorption phenomena, that value of the surface area is of the most direct significance which is obtained by adsorption methods. Adsorption from solutions and gas adsorption are now widely used for measuring the surface areas of finely divided and porous substances.

Besides visual and adsorption methods, surface areas can be determined by measuring rates of solution, heats of wetting, permeabilities and heat conductivities; they can also be evaluated by optical

methods and by x-ray diffraction methods. These methods are briefly discussed in the present chapter. The literature of particle size and surface area determination is so enormous that a detailed treatment of the subject can not be attempted here.

### VISUAL METHODS FOR DETERMINING SURFACE AREAS

The surface areas of some powders can be determined by observing the particles under a microscope, ultramicroscope, or electron microscope, and measuring the dimensions of the particles either directly under the microscope or on photomicrographs. If the particles have differing sizes and shapes, the surface determination, as described by Heywood,<sup>1</sup> consists of three steps. 1. One must determine experimentally the particle size distribution curve for the powder using sieve analysis for the coarser particles and sedimentation or elutriation methods for the finer ones. 2. Next the "shape factor" is calculated by examining representative particles of one of the larger fractions. The average particle size is first obtained by counting and weighing. Then from measurements of the areas and perimeters of projections of the particles on the field of view in the microscope one can calculate the shape factor according to a method suggested by Heywood. 3. Finally, assuming that the shape factor is independent of size, one can calculate the specific surface from the size distribution curve.

To obtain the size distribution curve one may use sieving methods down to particle diameters of about  $60\ \mu$ . Elutriation and sedimentation methods are applicable down to particles of  $1\text{--}2\ \mu$ , and with the help of the centrifuge and ultracentrifuge one can extend the limit to  $0.01\ \mu$ . We shall not discuss here Heywood's method of evaluating the shape factor.

The microscopic determination of surface area is a very laborious process; both the experimental procedure and the calculations involved are extremely time-consuming. Furthermore, the assumption that shape is independent of size may or may not be correct; a thorough experimental test of this assumption is as yet lacking. Finally, and this is the most important, the method gives the true surface only for smooth, non-porous substances. It will be seen that some of the other methods give the total surface area, including both the internal and external surfaces, of powders or any other finely divided materials with much greater ease and without any analysis of the sizes and shapes of the particles.

<sup>1</sup> H. Heywood, *Proc. Inst. Mech. Eng.*, 125, 383 (1933).

Naturally there are problems of practical importance in which the investigator is primarily interested in the external surfaces of particles; in such cases he may use Heywood's method or some other visual method. However, microscopic methods have often been used in the past for surface area determinations when the investigator was really interested in the total surface of the substance, rather than merely in its external surface. For example, in the combustion of coal or in the setting of cement the rate of the process depends on the access of small molecules (oxygen and water) to the surface of the substance. These molecules can certainly penetrate into whatever internal surfaces coal and cement have. In such cases the gas adsorption method would give an accurate estimate of the surface in which the chemical engineer is interested, while microscopic examination would not.

The use of the visual method may be illustrated by one of its more recent applications. Perhaps the most difficult step in the method is to estimate the surface areas of irregularly shaped particles. A new way of doing this was suggested by Kenrick.<sup>2</sup> He called attention to the fact that the average of the areas of the projections of a unit plane area of any shape in all random positions is one half. Since the surface of any solid in all random positions may be considered as made up of plane surface elements in all random positions, the sum of the averages of the projection areas of these will be equal to one half of the total surface area of the figure. If the figure possesses no re-entrant angles, half of the projection areas of the elements will be masked by the other half, so that the average projection area of any figure in all random positions is one quarter of the total surface area of the figure. For example, the average projection areas of a sphere of radius 1, a cube of edge 1, and a plate of dimensions  $1 \times 1 \times 0$  are  $\pi$ , 1.5 and 0.5, respectively, as compared to the actual surfaces of  $4\pi$ , 6 and 2.

Following Kenrick's method, Barrett, Birnie and Cohen<sup>3</sup> determined the specific surface of finely powdered silica. They prepared samples of mesh size 230-270 (0.065 and 0.053 mm.). If it was assumed that the particles were cubes with edges equal to the average size of the mesh openings, the surface area of the adsorbent was 460 sq. cm./g. The actual surface determination was performed by taking photomicrographs of the particles on a microscopic slide and projecting them on a screen giving a magnification of about 440 diameters. The outlines of about 300 particles were traced on the screen, and the areas

<sup>2</sup> F. B. Kenrick, *J. Am. Chem. Soc.*, 62, 2838 (1940).

<sup>3</sup> H. W. Barrett, A. W. Birnie, and M. Cohen, *J. Am. Chem. Soc.*, 62, 2839 (1940).

of the outlines were measured with a planimeter. The average projection area per particle was found to be  $6.13 \times 10^{-5}$  sq. cm., giving an average surface per particle of  $24.5 \times 10^{-5}$  sq. cm. Three different methods of suspending the particles on the slide were used to insure random orientation. The average particle areas determined by these methods agreed within 5%.

The number of particles per gram was obtained by weighing an evenly scattered layer of powder on a thinly greased cover glass and counting the particles in sample strips under a microscope. The average was  $2.275 \times 10^6$  particles per gram; the different determinations agreed within 3%. Thus the specific surface was found to be 558 sq. cm./g. This value is not quite accurate due to some occurrence of reentrant angles and to some fine grained roughness which escapes observation in the images. However, careful examination of a large number of particles showed that these two sources introduce only a small error in the surface determination.

To ascertain whether the surfaces of the silica particles were sub-microscopically uneven, Barrett, Birnie and Cohen decided to undertake adsorption experiments with methylene blue. For reasons which will be clear later, it is very unlikely that such dye adsorption experiments could give as accurate a measure of the true surface as one can get from the water vapor isotherms obtained by the same investigators on their 230–270 mesh silica samples. The isotherms are S-shaped, and a rough inspection of Figs. 3 and 4 in their paper suggests that the unimolecular layer corresponds to about  $1.5 \times 10^{-5}$  grams of water adsorbed per gram of powder.<sup>4</sup> Assuming that a water molecule covers  $11.5 \times 10^{-16}$  sq. cm. area<sup>5</sup> one obtains a specific surface of 576 sq. cm./g., in very good agreement with the microscopically determined value of 558 sq. cm./g. Further comparisons between the microscopic and other methods will be discussed later.

## SURFACE AREA DETERMINATION BY ADSORPTION FROM SOLUTIONS

### A. The Radioactive Indicator Method

The method was first applied by Paneth and Vorwerk<sup>6</sup> to the determination of the surface area of lead sulfate using a radioactive

<sup>4</sup> The estimate was made on the basis of "Point B" of the adsorption isotherms. (See the discussion of the gas adsorption method in the present chapter.)

<sup>5</sup> S. B. Hendricks, of the Bureau of Plant Industry, found that a unit cell of the layer crystal montmorillonite adsorbs four molecules of water. Thus the area covered by a water molecule is  $11.5 \text{ \AA}^2$ . Calculation of the area from the density of liquid water at 30° C. according to equation (7) of this chapter gives a value of  $10.5 \text{ \AA}^2$ .

<sup>6</sup> F. Paneth and W. Vorwerk, *Z. phys. Chem.*, 101, 445 (1922).

isotope of lead, thorium B, as the indicator. When thorium B is brought together with a saturated solution of lead sulfate containing an excess of solid, the radioactive ions distribute themselves between the lead atoms of the surface and those of the solution according to the law

$$(1) \quad \frac{\text{Th B (Surface)}}{\text{Th B (Solution)}} = \frac{\text{Pb (Surface)}}{\text{Pb (Solution)}}$$

The amount of thorium B adsorbed is determined by measuring with an electroscope the loss of radioactivity of the solution in contact with solid lead sulfate. This is compared with the loss of radioactivity of a blank solution containing no solid lead sulfate, and it is assumed that the difference corresponds to the amount of thorium B adsorbed. The amount of lead in solution is obtained by chemical analysis. Since the amount of thorium B in the original solution is known, one can calculate the amount of lead on the surface by means of equation (1). From the number of lead atoms on the surface one can estimate the absolute surface area of lead sulfate by assigning a reasonable area to a lead sulfate molecule.

The point of crucial importance is that the isotope leaving the solution should remain on the surface of the adsorbent and should not enter the inside of its crystal lattice, otherwise the method loses its validity. Paneth and Vorwerk found that the isotope ions continued to leave the solution for rather long periods. They attributed this effect partly to the breaking up of aggregates of lead sulfate crystallites and partly to diffusion of thorium B into cracks of the crystals. Since the drift was slow after three minutes they adopted, somewhat arbitrarily, the loss of  $\beta$ -ray activity after three minutes as the measure of the amount of isotope on the surface. It was shown later by Kolthoff and Rosenblum<sup>7</sup> that the drift was due to recrystallization of the precipitated lead sulfate, resulting in a penetration of thorium B into the lattice. Kolthoff and Eggertsen<sup>8</sup> determined the time-adsorption curve for several hours and extrapolated it back to zero time to obtain the isotope on the surface. They also made correction for the fact that the lead on the surface in equation (1) includes not merely the lead ions that are in the surface lattice of the crystallites, but also the adsorbed lead ions.

Paneth and Vorwerk<sup>6</sup> found that the surfaces of differently prepared lead sulfate samples contained from 6.4 to  $12.7 \times 10^{-4}$  g. of

<sup>7</sup> I. M. Kolthoff and C. Rosenblum, *J. Am. Chem. Soc.*, **56**, 1658 (1934).

<sup>8</sup> I. M. Kolthoff and F. T. Eggertsen, *J. Am. Chem. Soc.*, **62**, 2125 (1940).

lead per gram of adsorbent. In order to have an independent check on the method they determined microscopically the surface areas of two of the samples. One can make a comparison between the two methods if one assigns a definite surface area value to a  $\text{PbSO}_4$  molecule. Paneth and Vorwerk assumed that the molecules were cube-shaped; in other words, they obtained the area belonging to a molecule by

$$(2) \quad A = (M/\delta_s N_A)^{2/3}$$

where  $M$  and  $\delta_s$  are the molecular weight and density of the solid, and  $N_A$  is Avogadro's number. This gave an area of  $18.4\text{\AA}^2$  to a  $\text{PbSO}_4$  molecule. The radioactive surface thus obtained was roughly twice as large as the microscopic surface for both samples.

TABLE XXXVII  
SPECIFIC SURFACES OF CRYSTALS

Crystal		Microscopic Determination		Radioactive Determination	
		Specific Surface $\text{cm}^2 \times 10^{-2}$	Molecules $\times 10^{-16}$	Molecules $\times 10^{-16}$	
				by Thorium B	by Thorium X
$\text{PbSO}_4$	P	55	294	338	
	X	21	115	213	
	Y	16	88	187	87
	Z	3.6	19.5	25.8	44
	N	1.3	7.1	7.4	
$\text{PbCrO}_4$	I	0.57	2.9	2.0	
	II	0.49	2.5	2.3	
$\text{PbCl}_2$	A	28	151	163	
	B	12	63	100	
$\text{PbS}$	V	0.87	6.2	2.9	
	IV	0.81	5.8	4.1	
	II	0.57	4.1	1.8	
$\text{BaSO}_4$	X	233	1170	2770	1090
	Z	7	35	63	
$\text{SrSO}_4$	A	15	80	81	75
$\text{CaSO}_4$	A	34	136	7	13

Paneth and Thimann<sup>9</sup> made further comparisons between the microscopically determined surface areas and the radioactive indicator surface values of various crystals. Most of their results are shown in Table XXXVII. The thorium B values for the more finely divided crystals of  $\text{PbSO}_4$  and  $\text{PbCl}_2$  are larger than the microscopic values,

<sup>9</sup> F. Paneth and W. Thimann, *Berichte*, 57, 1215 (1924).

as a comparison between Columns 3 and 4 reveals, but for the coarser  $\text{PbCrO}_4$  and  $\text{PbS}$  crystals the reverse is true. The discrepancy is not great for  $\text{PbCrO}_4$  but for  $\text{PbS}$  it is quite large. As a matter of fact, naturally occurring  $\text{PbS}$  gave no isotope exchange at all, nor did it adsorb methylene blue. Paneth ascribed this to the great regularity of the naturally occurring crystals and suggested that isotope exchange on them can proceed only from the edges of crystals but not from the surface. Ratner,<sup>10</sup> however, ascribes the lack of exchange to adsorbed impurities on the surfaces of natural crystals. Whatever the cause, the fact clearly shows one of the serious limitations of the method.

Table XXXVII also shows that the radioactive method can be used with about equally good results for the determination of the surface areas of isomorphous crystals, such as  $\text{BaSO}_4$  and  $\text{SrSO}_4$ . Neither thorium B, nor thorium X is an isotope of barium or strontium; thorium X is an isotope of radium. For isomorphous crystals the equilibrium equation (1) was modified by Paneth to

$$(3) \quad k \frac{\text{Th B (Surface)}}{\text{Th B (Solution)}} = \frac{\text{Sr (Surface)}}{\text{Sr (Solution)}}$$

where  $k$ , the "solubility factor," is the ratio of the solubilities of the two salts in the saturated solutions used. Although the factor  $k$  is usually quite large, the correctness of its inclusion was confirmed later by a number of investigators, among them recently Chlopin and Kusnetzowa<sup>11</sup> who made a very thorough study of the adsorption of radium on lead sulfate.

Table XXXVII shows that the radioactive indicators thorium B and thorium X can not be used to determine the surface of  $\text{CaSO}_4 \cdot 2\text{H}_2\text{O}$ . The latter crystallizes in the monoclinic system, consequently it is not isomorphous with the orthorhombic lead, barium, and strontium sulfates. The radioactive indicators in this case can not enter the surface lattice of calcium sulfate, and the method becomes inapplicable.<sup>12</sup>

### B. The Dye Adsorption Method

This method was also originated by Paneth. Previous work of Marc<sup>13</sup> showed that the adsorption isotherms of dyes on crystal

<sup>10</sup> A. Ratner, *Acta Physiochim. U.R.S.S.*, 11, 475 (1939).

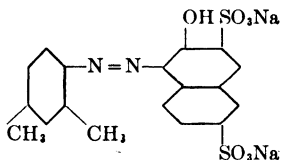
<sup>11</sup> V. Chlopin and W. Kusnetzowa, *Acta Physiochim. U.R.S.S.*, 11, 661 (1939).

<sup>12</sup> It is possible that the sizes of the ionic radii play an even more important role than isomorphism. The thorium B ion does not differ greatly in size from the lead, barium and strontium ions, but differs greatly from the calcium ion.

<sup>13</sup> R. Marc, *Z. phys. Chem.*, 75, 710 (1911).

powders—for example, on the sulfates of lead, barium, and strontium—tend toward definite saturation values. Paneth suspected that the maximum adsorption may correspond to a unimolecular layer, and he tested this by comparing the results of dye adsorption with those of the radioactive indicator method.

Paneth and Vorwerk<sup>14</sup> used a sample of 1.724 g. of  $\text{PbSO}_4$ , the surface of which according to the radioactive indicator method contained  $16.83 \times 10^{-4}$  g. of Pb, or  $4.95 \times 10^{18}$  molecules of Pb. Since the area assigned to a  $\text{PbSO}_4$  molecule was  $18.4 \text{ \AA}^2$ , the surface area of the crystal was 9100 sq. cm. At saturation the adsorption of the dye Ponceau Red 2R was  $3.6 \times 10^{-4}$  g. The structural formula of this dye is



The corresponding molecular weight is 480.34. If one assumes that the molecules of the dye are cube-shaped and calculates the area of a molecule by means of equation (2), one obtains  $62.4 \text{ \AA}^2$ . On this basis the dye at saturation adsorption covers only 31.3% of the lead sulfate surface. However, an inspection of the structural formula shows that the molecule of Ponceau 2R is not very likely to have a cubic shape; it is much more probable that the molecule lies flat on the surface, covering as much area as it possibly can. A rough estimate shows that the molecule lying flat covers an area of about  $200 \text{ \AA}^2$ , from which it follows that the dye covers the surface of  $\text{PbSO}_4$  with a complete unimolecular layer.

The testing of the method was continued by Paneth and Thimann<sup>9</sup> who used four dyes: Ponceau 2R, methylene blue, naphthol yellow, and methyl green. The dyes were selected because of their different structures (an azo, a thiazine, a nitro, and a triphenylmethane dye). They used two other molecules also: the alkaloid brucine and acetone. The results are shown in Table XXXVIII. The specific surface values given in Columns 2 and 3 were obtained by the radioactive indicator method, those in Columns 5 and 6 by the dye adsorption method. The surface area values given in Column 6 were calculated by assuming that the dye molecules are cube-shaped, which naturally leads to too low values. The percentage of the surface covered by the dye, given

<sup>14</sup> F. Paneth and W. Vorwerk, *Z. phys. Chem.*, 101, 480 (1922).



in the last column, is the ratio of the surface area values of Columns 6 and 3.

Table XXXVIII reveals some of the difficulties with the dye adsorption method. In the first place Ponceau 2R covers only 32% of the surface of  $\text{PbSO}_4$ , but as much as 84% of the surface of PbS. This may be explained by assuming that the dye molecules are differently oriented on the surfaces of the two different crystals, but it is also

TABLE XXXVIII  
ADSORPTION OF DYES ON CRYSTALS

Adsorbent	Specific Surface		Dye	Specific Surface		% Surface Covered by Dye
	in Molecules $\times 10^{-16}$	in $\text{cm}^2 \times 10^{-3}$		in Molecules $\times 10^{-16}$	in $\text{cm}^2 \times 10^{-3}$	
$\text{PbSO}_4$ H	290	53	Ponceau 2R	27	17	32
$\text{PbSO}_4$ J	180	32	Brucine	30	20	63
PbS A	800	116	Ponceau 2R	150	95	82
PbS D	430	61	Ponceau 2R	80	51	84
PbS E	2800	400	Ponceau 2R	540	340	85
PbS E	2800	400	Methylene blue B extra	490	270	68
PbS E	2800	400	Acetone	1560	380	95
PbS C	2580	374	Methylene blue HB	712	371	99
PbS C	2580	374	Methyl green	298	235	63
PbS F	1450	204	Acetone	735	179	88
$\text{Bi}_2\text{S}_3$	590	138	Ponceau 2R	131	82	59
$\text{BiPO}_4$	1400	258	Ponceau 2R	22	14	5.4
$\text{BiPO}_4$	1400	258	Naphthol yellow	52	23	8.8
$\text{BaSO}_4$ C	1580	306	Ponceau 2R	52	32	10

possible that the radioactive indicator method, used here as the standard, gives too small a value for the surface of PbS. The fact that methylene blue HB gives the same surface area for PbS as the radioactive indicator method does not mean that the cube-shaped structure assigned to the dye molecule by Paneth is correct, but rather that the dye adsorption and the radioactive methods both give too low surface area values, which in this instance accidentally check each other. Since the van der Waals energy of attraction between a molecule and a surface increases with the size of the molecule and is inversely proportional to the cube of the distance between the center of the molecule and the surface, one would expect that large molecules have a strong tendency to lie flat on the surface. This was demonstrated experi-

mentally by Hendricks<sup>15</sup> for a number of large organic molecules adsorbed on the layer crystal montmorillonite. It seems likely therefore that methylene blue HB lies flat on the surface of PbS and that the surface area value of 3.7 sq. m./g., obtained by both methods, is too low by a factor of two or three.

An even more serious difficulty with the dye adsorption method is indicated by the results obtained for BiPO<sub>4</sub> and BaSO<sub>4</sub>. Table XXXVIII shows that the dye adsorption surface values are only 5–10% of the radioactive indicator surface values. Thus the greatest part of the surface of either of these crystals does not adsorb dye, and the method breaks down completely.

Paneth and Radu<sup>16</sup> extended the method to non-crystalline substances, notably to the measurement of the surface areas of various charcoals and artificial silks. Four different charcoals were investigated using as adsorbates three dyes, lead nitrate, and acetone. The surface area values obtained for the same adsorbents differed 3.5 to 5 fold. The values obtained by the three dyes were considerably lower than the acetone values. It will be seen later that gas adsorption also gives larger surface area values than dye adsorption in all cases in which comparisons between the two methods are available. The main reason for this is that the much smaller gas molecules can penetrate to parts of the internal surfaces of porous adsorbents where the large dye molecules can not enter.

The results of Paneth and Radu for artificial silks are also interesting. The specific surface areas of a nitro, a cuproammonium, and an acetate silk microscopically determined were 0.12, 0.15 and 0.30 sq. m./g., respectively. The surface areas of the same three silks determined by the adsorption of methylene blue B extra were 18.2, 4.56 and 0.28 sq. m./g., respectively. Thus the dye adsorption for nitro silk gives 150 times as large surface area as the microscopic determination, for the cuproammonium silk a value 30 times as large, while for the acetate silk the two methods give equal values. The reason is, of course, that the microscopic examination reveals only the external surface of the silk, but the dye adsorption gives also a part or all of the internal surface. This is confirmed by the fact that the cross-sections of the fibers of the first two silks, viewed under the microscope, showed uniform blue coloration after the dye treatment, but the cross-section of the acetate silk fiber showed no coloring at all. One must conclude therefore that the acetate silk either has no internal

<sup>15</sup> S. B. Hendricks, *J. Phys. Chem.*, **45**, 65 (1941).

<sup>16</sup> F. Paneth and A. Radu, *Berichte*, **57**, 1221 (1924).

surface or that the pores within the fibers are so fine that the dye molecules can not penetrate into them.

A further difficulty with the dye adsorption method is that the maximum adsorption depends very strongly on the pH of the solution, as well as on the concentration of other foreign ions than hydrogen. The situation is illustrated in Fig. 99 representing the adsorption of the dye alizarine SW on chromic oxide, determined by Weiser and Porter.<sup>17</sup>

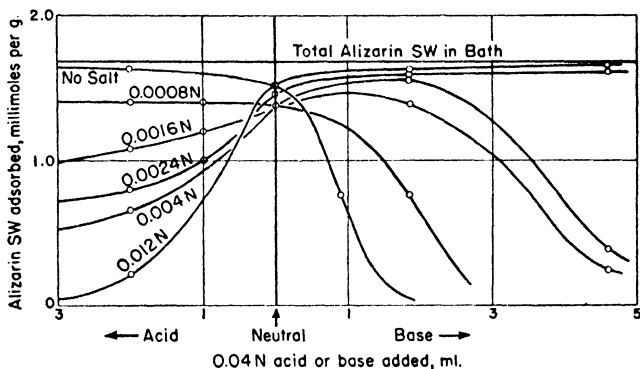


Fig. 99.—The effect of calcium sulfate on the adsorption of alizarin SW by chromic oxide at different hydrogen ion concentrations.

The curve marked "no salt" gives the effect of the hydrogen ion alone. It will be seen that the dye is well adsorbed in neutral and acid solution, but the adsorption rapidly decreases in alkaline solution. The effect of adding  $\text{CaSO}_4$  is to decrease the adsorption in acid solution and to increase it in alkaline solution. The curves represent the effect on the adsorption of a given concentration of alizarine SW, but similar results are obtained for other concentrations of the dye as well.

In spite of the many drawbacks of the dye adsorption method, it is probably the most widely used method of surface determination at present. This is because the experimental technique is very simple, and also because in industrial practice one is seldom interested in the absolute surface of a substance, but rather in the relative surface areas of different samples of the same or similar materials. For such purposes the dye adsorption method may serve very well, even though for absolute surface determination it is quite inaccurate and often entirely unreliable. It seems probable that dye adsorption occurs on

<sup>17</sup> H. B. Weiser and E. E. Porter, *J. Phys. Chem.*, **31**, 1824 (1927).

certain active groups of the surface rather than on the entire surface; it is therefore a specific "chemisorption" process. It was shown in Table XXXVIII that dye adsorption covers only a small fraction of the surfaces of  $\text{BiPO}_4$  and  $\text{BaSO}_4$ . Similarly, experiments performed in the Bureau of Plant Industry showed that some soil colloids having large surface areas as determined by the gas adsorption method adsorbed alizarine S very slightly or not at all.<sup>18</sup> If the surface of the adsorbent consists entirely of active groups, then the dye adsorption method may come close to determining the total surface area of the adsorbent. This, however, is more likely to be the exception than the rule.

The dye adsorption method of surface determination often can not be employed because the solution alters the surface of the adsorbent. For example, certain clays are dispersed in water solutions. Another objection to the method is that it always involves a competition for the surface between the solvent and the solute molecules. The low results obtained in comparison with the gas adsorption method may at least be partly explained on the basis that the surface adsorbs not only the solute molecules but the solvent molecules too.

### C. The Electrolytic Method

A far more accurate method of surface determination has been developed by Bowden and Rideal,<sup>19</sup> but it is applicable only to metals. It measures the surface area accessible to the smallest of all ions, the hydrogen ion.

When a metal is made the cathode in a dilute acid and current is passed through the solution the potential changes due to accumulation of hydrogen on the electrode. This phenomenon is called polarization. Bowden and Rideal noted that the change in potential was proportional to the amount of hydrogen deposited on the electrode

$$(4) \quad -\Delta E/\Delta\Gamma = K_A$$

or in the integrated form

$$(5) \quad -E = K_A\Gamma + \text{const.}$$

where  $E$  is the potential and  $\Gamma$  is the amount of hydrogen on the surface of the cathode. They also made the important discovery that  $K_A$  was not dependent on the nature of the metal but only on its surface area. All liquid metals investigated (mercury, amalgamated silver,

<sup>18</sup> These experiments were performed by S. B. Hendricks and R. A. Nelson.

<sup>19</sup> F. P. Bowden and E. K. Rideal, *Proc. Roy. Soc.*, A120, 59, 80 (1928).

platinized mercury, liquid gallium, liquid Wood's metal) required about  $6 \times 10^{-7}$  coulombs of electricity per square centimeter surface to produce a change of 100 millivolts in the electrode potential. It seemed therefore safe to assume for all metals that

$$(6) \quad -E = K_h \Gamma / A + \text{const.}$$

where  $A$  is the surface area accessible to hydrogen ions, and  $K_h/A$  is a constant for all metals.  $A$  will be referred to as the "true" surface of the metal.

In the electrolytic method of surface determination one measures the quantity of electricity necessary to produce a change of 100 millivolts in the electrode potential. When this value is divided by  $6 \times 10^{-7}$  coulombs one obtains the ratio between the true surface of the metal and its apparent surface. This involves the assumption that for liquid metals the true and apparent surfaces are identical, which is without doubt correct. The method is completely reversible; one can reverse the current and observe the decrease in the overvoltage as the hydrogen is removed from the surface.

The amount of hydrogen deposited in the experiments of Bowden and Rideal is very small, it covers only a fraction of one per cent of the surface. If it is assumed that the diameter of the hydrogen atom is  $1\text{\AA}$ , then  $1/3000$  of an atomic layer of hydrogen causes an increase of 100 millivolts in the potential. If on the other hand it is assumed that hydrogen is adsorbed on the metal atoms and the distance between the metal atoms of the surface is  $3\text{\AA}$ , then approximately  $1/300$  of the surface metal atoms is covered with hydrogen for a potential rise of 100 m.v.

The results of Bowden and Rideal<sup>19</sup> and Bowden and O'Connor<sup>20</sup> are collected in Table XXXIX. The table gives the ratios of the true surface, i.e., the surface accessible to hydrogen ions, to the apparent surface for metals exposed to different treatments. It will be noted that when the liquid metal solidifies the surface increases only slightly, from 1.0 to 1.4 for Wood's metal and 1.7 for gallium. Polishing caused a large increase in the surface; the ratio was 13.3 for nickel and 16 for silver. When polished nickel was electrolyzed for 20 hours the ratio decreased to 9.7. Activation of the nickel cathode by alternate oxidation and reduction (three times) increased the ratio to 46, but on ageing it decreased to 29. Annealing then decreased the surface to 10.8, and after 20 hours of electrolysis the surface decreased further to 7.7. After repolishing the cathode was electroplated with a thin coat-

<sup>20</sup> F. P. Bowden and E. A. O'Connor, *Proc. Roy. Soc., A128*, 317 (1930).

ing; the surface obtained was approximately the same as after polishing. Finally cold rolling reduced the surface to 5.8, and ageing to 3.5. Thus different treatments of nickel produced surface areas varying from 3.5 to 46 times the visible surface. Meantime the appearance of the surface remained practically unchanged. Sponge formation,

TABLE XXXIX  
THE RATIO OF TRUE SURFACE TO APPARENT SURFACE FOR METALS

Substance	Ratio
Silver; freshly etched with dil. $\text{HNO}_3$ (fine crystalline structure)	51
Silver; same, 20 hours old	37
Silver; polished with "flour" sandpaper	16
Silver; amalgam 1 hour old. Surface bright, resembling Hg	1.2
Silver; amalgam 20 hours old. Surface gray and solid	1.3
Silver; amalgam 150 hours old. Surface solid and rough	1.7
Platinum; smooth	2.1
Platinum black	1830
Carbon rod after 2 hours	328
Carbon rod after 20 hours	366
Nickel, polished, new	13.3
Nickel, polished, old	9.7
Nickel, activated, new	46
Nickel, activated, old	29
Nickel, annealed, new	10.8
Nickel, annealed, old	7.7
Nickel, electroplated, new	12
Nickel, electroplated, old	9.5
Nickel, rolled, new	5.8
Nickel, rolled, old	3.5
Wood's metal, solidified from liquid state	1.4
Wood's metal, surface rubbed with glass paper	6.3
Wood's metal, etched with $\text{HNO}_3$ until surface covered with metal sponge	800-1000
Gallium, solidified from liquid state	1.7

however, caused a visible change in the appearance of the surface of Wood's metal as well as a tremendous increase in its true surface. The ratio of true to apparent surface increased to 800-1000. The largest ratio was found for platinum black; the true surface exceeded the visible surface 1830 fold.

Using pieces of the same carbon rod for which the ratio of true to apparent surface is given in Table XXXIX, Bowden and Rideal made a comparison between the electrolytic and the dye adsorption method of surface determination. Methylene blue was used as the dye, and they found that the ratio of the surface area accessible to methylene blue to the apparent surface was 100 after 24 hours of immersion in the dye, 140 after 48 hours, 160 after 72 hours, and 165 after 96 hours.

Thus the dye molecules slowly penetrated into the pores of carbon, but even after 4 days only half of the surface accessible to hydrogen was reached by the dye.

The electrolytic method requires a rather elaborate electrical set-up, but it is one of the most accurate methods of surface determination. Unfortunately, it is applicable only to metals, and therefore it can not be used to measure the surface areas of the most important adsorbents.

#### SURFACE AREA DETERMINATION BY THE GAS ADSORPTION METHOD

In the discussion of the equations of Langmuir and of Williams, in Chapter IV, it was shown that both equations contain  $v_m$ , the constant that measures the surface of the adsorbent. In 1919 Williams<sup>21</sup> actually calculated from the van der Waals adsorption isotherms of Miss Homfray<sup>22</sup> the surface area of the charcoal she used, by means of his own equation. The value of 130 sq. m./g. was probably too low by at least a factor of 3. Markham and Benton,<sup>23</sup> using the Langmuir equation, evaluated  $v_m$  for silica from adsorption isotherms of oxygen, carbon monoxide and carbon dioxide, but obtained inconsistent surface values for the same adsorbent. The probable difficulties with these calculations were discussed in Chapter IV.<sup>24</sup>

In 1926 Benton<sup>25</sup> attempted to evaluate the surface area of platinum black by measuring the adsorption of hydrogen, carbon monoxide and oxygen at 25° C. The value he obtained, 6 sq. m./g., is probably much too low. Benton dealt with chemisorptions, and it is very difficult to get reliable surface area values by means of chemisorption experiments. Ordinarily chemisorbed gas covers only a part of the surface of the adsorbent, and it is always hard and often impossible to ascertain whether complete saturation of the surface has been reached.

In studying the physical adsorption of nitrogen on an iron catalyst, Benton and White<sup>26</sup> noticed two abrupt breaks in their S-shaped iso-

<sup>21</sup> A. M. Williams, *Proc. Roy. Soc.*, A96, 298 (1919).

<sup>22</sup> I. F. Homfray, *Z. phys. Chem.*, 74, 129 (1910).

<sup>23</sup> E. C. Markham and A. F. Benton, *J. Am. Chem. Soc.*, 53, 497 (1931).

<sup>24</sup> W. K  lberer and H. Mark (*Z. phys. Chem.*, A139, 159, 1928) suggested a method of calculating the surface of the adsorbent from the temperature dependence of the linear beginning portion of the adsorption isotherm. The suggestion did not prove successful; different gases gave inconsistent values for the same surface. The reason is that the method does not evaluate the total surface, but only the area of a relatively homogeneous fraction of the surface.

<sup>25</sup> A. F. Benton, *J. Am. Chem. Soc.*, 48, 1850 (1926).

<sup>26</sup> A. F. Benton and T. A. White, *J. Am. Chem. Soc.*, 54, 1820 (1932).

therm at  $-191.5^{\circ}\text{C}$ . They attributed these breaks to the completion of the first and second adsorbed layers. Although later work<sup>27</sup> has shown that the breaks disappear when correction is made for the deviation of nitrogen from the ideal gas laws, still this suggestion of Benton started the research conducted by Emmett and the author that led to the gas adsorption method for surface determination.<sup>27, 28, 29</sup>

Since at the time the investigations were started the theory of multimolecular adsorption was not yet developed, it was necessary to adopt an empirical approach to the problem. It was believed that

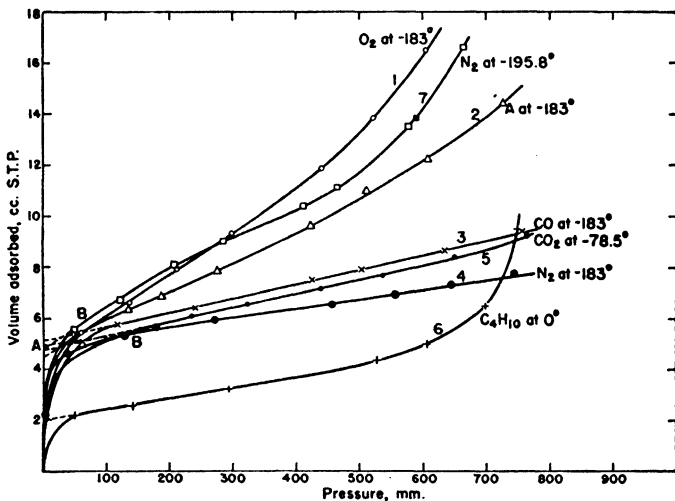


Fig. 100.—Determination of the surface area of an iron catalyst by the gas adsorption method.

if the van der Waals adsorption of a gas is measured close to its boiling point one obtains at sufficiently high relative pressures either multimolecular adsorption or capillary condensation. Since the forces of interaction in the first adsorbed layer operate between molecules of the adsorbent and adsorbate, while in the second adsorbed layer, and in capillary condensation also, between molecules of the adsorbate themselves, it seemed reasonable to expect that some point of the isotherm would indicate the completion of the first adsorbed layer.

<sup>27</sup> S. Brunauer and P. H. Emmett, *J. Am. Chem. Soc.*, **57**, 1754 (1935).

<sup>28</sup> P. H. Emmett and S. Brunauer, *J. Am. Chem. Soc.*, **59**, 1553 (1937).

<sup>29</sup> S. Brunauer and P. H. Emmett, *J. Am. Chem. Soc.*, **59**, 2682 (1937).



The first adsorbent investigated was an unpromoted iron synthetic ammonia catalyst, and the adsorption isotherms of six different gases at or near their boiling points were measured.<sup>27</sup> These are shown in Fig. 100. The isotherms are S-shaped with three distinct regions: the low pressure region is concave to the pressure axis, the high pressure region is convex, and between the two there is a linear portion. Some of the isotherms of Fig. 100 show only the concave and the straight line portions because the experiments were not carried up to high enough relative pressures. It will be noted that the five smaller molecules of approximately equal size ( $N_2$ ,  $O_2$ , A, CO and  $CO_2$ ) show approximately equal adsorptions around 50 mm. pressure, but at higher pressures the isotherms diverge widely. At first it was believed that the extrapolation of the intermediate straight line portion to zero pressure (Point A) corresponded to the volume of gas necessary to cover the surface with a unimolecular adsorbed layer,<sup>27</sup> but later the beginning of the straight line portion (Point B) was chosen as the most likely point to correspond to a monolayer.<sup>28</sup> Granted that Point B does give the number of molecules in a complete monolayer, we can calculate the absolute surface area of the catalyst if we know the area

TABLE XL  
THE SURFACE AREA OF AN IRON CATALYST  
Weight of sample = 46.2 g.

Gas	Temp. of Isotherm ° C.	Boiling Point of Gas ° C.	Point B cc. at S.T.P.	Calculated Area sq. m.	
				Solid Packing	Liquid Packing
$N_2$	-183	-195.8	5.5	20.5	25.3
$N_2$	-195.8	-195.8	5.5	20.5	24.1
CO	-183	-192.0	5.7	21.1	25.9
A	-183	-185.7	5.8	20.1	22.6
$O_2$	-183	-183.0	5.5	18.0	21.0
$CO_2$	-78.5	-78.5	5.95	22.7	27.4
$C_4H_{10}$	0	- 0.3	2.2	19.0	19.0

occupied by a molecule on the surface. Assuming that the adsorbed molecules have the same packing on the surface as the molecules of the solidified gas have in their plane of closest packing, we obtain for the area covered by a molecule

$$(7) \quad \text{Area (S)} = (4)(0.866) \left( \frac{M}{4\sqrt{2}N_A\delta_s} \right)^{2/3}$$

where  $M$  is the molecular weight of the gas,  $N_A$  is Avogadro's number, and  $\delta_s$  is the density of the solidified gas. Another possibility is that

the packing of the molecules on the surface approximates that of the liquefied gas; in that case we obtain Area (L) by substituting into equation (7)  $\delta_l$ , the density of the liquid.

Table XL represents the surface area values calculated from the isotherms of Fig. 100 on the assumption that Point B corresponds to a monolayer. The use of Area (S) values gives a better agreement in this case than the use of Area (L) values. However, this is not generally true, often Area (L) values give the better agreement. At any

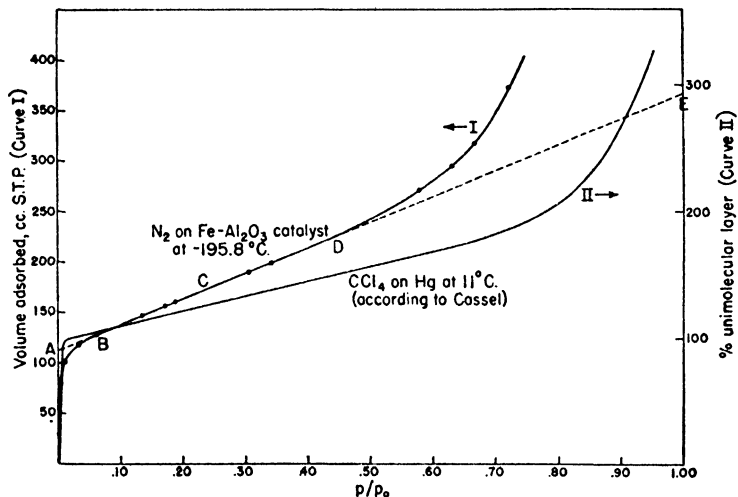


FIG. 101.—Adsorption isotherms of nitrogen on iron and carbon tetrachloride on mercury.

rate, in previous chapters sufficient evidence has been cited on the similarity between the adsorbed state and the liquid state to make the liquid-like packing the logical choice.

The selection of Point B, the beginning of the linear portion of the adsorption isotherm, as the point most likely to represent a monolayer was made for several reasons.

1. When the surface area of a given catalyst was calculated from adsorption isotherms of a number of gases using Point B as corresponding to a monolayer, better agreement was obtained between the calculated values than when Point A was used, or several other points that were tried. The five points for which calculations were made are shown in Fig. 101.<sup>28</sup> Curve I represents the adsorption isotherm of

nitrogen on an  $\text{Al}_2\text{O}_3$  promoted iron catalyst at  $-195.8^\circ\text{C}$ . Points A and B were defined before, Point C is the midpoint of the straight line portion, Point D is the end of the straight line, and Point E is the extrapolation of the straight line to the saturation pressure. Adsorption isotherms of 10 different gases on 10 different promoted and unpromoted iron catalysts showed that the *maximum* deviations of the Point B surface area values from the average ranged from 3 to 12%. For Point A the maximum deviations ranged from 7 to 28.4%, and the other three points also showed less good agreement than Point B.

Curve II in Fig. 101 represents an adsorption isotherm of carbon tetrachloride on liquid mercury at  $11^\circ\text{C}$ . It was obtained by Cassel,<sup>30</sup> using an unusual method of isotherm determination. He measured the decrease in the surface tension of mercury with increasing partial pressure of the surrounding carbon tetrachloride atmosphere and calculated the isotherm from the Gibbs equation<sup>31</sup>

$$(8) \quad a = - \frac{c}{RT} \frac{d\sigma}{dc}$$

where  $a$  is the amount of  $\text{CCl}_4$  adsorbed per square centimeter of mercury surface,  $c$  is the concentration of  $\text{CCl}_4$  in the gas phase, and  $\sigma$  is the surface tension. In the calculation it was assumed that the packing of  $\text{CCl}_4$  on the surface was the same as in the liquid state. There is a good deal of similarity between the two isotherms of Fig. 101. The most important point, however, is that Cassel also found that the beginning of the middle linear portion of the  $\text{CCl}_4$  isotherm corresponded to the completion of a unimolecular layer on the surface of mercury.

2. Another evidence that Point B corresponds to an adsorbed monolayer is shown in Fig. 102, representing the variation of the net heats of adsorption of nitrogen and argon on iron catalysts with the amounts of gas adsorbed. The heats of adsorption were calculated by means of the Clapeyron-Clausius equation from isotherms measured at  $-183$  and  $-195.8^\circ\text{C}$ . The Point B values for curves 1, 2 and 3 were 125, 115 and 6.5 cc., respectively. The curves, particularly those of nitrogen, show a sharp decrease in the net heat values in the vicinity of Point B. At an adsorbed volume 25% smaller than the Point B value the net heat of adsorption is of the order of 1200 calories per mole; at a volume 25% larger than Point B the net heat is only 100–300

<sup>30</sup> H. Cassel, *Trans. Far. Soc.*, 28, 177 (1932).

<sup>31</sup> For the derivation of the Gibbs equation see, for example, H. B. Weiser, *Colloid Chemistry*, New York, 1939, p. 18.

calories per mole. Since the isosteric heat of adsorption is equal to  $q_d + RT$  (Chapter VIII, equation 22), and  $RT$  here is about 170 calories,  $q_d$  for the second case is equal to the heat of liquefaction within the experimental error. Thus one can safely conclude from the curves of Fig. 102 that at an adsorption 25% larger than the Point B value adsorption is taking place already in the second layer.

3. A third corroborative evidence came from the discovery of the chemisorption of carbon monoxide on the unpromoted iron catalyst.<sup>27</sup> When the adsorption isotherm of carbon monoxide was determined at  $-183^\circ\text{C}$ . it was found that the Point B value was twice as large as

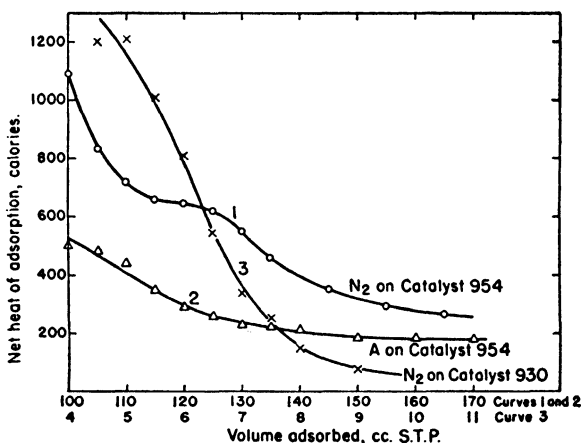


Fig. 102.—The net heats of adsorption of nitrogen and argon on iron catalysts.

expected. This is shown in Fig. 103, Curve 1A, representing the total adsorption of carbon monoxide. Actually, however, only about half of the amount taken up is physical adsorption, and this part can be pumped off readily at  $-78^\circ\text{C}$ . The other half, the chemisorbed carbon monoxide, comes off only at higher temperatures as iron carbonyl. If one saturates first the surface of the iron catalyst with chemisorbed carbon monoxide and then determines the adsorption isotherm at  $-183^\circ\text{C}$ ., one obtains Curve 1B, which represents the physical adsorption alone. The Point B value is now in complete agreement with the Point B values of the nitrogen, argon and carbon dioxide curves, as shown in Fig. 103. The difference between the Point B values of Curves 1A and 1B, i.e., the amount of chemisorbed carbon monoxide, is about 15% larger than the physical adsorption

corresponding to a monolayer. The chemisorption of carbon monoxide at  $-78^{\circ}\text{C}$ . is somewhat larger than at  $-183^{\circ}\text{C}$ ., it is about 25% larger than the van der Waals monolayer. However, this difference can be easily accounted for by assuming that chemisorbed carbon monoxide is more densely packed on the catalyst surface than van der Waals carbon monoxide or nitrogen.

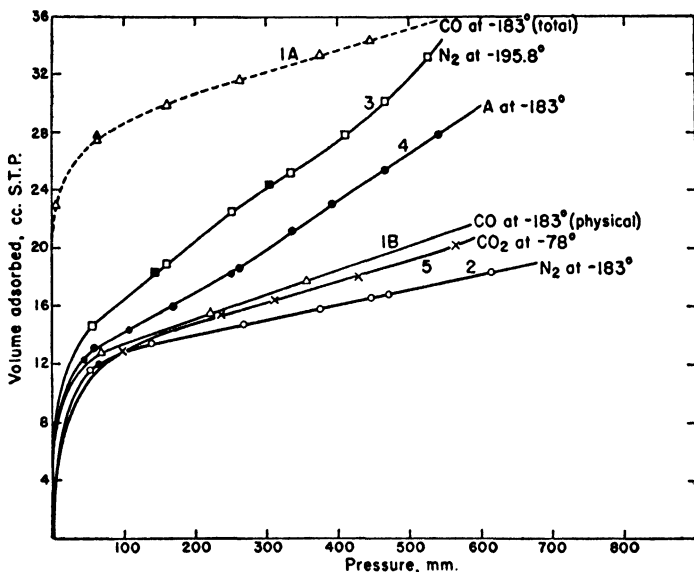


FIG. 103.—Checking of the physically adsorbed monolayer by means of the chemisorption of carbon monoxide on an iron catalyst.

Besides the three independent lines of empirical evidence, discussed above, a fourth and most decisive confirmation came from the development of the theory of multimolecular adsorption.<sup>32, 33</sup> It was shown in Chapter VI that a plot of equation (38) gives a straight line and that the constant  $v_m$ , giving the volume corresponding to a monolayer, can be calculated from the slope and intercept of the straight line. In Table XIV comparisons were made between the theoretical and experimental  $v_m$  values obtained from adsorption isotherms of nitrogen on twelve different adsorbents at  $90.1^{\circ}\text{K}$ . The experimental

<sup>32</sup> S. Brunauer, P. H. Emmett and E. Teller, *J. Am. Chem. Soc.*, 60, 309 (1938).

<sup>33</sup> S. Brunauer, L. S. Deming, W. E. Deming, and E. Teller, *J. Am. Chem. Soc.*, 62, 1723 (1940).

$v_m$  values are Point B values. The table shows that the two values seldom differ from each other by as much as 10%. This is true not merely for nitrogen, but also for oxygen, argon, carbon monoxide, and carbon dioxide, as was shown in Table XV. Only the butane values show a marked discrepancy, the Point B value being obviously too low. The reason for this becomes clear if one inspects Fig. 5 in Chapter II, giving the experimental isotherms of seven gases on silica gel. The butane isotherm approaches a Type III isotherm in shape, which makes the evaluation of Point B very difficult.

For gases that give distinct Type II and Type IV isotherms the Point B values are in excellent agreement with the theoretical  $v_m$  values. This can be regarded as a mutual confirmation of the empirical method of selecting the point on the isotherm corresponding to a monolayer and the fundamental assumptions underlying the derivation of equation (38). Although one can choose either method for surface determination, ordinarily the theoretical approach is preferable. One reason is that the empirical method breaks down in certain borderline cases, as for example in the above mentioned case of butane on silica gel, whereas the theory gives even in this case a consistent  $v_m$  value. Another reason is that the accurate determination of the beginning of the straight line portion in S-shaped isotherms requires a large number of experimental points, whereas for the determination of the straight line of equation (38) two points are sufficient, and three points already give a check value. In fact even one point at about  $p/p_0 = 0.3$  can give  $v_m$  quite accurately. The intercept,  $1/v_m c$ , is usually so small that one can simply connect the point with the origin and obtain  $v_m$  from the slope of the line, with an error less than 5%.<sup>32</sup> Occasionally the use of the empirical method is more convenient, notably if the isotherm is already available. In that case a simple inspection without any calculation can give Point B, at least approximately.

The theory of multimolecular adsorption provides a method for calculating the surface areas of adsorbents not only from Type II and IV isotherms, but from each of the five different isotherm types. Type III and V isotherms are not very common, but at least two important adsorbents yield Type I isotherms. Chabasite and some of the charcoals, among them coconut charcoal, give Type I isotherms. For such isotherms one can either calculate  $v_m$  by means of the Langmuir equation or take the amount adsorbed at the saturation pressure as the measure of the surface (Chapter IV). We may also recall at this point the excellent agreement between the surface area values obtained for

silica gel from the Type III isotherms of Reyerson and Cameron <sup>34</sup> and the Type II isotherms of Brunauer and Emmett <sup>29</sup> (Chapter VI).

Although the gas adsorption method of surface determination is relatively new, there are already a number of interesting comparisons available between it and other methods. A comparison with the ultramicroscopic method is shown in Table XLI, representing surface

TABLE XLI  
SURFACE AREAS OF DIFFERENT CARBON BLACKS

Material	Weight g.	$v_m$ cc. at S.T.P.	Specific Surface sq. m./g.	Average Particle Diameter Microns	
				Nitrogen Adsorption	Ultra- microscopic Count
Micronex	3.08	75.2	106.7	0.031	0.061
P-33	2.86	14.4	22.1	0.151	0.159
Arrow black	3.29	84.8	112.7	0.029	—
Wyex	2.95	74.2	110.2	0.030	—
Thermax	4.44	7.8	7.7	0.43	—
Thermatomic carbon	5.50	8.54	6.8	0.49	1.12
Acetylene black	0.792	11.68	64.5	0.052	0.130

area and average particle size determinations on seven different carbon blacks. The nitrogen adsorption values were obtained by Emmett and De Witt,<sup>35</sup> the ultramicroscopic values by Gehman and Morris.<sup>36</sup> The average particle size was obtained from the surface area determined by nitrogen adsorption by assuming that the carbon black particles are spheres with smooth surfaces. In this case

$$(9) \quad S = \frac{6}{\delta_s d}$$

where  $S$  is the specific surface of the adsorbent,  $\delta_s$  is its density, and  $d$  is the average particle diameter. Electron microscope photographs show that the carbon black particles actually have spheroidal shapes and nonserrated surfaces.<sup>37</sup>

A comparison between the last two columns of Table XLI shows that for P-33 the agreement is very good, but for three other carbons the nitrogen adsorption gives a smaller particle diameter, roughly by a factor of 2. The reason for the discrepancy may possibly be that the

<sup>34</sup> L. H. Reyerson and A. E. Cameron, *J. Phys. Chem.*, **39**, 181 (1935).

<sup>35</sup> P. H. Emmett and T. De Witt, *Ind. Eng. Chem., Anal. Ed.*, **13**, 28 (1941).

<sup>36</sup> S. C. Gehman and T. C. Morris, *Ind. Eng. Chem., Anal. Ed.*, **4**, 157 (1932).

<sup>37</sup> Columbian Carbon Co., *Ind. Eng. Chem., News Ed.*, **18**, 492 (1940).

smallest particles were beyond the resolving power of the ultramicroscope. For two of the carbon blacks electron microscopic particle size determinations were also made. For micronex the electron microscope<sup>37</sup> gave an average diameter of  $28\ \mu\mu$ , as compared to the nitrogen adsorption values of  $31\ \mu\mu$ , obtained by Emmett and De Witt,<sup>35</sup> and  $28.4\ \mu\mu$  obtained by Smith, Thornhill and Bray.<sup>38</sup> For acetylene black the electron microscope gave a particle size of  $51\ \mu\mu$ ,<sup>39</sup> as compared with the nitrogen adsorption values of  $52\ \mu\mu$ , obtained by Emmett and De Witt, and  $53.3\ \mu\mu$ , obtained by Smith, Thornhill and Bray. The nitrogen surface area values were calculated by assuming liquid-like packing of the molecules on the surface. The agreement between the two methods is so striking that it leaves little room for doubt about the validity of the linear equation (38), Chapter VI, for surface area determination.

Some further comparisons between visual microscopic determinations and nitrogen adsorption values are shown in Table XLII, repre-

TABLE XLII  
SURFACE AREAS OF ZINC OXIDE PIGMENTS

	Adsorbent		
	F-1601	K-1602	G-1603
Area by nitrogen adsorption sq. m./g.	9.48	8.80	3.88
Average particle diameter, microns			
1. By direct microscopic count	0.21	0.25	0.49
2. By ultramicroscopic count	0.135	0.16	0.26
3. By adsorption of methyl stearate	0.19	0.24	0.55
4. By adsorption of nitrogen	0.115	0.124	0.28
5. By permeability	0.12	0.15	0.25

senting the average particle diameters of three different types of zinc oxide pigments, obtained by five different methods. The nitrogen adsorption values were obtained by Emmett and De Witt, the microscopic and ultramicroscopic values were furnished by the New Jersey Zinc Company. The microscopic values are too large, doubtless because the smallest particles were beyond the resolving power of the microscope. The agreement between the ultramicroscopic values and the nitrogen adsorption values is quite satisfactory. There is excellent agreement between the gas adsorption and the permeability values; the deviations from the averages of the two methods are 2, 10 and

<sup>38</sup> W. R. Smith, F. S. Thornhill and R. I. Bray, *Ind. Eng. Chem., Ind. Ed.*, **33**, 1303 (1941).

<sup>39</sup> J. Hillier, *Am. Soc. Testing Materials Symposium*, Washington, D. C., 1941.



5.5% for the three samples. The permeability method will be discussed later.

Besides using carbon blacks and zinc oxide pigments Emmett<sup>40</sup> also used sized glass beads to compare the gas adsorption method with the microscopic method. The beads were prepared by Bloomquist and Clark.<sup>41</sup> The average diameter of the beads, as judged by microscopic examination, was 7  $\mu$ , nitrogen adsorption gave 4.5  $\mu$ . The difference was probably due to the fact that the beads were washed with cleaning solution prior to the nitrogen adsorption. Such washing etches the surface of glass and increases the area accessible to nitrogen molecules. Since according to equation (9) the apparent particle diameter is inversely proportional to the surface area, a 36% increase in surface due to the acid treatment would account for the particle diameter obtained by Emmett. To test the validity of this explanation the glass beads were further treated with cleaning solution; the nitrogen adsorption after this treatment gave a surface area 40% larger than before.

Two other comparisons may be mentioned between visual determinations and gas adsorption measurements of the same surfaces. One of these was discussed before: Barrett, Birnie, and Cohen<sup>3</sup> microscopically obtained for the specific surface of their silica powder the value of 560 sq. cm./g., while the Point B values of their water vapor isotherms give 580 sq. cm./g. The other can be obtained from an adsorption isotherm of benzene on mica sheets, determined by Bangham and Mosallam.<sup>42</sup> The isotherm is S-shaped, with a Point B value somewhat less than 0.3 cc. The differential heats of adsorption calculated by means of the Clapeyron-Clausius equation show a sudden drop in the vicinity of 0.27 cc. vapor adsorbed from 12,000 calories per mole to 8000 calories per mole, the latter being equal to the heat of liquefaction of benzene. Assuming that 0.27 cc. corresponds to a monolayer, and assuming liquid-like packing of the benzene molecules on the surface, the calculated area is 22,300 sq. cm. The geometrical surface of the mica sheets was 18,000 sq. cm. A slight roughness of the surface or a few cracks in the sheets could account for the small difference of 22%.

When the surface area of an adsorbent is determined by nitrogen adsorption and also by the adsorption of organic molecules from

<sup>40</sup> P. H. Emmett in E. O. Kraemer's "Advances in Colloid Science," New York, 1942, Chapter I.

<sup>41</sup> C. R. Bloomquist and A. Clark, *Ind. Eng. Chem., Anal. Ed.*, 12, 61 (1940).

<sup>42</sup> D. H. Bangham and S. Mosallam, *Proc. Roy. Soc., A166*, 558 (1938).

solutions, one invariably finds that the latter method gives the smaller surface area. An example of this was given in Table XLII. The methyl stearate values, obtained by Ewing,<sup>43</sup> indicate roughly half as large surface areas as the nitrogen adsorption does. One would be tempted to ascribe this to the inaccessibility of certain narrower cracks and pores to the large organic molecules, but the ultramicroscopic values preclude this possibility. The agreement between the nitrogen adsorption values and the ultramicroscopic determinations clearly indicates that the pigment particles could not have had large internal surfaces. The explanation must be, therefore, either that Ewing ascribed to a methyl stearate molecule an area that was too small by a

TABLE XLIII  
SURFACE AREA MEASUREMENTS

Material	Surface Area (in sq. m./g.) Obtained from			
	Adsorption of Nitrogen	Adsorption of Butane	Adsorption of Salicylic Acid	Radioactive Indicator
Graphite	30.73		3.96	
TiO <sub>2</sub>	9.88	6.58	5.55	
ZrSiO <sub>4</sub>	2.76		1.33	
BaSO <sub>4</sub>	4.30	2.68	1.73	2.2

factor of 2, or that the adsorption of methyl stearate is a specific chemisorption process, and only half of the zinc oxide surface contains the active groups that are capable of chemisorbing methyl stearate.

In Table XLIII, taken from Emmett and De Witt,<sup>35</sup> comparisons are shown between surface area values obtained by nitrogen adsorption and by salicylic acid adsorption.<sup>44</sup> The latter gives a smaller value in every case. The discrepancy for titanium oxide is less than two fold, for graphite more than eight fold. In this case it seems quite likely that the large organic molecules were unable to penetrate into the narrower cracks and pores of the adsorbent. This is indicated by the butane adsorption values; they are intermediate between the nitrogen and the salicylic acid values. Obviously in the case of butane the low values can not be due to chemisorption. The radioactive indicator value<sup>45</sup> is also too low by a factor of 2. It was pointed out before

<sup>43</sup> W. W. Ewing, *J. Am. Chem. Soc.*, **61**, 1317 (1939).

<sup>44</sup> The salicylic acid adsorption values were obtained by Dr. G. E. Boyd of the University of Chicago.

<sup>45</sup> This value was obtained by Professor I. M. Kolthoff of the University of Minnesota.

that the radioactive indicator method often gives surface area values that are too low.

Smith, Thornhill and Bray<sup>38</sup> determined the adsorption of diphenylguanidine on about 20 different carbon blacks and compared them with the surface areas of the same samples determined by nitrogen adsorption. They found, for example, that the four carbon blacks, graphitized black, grade 9 rubber black, carbolac 1 color black, and carbolac 1 calcined, had surface area values of 90, 100, 947 and 990 sq. m./g., respectively, while the adsorption of diphenylguanidine was 1.0, 10.2, 192.0 and 17.3 mg./g., respectively. Thus there seems to be no correlation between total surface area and the adsorption of this organic molecule. The investigators concluded therefore that the adsorption of diphenylguanidine was a chemisorption process.

In the discussion of other methods of surface area determination further comparisons are made with the gas adsorption method. At this point we shall summarize some of the advantages and limitations of the method.

1. The experimental technique of the gas adsorption method is simple; it is far simpler than that of any other method discussed in this chapter, with the exception of the unreliable dye adsorption method. Furthermore, if an inert gas like argon or nitrogen is used, the adsorbent sample is recovered after the surface area determination in exactly the same condition as it was before, which is a great advantage in many investigations.

2. The method is accurate; nitrogen adsorption can give the absolute surface area within 20%. Comparison with visual determinations, particularly with the electron microscopic values, indicates that this is a conservative estimate. Relative surface areas can be obtained to better than 10%. For example, the ratio of the surface area of an  $\text{Al}_2\text{O}_3$  promoted iron catalyst to that of an unpromoted iron catalyst obtained from Point B values was 22.0 (nitrogen isotherms at  $-183^\circ$ ), 23.3 (nitrogen at  $-195.8^\circ$ ), 22.8 (carbon monoxide at  $-183^\circ$ ), 22.0 (argon at  $-183^\circ$ ), and 22.7 (butane at  $0^\circ \text{C.}$ ). The maximum deviation from the average of these five values is less than 5%.

3. The method is quite universal; it can be applied to any porous or finely divided adsorbent. The universality of the method is illustrated in Table XLIV, representing the specific surface areas of 45 adsorbents. The data for adsorbents 1-30 were taken from Brunauer and Emmett,<sup>29</sup> for 31-34 from Smith, Thornhill, and Bray,<sup>38</sup> and for 35-45 from Emmett and De Witt.<sup>35</sup> The table reveals the striking

fact that the method of gas adsorption is applicable through a 100,000 fold variation in specific surface, from unreduced  $\text{Fe}_3\text{O}_4$  to Darco G.

4. The gas adsorption method is limited to finely divided substances; it can not measure the surfaces of coarse particles. Among the surface area values listed in Table XLIV that of  $\text{Fe}_3\text{O}_4$  is quite uncertain, the smallest reasonably accurate value is that of  $\text{CuSO}_4 \cdot 5\text{H}_2\text{O}$ . The surface area of this substance according to equation (9) corre-

TABLE XLIV  
SPECIFIC SURFACE AREAS OF VARIOUS ADSORBENTS

Adsorbent	Specific Surface sq. m./g.	Adsorbent	Specific Surface sq. m./g.
1. $\text{Fe}_3\text{O}_4$ catalyst (unreduced)	0.02	23. Glaucosil	82
2. Fe catalyst 973, sample I, unpromoted	0.55	24. Silica gel I (non-electrodialyzed)	584
3. Fe catalyst 973, sample II, unpromoted	1.24	25. Silica gel II (electrodialyzed)	614
4. Fe catalyst 954, 10.2% $\text{Al}_2\text{O}_3$	11.03	26. Dried bacteria	0.17
5. Fe catalyst 424, 1.03% $\text{Al}_2\text{O}_3$ , 0.19% $\text{ZrO}_2$	9.44	27. Dried bacteria (pulverized)	3.41
6. Fe catalyst 931, 1.3% $\text{Al}_2\text{O}_3$ , 1.59% $\text{K}_2\text{O}$	4.78	28. Granular Darco B	576
7. Fe catalyst 958, 0.35% $\text{Al}_2\text{O}_3$ , 0.08% $\text{K}_2\text{O}$	2.50	29. Granular Darco G	2123
8. Fe catalyst 930, 1.07% $\text{K}_2\text{O}$	0.56	30. Activated charcoal	775
9. Fused copper catalyst	0.23	31. Lampblack	28
10. Commercial copper catalyst	0.42	32. Acetylene black	64
11. Pumice	0.38	33. Grade 3 rubber black	135
12. Ni on pumice, 91.8% pumice	1.27	34. Carbolac 1 color black	947
13. NiO on pumice, 89.8% pumice	4.28	35. Graphite	30.7
14. $\text{Cr}_2\text{O}_3$ gel	228	36. Cuprene	20.7
15. $\text{Cr}_2\text{O}_3$ "glowed"	28.3	37. Paper	1.59
16. KCl (finer than 200 mesh)	0.24	38. Cement	1.08
17. $\text{CuSO}_4 \cdot 5\text{H}_2\text{O}$ (40-100 mesh)	0.16	39. $\text{TiO}_2$	7.88
18. $\text{CuSO}_4$ anhydrous	6.23	40. $\text{BaSO}_4$	4.30
19. Cecil soil, 9418	32.3	41. $\text{ZrSiO}_4$	2.76
20. Cecil soil colloid, 9418	58.6	42. Lithopone	34.8
21. Barnes soil, 10,308	44.2	43. Lithopone—calcined	1.37
22. Barnes soil colloid, 10,308	101.2	44. Lithopone—calcined and ground	3.43
		45. Porous glass	125.2

sponds to an average particle diameter of  $16.4 \mu$ . For particles larger than  $20 \mu$  the method becomes inaccurate because large dead space corrections must be applied to small adsorption values. This difficulty can be avoided if in place of the most frequently used nitrogen some other gas is employed, the vapor pressure of which at the temperature of the run is smaller than 1 mm. At such low pressures the dead space correction becomes negligible. Naturally in this case high vacuum technique must be used. Armbruster and Austin<sup>46</sup> measured

<sup>46</sup> M. H. Armbruster and J. B. Austin, *J. Am. Chem. Soc.*, 61, 1117 (1939).

in such manner the surface areas of steel sheets by the adsorption of ethyl iodide at room temperature.

There is no lower limit to the particle size that can be measured by the gas adsorption method. A simple calculation shows that at the point on the adsorption isotherm which corresponds to a monolayer one nitrogen molecule is adsorbed for every three molecules of  $\text{SiO}_2$  in silica gel, for every six atoms of carbon in charcoal, and for every two atoms of carbon in Darco G. Thus some of the substances of Table XLIV come quite close to the upper limit of surface area, or to the lower limit of particle size.

5. In order to get closest to the true surface of an adsorbent by the gas adsorption method one should use the smallest molecules. However, to obtain complete monolayers with helium, neon, and hydrogen, one must measure the adsorption at liquid helium and hydrogen temperatures. Since liquid helium and hydrogen are usually not available, while liquid air is easily obtained, one is forced to use the somewhat larger molecules of nitrogen and argon. These two molecules are particularly suitable because they are inert; no chemisorption complicates the determination of their van der Waals adsorption isotherms. Nitrogen is especially useful because of its ready availability. However, if an adsorbent contains exceedingly fine pores nitrogen adsorption may give wholly erroneous results about the true surface. Thus Emmett<sup>40</sup> found that 50% dehydrated chabazite adsorbs hydrogen at 77° K., but practically no nitrogen can enter the pores at that temperature.

In conclusion it may be emphasized that the gas adsorption method can be used to determine the average particle size only if the particles are smooth and possess no internal surfaces. If one is interested in the surface area of a finely divided substance, the gas adsorption method gives far more accurate results and is much less time-consuming than the microscopic methods. On the other hand, if one is interested in the particle size, it is best to use microscopic methods.

## MISCELLANEOUS METHODS OF SURFACE AREA DETERMINATION

### *A. Rate of Solution of a Powder*

The method was first applied by Wolff<sup>47</sup> to measure the surface areas of glass powders. He measured the rate of solution of a glass plate in a solvent, then the rate of solution of the same glass in powdered form in the same solvent. In both cases the rate of solution was measured by determining the loss in the weight of the glass in a given

<sup>47</sup> H. Wolff, *Z. angew. Chem.*, **35**, 138 (1922).

time. Assuming that the initial rate of solution is proportional to the surface exposed to the solvent, one can obtain the surface area of the powder if one knows that of the glass plate. Wolff simply assumed that the visible surface of the glass plate was equal to its true surface, but this is incorrect.

Wolff believed that the most troublesome step in the method was finding a suitable solvent. He first tried water for his glass samples, then hydrofluoric acid, but both were found unsuitable. He finally adopted a mixed solution of sodium carbonate and sodium hydroxide in water. The work of other investigators revealed, however, that the greatest difficulty lies not in the choice of the solvent but in obtaining a suitable standard of known surface area.

Wolff's research was continued and extended by Schmidt and Durau.<sup>48</sup> They found by the rate of solution method that different glass powders ground to the same mesh size gave different surface areas. The method did not work equally well for all glasses. For the window glass which was most suitable for the investigations they found that the amount of glass dissolved (both plate and powder) was: (1) independent of the velocity of stirring, (2) beginning with a definite concentration independent of the concentration of the solvent, and (3) proportional to the time of contact with the solvent. They concluded therefore that the solution of the plate and the powder proceeds in the same manner and that one can use for the surface area determination the equation

$$(10) \qquad W_1/S_1 = W_2/S_2$$

where  $W_1$  and  $W_2$  are the losses in weight of the plate and the powder in a given time, and  $S_1$  and  $S_2$  are the surface areas of the plate and the powder.

Schmidt and Durau then proceeded to compare Wolff's rate of solution method with Paneth's dye adsorption method. Using methyl violet they calculated from the number of dye molecules adsorbed at saturation and from the previously determined surface area of the glass powder that a dye molecule occupies an area of  $35.2\text{\AA}^2$  on the glass surface. If the dye molecules were cube-shaped, the area covered by a molecule would be  $69.0\text{\AA}^2$ . This calculation suggests therefore that the dye adsorption is at least two molecular layers thick. However, Schmidt and Durau point out that if one assumes that the dye molecule has the shape of a parallelepiped and is adsorbed with its small side on the surface, the adsorption may still be unimolecular. With

<sup>48</sup> G. C. Schmidt and F. Durau, *Z. phys. Chem.*, 108, 128 (1924).

another dye, diamond fuchsine, the same result was obtained as with methyl violet.

There is good reason to suppose that large organic molecules tend to lie flat on the surface rather than perpendicular to it, as was shown in the discussion of the dye adsorption method. This would mean that the adsorption of methyl violet and diamond fuchsine on glass was about six layers thick—if the standard used in the determination of the surface of the glass powder was correct. If, however, the true surface of the glass plate was six times as large as its visible surface, the dye adsorption was unimolecular. If the ratio of true surface to apparent surface was even greater than this, the dye adsorption covered only a fraction of the surface of glass powder.

Schelte<sup>49</sup> continued the investigations on window glass and lead glass. He used Wolff's method to determine the surface areas of the powders and measured the adsorption of four different dyes on each powder. The results are shown in Table XLV. They were calcu-

TABLE XLV  
ADSORPTION OF DYES ON POWDERED GLASS

Glass	% Surface Covering by			
	Methyl Violet	Ethyl Violet	Diamond Fuchsine	Methylene Blue
Window glass	196.6	164.8	198	136.4
Lead glass	192	140.3	75.2	79.5

lated by assuming that the dye molecules were cube-shaped and that the surface areas of the standard glass plates were equal to their geometrical surfaces. On this basis methyl violet appears to be two layers thick on both glasses; diamond fuchsine, on the other hand, two layers thick on window glass but only 3/4 of a layer thick on lead glass. Schelte therefore concluded that dye adsorption does not merely depend on the extent of the surface, but also on the chemical composition of the glass.

Miss Isselstein<sup>50</sup> used the lead glass powder, the surface of which was determined by Schelte, and measured the adsorption of carbon disulfide, pentane, and chloroform on it. She found for all three vapors that the adsorption layer in the vicinity of the saturation pressure was more than 30 molecules thick. An inspection of the

<sup>49</sup> F. Schelte, *Z. phys. Chem.*, **114**, 394 (1925).

<sup>50</sup> M. T. Isselstein, *Physical. Z.*, **29**, 873 (1928).

isotherms reveals that she actually did obtain multimolecular adsorption, but she overestimated the number of layers roughly by a factor of 5. This is again due to the fact that the true surface of the standard glass plate of Schelte was five times as large as its visible surface.

From the foregoing discussion it may be concluded that the rate of solution method of surface determination is greatly hampered by a lack of knowledge of the true surface area of the substance used as a standard. Another objection is that if there is a wide range of particle sizes in the powder, some of the finer particles may dissolve completely during the experiment. Besides, the rate of solution depends on the motion of the liquid in the immediate vicinity of the surface, and this may be different for the plate and the powder.

In spite of the above objections the rate of solution method can give quite accurate results with proper care. This is shown by the work of Palmer and Clark,<sup>61</sup> who determined the surface area of vitreous silica powder by measuring the rate of solution in hydrofluoric acid. The success of their work was due mainly to two factors. In the first place the rate of solution was determined not by the loss in the weight of the adsorbent but by the change in the electrolytic conductivity of the solution. The difference between the degrees of ionization of the original hydrofluoric acid and the product hydrofluosilicic acid is so great that the method is very sensitive, especially in the important initial stages. In the second place the standardization was very carefully done by determining the rate of solution of several clear fused quartz rods having easily measurable geometrical surfaces.

Since Palmer and Clark determined the adsorption of acetone and several other organic vapors on their fused silica samples, one can calculate the surface areas of the powders from the adsorption isotherms and compare them with the values obtained from rate of solution measurements. If one plots the 25° C. acetone isotherm according to the linear equation (38), Chapter VI, one obtains an excellent straight line, giving a  $v_m$  value of 50.6 micromoles of acetone on a 14.67 g. sample of vitreous silica. The specific surface of this same sample was 4690 sq. cm./g. according to the rate of solution measurements. If one uses for the area occupied by an acetone molecule on the surface the value  $26.9\text{\AA}^2$ , obtained from the density of liquid acetone at 25° C., one calculates from the above  $v_m$  value a specific surface of 5640 sq. cm./g., which is 20% larger than the value of Palmer and Clark. If on the other hand one uses for the area occupied by an acetone

<sup>61</sup> W. G. Palmer and R. E. D. Clark, *Proc. Roy. Soc.*, A149, 360 (1935).



molecule the value  $20.5\text{\AA}^2$ , given by Adam<sup>52</sup> for close-packed films on water of long chain compounds terminating in the  $\text{CO}-\text{CH}_3$  group, one obtains for the specific surface  $4290\text{ sq. cm./g.}$ , which is about 8% smaller than the value of Palmer and Clark. Thus the agreement between the surface area values obtained by measuring the rate of solution of silica in hydrofluoric acid and by measuring the adsorption isotherm of acetone on silica is very good. This can be considered a mutual confirmation of both methods of surface determination.

### B. The Permeability Method

D'Arcy's law states that the rate of flow of a liquid through a bed of material is proportional to the pressure gradient across the bed

$$(11) \quad \frac{Q}{A} = K_p \frac{h}{L}$$

where  $Q$  is the volume of liquid passing through the bed in unit time,  $A$  is the cross-section of the bed, and  $h$  is the loss of head of the liquid in passing through a thickness  $L$  of the bed. Writing  $u = Q/A$  for the linear rate of flow through the bed and  $i = h/L$  for the hydraulic gradient, equation (11) becomes

$$(12) \quad u = K_p i$$

The proportionality constant  $K_p$  represents the apparent linear rate of flow for unit hydraulic gradient, and it is called the permeability of the bed. D'Arcy's law has been tested for a great variety of porous media and powders, and it has been found valid in every instance.

Kozeny<sup>53</sup> derived a semi-empirical equation for the permeability, which was utilized by Carman<sup>54,55</sup> to evaluate the surface areas of powders. The equation is

$$(13) \quad S_0 = 14 \sqrt{\frac{1}{K_p \nu} \cdot \frac{\epsilon^3}{(1 - \epsilon)^2}}$$

where  $S_0$  is the specific surface area, referred to 1 cc., (instead of 1 g.) of powder,  $\nu$  is the kinematic viscosity (in stokes) of the liquid which is used in the determination of the permeability  $K_p$ , and  $\epsilon$  is the porosity of the bed, i.e., the volume of pore space per unit volume of the bed. To obtain the porosity of the bed one must know its total volume as

<sup>52</sup> N. K. Adam, *The Physics and Chemistry of Surfaces*, Oxford, 1930, p. 50.

<sup>53</sup> J. Kozeny, *Ber. Wien Akad.*, 136A, 271 (1927).

<sup>54</sup> P. C. Carman, *J. Soc. Chem. Ind.*, 57, 225 (1938).

<sup>55</sup> P. C. Carman, *J. Soc. Chem. Ind.*, 58, 1 (1939).

well as the volume of the solid particles in it; the latter is calculated from the weight and the true density of the solid. The surface determination therefore involves the measurement of the viscosity of the liquid, the density of the solid, and the permeability of the bed.

The validity of equation (13) has been thoroughly tested by Carman down to an average particle size of  $2\ \mu$ . One of the tests was made on spherical glass particles in the size-range 10–100  $\mu$ . The powder was divided into three fractions and each fraction was examined microscopically. The size analyses are given in Table XLVI; each was

TABLE XLVI  
SIZE ANALYSES OF SPHERICAL GLASS PARTICLES

Size Range in Microns	Average $d$ in Range, Microns	Number of Particles $N$		
		Fraction I	Fraction II	Fraction III
2– 5	3.5	38	—	—
5– 10	7.5	109	—	—
10– 20	15	331	103	90
20– 30	25	404	96	
30– 40	35	97	125	
40– 60	50	19	426	261
60– 90	75	2	235	307
90–110	100	—	15	266
110–140	125	—	—	76
Totals		1000	1000	1000
Specific surface, $S_0$ cm. <sup>2</sup> /cm. <sup>3</sup>		2070	950	653
Average particle size, $d_m$ microns		29 $\mu$	63 $\mu$	92 $\mu$

based on a count of 1000 particles. Since the total surface area of the 1000 particles is  $\pi \sum_i N_i d_i^2$ , and the total volume is  $\pi/6 \sum_i N_i d_i^3$ , the specific surface  $S_0$ , expressed in cm.<sup>2</sup>/cm.<sup>3</sup>, is given by

$$(14) \quad S_0 = 6 \frac{\sum_i N_i d_i^2}{\sum_i N_i d_i^3}$$

If the average particle size  $d_m$  is defined as the diameter of equal spheres which would give the same specific surface as the powder, then

$$(15) \quad d_m = 6/S_0$$

The values of  $S_0$  and  $d_m$  for the three fractions are given in Table XLVI.

Carman performed permeability measurements on each fraction using acetone and alcohol as the liquids. The viscosities of the two liquids differ four fold, as seen in Table XLVII, Column 3. A comparison between the  $S_0$  and  $d_m$  values of Tables XLVI and XLVII shows an excellent agreement. At the same time this agreement

shows that the permeability method measures only the external surfaces of the glass spheres and not their true surfaces. Acid washing, or even washing with water, makes the surface of glass rough on a molecular scale, but this roughness is not indicated by the permeability method. The reason is that the liquid used in the measurements tends to flow through the large channels between the particles, and only a negligible fraction flows through the extremely fine pores produced in the washing process. We may recall that the permeability

TABLE XLVII  
PERMEABILITY MEASUREMENTS ON SPHERICAL GLASS PARTICLES

Material	Liquid	Viscosity $\nu$	Porosity $\epsilon$	Permeability $K_p$	$S_0$ cm. <sup>3</sup> /cm. <sup>2</sup>	$S_0$ Average	$d_m$ Microns
Fraction I	Acetone	0.00415	0.338	0.00102	2020	2090	28.7
Fraction I	Acetone	0.00415	0.360	0.00120	2120		
Fraction I	Alcohol	0.0154	0.360	0.000321	2120		
Fraction I	Alcohol	0.0154	0.370	0.000365	2110		
Fraction II	Acetone	0.00415	0.390	0.0077	990	987	61
Fraction II	Alcohol	0.0154	0.384	0.00201	975		
Fraction III	Acetone	0.00415	0.375	0.01505	651	653	92
Fraction III	Alcohol	0.0154	0.392	0.00482	656		

method and the gas adsorption method gave excellent agreement for zinc oxide pigments (Table XLII). However, in that case the surfaces of the pigment particles were smooth, and the true surface and the external surface were identical. This was evidenced by the fact that the ultramicroscopic determinations also checked the other two methods very well.

Lea and Nurse<sup>56</sup> used air and water as fluids in their determinations of the surface areas of cements and sands by the permeability method. They found that the values obtained with water were 20–40% higher than the air permeability values. Determination of the surface by the Andreasen sedimentation method<sup>57</sup> gave good agreement with the air permeability values. Gooden and Smith<sup>58</sup> used a self-calculating air permeability apparatus to measure the average particle diameter of silica powders. Comparison with the microscopic method showed good agreement down to a particle diameter of 3  $\mu$ , but for the finest fraction (0.3–3  $\mu$ ) the air permeability method gave a value that was 58% higher than the microscopic value.

The permeability method can be used successfully for the determination of the surface areas of powders which have too coarse particles

<sup>56</sup> F. M. Lea and R. V. Nurse, *J. Soc. Chem. Ind.*, 58, 277 (1939).

<sup>57</sup> A. H. M. Andreasen, *Kolloid Z.*, 49, 48, 252 (1929).

<sup>58</sup> E. L. Gooden and C. M. Smith, *Ind. Eng. Chem., Anal. Ed.*, 12, 479 (1940).

to give accurate nitrogen adsorption values. For an average particle size greater than  $10\ \mu$  the permeability method is more accurate than the gas adsorption method. It is also far superior to the laborious microscopic methods. On the other hand the method can not be used at all for very fine powders. Carman<sup>55</sup> estimated that the theoretical lower limit of the validity of the method is in the neighborhood of  $0.1\ \mu$ . The zinc oxide particles of Table XLII, therefore, were fairly near to the lower size limit. The method can not be applied to such fine particles as some carbon blacks, the surface areas of which were determined by Smith, Thornhill and Bray<sup>38</sup> by the nitrogen adsorption method.

In a critical estimate of the permeability method Sullivan and Hertel<sup>59</sup> state: "From the rather extensive data supplied by the various workers in the field it appears that where proper technique is employed the specific surface, the surface per gram, or the surface weighted average particle diameter may be calculated with high reproducibility and good accuracy from permeability measurements on powders, sands, textile fibers and other non-consolidated porous media. Where the media are consolidated (such as porous carbon, natural sandstone and the like) or where the media contain bridging, agglomeration, or considerable channelling, it is not certain how much of the surface is actually exposed to flow. Therefore specific surface calculations for such media are likely to be in error or of doubtful significance."

### C. The Heat of Wetting of a Powder

This method of surface determination was originated by Bartell and Fu.<sup>60</sup> By thermodynamic reasoning they derived the equation

$$(16) \quad S = \frac{-q_w}{K_a \left( \sigma - T \frac{d\sigma}{dT} \right)}$$

where  $S$  is the surface of the powder,  $-q_w$  is the heat of wetting of the adsorbent by a given liquid,  $\sigma$  is the surface tension of that liquid, and  $K_a$  is a constant. The value of  $K_a$  is obtained from the equation

$$(17) \quad \sigma_s - \sigma_{sl} = K_a \sigma$$

where  $\sigma_s$  is the surface tension of the solid adsorbent against air, and  $\sigma_{sl}$  is the interfacial tension between the solid and the liquid. Neither

<sup>59</sup> R. R. Sullivan and K. L. Hertel in E. O. Kraemer's "Advances in Colloid Science," New York, 1942, Chapter II.

<sup>60</sup> F. E. Bartell and Y. Fu, *Colloid Symposium Monograph*, 7, 138 (1930).

$\sigma_s$  nor  $\sigma_{sl}$  is readily measurable, but Bartell and Osterhof<sup>61</sup> developed a method for measuring their difference. The determination of the surface area of an adsorbent thus necessitates the knowledge of  $\sigma$  and  $d\sigma/dT$  for the liquid used, as well as the experimental determination of  $q_w$  and  $K_a$ . The measurement of the heat of wetting is done calorimetrically, while the determination of  $K_a$  involves the measuring of three displacement pressures.

The term  $\sigma_s - \sigma_{sl}$  in equation (17) is called the adhesion tension between the solid and the liquid; it is the decrease in free energy that occurs when a unit interface solid-liquid is substituted in place of a unit interface solid-air. The determination of the adhesion tension according to the method of Bartell and Osterhof begins with the grinding of the adsorbent to a very fine powder, 300 mesh or finer. Let us say that the adsorbent is carbon. The carbon powder is subjected to a uniform compression in a displacement cell, the pressure having a definite value between 100 and 200 atmospheres. A liquid which is known to have zero contact angle with carbon, for example benzene, is then brought in contact with the solid in the cell. Air begins to be displaced by the liquid toward the manometer side. The air pressure is increased on that side until the movement of the liquid in the capillary spaces ceases. The equilibrium pressure is read on the manometer. This gives the displacement pressure of air by benzene, the first of the three pressures necessary for calculating the adhesion tension. The second is the displacement pressure of air by a liquid which gives a definite contact angle with carbon, such as water. The third is the displacement pressure of water by benzene. The three values give the adhesion tensions of both carbon-benzene and carbon-water. The values of the constant  $K_a$  can be obtained by means of equation (17), using the known surface tensions of benzene and water.

The results of Bartell and Fu<sup>60</sup> for sugar charcoal and dehydrated silica gel are shown in Table XLVIII. The specific surface areas obtained by the use of five different liquids for each adsorbent show excellent agreement with one another. The average value for the charcoal is 630 sq. m./g., for the silica 450 sq. m./g. A silica gel sample containing 4% water gave an average specific surface of 720 sq. m./g. In the light of gas adsorption experiments that were performed on various charcoals and silica gels all three values seem reasonable. For example, the silica gel used by Reyerson and Cameron<sup>24</sup> and by Brunauer and Emmett<sup>29</sup> had a specific surface of

<sup>61</sup> F. E. Bartell and H. J. Osterhof, *Colloid Symposium Monograph*, 5, 113 (1927).

about 500 sq. m./g., while the most active gel used by McGavack and Patrick <sup>62</sup> had a surface area of about 660 sq. m./g. <sup>63</sup> This latter value is about 10% smaller than that of Bartell and Fu for the gel containing 4% water, but the methods of preparation of the two gels were somewhat different.

In contrast with the gas adsorption method, the heat of wetting method makes no assumptions with regard to the packing of the

TABLE XLVIII  
SURFACE AREAS OF SUGAR CHARCOAL AND SILICA

Liquid	$-q_w$ Calories/g.	$\sigma_s - \sigma_{sl}$	$K_a$	$-d\sigma/dT$	$S$ sq. m./g.
Charcoal					
C <sub>6</sub> H <sub>6</sub>	28.56	81.1	2.87	0.130	620
CHCl <sub>3</sub>	30.1	79.83	3.04	0.134	630
CS <sub>2</sub>	31.2	89.45	2.65	0.161	610
(C <sub>2</sub> H <sub>5</sub> ) <sub>2</sub> CO <sub>2</sub>	26.4	65.55	2.54	0.122	680
CCl <sub>4</sub>	30.97	86.37	3.3	0.120	630
Silica					
H <sub>2</sub> O	15.91	82.82	1.15	0.1511	500
C <sub>6</sub> H <sub>6</sub>	12.66	42.43	1.85	0.140	430
CHCl <sub>3</sub>	14.52	59.95	2.25	0.113	450
C <sub>6</sub> H <sub>5</sub> NO <sub>2</sub>	12.3	63.45	1.48	0.114	450
CCl <sub>4</sub>	10.0	40.7	1.56	0.128	430

molecules on the surface of the adsorbent. On the other hand certain other assumptions enter into the method, which introduce elements of uncertainty. In the first place, it is assumed that the pores between the particles of the powder which serve as capillary tubes remain constant in size during the three displacement pressure determinations. It was pointed out by McBain <sup>64</sup> that this is not quite true. In the second place, it is assumed in the derivation of equation (16) that  $K_a$  is independent of the temperature. Since according to equation (17)  $K_a$  depends on three surface tension terms, each of which is dependent on the temperature, it seems likely that  $K_a$  also depends on the temperature.

<sup>62</sup> J. McGavack and W. A. Patrick, *J. Am. Chem. Soc.*, **42**, 946 (1920).

<sup>63</sup> Estimated on the basis of the theory of multimolecular adsorption (equation 38, Chapter VI).

<sup>64</sup> J. W. McBain, *The Sorption of Gases and Vapors by Solids*, London, 1932, p. 346.

The method of Bartell and Fu measures only that part of the surface of a porous substance to which the large organic molecules used in the heat of wetting determinations have access. Gas adsorption experiments show that butane gives a smaller specific surface for both charcoal and silica gel than nitrogen or other smaller molecules. The larger specific surface obtained for silica by water than by the four organic molecules, shown in Table XLVIII, may be due to the smaller size of the water molecules.

The main drawback of the method is its great complexity, particularly compared with the gas adsorption method. Nevertheless, since the heat of wetting method seems also to give quite accurate surface area values, it would be of interest to check the two methods against each other, using the same adsorbent for both determinations.

#### *D. The Interference Method*

Constable<sup>65,66</sup> developed a method of determining the surface areas of metals by studying the interference colors formed when metal is oxidized. Actually the interference colors give only the thickness of the oxide layer formed, but if the volume of the layer can be determined one can divide it by the thickness and obtain the surface area. The volume of the oxide layer is calculated from its weight and its density; the weight of the layer is obtained by measuring the conductivity of the metal before and after oxidation. The decrease in conductivity is ascribed to the conversion of part of the metal to the oxide.

Since the smallest film thickness measurable by the interference method is in the neighborhood of 500 Å, one must oxidize about 200 layers of the metal before its surface can be determined. It may well be that the oxidation alters the surface of the metal. Brunauer and Emmett<sup>27,28,67</sup> found by the nitrogen adsorption method that oxidation of the upper 5–10 layers of iron atoms alters the surface of an iron catalyst only very slightly. However, this may not be true for all metals, nor can one say with certainty what would have happened to the surfaces of the iron catalysts if the oxidation had penetrated 200 layers deep.

The interference method is rather inaccurate; it is probably the least accurate among the methods discussed in this chapter. This is illustrated in Table XLIX, which gives some comparisons between

<sup>65</sup> F. H. Constable, *Nature*, 118, 730 (1926).

<sup>66</sup> F. H. Constable, *Proc. Roy. Soc.*, A119, 196, 202 (1928).

<sup>67</sup> S. Brunauer and P. H. Emmett, *J. Am. Chem. Soc.*, 62, 1732 (1940).

the interference, the electrolytic, and the adsorption from solution methods, obtained by Constable.<sup>68</sup> For copper and nickel the interference values compared with the electrolytic values are too low by a factor of 10. For copper granules the adsorption of palmitic acid gives a surface area that is more than half as large as the electrolytic value and seven times as large as the interference value. For the oxidized copper, however, the interference value is only about 20%

TABLE XLIX  
THE RATIO OF TRUE SURFACE AND APPARENT SURFACE FOR METALS

Substance	Interference	Electrolytic	Adsorption
Copper	1.52	10.4	
	2.26	25.3	
	2.40	26.8	
Nickel	1.33	9.0	
	2.00	18.2	
	2.70	22.4	
Copper granules (absolute area 1000 cm. <sup>2</sup> )	4.5	55.2	30.7
Copper granules, slightly oxidized (film c. 10 <sup>-6</sup> cm.)	4.8	—	6.1

smaller than the palmitic acid adsorption value. (Naturally the electrolytic method is not applicable to the determination of the surface areas of oxides.)<sup>69</sup>

#### E. The X-ray Diffraction Method

The method of determining the particle size of crystals by means of x-ray diffraction was originated by Scherrer.<sup>70</sup> He pointed out the fact that very small crystals give rise to broad diffraction lines in the powder diagram, and derived the theoretical relation between line breadth and particle size for cubic crystals. This is given by

$$(18) \quad B = 2 \sqrt{\frac{\ln 2}{\pi}} \frac{\lambda}{D \cos \theta/2} + b$$

where  $B$  is the line breadth divided by  $R$ , the radius of the camera,  $\lambda$  is the wave length of the x-rays,  $D$  is the length of the edge of the

<sup>68</sup> F. H. Constable, *Nature*, 144, 630 (1939).

<sup>69</sup> Another optical method of particle size and surface area determination is the method of turbidimetric analysis. It is widely used in industry because it gives reliable relative surface area values. For a recent discussion of the method see H. E. Schweyer and L. T. Work, "Methods for Determining Particle Size Distribution," A. S. T. M. Symposium, Washington, 1941, p. 11.

<sup>70</sup> P. Scherrer, *Nachr. Ges. Wiss. Göttingen*, 1918, p. 98.



cube-shaped crystal particle,  $\theta/2$  is the angle between the incident and diffracted beams, and  $b$  is a constant depending on the dimensions of the apparatus. The line breadth is defined as the ratio of the integral of the intensity across the diffraction line to the maximum intensity. Since it would be difficult to evaluate this in practice, one usually measures the distance between two points on the line where the intensity is half the maximum. The two definitions are identical for certain shapes of the diffraction lines.

Scherrer estimated the particle size of colloidal gold with the help of equation (18). The gold preparations were in the form of dry powders protected by gelatine. Each diffraction line gives a value for  $\cos \theta/2$  and for  $B$ , and if one plots  $B$  against  $1/\cos \theta/2$  according to equation (18) one obtains a straight line, the slope of which gives  $D$ . A certain gold preparation that was specified by its maker to have an average particle size of  $10 \mu\mu$  gave a  $D$  value of  $8.62 \mu\mu$ . Another preparation gave a  $D$  value of  $1.86 \mu\mu$ . A cube of gold having this edge contains only 380 atoms, and yet the diffraction pattern has lines identical in position with those obtained from large crystals.

The method of Scherrer was extended by Laue,<sup>71</sup> by Brill,<sup>72</sup> and by Brill and Pelzer<sup>73</sup> to apply to crystals of any shape. An interesting application of their method was made by Hofmann and Wilm<sup>74,75</sup> in the determination of the specific surface areas of various activated carbons. They used the so-called solid cylinder method, i.e., the powder sample was arranged in the form of a small rod. For this case Laue gave the formula

$$(19) \quad \eta = 0.0884 \left[ B \cos \theta - \frac{1}{B} \left( \frac{\pi r}{R} \right)^2 \cos^3 \theta \right]$$

where  $B$  is the half intensity breadth,  $\theta$  is the glancing angle,  $r$  is the radius of the preparation,  $R$  is the radius of the camera, and  $\eta$  is a number of measurement from which one can obtain the average size and shape of the little crystal particles. For orthorhombic crystals

$$(20) \quad \eta_{h,k,l} = \frac{\lambda}{4\pi} \sqrt{\frac{\left(\frac{h}{m_1 a^2}\right)^2 + \left(\frac{k}{m_2 b^2}\right)^2 + \left(\frac{l}{m_3 c^2}\right)^2}{\left(\frac{h}{a}\right)^2 + \left(\frac{k}{b}\right)^2 + \left(\frac{l}{c}\right)^2}}$$

<sup>71</sup> M. von Laue, *Z. Krist.*, **64**, 115 (1926).

<sup>72</sup> R. Brill, *Z. Krist.*, **68**, 387 (1928).

<sup>73</sup> R. Brill and H. Pelzer, *Z. Krist.*, **72**, 398 (1929), **74**, 147 (1930).

<sup>74</sup> U. Hofmann and D. Wilm, *Z. phys. Chem.*, **B18**, 401 (1932).

<sup>75</sup> U. Hofmann and D. Wilm, *Z. Elektrochem.*, **42**, 504 (1936).

where  $\lambda$  is the wave length of the x-rays;  $h, k, l$  are the Miller indices of the interference;  $a, b$ , and  $c$  are the orthorhombic axes; and  $m_1a$ ,  $m_2b$ , and  $m_3c$  are the extensions of the crystal particle along the three axes.

All activated carbons have the diffraction pattern of graphite. The three most important interferences are (002), (200), and (020). For the first of these equation (20) reduces to

$$(21) \quad \eta_{(002)} = \frac{\lambda}{4\pi m_3c}$$

so that one can evaluate  $m_3c$ , one of the dimensions of the crystal. The two other dimensions are obtained from the two other interferences in the same manner.

The graphite crystal has the form of a hexagonal prism. One can distinguish only between two directions: the extension along the

TABLE L  
CRYSTAL FORMS AND CRYSTAL SIZES OF VARIOUS CARBONS

Substance	Height of Crystal (Å)	Diameter of Crystal (Å)		
	$m_3c$	$m_1a$	$m_2b$	Average
Carbon from CO, 700°	113	190	203	196
550°	62	—	115	115
400°	36	39	38.5	39
Retort graphite	25	25	25	25
Benzine soot 950°	12	17	17	17
coked	13	23	23	23
850°	12	14	14	14
Acetylene soot	15	20	19	20
Carboraffin	10	20.5	21	21
Gas mask charcoal	10	20	19.5	20
Active carbon IV	10.5	18	17.5	18
Supranorite	7.5	23.5	22.5	23

$c$ -axis and that perpendicular to it; one can not distinguish between the  $a$  and  $b$  axes. Hofmann and Wilm concluded that the shape of all very finely divided carbons is that of a hexagonal prism with strongly rounded edges; in fact, more like a cylinder than a prism with sharp edges. They therefore described the crystallites in terms of two dimensions:  $m_3c$ , the height of the cylinder, and  $m_1a = m_2b$ , the diameter of its base.

A collection of the dimensions of various carbons is given in Table L. It will be noted that the particles are flat cylinders, the height being usually smaller than the diameter of the base. The flat-

test is supranorite, the height of which is one third of the diameter, the tallest is retort graphite with height and diameter equal. The average shape shows that the growth of the crystal is more rapid in the direction of the layer planes than perpendicular to it. This is not surprising since the forces in the plane are large homopolar valence forces, whereas perpendicular to the layers the much smaller van der Waals forces are operative.

Table L shows that the temperature of preparation influences the crystal size; the lower the temperature, the smaller are the crystals. Carbon, obtained from the decomposition of carbon monoxide over iron, shows great differences in size when prepared at 400, 550, and 700° C. There is a noticeable difference also between the diameters of benzine soot prepared at 850 and 950° C. Coking increases the particle size.

The dimensions of the most active carbons, which have the smallest crystals, are striking. Supranorite crystals have an average height of

TABLE LI  
SURFACE AREAS OF VARIOUS CARBONS

Substance	Surface Area in sq. m./g.			
	From Crystal Dimensions		From Adsorption of	
	Lateral Area of Cylinder	Total Surface	Methylene Blue	Phenol
Carbon from CO, 700°	90	170	—	61
550°	155	300	—	107
400°	470	720	210	230.
Retort graphite	750	1110	<20	about 15
Benzine soot, 950°	1085	1840	500	540
coked	800	1500	—	125
850°	1320	2110	—	>550
Acetylene soot	950	1570	130	185
Carboraffin	900	1860	850	905
Gas mask charcoal	960	1940	670	765
Active carbon IV	1080	2000	580	750
Supranorite	830	2130	750	935

only 7.5 Å. This means that most of the crystallites consist of only two layers since the distance between layers is 3.5 Å. It is questionable whether the equations of Laue are applicable when one deals with two or three lattice planes only. Hofmann and Wilm admit that the values obtained for the heights of the smallest crystals are certainly too small, possibly by a factor of 2. The diameter is more certain; if for no other reason because the values obtained from the

two different interferences check each other very well. This is shown in Table L, Columns 3 and 4. If the values of the table are correct the average supranorite crystal contains only about 200 carbon atoms.

From the data of Table L Hofmann and Wilm calculated the specific areas of the different carbons. These are given in Table LI. The table also lists the surface area values obtained from the adsorption of methylene blue and of phenol. The phenol values are invariably higher than the methylene blue values, probably because of the smaller size of the phenol molecule. The discrepancy between the x-ray values and the adsorption values is very large for retort graphite, but not quite so large for the porous carbons. Hofmann and Wilm suggest that the adsorption on carboraffin, gas mask charcoal, active carbon IV, and supranorite occurs only on the prismatic faces, or the lateral area of the cylinder, because large chemical forces are active there. As a matter of fact, there seems to be a fair agreement between the surface area values given in Columns 2, 4, and 5 for these four substances. On the other hand the crystallites of retort graphite seem to form aggregates with too small gaps in-between to permit the penetration of methylene blue and phenol.

There are no direct comparisons available between x-ray surface area values and gas adsorption values, but doubtless the former would indicate larger surface values than the latter. It is quite possible that there are pore spaces in activated carbons so narrow that even nitrogen molecules can not penetrate into them. At the same time it should be kept in mind that the surface area values given in Table LI, Column 3, are maximum values.<sup>76</sup> If the heights of the crystallites determined by Hofmann and Wilm are too small by a factor of 2, then the true surface area values for carboraffin, gas mask charcoal, active carbon IV, and supranorite become 1365, 1450, 1540, and 1480 sq. m./g., respectively. For two different coconut charcoals Deitz and Gleysteen<sup>77</sup> found surface area values of 1400 and 1850 sq. m./g. by the nitrogen adsorption method. It seems therefore quite possible that surface area determinations on the same adsorbent by the x-ray method and the nitrogen adsorption method would give good agreement.

<sup>76</sup> On the basis of careful study, G. H. Cameron concludes that particle size values obtained by x-ray determination may be in error by a factor of 2. (*Physics*, 3, 57, 1932.)

<sup>77</sup> V. R. Deitz and L. F. Gleysteen, To be published in the *Journal of Research* of the National Bureau of Standards.

*F. The Heat Conductivity Method*

The most recent method uses heat conductivity measurements for the determination of surface area. Its development is due to Kistler.<sup>78</sup>

The fundamental idea of the method is that the average diameter of the pores of an adsorbent can be characterized by a number that represents the mean free path of a gas in the pores at such low pressures that practically every collision of each molecule is with the walls. This mean free path, characteristic of the particular porous solid, can be calculated from measurements of the heat conductivity of the solid at three different pressures.

The heat conductivity of a porous solid can be resolved into three conductivities: that of the solid structure  $k_s$ , that of the gas in the pores  $k_g$ , and that of a film  $k_i$ , due to imperfect fit between calorimeter plates and porous solid. The three conductivities are related to each other and to the measured conductivity  $k$  by the equation

$$(22) \quad \frac{1}{k_s + k_g} + \frac{1}{k_i} = \frac{1}{k}$$

Only the conductivity of the gas,  $k_g$ , is pressure dependent, and its dependence is given by the equation

$$(23) \quad k_g = K \frac{L}{L + \frac{l_0}{p}}$$

where  $K$  is the normal conductivity of the gas,  $L$  is the above defined "mean free path of the adsorbent,"  $l_0$  is the normal mean free path of the gas at 1 mm. pressure, and  $p$  is the pressure in millimeters.

The relation between  $L$  and  $A_g$ , the projected area of all the structure elements, is given by the equation

$$(24) \quad L = \frac{1}{A_g} (V - 0.62b)$$

where  $V$  is the apparent volume of 1 g. of adsorbent, and  $b$  is the true specific volume. The coefficient of  $b$ , 0.62, is obtained on the assumption that all of the structure elements are cylindrical in shape. This coefficient is very insensitive to shape; its value for a sphere is 0.59, and for a rectangular parallelepiped five times as long as wide it is 0.73.

From the value of  $L$  one obtains the value of  $A_g$ . As we discussed in the section on the visual determination of the surface area, it was

<sup>78</sup> S. S. Kistler, *J. Phys. Chem.*, **46**, 19 (1942).

shown by Kenrick<sup>2</sup> that the actual surface area is equal to four times  $A_g$ .

The method is sufficiently sensitive only if the heat conductivity of the solid structure is not too large to mask that of the gas in the pore spaces. It is therefore particularly suitable for very light, highly porous substances, like aerogels and xerogels. Kistler found that  $L$  for silica aerogel was  $7.8 \times 10^{-6}$  cm., giving for the specific surface of the aerogel the value of 260 sq. m./g. Since water vapor adsorption isotherms were previously determined on this sample he was able to check the heat conductivity method against the gas adsorption method. The Point B value of the water isotherm gave a specific surface of 240 sq. m./g., using  $11 \text{ \AA}^2$  for the surface area covered by a water molecule. For a second aerogel sample Kistler measured by the heat conductivity method a specific surface of 410 sq. m./g. He did not obtain a water adsorption isotherm on this sample, but he had an isotherm on another similar sample. The Point B value in this case gave a specific surface of 470 sq. m./g. It seems, therefore, that the heat conductivity method gives approximately correct surface area values for aerogels.

## CHAPTER X

### THE SURFACE OF THE ADSORBENT II

From the point of view of physical adsorption the extent of the surface area is probably the most important characteristic of the adsorbent, but it is not the only important one. The heterogeneity of the surface plays an essential role, particularly in the adsorption of gases at low pressures, as was pointed out in previous chapters. The first part of the present chapter deals with the effect of the heterogeneity of the surface on van der Waals adsorption. This part includes the adsorption experiments performed on plane or supposedly plane surfaces, a subject of great theoretical importance.

The surface of an adsorbent can be greatly altered by subjecting it to different physical and chemical treatments. In Chapter IX we discussed briefly the effects of various treatments on the extent of the surface areas of nickel, platinum, silver, and other substances. In the second part of the present chapter we discuss further the influence of activation, sintering, and other treatments on the total surface area, as well as on the more active portion of the surface. This part treats also the alteration produced in the surfaces of certain adsorbents by the adsorption process itself.

#### ADSORPTION ON A PLANE SURFACE

The adsorption of gas on a plane uniform surface can be calculated if one knows the extent of the surface area and the energy of interaction between the surface and the gas. Since the former can be measured visually for a plane, and the latter can be calculated from fundamental physical considerations according to the methods discussed in Chapter VII, one can obtain the adsorption isotherm with the help of a ruler, a pencil, and paper—in principle. Unfortunately, in practice our methods for calculating the heats of adsorption are as yet too crude, and our theories of the adsorption isotherm are also only approximations. Nor have we at our disposal ideal plane surfaces large enough to test our adsorption theories with our present experimental technique.

Probably the closest approximation to an ideal uniform surface is a crystal plane; for example, the (100) plane of a sodium chloride crystal. Another approximation is the plane surface of a liquid. At

any particular instant the heat of adsorption varies over the different parts of the surface due to the varying distances between the neighboring molecules of the liquid surface. However, the time average of the interaction energy between a surface element and a gas molecule is the same for all surface elements because of the constant motion of the molecules of the liquid. Glass presents still another approximation. The surface of a glass resembles more the instantaneous picture of a liquid surface than the time average picture; nevertheless the variation in the heat of adsorption from point to point is probably slight.

Investigation of the adsorption of vapors on plane surfaces is of great theoretical importance, since it can decide between some of the rival theories of adsorption discussed in Chapters IV, V, and VI. Even though the present experimental technique is not accurate enough to check in detail the course of the isotherm against the predictions of the different theories, it is at least capable of deciding whether adsorption on a plane surface is unimolecular or multimolecular. The thickness of the adsorbed layer is one of the most crucial problems in the study of adsorption.

Langmuir,<sup>1</sup> in his fundamental investigations of the adsorption of gases on plane surfaces of glass and mica, found that the adsorption was less than that corresponding to a unimolecular layer. His isotherms were measured at very low pressures; he did not use pressures at which one would expect the formation of a second adsorbed layer. In spite of the fact that Langmuir himself in some of his later papers<sup>2,3</sup> discussed adsorption in the second layer, a great number of investigators in the field have adopted the idea that adsorption is always unimolecular. Some of them admit the possibility of capillary condensation in porous adsorbents at high relative pressures.

Many advocates of the capillary condensation theory maintain that adsorption in porous bodies is largely due to capillary condensation, although they do not deny the existence of unimolecular adsorption. The two schools of thought meet on a common ground, namely, that adsorption on a plane surface—where capillaries do not exist—must be unimolecular. In contrast with this the theory of multimolecular adsorption maintains that adsorption on a plane surface is multimolecular.<sup>4</sup> Accordingly, multimolecular adsorption on a plane sur-

<sup>1</sup> I. Langmuir, *J. Am. Chem. Soc.*, 40, 1361 (1918).

<sup>2</sup> I. Langmuir, *J. Am. Chem. Soc.*, 54, 2798 (1932).

<sup>3</sup> I. Langmuir, *Surface Chemistry*, Nobel Lecture, 1932.

<sup>4</sup> S. Brunauer, P. H. Emmett, and E. Teller, *J. Am. Chem. Soc.*, 60, 309 (1938).



face should not give Type I isotherms but Type II or III isotherms, depending on whether the net heat of adsorption is positive or negative.<sup>5</sup>

In previous chapters numerous contributions of the theory of multimolecular adsorption were discussed. At this point we may recall the remarkably close agreement between the electron microscopic particle size values and those obtained from nitrogen adsorption experiments for certain carbon blacks.<sup>6,7</sup> This agreement proves in the first place that the visible surfaces of these particles are identical with their adsorptive surfaces; in the second place it proves that adsorption on these non-porous bodies is multimolecular. Nevertheless, an ardent advocate of the capillary condensation theory might maintain that even though the carbon black particles are non-porous capillary condensation may occur in the narrow spaces between them, and that the agreement between the theoretical and experimental surface areas is merely a case of remarkable coincidence, infrequent but not absent in scientific research. Only experiments performed on an unquestionably plane surface can give the crucial decision as to whether adsorption is unimolecular or multimolecular.

Several investigators tried to ascertain the thickness of the adsorbed layer on the surface of liquid mercury. Due to the smallness of the quantity adsorbed indirect methods had to be used in all of these experiments. Oliphant<sup>8</sup> found that the adsorbed layer of carbon dioxide on mercury was about one layer thick. However, at the temperature and maximum partial pressure of CO<sub>2</sub> used (16° C. and 0.5 atm.) one would not expect more than one layer adsorbed. Iredale,<sup>9</sup> using surface tension measurements and the Gibbs equation to determine the adsorption of certain organic vapors on mercury, obtained also approximately unimolecular adsorption, but his results show certain strange peculiarities that are hard to understand. For example, he found that the adsorption of benzene reaches a maximum and then *decreases* with increasing pressure. Although a firm believer in unimolecular adsorption he admits that at saturation the adsorption obtained was sometimes many molecular layers thick. The much

<sup>5</sup> S. Brunauer, L. S. Deming, W. E. Deming, and E. Teller, *J. Am. Chem. Soc.*, **62**, 1723 (1940).

<sup>6</sup> P. H. Emmett and T. DeWitt, *Ind. Eng. Chem., Anal. Ed.*, **13**, 28 (1941).

<sup>7</sup> W. R. Smith, F. S. Thornhill and R. I. Bray, *Ind. Eng. Chem., Ind. Ed.*, **33**, 1303 (1941).

<sup>8</sup> M. L. Oliphant, *Phil. Mag.*, (7), **6**, 422 (1928).

<sup>9</sup> T. Iredale, *Phil. Mag.*, (6), **45**, 1088 (1923); **48**, 177 (1924); **49**, 603 (1925).

more reliable experiments of Cassel,<sup>10</sup> who also used surface tension measurements and the Gibbs equation, clearly indicate multimolecular adsorption of carbon tetrachloride on mercury. His S-shaped isotherm was shown in Fig. 101.

Bangham and Mosallam<sup>11</sup> obtained S-shaped adsorption isotherms for benzene on mica sheets and the surface area evaluated from the isotherms agreed well with the geometrical surface of the sheets. Armbruster and Austin<sup>12</sup> measured the adsorption of ethyl iodide on cold-rolled steel wires, and the Point B values gave surface areas approximately equal to the geometrical surface. Likewise Itterbeek and Vereycken<sup>13</sup> found very good agreement between the geometrical surface and surface area values calculated by means of the theory of multimolecular adsorption from isotherms of methane, carbon disulfide, acetone, water and deuterium oxide on glass plates. In all these cases adsorption was measured up to pressures at which several adsorbed layers were built up on the plane surfaces of mercury, mica, steel and glass.

In 1927 Frazer, Patrick, and Smith<sup>14</sup> performed an important experiment to ascertain the thickness of the adsorbed layer on a plane glass surface. The investigators concluded: "It has been shown that the thickness of the adsorbed film of toluene on a plane surface is never greater than unimolecular, even at saturation pressures." If this conclusion were correct, the theory of multimolecular adsorption would lose its foundation. Because of the decisive importance of these experiments they will be discussed here in some detail.

In 1925 McHaffie and Lenher<sup>15</sup> originated a method for determining the thickness of the adsorbed layer. It consists simply in measuring at different temperatures the pressure of a known amount of vapor enclosed in a vessel of known volume and surface area. At the lower temperatures part of the vapor must be in the liquid form, at the higher temperatures all must be in the gaseous state. Under these conditions a plot of the pressure against the temperature is shown in Fig. 104, taken from Frazer, Patrick, and Smith.<sup>14</sup> If there is no adsorption on the wall of the container, the course of the experiment will be represented by the curve COA. At the higher

<sup>10</sup> H. Cassel, *Trans. Far. Soc.*, **28**, 177 (1932).

<sup>11</sup> D. H. Bangham and S. Mosallam, *Proc. Roy. Soc.*, **A166**, 558 (1938).

<sup>12</sup> M. H. Armbruster and J. B. Austin, *J. Am. Chem. Soc.*, **61**, 1117 (1939).

<sup>13</sup> A. van Itterbeek and W. Vereycken, *Z. phys. Chem.*, **B48**, 131 (1941).

<sup>14</sup> J. C. W. Frazer, W. A. Patrick, and H. E. Smith, *J. Phys. Chem.*, **31**, 897 (1927).

<sup>15</sup> I. R. McHaffie and S. Lenher, *J. Chem. Soc.*, **127**, 1559 (1925).

temperatures the vapor follows the ideal gas laws, and so one obtains the straight line  $CO$ . At the point  $O$  some of the vapor condenses; therefore at lower temperatures one measures the vapor pressure curve of the liquid  $OA$ . If there is adsorption on the walls, the two curves will not have a sharp intersection at  $O$  but there will be

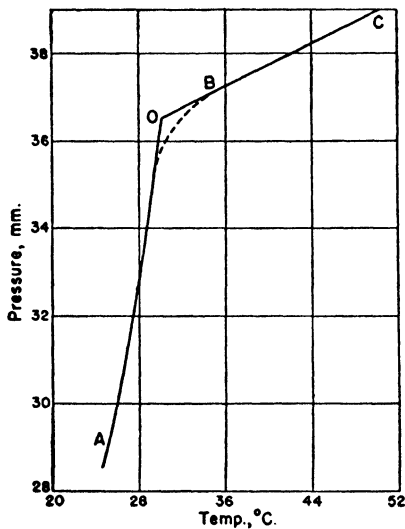


FIG. 104.—Determination of the thickness of the adsorbed layer by the method of McHaffie and Lenher.

a gradual transition represented by the curve  $CBA$ . From the pressure drop shown by the dotted curve one can readily calculate the amount of vapor adsorbed at different pressures and temperatures.

The results of McHaffie and Lenher<sup>15</sup> for the adsorption of water vapor on glass are shown in Fig. 105. The curves clearly indicate that the adsorption is many molecular layers thick. If one assumes that the true surface of the glass container was identical with its geometrical surface, the point on curve 3 at 310° K. indicates 7.2 layers adsorbed ( $p/p_0 = 0.77$ ), and the point on curve 4 at the same temperature indicates 46.3 layers adsorbed ( $p/p_0 = 0.92$ ). Each of the four curves in the low temperature region falls below the true vapor pressure curve of water  $ao$ . Curves 1–4 at 298° K. indicate 52–184 adsorbed layers.

Figure 106 gives a composite isotherm including the data of all four curves, taken from McBain.<sup>16</sup> It is a Type III isotherm with very slight adsorption below  $p/p_0 = 0.60$ . Frazer, Patrick, and Smith pointed out that the main weakness in the work of McHaffie and Lenher was the lack of knowledge of the true surface area of their

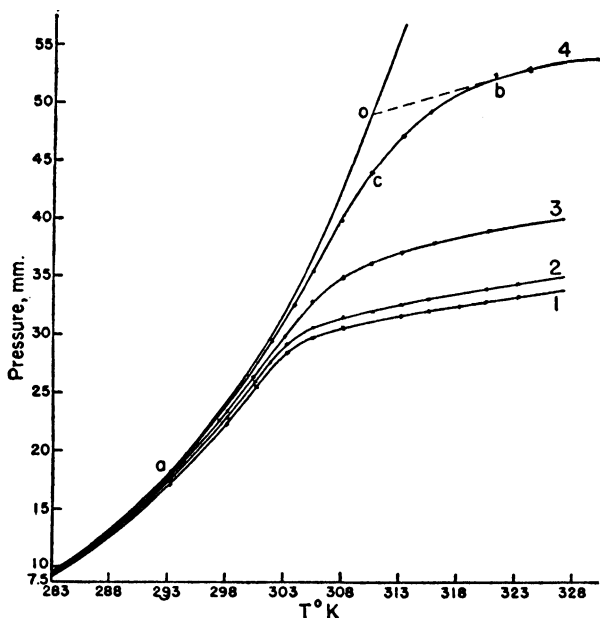


FIG. 105.—Determination of the thickness of the adsorbed film of water vapor on a glass surface.

glass bulb. Glass washed with chromic acid may have a surface many times as large as the visible one. Unless one knows the true surface, one can not make any assertions about the thickness of the adsorbed layer. The absolute values of the ordinates in Fig. 106 therefore are doubtless incorrect. Nevertheless, unless the acid washing increased the surface of glass 180 fold the curve indicates multimolecular adsorption.

Emmett<sup>17</sup> found by nitrogen adsorption that washing small glass spheres with chromic acid increased their surface by 40%. Further

<sup>16</sup> J. W. McBain, "Sorption of Gases and Vapours by Solids," London, 1932, p. 228.

<sup>17</sup> P. H. Emmett in E. O. Kraemer's "Advances in Colloid Science," New York, 1942, Chapter I.

washing with chromic acid increased the surface again by about 40%. Frank<sup>18</sup> found by water adsorption that treating Pyrex glass with chromic acid cleaning solution for a week, during which the acid was heated to boiling a number of times, made the true surface several times larger than the geometrical surface. One may venture the very rough guess that the glass bulb of McHaffie and Lenher had a true surface area about 7 times as large as the visible one. Probably this guess is not in error by a factor greater than 2. This would mean that the adsorption at the two points mentioned above, namely at

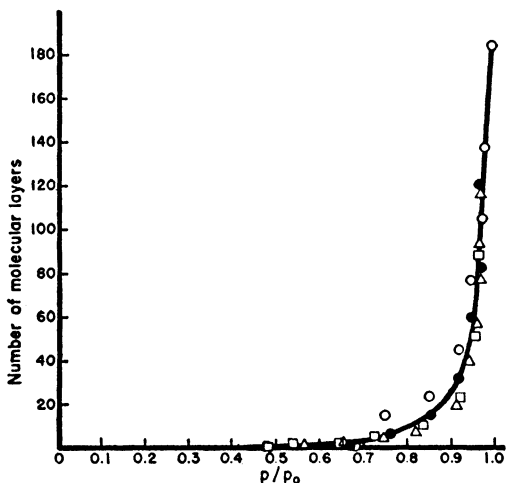


FIG. 106.—Adsorption isotherm of water vapor on glass.

$p/p_0 = 0.77$  and  $0.92$ , was actually 1 and 6.5 molecular layers thick. Lenher<sup>19</sup> found that the isosteric heats of adsorption of water vapor on fused silica, calculated by means of the Clapeyron-Clausius equation, ranged from values that were about 1000 calories lower than the heat of liquefaction up to values that were about equal to it. If one assumes that the heat of adsorption of water on the glass used by McHaffie and Lenher was 1000 calories lower than the heat of liquefaction, then according to the theory of multimolecular adsorption at the relative pressures of 0.7 and 0.9 the adsorption should be approximately 1 and 6.5 molecular layers thick. This very crude calculation

<sup>18</sup> H. S. Frank, *J. Phys. Chem.*, **33**, 970 (1929).

<sup>19</sup> S. Lenher, *J. Chem. Soc.*, 1926, 1785.

indicates that the results of McHaffie and Lenher can be interpreted without difficulty in terms of the theory of multimolecular adsorption.

Since the washing of glass roughens its surface, Frazer, Patrick and Smith<sup>14</sup> performed the experiment of McHaffie and Lenher with a "virgin" glass bulb, i.e., with a bulb freshly blown with dry air and not washed even with water. The results of the first adsorption run

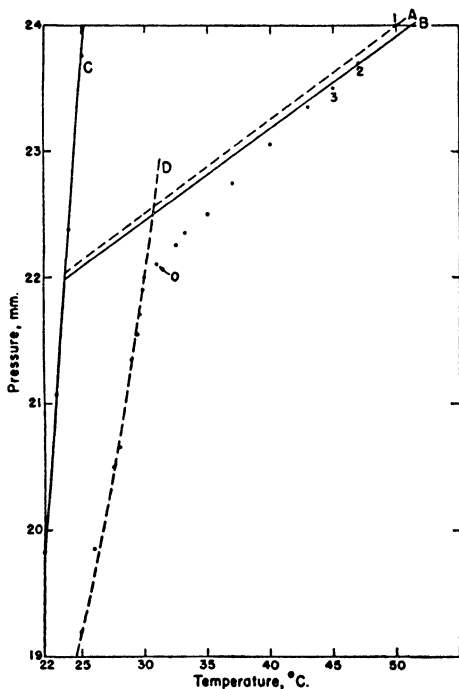


Fig. 107.—Determination of the thickness of the adsorbed layer of water on virgin glass.

with water (given in Table IV of their paper), are plotted in Fig. 107. Curve A gives the variation of the pressure with the temperature according to the ideal gas law, calculated on the basis of point 1. Curve B gives the same, calculated from the average of the first three experimental points. Curve C represents the vapor pressure curve of water according to the International Critical Tables.<sup>20</sup> Frazer, Patrick, and Smith showed experimentally that water dissolves some

<sup>20</sup> International Critical Tables, III, 210.

alkali in virgin glass, which results in a lowering of the vapor pressure. If we make the extreme assumption that the entire vapor pressure lowering found by the investigators was due to dissolved alkali and none of it to adsorption, then curve *D* gives the variation of the vapor pressure of the solution with the temperature. It is clear from the

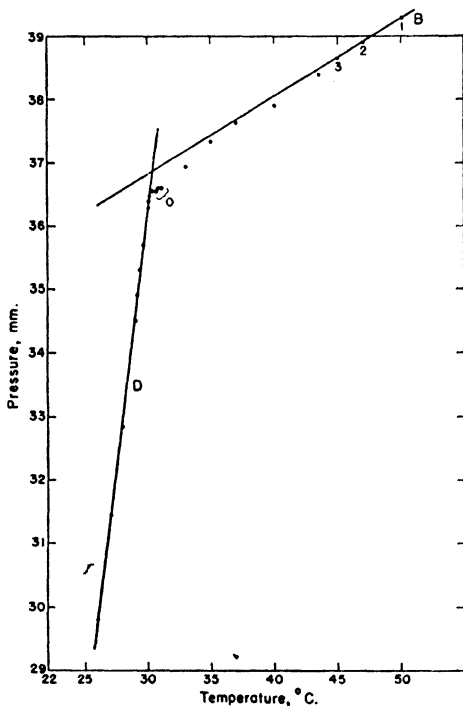


FIG. 108.—Determination of the thickness of the adsorbed film of toluene on virgin glass.

figure that even then the adsorption of water on virgin glass is multimolecular, the point *O* corresponding to at least 10 adsorbed layers at a relative pressure of 0.965. According to the theory of multimolecular adsorption if we assume that the heat of adsorption of water on virgin glass is about 8000 calories per mole—which is equivalent to a negative net heat of about 2500 calories—the adsorption at  $p/p_0 = 0.965$  should be about 9 molecular layers. Because the true vapor pressure curve of the solution is probably not curve *D* but lies somewhere

between curves *C* and *D*, the adsorption at *O* is more than 10 layers thick. This means that a smaller negative net heat than 2500 calories can account for the results.

Since water even in the first adsorption run might have corroded the virgin glass surface producing capillaries and capillary condensation, the results of Frazer, Patrick, and Smith with toluene are of greater interest. Figure 108 represents the plot of the data given in their Table I. Curve *B* gives the variation of pressure with temperature according to the ideal gas law, calculated on the basis of the first three experimental points. Since accurate independent measurements on the vapor pressure of toluene are not available curve *D* was drawn through the experimental points of Frazer, Patrick, and Smith. Here

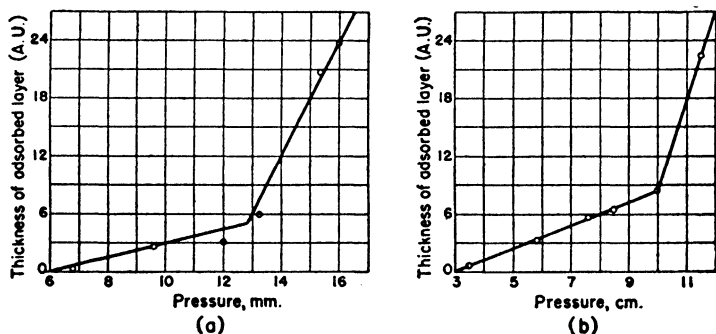


FIG. 109.—Measurement of the thickness of the adsorbed layer by the optical method.  
(a) Water on glass. (b) Methyl alcohol on glass.

again the average of the four points at *O* corresponds to about 20 adsorbed layers at  $p/p_0 = 0.98$ .

The above considerations were based on the assumption that the vapor of water and of toluene obey the ideal gas laws. This was assumed by McHaffie and Lenher and also by Frazer, Patrick, and Smith. If there is any deviation from the ideal gas laws, the adsorption is smaller than the above calculations indicate, but the correction probably would amount at most to about one molecular layer. Thus the results of Frazer, Patrick, and Smith, as well as the results of McHaffie and Lenher, can be interpreted as Type III isotherms representing multimolecular adsorption.

A very striking confirmation of this view comes from a reinterpretation of the results of J. H. Frazer.<sup>21</sup> He studied the adsorption of

<sup>21</sup> J. H. Frazer, *Phys. Rev.*, (2), 33, 97 (1929).



water and methyl alcohol on virgin glass by the optical method described in Chapter III. His results are shown in Fig. 109 (a) and (b). In the curves the thickness of the adsorbed layer in Angstrom units is plotted against the pressure. It will be noted that both curves resemble Type III isotherms. Although there is an apparent break in each curve, one could draw smooth curves in place of the straight lines just about as well. Frazer attributed the break to the completion of a unimolecular layer, but this explanation can not be correct since in the methyl alcohol curve the break comes at a thickness of 9 Å. This would correspond to more than two adsorbed layers.

There are two conclusions that can be drawn from the curves of Fig. 109. In the first place, the water curve shows very little adsorption up to about  $p/p_0 = 0.4$ , in good qualitative agreement with the water isotherm of McHaffie and Lenher shown in Fig. 106. Likewise, the methyl alcohol curve shows little adsorption up to about  $p/p_0 = 0.3$ . In the second place, and this is of great importance, the curves prove beyond question that the adsorption of both vapors on virgin glass is multimolecular. In the experiments of McHaffie, and even in those of Frazer, Patrick, and Smith, the thickness of the adsorbed layer was uncertain since the investigators did not know definitely the true surface areas of their glass bulbs. In the experiments of J. H. Frazer, however, the thickness of the adsorbed layer was measured *directly*. It can be safely concluded therefore that at a pressure of 16 mm. the adsorbed water layer was 6 or 7 molecular diameters thick.

Since water dissolves some alkali out of virgin glass J. H. Frazer suggested that this alkali might lower the vapor pressure of water, causing condensation already at 13 mm. pressure. ( $P_0$  was 18 mm.) However, he himself pointed out that the results were completely reversible; pumping removed the adsorbed water from the glass, and the ellipticity returned to its original value. This could happen only if the alkali recombined with the glass after the removal of the water. The same result was obtained with methyl alcohol. It seems therefore that the most plausible explanation of J. H. Frazer's results for virgin glass is that his curves represent multimolecular Type III isotherms.<sup>22</sup>

After virgin glass is washed with water it adsorbs water and other vapors in much larger amounts. Washing causes a roughening of the

<sup>22</sup> Using the optical method of Frazer and Herzfeld, S. Silverman (*Phys. Rev.*, **36**, 311, 1930) investigated the adsorption of methyl alcohol on a cleavage plane of rock salt. His results for pressures from 2 cm. upward are similar to Type II isotherms. He also found that at a pressure between  $10^{-4}$  and  $10^{-5}$  mm. a monolayer of adsorbed methyl alcohol forms on rock salt. This is doubtless a chemisorbed layer.

surface with an increase of the true surface area. However, this is probably not the complete explanation. Frazer, Patrick, and Smith suggest that a layer of silica gel may form on top of the glass. This would result in changing not merely the extent of the surface area but also its nature. The adsorption of water on silica gel gives Type II isotherms, whereas on fire polished glass it gives Type III isotherms. A change from the glass to the silica gel surface would therefore produce great changes in the amount of water vapor adsorbed, especially at lower relative pressures. A relatively small change in the heat of adsorption could produce a great change in the amount adsorbed. Assuming that the heat of adsorption of water on silica gel is 11,500 calories per mole, while that on virgin glass is 9500 calories per mole (a positive net heat of 1000 calories in the first case, and a negative net heat of 1000 calories in the second), the adsorption at 31° C. and  $p/p_0 = 0.3$  would correspond approximately to one complete layer on silica gel but only to about 8% surface covering on glass.

So far nobody attempted to make a fundamental theoretical calculation of the heat of van der Waals adsorption on amorphous surfaces. Glass and silica gel are both amorphous substances. It seems probable that the difference between their heats of adsorption for water vapor has something to do with the water content of their surfaces. The cohesive forces between water molecules are apparently larger than the adhesive forces between sodium silicate and water molecules. In silica gel, even when dehydrated, a considerable fraction of the surface may be covered with water, either chemisorbed or water of constitution. Due to the attraction between the water molecules of the surface and the water molecules in the vapor phase adsorption on such a surface proceeds readily even at low pressures, giving Type II isotherms. On the other hand, fire polished glass may be completely devoid of water nuclei upon which adsorption could originate. In this case higher relative pressures must be reached before the first adsorbed layer is established. After a considerable fraction of the first layer is formed the rest goes easily. The experiments of Trouton<sup>23</sup> on glass wool may be cited in support of this view. He found that glass wool, dried in vacuum at 160° C. for 70 hours over phosphorous pentoxide, adsorbed water vapor with great difficulty. When it was less thoroughly dried the effect was partly or completely eliminated, as though nuclei were present which could originate the adsorption process.

<sup>23</sup> F. T. Trouton, *Proc. Roy. Soc.*, A79, 383 (1907).

Besides glass, amalgamated metal surfaces have also been used by some investigators to test the thickness of the adsorbed layer. Smith<sup>24</sup> performed the McHaffie-Lenher experiment using a platinum bulb amalgamated with sodium amalgam. He obtained as many as 42 adsorbed layers with water and 312 layers with benzene. Latham<sup>25</sup> amalgamated the surface of platinum electrolytically and found that the adsorption of water vapor was 30 molecular layers thick. With amalgamated silver, however, he found considerably smaller adsorption, amounting to only about 6 layers in the neighborhood of the saturation pressure. He ascribed this adsorption to the glass parts of the apparatus and concluded that on the silver amalgam only a unimolecular layer was adsorbed. He further concluded that the large adsorption on the amalgamated platinum bulb indicated that the surface of the bulb was not smooth. To be sure, it is possible that the surface of amalgamated platinum is not quite as smooth as that of liquid mercury, nevertheless, it would be very hard to account for the factor of 300 in the benzene adsorption of Smith, or even for the factor of 30 in Latham's own water vapor adsorption experiments. It seems much more likely that the difference between the number of layers of vapor adsorbed on amalgamated platinum and silver in the neighborhood of the saturation pressure is largely due to relatively small differences in the heats of adsorption rather than to tremendous discrepancies between the true and apparent surface areas.

Although the problem of the thickness of the adsorbed layer on a plane surface can not be considered completely settled yet, the weight of the evidence at present is in favor of multimolecular adsorption at high relative pressures.

## ADSORPTION ON HETEROGENEOUS SURFACES

### *A. Specificity in Physical Adsorption*

Chemisorption is often called "specific," van der Waals adsorption "non-specific." The term "specific" is somewhat vague, it has never been accurately defined. Perhaps we can come closer to the true meaning of the term if we consider that adsorption in the first layer—whether chemisorption or physical adsorption—depends on two factors: the extent of the surface area and the energy of interaction between the surface and the gas. The former is the "non-specific" factor, the latter the "specific" factor in adsorption. In van der Waals

<sup>24</sup> J. W. Smith, *J. Chem. Soc.*, 1928, 2045

<sup>25</sup> G. H. Latham, *J. Am. Chem. Soc.*, 50, 2987 (1928).

adsorption the energies of interaction between a given gas and different adsorbents are not very different, and so the surface factor is of greater importance than the energy factor. In chemisorption the reverse is true, the energy factor is more important. Strictly speaking it is incorrect to say, therefore, that one adsorption is non-specific, the

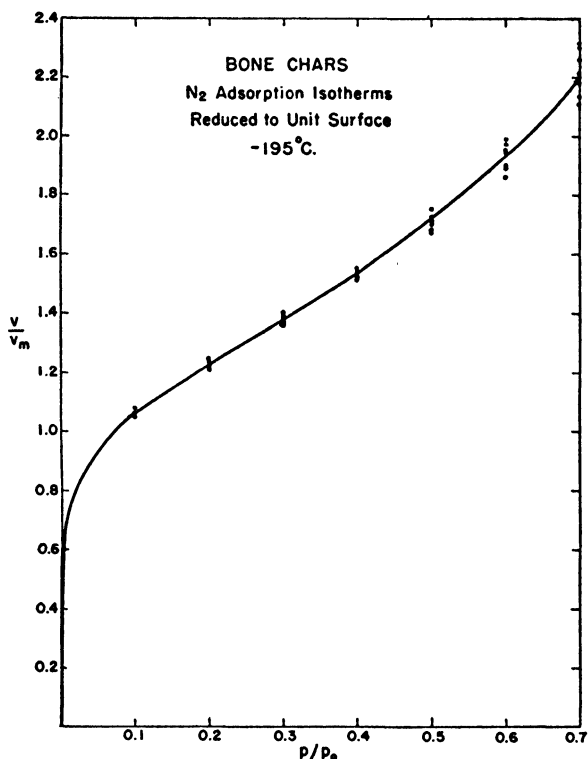


FIG. 110.—Adsorption isotherms of nitrogen on twelve different bone chars reduced to unit surface.

other specific; it would be more correct to say that van der Waals adsorption is only slightly specific while chemisorption is strongly specific.

If physical adsorption were completely non-specific, the nature of the adsorbent would be entirely immaterial and only the extent of the surface area would matter. Whether one measures the adsorption on an ionic crystal like sodium chloride, on a semi-conductor like

graphite, or on a metallic conductor like iron, the adsorption per unit surface would then be the same. If a sample of charcoal had 100 times the specific surface of a sample of an iron catalyst, the adsorption isotherms of nitrogen plotted for 1 g. of iron and for 0.01 g. of charcoal on the same paper would exactly coincide, at least in the lower pressure region. (At higher pressures differences in the pore structure would make the isotherms different.) Of course, this does not happen. The isotherms do not coincide, because even the slight differences in the heats of adsorption bring a certain amount of specificity into van der Waals adsorption.

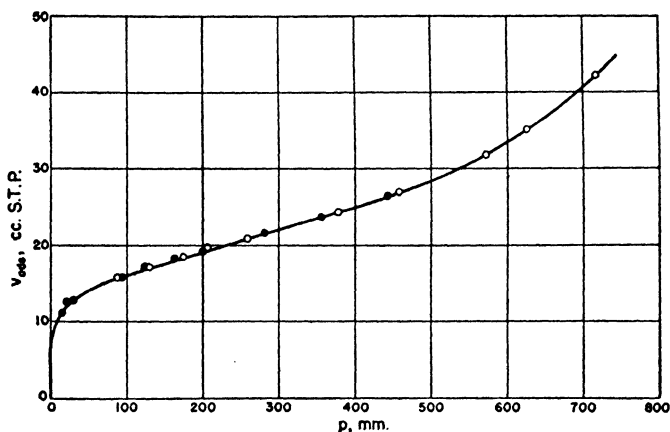


FIG. 111.—Adsorption isotherms of nitrogen on barium sulfate and titanium oxide.

That occasionally a high degree of non-specificity exists can be illustrated by two examples. Figure 110 gives the adsorption isotherms of nitrogen at  $-195^{\circ}\text{C}$ . on twelve different bone chars, obtained by Deitz and Gleysteen.<sup>28</sup> The adsorption values have been reduced to unit surface; in other words,  $v/v_m$  is plotted against the relative pressure. The data for four different new chars, seven different service chars, and one spent char all fall on the same curve. The surface of the best new char is six and a half times as great as that of the spent char;  $v_m$  is 27.60 cc./g. for the former and 4.25 cc./g. for the latter. The  $v_m$  values for the four new chars range from 23.26 to 27.60 cc., for the seven service chars from 8.17 to 19.28 cc. The

<sup>28</sup> V. R. Deitz and L. F. Gleysteen, To be published in the *Journal of Research of the National Bureau of Standards*.

greater range in the latter case is due to the fact that some of the service chars were used only a short time while others were used for several months and were close to the end of their usefulness. In spite of the six and a half fold variation in surface area there is not a single experimental point that is off the curve by as much as 5%.

Another example of the non-specificity of van der Waals adsorption is shown in Fig. 111, taken from Emmett and DeWitt.<sup>6</sup> The curve represents two nitrogen isotherms at  $-195.8^{\circ}\text{C.}$  that coincide with each other; the adsorbent was 14.88 g. of barium sulfate in one case and 6.60 g. of titanium oxide in the other. The specific surface of the latter is 2.25 times as large as that of the former, but the adsorption per unit surface is identical on the two different ionic crystals. It should be noted, however, that all adsorption points in Figs. 110 and 111 correspond to  $v/v_m$  values greater than 0.8. It is probable that adsorption at lower pressures, on the more active parts of the surfaces of these adsorbents, would exhibit a certain amount of specificity.

In contrast with the above examples van der Waals adsorption sometimes shows a high degree of specificity, comparable to that encountered in chemisorption. Perhaps the best known example of such specificity is found in the difference between the actions of charcoal and silica gel toward benzene and water. It was pointed out by Chaney, Ray, and St. John<sup>27</sup> that if one shakes up a mixture of water and benzene with charcoal and silica gel, the charcoal will adsorb the benzene, and if enough benzene is present to saturate the charcoal water will not be taken up at all. On the other hand, the silica gel will adsorb the water and leave the benzene unadsorbed. This specificity can be understood if we consider the heats of adsorption of the two vapors on the two adsorbents. Although the heat of adsorption of water on silica gel is not much greater than on charcoal, the net heat of adsorption is positive on the former but negative on the latter. For this reason the amounts of water taken up by the two adsorbents differ widely, especially in the initial stages of the adsorption. The net heat of adsorption of benzene is positive on both adsorbents but is greater on charcoal than on silica gel. Thus even though we deal here with clear-cut examples of van der Waals adsorption a rather striking specificity is produced by not very great differences between the energies of interaction of the two adsorbents and the two adsorbates. Incidentally, this specificity is responsible for certain important practical uses of silica gel and charcoal. Silica gel is used in the recovery of organic solvents, because the solvents

<sup>27</sup> N. K. Chaney, A. B. Ray, and A. St. John, *Ind. Eng. Chem.*, 15, 1244 (1923).

can be displaced from the gel by water. On the other hand, the high heat of adsorption of organic vapors on charcoal makes the latter much better suited for the adsorption of war gases. This point will be discussed further in this chapter.

Another example of specificity in physical adsorption is shown in Figs. 112 and 113, taken from Pearce and Rice.<sup>28</sup> Figure 112 represents adsorption isotherms of water at 99.4° C. on four ionic adsorbents: thorium oxide, aluminum oxide, tungstic oxide, and zirconium oxide. The full curves represent the volume of gas adsorbed per cc. of ad-

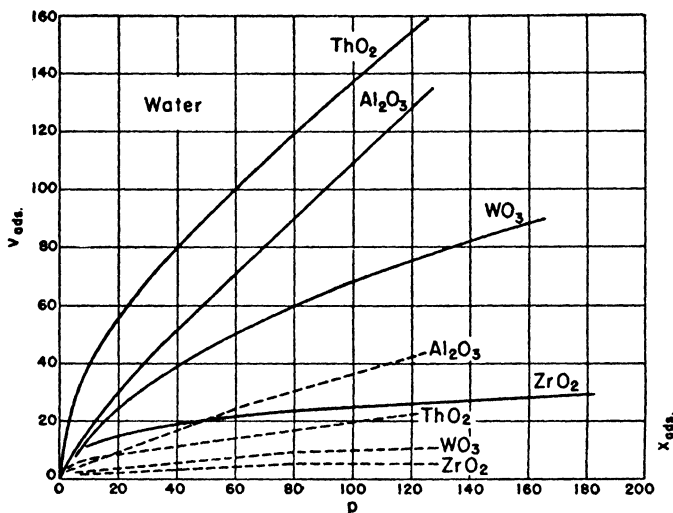


Fig. 112.—Adsorption isotherms of water on four ionic adsorbents at 99.4° C.

sorbent, the dotted curves the volume adsorbed per g. of adsorbent. Figure 113 gives the adsorption isotherms of alcohol on the same four adsorbents at the same temperature. At 140 mm. pressure ZrO<sub>2</sub> is the best adsorbent among the four oxides for alcohol but the poorest for water, whether judged on volume or weight basis. On volume basis the order of the four adsorbents for water at 140 mm. is ThO<sub>2</sub>, Al<sub>2</sub>O<sub>3</sub>, WO<sub>3</sub>, and ZrO<sub>2</sub>, whereas for alcohol it is exactly the reverse. Clearly, we deal here with a high degree of specificity, which is more surprising than that found for the charcoal-silica gel-benzene-water system. After all, benzene and water are very different substances,

<sup>28</sup> J. N. Pearce and M. J. Rice, *J. Phys. Chem.*, **33**, 692 (1929).

and so are charcoal and silica gel, but water and alcohol are similar dipole molecules, and the four oxides are similar ionic crystals.

The adsorption isotherms shown in Figs. 112 and 113 represent borderline cases between chemisorption and van der Waals adsorption. The exchange forces that exist, for example, between the two atoms of a hydrogen molecule and the Coulomb forces that attract two ions of opposite charge, as in a sodium chloride crystal, are examples of chemical valence forces—the former are homopolar or covalence forces, the latter electrovalence forces. On the other hand, the much weaker

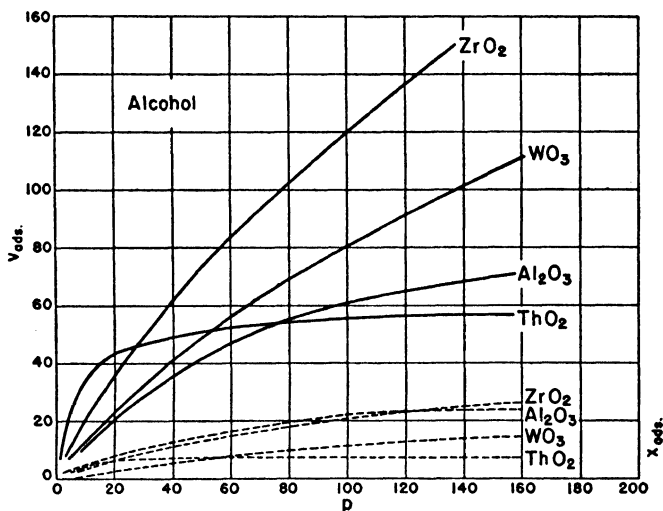


Fig. 113.—Adsorption isotherms of alcohol on four ionic adsorbents at 99.4° C.

electrostatic attraction between two dipoles is classified as a van der Waals force. Between the ion-ion and the dipole-dipole interaction is the ion-dipole interaction, representing the borderline between chemical and van der Waals forces. The ion-induced dipole interaction is still clearly classifiable with the van der Waals forces, but the ion-permanent dipole interaction can be regarded as either the upper limit of van der Waals forces or the lower limit of chemical forces. The binding energy of the water molecules to the cupric ion in  $\text{CuSO}_4 \cdot 5\text{H}_2\text{O}$  is an ion-dipole interaction; it is an example of the “secondary valence” forces.

The adsorption of nitrogen atoms on an iron catalyst and of cesium ions on a tungsten surface are examples of chemisorption. The



adsorption of argon on potassium chloride is still pure van der Waals adsorption (ion-induced dipole interaction). Although the adsorption of water and alcohol by  $\text{Al}_2\text{O}_3$  and  $\text{ZrO}_2$  can still be considered van der Waals adsorption (ion-permanent dipole interaction), it is so close to chemisorption that a considerable amount of specificity is not very surprising. This is particularly true of the adsorption of water. From the point of view of adsorption water is the strongest dipole molecule. Actually, the absolute values of the dipoles of many other molecules are greater than that of water, but water has the largest dipole moment per unit surface. If one divides the dipole moment by the area occupied by the molecule on the surface of the adsorbent (using liquid-like packing), one obtains a larger value for water than for any other molecule except *p*-nitroaniline. Some others have almost as large values as water, notably, nitroethane, nitromethane, *p*-nitrophenol, and acetonitrile, but none of these substances is used much as an adsorbate. The dipole moment of water per unit surface is almost twice as large as that of methyl alcohol and almost two and a half times as large as that of ethyl alcohol; it is more than one and a half times as large as that of ammonia and more than twice as large as that of sulfur dioxide. Thus the adsorption of water on ionic adsorbents occupies a rather unique place in van der Waals adsorption.

### *B. The Homogeneous and the Heterogeneous Parts of the Surface*

An inspection of Fig. 85, Chapter VIII, shows that the heat of adsorption of nitrogen and argon on graphite at first falls very sharply with the amount of gas adsorbed, then attains an almost constant value. The adsorption of the first 20 cc. of gas takes place on a strongly heterogeneous surface, but beyond that the surface is approximately homogeneous. Since Barrer's<sup>29</sup> nitrogen and argon isotherms show that 20 cc. of gas covers less than one-sixth of the surface of graphite, in this instance more than five-sixths of the surface can be characterized by a uniform heat of adsorption.

In Table XXXIV, Chapter VIII, it was shown that the integral heats of adsorption of carbon dioxide on different charcoals were the same for the pressure range up to 760 mm. The average value of the integral heats for seven widely different charcoals was 0.310 calories per cc. In contrast to this Krut and Modderman<sup>30</sup> pointed out that the initial differential heats of adsorption on these charcoals

<sup>29</sup> R. M. Barrer, *Proc. Roy. Soc., A161*, 476 (1937).

<sup>30</sup> H. R. Krut and J. G. Modderman, *Chem. Rev.*, 7, 259 (1930).

were very different. For example, Magnus and Kälberer<sup>31</sup> found that the initial heat on a charcoal outgassed at 600° C. was 0.558 calories per cc., but for the same charcoal outgassed at 100° C. it was 0.378 calories per cc. (The integral heats were 0.313 and 0.308 calories per cc., respectively.) It seems, therefore, that the surface of such charcoals is made up of two parts: a smaller, energetically heterogeneous fraction and a larger approximately homogeneous fraction.

The above examples are merely illustrations of the fact that the surfaces of adsorbents can usually be divided into two parts: a heterogeneous part possessing higher heats of adsorption, and a homogeneous part with a smaller approximately constant heat of adsorption. It was pointed out in Chapter VI that the straight line equation (38) of the theory of multimolecular adsorption breaks down for  $p/p_0$  values smaller than 0.05 to 0.10. The reason is that the adsorption takes place on the strongly heterogeneous fraction of the surface, which can not be characterized by a constant heat of adsorption. On the other hand, the fact that usually very good straight lines are obtained for adsorptions up to  $p/p_0 = 0.35$  indicates that most adsorbents possess a less active fraction of the surface, with a nearly uniform heat of adsorption,  $E_1$ . As a matter of fact, the value of  $E_1$  does not differ much even from adsorbent to adsorbent. An extreme example of this was shown in Fig. 110, in which adsorption isotherms of 12 different bone chars fell on the same curve. This means that the chars differ from each other only with respect to the extent of the surface area, but the  $E_1$  values are the same for all of them.

In the present book most data deal with adsorption below the critical temperature of the gas, i.e., with the adsorption of vapors. This is not due to a scarcity of data above the critical temperature, but rather to the fact that the available theories can handle the adsorption of vapors much better than the adsorption of gases. Actually, there exists a great mass of experimental data on adsorption above the critical temperature. Most of these refer to adsorption on the active and energetically heterogeneous part of the surface; all refer to adsorption in a unimolecular layer.

Adsorption above the critical temperature is probably always unimolecular. All data available at present on adsorbents of known surface areas indicate less than a complete layer adsorbed. Data obtained on adsorbents with unknown surface areas suggest uni-

<sup>31</sup> A. Magnus and W. Kälberer, *Z. anorg. allgem. Chem.*, 164, 345, 357 (1927).

molecular adsorption by the shapes of the isotherms. Only Maass<sup>32,33</sup> and his collaborators obtained multimolecular S-shaped isotherms at temperatures as high as 15 degrees above the critical temperature. However, it will be shown in Chapter XII that in the terms of Mayer's<sup>34</sup> statistical theory of condensation these temperatures can still probably be considered to be below the *true* critical temperature. The isotherms of all other investigators have the shapes of the lower

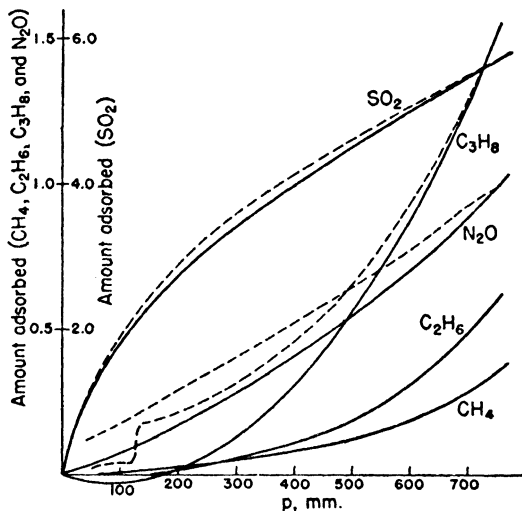


FIG. 114.—Adsorption isotherms of five gases on sodium chloride.

portions of Type II and III isotherms. The great majority of the data belong to the former group, but occasionally the isotherms are convex with respect to the pressure axis. An example of this is shown in Fig. 114, representing the adsorption isotherms of five gases on sodium chloride, obtained by Durau.<sup>35</sup> Since they were measured at 18° C., only methane was above its critical temperature but ethane and nitrous oxide were close to theirs. Four of the five gases give isotherms convex to the pressure axis, indicating negative net heats of adsorption; only sulfur dioxide gives the customary concave curve.

<sup>32</sup> H. E. Morris and O. Maass, *Can. J. Res.*, 9, 240 (1933).

<sup>33</sup> J. Edwards and O. Maass, *Can. J. Res.*, 13B, 133 (1935).

<sup>34</sup> J. E. Mayer and M. G. Mayer, *Statistical Mechanics*, New York, 1940, p. 312.

<sup>35</sup> F. Durau, *Ann. der Phys.*, (4), 87, 307 (1928).

Even the highest adsorptions obtained correspond to only a fraction of the surface covered with gas.

Most isotherms obtained for gases above their critical temperatures represent adsorption on the heterogeneous part of the surface. The theoretical treatment of this case is difficult, as we have seen in previous chapters. Sometimes the isotherms obey the Freundlich equation. In other cases the Langmuir equation is obeyed, either because the heat of adsorption is at least roughly constant for a portion of the active surface, or because the variation in the heat of adsorption is compensated by an opposite and approximately equal variation in the partition function of the adsorbed states (equation 35, Chapter IV).<sup>36</sup> Since the variation in the heat of adsorption with the amount adsorbed is usually great, the theory best equipped to handle the situation is the potential theory of Polanyi.<sup>37</sup> It was shown in Chapter V that the potential theory has been successfully applied in a number of cases to the adsorption of gases above their critical temperatures.

If the adsorption of a gas is measured considerably above the critical temperature, saturation of the surface with a unimolecular layer is attained only at high pressures. Adsorption data at high pressures are very scarce. The best among them are those of McBain and Britton<sup>38</sup> on the adsorption of nitrous oxide, ethylene and nitrogen by charcoal, and the results of Maass and his collaborators<sup>32,33</sup> on the adsorption of propylene and dimethyl ether by alumina.

Figure 115 gives an example of the results obtained by McBain and Britton. It represents adsorption isotherms of nitrogen on charcoal at  $-77$  and  $20^{\circ}\text{C}$ . These temperatures are far above the critical temperature of nitrogen,  $-146^{\circ}\text{C}$ . The  $-77^{\circ}\text{C}$ . isotherms show that practically complete saturation of the surface is reached around 35 atm. pressure. Plots of the isotherms according to the Langmuir equation give good agreement for the higher pressure region but poor agreement at lower pressures. Roughly half of the surface of the charcoal used is heterogeneous, with high heats of adsorption; the other half is homogeneous, with a lower constant heat of adsorption. The adsorption on the second half obeys the Langmuir equation.

\* H. Dohse and H. Mark (*Die Adsorption von Gasen und Dämpfen an festen Körpern*, Leipzig, 1935, p. 26) discuss adsorption on a composite surface containing two different types of adsorbing centers.

<sup>37</sup> G. E. Cunningham (*J. Phys. Chem.*, 39, 69, 1935) proposed a new theoretical approach to the adsorption of gases on heterogeneous surfaces. Although his treatment appeared promising, it has not been followed up either by him or by others.

<sup>38</sup> J. W. McBain and G. T. Britton, *J. Am. Chem. Soc.*, 52, 2198 (1930).

The isotherms of Graham<sup>39</sup> for the adsorption of carbon dioxide, methane and nitrogen on coal at 10.8° C. and up to 32 atm. pressure, as well as the isotherms of Briggs and Cooper<sup>40</sup> for the adsorption of nitrogen and hydrogen by coconut charcoal at 15° C. and up to 100 atm. pressure show no tendency toward saturation; they resemble the 20° C. isotherms of Fig. 115.

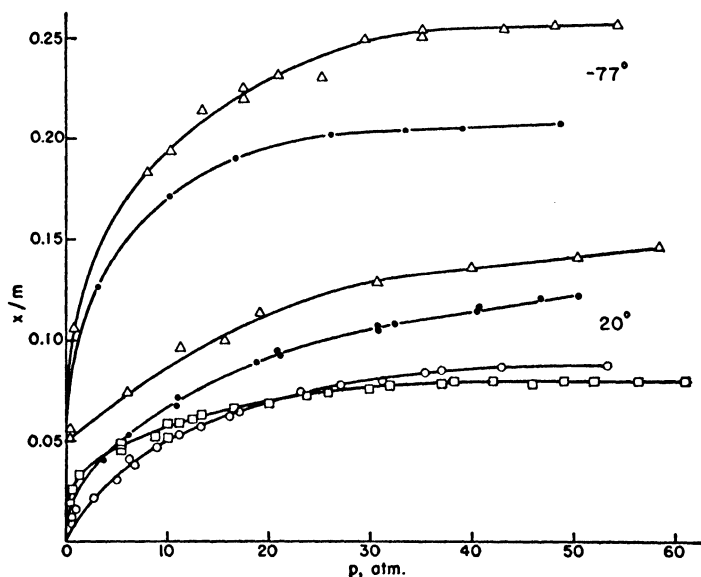


FIG. 115.—Adsorption isotherms of nitrogen on charcoal at high pressures.

The fact that the charcoals of McBain and Britton and of Briggs and Cooper gave unimolecular adsorption above the critical temperature even at high pressures is no definite proof that multimolecular adsorption does not occur above the critical temperature. The charcoals used contain such exceedingly fine pores that multimolecular adsorption can not be obtained on them even below the critical temperature and close to the saturation pressures. Silica gel would be better suited for the investigation of adsorption at high pressures. The determination of a nitrogen isotherm at  $-78^{\circ}$  C. and up to 100 atm. or higher pressures would probably reveal whether the building up of a multilayer is possible above the critical temperature.

<sup>39</sup> J. I. Graham, *Colliery Guardian*, 122, 810 (1921).

<sup>40</sup> H. Briggs and W. Cooper, *Proc. Roy. Soc. Edin.*, 41, 119 (1921).

*C. Effect of the Heterogeneity of the Surface on Physical Adsorption*

The heterogeneity of the adsorbent surface has a much more marked effect on chemisorption than on van der Waals adsorption. The effect on chemisorption will be discussed in detail in Volume II; at this point it will be illustrated only with two examples. In the first place, Brunauer and Emmett<sup>41</sup> found that if part of the surface of an iron catalyst is covered with a layer of oxygen, the physical adsorption of nitrogen (or of any other gas) proceeds just as readily on the oxygen covered part as on the unoxidized iron atoms of the surface, but the chemisorption of hydrogen or of carbon monoxide is eliminated on the oxidized portion and proceeds only on the iron, atoms. If the entire surface is covered with oxygen, the chemisorption of hydrogen at  $-78^{\circ}\text{C}$ . or of carbon monoxide at  $-183^{\circ}\text{C}$ . is almost completely eliminated, but the physical adsorption of nitrogen remains practically unaffected by the oxidation. In the second place Emmett and Brunauer<sup>42</sup> found that the surface of an aluminum oxide promoted iron catalyst contains both iron atoms and  $\text{Al}_2\text{O}_3$  molecules. Chemisorption of carbon monoxide occurs only on the iron atoms of the surface but not on the  $\text{Al}_2\text{O}_3$  molecules. On the other hand, the physical adsorption of nitrogen, or carbon monoxide, or any other gas, takes place just as readily on the  $\text{Al}_2\text{O}_3$  molecules as on the iron atoms. (This fact enables one to determine the fraction of the catalyst surface covered by the promoter.)

Although the effect of the non-uniformity of the surface on van der Waals adsorption is not as pronounced as on chemisorption it is by no means negligible. We have seen in previous chapters that the theoretically calculated heats of adsorption of a gas on the surfaces of carbon, a metal, or an ionic crystal are not very different, and that experimental evidence corroborates the theory for the less active homogeneous part of the surface. However, even though the heat of adsorption of a molecule is about the same on the plane surfaces of carbon and iron, it makes a great difference whether the molecule is attracted by two carbon surfaces or by one. In other words, the heat of adsorption in narrow cracks and crevices differs strongly from that on the plane surface of the adsorbent.

There are other causes besides narrow pore spaces that can give rise to high heats of adsorption. Atoms located on the edges and corners of crystals have different degrees of unsaturation from those

<sup>41</sup> S. Brunauer and P. H. Emmett, *J. Am. Chem. Soc.*, **62**, 1732 (1940).

<sup>42</sup> P. H. Emmett and S. Brunauer, *J. Am. Chem. Soc.*, **59**, 1553 (1937).

located in the surface planes, therefore their interaction energies with a gas molecule will be different. Even plane surfaces of a crystal will have different heats of adsorption depending on the distances and geometrical configurations of the atoms composing the plane. The attraction of a molecule by the (100), (110), and (111) faces of the same crystal will obviously be different. Finally, incompletely crystallized and amorphous patches on the surfaces of crystals may also produce higher heats of adsorption. In a two-component adsorbent, such as an  $\text{Al}_2\text{O}_3$  promoted iron catalyst, each of the above causes may create varying heats of adsorption for each of the components. Moreover, the boundary lines between patches of catalyst atoms and promoter molecules on the surface will interact with gas molecules differently than either of the components. Each of these causes may and probably does play some role in producing the observed variation in the heat of van der Waals adsorption.<sup>43</sup> However, it is very difficult to say at present what part of the variation is caused by each factor individually.

A number of attempts have been made to attack the problem theoretically, some of which were discussed in Chapters VII and VIII. Barrer<sup>29</sup> pointed out that if a molecule is adsorbed in a crack so narrow that it touches two parallel walls, the heat of adsorption is twice as large as on a plane surface. De Boer and Custers<sup>44</sup> showed that in pockets, tubes, and cavities of the adsorbent the heat of adsorption may be several times as large as on a plane surface. Lenel<sup>45</sup> calculated that the heat of adsorption of argon on cesium chloride is 3500 calories per mole for the (100) face, but only 2500 calories per mole for the (110) face. In this crystal the (100) face contains only one type of ions, the (110) face both types; the value given above is for the (100) face composed of cesium ions. Orr<sup>46</sup> calculated that the heat of adsorption of argon on cesium iodide is 3170 calories per mole for the (100) face made up of cesium ions, and 2680 calories per mole for the same face composed of iodide ions. Barrer<sup>29</sup> calculated that the heat of adsorption on the basal surfaces of graphite is larger than on the prismatic surfaces.

<sup>43</sup> Besides the heterogeneity of the surface, forces of interaction between the adsorbed molecules also produce variation in the heats of adsorption. This subject was discussed in Chapter VIII.

<sup>44</sup> J. H. de Boer and J. F. H. Custers, *Z. phys. Chem.*, **B25**, 225 (1934).

<sup>45</sup> F. V. Lenel, *Z. phys. Chem.*, **B23**, 379 (1933).

<sup>46</sup> W. C. J. Orr, *Trans. Far. Soc.*, **35**, 1247 (1939).

The importance of the distances and geometrical configurations of the surface atoms for catalysis was first emphasized by Burk<sup>47</sup> in his "multiple adsorption" theory. His ideas were further developed by Balandin.<sup>48</sup> Sherman and Eyring<sup>49</sup> showed by quantum-mechanical calculations that the energy of activation of the chemisorption of hydrogen on carbon depends strongly on the distances of the carbon atoms from each other. Beeck, Smith, and Wheeler<sup>50</sup> proved experimentally that certain crystal faces have higher catalytic activity than others. These investigations will be further discussed in Volume II. The effect of the different crystal faces on physical adsorption has been treated theoretically in the above-mentioned papers of Lenel,<sup>45</sup> Barrer,<sup>29</sup> and Orr.<sup>46</sup> So far nobody has measured experimentally the heat of adsorption on a definite face of a crystal.

The role of crystal edges in catalysis was discussed by Schwab and Pietsch<sup>51</sup> in their "adlineation" theory. The importance of edges and corners in adsorption can be gauged from the work of Stranski,<sup>52</sup> who calculated the energy of attachment of an ion to different positions in a sodium chloride type lattice. The values are given in Table LII.

TABLE LII  
ENERGIES OF ATTACHMENT TO AN NaCl-TYPE LATTICE

Number in Fig. 116	Position	Energy of Attachment
1	Inside edge	$0.313e^2/d$
2	End of inside edge	0.675
3	Inside corner	0.807
4	Surface	0.132
5	Edge	0.181
6	Corner	0.494

The numbers in the first column refer to the numbers in Fig. 116. The energies are given in units of  $e^2/d$ , where  $e$  is the charge of an electron and  $d$  is the lattice distance. Although Stranski did not calculate the heats of adsorption of a molecule attached to the six different positions indicated in Fig. 116, it is obvious that the values would be different.

<sup>47</sup> R. E. Burk, *J. Phys. Chem.*, **30**, 1134 (1926).

<sup>48</sup> A. A. Balandin, *Z. phys. Chem.*, **126**, 267 (1927), **B2**, 289 (1928), **B3**, 167 (1929).

<sup>49</sup> A. Sherman and H. Eyring, *J. Am. Chem. Soc.*, **54**, 2661 (1932).

<sup>50</sup> O. Beeck, A. E. Smith, and A. Wheeler, *Proc. Roy. Soc.*, **A177**, 62 (1940).

<sup>51</sup> G. M. Schwab and E. Pietsch, *Z. phys. Chem.*, **B1**, 385 (1929); *Z. Elektrochem.*, **35**, 573 (1929).

<sup>52</sup> I. N. Stranski, *Z. Elektrochem.*, **36**, 25 (1930).



The existence of incompletely crystallized atom groups on the surfaces of catalysts was first suggested by Taylor<sup>53</sup> in his theory of active centers. The question of the stability of such atom groups was investigated quantum-mechanically by Taylor, Eyring, and Sherman.<sup>54</sup> They came to the conclusion that small groups of atoms tend to form non-symmetrical arrays (such as linear filaments), and also that atoms readily attach themselves to the corners of crystals, projecting

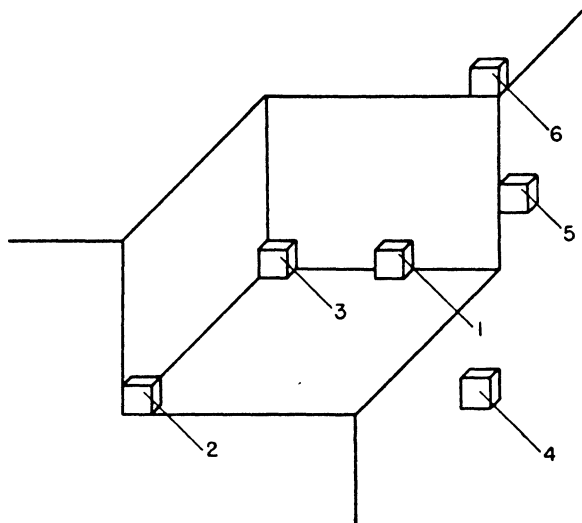


FIG. 116.—Six different positions in a sodium chloride type crystal having different energies of attachment of the ions.

out into space. These non-lattice arrangements have a certain degree of stability, and a definite amount of activation energy must be supplied to take the system over into the thermodynamically stable lattice arrangement.

Although at present we have practically no information as to the relative importance of the above discussed factors in van der Waals adsorption, it is possible to draw at least a few tentative conclusions. Incompletely crystallized atom groups probably make up only a small fraction of the surface of crystalline adsorbents. They may play an important part in catalysis but their role in physical adsorption

<sup>53</sup> H. S. Taylor, *Proc. Roy. Soc.*, A108, 105 (1925); *J. Phys. Chem.*, 30, 145 (1926).

<sup>54</sup> H. S. Taylor, H. Eyring, and A. Sherman, *J. Chem. Phys.*, 1, 68 (1933).

is probably small. Likewise, atoms located on the edges and corners of crystals do not constitute a large fraction of the surface atoms, except possibly in the most finely divided substances. Some of these, like silica gel, are amorphous anyhow, and so it is questionable whether one can speak at all about the edges and corners of such adsorbents.

The varying distances and configurations of surface atoms may play an important role in bringing about varying heats of adsorption. In the case of amorphous adsorbents there exist no regular geometrical

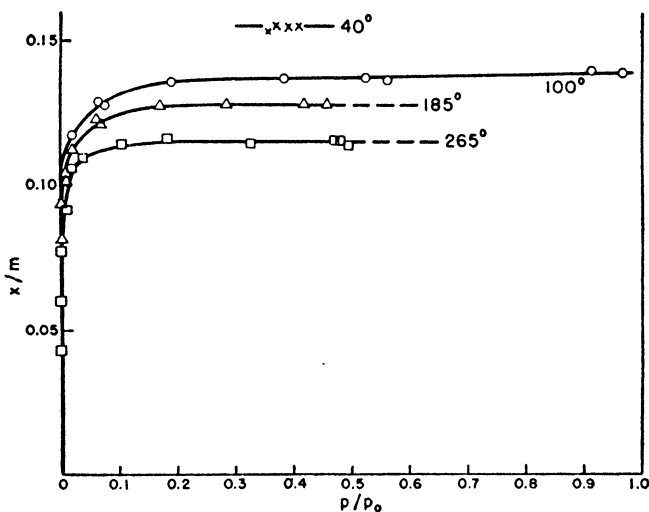


FIG. 117.—Adsorption isotherms of benzene on charcoal.

arrangements of the surface atoms as in crystals; nevertheless in the random distribution of the distances and configurations of the molecules composing the surface there will be some more favorable and others less favorable for adsorption. On the basis of this factor alone one would expect a more continuous and more gradual distribution of the heat of adsorption for amorphous than for crystalline adsorbents. However, other factors, especially narrow cracks and capillaries, can completely alter the picture.

The influence of the pore structure on the heat of adsorption can perhaps be best illustrated by comparing the adsorptive behavior of charcoal and silica gel at low pressures. The greatest part of the adsorption of an organic vapor on charcoal takes place at very low relative pressures. This is shown in Fig. 117 representing adsorption

isotherms of benzene on air activated sugar charcoal, obtained by McBain, Jackman, Bakr, and Smith.<sup>55</sup> In contrast with this, adsorption isotherms of benzene and other organic vapors on silica gel exhibit no such sharp rise at low pressures; the increase is much more gradual. This is further illustrated in Table LIII, taken from Chaney Ray, and St. John.<sup>27</sup> It gives the total adsorptive capacities and retentivities of various activated carbons and silica gels for carbon tetrachloride. The total adsorptive capacities were determined by saturation with the pure vapor at 25° C.; the retentivities represent the amount of adsorbed carbon tetrachloride retained at 100° C. and

TABLE LIII

TOTAL ADSORPTIVE CAPACITIES AND RETENTIVITIES OF ACTIVATED CARBONS AND SILICA GELS FOR CARBON TETRACHLORIDE

Adsorbent	Total Adsorptive Capacity Grams of CCl <sub>4</sub> per 100 g. of Adsorbent	Retentivity
Activated carbon <i>A</i>	110.9	30.0
Activated carbon <i>B</i>	103.8	28.5
Activated carbon <i>C</i>	95.7	27.0
Activated carbon <i>D</i>	79.5	28.0
Silica gel <i>A</i>	19.8	2.0
Silica gel <i>B</i>	39.2	1.5
Silico-cel	12.3	2.0

3 mm. pressure. The four carbons retain 27 to 35% of the amount held at the saturation pressure, whereas the two silica gels retain only 4 to 10% of the vapor.

It is probable that this difference between the retentivities of two of our most important industrial adsorbents is due to differences in the heats of adsorption on the most active parts of the surface, which are in turn due to differences in the pore structures. A large fraction of the pores in charcoal are probably between one and two molecular diameters wide. This means that the adsorbed molecules are attracted on both sides either by the walls of the capillaries or by one wall and the molecules already adsorbed on the opposite wall. On the other hand, in silica gel the structure is open; most of the pores are at least several molecular diameters wide, so that the adsorbed molecules are in contact with only one wall of the adsorbent. Of course, there are some fine pores in silica gel also, and probably these give rise to the 4 to 10% retentivity shown in Table LIII. Thus for adsorbents composed of extremely fine pores (e.g., charcoal and chabasite) perhaps

<sup>55</sup> J. W. McBain, D. N. Jackman, A. M. Bakr, and H. G. Smith, *J. Phys. Chem.*, **34**, 1439 (1930).

the most important factor in producing variation in the heat of adsorption is the structure of the pores.<sup>56</sup>

#### D. Stepwise Isotherms

There is a curious phenomenon in physical adsorption which is without adequate explanation as yet. It was noted by Allmand and his collaborators<sup>57</sup> that adsorption isotherms of vapors on charcoal and silica gel showed discontinuities if the experimental points were measured in sufficiently small pressure intervals. The curves were not smooth but rather wavy in shape. Benton and White<sup>58</sup> obtained similar stepwise isotherms for the van der Waals adsorption of hydrogen, nitrogen, and carbon monoxide on iron, copper, and nickel catalysts. Figure 118 shows an example of their results. It represents adsorption isotherms of hydrogen on iron at  $-195$ ,  $-183$ , and  $-78^{\circ}\text{C}$ . The discontinuities are considerably larger than the experimental error; there is little doubt therefore about the existence of the steps shown in the figure.<sup>59</sup>

Allmand attempted to explain the breaks by assuming that adsorption starts out from certain "active centers," from which liquid islands of the adsorbate spread out, in the sense suggested by Goldmann and Polanyi<sup>60</sup> and discussed in Chapter V. An island is composed of a

<sup>56</sup> Interesting possibilities for the study of the heterogeneity of the surface are presented by the adsorbent siloxene,  $\text{Si}_6\text{H}_6\text{O}_3$ , and its bromine derivatives,  $\text{Si}_6\text{H}_5\text{O}_3\text{Br}$  and  $\text{Si}_6\text{H}_4\text{O}_3\text{Br}_2$ . H. Kautsky and F. Greiff (*Z. anorg. allgem. Chem.*, **236**, 124, 1938) find that siloxene has only one type of adsorption center, which is evidenced by the fact that isotherms of methane, ethane and propane obey the Langmuir equation. On the other hand, the surfaces of the bromine derivatives are composite, consisting of at least two types of adsorption centers: siloxene and bromine. The bromine atoms have two antagonistic effects on the adsorption of hydrocarbons: they increase the heat of adsorption, but they also block the access to part of the surface because of their large size. The first of these effects outweighs the second for the tribromoderivative, but the second outweighs the first for the monobromo-derivative (except at low pressures). Thus at equal pressures tribromosiloxene adsorbs more gas than siloxene, but siloxene adsorbs more gas than monobromosiloxene.

<sup>57</sup> A. J. Allmand, L. J. Burrage, and R. Chaplin, *Trans. Far. Soc.*, **28**, 218 (1932).

<sup>58</sup> A. F. Benton and T. A. White, *J. Am. Chem. Soc.*, **53**, 3301 (1931).

<sup>59</sup> Although there is no doubt that the phenomenon of stepwise isotherms exists, there is considerable disagreement about the existence of steps in certain individual instances. Thus L. J. Burrage (*J. Phys. Chem.*, **37**, 33, 1933), using the dynamic retentivity method, finds regular rectangular steps in the adsorption of vapors by silica gel; A. G. Foster (*Trans. Far. Soc.*, **32**, 1559 1936), using the static vacuum method, finds no steps at all; and H. H. Chambers and A. King (*J. Chem. Soc.*, 1940, 156), using their own "hydrometer" method, find discontinuities, but neither regular nor rectangular steps.

<sup>60</sup> F. Goldmann and M. Polanyi, *Z. phys. Chem.*, **A132**, 313 (1928).

series of concentric rings, and the completion of a ring and the starting of a new one is marked by a break in the curve. Since the rings constantly increase in size, one would expect the height of the steps to increase with increasing pressure, but there is no evidence of this in the isotherms. Furthermore, Benton and White pointed out that stepwise isotherms occur even above the critical temperature of the adsorbate, which would make an explanation based on liquid formation improbable.

Benton and White suggested a different explanation for their results on metal catalysts. They assumed that the surfaces of their

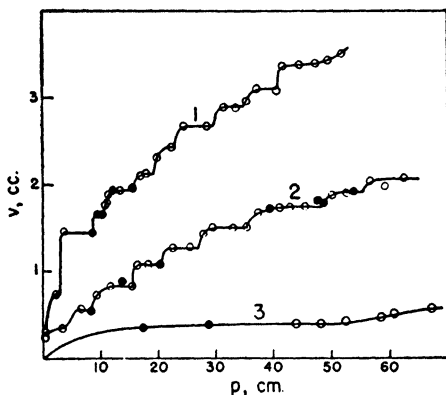


FIG. 118.—Stepwise isotherms of hydrogen on iron.

adsorbents were essentially composed of plane crystal faces. For a given kind of face, such as the (100) face, a step in the isotherm represents the completion of a row of adsorbed molecules parallel to the edges. The first row is formed at the edges, the next row forms next to these, and the process continues until the face is completely covered. According to this hypothesis each step ought to be smaller than the preceding one, but in the isotherms of Allmand and of Benton there is no evidence of this, either.

Benton and White found that the steps in some of their isotherms were approximately equal. In Curve 1, Fig. 118 they assigned to each step 0.24 cc. of hydrogen adsorbed. The first two steps in the isotherm are much larger, but these correspond to the adsorption of about  $3 \times 0.24$  cc. of hydrogen. On the basis of their hypothesis such equality of steps would be obtained if all the crystallites composing

the iron catalyst were approximately equal in size and if all the developed faces on the surface were of the same type. Besides this the crystallites must be fairly large, otherwise the differences in the steps would show up.

From the amount of hydrogen adsorbed in one step one can calculate the size of the crystal edge. Benton and White found this to be  $0.27 \mu$  for iron, which means that 750 hydrogen molecules are adsorbed along one edge of the cube. Of course, for such a large crystal the differences in the size of the steps would not show up in the first 10–15 steps. However, this calculation would lead to a surface area for the iron catalyst *at least* five times as large as it could have possessed. Moreover, if one can speak at all about the edges of the ultimate particles of charcoal and silica gel, the decrease in the size of the steps should show up for these adsorbents because of the very small size of the particles. However, no such decrease is found in the isotherms of Allmand, Burrage, and Chaplin.<sup>67</sup>

Although there has been no completely satisfactory theory advanced so far for the stepwise isotherms,<sup>61</sup> it seems probable that they are due to a discontinuous distribution of the heat of adsorption over the surface of the adsorbent, regardless of the cause of the discontinuity. Any of the factors producing variation in the heat of adsorption, discussed in the previous section, can produce a discontinuous variation. For example, on the surface of an iron catalyst the heat of adsorption of a gas will be different for the (100), (110), (111), (211) and the other crystal faces. If the heterogeneity were due to this cause alone, the heat of adsorption would have a finite and not very large number of discrete values. The adsorption isotherm would then have as many steps as there are different developed crystal faces on the surface. Naturally, this hypothesis would not lead to equal steps, but the fact is that most of the isotherms of Allmand and Benton show really no equality of steps. Only some of the isotherms show a rough equality which may possibly be accidental.

<sup>61</sup> F. J. Wilkins (*Trans. Far. Soc.*, **28**, 424, 1932) suggests that the discontinuities are due to accumulation of the gas in the cracks of the adsorbent, and to the fact that these cracks split wider open at certain definite pressures. G. H. Piper (*Trans. Far. Soc.*, **29**, 538, 1933) advances a similar explanation: he assumes that the adsorbent atoms situated on opposite sides of a capillary form weak bonds between themselves, the breaking of these bonds at definite pressures giving rise to the steps. Both explanations imply that all or most of the ultimate particles have identical pore structures; otherwise the steps would be immeasurably small.

*E. Effect of Impurities on Physical Adsorption*

Besides such causes as are inherent in the structure of the adsorbent itself there are other extraneous causes producing heterogeneity in the surface. Impurities adsorbed on parts of the surface create differences in the heats of adsorption. The effect of an impurity is usually to cut down the physical adsorption of a gas or to leave it unchanged. Occasionally the impurity may even cause an increase in adsorption, both chemical and physical. Thus Griffin<sup>62</sup> found that chemisorption of carbon monoxide on copper increased the chemisorption of hydrogen and ethylene at low pressures at 0 and 20° C. Brunauer and Emmett<sup>41</sup> found that the activated adsorption of nitrogen increased the activated adsorption of hydrogen at 100° C. on an  $\text{Al}_2\text{O}_3$  promoted iron catalyst. An example of an impurity promoting physical adsorption is given later.

The effect of impurities is greater on chemisorption than on van der Waals adsorption. As one would expect, the effect on van der Waals adsorption is most marked at lower pressures but small or negligible at higher pressures. Brunauer and Emmett<sup>41</sup> found that the isotherms of nitrogen on iron catalysts at -183° C. were the same whether adsorption took place on the pure surface or on surfaces covered with chemisorbed hydrogen, nitrogen, or oxygen atoms. Since no adsorption points were taken at low enough pressures to include the most active parts of the surface this result is not very surprising. Atomic chemisorptions do not cut down appreciably the extent of the surface area of the catalyst, and they do not change much the heat of adsorption on the less active part of the surface. Since the heat of adsorption of nitrogen on iron is about the same as on silica gel, one would not expect it to be very different on iron oxide, iron nitride, or iron hydride.

The purpose of evacuation prior to any adsorption run is to remove adsorbed impurities from the surface. The importance of thorough evacuation has been emphasized by many investigators. Raising the temperature helps to remove the impurities. The temperature of evacuation affects the adsorption more strongly at lower pressures than at higher pressures. We may recall the finding of Magnus and Kälberer<sup>31</sup> that the initial heat of adsorption of carbon dioxide on a charcoal evacuated at 600° C. was about 50% larger than that on the same charcoal evacuated at 100° C., but the integral heat of adsorption up to 760 mm. pressure was only 1.6% larger.

<sup>62</sup> C. W. Griffin, *J. Am. Chem. Soc.*, **49**, 2136 (1927).

One of the most effective methods of liberating the surface from impurities is to treat it with the adsorbate and then to remove the latter by evacuation. McBain <sup>63</sup> found, for example, that after evacuating sugar charcoal at 450° C. for five hours to a vacuum of  $10^{-5}$  mm. it adsorbed a maximum of 19.8% of its weight of nitrous oxide. After saturation with nitrous oxide had been reached he evacuated the charcoal again at 450° C. and redetermined the adsorption. The maximum amount of nitrous oxide taken up now was 26.5% of the weight of charcoal. Thus preliminary treatment of the adsorbent with the vapor increased the adsorption by 34%.

Berl and Address <sup>64</sup> actually measured the amount of air removed from the surface of charcoal by adsorbed ether. Their results are given in Table LIV. The adsorption is expressed as per cent of the weight

TABLE LIV  
THE REMOVAL OF ADSORBED AIR BY ADSORBED ETHER FROM CHARCOAL

Adsorbed Ether	Adsorbed Air	Adsorbed Ether	Adsorbed Air
% by Weight		% by Weight	
0.5	0.08	10	0.58
1	0.13	12	0.64
2	0.22	14	0.67
3	0.28	16	0.71
4	0.32	18	0.74
5	0.38	20	0.77
6	0.43	25	0.81
8	0.52	30	0.82

of charcoal. The table shows that the first additions of ether remove more air than the subsequent additions. When the adsorption of ether is about 6% of the weight of charcoal about half of the air is already removed. This occurs at less than 1 mm. pressure. At about 10 mm. pressure the adsorption of ether is about 16%, and 87% of the air is removed. The final amount of air removed is less than 1% of the weight of charcoal.

Allmand and Chaplin <sup>65</sup> noted that the quantity of gas displaced from charcoal by carbon tetrachloride was very small compared with the increase in the amount of vapor adsorbed caused by the removal of the impurity. They suggested as an explanation that the removal

<sup>63</sup> J. W. McBain, *Nature*, 117, 550 (1926).

<sup>64</sup> E. Berl and K. Address, *Z. angew. Chem.*, 34, 377 (1921).

<sup>65</sup> A. J. Allmand and R. Chaplin, *Proc. Roy. Soc.*, A129, 252 (1930).



of gas unmasks active centers capable of adsorbing large quantities of carbon tetrachloride. According to our present views of physical adsorption such an explanation is untenable. It is quite possible, however, that a foreign molecule, like carbon dioxide, chemisorbed at the entrance of a very narrow capillary, may block the penetration of carbon tetrachloride molecules into the capillary. The removal of the carbon dioxide molecule would then cause a large increase in the adsorption of carbon tetrachloride.

Although preliminary treatment of the adsorbent with the adsorbate is ordinarily very useful for the purification of the surface, occasionally it can injure the surface almost as badly as sintering. An example of this is given in the next section.

The phenomenon of hysteresis (discussed in Chapters V and XI) has been attributed by some investigators to adsorbed impurities, particularly to adsorbed permanent gases. The isotherms of water on silica gel usually show very marked hysteresis loops, but Patrick<sup>66</sup> found that these loops disappear if the gel is first evacuated at 350° C. until no further gases are evolved. His results are shown in Fig. 119. The curves represent both the adsorption and desorption points. The evacuation did not only remove the hysteresis loops, but also changed the shapes of the isotherms. Water on silica gel ordinarily gives S-shaped isotherms, but the curves of Fig. 119 resemble Langmuir isotherms. Similarly, Lambert and Clark<sup>67</sup> obtained Type I isotherms for the adsorption of benzene on thoroughly evacuated silica gel. These isotherms were also completely reversible, showing no hysteresis.

It seems probable that the disappearance of the hysteresis loop is connected with the change in the shape of the isotherm. Drastic evacuation at 350° C.—which not only removes the adsorbed permanent gases, but also part of the water content of silica gel—apparently changes the structure of the gel, reducing the diameter of the pores. The curves of Fig. 119 may indicate unimolecular adsorption, but more likely they are pseudo-unimolecular isotherms in the sense discussed in Chapter VI. Even so, they indicate a relatively small average pore diameter with an  $n$  value of 2 or 3, in contrast with the silica gels of Reyerson and Cameron<sup>68</sup> and Brunauer and Emmett<sup>69</sup> which had  $n$

<sup>66</sup> W. A. Patrick, *Colloid Symposium Annual*, 7, 129 (1930).

<sup>67</sup> B. Lambert and A. M. Clark, *Proc. Roy. Soc., A122*, 497 (1929).

<sup>68</sup> L. H. Reyerson and A. E. Cameron, *J. Phys. Chem.*, 39, 181 (1935).

<sup>69</sup> S. Brunauer and P. H. Emmett, *J. Am. Chem. Soc.*, 59, 2682 (1937).

values of 8 or 9. The reduction in pore size is accompanied by elimination of the hysteresis. The reason for this is discussed in Chapter XI.

Silica gel is ordinarily considered an adsorbent with rather wide pores, while charcoal is regarded as an adsorbent possessing narrow pores. Most of the common vapors adsorbed on the different types of silica gel give S-shaped isotherms, while many charcoals almost invariably give Langmuir isotherms. Nevertheless, some silica gels

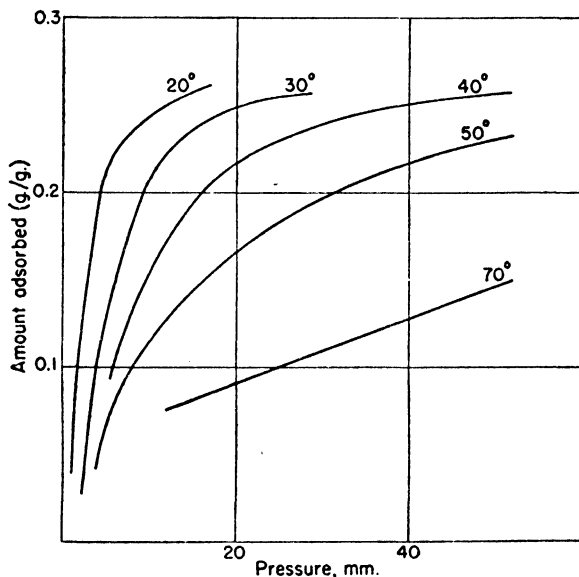


FIG. 119.—Adsorption isotherms of water on silica gel, illustrating the disappearance of hysteresis.

have narrow pores, as the above examples indicate, and likewise some charcoals have wider pores. Isotherms indicating multimolecular adsorption on charcoals of certain types are by no means infrequent.

Allmand and his collaborators investigated the adsorption of water vapor on several different charcoals and obtained hysteresis both in the presence and the absence of permanent gases. Allmand, Chaplin, and Shiels <sup>70</sup> studied the adsorption in the presence of measured amounts of air, Allmand and Hand <sup>71</sup> in the presence of nitrogen, and Allmand,

<sup>70</sup> A. J. Allmand, R. Chaplin, and D. O. Shiels, *J. Phys. Chem.*, **33**, 1151 (1929).

<sup>71</sup> A. J. Allmand and P. G. T. Hand, *J. Phys. Chem.*, **33**, 1161 (1929).

Hand, Manning, and Shiels<sup>72</sup> in the absence of any impurities. Although some of the isotherms show certain peculiarities they can probably all be labelled as Type V isotherms. All of them, without exception, show marked hysteresis loops, even those determined after  $7\frac{1}{2}$  hours of evacuation at  $800^{\circ}\text{C}$ . The presence of nitrogen and air has some influence on the sizes and shapes of the hysteresis loops, but only a relatively small influence. There seems to be little doubt that hysteresis in this case is not due to the presence of adsorbed impurities.

The effect of impurities held to the surface by physical adsorption is essentially to cut down the surface available for the adsorption of other molecules. This is actually a special case of mixed physical adsorption, discussed in detail in Chapter XIV. The effect of chemisorbed impurities is sometimes large, for example, the blocking of the entrance to a narrow pore may cut out adsorption in the entire pore. In wider pores the effect may vary from a 1 : 1 decrease in adsorption to no decrease at all. If the chemisorbed particles are atoms, there is no decrease on the less active part of the surface, as has been pointed out before. On the more active parts of the surface even atoms can cause inhibition.

Howard<sup>73</sup> investigated the effect of the activated adsorption of hydrogen on the physical adsorption of hydrogen at  $-78.5^{\circ}$  and on the physical adsorption of nitrogen at  $0^{\circ}\text{C}$ . The adsorbent was chromium oxide gel, and the adsorption was measured up to atmospheric pressure. The results for hydrogen at  $-78.5^{\circ}\text{C}$ . are given in Fig. 120. Each isotherm shows a definite decrease in the hydrogen adsorption. The first 5 cc. of chemisorbed hydrogen causes the largest decrease, about 2.5 cc., the next 17.7 cc. of chemisorbed hydrogen causes a decrease of about 5 cc., the next 25.3 cc. decreases the adsorption by about 4 cc., and the final 27 cc. by about 2.5 cc. The decrease in physical adsorption is thus less than 1 : 1 even for the first 5 cc. of hydrogen chemisorbed, and less than 1 : 10 for the last addition.

The surface of Howard's chromium oxide gel is not known, but Brunauer and Emmett<sup>69</sup> prepared chromium oxide gel by the same method and obtained its surface by nitrogen adsorption. Assuming that the two gels had equal specific surface areas the maximum hydrogen adsorption in Fig. 120 corresponds to less than 1.5% of the surface covered. Even if there were a several fold difference in the specific surfaces, the adsorption values of Howard would still correspond to

<sup>72</sup> A. J. Allmand, P. G. T. Hand, J. E. Manning, and D. O. Shiels, *J. Phys. Chem.*, **33**, 1682 (1929).

<sup>73</sup> J. Howard, *Trans. Far. Soc.*, **30**, 278 (1934).

only a small fraction of the surface covered. The maximum amount of chemisorbed hydrogen put on the surface was 75 cc. This is probably atomic hydrogen, and covers about 10% of the surface. The decrease caused in the van der Waals adsorption of hydrogen at  $-78.5^{\circ}\text{C}$ . and 760 mm. pressure is about 50%. The adsorption at a given

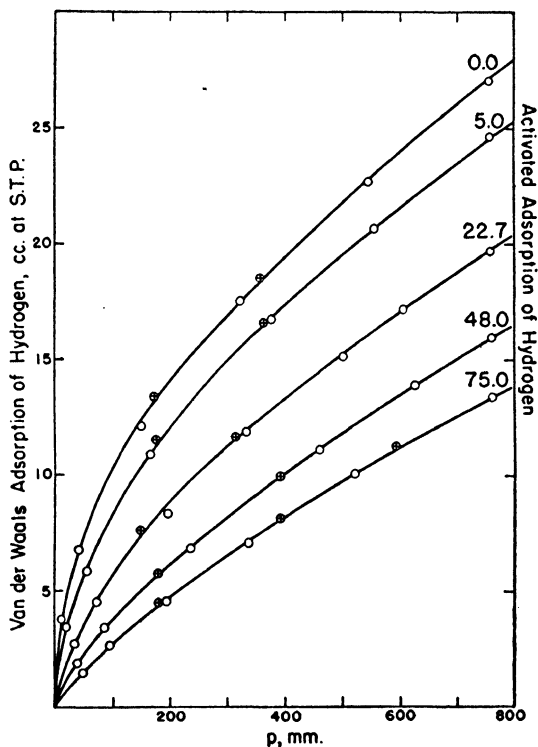


FIG. 120.—The effect of the activated adsorption of hydrogen on the physical adsorption of hydrogen.

pressure is directly proportional to the surface area but varies exponentially with the heat of adsorption. A 10% decrease in the available surface could therefore account for only a 10% decrease in adsorption, but a slight decrease in the heat of adsorption caused by hydrogen chemisorbed on the oxide surface can easily account for the 50% decrease. The results of Howard for nitrogen were very similar to those obtained for hydrogen.

Hendricks, Nelson, and Alexander<sup>74</sup> investigated the effect of chemisorbed cations on the adsorption of water by the clay mineral montmorillonite. This substance acts as an acid radical, and its free negative charges can be neutralized by the adsorption of cations between the layers of which it is composed. The different samples of montmorillonite had the same specific surface areas and the same number of equivalents of positive ions adsorbed but differed from each other with respect to the nature of the positive ions. The investigators found that the adsorption of water at equal relative pressures depended strongly on the nature of the adsorbed positive ions; particularly great was the difference at low relative pressures. Thus at  $p/p_0 = 0.05$  the adsorption of water per g. of adsorbent was 0.085 g. when the surface contained 0.95 milliequivalents of magnesium ions per g., 0.070 g. when it contained the same milliequivalents of calcium ions, 0.050 g. for strontium, 0.050 g. for barium, 0.065 g. for lithium, 0.045 g. for hydrogen, 0.025 g. for sodium, 0.015 g. for potassium, and 0.020 g. for cesium ions. There is an almost six fold difference between the amounts of water adsorbed on magnesium and on potassium montmorillonite. The differences between the amounts adsorbed get smaller as the relative pressure increases. Hendricks, Nelson, and Alexander ascribed the differences to different degrees of hydration of the positive ions on the surface, the larger alkali ions,  $\text{Na}^+$ ,  $\text{K}^+$ , and  $\text{Cs}^+$  showing no hydration,  $\text{Li}^+$ ,  $\text{Mg}^{++}$ , and the alkali earth ions showing considerable hydration. This hydration of the adsorbed ions is one of the few examples known which indicate promotion rather than inhibition of van der Waals adsorption by adsorbed particles. Further examples are given in Chapter XIV.

#### ALTERATION OF THE SURFACE OF THE ADSORBENT

Alteration in the surface of an adsorbent can be caused by external factors, such as heat, impurities, etc., or by the adsorption process itself. Fortunately for the understanding of adsorption adsorbents can usually be regarded as having rigid structures, uninfluenced or at worst only slightly influenced by the adsorbate. Occasionally, however, this is not the case.

A striking example of the adsorption process altering the structure of the adsorbent is shown in Fig. 121. The curves represent isotherms of chloroform on chromic oxide obtained by Harbard and King.<sup>75</sup>

<sup>74</sup> S. B. Hendricks, R. A. Nelson, and L. T. Alexander, *J. Am. Chem. Soc.*, **62**, 1457 (1940).

<sup>75</sup> E. H. Harbard and A. King, *J. Chem. Soc.*, 1940, 19.

Curve 1 gives the first isotherm, the other curves give isotherms after a certain number of flushings of the adsorbent with the adsorbate. Curve 2 was obtained after 2, curve 3 after 5, curve 4 after 10, and curve 5 after 20 flushings. Since adsorbed impurities were doubtless removed in the first two or three flushings, the alteration in the shapes of the curves must be due to the repeated adsorption of chloroform itself. The investigators did not state either the temperature of these

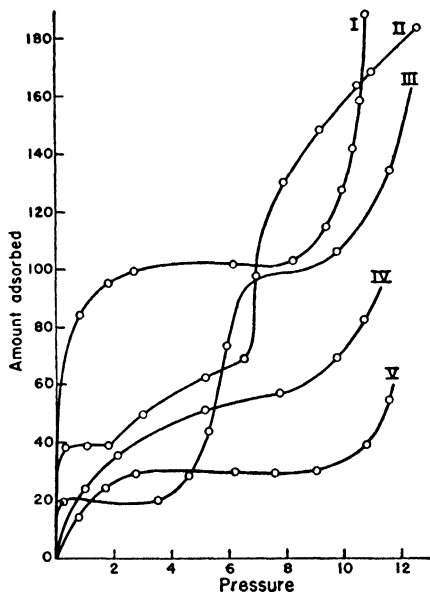


FIG. 121.—The effect of repeated flushing on the adsorption of chloroform by chromic oxide.

runs or the temperature of evacuation between runs, and so there is no way to tell to what extent heat might have been responsible for the results. Harbard and King attribute the changes to a progressive destruction of the small capillaries by the process of adsorption. A great deal more careful experimental work must be performed along similar lines before an attempt at the theoretical analysis of such complicated curves becomes worth while.

A more clear-cut example of adsorption influencing the adsorbent surface was found in the determination of the surface area of montmorillonite by the adsorption of nitrogen and of water vapor. Hend-

ricks, Nelson, and Alexander's <sup>74</sup> water adsorption isotherms indicate a specific surface of 400 sq. m./g., whereas the nitrogen and oxygen isotherms of Makower, Shaw, and Alexander <sup>76</sup> give a surface area only 1/25 as large. Obviously, water is able to penetrate between the layers of montmorillonite, while nitrogen and oxygen merely measure the external surface areas of the organized crystal particles. A similar comparison is available for the colloid of Barnes soil. The surface area evaluated from a water vapor isotherm of Alexander and Haring <sup>77</sup> is four times as large as that obtained from nitrogen isotherms by Emmett, Brunauer, and Love.<sup>78</sup> Since montmorillonite is one of the principal constituents of Barnes colloid these results are easily understandable.

In Chapter VI we have discussed the discrepancy between the surface area values calculated from the isotherms of Coolidge <sup>79</sup> for the adsorption of benzene and water vapor on charcoal. Benzene gives a surface area value about five times as large as water. One of the explanations advanced in Chapter VI was similar to that given above for montmorillonite. Charcoal is a layer crystal like graphite. Benzene penetrates readily between the layers, but water has difficulty in penetrating because of the negative net heat of adsorption.

The above examples will suffice to show that occasionally adsorption does alter the structure of the adsorbent. Ordinarily, however, the adsorbent presents a fairly rigid structure and a constant surface to the adsorption of different gases and vapors, as we have seen in a large number of examples discussed in this book. External factors can alter the surface in both the positive and the negative sense. The process of increasing the surface is called activation. The process of decreasing the surface by heat is called sintering.

Every adsorbent sinters if heated to high enough temperatures. A pure iron catalyst used for ammonia synthesis begins to sinter at 350° C., even though the melting point of iron is 1530° C.<sup>80</sup> Nickel catalysts, prepared by Beeck, Smith, and Wheeler <sup>50</sup> by condensing the metal atoms on a glass surface, sinter already around 100° C. On the other hand, charcoal begins to sinter only above 1000° C.

The mechanism of sintering is not the same for all adsorbents. Probably the most common cause is growth in particle size. High

<sup>76</sup> B. Makower, T. M. Shaw, and L. T. Alexander, *Proc. Soil Sci. Soc. Am.*, 2, 101 (1937).

<sup>77</sup> L. T. Alexander and M. M. Haring, *J. Phys. Chem.*, 40, 145 (1936).

<sup>78</sup> P. H. Emmett, S. Brunauer, and K. S. Love, *Soil Science*, 45, 57 (1938).

<sup>79</sup> A. S. Coolidge, *J. Am. Chem. Soc.*, 46, 596 (1924).

<sup>80</sup> Unpublished results of P. H. Emmett and the author.

temperature causes the small particles composing the adsorbent to fuse together into larger ones. This results in a decrease of the surface. Wyckoff and Crittenden<sup>81</sup> were the first to show by x-ray diffraction photographs that sintering is accompanied by particle size growth. After the reduction of iron oxide they took powder photographs of a promoted and an unpromoted iron catalyst and obtained very clear patterns of  $\alpha$ -iron. This indicates that the length of the edge of the cubic crystals was somewhere between  $10^{-3}$  and  $10^{-6}$  cm. They then heated the catalysts in hydrogen at  $650^{\circ}\text{C}$ . for four hours and took photographs again. The promoted catalyst now showed a few streaks characteristic of large crystals, while the unpromoted catalyst showed so many such streaks that the position of the diffraction lines could scarcely be distinguished. These experiments indicate not only that sintering is accompanied by crystal growth, but also that one of the functions of the promoter is to prevent crystal growth in the catalyst.

The qualitative findings of Wyckoff and Crittenden were quantitatively confirmed by P. H. Emmett and the author,<sup>80</sup> who determined by nitrogen adsorption the surface areas of promoted and unpromoted iron catalysts at different stages of reduction and sintering. They have found that in the course of a very slow reduction of  $\text{Fe}_3\text{O}_4$ , containing no promoter, the crystals split into such small particles that the specific surface of the reduced iron is more than 100 times as large as that of the original oxide. However, even before the reduction is complete at  $350^{\circ}\text{C}$ . the iron begins to sinter. Continued heating of the catalyst at  $450$ – $500^{\circ}\text{C}$ . cuts down the surface area to one-fourth of its original value, and heating at higher temperatures destroys it still further. The promoted iron catalysts are much more resistant to sintering. A singly promoted  $\text{Fe}_3\text{O}_4$  catalyst, containing about 10%  $\text{Al}_2\text{O}_3$ , yields on reduction at  $450^{\circ}\text{C}$ . a specific surface area that is about six times as large as that of the pure iron catalyst at its maximum. On continued heating at  $575^{\circ}\text{C}$ . the catalyst sinters slightly, but only about one-fourth to one-third of its surface is destroyed. The mechanism of promoter action in this instance is clear. Before reduction the  $\text{Al}_2\text{O}_3$  promoter is in solid solution in  $\text{Fe}_3\text{O}_4$ , as was shown by Brill.<sup>82</sup> When  $\text{Fe}_3\text{O}_4$  is reduced it is split up into tiny crystallites, and the splitting occurs preferentially around the places where the unreducible  $\text{Al}_2\text{O}_3$  is located. This is the reason why the promoted catalyst has smaller crystallites than the pure iron catalyst. When the reduced promoted catalyst is heated to high temperatures, the  $\text{Al}_2\text{O}_3$  grains

<sup>81</sup> R. W. G. Wyckoff and E. D. Crittenden, *J. Am. Chem. Soc.*, 47, 2866 (1925).

<sup>82</sup> R. Brill, *Z. Elektrochem.*, 38, 669 (1932).



on the surface prevent the iron crystallites from growing together into larger particles, and so sintering is very strongly reduced.

There are other factors besides crystal growth that may bring about sintering. Table LV shows the sintering of coconut charcoal, determined by Howard and Hulett.<sup>53</sup> Samples of charcoal were heated for half an hour in the temperature range indicated in the first column, then the densities were determined with helium, and the nitrogen adsorption was measured at 25° C. and 760 mm. pressure. There is considerable sintering around 1100–1200° C. and an almost complete loss of adsorptive power around 1600° C. At the same time

TABLE LV  
THE SINTERING OF CHARCOAL

Temperature ° C.	Density g./cc.	Nitrogen Adsorption cc. at S.T.P./g.
900–1000	2.22	8.2
1100–1200	2.26	3.9
1300–1400	2.13	3.8
approx. 1600	1.44	0.2
approx. 2000	1.35	0.2

there is a large decrease in density also. Howard and Hulett suggest the explanation that carbon deposited from the cracking of hydrocarbons plugs the entrance of the pores of charcoal, thereby preventing the penetration of both helium and nitrogen. The decrease in the surface areas of bone chars on continued use, mentioned before, may be due either to a slow growth of the particles in the revivification process around 400° C., or to the plugging of the pores by impurities.

Heating an adsorbent to a high temperature may alter not only the extent of its surface area but also the structure of the surface. For example, one type of developed crystal face may be replaced by another, with a resulting change in the heat of adsorption. Such effects are much more marked in chemisorption than in physical adsorption, consequently they will be discussed in detail in Volume II. We mention here only one example. Brunauer and Emmett<sup>41</sup> investigated the effect of sintering of iron catalysts on the chemisorptions of different gases. They were able to explain their results by postulating that sintering does not merely reduce the total surface of the catalyst, but also changes loosely packed crystal planes, like the (111) face of iron, into densely packed planes, like the (110) face.

Heating may also change the chemical nature of the surface, which in turn may cause a change in the heat of adsorption. McGavack

<sup>53</sup> H. C. Howard and G. A. Hulett, *J. Phys. Chem.*, **28**, 1082 (1924).

and Patrick <sup>84</sup> found that the adsorbing power of silica gel depends on its water content. Thus three different gels, containing 4.87, 3.51, and 2.31% water, adsorbed at 40° C. and 400 mm. pressure 64, 54.5, and 48 cc. of sulfur dioxide, respectively. The different samples were obtained by heating silica gel at various temperatures and for various lengths of time. It seems likely that the decrease in adsorption was not due to a decrease in the surface caused by particle growth, but rather to a decrease in the heat of adsorption produced by changing the chemical composition of the surface. The work of Patrick, Frazer, and Rush <sup>85</sup> indicates that sintering of silica gel by particle size growth begins only around 900° C.

Krieger <sup>86</sup> investigated the sintering of aluminum oxide and found that heating the adsorbent at 700° C. and higher temperatures destroys part of the surface, but it *increases* the heat of adsorption of nitrogen at 77.3° K. The increase in the heat of adsorption may be due to removal of impurities or to an alteration in the structure of the surface. Perhaps the second reason is the more probable one, since the greatest change in the surface and the heat of adsorption occurs after heating the adsorbent to 938° C., and there is an isomeric change in aluminum oxide at 925° C.

Since the use of too high temperatures injures the surface the adsorbent should always be prepared at the lowest possible temperature. This fact is of utmost importance in preparing active catalysts. Although the temperature of preparation is not quite so crucial in physical adsorption, nevertheless it is of some importance. We may recall that carbon obtained from the decomposition of carbon monoxide showed great differences in particle size when prepared at 400, 550, and 700° C. (Table L).

Sintering is by far the most common method of destroying the surface of an adsorbent, but it is not the only one. An example of a different method may be recalled here: Bowden and Rideal <sup>87</sup> found that cold rolling reduced the true surface of a polished nickel plate to less than half of its original value (Table XXXIX).

Activation is the opposite of sintering; it is the increasing of the adsorptive power of a substance. Like sintering, it may be produced by heat alone; more often, however, chemical agents are used along

<sup>84</sup> J. McGavack and W. A. Patrick, *J. Am. Chem. Soc.*, **42**, 946 (1920).

<sup>85</sup> W. A. Patrick, J. C. W. Frazer, and R. I. Rush, *J. Phys. Chem.*, **31**, 1511 (1927).

<sup>86</sup> K. A. Krieger, *J. Am. Chem. Soc.*, **63**, 2712 (1941).

<sup>87</sup> F. P. Bowden and E. K. Rideal, *Proc. Roy. Soc.*, **A120**, 80 (1928).

with heat. Thus charcoal can be activated to some extent by heat and evacuation alone, but to get the most active product one must use air, steam, chlorine, or some other activating agent.

Activation is always accompanied by an increase in the surface area of the adsorbent. One of the most common methods of activating metallic catalysts is alternate oxidation and reduction. We have seen that reduction increases the surface of an  $\text{Fe}_3\text{O}_4$  catalyst about 100-fold. While alternate oxidation and reduction seems to have no effect on this particular catalyst, it produces highly active copper and nickel catalysts. Bowden and Rideal<sup>87</sup> found, for example, that oxidizing and reducing their nickel plate three times made the true surface 46 times as large as the apparent surface. The action of  $\text{Al}_2\text{O}_3$  promoter in an iron catalyst gives another example of activation by increasing the surface area. In a wider sense even the polishing of a metal or the washing of glass with cleaning solution can be considered activation. These treatments impart a certain degree of roughness on a molecular scale to a smooth surface, thereby causing an increase in its adsorptive capacity.

Another activating mechanism consists in removing a part of the adsorbent to create a large internal surface, or in removing certain adsorbed impurities that block the entrance to an already existing internal surface. This is the most frequent method of activation in physical adsorption. The removal of the water of crystallization from a hydrate usually creates a large internal surface. Brunauer and Emmett<sup>69</sup> found that dehydration of  $\text{CuSO}_4 \cdot 5\text{H}_2\text{O}$  at  $350^\circ\text{C}$ . increased the specific surface 39-fold. Dehydration of gibbsite,  $\text{Al}(\text{OH})_3$ , increased its surface area 300-fold.<sup>88</sup> An outstanding example of this class is the dehydration of chabasite,  $\text{CaAl}_2\text{Si}_4\text{O}_{12} \cdot 6\text{H}_2\text{O}$ . The hydrate has practically no adsorptive capacity, whereas dehydrated chabasite has an internal surface rivalling that of charcoal.<sup>89</sup>

While the activation mechanism in the above mentioned examples is quite clear, it is not so well understood in the case of charcoal and some other activated carbons. The activation process probably consists in the removal of certain substances in contact with the carbon atoms, but it is hard to tell just what these substances are. Chaney<sup>90</sup> believes that during the primary carbonization of wood certain oily

<sup>88</sup> Unpublished results of R. A. Nelson and the author.

<sup>89</sup> Removal of water plays a very important role in the activation of silica gel too. See, for example, F. E. Bartell and E. G. Almy, *J. Phys. Chem.*, **36**, 475 (1932).

<sup>90</sup> N. K. Chaney, *Trans. Electrochem. Soc.*, **36**, 91 (1919).

hydrocarbons are formed and are adsorbed strongly on the carbon surfaces, blocking the narrow capillary spaces. Activation consists in burning off these hydrocarbons with air or steam at high enough temperatures but not so high as to burn the adsorbent itself. If too high temperatures are used the hydrocarbons may crack, depositing carbon in the narrow capillaries of the charcoal and destroying its adsorptive capacity.

Table LVI, taken from Barker,<sup>91</sup> illustrates the effect of activation on various charcoals. Barker points out that the granule density of activated charcoal is lower than that of primary charcoal, whereas

TABLE LVI  
THE ACTIVATION OF CHARCOAL

Charcoal	Adsorption of CCl <sub>4</sub> mg. per g.	Granule Density g./cc.	True Density g./cc.	Volume cc./g.	Charcoal Substance cc./g.	Pore Space cc./g.	Pore Space Filled by Adsorbed CCl <sub>4</sub>	
							cc./g.	%
Primary coconut	47	0.96	1.46	1.04	0.685	0.355	0.032	9.1
Activated coconut	630	0.84	2.15	1.19	0.465	0.725	0.420	58
Primary ironwood	30	0.89	1.46	1.123	0.685	0.438	0.020	4.6
Activated ironwood	1160	0.72	2.15	1.39	0.465	0.925	0.774	83.6
Primary lignite	30	1.09	1.43	0.92	0.70	0.220	0.020	9.1
Activated lignite	640	0.89	2.15	1.12	0.465	0.655	0.426	65
Extremely activated lignite	2715	0.31	2.15	3.23	0.465	2.765	1.81	65

the true density of the activated charcoal substance (determined with helium) is considerably higher than that of the primary carbon. This indicates an increase in the pore space during the process of activation. However, Column 7 shows that this increase is only two-fold, whereas the increase in the adsorption of carbon tetrachloride at 24° C. and saturation pressure, shown in Column 2, is from 13 to 39-fold. The last column shows that in the primary charcoals only 5–10% of the pore space is filled with the adsorbate at the saturation pressure. Since at saturation the adsorbate fills all the pores to which the molecules have access, it seems that most of the pores of the primary carbons are clogged up with some substance that prevents the entrance of the carbon tetrachloride molecules. It is also possible that the pores are not blocked by impurities but are too narrow to admit the adsorbate molecules. If this is true, the process of activation consists in the widening of the pores by burning off a layer of carbon atoms. Whatever be the substance removed Barker's work

<sup>91</sup> M. E. Barker, *Ind. Eng. Chem.*, 22, 926 (1930).

clearly indicates that activation makes the pores accessible to the adsorbate molecules and thus opens up the tremendous internal surface of charcoal for adsorption.

Heating charcoal in vacuum results in the removal of some oxygen in the form of carbon monoxide and carbon dioxide. This alone is sufficient to activate charcoal to some extent. Driver and Firth<sup>92</sup> found that the heating of animal charcoal and sugar charcoal to 900° C. for 48 hours increased the adsorption of benzene and chloroform at the saturation pressure by about 100%. In this case also the removal of some of the carbon, along with oxygen and hydrogen, produced a widening in the pores of the charcoals. Barker<sup>91</sup> noted that in the activation process the oxygen and hydrogen content of charcoals decreases to some extent, but even the best activated charcoals contain considerable amounts of both hydrogen and oxygen.

Activation, like sintering, can alter not merely the extent of the surface, but also its structure. Barker found, for example, that primary carbons were amorphous to x-rays and gave no diffraction patterns, but activated charcoals were crystalline and showed the graphite pattern. Although such change in structure doubtless results in some change in the heat of adsorption, probably the effect on the adsorption of vapors would not be very great. The point of vital importance is that activation makes the internal surface of charcoal accessible to the adsorbate molecules. In the sintering of silica gel just the opposite happens. Patrick, Frazer, and Rush<sup>93</sup> found that amorphous silica gel was a very good adsorbent for carbon tetrachloride, but when heated to 1000° C. it crystallized and lost its adsorptive power. Here again the important factor for physical adsorption is not the crystalline or amorphous nature of the adsorbent, but the fact that heating to 1000° C. closes up the pores and destroys the internal surface of silica gel.

Activation often produces chemical changes in the surface. Dehydration of a substance changes not only the extent of the surface area but the composition of the surface as well. Removal of oxide layers, or of other impurities, also changes the chemical nature of the surface. Some investigators believe that the high adsorptive power of charcoal depends on the degree of unsaturation of the carbon atoms of the surface. Lowry and Morgan<sup>93</sup> found that finely divided graphite, produced by the explosion of graphitic acid, had an adsorptive power that depended on the state of oxidation of the original graphitic

<sup>92</sup> J. Driver and J. B. Firth, *J. Chem. Soc.*, 121, 2409 (1922).

<sup>93</sup> H. H. Lowry and S. O. Morgan, *J. Phys. Chem.*, 29, 1105 (1925).

acid. The most highly oxidized sample gave the best adsorbent, the least oxidized the poorest, although there was no exact quantitative relationship between the state of oxidation and the amount of gas adsorbed. They measured the adsorption of nitrogen and carbon dioxide from 0 to 100° C., and the adsorption of hydrogen at - 191° C. up to atmospheric pressure on the graphite samples. Since at these temperatures and pressures only the active part of the surface is covered with adsorbed gas, it is not surprising to find that the degree of saturation of the surface atoms had some, although not very great influence on physical adsorption.

A more striking example of the effect of activation on the chemical composition of the surface is found in a work of Bartell and Lloyd.<sup>94</sup> They activated sugar charcoal by means of different gases at different temperatures and measured interferometrically the adsorption of benzene-ethanol mixtures on the samples. They were able to show that the surface of the charcoal can be changed from extremely organophilic to more and more hydrophilic, until it approaches in its adsorptive properties the surface of silica.

<sup>94</sup> F. E. Bartell and L. E. Lloyd, *J. Am. Chem. Soc.*, 60, 2120 (1938).

## CHAPTER XI

### THE PORE STRUCTURE OF THE ADSORBENT

The adsorption of gases above the critical temperature is probably unimolecular, although experiments carried to higher pressures than those performed so far may yet reveal multimolecular adsorption. In unimolecular adsorption the pore structure of the adsorbent plays a part only if an appreciable fraction of the surface is located in pores that are not more than one or two molecular diameters wide. In such narrow pores the heat of adsorption is greater than on a plane surface since the gas molecule is subjected to attractive forces on more than one side. This results in enhanced adsorption at lower pressures. On the other hand, if the pores are too narrow the molecules may not be able to penetrate into them. In this case the adsorption may be cut down considerably and possibly even eliminated completely. Adsorbents with very fine pores act as molecular sieves, allowing smaller molecules to penetrate into their pores and shutting out the larger ones. McBain<sup>1</sup> called this phenomenon "persorption."

All porous adsorbents contain some fine pores, therefore they all exhibit persorption to some extent. We have seen in Chapter IX that the surface area determined by gas or dye adsorption methods is always a function of the size of the molecule used for the determination. Larger molecules always give smaller surface area values, doubtless because they can not penetrate into the narrowest pores of the adsorbent. Another evidence of fine pores in adsorbents with fairly large average pore diameters is found in the 4-10% retentivity exhibited by silica gels at low pressures and high temperatures (Table LIII, Chapter X).

Adsorption below the critical temperature is multimolecular, and the pore structure of the adsorbent plays a vital role in multimolecular adsorption. The size of the pore sets an upper limit to the number of layers that can be adsorbed within it. Narrower pores fill at lower relative pressures, wider pores at higher pressures, and the entire pore space is filled at the saturation pressure. These facts are true whether adsorption beyond the first layer is interpreted in terms of the capillary condensation theory or the theory of multimolecular adsorption. With

<sup>1</sup> J. W. McBain, *Colloid Symposium Monograph*, 4, 1 (1926).

the help of an exact theory one could calculate the entire pore size distribution of an adsorbent from a single complete adsorption isotherm. Unfortunately such an exact theory does not exist; the best we can do therefore is to use the existing theories to obtain an approximate picture of the pore structure.

Many adsorption isotherms at higher relative pressures exhibit the phenomenon of hysteresis (discussed to some extent in Chapters V and X). Hysteresis seems to depend on the sizes and shapes of the pores of the adsorbent and so study of it can furnish valuable information about the pore structure. In the present chapter we discuss the information acquired from persorption experiments, adsorption isotherms, density measurements, and other lines of investigation about the pore size distribution of the most important adsorbents. We discuss also the alterations in the pore structure caused by the adsorption process itself, as well as by such external treatments as activation and sintering.

#### PERSORPTION

Persorption may be defined as adsorption in pores that are only slightly wider than the diameter of the adsorbate molecule. By using molecules of different diameters and noting the extent to which adsorption under given experimental conditions decreases as the size of the molecule increases one can study the structure of the finest pores of the adsorbent.

The adsorbent *par excellence* for the study of persorption is chabasite, a mineral belonging to the class of zeolites. Its formula is  $\text{CaAl}_2\text{Si}_4\text{O}_{12} \cdot 6\text{H}_2\text{O}$ . Crystallographically it is based on a three-dimensional network of silica tetrahedra, in which one-third of the silicon is replaced by aluminum ions. The replacement gives rise to an excess negative charge, which is balanced by the incorporation of positive ions. In nature calcium is the most common among these but it can be substituted by other positive ions, such as copper, sodium, barium, cadmium, etc. The phenomenon of a positive ion replacing an equivalent quantity of another positive ion is called *base exchange*.

The six molecules of water can be removed from the chabasite crystal by simultaneous heating and evacuation. The dehydration leaves the framework of the crystal unchanged; only when 93% of the water is removed does the structure begin to collapse. Dehydrated chabasite is an adsorbent with very fine pores and a tremendous internal surface; its specific surface area approaches that of coconut charcoal.



Weigel and Steinhof<sup>2</sup> found that dehydrated chabasite adsorbs water, methyl alcohol, ethyl alcohol, and formic acid in large quantities, but acetone, benzene, and ether are only slightly adsorbed or not at all. McBain<sup>1</sup> concluded from this that the pore diameter of chabasite must be 5Å or less. Schmidt<sup>3</sup> investigated the adsorption of 17 gases by chabasite and found that the 9 smaller molecules gave normal adsorption values, but the 8 larger molecules showed smaller adsorption than expected or none at all. This is shown in Table LVII.

TABLE LVII  
ADSORPTION OF GASES BY DEHYDRATED CHABASITE

Gas	Molecular Volume cc.	Molecular Diameter Å	Gas Adsorbed, cc. S.T.P. on 0.2 g. Chabasite at 100° C. and 760 mm.
NH <sub>3</sub>	25.2	3.65	37.0
O <sub>2</sub>	28.0	3.8	0.6
A	28.3	3.8	0.4
H <sub>2</sub>	28.6	3.8	0.1
N <sub>2</sub>	34.5	4.05	1.2
CO	35.4	4.1	1.6
CO <sub>2</sub>	35.1	4.1	13.3
CH <sub>4</sub>	33.0	4.0	1.9
C <sub>2</sub> H <sub>4</sub>	44.0	4.4	8.3
C <sub>2</sub> H <sub>6</sub>	55.0	4.7	6.6
C <sub>3</sub> H <sub>8</sub>	67.0	5.05	4.0
C <sub>4</sub> H <sub>10</sub>	90	5.6	0.8
C <sub>4</sub> H <sub>8</sub>	88	5.5	1.4
C <sub>5</sub> H <sub>12</sub>	96	5.7	0.0
C <sub>6</sub> H <sub>14</sub>	102	5.8	0.3
(C <sub>2</sub> H <sub>5</sub> ) <sub>2</sub> O	107	5.9	0.0
C <sub>8</sub> H <sub>18</sub>	117	6.1	0.0

Ethylene is the largest molecule that gives normal adsorption; its molecular volume is 44.0, its molecular diameter is 4.4Å. Since the adsorption values given in Column 4 were measured on equal surface areas, the amount adsorbed should increase with increasing heat of adsorption. The heat of adsorption increases as the size of the molecule increases, therefore the molecules below ethylene should exhibit larger and larger adsorption. Actually, as the table shows, the adsorption becomes less and less as the size increases. Ethane, with a molecular volume of 55.0 and a diameter of 4.7Å, already has difficulty in penetrating into the pores, and the larger molecules of ether, benzene, and hexamethylene can not penetrate at all. It seems therefore

<sup>1</sup> O. Weigel and E. Steinhof, *Z. Krist.*, 61, 125 (1925).

<sup>2</sup> O. Schmidt, *Z. phys. Chem.*, 133, 263 (1928).

that the main pore diameter of chabasite is somewhere between 4.4 and 4.7Å. The smaller adsorption of the larger molecules occurs either on the external surfaces of the crystallites or, what is more probable, the adsorbent contains a small percentage of larger sized pores.

Baba <sup>4</sup> continued the persorption experiments on chabasite using additional gases besides some of those already mentioned. He found no adsorption with pentane, benzene, ether, chloroform, carbon tetrachloride and acetone. Large adsorption was obtained with carbon dioxide, methyl alcohol, and methyl amine, very small adsorption with ethyl alcohol and ethyl amine. Here again the dividing line is at a molecular diameter of 4.4Å, that of methyl amine. Propyl and butyl amine were also adsorbed slightly, probably indicating a small fraction of larger pores.

The above experiments clearly prove that a large fraction of the pores in dehydrated chabasite have diameters of 4.4Å or less. There is a further distribution of pore sizes even below this limit. Rabinowitsch <sup>5</sup> states that at liquid air temperature and 300–400 mm. pressure chabasite adsorbs more hydrogen than nitrogen. Since the adsorption of nitrogen should be much greater than that of hydrogen, this can be explained only if we assume that the surface available for hydrogen adsorption is much larger than the surface available for nitrogen. This means that a considerable fraction of the pores can admit hydrogen molecules but are too narrow to admit nitrogen. Emmett <sup>6</sup> found similar results for 50% dehydrated chabasite. Large quantities of hydrogen are adsorbed at 77° K., but practically no nitrogen is taken up at the same temperature.

Rabinowitsch and Wood <sup>7</sup> investigated the effect of base exchange on the adsorptive capacity of chabasite. They found that the replacement of calcium by sodium ions had only slight effect on the hydrogen adsorption, but it eliminated almost completely the nitrogen adsorption. Replacement of calcium by potassium ions cut down very strongly both the hydrogen and nitrogen adsorption. These results are readily understandable if we consider the sizes of the three ions. The sodium ion is slightly smaller than the calcium ion (the radii are 0.98 and 1.06Å according to Goldschmidt), but each calcium

<sup>4</sup> T. Baba, *Bull. Chem. Soc. Japan*, 5, 190 (1930).

<sup>5</sup> E. Rabinowitsch, *Z. phys. Chem.*, B16, 43 (1932).

<sup>6</sup> P. H. Emmett, in E. O. Kraemer's "Advances in Colloid Chemistry," New York, 1942, Chapter I.

<sup>7</sup> E. Rabinowitsch and W. C. Wood, *Trans. Far. Soc.*, 32, 947 (1936).

ion is replaced by two sodium ions in the base exchange. This is sufficient to prevent the penetration of the larger nitrogen molecules into the very fine pores of chabasite, but hydrogen can still enter readily. The potassium ion is larger than the calcium ion (its radius is  $1.33\text{\AA}$ ); it is large enough to cut out even the adsorption of the smaller hydrogen molecules.

Lamb and Woodhouse<sup>8</sup> determined the adsorption of hydrogen, nitrogen and carbon dioxide on chabasite during different stages of dehydration. Figure 122 shows the effect of dehydration on the

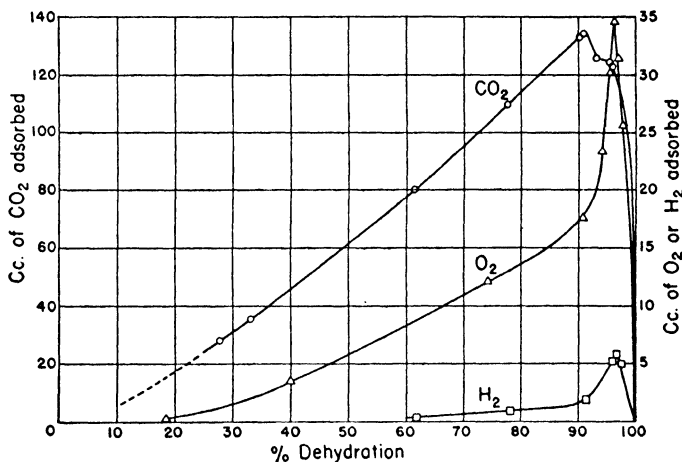


FIG. 122.—The effect of the dehydration of chabasite on the adsorption of hydrogen, oxygen and carbon dioxide.

adsorption of the three gases at  $0^{\circ}\text{C}$ . and 1600 mm. pressure. As the water is removed the adsorption increases because the pore space and the inner surface increase in extent. This lasts as long as the original crystal lattice remains intact. The dehydration is carried out at progressively increasing temperatures. To remove the last few per cent of water temperatures above  $640^{\circ}\text{C}$ . must be used. At these temperatures the crystal structure begins to collapse, with a decrease in the adsorbing power. As the figure shows, the sintering takes place in a narrow range of water content.

Figure 122 has some very interesting and at first sight rather puzzling aspects. Carbon dioxide adsorption begins around 5%

<sup>8</sup> A. B. Lamb and J. C. Woodhouse, *J. Am. Chem. Soc.*, 58, 2637 (1936).

dehydration, oxygen adsorption around 17%, hydrogen around 50%. Obviously, this can not have anything to do with an increase in the pore size upon increasing dehydration, since the smaller hydrogen and oxygen molecules must be able to penetrate into any pore where carbon dioxide can enter. We must assume therefore that the same surface is available for all three molecules. Yet at 17% dehydration about 75 times as much carbon dioxide is adsorbed as oxygen, and at 50% dehydration 60 times as much oxygen is adsorbed as hydrogen. Because of differences in the heats of adsorption at a given temperature and pressure carbon dioxide is adsorbed in larger amounts than oxygen, and oxygen in larger amounts than hydrogen. However, the ratio of the adsorbabilities of these gases on other adsorbents is much smaller; for example, it is only about 4 : 1 on charcoal. On chabasite the ratio is about 15 times as large as this.

Lamb and Woodhouse suggest that the disparity between the ratio of 60 : 1 on partly dehydrated chabasite and 4 : 1 on charcoal is due to differences in the pore sizes of the two adsorbents. If one assumes that in chabasite the gases have access to all pores while in charcoal many of the finer pores are accessible only to the smaller molecules, the latter will appear a relatively better adsorbent for the smaller and less adsorbable molecules. This factor may account for part of the discrepancy, but probably the greater part is not due to differences in the available surface, but to differences in the heats of adsorption. As we shall see, the heats of adsorption of gases on chabasite are about twice as large as on charcoal. This would make the adsorbability ratios on chabasite  $e^2$ , or about seven times as large as on charcoal. The rest of the discrepancy, i.e., a factor of 2, is probably due to the cause suggested by Lamb and Woodhouse.

Another interesting feature of Fig. 122 is the location of the maxima for the three gases. The maximum for hydrogen adsorption is located at 97.8% dehydration, for oxygen at 96.9%, and for carbon dioxide at 92.9%. The maxima result from two opposing effects of the dehydration: removal of the water keeps on increasing the inner surface, but the collapse of the structure decreases the surface. If, as expected, the walls of the coarser pores collapse first, carbon dioxide reaches its maximum first. Beyond 92.9% dehydration there is still a continued opening up of the finer pores even though the coarser pores begin to disappear. Beyond 96.9% dehydration the pores that are wide enough to hold oxygen but not carbon dioxide also begin to

collapse, but the finer pores still keep on increasing in number. Finally at 97.8% dehydration even the finest pores begin to collapse.<sup>9</sup>

It is worthy of note that water is held so firmly in partly dehydrated chabasite that adsorbed hydrogen, oxygen, and carbon dioxide do not carry away water molecules on desorption. This is not true of organic vapors. Lamb and Ohl<sup>10</sup> found that organic vapors on desorption do remove some water.

Barrer<sup>11</sup> determined the isosteric differential heats of adsorption of nitrogen, argon, and hydrogen on chabasite. The isotherms ranged from 104 to 237° K. He found very large heat values, probably the largest recorded for physical adsorption. Just as for graphite (Chapter VIII), he found that the differential heats decreased at first with the amount of gas adsorbed, then reached an apparent limiting value. However, both the initial and the limiting heat values were about twice as large for chabasite as for graphite. For nitrogen, argon, and hydrogen the initial heats of adsorption were 8800, 6000, and 4000 calories per mole, respectively. According to the calculations of de Boer and Custers<sup>12</sup> the van der Waals dispersion energy may be six times as large in long cylindrical channels as on a plane surface, and actually the initial heat of adsorption of nitrogen on chabasite is about four times as large as would be calculated from London's equation (65) in Chapter VII. The heats of adsorption of nitrogen and argon on graphite differ from each other only slightly (4600 and 4100 calories per mole, respectively), but on chabasite the difference is very large. Probably this is also due to the size of the pore. If the width of the pore is just sufficient for a nitrogen molecule having a diameter of 4.08 Å to squeeze in, then an argon atom with a diameter of 3.83 Å will be adsorbed near to one wall, but farther away from the other. Since the dispersion energy decreases as the cube of the distance from the wall, this may possibly explain the considerably smaller heat value obtained for argon.

Lamb and Ohl<sup>10</sup> determined the integral heats of adsorption of a number of vapors on chabasite, and they also found values that were

<sup>9</sup> A. B. Lamb and C. D. West (*J. Am. Chem. Soc.*, **62**, 3176, 1940) investigated the effect of dehydration of  $\text{Mg}(\text{OH})_2$ ,  $\text{Ca}(\text{OH})_2$  and  $\text{Zn}(\text{OH})_2$  on the adsorption of nitrous oxide. Although these substances are much poorer adsorbents than chabasite, the shapes of the curves are very similar to those of Fig. 122. The cause of the maxima is also probably the same as in the case of chabasite.

<sup>10</sup> A. B. Lamb and E. N. Ohl, *J. Am. Chem. Soc.*, **57**, 2154 (1935).

<sup>11</sup> R. M. Barrer, *Proc. Roy. Soc.*, **A167**, 392 (1938).

<sup>12</sup> J. H. de Boer and J. F. H. Custers, *Z. phys. Chem.*, **B25**, 225 (1934).

considerably larger than those obtained for the same vapors on charcoal. For carbon dioxide, nitrous oxide, methyl chloride, and methyl alcohol the integral heats <sup>13</sup> on chabasite are 12.41, 12.83, 13.47 and 23.32 kcal. per mole, respectively, while on charcoal the corresponding values are 7.7, 7.76, 7.18 and 14.3 kcal. per mole, respectively. These vapors are adsorbed in large quantities since the molecules are small enough to penetrate into the pores of chabasite. In contrast with this, ethyl alcohol and ethyl chloride are only slightly adsorbed; the molecules are too large to enter the pores and their heats of adsorption are smaller than on charcoal. The integral heat values for ethyl alcohol and ethyl chloride on chabasite are 9.27 and 11.06 kcal. per mole, on charcoal 16.4 and 13.49 kcal. per mole, respectively. Lamb and Ohl suggest that the adsorption of these two vapors takes place on the external surface of the chabasite crystals.

The other zeolites do not exhibit the remarkable adsorptive properties of chabasite. There are three types of zeolites: three-dimensional networks (chabasite, analcite), plate-like structures (heulandite), and fibrous structures (natrolite, scolecite). Barrer <sup>11</sup> investigated the adsorption of nitrogen, argon, and hydrogen on these five zeolites. Analcite, dehydrated in vacuum at 330° C. for three days, shows less than one-fifth as large nitrogen adsorption at liquid air temperature as chabasite. This indicates either that the pores are finer than in chabasite or that the crystal structure had already collapsed to a large extent at 330° C. The heats of adsorption are exceptionally uniform for different amounts of gas adsorbed; the initial and limiting values for nitrogen, argon and hydrogen are 5500 and 5000, 3700 and 3300, and 1500 and 1400 calories per mole, respectively.

In the laminar crystal heulandite the water of crystallization is held between the layers. Dehydration takes place very easily and is accompanied by a great shrinkage in a direction normal to the layers. Because of this shrinkage the interlaminar space does not become available for gas adsorption. Both partly and completely dehydrated heulandite show negligibly small nitrogen and argon adsorption. The two fibrous zeolites likewise admit no gas into the channels from which water has been removed.

Probably all adsorbents exhibit persorption to some extent. This shows up when one determines the surface area by the adsorption of molecules of different sizes. Thus Brunauer and Emmett <sup>14</sup> found that

<sup>13</sup> These values represent the integral heat of adsorption of 1 mole of gas on 500 g. of adsorbent.

<sup>14</sup> S. Brunauer and P. H. Emmett, *J. Am. Chem. Soc.*, **59**, 2682 (1937).

the surface area of silica gel determined by means of butane was 22.5% smaller than the average value obtained from isotherms of five smaller molecules (argon, nitrogen, oxygen, carbon monoxide and carbon dioxide). The difference was even greater for a charcoal sample, about 34%. Although there is some uncertainty as to the area occupied by a butane molecule on these surfaces, nevertheless it is safe to conclude that both charcoal and silica gel contain a considerable number of pores that are too narrow to allow the penetration of butane. By employing a series of molecules of different sizes to determine the surface of an adsorbent one can evaluate the fraction of the surface located in pores smaller than the diameter of any given molecule used.

### THE PORE SPACE OF THE ADSORBENT

When an adsorbent is placed in a vessel, the vessel contains solid matter and space filled with air. Manegold<sup>15</sup> divides the space into three parts: empty space, capillary space, and force space. If the width of the space is so great that the forces emanating from the adsorbent influence only a negligibly small portion of the matter which fills it, it is called empty space. The word "empty" here does not refer to matter but rather to the fact that the space is force-free. Such a space can be filled or emptied quantitatively without difficulty. If the width of the space is so small that the forces originating from the adsorbent influence most of the matter within it, it is called capillary space. Such a space can be emptied only with difficulty. Finally, the space between the atoms of the adsorbent and within the atoms constitutes the force space. To obtain the pore space of the adsorbent one must be able to separate the empty space from the capillary space; the force space usually introduces no difficulty.

A simple way of determining the pore space is by immersing the adsorbent in some liquid, drying the granules, and weighing them at the moment when their external surface appears to be dry. The increase in the weight of the adsorbent divided by the density of the liquid gives the volume of the total pore space. Table LVIII, taken from Kubelka,<sup>16</sup> represents pore space determinations on ten different charcoals. He used water and alcohol as the liquids, and the values given in Column 4 are the averages of the two determinations. The bulk density in Column 2 gives the weight of the charcoal per unit volume of the container. The volume of the charcoal substance was calculated from the bulk density with the assumption that the true

<sup>15</sup> E. Manegold, *Kolloid Z.*, 80, 253 (1937).

<sup>16</sup> P. Kubelka, *Kolloid Z.*, 55, 129 (1931).

density of charcoal is 2.0. The empty space, or the space between the granules, is the difference between 1 and the sum of the volumes of the charcoal substance and the pores. It is approximately the same for all of the charcoals since the granules had the same size, between 1.25 and 2.5 mm. The value of 0.32 cc. per cc. is not far from the space calculated for the close-packing of spheres.

Another way of obtaining the pore space is to determine the adsorption isotherm of a vapor up to saturation pressure. At saturation pressure all pores ought to be filled, so that one ought to be able to check the values obtained by immersion of the charcoal in the liquids. As a matter of fact, the values determined by the two different methods usually do not check with each other. For the first three charcoals of Table LVIII Kubelka obtained from benzene adsorption isotherms the

TABLE LVIII  
THE PORE VOLUME OF CHARCOALS

Charcoal	Bulk Density g./cc.	Charcoal Substance cc./cc.	Pore Volume cc./cc.	Space between Granules cc./cc.
Aussig old I	0.240	0.12	0.57	0.31
Aussig old II	0.274	0.14	0.54	0.32
Aussig G 1000	0.530	0.27	0.39	0.34
Leverkusen	0.332	0.17	0.52	0.31
Höchst	0.248	0.12	0.55	0.33
BASF	0.338	0.17	0.51	0.32
Urbain	0.282	0.14	0.57	0.29
1010	0.640	0.32	0.36	0.32
Nk 161	0.530	0.27	0.41	0.32
Nk 64	0.521	0.26	0.42	0.32

values of 0.196, 0.236 and 0.248 cc. per cc. for the capillary space, instead of the values of 0.57, 0.54 and 0.39 cc. per cc., respectively. The discrepancy can be explained by assuming that the pore space is divided into two parts: capillaries and coarse non-capillary pores, and that adsorption occurs predominantly in the former. For the first three charcoals the capillaries constitute 34, 44 and 64% of the total pore space, respectively. At exactly 100% saturation even the coarsest pores will fill if sufficient time is allowed to establish equilibrium. However, capillaries greater than  $0.15\ \mu$  in radius fill with benzene only if  $p/p_0$  is greater than 0.99, according to the Kelvin equation (Chapter V). This region of the isotherm is difficult to investigate, and so the adsorption at saturation is usually obtained by extrapolation of the adsorption values obtained at somewhat lower relative pressures.



It is customary to divide the pore space of the adsorbent into macropores and micropores, which means literally large pores and small pores. For isotherms that indicate an approach to saturation at a pressure considerably lower than the vapor pressure of the adsorbate (Types I, IV, and V) the two pore systems are sharply separated, but for isotherms that show indefinitely increasing adsorption near saturation (Types II and III) the separation is difficult.

Table LIX gives the pore space data for two charcoals and two silica gels, determined by Wicke.<sup>17</sup> The total pore space was determined by immersion in benzene, the volume of the micropores from

TABLE LIX  
PORE SPACE DATA ON CHARCOALS AND SILICA GELS

Substance	Bulk Density g./cc.	Appar- ent Density g./cc.	True Density g./cc.	Volume of Sub- stance cc./g.	Total Pore Space cc./g.	Macro- pore Volume cc./g.	Micro- pore Volume cc./g.
Charcoal KA	0.36	0.55	1.81	0.55	1.27	0.60	0.67
Charcoal KB	0.53	0.89	2.08	0.48	0.65	0.41	0.24
Silica gel E	0.85	1.10	2.38	0.42	0.49	0.35	0.14
Silica gel W	0.47	0.76	2.28	0.44	9.87	—	—

benzene adsorption isotherms. Since Silica Gel W gave Type II isotherms the separation into macro- and micropores was impossible. For the three other adsorbents Wicke estimated from the adsorption isotherms, using the Kelvin equation, that practically all of the micropores had radii smaller than 30Å, the average being roughly 10Å. The smallest macropores had radii of about 0.1  $\mu$  and he estimated that the average was about 1  $\mu$ . Using these values one can calculate the inner surfaces located in the micropores and in the macropores. For a sphere the surface is equal to  $3V/\bar{r}$ , and for the side of a cylinder it is  $2V/\bar{r}$ . Wicke assumed that the surface within the pores is given by

$$(1) \quad S = 2.5V/\bar{r}$$

where  $V$  is the volume of the pore space, and  $\bar{r}$  is the average radius. Using the  $V$  values given in the last two columns of Table LIX, and  $\bar{r} = 10^{-7}$  for the micropores and  $10^{-4}$  for the macropores, he obtained for the surface area in the micropores 900 to 1500 sq. m./g., and for the surface in the macropores 0.35 to 1.7 sq. m./g. This rough order of magnitude calculation indicates that surface adsorption in the macropores is negligible compared to adsorption in the micropores. However, this does not mean that the macropores play a negligible part in

<sup>17</sup> E. Wicke, *Kolloid Z.*, **86**, 167 (1939).

adsorption. Actually they play a vital role in determining the rate of adsorption. As we shall see in Chapter XIII, the rate of adsorption in long and very narrow pores is slow. If pores of large diameter alternate with narrow pores, the distance through which molecules must travel in the micropores is shortened, and the rate of adsorption becomes much faster.

For Type II and III isotherms the size of the pores increases continuously, and always larger pores fill up as saturation is approached. Because of this the macro- and micropores do not constitute two sharply defined systems, but gradually shade into each other. Doubtless this is the explanation of the fact that Bachmann<sup>18</sup> obtained the same pore volume for silica gel samples by immersion in the liquid and by determining the adsorption of the vapor at saturation pressure. Table LX shows the excellent agreement between the two methods.

TABLE LX  
TOTAL PORE VOLUME OF SILICA GELS

Gel Number	Measuring Liquid	Method of Determination	Total Pore Volume, cc./cc.
3	CHCl <sub>3</sub>	Vapor	0.374
	C <sub>2</sub> H <sub>5</sub> I	Vapor	0.377
	CHCl <sub>3</sub>	Vapor	0.374
5	H <sub>2</sub> O	Vapor	0.426
	C <sub>6</sub> H <sub>6</sub>	Vapor	0.420
2	H <sub>2</sub> O	Liquid	0.564
	H <sub>2</sub> O	Vapor	0.561
	C <sub>6</sub> H <sub>6</sub>	Vapor	0.562
	C <sub>2</sub> H <sub>5</sub> Br <sub>4</sub>	Liquid	0.560
	H <sub>2</sub> O	Vapor	0.560

It also shows how accurately the pore volumes obtained for the same gel sample agree when determined by different liquids and vapors. The three different gel samples, however, show a considerable variation in the total pore volume.

In the above discussed works of Kubelka,<sup>16</sup> Wicke,<sup>17</sup> and Bachmann<sup>18</sup> the size of the micro- and macropores was not defined exactly. The present usage is to call micropores those that have radii smaller than 100Å. Rabinowitsch and Fortunatow<sup>19</sup> determined the adsorption isotherms of water vapor on a number of substances and calculated the amount adsorbed in capillaries smaller than 10<sup>-6</sup> cm.

<sup>18</sup> W. Bachmann, *Z. anorg. allgem. Chem.*, 79, 202 (1913).

<sup>19</sup> M. Rabinowitsch and N. Fortunatow, *Z. angew. Chem.*, 41, 1222 (1928).

in radius by means of the Kelvin equation. Their results are shown in Table LXI. The three active carbons have about the same total pore space but the micropore space is very different. Birchwood charcoal has about 85% greater micropore volume than pinewood charcoal. The activated carbon has the smallest total pore space but the largest micropore space; in fact, it consists almost completely of micropores. The two graphites show approximately equal micropore volumes but the macropore space is different. Rabinowitsch

TABLE LXI  
PORE VOLUMES OF DIFFERENT SUBSTANCES

Substance	Specific Gravity	Total Pore Volume, cc./cc.	Micropore Volume, cc./cc.	% Micropores
Pinewood charcoal	1.72	0.883	0.354	40.2
Birchwood charcoal	1.72	0.936	0.656	70.0
Activated carbon	1.78	0.870	0.858	98.6
Acheson graphite	2.23	0.246	0.166	67.5
German graphite	1.99	0.163	0.157	96.3
Kaolinite	2.37	0.369	0.126	34.1
Porcelain	2.53	0.031	0.0034	10.9

and Fortunatow believe that the macropores in the German graphite were clogged up, probably with amorphous carbon. As an evidence they cite the much lower apparent density of this graphite. The last two adsorbents, kaolinite and porcelain, differ in the sizes of both macro- and micropores. The difference in the micropore volume is greater; only 11% of the total pore space in porcelain consists of micropores.

Determination of the densities of certain zeolites leads to some interesting correlations between pore volume and adsorptive power. Rabinowitsch<sup>6</sup> obtained for the densities of calcium-chabasite, potassium-chabasite, and heulandite the values of 2.15, 2.3 and 2.3, while for the densities of the same substances in the dehydrated state he obtained 1.7, 1.85 and 1.9 respectively. If we assume that the undehydrated zeolites had negligible pore volumes, we can calculate the pore volumes after dehydration by means of the equation

$$(2) \quad V = 1 - d_d/d_u$$

where  $d_d$  is the density of the dehydrated,  $d_u$  that of the undehydrated substance. The calculation gives the values of 0.21, 0.195 and 0.175 cc./cc. for natural chabasite, potassium chabasite and heulandite, respectively. We have seen that these three substances have very different adsorptive properties. It seems probable that the decrease in

pore volume from chabasite to heulandite occurs at the expense of the width of the capillaries rather than their length, otherwise the three adsorbents would exhibit only slight differences in their adsorptive power. The decrease in cross-section, indicated by the above pore space values, is sufficient to decrease hydrogen and nitrogen adsorption very strongly on potassium-chabasite, and to eliminate them almost completely on heulandite.

We have seen in the discussion of the adsorption isotherm that the capillary condensation theory, the potential theory, and the theory of multimolecular adsorption ascribe liquid like characteristics to the adsorbate. It follows from each of these theories that at the saturation pressure the pores of the adsorbent are completely filled with the liquid-like adsorbate. If one determines the amounts of different vapors adsorbed at their saturation pressures on the same adsorbent and calculates the volumes of liquid corresponding to these adsorptions, one should obtain identical values. As we have seen in Table VII, Chapter V, Goldmann and Polanyi<sup>20</sup> determined the adsorption space—or the capillary pore volume—of their charcoal by means of four different vapors, and found a maximum deviation from the average of only 0.4%. Coolidge<sup>21</sup> studied the adsorption of eight vapors on charcoal; the maximum deviation from the average pore volume in his experiments was about 8%. The data of Bachmann<sup>18</sup> in Table LX show a very striking agreement between the pore volumes of silica gel samples obtained by two different methods. Foster<sup>22</sup> found that ferric oxide gel had a pore volume of 0.284 cc./g. when alcohol was used as adsorbate, and 0.274 cc./g. when benzene was used. For a water treated ferric oxide gel sample alcohol and benzene gave 0.215 and 0.205 cc./g., respectively. The maximum deviation from the average in this case is 2.4%. These are only a few examples from a great mass of experimental data.

The above examples also show that although the agreement between the values of the pore volume obtained from the saturation adsorption of different vapors is very good, nevertheless the differences are almost always greater than the experimental error. This is not surprising, because although the adsorbate is similar in many respects to the liquid the two are not identical in all of their properties. In fact, the study of these slight differences is very useful in giving us information about the mechanism of the adsorption process.

<sup>20</sup> F. Goldmann and M. Polanyi, *Z. phys. Chem.*, **132**, 321 (1921).

<sup>21</sup> A. S. Coolidge, *J. Am. Chem. Soc.*, **48**, 1795 (1926).

<sup>22</sup> A. G. Foster, *Trans. Far. Soc.*, **28**, 645 (1932).

Kubelka<sup>16</sup> determined the total capillary volumes of the ten charcoals previously discussed by means of the saturation adsorptions of benzene, ether, chloropicrin, and water. He obtained the usual good agreement, but the slight deviations showed an unquestionable trend. If one takes the values obtained by means of benzene as the standard, all the water values are lower, and all the ether and chloropicrin values (with one exception) are higher. This is shown in Table LXII. Kubelka realized that the least compressible liquid, water, gave the smallest pore volume, and the most compressible one, ether, the largest. He concluded from this that the liquids in the pores must be under great compression. However, he mistakenly took this as a confirma-

TABLE LXII

DEVIATIONS OF THE CAPILLARY VOLUMES OBTAINED BY DIFFERENT VAPORS

Charcoal	% Deviation from the Benzene Values		
	Ether	Chloropicrin	Water
Aussig old I		+1	- 3
Aussig old II	+ 3	0	- 3
Aussig G1000	+ 7	+2	- 3
Leverkusen	0	+1	-10
Höchst	+11		
BASF	- 5		
Urbain	+ 1		
1010	+ 5		
Nk 161	+ 2		
Nk 64	+ 5		
Average	+ 3	+1	- 5

tion of the capillary condensation theory, whereas it is actually in contradiction to that theory. A liquid having a concave meniscus in a capillary is under tension and not compression; its density should therefore be smaller than that of the normal liquid and not larger. On the other hand, the potential theory postulates a compression of the adsorbed liquid, which is in agreement with the data of Table LXII. In a later paper Kubelka and Müller<sup>23</sup> obtained similar results using other adsorbates and other charcoals. The more compressible hexane and benzene gave larger pore volumes than the less compressible methyl and ethyl alcohol.

Besides comparing the amounts of the different liquids adsorbed at saturation pressure in the capillaries of the adsorbent there are other types of experiments that seem to indicate that the adsorbate is under

<sup>23</sup> P. Kubelka and M. Müller, *Kolloid Z.*, 58, 189 (1932).

compression in the pores and not under tension. Measuring the density of a given adsorbent by the displacement of different liquids led a number of investigators to the conclusion, already discussed in Chapter V, that the adsorbed phase is under very high compression. Also, experiments performed on the expansion of the adsorbent under the effect of the adsorbate lead to the same conclusion.

#### THE DENSITY OF THE ADSORBENT

Density determinations can convey much valuable information about the pore structure of the adsorbent. If one knows the apparent and the true density of an adsorbent, one can calculate at once the total pore volume. McBain<sup>24</sup> distinguishes between four different densities. The bulk density (or volume weight) is the weight of the adsorbent per unit volume of the container; the apparent density (or granule density) is determined by displacement of mercury, a liquid that can not enter the pores of the adsorbent; the specific gravity (sometimes called real density) is determined by displacement of liquids that penetrate partially or completely into the pores; and finally, true density refers to the compact solid matter of which the adsorbent is composed. A gas that would penetrate into all of the pores of an adsorbent without being adsorbed, or a liquid that would penetrate into all pores without being compressed, would give the true density; probably helium comes the closest among all fluids to giving the correct value.

In Table LIX Wicke<sup>17</sup> gave three different densities for each of the adsorbents he investigated. The so-called true density values in Column 4 were actually determined by displacement of benzene. Since it is quite likely that benzene does not penetrate into all of the pores, it would be more correct to call them specific gravity values according to the terminology of McBain.

It is interesting to compare the four densities of different charcoals. McBain gives the following values: the bulk densities range from 0.03 to about 1.0, apparent densities from 0.3 to 1.3, specific gravities from 1.2 to 2.1, and true densities from 2.2 to 2.3. The density of graphite is 2.25 to 2.27. Thus the true density of charcoal, i.e., the density of the compact solid matter itself, is quite close to that of graphite. The other, smaller density values refer to the charcoal including some or all of the pore space: the specific gravity value includes some of the capillary pores, the apparent density includes the entire pore volume, and

<sup>24</sup> J. W. McBain, *The Sorption of Gases and Vapours by Solids*, London, 1932, p. 79.

the bulk density includes even the volume of the space between the granules.

It has been noted by many investigators that if the specific gravity of a given charcoal sample is determined by displacement of different liquids different values are obtained. Harkins and Ewing<sup>25</sup> measured the density of a coconut shell gas mask charcoal in 11 different liquids and obtained the results shown in Table LXIII. The mercury value

TABLE LXIII  
SPECIFIC GRAVITY AND PORE VOLUME OF CHARCOAL

Liquid	Specific Gravity	Pore Volume cc./cc.	Per Cent Compressed at 12,000 atm.	$\sigma/\eta$
Mercury	0.865	—	—	—
Water	1.843	0.534	20.51	7200
Propyl alcohol	1.960	0.559	22.93	1062
Chloroform	1.992	0.566		4760
Benzene	2.008	0.568		4510
p-Xylene	2.018	0.571		4430
Petroleum ether	2.042	0.579		—
Carbon disulfide	2.057	0.580	25.75	8480
Acetone	2.112	0.590	27.0	7120
Ether	2.120	0.592	30.0	7125
Pentane	2.129	0.593	More than ether	6200

represents the granule density; the other ten values indicate penetration of the liquids into the pores. The total pore volume, calculated on the assumptions that each of the ten liquids penetrates into all of the pores and has its normal density in the pores, is given in Column 3. If we take benzene as the reference substance, the water value shows a deviation of  $-6\%$ , the ether value  $+4\%$ , in good agreement with the average values given in Table LXII. There are two ways to explain the variation in the calculated pore volume: either the different liquids do not penetrate into all of the pores, water entering the smallest number of pores, pentane the largest number; or the liquids do penetrate into all of the pores but their densities in the pores are different from their normal densities. Harkins and Ewing pointed out that if the first of these explanations were the correct one, the order of penetration of the liquids should be determined by the ratio  $\sigma/\eta$ , because  $\sigma$ , the surface tension, is the driving force of penetration, and  $\eta$ , the viscosity, is the retarding force. As the last column shows there is absolutely no correlation between the specific gravity and  $\sigma/\eta$ ; particularly propyl alcohol is quite absurdly out of line. If on the

<sup>25</sup> W. D. Harkins and D. T. Ewing, *J. Am. Chem. Soc.*, 43, 1787 (1921).

other hand the second explanation is correct, then the order of the specific gravities should be the same as the order of the compressibilities of the liquids. Column 4 shows that if a compression of about 12,000 atm. is assumed the six liquids for which compressibility data were available at the time of the experiments fall excellently in line. The investigators also stated that compressibility data on chloroform, benzene, and *p*-xylene for lower pressures indicate that these liquids are in their proper order, and further that the experiments of C. E. Monroe on five other liquids place these also in the right order.

In spite of the strong appeal of the data of Harkins and Ewing, their conclusions can not be accepted completely. Their calculations involve the assumption that the true density of their charcoal is 1.6, and that the high specific gravity values of Column 2 are due to the fact that the liquids are under tremendous compression in the pores. We now know that the true density of coconut charcoal is certainly greater than 2.0. Howard and Hulett<sup>26</sup> measured the densities of different carbons with helium at 25° C. Their results are shown in Table LXIV. Except for samples 6, 7 and 8 the densities approach

TABLE LXIV  
DENSITIES OF CARBONS DETERMINED BY HELIUM

Sample Number	Type of Carbon	Density in Helium	Nitrogen Adsorption 25° C., 760 mm.
1	Coconut charcoal	2.12	8.8 cc.
2	Sugar charcoal	2.26	6.2
3	Kelp charcoal	2.28	5.2
4	Carbon black	2.05	5.5
5	Coconut charcoal	2.14	8.2
6	Willow charcoal	1.44	2.8
7	Petroleum coke	1.43	0.3
8	Coke from bituminous coal	1.51	0.5
9	Ceylon graphite	2.28	None

that of graphite. These three samples were probably incompletely freed from hydrocarbons, which is evidenced also by the low nitrogen adsorption values given in the last column. The calculated densities are based on the assumption that the adsorption of helium at room temperature is negligible. The investigators advanced a number of sound arguments to prove this point. Although it is very difficult to give a complete proof of the absence of any adsorption, nevertheless it seems probable that there is very little adsorption of helium on any adsorbent at 25° C. and higher temperatures.

<sup>26</sup> H. C. Howard and G. A. Hulett, *J. Phys. Chem.*, **28**, 1082 (1924).



Howard and Hulett noticed that there was a very definite drift with time in the volume of helium required to fill the pore space of charcoal. This is shown in Fig. 123, representing the increase with time in the apparent specific gravity of coconut charcoal. The value of about 2.07 was reached very rapidly, but the final value of 2.15 took about 15 hours. This shows that charcoal has some exceedingly fine pores, into which even helium atoms penetrate only with difficulty.

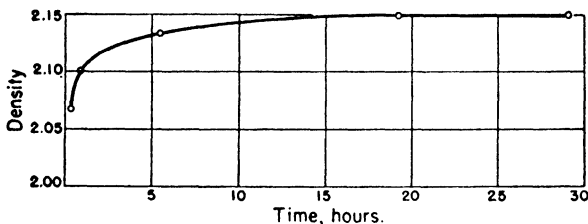


FIG. 123.—The change with time in the apparent specific gravity of charcoal determined with helium.

Although some investigators are inclined to ascribe entirely to compression effects and others entirely to penetration effects the differences in the apparent specific gravities of adsorbents when measured with different liquids, it seems very probable that both effects play important roles. It is quite certain that the true density value of 1.6 assumed by Harkins and Ewing<sup>25</sup> is too low, and that the calculated compression of 12,000 atm. is too high; nevertheless the striking parallelism between compressibilities and specific gravities can not be disregarded. The work of Culbertson and his collaborators clearly shows that both effects must be considered.

TABLE LXV  
SPECIFIC GRAVITIES OF CHARCOAL AND SILICA GEL

Liquid	Charcoal g./cc.	Silica Gel g./cc.
Water	1.821	2.246
Benzene	1.994	2.149
Carbon tetrachloride	1.860	2.132
Petroleum ether	2.083	2.125

Culbertson and Dunbar<sup>27</sup> determined the specific gravities of charcoal and silica gel in four different liquids. The results are shown in Table LXV. The table reveals the striking fact that water gives

<sup>27</sup> J. L. Culbertson and A. Dunbar, *J. Am. Chem. Soc.*, 59, 306 (1937).

the highest density for silica gel and the lowest for charcoal, while petroleum ether gives the lowest density for silica gel and the highest for charcoal. Obviously, neither penetration nor compression of the liquid, alone, can explain these results. If the density values depended only on such factors as the surface tension, viscosity, or compressibility of the *liquid*, then the order of the specific gravities ought to be the same for both adsorbents. However, the data of the table show clearly that the forces of interaction between the adsorbent and the liquid must be of great importance in determining the specific gravity. These forces doubtless compress the liquids at the interface and also strongly influence the penetration into the pores.

Culbertson and Weber<sup>28</sup> used nine liquids to determine the densities of charcoal and silica gel. In agreement with Harkins and Ewing<sup>25</sup> they found that for charcoal the liquids followed the order of their compressibilities. However, this was not true for silica gel; the liquids with dipole moments gave high density values, the non-polar liquids gave low values. Acetone, for example, with large dipole moment and high compressibility, gave high density values for both charcoal and silica gel; water, with large dipole moment and low compressibility, gave high density for silica gel and low for charcoal; petroleum ether, with high compressibility and zero dipole moment, gave high value for charcoal and low for silica gel. It seems therefore that the ion-dipole attraction between the silica surface and water produces a greater compression than the dispersion forces produce between silica and petroleum ether, even though petroleum ether is much more compressible than water.

The above data can also be explained by assuming that the degree of penetrability of the pores by the different liquids is strongly influenced by the nature of the forces of interaction between the adsorbent and the adsorbate. To test this possibility Culbertson and Weber determined the density of ground quartz with water and benzene. After about 50 hours of grinding the density of the quartz powder began to fall off in both liquids but the values remained equal. After about 300 hours of grinding the density in benzene began to fall below the value in water, and the discrepancy increased as the grinding was continued. If the quartz powder retains its non-porous character after such a long grinding, the results can be explained only on the basis of a stronger compression of the water at the interface. However, it is impossible to know whether the quartz particles did or did not develop cracks of molecular dimensions in the grinding process.

<sup>28</sup> J. L. Culbertson and M. K. Weber, *J. Am. Chem. Soc.*, **60**, 2695 (1938).

The conclusion from the above considerations is that probably both compression and penetration effects play a part in producing different apparent specific gravities when different liquids are used for the determination.<sup>29</sup> The potential theory predicts compression, the capillary condensation theory predicts dilation of the liquids in the pores. So far nobody has cited any experimental evidence that would indicate that the adsorbed liquid in the pores has a smaller density than the bulk liquid. Nevertheless this does not exclude the possibility that capillary condensation exists at high relative pressures. Even if in the adsorption process at high pressures multimolecular adsorption is followed by capillary condensation, the compression effect due to the adsorption may still overbalance the tension effect due to the condensation, giving a net compression. Particularly in adsorbents with very narrow pores, such as charcoal, would the compression effect predominate over the tension effect. It is possible that at least a part of Culbertson's results for silica gel are due to the increased importance of capillary condensation in an adsorbent with wider pores. It is interesting to note in this connection that in Table LXII, Column 2, the only charcoal that gave a negative deviation for ether was *BASF*, the one that has by far the largest pore diameter, as we shall see in the next section.

#### THE PORE SIZE DISTRIBUTION OF THE ADSORBENT

The pores of the adsorbent may be divided into macro- and micropores. The adsorption that takes place in the macropores is negligible, consequently the size distribution of the macropores is unimportant from the point of view of adsorption investigations. The size distribution of the micropores plays a vital role in adsorption; beyond unimolecular adsorption it is the main factor in determining the shape of the isotherm. Conversely, from the adsorption isotherm one can draw conclusions relative to the distribution of the micropores of the adsorbent.

<sup>29</sup> G. F. Davidson (*J. Text. Inst.*, 18, T175, 1927) found that the specific gravity of cotton determined in organic liquids was lower than in helium, but water gave a higher value than helium. If the helium value is taken as the true density the low values obtained with organic liquids can be ascribed to incomplete penetration, but the high water value must be due to compression of the adsorbate. Davidson calculates that a compression of 2000 atm. can account for the results. A. J. Stamm and R. M. Seborg (*J. Phys. Chem.*, 39, 133, 1935) determined the compression of water adsorbed on cellulose and wood, and came to the conclusion that it is of the order of 3-4000 atm.

At present there are two theories that give information about the pore distribution of the adsorbent, neither of which is completely satisfactory. The capillary condensation theory enables us to evaluate the pore radius distribution only if we assume that *all* adsorption is due to capillary condensation; on the other hand, the theory of multi-molecular adsorption in its simpler form (equation 41, Chapter VI) neglects completely whatever capillary condensation takes place at higher relative pressures, and even in its improved form (equation 47, Chapter VI) takes account of it only in an incomplete manner. However, the two theories together give us at least a crude, semi-quantitative picture of the pore distribution in adsorbents.

Anderson<sup>30</sup> was the first to calculate the sizes of the capillaries in an adsorbent from isotherm data, using Zsigmondy's capillary condensation theory. He determined the adsorption isotherms of water, alcohol, and benzene on silica gel and obtained the curves shown in Fig. 124. The amount adsorbed is plotted as the volume of liquid per 100 grams of gel, consequently the adsorption at the saturation pressure ought to be the same for the three adsorbates. The volumes of water, alcohol, and benzene adsorbed at saturation were 56.48, 56.79, and 55.30 cc. per 100 grams of gel; the average is 56.19 cc., the maximum deviation is less than 2%. Each isotherm shows a marked hysteresis loop. According to Zsigmondy the desorption branch of the isotherm corresponds to true equilibrium, as we shall see in the next section. Anderson, using the Kelvin equation, calculated the capillary radius corresponding to the point O, the turning point of the desorption branch. For water, alcohol, and benzene he obtained the values 27.46, 25.87, and 29.90 Å, respectively. The average is 27.74 Å; thus the diameter of these capillaries is 55.5 Å.

The lowest, reversible portion of the isotherm corresponds to adsorption according to Zsigmondy, and so the point O<sub>1</sub> marks the beginning of capillary condensation. From the water, alcohol, and benzene isotherms Anderson calculated radii of 13.76, 12.12, and 13.51 Å, respectively, for these points. The average of the three values is 13.13 Å. This is the radius of the smallest capillaries in the gel, while 27.74 Å is that of the largest capillaries. The average capillary radius is therefore 20.43 Å. Anderson realized that his value is too low, because it neglects the adsorption occurring on the walls of the capillaries. He estimated that the error was somewhere between 1.5 and 16 Å.

<sup>30</sup> J. S. Anderson, *Z. phys. Chem.*, **88**, 191 (1914).

Although one can calculate the average capillary diameter from an adsorption isotherm with the help of the capillary condensation theory, the process can not be reversed. One can not calculate the adsorption isotherm from a knowledge of the average pore diameter; in fact, the average diameter gives no clue at all to the shape of the isotherm. On the other hand, the theory of multimolecular adsorption enables

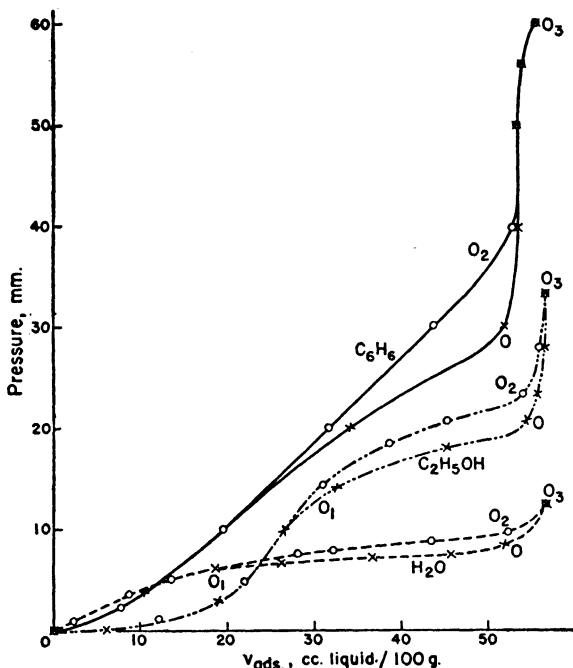


FIG. 124.—Determination of the average capillary radius of silica gel by means of adsorption isotherms of water, alcohol and benzene.

one to predict the shape of the entire isotherm beyond unimolecular adsorption if the average pore size is known. This is illustrated in Fig. 125, taken from Deitz and Gleysteen.<sup>31</sup> The curves represent nitrogen adsorption isotherms at  $-195.8^{\circ}\text{C}$ . calculated from equation (41), Chapter VI. It will be seen that the value of  $n$ , the maximum number of layers that can be adsorbed on one wall of the average

<sup>31</sup> V. R. Deitz and L. F. Gleysteen, To be published in the *Journal of Research* of the National Bureau of Standards.

sized capillary, determines the shape of the isotherm. Deitz and Gleysteen found that the nitrogen isotherms on a variety of active carbons had the shapes of the curves shown in Fig. 125. Two coconut charcoals followed the curve with  $n = 1$ , two activated carbons had  $n$  values of 1.5, three others had  $n$  values of 2, a carbon black had  $n = 4$ , and a series of bone chars, new, used, and spent, had  $n$  values of 4 and 5. Up to  $p/p_0 = 0.6$  the isotherms followed these curves quantitatively, but at higher relative pressures there were increasingly greater deviations.

If the sizes of the capillaries do not deviate very much from the average size, the theory of multimolecular adsorption can give a fair

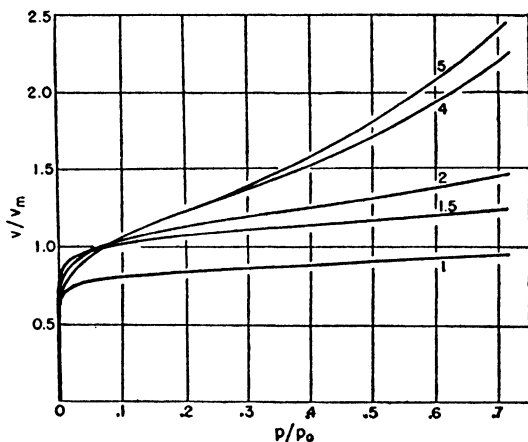


FIG. 125.—Effect of the average capillary size on the shape of the adsorption isotherm according to the theory of multimolecular adsorption.

fit for the entire adsorption isotherm up to saturation pressure. Thus Brunauer, Emmett and Teller<sup>32</sup> found that isotherms of gases on a charcoal sample obeyed equation (41), Chapter VI, with  $n = 1$ , and on the adsorbent Darco G with  $n = 2.2$ , almost up to the saturation pressure. Similarly Brunauer, Deming, Deming and Teller<sup>33</sup> found that the isotherms of benzene on ferric oxide gel obtained by Lambert and Clark<sup>34</sup> obeyed equation (47), Chapter VI, with  $n = 3$  up to the saturation pressure.<sup>35</sup> However, if there are considerable

<sup>32</sup> S. Brunauer, P. H. Emmett and E. Teller, *J. Am. Chem. Soc.*, **60**, 309 (1938).

<sup>33</sup> S. Brunauer, L. S. Deming, W. E. Deming and E. Teller, *J. Am. Chem. Soc.*, **62**, 1723 (1940).

<sup>34</sup> B. Lambert and A. M. Clark, *Proc. Roy. Soc.*, **A122**, 497 (1929).

<sup>35</sup> This is the same as  $n = 6$  in equation (47), Chapter VI.

deviations from the average, the calculation of the entire isotherm from the average pore width can give only a rough semi-quantitative fit.

Most adsorbents contain capillaries of different sizes. Both the theory of multimolecular adsorption and the capillary condensation theory agree that the narrower pores fill up at lower relative pressures, the wider pores at higher pressures. Figure 126 expresses this fact in terms of the theory of multimolecular adsorption. The curve represents a nitrogen adsorption isotherm on bone char at  $-195.8^{\circ}\text{C.}$ ,

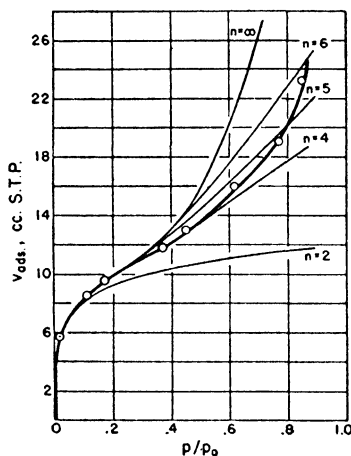


Fig. 126.—Effect of varying capillary sizes on the shape of the adsorption isotherm according to the theory of multimolecular adsorption.

obtained by Deitz and Gleysteen.<sup>31</sup> With  $n = 4$  the isotherm can be reproduced correctly up to  $p/p_0 = 0.5$ , but at  $p/p_0 = 0.8$  the value of  $n$  is 5, and it increases further at higher relative pressures. The reason for this is that the narrower capillaries fill at lower pressures, and so the average width of the pores that still participate in adsorption gets larger as the pressure increases. In terms of the capillary condensation theory every value of  $p/p_0$  corresponds to a capillary radius that can be calculated from the Kelvin equation. As the relative pressure increases, the radius increases; in other words, at higher pressures the larger capillaries fill with liquid.

Kubelka<sup>16</sup> examined the pore distribution in ten different charcoals by determining the adsorption isotherms of five different vapors on each and interpreting the results in terms of the capillary condensation theory. The pore volumes of these charcoals were given in Table LXVIII.

The adsorption isotherms of benzene at 20° C. are shown in Fig. 127. The adsorption values are plotted as fractions of the saturation adsorption,  $v_s$ . A casual inspection of the curves suffices to suggest a variety of pore distributions. Several of the charcoals indicate hardly more than unimolecular adsorption even at the saturation pressure. At the other extreme charcoal *BASF* shows completion of the monolayer at  $p/p_0$  less than 0.1, and at least five layers adsorbed

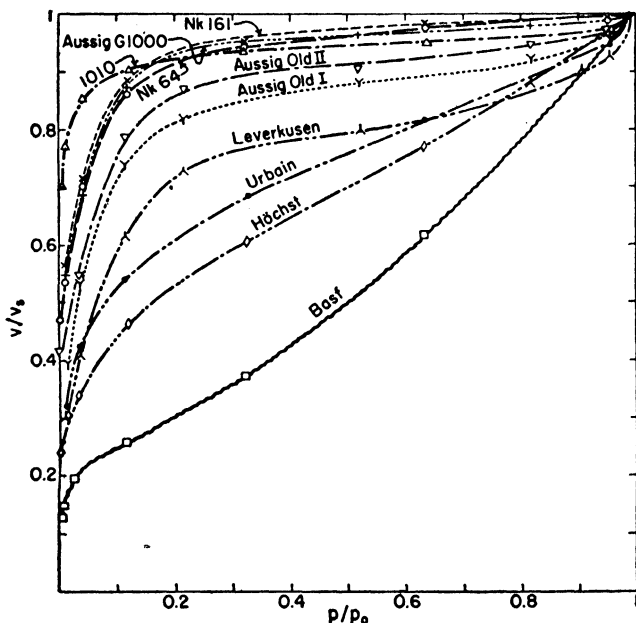


FIG. 127.—Adsorption isotherms of benzene on ten different charcoals.

at saturation. The other charcoals indicate intermediate average pore sizes.

According to the capillary condensation theory one can evaluate the structure curve of an adsorbent from an isotherm by calculating the capillary radius corresponding to each value of  $p/p_0$  by means of the Kelvin equation, and plotting the volume adsorbed as liquid against the capillary radius. Such a structure curve was shown in Fig. 63, Chapter V. The structure curves used by Kubelka are somewhat different; he plotted  $v/v_s$  against the logarithm of the capillary diameter. For one of his charcoals, Aussig G 1000, he obtained the



curve shown in Fig. 128. This curve was calculated from isotherms of five different vapors, but only the points obtained from the benzene isotherm were calculated by means of the Kelvin equation. The capillary radii for the four other vapors (ether, chloropicrin, water, and carbon dioxide) were calculated from Kubelka's own semi-empirical equation (32), Chapter V. The value of the constant  $B$  in that equation was so chosen for each vapor as to bring one point in coincidence with the benzene curve. The figure also reveals that the capillary condensation theory and the theory of multimolecular adsorption picture different pore distributions in this charcoal. According to the former at  $\log D = 0$  the capillary diameter is  $10\text{\AA}$ , and the amount

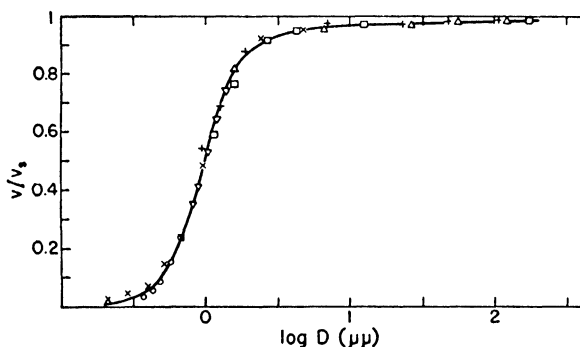


Fig. 128.—The structure curve of charcoal Aussig G 1000.

adsorbed is about 55% of the saturation value. Judging on the basis of the benzene isotherm in Fig. 131, the theory of multimolecular adsorption would predict that more than 90% of the saturation adsorption takes place in capillaries  $10\text{\AA}$  in width or less. On the other hand, 90% adsorption according to the capillary condensation theory corresponds to a radius of about  $26\text{\AA}$ , as Fig. 128 shows.

Although there is no quantitative agreement between the pore size distribution data obtained from the two theories, qualitatively the results show a good deal of similarity. The structure curve of Kubelka and Müller<sup>23</sup> for a silica gel sample indicates that only about 15% of the saturation adsorption takes place in capillaries less than  $10\text{\AA}$  in diameter, as compared to 55% in the charcoal of Fig. 128. In their silica gel sample 55% of the saturation adsorption corresponds to capillaries of about  $30\text{\AA}$  in diameter, 80% adsorption to capillaries of about  $50\text{\AA}$ . The theory of multimolecular adsorption indicates pore

sizes that are not very far from these values. Activated charcoals with fine pores have  $n$  values of 1 or 2 for nitrogen while some silica gels have as high  $n$  values as 8 or 9. The former correspond to capillary sizes of about  $15\text{\AA}$ , the latter to about  $70\text{\AA}$ .<sup>36</sup>

The pore size distributions of Kubelka's charcoals can be better visualized from the *differentiated structure curves*, i.e., from plots of the slopes of his structure curves against  $\log D$ . These curves are shown in Fig. 129. The ordinates are proportional to the frequency of occurrence of the capillary having diameter  $D$  in the given adsorbent. The curves resemble typical probability curves. The

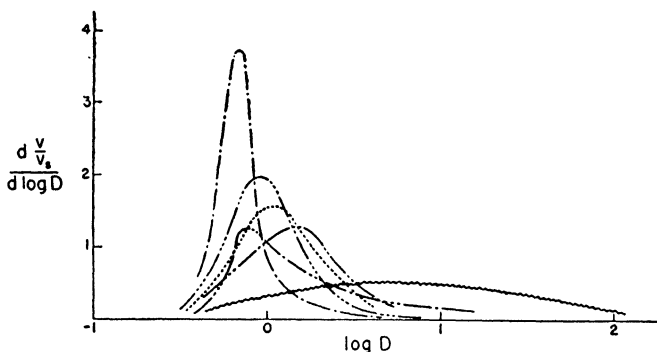


FIG. 129.—The differentiated structure curves of six of the charcoals of Fig. 127.

abscissa corresponding to the maximum of the curve gives the main capillary diameter, i.e., the capillary diameter that occurs most frequently in the adsorbent. The curves of Fig. 129 bring out even more clearly the similarity between the results of the two theories. The charcoals of finer pores have main diameters of  $10\text{\AA}$  and even less, while charcoal *BASF* has a main diameter of about  $50\text{\AA}$ . As we pointed out before, an inspection of the isotherms of Fig. 127 leads to the conclusion, on the basis of the theory of multimolecular adsorption, that the charcoals of finer pores have only slightly greater than unimolecular adsorption, while charcoal *BASF* has at least five layers adsorbed at saturation. Thus the width of the average pore is about  $10\text{\AA}$  for the former, and at least  $40\text{\AA}$  for the latter.

<sup>36</sup> It should be remembered that the theory of multimolecular adsorption pictures the capillary as consisting of two plane parallel walls, and  $n$  is the maximum number of layers that can be adsorbed on *one* of the walls.

Schuchowitzki<sup>37</sup> criticized Kubelka's structure curves on the ground that neglecting adsorption in comparison with capillary condensation leads to wholly erroneous results. If one takes account of both adsorption and capillary condensation according to Schuchowitzki's method, discussed in Chapter V, one obtains very different structure curves. This is shown qualitatively in Fig. 130. Curve 1 represents the differentiated structure curve obtained by Kubelka's method, while curve 2 gives the correct curve, taking adsorption into account. Neglecting the adsorption introduces two errors. In the first place, the curve shifts to the left, i.e., for any given value of  $v/v_s$ ,

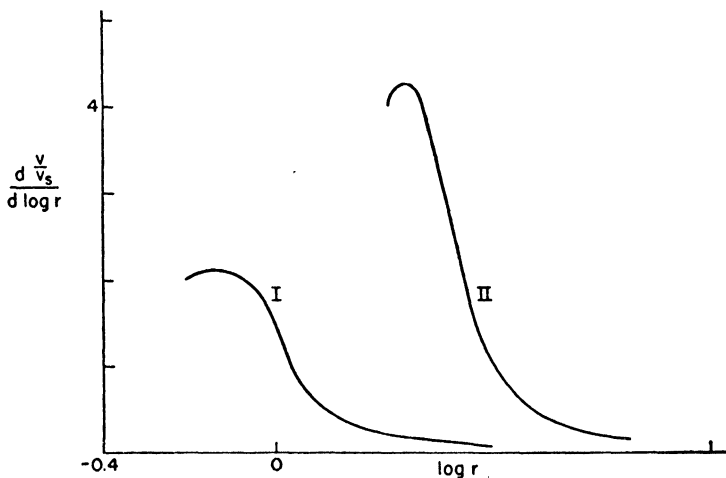


FIG. 130.—The distortion in the differentiated structure curve caused by neglecting adsorption in comparison with capillary condensation.

the capillary condensation theory gives too low a value for  $r$  since it neglects the thickness of the adsorbed layer. In the second place, the curve is deformed since the use of the capillary condensation theory alone leads to greater errors at low pressures than at high pressures. As a matter of fact, at low pressures adsorption is certainly more important than capillary condensation, whereas at high pressures capillary condensation takes on increasing importance. Although Schuchowitzki's criticism is entirely justified, nevertheless the methods discussed in this section can give at least a rough estimate of the pore size distribution of adsorbents.

<sup>37</sup> A. A. Schuchowitzki, *Kolloid Z.*, **66**, 139 (1934).

## HYSTERESIS AND THE STRUCTURE OF PORES

Typical examples of isotherms exhibiting hysteresis were given in Fig. 63, Chapter V, and in Fig. 124 of this chapter. The desorption branch of the hysteresis loop always corresponds to larger adsorption at a given pressure or, what is the same thing, to a lower pressure for a given amount of vapor adsorbed. Hysteresis may be reversible or irreversible; it is reversible if on repetition of the experiment the adsorption isotherm is completely reproduced, irreversible if the second experiment gives a different curve.

Physical adsorption occurring on the surface of the adsorbent is usually completely reversible. Hysteresis in most cases begins at higher relative pressures, in the region of multimolecular adsorption. The first explanation of hysteresis was advanced by Zsigmondy<sup>38</sup> in terms of the capillary condensation theory, and although several other explanations have been offered since the only satisfactory ones are still based on the capillary condensation theory.

Zsigmondy assumed that during adsorption the vapor does not wet the wall of the adsorbent completely. Since the wetting angle  $\theta$  is not zero, the equilibrium pressure is given by the Kelvin equation

$$(3) \quad p_a = p_0 e^{-2\sigma V \cos \theta / rRT}$$

where  $p_a$  is the observed pressure on the adsorption branch of the curve,  $p_0$ ,  $\sigma$  and  $V$  are the vapor pressure, surface tension, and molar volume of the adsorbed liquid, and  $r$  is the radius of the capillary in which the adsorption is taking place. The incomplete wetting is caused by impurities adsorbed on the walls of the capillary, mostly permanent gases, particularly air. As the pressure is raised more and more of these impurities are displaced by the vapor, and finally at saturation complete wetting takes place. The desorption equilibria therefore correspond to zero wetting angle or

$$(4) \quad p_d = p_0 e^{-2\sigma V / rRT}$$

A comparison of equations (3) and (4) reveals that  $p_a > p_d$ .

It follows from Zsigmondy's explanation that hysteresis should extend back to very low pressures. This is because permanent gases or other impurities inhibit not only capillary condensation but also adsorption at low pressures, as we have seen in Chapter X. Furthermore, repetition of the isotherm should show a drift with respect to the first determination, since the permanent gases should be partly or

<sup>38</sup> R. Zsigmondy, *Z. anorg. allgem. Chem.*, 71, 356 (1911).

completely removed from the system in the course of determining the first isotherm. These consequences of Zsigmondy's theory are actually fulfilled in the isotherms shown in Fig. 131. The curves represent the adsorption of water on silica gel at 28° C., determined by Cohan.<sup>39</sup> It also follows from the theory that drastic evacuation and cleansing of the surface should remove hysteresis. This also has been found

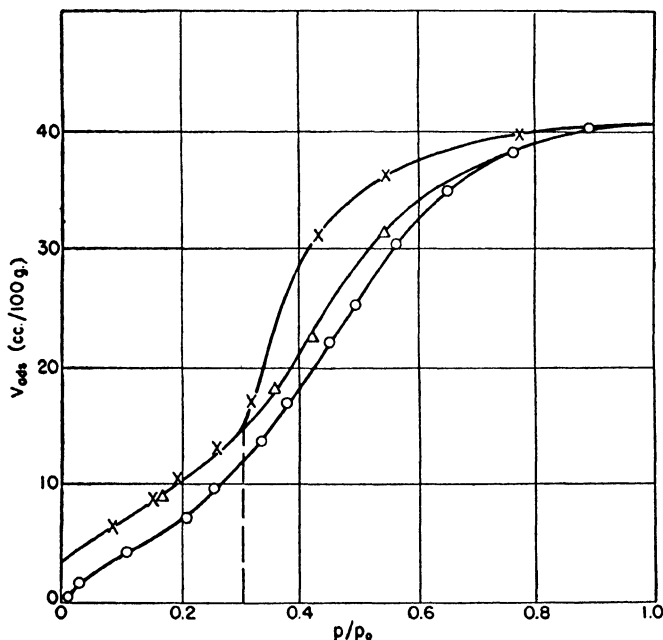


FIG. 131.—Irreversible hysteresis in the adsorption of water on silica gel.

true in a number of cases; for example, Patrick<sup>40</sup> found that the hysteresis in the adsorption of water by silica gel disappeared on thorough evacuation (Chapter X).

According to Zsigmondy's view hysteresis is not a property of the adsorbent-adsorbate system but is due to extraneous factors, i.e., to impurities. The true equilibrium curve is the desorption branch since it represents complete wetting after the removal of the impurities. Although Zsigmondy's explanation is probably correct for irreversible

<sup>39</sup> L. H. Cohan, To be published in the *J. Am. Chem. Soc.*

<sup>40</sup> W. A. Patrick, *Colloid Symposium Annual*, 7, 129 (1930).

hysteresis, there is another type of hysteresis which is completely reversible and requires therefore a different explanation.

Although Patrick succeeded in eliminating the hysteresis loop from his water-silica gel system, other investigators, using equally thorough and sometimes even a more drastic evacuation technique, still obtained very definite hysteresis. Urquhart,<sup>41</sup> Lambert and Foster,<sup>42</sup> Pidgeon,<sup>43</sup> and Rao<sup>44</sup> established beyond question the reality and reversibility of hysteresis in the adsorption of water on silica gel. On the other hand, the situation with respect to the adsorption of benzene and alcohol on silica gel seemed to develop the opposite way. Anderson,<sup>30</sup> the original investigator, found hysteresis for both (Fig. 124), whereas the later investigators, Lambert and Clark,<sup>34</sup> and Pidgeon<sup>43</sup> found no hysteresis for either. At first sight this seems very confusing but, as we shall see later, all of these facts can be explained satisfactorily by assuming different pore size distributions in the different silica gel samples used by the above investigators.

Pidgeon<sup>43</sup> offered a simple and convincing explanation for Patrick's results on the water-silica gel system. In Patrick's experiments the pressure was altered by direct addition or removal of water vapor. However, when vapor is added directly the pressure is at first greater than the equilibrium value, so that adsorption occurs under falling pressure. Some parts of the gel will equilibrate quickly with the higher pressure, and the final equilibrium will be established by desorption from these parts and adsorption on the less accessible parts. Thus the processes of adsorption and desorption are taking place simultaneously. The reverse of this takes place on desorption; first the pressure is lowered below the equilibrium value, and then it rises as equilibrium is approached. This effect of mixing adsorption with desorption, and vice-versa, is particularly great if there is a large quantity of gel in the apparatus, as was the case in Patrick's experiments. According to Pidgeon this explains the apparent disappearance of the hysteresis loop.

There is no doubt that Pidgeon's explanation may account for part of Patrick's results, and his considerations are well worth keeping in mind by all who investigate adsorption at higher relative pressures. However, it was pointed out in Chapter X that Patrick's isotherms had different shapes from the usual water-silica gel isotherms; they were

<sup>41</sup> A. R. Urquhart, *J. Textile Inst.*, **20**, T117 (1929).

<sup>42</sup> B. Lambert and A. G. Foster, *Proc. Roy. Soc.*, **A134**, 246 (1931).

<sup>43</sup> L. M. Pidgeon, *Can. J. Res.*, **10**, 713 (1934).

<sup>44</sup> K. S. Rao, *J. Phys. Chem.*, **45**, 513 (1941).

not S-shaped, but apparently Langmuir-type. This indicates a difference in the pore structure that alone suffices to account for the disappearance of hysteresis, as we shall see later.

The phenomenon of reversible hysteresis is most strikingly shown in the work of Rao.<sup>44</sup> Figure 132 gives his water isotherms on silica gel at 30° C. Curve *A* represents the first adsorption-desorption isotherm, *B* the second, *C* the third and *D* the nineteenth. The first curve is obviously different from the others; it shows irreversible hysteresis due to the displacement of permanent gases. The water retained at zero pressure is probably chemisorbed by the gel. From

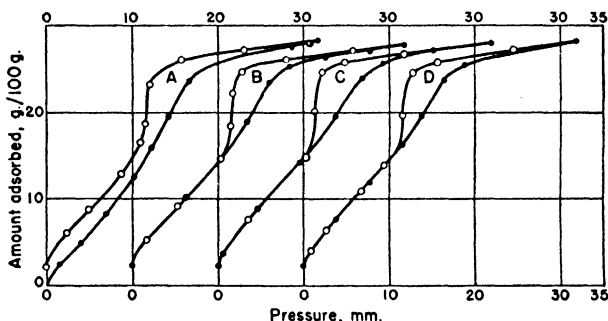


FIG. 132.—Reversible and irreversible hysteresis in the adsorption of water on silica gel.

the second curve on the adsorption-desorption isotherms remain unchanged; there is no tendency to drift. The third and the nineteenth hysteresis loops are identical with the second, even though a period of two months elapsed between the first and the last run.

A second illustration of the remarkable constancy of the hysteresis loops is shown in Fig. 133, representing adsorption isotherms of carbon tetrachloride on silica gel at 30° C., obtained by Rao.<sup>45</sup> The shapes of these curves are quite different from the water isotherms, but the shapes of the hysteresis loops are similar to the water hysteresis loops. Curves *A*, *B*, *C* and *D* represent the first, second, third and eighth adsorption-desorption isotherms. In this case all four curves are identical; not excepting even the first one. Incidentally, the total capillary volume of the silica gel is quite different when calculated from the saturation adsorptions of water and carbon tetrachloride. The former gives 28.0 cc. per 100 g. of gel, the latter 23.5 cc. This

<sup>45</sup> K. S. Rao, *J. Phys. Chem.*, **45**, 517 (1941).

indicates that Rao's gel had a large number of pores inaccessible to the bigger carbon tetrachloride molecules.

Rao <sup>46</sup> investigated the hysteresis loop by a process which he called "scanning" the loop. This is illustrated in Fig. 134. If one starts from any point on the adsorption branch and reduces the pressure, the loop is crossed and the desorption branch is reached. Starting from (1) experimental points are obtained along curve *B* until (2) is reached. If, however, one starts from the desorption branch and increases the pressure, the main adsorption branch is not reached, but a different curve is followed which joins the adsorption branch only at the

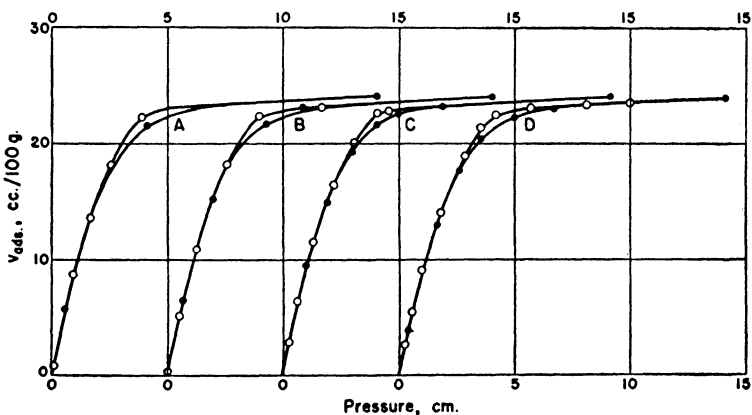


FIG. 133.—Reversible hysteresis in the adsorption of carbon tetrachloride on silica gel.

saturation pressure. Thus starting from (3) experimental points are obtained along curve *A* until (4) is reached. These curious results were explained by Rao in terms of a second theory of hysteresis, the so-called "ink-bottle" theory.

It was suggested by Kraemer <sup>47</sup> and elaborated in more detail by McBain <sup>48</sup> that the phenomenon of reversible hysteresis can be explained by the assumption that the pores are shaped like ink-bottles, having narrow necks and wide bodies. On the adsorption side the narrow neck will fill at relatively low pressures, but condensation in the

<sup>46</sup> K. S. Rao, *J. Phys. Chem.*, **45**, 506 (1941).

<sup>47</sup> E. O. Kraemer, in H. S. Taylor's "A Treatise on Physical Chemistry," New York, 1931, Chapter XX, p. 1661.

<sup>48</sup> J. W. McBain, *J. Am. Chem. Soc.*, **57**, 699 (1935).



body takes place only when

$$(5) \quad p_a = p_0 e^{-2\sigma V/r_b RT}$$

where  $r_b$  is the radius of the body of the capillary. On the desorption side, however, the pore will empty only when the pressure is reduced so far that the liquid in the neck of the pore will become unstable, i.e.,

$$(6) \quad p_d = p_0 e^{-2\sigma V/r_n RT}$$

where  $r_n$  is the radius of the neck of the pore. Since  $r_n^{\text{②}}$  is smaller than  $r_b$ ,  $p_a$  will be larger than  $p_d$ . In this theory the true equilibrium

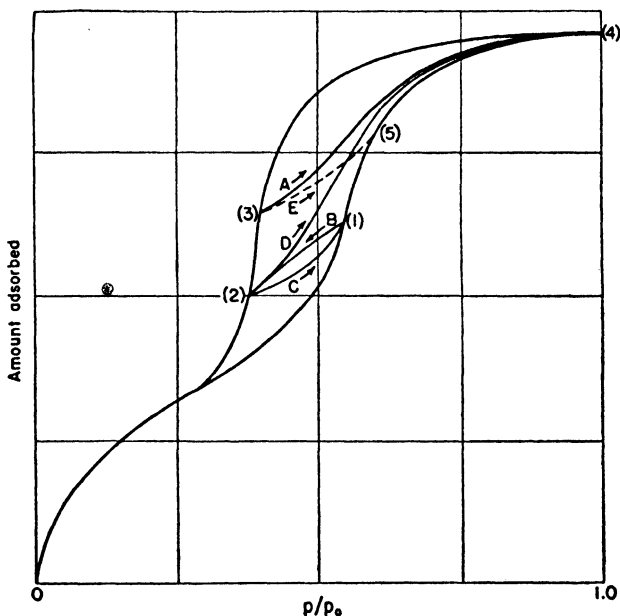


FIG. 134.—Scanning the hysteresis loop.

corresponds to the adsorption points since the important part of the liquid, that contained in the body of the pore, is in equilibrium with the vapor only on the adsorption side but not on the desorption side.

Rao <sup>46</sup> assumed that there are two types of pores in adsorbents: V-shaped pores and pores with constricted ends, shaped like ink-bottles or Erlenmeyer flasks. The V-shaped pores fill and empty reversibly, the others are responsible for hysteresis. At any point

along the main adsorption branch of the hysteresis loop there are some pores filled with liquid, some partly filled, and some empty. If in Fig. 134 one starts from (1) and reduces the pressure the partly filled capillaries will empty reversibly as one passes along curve *B* to (2). However, the completely filled pores will retain the water until the pressure is lowered to  $p_a$ , the equilibrium pressure of the liquid condensed in the neck. Thus the hysteresis loop is crossed until the desorption branch is reached. At lower pressures all of the pores empty completely.

At any point along the main desorption branch the pores are either completely full or completely empty, there are no partly filled pores. If one starts from some intermediate point (3) and increases the pressure the empty pores fill again as one passes along curve *A* to (4). At (3) all pores having neck radii smaller than a given value,  $r_n$ , are still full, and these pores have body radii ranging from small to large values. Because some of the pores with large bodies are full one does not obtain a curve like curve *E* rejoining the adsorption branch at (5). Obviously, such a curve would imply that the pores having the largest body radii were all empty at the starting point (3).<sup>49</sup>

The above considerations show that the ink bottle theory can account qualitatively for Rao's experimental results on hysteresis. So far the theory has not been formulated quantitatively, and probably such formulation would be very difficult. The adsorption and desorption pressures depend upon the radii of the body and the neck of the pore. Since there is no reason to expect any relation between  $r_b$  and  $r_n$ , there is no reason to expect any between  $p_a$  and  $p_d$ . However, the third theory of hysteresis, the open pore theory, does lead to a relation between  $p_a$  and  $p_d$  that can be tested experimentally. It is the only theory of hysteresis advanced to date that received a quantitative formulation, and some of its predictions are born out fairly well by experiment. The open pore theory does not give a complete explanation of hysteresis in all of its forms; it can not explain irreversible hysteresis, nor all of Rao's results on scanning the hysteresis loop. It does not include the theory of incomplete wetting and the ink bottle theory as special cases. Nevertheless, the three theories *together* can

<sup>49</sup> L. H. Cohan suggests an alternative explanation for Rao's results on adsorption following desorption. If the adsorbent contains some narrow pores with plane parallel walls the pore will not fill until the saturation pressure is reached, and it will not empty until the pressure is reduced to a value that depends on the width of the pore. In this case also if one starts from point (3) and increases the pressure, the adsorption curve will not join the main adsorption branch until the saturation pressure is reached. (To be published in the *J. Am. Chem. Soc.*)

give a reasonable explanation of the diverse facts of hysteresis in adsorption.

Foster<sup>22</sup> suggested that hysteresis was due to a delay in the formation of the meniscus in open pores<sup>50</sup> during the adsorption process. At the beginning of the hysteresis region there is an adsorbed film on the walls of the capillaries, at most only a few molecules thick. As the pressure is increased more adsorption takes place, but the meniscus does not form until the adsorbed film is thick enough to block the pore at its narrowest point. When this happens capillary condensation occurs immediately, but the wider pores still have only adsorbed liquid. At saturation all capillaries fill, and since this involves the formation of meniscus in every pore the desorption branch obeys the Kelvin equation. Thus the ascending branch of the loop corresponds to adsorption and capillary condensation occurring simultaneously, but the descending branch represents capillary condensation only.

It was pointed out in Chapter V that the potential of capillary condensation is temperature dependent, whereas the Polanyi adsorption potential is independent of temperature. Foster's calculations for the benzene-ferric oxide gel system, given in Table XII, Chapter V, show how accurately the descending branch of the hysteresis loop obeys the Kelvin equation. The ascending branch has a potential approximately independent of temperature, which seems to indicate that adsorption plays a considerably more important role along this branch than capillary condensation. The differential heats of adsorption calculated from the ascending branches were lower than those obtained from the descending branches, the difference being due to the heat of capillary condensation.

Foster obtained the structure curves of ferric oxide gel and silica gel by plotting the capillary radius, calculated from the Kelvin equation, against the volume of liquid adsorbed. His plot for benzene on ferric oxide gel was given in Fig. 63, Chapter V. Another plot, for alcohol on a water treated ferric oxide is shown in Fig. 135. It was calculated from the isotherms of Lambert and Foster.<sup>51</sup> A comparison of the two figures shows that the water treated gel has much wider pores than the normal gel. There are two important differences between the structure curves of Foster and those of Kubelka<sup>16</sup> (Fig. 128). In the first place, Foster's curves are plotted on the basis of the Kelvin equation, Kubelka's on the basis of his own semi-empirical

<sup>50</sup> The term "open pore" designates here a pore which is open on *both sides*. V-shaped and ink bottle shaped pores are not considered open pores.

<sup>51</sup> B. Lambert and A. G. Foster, *Proc. Roy. Soc., A136*, 363 (1932).

method. In the second place, Foster plotted the structure curves only for the hysteresis region in which capillary condensation is likely to play an important role, while Kubelka plotted them for the entire adsorption isotherm, including even the range of unimolecular adsorption, in which capillary condensation can play no part at all.

An inspection of either Fig. 63, or Fig. 135 shows that the desorption branch of the hysteresis loop has a point of inflection which corresponds approximately to the mean capillary radius. Thus in Fig. 63 the smallest capillary radius, that corresponding to the beginning of the

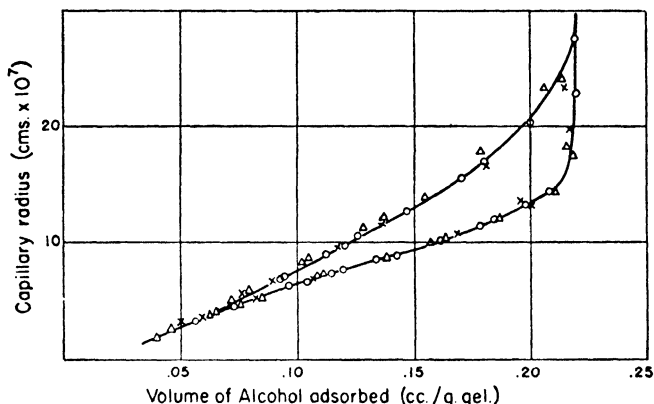


FIG. 135.—The structure curve of water treated ferric oxide gel, calculated from alcohol isotherms.

hysteresis loop, is  $14\text{\AA}$ ; the largest radius, that at the point where the desorption branch turns upward, is  $18\text{\AA}$ ; and the point of inflection is at  $16\text{\AA}$ . Likewise, in Fig. 135 the smallest radius is  $40\text{\AA}$ , the largest is  $140\text{\AA}$ , and the point of inflection is at  $90\text{\AA}$ . The reason for this point of inflection becomes clear if one plots the differentiated structure curve, or the pore frequency curve, for the desorption branch. On the structure curve each point gives the volume of the liquid  $v$ , necessary to fill all the pores having radii equal to or less than  $r$ . An addition of a small amount of liquid  $dv$  fills up the pores having radii between  $r$  and  $r + dr$ , so the curve obtained by plotting  $dv/dr$  against  $r$  shows the contribution of the pores of radius  $r$  to the total capillary volume of the gel. Such a curve, calculated from Fig. 63, is given in Fig. 136. The shape of the curve, like the shapes of Kubelka's curves in Fig. 129, resembles the Gauss error curve and implies that

the pores are distributed according to the laws of probability. The peak of the curve corresponds to the point of inflection on the desorption branch. Thus the capillary radius corresponding to the point of inflection is the most frequently occurring radius in the gel.<sup>52</sup>

To obtain the mean radius of an adsorbent one does not need to plot the differentiated structure curve, nor even the structure curve.

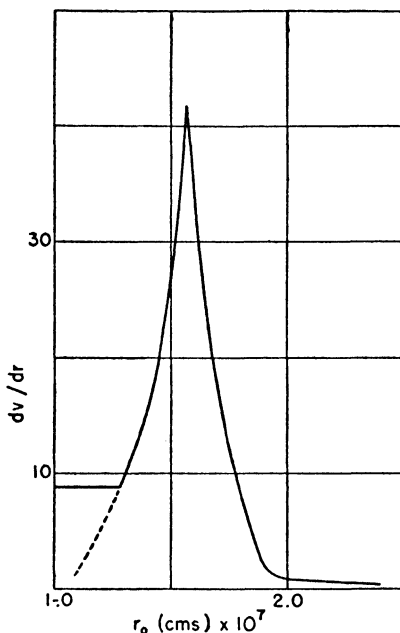


FIG. 136.—Differentiated structure curve, calculated from the structure curve of Fig. 63.

The point of inflection on the desorption branch of the hysteresis loop can be easily read off from the original isotherm, and the radius can be calculated from the Kelvin equation. Foster determined the adsorption isotherms of five different alcohols on ferric oxide gel<sup>53</sup> and on silica gel<sup>54</sup> up to saturation pressure, and calculated the mean radius from the point of inflection. His results are given in Table

<sup>53</sup> The frequency curve calculated from Fig. 139 for the water treated gel has a lower and less sharp peak.

<sup>54</sup> A. G. Foster, *Proc. Roy. Soc.*, A147, 128 (1934).

<sup>54</sup> A. G. Foster, *Proc. Roy. Soc.*, A150, 77 (1935).

LXVI. The agreement between the values obtained from different alcohols for the same adsorbent is very good. Of the two adsorbents silica gel has the narrower pores, but still its total capillary volume is almost 50% larger than that of the ferric oxide gel. This is, of course, due to the much larger surface of silica gel. Assuming that the beginning of the hysteresis loop indicates the beginning of capillary condensation, in the silica gel sample 85% of the saturation adsorption has already taken place when capillary condensation begins, in the ferric oxide gel only 46%.<sup>55</sup> An inspection of Foster's isotherms

TABLE LXVI  
THE MEAN CAPILLARY RADII OF FERRIC OXIDE GEL AND SILICA GEL

Alcohol	Ferric Oxide Gel		Silica Gel	
	Relative Pressure	Capillary Radius	Relative Pressure	Capillary Radius
Methyl	0.73	22.9 Å	0.64	16.3 Å
Ethyl	0.60	19.9	0.49	14.3
n-Propyl	0.55	22.9	0.38	14.1
iso-Propyl	0.56	21.8	0.44	15.6
n-Butyl	0.47	22.9	0.29	14.1

suggests that the beginning of the hysteresis loop corresponds roughly to two adsorbed layers on both silica gel and ferric oxide gel.

Mrs. Coelingh<sup>56</sup> used an optical method to investigate the adsorption of vapors on weathered glass. She noted that interference colors on the wall of a glass flask exhibited abrupt changes as the temperature was changed. She interpreted these color changes as being due to the sudden emptying or filling of capillaries in the glass. The changes in temperature produce changes in the relative pressure of the vapor. If the pore size distribution is discontinuous, capillaries of a given size suddenly empty or fill when a certain relative pressure is reached. This causes a sudden change in the interference color. Noting the relative pressure at which the color change occurs one can calculate the capillary radius from the Kelvin equation.

By using alcohol, benzene, carbon tetrachloride, water, ether and acetone to determine the radius of a certain group of capillaries Mrs. Coelingh obtained the values 6.93, 6.9, 7.1, 6.81, 6.7 and 6.6  $\mu\mu$ , respectively. These values were obtained on desorption, and the agreement between them is very good. Using the same vapors on

<sup>55</sup> On the water treated ferric oxide gel sample (Fig. 139) hysteresis begins when only 27% of the saturation adsorption has taken place.

<sup>56</sup> M. B. Coelingh, *Kolloid Z.*, **7**, 251 (1939).

adsorption she obtained the values 12.5, 12.5, 12.5, 12.6, 12.2 and 12.0  $\mu\mu$  for the *same* group of capillaries. The agreement between the six values is again excellent, but the calculated radii for the adsorption process are roughly twice as large as for the desorption process. For other groups of capillaries she also found the same approximately two fold discrepancy. As an explanation she suggested that the meniscus of the liquid condensed in the capillary has a cylindrical shape on adsorption, and a spherical shape on desorption. The vapor pressure lowering is calculated from the main radii of curvature  $r_1$  and  $r_2$ , and is a function of  $1/r_1 + 1/r_2$ . For a cylinder this gives  $1/r_1 + 1/\infty = 1/r_1$ ; for a sphere  $1/r_1 + 1/r_1 = 2/r_1$ . Thus the radius of curvature of the spherical meniscus is only half as large as that of the cylindrical meniscus, which results in a greater vapor pressure lowering on desorption than on adsorption. Although this suggestion accounts for the fact that the radii calculated from the adsorption experiments were twice as large as the radii obtained from the desorption side, it does not explain *why* the meniscus is cylindrical on adsorption and spherical on desorption.

Independently and somewhat before Mrs. Coelingh, Cohan<sup>57</sup> deduced a relation between  $p_a$  and  $p_d$ , the pressures at which a given capillary fills and empties, which also leads to the result that the radius of curvature during the adsorption process is twice as large as during desorption. His formulation is more successful than Mrs. Coelingh's since it gives a clear picture of the mechanism of filling and emptying of capillaries.

Cohan starts out with Foster's<sup>22</sup> idea that a delay in the formation of the meniscus during adsorption is responsible for the phenomenon of hysteresis. If a capillary is open at both ends the meniscus can not form during the adsorption process. In a cylindrical capillary condensation will occur if the pressure of the vapor is raised to a high enough value to form an annular ring of condensed liquid on the wall. When this pressure  $p_r$  is reached, not only will this ring of liquid form but the capillary will fill completely, since any inner annular ring has a lower vapor pressure than the outermost one. Cohan shows that the pressure at which the ring forms on the wall, i.e., the pressure at which the capillary fills during adsorption, is given by

$$(7) \quad p_a = p_r = p_0 e^{-\sigma V/rRT}$$

where  $r$  is the radius of the annular ring. If the capillary is wide and the adsorbed film is thin,  $r$  may be considered the radius of the capillary

<sup>57</sup> L. H. Cohan, *J. Am. Chem. Soc.*, 60, 433 (1938).

itself. When the capillary is full the meniscus forms, therefore during desorption the Kelvin equation is obeyed

$$(8) \quad p_d = p_0 e^{-2\sigma V/r'RT}$$

where  $r'$  is the radius of curvature of the meniscus. If the wetting is complete  $r' = r$ . A comparison of equations (7) and (8) shows that the radius of curvature corresponding to adsorption is twice as large as the desorption radius, and that  $p_a$  and  $p_d$  are related by the equation

$$(9) \quad p_a^2 = p_0 p_d$$

For narrower capillaries the thickness of the adsorbed film  $D$  can not be neglected in comparison with  $r$ . In equation (7) one must therefore use  $r - D$  in the denominator, instead of  $r$

$$(10) \quad p_a = p_0 e^{-\sigma V/(r-D)RT}$$

The relation between  $p_a$  and  $p_d$  becomes

$$(11) \quad p_d/p_0 = (p_a/p_0)^{2-2D/r}$$

A comparison of equations (8) and (10) shows that  $p_d$  becomes equal to  $p_a$  if

$$(12) \quad r = 2D$$

i.e., if the radius of the capillary is equal to twice the thickness of the adsorbed layer. Since the smallest possible value of  $D$  is the diameter of a molecule, equation (12) means that hysteresis can not occur in capillaries narrower than four molecular diameters. At the same time it follows from the equation that in open cylindrical capillaries hysteresis starts when  $r$  becomes greater than  $2D$ . One can therefore get the thickness of the adsorbed layer at the beginning of the capillary condensation from the equation

$$(13) \quad D = r_h/2$$

where  $r_h$  is the radius of the capillary corresponding to the beginning of the hysteresis loop, calculated from the Kelvin equation. Cohan<sup>39</sup> gives a detailed table containing  $r_h/2$  values calculated from the experiments of a number of investigators. The thickness of the adsorbed layer in this table ranges from values smaller than one molecular diameter to values somewhat larger than two molecular diameters. However, the beginning of hysteresis often indicates thicker adsorbed layers. Thus in Fig. 135  $r_h/2$  for water treated



ferric oxide gel is about  $20\text{\AA}$ , which corresponds to about four adsorbed layers of alcohol at the start of capillary condensation.

The correctness of Cohan's equation can be tested by investigating the relation between  $p_a$  and  $p_d$ . For wide pores this is given by equation (9), for narrow pores by equation (11). Equation (11) has not been tested yet satisfactorily.<sup>58</sup> Emmett<sup>59</sup> tested equation (9) and found that some of his data obey it reasonably well above  $p/p_0 = 0.8$ . Fairly good agreement with equation (9) is found also in the experiments of Mrs. Coelingh,<sup>56</sup> as we have seen before.<sup>60</sup>

Cohan's theory can explain at once why certain vapors exhibit hysteresis on a given adsorbent while other vapors show no hysteresis on the same adsorbent. Hysteresis occurs only in capillaries more than four molecular diameters wide. If a capillary is fairly narrow, it can be more than four molecular diameters wide for a small molecule, like water, but less than four molecular diameters wide for a large molecule, like benzene. Thus water will show hysteresis while benzene will not. We may recall that Anderson's<sup>30</sup> silica gel showed hysteresis for both water and benzene while Lambert's<sup>34, 42</sup> showed hysteresis only for water but not for benzene. This would indicate that Lambert's silica gel had narrower pores than Anderson's. Judging on the basis of the saturation adsorption of benzene the total pore volume of Lambert's gel was 0.203 cc./g. while that of Anderson's was 0.553 cc./g. Although there are undoubtedly differences in the surface areas, probably the greatest part of the difference between the pore volumes comes from the different average pore diameters of the two gels.

Following Mrs. Coelingh<sup>56</sup> we may subdivide all adsorbents into four groups according to the average pore radius. To the first group belong adsorbents that have very narrow pores, like chabasite and some charcoals. These exhibit only adsorption but no capillary condensation, consequently isotherms of even the smallest molecules show no hysteresis. In the second group are the adsorbents with

<sup>58</sup> L. H. Cohan (Footnote 39) tested equation (11) in a very unsatisfactory manner. He took the data of Rao's experiments (Footnotes 41, 42, 43), but instead of calculating  $D$ , the thickness of the adsorbed layer, from Rao's curves, he calculated it from Higuti's experiments. [I. Higuti, *Bull. Inst. Phys. Chem. Res. (Tokyo)*, 18, 657 (1939); 19, 951 (1940); 20, 130 (1941).] This unjustified procedure makes Cohan's calculations meaningless.

<sup>59</sup> P. H. Emmett, in E. O. Kraemer's "Advances in Colloid Science," New York, 1942, Chapter I.

<sup>60</sup> Finding the radius of curvature on adsorption twice as large as on desorption is equivalent to a proof of equation (9).

somewhat wider pores, with radii in the vicinity of  $10\text{\AA}$ . Charcoals of wider pores and silica gels of narrower pores belong to this group. These adsorbents show hysteresis for small molecules, like water, but no hysteresis for large molecules, like benzene. In the third group are the adsorbents with still larger pores, which show hysteresis for all vapors. (Lambert's silica gel belongs to the second group, Anderson's to the third group. Mrs. Coelingh's weathered glass also belongs to the third group.) Finally, in adsorbents with very large pores capillary condensation occurs so close to the saturation pressure that the hysteresis loop can not be determined at all. To this fourth group belong some of the gels of van Bemmelen,<sup>61</sup> which on ageing showed a widening of the pores until hysteresis completely disappeared.

Several investigators noted discontinuities in the desorption branch of the hysteresis loop similar to those found in the stepwise isotherms, discussed in Chapter X. These steps were experimentally investigated by Burrage,<sup>62</sup> Foster,<sup>53,54</sup> Mrs. Coelingh,<sup>56</sup> Radulescu and Tilenschi,<sup>63</sup> and others. Probably the explanation of the phenomenon is found in a discontinuous distribution of the capillary diameters.

Radulescu and Radulescu<sup>64</sup> assumed that the radius of curvature of the meniscus is an integral multiple of the radius of the adsorbent molecule, i.e.,

$$(14) \quad r = nr_m$$

where  $r_m$  is the radius of the molecule and  $n$  is an integer. Naturally, this assumption would lead to discontinuities in the desorption branch of the hysteresis loop. With the help of a number of other assumptions the investigators calculated  $r_m$  for benzene, carbon tetrachloride and benzyl chloride from the discontinuities of the desorption isotherms of these vapors on charcoal. The values came out lower than the molecular radii calculated from liquid densities. Although Radulescu and Radulescu offered certain explanations for these low values, it seems safer to conclude that the relation suggested in equation (14) is not yet proven.

#### ALTERATION OF THE PORE STRUCTURE OF THE ADSORBENT

Changes in the pore structure of the adsorbent, like changes in the surface, can be produced by external factors, such as heat, chemical agents, etc., or by the adsorption process itself. As a matter of fact,

<sup>61</sup> J. M. van Bemmelen, *Z. anorg. allgem. Chem.*, **13**, 239 (1896).

<sup>62</sup> L. J. Burrage, *Trans. Far. Soc.*, **29**, 570 (1933); **30**, 317 (1934).

<sup>63</sup> D. Radulescu and S. Tilenschi, *Z. phys. Chem.*, **A179**, 210 (1937).

<sup>64</sup> D. Radulescu and F. Radulescu, *Kolloid Z.*, **87**, 241 (1939).

even though adsorbents are usually regarded as rigid bodies the adsorption process quite often, perhaps always, causes a change in the pore volume. The change caused by the adsorbate is either reversible or irreversible.

An example of an irreversible effect is shown in Fig. 137, representing adsorption isotherms of water on ferric oxide gel at 30° C., obtained by Rao.<sup>65</sup> The first five runs are not shown in the figure; the curves represent the sixth, seventh, eighth, ninth and tenth adsorption runs. The ten runs extended over a period of four months. There is clearly a very definite drift in the hysteresis loop. The

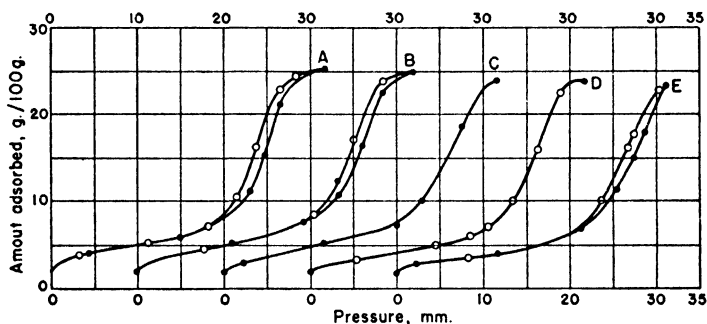


FIG. 137.—Drift in the hysteresis loops of water isotherms on ferric oxide gel.

adsorption at saturation pressure decreases in every consecutive experiment indicating a gradual decrease in the total capillary volume. The saturation adsorption was 0.267 grams per gram of gel in the first run, and 0.232 g./g. in the last. Rao obtained no such drift in the adsorption isotherms of water on silica, titania and alumina gels; the hysteresis loops were completely reproducible. He believes that the drift in the case of the ferric oxide gel is due to a growth of the particles. This growth results in larger sized capillaries, fewer in number.

Much greater alterations in the structure of a gel were obtained in consecutive adsorption runs by Harbard and King.<sup>66</sup> Their results for the adsorption of chloroform on chromic oxide gel were shown in Fig. 121. The drastic changes that occurred in the shapes of the isotherms and in the amounts adsorbed at low and high pressures.

<sup>65</sup> K. S. Rao, *J. Phys. Chem.*, **45**, 522 (1941).

<sup>66</sup> E. H. Harbard and A. King, *J. Chem. Soc.*, 1940, 19.

indicated marked changes both in the surface and in the pore structure of the gel.

Irreversible alterations in the structure of the adsorbent are rather unusual, but reversible changes probably always occur during the adsorption process. Not only gels, but even charcoal expands during adsorption, and then contracts to its original dimensions when the adsorbate is removed. Meehan<sup>67</sup> was the first to measure the expansion of charcoal caused by the adsorption of carbon dioxide. He found that the expansion of wood charcoal was isotropic, i.e., independent of the direction of the grain; he obtained the same values whether he measured the expansion along the grain, radially, or tangentially. This behavior is very different from the expansion of wood due to adsorption of moisture, and it indicates that the fibrous structure of wood is destroyed in the process of carbonization. The cubical coefficient of expansion for the adsorption of 1 atm. of carbon dioxide was 0.66% at 16.4° and 0.75% at 10.0° C., doubtless because at the lower temperature the adsorption is greater. As a matter of fact, the variation of the linear expansion with pressure at constant temperature followed in general the shape of an adsorption isotherm. Meehan found that the variation of the expansion with pressure and with temperature could be represented reasonably well by equations formally identical with the isotherm and isobar equations of Williams and Henry (Chapter IV).

McBain<sup>68</sup> pointed out that according to the capillary condensation theory the adsorbate should cause a contraction of the adsorbent, rather than an expansion. The liquid under a concave meniscus is subjected to a tension, not a compression, and this tension should contract the adsorbent. McBain states that the fact that all investigators found expansion for charcoal, and not contraction, disproves the capillary condensation theory for this adsorbent. Perhaps it would be more correct to say that capillary condensation plays a subordinate role or is completely absent in the adsorption of vapors on certain charcoals, particularly on those containing very narrow pores.

McBain, Porter and Sessions<sup>69</sup> measured the expansion of charcoal caused by the adsorption of benzene, heptane and water. The

<sup>67</sup> F. T. Meehan, *Proc. Roy. Soc.*, A115, 199 (1927).

<sup>68</sup> J. W. McBain. *The Sorption of Gases and Vapors by Solids*, London, 1932, p. 148.

<sup>69</sup> J. W. McBain, J. L. Porter and R. F. Sessions, *J. Am. Chem. Soc.*, 55, 2294 (1933).

expansion follows the general shape of the adsorption isotherm: with the organic vapors large expansion occurs at low relative pressures, while with water most of the expansion occurs at higher relative pressures. Temperature has a curious effect in the experiments with water. When the charcoal is heated to a few degrees above room temperature it contracts, then on cooling expands again. The reason for this is that the volume change caused by the adsorption and the desorption of water is much greater than that due to the heat expansion of charcoal.

Bangham and his collaborators made probably the most extensive study of the expansion of charcoal due to adsorption of vapors. Their results on the whole agree well with the results discussed above. However, Bangham, Fakhoury and Mohamed <sup>70</sup> observed that in the adsorption of benzene and pyridine at low pressures the initial expansion of the charcoal was followed by a slight contraction that went on for hours. McBain, Porter and Sessions <sup>69</sup> obtained no such relaxation effect with benzene. They ascribed the findings of Bangham and his collaborators to incomplete evacuation of the charcoal and to the displacement of the adsorbed air by the organic vapor.

Bangham and Razouk <sup>71</sup> attribute the expansion of charcoal to the surface pressure of the adsorbed gas. They developed a method for finding the two-dimensional equation of state for the adsorbed film and used it for expressing the adsorption data of Coolidge <sup>72</sup> for benzene, methyl alcohol and water on charcoal. They made a semi-empirical comparison between these data and the results that Bangham, Fakhoury and Mohamed <sup>70</sup> obtained for the expansion of charcoal caused by the same three vapors, and found a tolerably good agreement.<sup>73</sup>

In the experiments on charcoal the overall linear expansion of a block of the adsorbent is always measured, so that one can draw only indirect conclusions as to what happens with the individual capillaries. For some other adsorbents, however, the expansion of the pores due to adsorbed vapor can be determined directly by means of x-ray diffraction photographs. Some layer crystals, notably graphitic acid and

<sup>70</sup> D. H. Bangham, N. Fakhoury and A. F. Mohamed, *Proc. Roy. Soc.*, **A138**, 162 (1932).

<sup>71</sup> D. H. Bangham and R. I. Razouk, *Trans. Far. Soc.*, **33**, 1463 (1937).

<sup>72</sup> A. S. Coolidge, *J. Am. Chem. Soc.*, **46**, 596 (1924).

<sup>73</sup> W. Lemcke and U. Hofmann (*Angew. Chem.*, **47**, 37, 1934) connect the hysteresis found in the adsorption isotherms of carbon tetrachloride on certain activated carbons with the volume expansion of the adsorbent, and attribute it to a dilation of the grain pores of the carbon.

montmorillonite, adsorb water between the layers, and the resulting increase in the spacing can be measured by x-ray diffraction. The interferences due to the arrangement of the carbon and oxygen atoms constituting a layer of graphitic acid remain unchanged as water is adsorbed but the distance between the layers increases. Thus according to Hofmann <sup>74</sup> in dry graphitic acid (containing 9% water) the distance between layers is  $6.1\text{\AA}$ , but when the adsorbent contains 35% water the distance is  $10\text{\AA}$ . Observing under a microscope a single crystal of graphitic acid one can directly see the expansion;

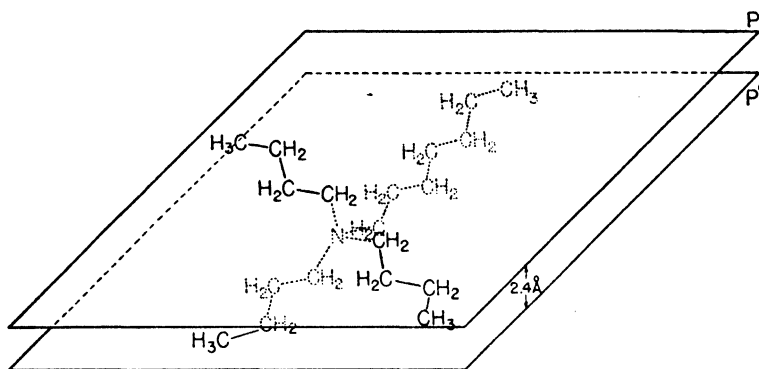


FIG. 138.—Increase in the spacing of montmorillonite layers caused by the adsorption of a heptyltributylammonium ion.

the adsorbent opens up just like an accordion. The swelling is completely reversible; on drying the layers contract to their original spacing. The expansion found by Hofmann probably corresponds to a monolayer of water adsorbed on each side of the graphitic acid layer.

The hydrous magnesium aluminum silicate mineral montmorillonite is likewise composed of layers that undergo expansion when water or some other substance is adsorbed between them. Hendricks, Nelson and Alexander <sup>75</sup> followed by x-ray diffraction photographs and by differential thermal analysis the changes occurring in montmorillonite with increasing relative pressure of water, and noted the building up of several adsorbed layers. Hendricks <sup>76</sup> measured the increase in the spacing of montmorillonite layers due to the adsorption

<sup>74</sup> U. Hofmann, *Kolloid Z.*, **69**, 351 (1934).

<sup>75</sup> S. B. Hendricks, R. A. Nelson and L. T. Alexander, *J. Am. Chem. Soc.*, **62**, 1457 (1940).

<sup>76</sup> S. B. Hendricks, *J. Phys. Chem.*, **45**, 65 (1941).

of various organic cations. From the observed increase he was able to conclude that organic molecules tend to lie flat on the surface, occupying the maximum possible surface and the minimum possible thickness. This is illustrated in Fig. 138, representing the adsorption of a heptyltributylammonium ion between two montmorillonite layers.

Some of our most important industrial materials are capable of taking up large quantities of water and other vapors, meantime undergoing considerable swelling. The fibres of cellulose deform and swell on the adsorption of water. McBain <sup>77</sup> found that substances which are known to be good solvents for nitrocellulose are taken up by it in large quantities, causing a large swelling, while poor solvents are taken up only slightly. For example, the solvents methyl and ethyl alcohol increase the volume of a dry film of nitrocellulose by 1939% and 1377%, respectively, while benzene and toluene cause a volume increase of only 1.4 and 1.2%, respectively. Speakman <sup>78</sup> determined the swelling of wool fiber caused by water. He found that the length of the fiber increased only 1.1%, but the cross-section increased 18%. The pore width in the dry fiber is about equal to the length of a propyl alcohol molecule. Butyl and amyl alcohol molecules therefore can not enter the pores, but methyl alcohol and ethylene glycol molecules can enter readily. When these smaller molecules enter the pores they cause such a great swelling that afterwards even octyl alcohol molecules can penetrate.

If montmorillonite is completely immersed in water the swelling is carried to such an extreme that the individual layers separate and form a colloidal solution. Disintegration caused by sudden swelling was demonstrated by Zsigmondy <sup>38</sup> for silica gel. When a dry sample is thrown into water it bursts from the sudden local strains. McBain <sup>79</sup> states that Porter in his laboratory made dehydrated chabasite disintegrate by too rapid exposure to water. Evans <sup>80</sup> finds that the adsorption of ammonia breaks up dehydrated chabasite into a fine crystalline powder. Apparently, the ammonia molecules can penetrate to all the places where the smaller water molecules were located before dehydration, but the penetration sets up great strains that shatter the adsorbent.

<sup>77</sup> J. W. McBain, *The Sorption of Gases and Vapours by Solids*, London, 1932, p. 373.

<sup>78</sup> J. B. Speakman, *Nature*, 126, 565 (1930).

<sup>79</sup> J. W. McBain, *The Sorption of Gases and Vapours by Solids*, London, 1932, p. 394.

<sup>80</sup> M. G. Evans, *Proc. Roy. Soc., A134*, 97 (1931).

Some adsorbents must be carefully protected from contact with certain adsorbates, otherwise a chemical reaction results that may injure or completely destroy the adsorbent. Thus siloxene,  $\text{Si}_6\text{O}_5\text{H}_6$ , an adsorbent prepared by Kautsky,<sup>81</sup> is spontaneously inflammable when exposed to air.

The examples discussed so far illustrate reversible and irreversible alterations in the adsorbent caused by the adsorption process itself. Alterations may also be caused by heat, chemical agents and other factors, both in the positive and negative sense, i.e., with a resulting increase or decrease in the pore volume of the adsorbent. Ordinarily, an increase or decrease of the pore volume goes hand in hand with an increase or decrease of the surface; in such cases one deals with clear-cut examples of activation or sintering. Occasionally, however, an increase in the pore volume is produced at the expense of decreasing the surface. An example of this is shown in Fig. 139, representing the adsorption of benzene on four differently prepared silica gels, taken from Holmes and Elder.<sup>82</sup> Gel 1 is a "vitreous" gel prepared by the method of Patrick,<sup>83</sup> i.e., by mixing hot sodium silicate with an equal volume of 10% hydrochloric acid, allowing the gel to set, washing out the excess acid and salt, and drying the product in air. Gel 3 is a "chalky" gel prepared by the method of Holmes, i.e., by adding ferric chloride to a sodium silicate solution, drying the gel to a moisture content of 55–60%, and removing the iron oxide by treatment with acid. Gel 4 was prepared like Gel 3, except that copper sulfate was used in place of ferric chloride.

The adsorption of benzene from an air stream carrying different partial pressures of the vapor was measured. As Fig. 139 shows, the four gels give very different adsorption isotherms. Particularly sharp is the contrast between Gels 1 and 4. At 25% saturation Gel 1 has twice as large adsorption as Gel 4, but at 100% saturation only one-fifth as large adsorption. This means that the surface of Gel 1 is about twice as large as that of Gel 4, but the pore volume of the latter is five times as large as that of the former. The two other gels are intermediate both in surface and in pore volume.

In Patrick's process the activation of the gel consists in removing water, just as in the dehydration of chabasite, and this leaves an adsorbent with relatively fine pores.<sup>84</sup> In Holmes' process the much

<sup>81</sup> H. Kautsky and G. Blinoff, *Z. phys. Chem.*, **A139**, 497 (1928).

<sup>82</sup> H. N. Holmes and A. L. Elder, *J. Phys. Chem.*, **35**, 82 (1931).

<sup>83</sup> W. A. Patrick, U. S. Patent 1,297,724.

<sup>84</sup> However, F. E. Bartell and E. G. Almy (*J. Phys. Chem.*, **36**, 475, 1932) find that if too much of the water is removed the gel structure collapses. According to



larger iron oxide molecules are removed, and the pores are consequently much wider. An activation process similar to that of Holmes was used by Wolochow in preparing active silica from the mineral serpentine,  $3\text{MgO} \cdot 2\text{SiO}_2 \cdot 2\text{H}_2\text{O}$ . Dilute acids remove the magnesium oxide

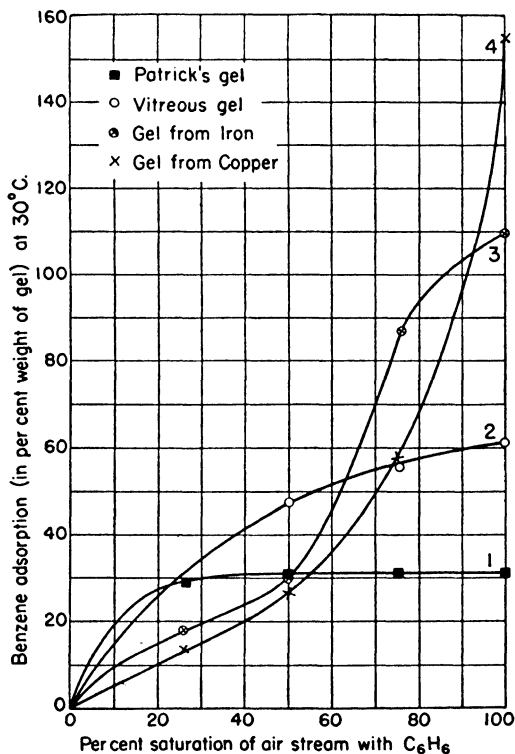


FIG. 139.—Adsorption of benzene on four different silica gels.

and the water, leaving only the silica framework. This retains the same spatial arrangement after the acid treatment as it had before, and so a porous structure is obtained. The effect of acid treatment on the adsorption of water by this active silica is shown in Table

these investigators water is held in at least two forms. Part of it is held in large capillaries; this part can be easily removed, with a resulting increase in the pore space and the surface of the gel. The rest is held in very fine capillary spaces; this is removed with difficulty, with a resulting collapse of the pore structure and decrease in the surface.

LXVII, taken from Pidgeon.<sup>85</sup> In the formula of serpentine the  $\text{SiO}_2$  corresponds to 43.3% of the original weight of the material. As Column 4 shows, the closer this theoretical limit is approached, the greater the adsorptive power of the silica. There is not much difference between the actions of hydrochloric acid and sulfuric acid, but nitric acid seems to give a poorer adsorbent. This is probably

TABLE LXVII  
EFFECT OF ACID TREATMENT ON ADSORPTION OF WATER BY ACTIVE SILICA

Acid	Conc.	Time of Boiling hr.	% Recovery	Amount Adsorbed at $p/p_0$			
				0.20	0.50	0.70	0.95
$\text{H}_2\text{SO}_4$	1 : 3	3	47.8	5.8	10.5	13.2	—
$\text{H}_2\text{SO}_4$	1 : 3	6	44.5	6.1	11.0	15.4	22.5
$\text{H}_2\text{SO}_4$	1 : 3	16	42.7	5.6	10.0	14.2	19.2
$\text{H}_2\text{SO}_4$	1 : 3.5	3	46.3	5.4	10.0	13.8	19.0
$\text{H}_2\text{SO}_4$	1 : 2.75	3	45.6	4.5	9.0	12.6	18.2
HCl	20%	2	47.8	5.9	10.5	15.8	22.7
HCl	20%	4	46.2	5.0	10.2	14.5	20.8
$\text{HNO}_3$	35%	2	51.7	4.5	8.8	12.0	16.8
$\text{HNO}_3$	40%	3 *	57.3	4.0	8.0	10.7	14.0

\* 60–90° C.

because the mineral is less soluble in nitric acid; as Column 4 shows, the percentage recovery is quite far from the theoretical limit.

Barker<sup>86</sup> showed that in the activation of charcoal the pore space increases by a factor of 2 (Table LVI, Chapter X). However, activation does not merely increase the total pore volume, it also makes the capillaries more accessible to the adsorbate, either by burning off hydrocarbon impurities that clog up their entrance or by removing a layer of carbon atoms with a resulting widening of the pores. King<sup>87</sup> also came to the conclusion that activation widens the pores of charcoal. For the activation he used oxygen at different temperatures and for various lengths of time. With increasing activation he obtained adsorption of larger and larger molecules in increasing amounts. His results for activation at 950° C. are given in Table LXVIII. The adsorption values are given in  $10^{-5}$  equivalents per gram of charcoal, adsorbed from an  $N/50$  solution of the acid. It will be noted that the three smallest molecules give large adsorption values even before activation, then a gradual increase in the course of activation. Phenylpropionic acid (Column 5) has a small adsorption before activation and a large increase after a short activation. H-acid (aminonaphthol-

<sup>85</sup> L. M. Pidgeon, *Can. J. Res.*, 12, 41 (1935).

<sup>86</sup> M. E. Barker, *Ind. Eng. Chem.*, 22, 296 (1930).

<sup>87</sup> A. King, *J. Chem. Soc.*, 1934, 1975.

disulfonic acid) shows no adsorption before activation but a considerable adsorption after 2 hours, while eosin shows adsorption only after 4 hours of activation, and Congo Red only after 11 hours. It is clear from these facts that activation by means of oxygen widens the pores of charcoal. Too long activation leads to graphitization and destruction of the pores. Just as in the case of chabasite the largest

TABLE LXVIII  
ADSORPTION ON CHARCOAL AFTER OXYGEN ACTIVATION AT 950° C.

Time of Activation Hours	CH <sub>3</sub> COOH	C <sub>6</sub> H <sub>5</sub> COOH	C <sub>6</sub> H <sub>5</sub> CH <sub>2</sub> COOH	C <sub>6</sub> H <sub>5</sub> C <sub>7</sub> H <sub>4</sub> COOH	H-Acid	Eosin	Congo Red
0	24.6	51.8	45.4	6.7	0	0	0
2	46.0	69.4	61.5	51.4	11.8	0	0
4	53.7	88.3	87.1	77.0	18.3	2.0	0
7	60.4	104.8	115.0	97.4	28.0	3.7	0
11	63.7	141.3	128.9	125.4	35.6	5.9	1.2
21	73.4	180.4	185	194	44.6	8.1	15.0
30	78.2	226	228	230	64.4	19	17.5
48	79.0	226	228	234	55.8	13	16.9

pores collapse first. After 48 hours of activation the adsorption of the four smallest molecules remains practically the same as it was after 30 hours, but the three largest molecules show a decrease in the adsorption.

There are several ways to diminish or to destroy the pore structure of an adsorbent, the most common being the use of heat. Sufficiently high temperatures destroy the pore structure of any adsorbent. Lamb and Woodhouse<sup>8</sup> found that the pores in chabasite begin to collapse around 510° and the destruction proceeds rapidly around 640° C. Howard and Hulett<sup>26</sup> noted a decrease in the surface and the pore volume of coconut charcoal around 1100–1200° C. and complete graphitization around 1600° C. Patrick, Frazer and Rush<sup>88</sup> encountered an appreciable diminution in the pore volume of silica gel around 800° and a very strong sintering around 1000° C. Figure 140 illustrates their results. Curve 1 gives the total pore volume obtained from determination of the apparent density by displacement of mercury. Curve 2 gives the adsorption of carbon tetrachloride from an air stream 43% saturated with the vapor. As the curves show, the total pore volume begins to decrease at a lower temperature than the adsorptive capacity. This is reasonable since the macropores are likely to collapse first, and the adsorption in them constitutes only a negligible fraction of the total.

<sup>88</sup> W. A. Patrick, J. C. W. Frazer and R. I. Rush, *J. Phys. Chem.*, **31**, 1511 (1937).

Ageing also changes the pore volume of a gel. Manegold<sup>39</sup> reports that three silica gel samples of van Bemmelen, one fresh, one 6 months old, and one 5 years old had pore volumes of 0.410, 0.485 and 0.570 cc./g., respectively, judged on the basis of density measurements. Ageing, therefore, in this instance increased the *total* pore volume. On the other hand Holmes and Elder<sup>32</sup> noted the effect of ageing on eleven samples of silica gel and found in every case a decrease in the *capillary* volume. This was determined by the saturation adsorption of benzene at 30° C. The decrease in adsorption ranged from 2 to

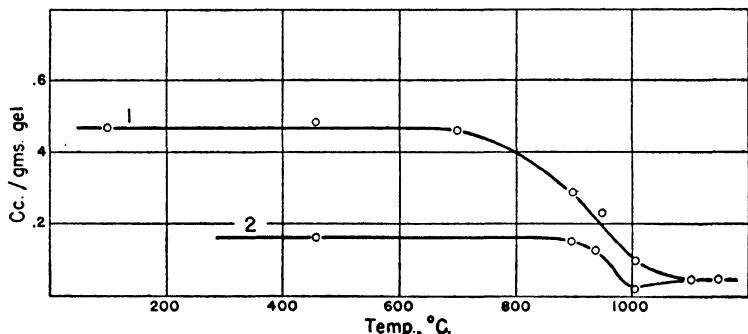


FIG. 140.—Effect of heat treatment on (1) the total pore volume of silica gel and (2) on the adsorption of carbon tetrachloride.

34%. These two results together may mean that ageing decreases the pore volume in some cases and increases it in others, but they may also mean that ageing decreases the volume of the micropores and increases the volume of the macropores and of the total pore space. Only determinations of the capillary pore space and of the total pore space performed on the same gel sample can settle this question definitely.

Treating a gel with water alters considerably the pore structure. Lambert and his collaborators<sup>34, 42</sup> find that water-treated ferric oxide gel has a smaller capillary volume than the untreated gel. The saturation adsorptions of alcohol and benzene on the normal gel were 0.284 and 0.274 cc. of liquid per gram; on the water treated gel they were 0.215 and 0.205 cc. per gram, respectively. On the other hand, the average capillary diameter of the water treated gel is about 5 or 6 times as large as that of the untreated gel, as we have seen before. These results are not contradictory; they simply mean that the water treated gel has a much smaller number of capillaries.

<sup>39</sup> F. Manegold, *Kolloid Z.*, 81, 19 (1937).

## CHAPTER XII

### THE ADSORBATE

In the three preceding chapters we discussed the information obtained about the adsorbent from physical adsorption investigations, particularly about the extent and structure of its surface, and the sizes and distribution of its pores. The present chapter deals with the nature of the adsorbate. Much of what is known about the properties of the adsorbed phase has already been presented in the chapters on the adsorption isotherm. The forces of interaction between the adsorbent and the adsorbate were examined in the chapters on the heat of adsorption.

The similarity between the behavior of the adsorbate and of a non-ideal gas or a liquid has been repeatedly emphasized. In the present chapter we point out further similarities and also dissimilarities. The first part is devoted mostly to experimental investigations of the physical properties of the adsorbate, such as its density, specific heat, light absorption, etc. The second part deals with various attempts to find a suitable equation of state for the adsorbate. The third part discusses the phase changes in the adsorbate.

#### SOME PHYSICAL PROPERTIES OF THE ADSORBATE

We have seen in Chapter V that the density distribution in the adsorbed phase can be evaluated by means of the potential theory. The first direct experimental determinations of the density of the adsorbate were made by Ewing and Spurway<sup>1</sup> and by De Vries.<sup>2</sup> In both investigations helium was used as the displaced fluid.

Ewing and Spurway<sup>1</sup> determined the density of water adsorbed on silica gel at 25° C. Using a gel sample of 38.65 g. they obtained for the adsorption of 0.40, 0.64 and 1.69 g. of water the density values of 1.0195, 1.0270 and 1.0285 g./cc., respectively. These values are greater than the density of liquid water; they correspond to the density of water compressed to about 750 atmospheres. At these adsorptions the residual pressure of water was so low that it could not be read on a manometer. For the adsorption of 2.11 and 2.57 g. of water they

<sup>1</sup> D. T. Ewing and C. H. Spurway, *J. Am. Chem. Soc.*, **52**, 4635 (1930).

<sup>2</sup> T. De Vries, *J. Am. Chem. Soc.*, **57**, 1771 (1935).

measured densities of 0.8305 and 0.5408 g./cc., respectively; the residual pressure of water was about 4 mm. The density values indicate that the adsorbate is composed of two phases: liquid and compressed vapor.

De Vries<sup>2</sup> determined the density of carbon dioxide absorbed by charcoal at 30° C. and at different pressures, and compared it with the average density calculated from the potential theory. In the calculations he used the method of Lowry and Olmstead,<sup>3</sup> discussed in Chapter V. Comparisons between the theoretical and experimental values showed that helium did not penetrate the adsorbed carbon dioxide layer when its density was greater than 0.09 g./cc. Furthermore, the theoretical and experimental values agreed well with each other if the assumption was made that helium penetrated the outer 10% of the adsorbate.

Danforth and De Vries<sup>4</sup> determined the densities of carbon tetrachloride and acetone adsorbed on charcoal at 30° C. over the entire isotherm up to the vicinity of the saturation pressure. Their results for carbon tetrachloride are shown in Fig. 141. At first there is a very sharp decrease with the amount adsorbed, followed by a gradual increase. The density of the normal liquid is 1.576 g./cc. The very high initial values doubtless indicate that the vapor adsorbed on the most active part of the charcoal is under very great compression. Perhaps the vapor is adsorbed in the narrowest pores, not much more than one molecular diameter wide. The rising part of the curve probably corresponds to adsorption on the normal charcoal surface. At lower pressures the adsorbate consists of a liquid and a vapor phase; with increasing pressure more of the liquid forms. Danforth and De Vries calculated the surface of their charcoal by means of the straight line equation of the multimolecular adsorption theory,<sup>5</sup> and found that the density corresponding to the adsorption of a complete monolayer was equal to the density of the normal liquid. Acetone gave similar results. The minima in the density curves of carbon tetrachloride and acetone correspond to 15–20% covering of the surface.

- Determination of the specific heat of the adsorbate supplies further interesting information about the state of adsorbed matter. Porter and Swain<sup>6</sup> reported that S. B. Thomas obtained a specific heat of

<sup>2</sup> H. H. Lowry and P. S. Olmstead, *J. Phys. Chem.*, **31**, 1601 (1927).

<sup>3</sup> J. D. Danforth and T. De Vries, *J. Am. Chem. Soc.*, **61**, 873 (1939).

<sup>5</sup> S. Brunauer, P. H. Emmett and E. Teller, *J. Am. Chem. Soc.*, **60**, 309 (1938).

<sup>6</sup> J. L. Porter and R. C. Swain, *J. Am. Chem. Soc.*, **55**, 2792 (1933).

8.5 calories for 6 g. of water adsorbed on 18 g. of highly active sugar charcoal at 10° C. If one assumes that charcoal has the same specific heat as graphite, one gets  $5.6 \pm 0.2$  calories for the specific heat of the 6 g. of adsorbed water. Since the specific heat of ice is only 0.5, it is clear that the adsorbate is very much like liquid water under compression. At 0° C. and 4000 atm. pressure the specific heat of water is 0.92.

More reliable data for the specific heat of the adsorbate were obtained by Simon and Swain.<sup>7</sup> They determined the specific heats

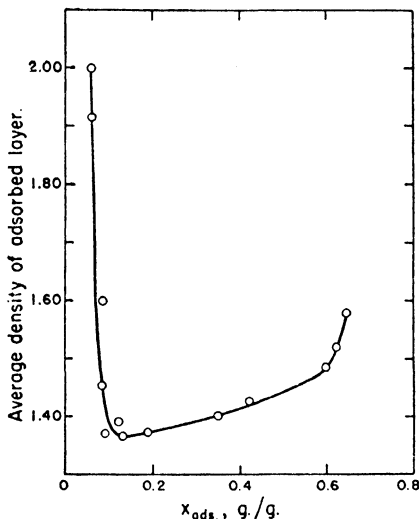


Fig. 141.—Density of carbon tetrachloride adsorbed on charcoal.

of argon and hydrogen on charcoal at very low temperatures. The advantage of using low temperatures is that the specific heat of the solid adsorbent decreases to a low value while that of the adsorbate remains relatively high. The results with hydrogen were ambiguous because the determination was complicated by the simultaneous occurrence of the ortho-para conversion reaction. The results with argon, however, were clear cut. They are shown in Fig. 142. The specific heat of the adsorbate is much smaller than that of solid argon; it is only 2 cal./deg. between 60 and 80° K. Since each translational degree of freedom contributes  $R/2$  calories to the specific heat, Simon

<sup>7</sup> F. Simon and R. L. Swain, *Z. phys. Chem.*, B28, 189 (1935).

and Swain believed that the result indicated free motion of the argon atoms over the surface in two dimensions. Cassel<sup>8</sup> interprets the results differently. If the movement of the adsorbed argon atoms were two-dimensional translation the specific heat would indeed be  $R$  calories, but it would remain the same down to very low temperatures. If the movement were two-dimensional oscillation the specific

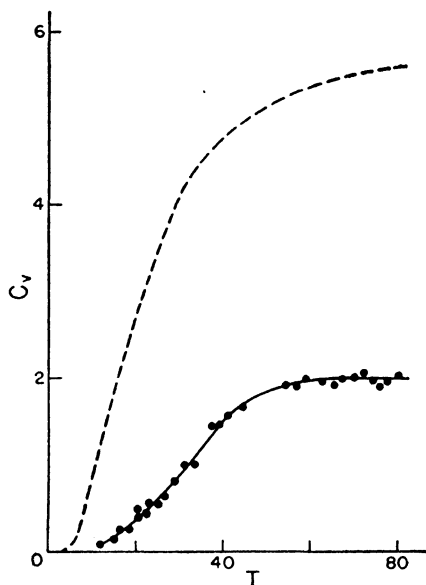


FIG. 142.—Specific heat of argon adsorbed on charcoal. The broken curve gives the specific heat of solid argon.

heat would be  $2R$ , decreasing with temperature as the Debye function of a two-dimensional oscillator. The specific heat curve of adsorbed argon does not follow either of these possibilities; it resembles the Debye function of a one-dimensional oscillator. If the argon atom is adsorbed in such narrow crevices that it is bound by two neighboring surfaces, at low temperatures it will be able to execute only one-dimensional vibrations parallel to both surfaces. Thus according to Cassel argon adsorbed on charcoal below  $80^{\circ}\text{K.}$  must be regarded as a solid, with no mobility over the surface. (The melting point of the normal solid is  $85.2^{\circ}\text{K.}$ )

<sup>8</sup> H. Cassel, *J. Am. Chem. Soc.*, 57, 2724 (1935).



The coefficient of thermal expansion of the adsorbed layer was experimentally measured by Goldmann and Polanyi.<sup>9</sup> The determination consisted in measuring the apparent specific gravity of charcoal by immersion in the liquid adsorbate at two different temperatures, 0 and 5.3° C. The values of  $\alpha_b$  (Chapter V) thus obtained agreed well with those calculated by the potential theory from adsorption isotherms. For ethyl chloride, ether and *n*-pentane the coefficient of thermal expansion of the adsorbate was about 20% smaller than that of the normal liquid in the same temperature range. It should be recalled, however, that according to the potential theory the adsorbates were under a compression of about 1000 atmospheres, and at that pressure the thermal expansion of the liquid is about 40% less than at atmospheric pressure. Interestingly, water, like the organic liquids, showed a positive thermal expansion between 0 and 5° C., even though in this temperature range the thermal expansion of the normal liquid is negative. This indicates that adsorbed water is similar to liquid water under great compression.

#### MUTUAL POLARIZATION OF ADSORBENT AND ADSORBATE

When a molecule is adsorbed by van der Waals forces its electrical charges are shifted by the process, as we have seen in Chapter VII. One would expect that this polarization would lead to changes in the optical and electrical properties of the adsorbed molecule, and such is actually the case. At the same time the adsorbate also influences the electrical properties of the surface.

de Boer and Custers<sup>10</sup> investigated the light absorption of iodine adsorbed on vacuum sublimed layers of calcium, strontium and barium fluoride. A comparison between the light absorption of a molecule in the free state and in the adsorbed state is possible only if the adsorbent does not absorb much light in the spectral range investigated, and if the adsorbate possesses particularly great light absorbing capacity. These conditions were fulfilled in the systems investigated by de Boer and Custers.

Free iodine possesses a strong absorption maximum at 499.5  $\mu\mu$  and a very weak one at 732  $\mu\mu$ . Iodine adsorbed on a  $\text{CaF}_2$  surface also has two maxima but at different wave lengths: at very low surface covering they are at 284 and 343  $\mu\mu$ . The first adsorbed molecules have a very high absorption coefficient, more than 100 times

<sup>9</sup> F. Goldmann and M. Polanyi, *Z. phys. Chem.*, **132**, 321 (1928).

<sup>10</sup> J. H. de Boer and J. F. H. Custers, *Z. phys. Chem.*, **B21**, 208 (1933); *Physica*, **3**, 1021 (1936).

as high as free iodine vapor. When more than 0.5% of the saturation adsorption is reached the adsorption coefficient suddenly falls to a value which at the maxima is about equal to that of solid iodine, but the maxima are still shifted to shorter wave lengths. As the adsorption increases the maxima shift toward longer wave lengths; the shift is particularly great for the long wave length maximum. At the highest adsorptions measured this maximum becomes very weak, like the weak long wave length maximum of free iodine. de Boer and Custers attribute the initial adsorption to electrostatic polarization of the iodine molecules by the fluoride ions of the surface layer.<sup>11</sup> The binding is rather similar to that of an iodine molecule to an iodide ion in solution, and the spectrum is actually similar to that given by the  $I_3^-$  ion. However, this can not be the complete explanation since it does not account for the sudden very great change after only 0.5% of the saturation adsorption has taken place. It seems probable that the initial strong adsorption occurs in the narrowest cracks or on the edges and corners of the crystals.

Subsequently de Boer and Custers<sup>12</sup> showed that on vacuum sublimed alkali and alkaline earth halides adsorbed iodine gives a brown color and adsorbed cesium a blue color, but vacuum sublimed  $SiO_2$ ,  $Al_2O_3$ ,  $ZrO_2$  and  $AgCl$  layers show no change in color when they adsorb iodine or cesium. The first group of adsorbents is porous, possessing a laminated structure; the second group has a compact structure. When the adsorbents of the second group are pulverized the adsorption of iodine or cesium is accompanied by development of color. de Boer and Custers contend that the color results from adsorption by means of dispersion forces, and that such adsorption takes place only in porous bodies. Dispersion forces alone on a plane surface are insufficient to account for the heat of physical adsorption but in a porous body, where two or more of the adsorbent atoms or molecules are in contact with an adsorbate molecule, they may account for the observed binding energies (Chapter VII). The colorless adsorption of iodine and cesium on the second group of adsorbents is similar to the active center adsorption on the first group; de Boer and Custers attribute it to the influence forces (ion-induced dipole attraction).

While the adsorbent produces a shift in the electrical charges of the adsorbate, the adsorbate likewise alters the electrical properties

<sup>11</sup> It was found by de Boer and Custers previously that the surface layer of vacuum sublimed  $CaF_2$  consists only of fluoride ions.

<sup>12</sup> J. H. de Boer and J. F. H. Custers, *Physica*, 4, 1017 (1937).

of the surface. It has been shown that adsorbed gases have a strong influence on the thermionic and the photoelectric emissivity of a surface. Since thermionic emission can be studied only at high temperatures and low pressures, where physical adsorption is necessarily small, only the effect of chemisorption has been investigated so far. This will be discussed in Volume II. Photoelectric emission, however, can be studied at ordinary temperatures. If a gas with low

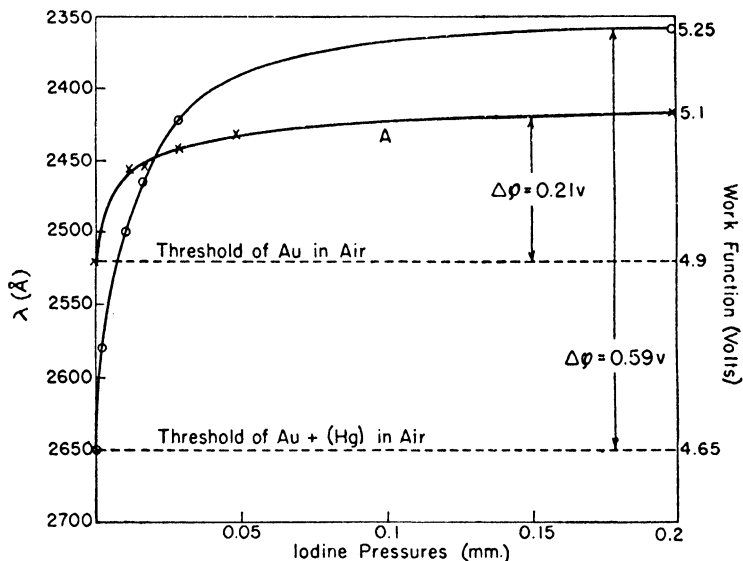


FIG. 143.—The shift in the photoelectric threshold of gold in the presence of adsorbed iodine.

vapor pressure is selected as the adsorbate, the effect of its physical adsorption on the photoelectric emissivity of the surface can be readily investigated.

Ouellet and Rideal<sup>13</sup> determined the photoelectric emission of a gold surface on which iodine and various organic vapors were adsorbed. A photoelectric tube counter of special design was used in the experiments. When iodine is admitted to the gold surface the threshold shifts to shorter wave lengths by an amount that increases with the iodine pressure. This is shown in Fig. 143, Curve A. The ordinate on the left gives the threshold, that on the right the work function.

<sup>13</sup> C. Ouellet and E. K. Rideal, *J. Chem. Phys.*, 3, 150 (1935).

Since iodine is an electronegative gas the work function is raised by its adsorption; i.e., it requires more energy to pull an electron out of the surface. The curves resemble Langmuir isotherms. This may mean that the adsorption of iodine on gold is unimolecular, but it more probably means that iodine adsorbed in the second layer has a negligibly small effect on the work function of the surface. Even the effect of the first layer is small; at saturation the increase in the work function is only 0.2 volt. This value is almost attained already at 25% of the saturation pressure.

Ethyl alcohol adsorbed on gold behaves differently. It gives a double threshold: one corresponding to the original threshold of gold, the other to a decrease of 0.49 volt in the work function. This second threshold, although obviously due to the adsorbed alcohol, does not shift with the pressure of the adsorbate as did the threshold of iodine on gold, but the intensity of the emission at this threshold increases with increasing pressure. Ouellet and Rideal suggest that the two thresholds are due to two emitting surfaces: one is bare gold surface or a surface covered with adsorbed vapor, the other is covered with two-dimensional liquid islands. The area covered by these islands increases with pressure causing the increase in the intensity of emission.

Adsorbed vapors also cause a change in the surface electrical potential which can be measured by various methods. Frost and Hurka<sup>14</sup> used two different methods to measure the potential differences arising from the adsorption of ethyl acetate, chloroform and benzene on paraffin and *p*-nitroaniline surfaces, and they obtained changes of 5 to 500 millivolts. The method is only in a semi-quantitative stage as yet, therefore no reliable conclusions can be drawn from the results as to the mechanism of the adsorption process.

#### THE EQUATION OF STATE OF THE ADSORBATE

Since the adsorbate under certain conditions behaves very much like a compressed gas, several investigators attempted to express its pressure-volume-temperature relations by a suitable equation of state. As a matter of fact, the potential theory used simply the ordinary equation of state of the gas with considerable success. We may recall as an example that Lowry and Olmstead<sup>3</sup> utilized van Laar's equation of state to calculate the adsorption of carbon dioxide by charcoal, and found very good agreement between theory and experiment (Chapter V).

<sup>14</sup> A. A. Frost and V. R. Hurka, *J. Am. Chem. Soc.*, **62**, 3335 (1940).

If the adsorption is unimolecular the motion of the gas is restricted to two dimensions. Since in this case the three-dimensional equations of state can not be valid, attempts have been made to try out their two-dimensional analogues. In the simplest case, when there are no forces of interaction between the adsorbed molecules, it was suggested that a two-dimensional ideal gas law should apply

$$(1) \quad F = sRT$$

which is the counterpart of the three-dimensional ideal gas law

$$(2) \quad p = cRT$$

The surface pressure or spreading force  $F$  is analogous to the pressure  $p$ , and the surface concentration  $s$  is analogous to the bulk concentration  $c$ .

It was shown by Traube<sup>15</sup> that in very dilute solutions the lowering of the surface tension was proportional to the concentration. The lowering of the surface tension is due to the spreading force of the molecules in the adsorbed layer

$$(3) \quad F = \sigma_0 - \sigma$$

where  $\sigma_0$  and  $\sigma$  are the surface tensions of the pure solvent and the solution, respectively. Langmuir<sup>16</sup> combined Traube's result

$$(4) \quad F = kp$$

with the Gibbs adsorption equation<sup>17</sup>

$$(5) \quad \frac{dF}{d \ln p} = sRT$$

and obtained equation (1). This equation can be written in the form

$$(6) \quad FA = RT$$

where  $A = 1/s$  is the surface area divided by the number of moles of gas adsorbed. Equations (1) or (6) are obeyed in the low pressure linear region of the adsorption isotherm.

Recently Innes and Rowley<sup>18</sup> investigated the relation between the equation of state and the adsorption isotherm and deduced the

<sup>15</sup> J. Traube, *Annalen*, 256, 27 (1891).

<sup>16</sup> I. Langmuir, *J. Am. Chem. Soc.*, 39, 1888 (1917).

<sup>17</sup> For the derivation of this much discussed but little tested equation see, for example, H. Freundlich, *Colloid and Capillary Chemistry*, London, 1926, p. 46. The equation found little use so far in the study of the adsorption of gases by solids, since the change in  $F$  can not be measured directly.

<sup>18</sup> W. B. Innes and H. H. Rowley, *J. Phys. Chem.*, 45, 158 (1941).

expression

$$(7) \quad \frac{nd(RT \ln p)}{dn} = S \frac{dF}{dn}$$

where  $n$  is the number of moles of gas adsorbed at pressure  $p$ , and  $S$  is the surface area of the adsorbent ( $S = An$ ). This equation enables one to evaluate the adsorption isotherm from the equation of state, and *vice versa*. For example, substituting the equation of state (6) into equation (7) one gets the isotherm equation

$$(8) \quad n = Kp$$

Thus, the two-dimensional ideal gas law (6) is equivalent to the linear adsorption isotherm (8). We have seen in Chapter IV that linear isotherms are obtained only at low pressures, and often even the lowest pressure region of the isotherm is non-linear.

At higher pressures one must take into account the forces of interaction between the adsorbed molecules. The short range repulsive forces were introduced in the equation of state by Volmer<sup>19</sup> and by Langmuir<sup>20</sup> independently. They suggested the equation

$$(9) \quad F(A - A_0) = RT$$

where  $A_0 = 1/s_1$  is the surface area divided by the number of moles of gas adsorbed at complete covering of the surface. The term  $A_0$  represents the part of the surface not available for the two-dimensional motion of the molecules; it is analogous to the van der Waals constant  $b$ . For large values of  $A$ , or small values of  $s$ , equation (9) reduces to the Langmuir isotherm equation.<sup>21</sup>

If one substitutes the Langmuir equation into equation (7) of Innes and Rowley,<sup>18</sup> one obtains the equation of state

$$(10) \quad \frac{FA}{RT} = \left( 1 + \frac{\theta}{2} + \frac{\theta^2}{3} + \frac{\theta^3}{4} + \cdots \right)$$

Figure 144 shows a plot of equation (10) compared with the two-dimensional ideal gas law (the dotted line). The deviation at  $\theta = 0.1$  is somewhat more than 5%.

Equation (9) can be written in the form

$$(11) \quad F = \frac{s_1 RT \theta}{1 - \theta}$$

<sup>19</sup> M. Volmer, *Z. phys. Chem.*, 115, 253 (1925).

<sup>20</sup> I. Langmuir, *Colloid Symposium Monograph*, 3, 72 (1925).

<sup>21</sup> See Volmer's thermodynamic derivation of the Langmuir equation in Chapter IV.

According to Langmuir<sup>22</sup> this equation often serves as a useful approximation. If we want to compare different equations of state, derived on the basis of different assumptions about the forces of interaction, we may use the more general equation

$$(12) \quad F = \frac{s_1 RT \theta}{Y(\theta)}$$

where  $Y(\theta)$  is a function of  $\theta$  that approaches unity when  $\theta$  is small, and it approaches zero when  $\theta$  approaches unity. Equation (11) represents the simplest case, namely, when  $Y(\theta) = 1 - \theta$ .

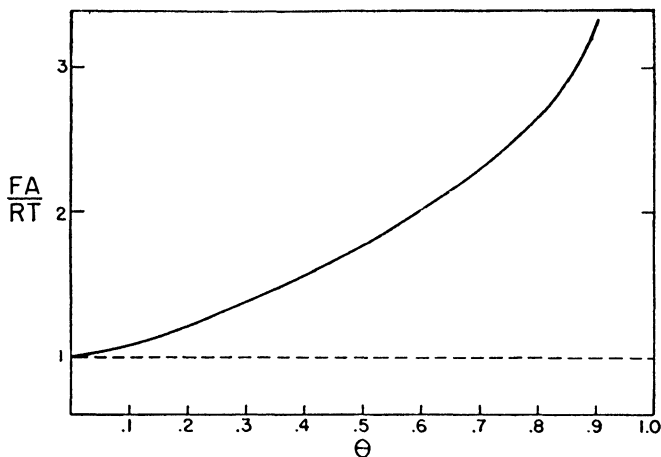


FIG. 144.—The plot of equation (10).

Tonks<sup>23</sup> derived the two-dimensional equation of state for molecules assumed to be hard, elastic spheres. For small values of  $\theta$  he obtains equation (12) with

$$(13) \quad Y(\theta) = 1 - 1.814\theta + 0.72\theta^2$$

and for large values of  $\theta$

$$(14) \quad Y(\theta) = 1 - \theta^{1/2}$$

When  $\theta$  is large the adsorbed molecules form approximately hexagonal close-packed arrangements, and the center of each molecule is able to move only within a small hexagonal region.

<sup>22</sup> I. Langmuir, *J. Chem. Soc.*, 1940, 511.

<sup>23</sup> L. Tonks, *Phys. Rev.*, (2), 50, 955 (1936).

While the Volmer-Langmuir equation (9) takes account of the short range repulsive forces between the adsorbed molecules, it does not consider the attractive (or cohesive) forces existing in the adsorbed layer. Schofield and Rideal<sup>24</sup> were the first to incorporate the attractive forces in the equation of state. They proposed an equation analogous to that of Amagat

$$(15) \quad F(A - A_0) = iRT$$

where  $i$  is a constant depending upon the cohesive forces; in the absence of cohesion it is equal to unity.

Semenoff<sup>25</sup> employed an equation of state completely analogous to that of van der Waals

$$(16) \quad \left( F + \frac{c}{A^2} \right) (A - A_0) = RT$$

The constant  $c$  is a measure of the attractive forces between the adsorbed molecules; it is analogous to the van der Waals constant  $a$ . According to Semenoff the cohesive forces cause condensation of the two-dimensional vapor to a two-dimensional liquid when  $F$  is increased beyond a certain value. The phase changes occurring in the adsorbate are discussed in the next section.

Magnus<sup>26</sup> used the equation of state

$$(17) \quad \left( F - \frac{\alpha}{A^2} \right) (A - A_0) = RT$$

This is formally similar to equation (16), except that the constant  $\alpha$  has a negative sign. According to the theory of Magnus the surface induces dipoles in the adsorbate molecules, and the dipoles are lined up by the surface parallel and oriented in the same direction. This results in repulsion between the molecules, giving a negative sign to the constant  $\alpha$ . The derivation of the isotherm equation of Magnus from equation (17) has been discussed in Chapter IV.

Palmer<sup>27</sup> advanced an equation of state for the adsorbate based on his empirical finding that the logarithm of the Polanyi potential varies linearly with the amount of vapor adsorbed<sup>28</sup>

$$(18) \quad -\log \epsilon/\epsilon_0 = ma$$

<sup>24</sup> R. K. Schofield and E. K. Rideal, *Proc. Roy. Soc., A109*, 57 (1925).

<sup>25</sup> N. Semenoff, *Z. phys. Chem.*, **B7**, 471 (1930).

<sup>26</sup> A. Magnus, *Z. phys. Chem.*, **A142**, 401 (1929).

<sup>27</sup> W. G. Palmer, *Proc. Roy. Soc., A160*, 254 (1937).

<sup>28</sup> See Chapter VI.



where  $\epsilon$  is the potential ( $RT \ln p_0/p$ ),  $a$  is the amount adsorbed,  $m$  is the slope of the straight line, and  $\log \epsilon_0$  is the intercept. The equation can also be written in the form

$$(19) \quad \epsilon = \epsilon_0 e^{-ma}$$

Combining equation (19) with the Gibbs equation (5) and integrating we get

$$(20) \quad F = k\epsilon_0 e^{-ma}(a + 1/m) + I_0$$

where  $k$  is a numerical constant converting to the appropriate unit, and  $I_0$  is the constant of integration.

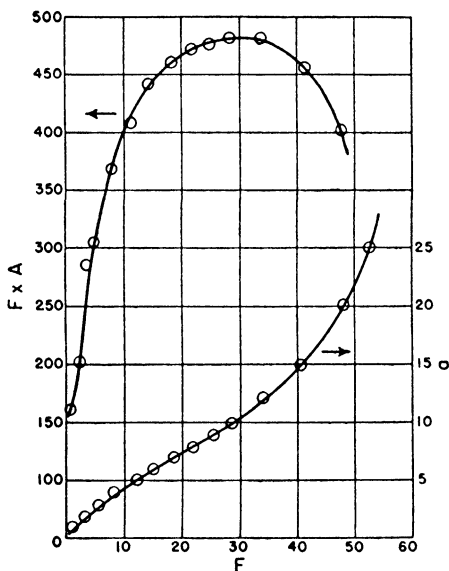


FIG. 145.—FA—F curve of benzene on vitreous silica.

The two-dimensional counterpart of the  $pv - p$  curve is the  $FA - F$  curve. Palmer measured the surface area of his vitreous silica adsorbent by the rate of solution method,<sup>29</sup> therefore he was able to calculate  $A$  from  $a$ ; and he calculated  $F$  by means of equation (20). His results for benzene are shown in Fig. 145. According to Palmer the rapid rise of the  $FA - F$  curve for small values of  $F$  and the

<sup>29</sup> See Chapter IX.

marked convexity to the  $FA$  axis demand for small adsorptions an equation of state of the form

$$(21) \quad \left( F - \frac{\alpha}{A^2} \right) (A - A_0) = iRT$$

which is a combination of the Magnus equation (17) and the Schofield-Rideal equation (15). The term  $-\alpha/A^2$  allows for repulsive forces between the induced dipoles, and the constant  $i$  allows for cohesive forces. For large adsorptions Palmer suggests the equation

$$(22) \quad F = \text{constant} (1/A - 1/A_0)$$

The lower curve in Fig. 145 represents the variation of the surface pressure with the amount adsorbed.<sup>30</sup>

#### TESTING OF THE EQUATION OF STATE

None of the equations discussed has been tested directly because  $F$ , the surface pressure, can not be measured directly. The nearest approach to direct testing of some of the equations is found in the works of Bangham and his collaborators, who measured an experimental quantity which appears to be proportional to the surface pressure. This quantity is the expansion of the adsorbent.

Bangham and Fakhoury<sup>31</sup> studied the expansion of unactivated wood charcoal<sup>32</sup> due to adsorption of water vapor, carbon dioxide, ammonia and sulfur dioxide. They noted that their results over certain ranges of concentrations could be expressed by an equation identical with the Schofield-Rideal equation (15), provided that a direct proportionality is assumed between the surface pressure  $F$  and the percentage linear expansion  $x$

$$(23) \quad x = \lambda F$$

where  $\lambda$  is a constant. Their interpretation of this result was that the expansion of charcoal was due to the two-dimensional pressure exerted by the adsorbate. Further investigation by Bangham, Fakhoury and Mohamed<sup>33</sup> on the expansion of charcoal caused by

<sup>30</sup> Miss Marion H. Armbruster and J. B. Austin (*J. Am. Chem. Soc.*, **60**, 467, 1938; **61**, 1117, 1939) used Palmer's equation of state (20) to interpret their adsorption results for carbon monoxide on mica and ethyl iodide on iron.

<sup>31</sup> D. H. Bangham and N. Fakhoury, *Proc. Roy. Soc.*, **A130**, 81 (1930).

<sup>32</sup> See Chapter XI.

<sup>33</sup> D. H. Bangham, N. Fakhoury and A. F. Mohamed, *Proc. Roy. Soc.*, **A138**, 162 (1932); **A147**, 152 (1934).

pyridine, benzene, water and the lower alcohols revealed that in most cases the Gibbs isotherm equation (5) was also obeyed if equation (23) was assumed to be true. The results for water did not obey the Gibbs equation. They attributed this to condensation of the two-dimensional gas to a two-dimensional liquid; the Gibbs equation is valid if only one surface phase is present.

Bangham<sup>34</sup> compared the  $FA - F$  curves obtained by Cassel and Salditt<sup>35</sup> for the adsorption of various alcohols on mercury with his own  $x/s - x$  plots, obtained by measuring the expansion of wood charcoal caused by the same alcohols. The great similarity between the two sets of data led him to the conclusion that the adsorption of alcohols on mercury and on charcoal obeys the same equation of state. With the help of certain deductions based on the similarity of the data he calculated that the surface area of his unactivated wood charcoal was 180 sq. m./g. The different alcohols gave consistent surface area values.

Bangham and Razouk<sup>36</sup> made further comparisons between the surface pressure and the expansion of the adsorbent. The surface pressure can be evaluated from the adsorption isotherm by integrating the Gibbs equation (5)

$$(24) \quad F = RT \int_0^p s d \ln p$$

It can also be obtained from expansion measurements according to equation (23). Unfortunately, Bangham and his collaborators did not measure the adsorption isotherms of the vapors they used in the expansion experiments. They had to be satisfied, therefore, with comparing their expansion data with the isotherms of Coolidge.<sup>37</sup>

To be able to compare the two sets of data one must know the surface area of the adsorbent (since  $s$  is the number of moles of gas adsorbed on unit surface) and the value of the constant  $\lambda$ . The latter was known from previous work.<sup>33</sup> The surface of Coolidge's charcoal was estimated by assuming that it had the same ratio to Bangham's charcoal as the amounts of vapor adsorbed by the two charcoals at saturation pressure. The surface area values thus obtained are shown in Table LXIX, Column 3. The three vapors do not give very good agreement. This is not surprising since the calculation involved the tacit assumption that the steam activated coconut charcoal of

<sup>34</sup> D. H. Bangham, *Proc. Roy. Soc.*, A147, 175 (1934).

<sup>35</sup> H. Cassel and F. Salditt, *Z. phys. Chem.*, A155, 321 (1931).

<sup>36</sup> D. H. Bangham and R. I. Razouk, *Trans. Far. Soc.*, 33, 1459, 1463 (1937).

<sup>37</sup> A. S. Coolidge, *J. Am. Chem. Soc.*, 46, 596 (1924).

Coolidge had the same pore structure as the unactivated wood charcoal of Bangham.

Bangham and Razouk<sup>36</sup> made two comparisons between the adsorption and the expansion data. The surface pressure at saturation,  $F_s$ , can be obtained by integrating equation (24) to  $p_0$  as the upper limit. Columns 4 and 6 in Table LXIX give the  $F_s$  values obtained from the adsorption data of Coolidge<sup>37</sup> and the expansion data of Bangham, Fakhoury and Mohamed,<sup>33</sup> respectively. There is a fair agreement between the values. Columns 5 and 7 give the

TABLE LXIX  
COMPARISON OF ADSORPTION AND EXPANSION DATA ON CHARCOAL

Vapor	Temperature °C.	Activated Coconut Charcoal			Unactivated Wood Charcoal	
		$S(\text{sq. m./g.})$	$F_s$	$F_s A_s$	$F_s$	$F_s A_s$
Benzene	0	510	—	—	219*	3500
	88.6	—	172	3010	—	—
Methyl alcohol	0	420	—	—	202*	1240
	59.5	—	199	1320	—	—
Water	23	558	—	—	77	310
	0	—	88	352	—	—

\* Decreases slowly with increasing temperature.

products  $F_s A_s$ , where  $A_s$  is the area per molecule at saturation. The rough agreement is even more significant than the agreement between the  $F_s$  values since the product  $F_s A_s$  is independent of the specific surface area assigned to Coolidge's charcoal.

The second comparison is shown in Fig. 146. The ordinates represent the integral  $I = k \int_p^{p_0} s d \ln p$ , the abscissae  $p/p_0$ .  $I$  is proportional to  $F_s - F$ . The curves were calculated from the isotherms; the points give the expansion data. The two sets of values were brought into coincidence at  $p/p_0 = 1$ , and the value of  $k$  was so chosen as to give the best fit with the methyl alcohol and benzene expansion data. There is at least a rough semi-quantitative agreement.

The results of Bangham and his collaborators seem to indicate that the adsorbate on charcoal behaves more like a two-dimensional compressed gas than a two-dimensional liquid even close to the saturation pressure. Bangham and Razouk<sup>33</sup> measured the expansion of wood charcoal exposed to the exactly saturated vapor of methyl

<sup>33</sup> D. H. Bangham and R. I. Razouk, *Proc. Roy. Soc., A166*, 572 (1938).

alcohol, and also when it was immersed in the liquid, and found an additional expansion on immersion. Other experiments<sup>36</sup> revealed that the *macropores* of wood charcoal did not fill with liquid even when exposed to the saturated vapor for weeks. Thus the adsorbed layers existing on the surfaces of the macropores are unable to function as condensation nuclei for the vapor, which in turn must mean that the adsorbed layer is different from the bulk liquid. Bangham and

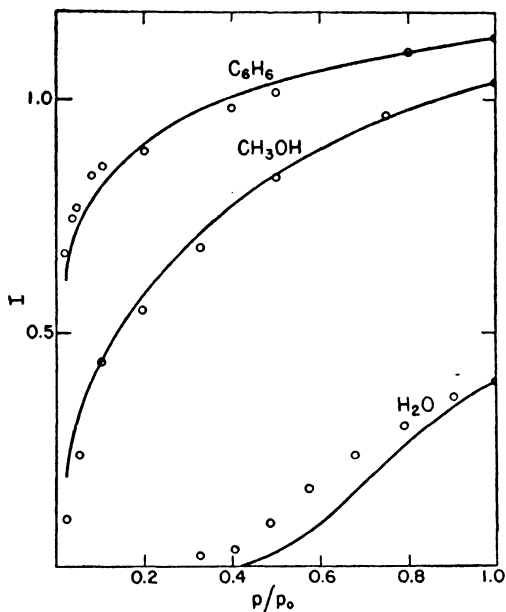


FIG. 146.—Comparison between adsorption and expansion data for three vapors on charcoal.

Razouk judiciously conclude: "It is not suggested that the inability of the films to act as condensation nuclei implies necessarily a very wide divergence of properties between them and the bulk liquids. The fact alone that as saturation is approached the quantities of different vapours adsorbed more and more nearly represent equal volumes of the liquids is sufficient to discount such an extreme view."

In some recent experiments Razouk<sup>39</sup> found that there is no measurable amount of heat evolved when charcoal saturated with a

<sup>39</sup> R. I. Razouk, *J. Phys. Chem.*, **45**, 179, 190 (1941).

vapor is plunged into the liquid adsorbate. This is another evidence that the properties of the adsorbate are very similar to those of the liquid.<sup>40</sup> Above the critical temperature the adsorbate should probably be regarded as a compressed gas, even at high pressures. We have seen in Chapter IV that  $v_m$ , the amount of gas necessary to cover the surface of the adsorbent with a complete monolayer, varied with temperature in the experiments of Miss Homfray,<sup>41</sup> Titoff,<sup>42</sup> and Richardson<sup>43</sup> much more strongly than would correspond to a liquid-like expansion of the adsorbate. Most of the isotherms determined by these investigators were measured well above the critical temperatures of the gases. If the adsorbate is similar to a compressed gas its thermal expansion should also be like that of a gas. Wilkins and Ward<sup>44</sup> pointed out that the decrease in  $v_m$  with increasing temperature is equivalent to the decrease in the mass of a gas that a given volume can hold at a constant pressure and increasing temperature. This means that  $1/v_m$  should increase linearly with the temperature, and that  $-dv_m/v_m dT$  should have the same order of magnitude as the coefficient of thermal expansion of a gas. Wilkins and Ward showed that in the results of a number of investigators both consequences are approximately fulfilled.

The use of equations of state proved particularly successful in the study of insoluble films adsorbed on liquid surfaces.<sup>45</sup> In the field of gas adsorption on solids this line of attack did not progress very far. Although, as we have seen, a number of equations have been proposed, none of them received sufficient experimental support to establish its validity. In general, the equation of state seems to be a less fruitful approach to the interpretation of experimental data than the adsorption isotherm equation. The isotherm equation contains only vari-

<sup>40</sup> W. G. Palmer (*Proc. Roy. Soc.*, A168, 190, 1938) calculated the coefficient of thermal expansion  $\alpha$  and the compressibility  $\beta$  of benzene, acetone and methyl alcohol films adsorbed on vitreous silica. He came to the conclusion that the state of the film resembled more nearly a compressed gas than a liquid. D. H. Bangham (*Proc. Roy. Soc.*, A147, 175, 1934) calculated  $\alpha$  and  $\beta$  for the lower alcohols adsorbed on charcoal at high relative pressures, and he came to the same conclusion. Against these calculations, inadequately supported by theory and experiment, we may cite the overwhelming evidence presented in previous chapters about the similarity between adsorbate and liquid, particularly near the saturation pressure.

<sup>41</sup> I. F. Homfray, *Z. phys. Chem.*, 74, 129 (1910).

<sup>42</sup> A. Titoff, *Z. phys. Chem.*, 74, 641 (1910).

<sup>43</sup> L. B. Richardson, *J. Am. Chem. Soc.*, 39, 1828 (1917).

<sup>44</sup> F. J. Wilkins and A. F. H. Ward, *Z. phys. Chem.*, A144, 259 (1929).

<sup>45</sup> The reason is that both the surface tension and the surface area of a liquid are readily measurable.

ables that can be directly measured, therefore its validity can be readily tested. In contrast, the equation of state contains the variables  $A$  and  $F$ , the first of which can be only approximately determined, while the second can not be measured directly at all. Nevertheless, the method is well worth following up, and the future will doubtless bring interesting developments in this field too.<sup>46</sup>

### PHASE CHANGES IN THE ADSORBATE

From all the facts presented so far it seems clear that there is no great difference between the adsorbate and a compressed gas or liquid. There is also some evidence that at low enough temperatures the adsorbate behaves like a solid. In the present section we investigate the conditions of existence of the three phases and compare them with those of the bulk phases.

#### A. The Condensation Point

Polanyi and Welke<sup>47</sup> in their experiments on the adsorption of sulfur dioxide by charcoal encountered a phenomenon that they attributed to condensation of the two-dimensional gas to a two-dimensional liquid (Chapter VIII). As Fig. 90 shows, the heat of adsorption at very low pressures at first drops sharply, then begins to rise. They explained the rising portion by suggesting that it was due to the heat given out in the two-dimensional condensation process. If this is true, condensation begins at very low pressures and small adsorptions: in their experiments the adsorbed layer covered less than 1% of the surface and the pressure was about 0.2 mm.

The theory of two-dimensional condensation was developed by Semenoff.<sup>25</sup> He built it on the experimental findings of Wood<sup>48</sup> and Knudsen.<sup>49</sup> These investigators directed a stream of metallic vapor at a cooled glass surface and found that if the temperature of the glass was higher than a given value,  $T_w$ , practically all metal atoms were reflected from the surface, whereas if the temperature was lower than  $T_w$  almost all of the atoms condensed. They called  $T_w$  the critical temperature of condensation but it is better to call it simply the condensation temperature. It is not a critical temperature because

<sup>46</sup> W. B. Innes and H. H. Rowley (*J. Phys. Chem.*, 46, 537, 548, 694; 1942).

<sup>47</sup> M. Polanyi and K. Welke, *Z. phys. Chem.*, A132, 371 (1928).

<sup>48</sup> R. W. Wood, *Phil. Mag.*, (6), 32, 365 (1916).

<sup>49</sup> M. Knudsen, *Ann. der Phys.*, (4), 50, 472 (1916).

it depends on the pressure of the gas stream.<sup>50</sup> Estermann<sup>51</sup> found that the relationship can be expressed by the empirical equation

$$(25) \quad p = a_1 e^{-b_1/T_w}$$

where  $a_1$  and  $b_1$  are constants. The pressure  $p$  at which condensation of metallic vapors occurs on glass is always much higher than  $p_0$ , the vapor pressure of the metal.

Semenoff<sup>25</sup> assumes that the metal can condense only if a two-dimensional condensed layer forms first. The condensation is caused by cohesive forces existing between the adsorbed molecules; he expressed this in his equation of state (16). With increasing  $F$  a point is reached where condensation begins and the adsorbed gas liquefies. The variation of the two-dimensional vapor pressure with temperature is given by

$$(26) \quad F = a_2 e^{-\Delta/RT}$$

where  $a_2$  is a constant and  $\Delta$  is the two-dimensional heat of vaporization.

Using the Langmuir isotherm equation Semenoff derived the relation

$$(27) \quad p^* = a_3 e^{-(q+\Delta)/RT}$$

where  $p^*$  is the pressure at which condensation takes place at temperature  $T$ , and  $q$  is the heat of adsorption. Since for metal vapors  $p^*$  is greater than  $p_0$ , the two-dimensional condensed layer is unstable, and as soon as it forms three-dimensional condensation follows. The pressure drops to  $p_0$  and remains constant until the condensation is complete.

Equation (27) is valid for adsorption phenomena in general, but ordinarily  $p^*$  is smaller than  $p_0$ . If  $q$  were constant over the surface condensation would occur when  $p^*$  is reached, and the pressure would remain constant until the entire two-dimensional gas is converted into a two-dimensional liquid.<sup>52</sup> However, since  $q$  varies over

<sup>50</sup> This was first shown by J. Chariton and N. Semenoff (*Z. Physik.*, 25, 287, 1924). They also found that the metal atoms were not elastically reflected above  $T_w$  but first adsorbed then reflected, in agreement with Langmuir's views. Below  $T_w$  the metal condenses in bulk.

<sup>51</sup> I. Estermann, *Z. Elektrochem.*, 31, 441 (1925).

<sup>52</sup> H. H. Rowley and W. B. Innes (*J. Phys. Chem.*, 46, 537, 1942) proposed the following phase rule for equilibria between two- and three-dimensional systems

$$F = C - (P + p) + 3$$

where  $F$  is the number of degrees of freedom,  $C$  is the number of components,  $P$  is the number of three-dimensional phases, and  $p$  is the number of two-dimensional



the surface, condensation occurs at quite low pressures on the most active places; then with increasing pressure the condensation spreads to places of lower heats of adsorption. Thus Semenoff's theory explains the formation of islands of liquid on the surface, suggested by Goldmann and Polanyi<sup>9</sup> (Chapter V).

A different type of evidence for condensation in the adsorbed layer was presented by Weingaertner.<sup>53</sup> Since the works of Semenoff and

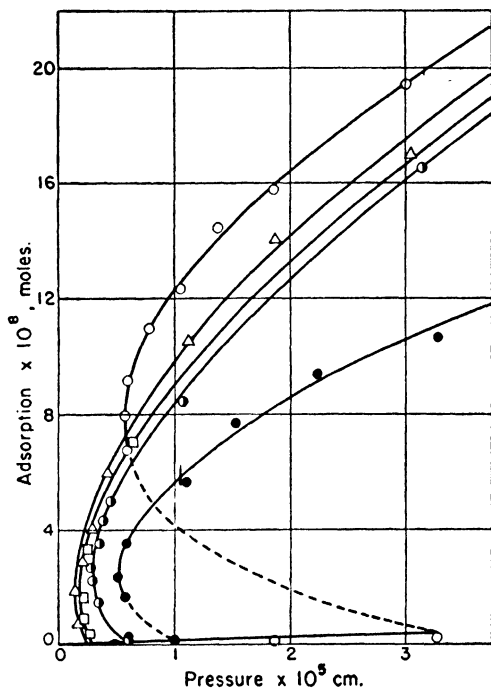


FIG. 147.—Supersaturation in the adsorption of nitrogen on glass spheres.

Polanyi indicated that condensation occurs at very low pressures, he looked for signs of condensation in the low pressure linear region of the adsorption isotherm. He measured the adsorption isotherms of methane, ethane and propane on charcoal in the linear region, and

phases. If this phase rule is correct two-dimensional condensation does not take place at a constant pressure even on a uniform surface. Since for the adsorption of one gas  $C = 2$ ,  $P = 2$ , and  $p = 2$ , the system still has one degree of freedom.

<sup>53</sup> E. Weingaertner, *Z. Elektrochem.*, **42**, 599 (1936).

found that the slopes of the isotherms determined below the critical temperatures of the gases showed certain marked characteristic fluctuations about their mean values. (The deviations of the slopes above the critical temperature were small and irregular.) If the distribution of the heat of adsorption over the surface is discontinuous, and if condensation on the different regions takes place according to Semenoff's equation (27), one might obtain such fluctuations in the slopes of the isotherms as were found by Weingaertner. The fluctuations occurred at pressures less than 0.01 mm.

That supersaturation may exist in the adsorbed phase is clearly indicated by the experiments of Shereshefsky and Weir,<sup>54</sup> shown in Fig. 147. The curves represent isotherms of nitrogen on glass spheres at liquid air temperatures and very low pressures. At first the adsorption is very slight and increases linearly with pressure according to Henry's law. Then at a pressure of about  $10^{-4}$  mm. suddenly a large adsorption occurs with a drop in pressure. This can be explained by assuming that two-dimensional condensation sets in, the pressure drop indicating that in the initial state the vapor was supersaturated.

### B. The Critical Point

The above discussed experiments all indicate that at a given temperature condensation in two dimensions sets in at much lower pressures than bulk condensation. For example, in the experiments of Shereshefsky and Weir<sup>54</sup> the bulk vapor pressure of nitrogen was several atmospheres, whereas condensation in the adsorbed film seemed to occur at a small fraction of 1 mm. pressure.<sup>55</sup> The next question is, how far does the condensed phase extend on the temperature scale; in other words, what is the two-dimensional critical temperature? At present this question can not be answered with any degree

<sup>54</sup> J. L. Shereshefsky and C. E. Weir, *J. Am. Chem. Soc.*, 58, 2022 (1936).

<sup>55</sup> The theory of multimolecular adsorption regards the adsorbate as being similar to a condensed phase. Recently H. H. Rowley and W. B. Innes (*J. Phys. Chem.*, 46, 694, 1942) raised an objection to this view. They argue that if each adsorbed layer is considered a separate two-dimensional condensed phase, there should belong to each condensed phase a two-dimensional vapor phase if the layers are incomplete. However, according to an extension of their phase rule (footnote 52) such a system would possess no variance. Aside from the fact that the validity of this phase rule has not been proven yet, it seems absurd to consider each adsorbed layer a separate system consisting of two phases. One would certainly not expect a boundary surface to exist between a group of molecules adsorbed in the fourth layer and the underlying molecules adsorbed in the third layer. It is much simpler to look upon the multimolecular adsorbate as one three-dimensional phase, obeying the phase rule of Gibbs.

of assurance. Devonshire<sup>56</sup> estimates on theoretical grounds that the critical temperature of a gas in two dimensions should be about half the critical temperature of the same gas in three dimensions. However, experimental confirmation of this view is completely lacking. In fact, the fluctuations noticed by Weingaertner<sup>53</sup> begin just about at the normal critical temperature; if these really indicate two-dimensional condensation the two-dimensional critical temperature is the same as the three-dimensional one.

At higher pressures unimolecular adsorption is followed by multimolecular adsorption, and at still higher pressures by capillary condensation. The three-dimensional adsorbate is very similar to a liquid; its critical temperature therefore should not be far from that of the liquid. Since adsorption usually takes place in porous solids some investigators attempted to find out whether the pore structure has any influence on the critical temperature of the adsorbate. Patrick, Preston and Owens<sup>57</sup> found that the adsorption isotherms of carbon dioxide and nitrous oxide are very similar at 30 and 40° C., in spite of the fact that the critical temperatures of both gases lie between these temperatures. (The critical temperature of carbon dioxide is 31.0, that of nitrous oxide 36.5° C.) On the basis of the belief that the adsorption was due to capillary condensation they concluded that in the pores of the gel liquid exists above the normal critical temperature. However, the shapes of the isotherms and the amounts adsorbed show that in these experiments both at 30 and 40° C. only a fraction of a monolayer was adsorbed, and so the investigators did not deal with capillary condensation.

Urry<sup>58</sup> measured the adsorption of argon, oxygen and methane on silica gel in the temperature range 90 to 273° K. He found that the isotherms obeyed the Freundlich equation. When he plotted the constants  $1/n$  and  $\log K$  against the temperature, he obtained very definite breaks in the vicinity of 195° K. This is illustrated in Fig. 148, representing plots of  $1/n$  against  $T$  for the three gases. Urry believed that the break-points corresponded to the critical temperatures of the gases and concluded that in the pores of silica gel the critical temperature is raised by about 40 degrees. However, there is no sound reason to believe that the break-point does actually correspond to the critical temperature. The value of  $1/n$  is unity for linear adsorption isotherms, and such isotherms are found at small

<sup>56</sup> A. F. Devonshire, *Proc. Roy. Soc.*, A163, 132 (1937).

<sup>57</sup> W. A. Patrick, W. C. Preston and A. E. Owens, *J. Phys. Chem.*, 29, 421 (1925).

<sup>58</sup> W. D. Urry, *J. Phys. Chem.*, 36, 1831 (1932).

enough adsorptions both far above and far below the critical temperature. Likewise fractional values of  $1/n$  are also found far above and below the critical temperature. A more plausible interpretation of the break-points is found in the theory that Zeldowitsh<sup>59</sup> advanced for the Freundlich equation (Chapter IV).

The most interesting investigations on the critical point of the adsorbate were made by Maass and his collaborators. Morris and

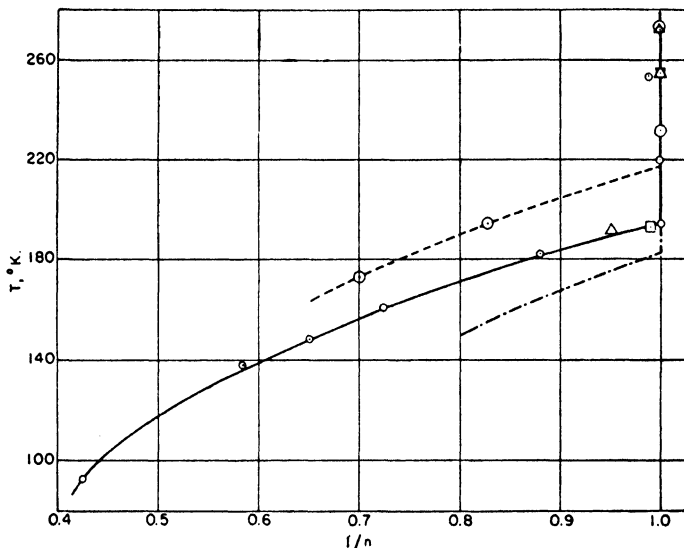


Fig. 148.—Variation of the constant  $1/n$  with temperature.

Maass<sup>60</sup> investigated the adsorption of propylene on alumina, and Edwards and Maass<sup>61</sup> the adsorption of dimethyl ether on alumina. The experiments were performed not only in the neighborhood of the critical temperature but also near the critical pressure. The adsorption isobars exhibit no break at the critical temperature, as Fig. 149 shows. The critical temperature of dimethyl ether is  $127^\circ\text{C}$ ., and the experiments were carried up to  $136^\circ\text{C}$ . The isotherms are S-shaped, clearly indicating multimolecular adsorption even 9 degrees above the critical temperature. The adsorption isobars of propylene show no breaks up to 15 degrees above the critical temperature.

<sup>59</sup> J. Zeldowitsh, *Acta Physicochim. U.R.S.S.*, 1, 961 (1935).

<sup>60</sup> H. E. Morris and O. Maass, *Can. J. Res.*, 9, 240 (1933).

<sup>61</sup> J. Edwards and O. Maass, *Can. J. Res.*, 13B, 133 (1935).

Although these experiments seem to suggest that the critical temperature of the adsorbate is higher than that of the bulk liquid, this is not necessarily true in the light of some other experimental and theoretical considerations. Tapp, Steacie and Maass<sup>62</sup> found that on raising the temperature of a liquid-vapor system one does not obtain a homogeneous phase immediately when the critical point is passed and the meniscus disappears, but a denser phase and a less

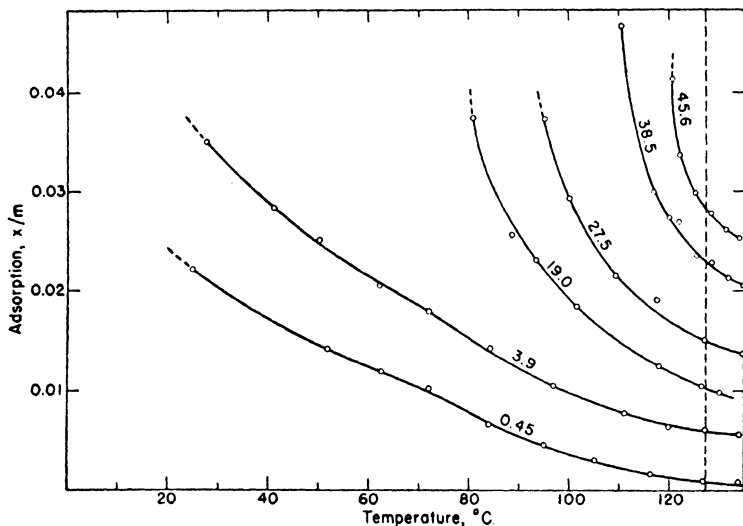


FIG. 149.—Adsorption isobars of dimethyl ether on alumina in the neighborhood of the critical point.

dense phase instead. Mayer<sup>63</sup> explained this phenomenon in terms of his statistical theory of condensing systems. According to him the temperature at which the meniscus disappears,  $T_m$ , is not the true critical temperature. Above  $T_m$  condensation and surface tension disappear, and yet one does not obtain an ordinary gas, but rather a system consisting of molecular clusters of various sizes. Experimental evidence shows that these clusters do not disappear until a temperature 10 to 15 degrees above  $T_m$  is reached. Mayer calls this higher temperature the true critical temperature,  $T_c$ .

Since the formation of multimolecular layers is similar to the formation of multimolecular clusters in imperfect gases,<sup>5</sup> there is no

<sup>62</sup> J. S. Tapp, E. W. R. Steacie and O. Maass, *Can. J. Res.*, 9, 217 (1933).

<sup>63</sup> J. E. Mayer and M. G. Mayer, *Statistical Mechanics*, New York, 1940, p. 312.

reason to expect that multimolecular adsorption should cease between  $T_m$  and  $T_c$ . It would be interesting to carry the experiments of Maass to higher temperatures to see whether multimolecular adsorption disappears above  $T_c$ , and if it does not disappear to find the critical temperature of the adsorbate.

### C. The Melting Point

It is definitely established that the melting point of the adsorbate is lower than that of the bulk substance. We may recall that the  $-183$  and the  $-195.8^\circ\text{C}$ . affinity curves of argon adsorbed on an aluminum oxide promoted iron catalyst coincided.<sup>64</sup> (Fig. 56.) We may also remember that the  $-195.8^\circ\text{C}$ . argon isotherm was calculated from the  $-183^\circ\text{C}$ . isotherm on the basis of the theory of multimolecular adsorption.<sup>6</sup> (Fig. 72.) The melting point of argon is  $-189.2^\circ\text{C}$ . In both calculations it was assumed that the adsorbate was in the liquid state even at the lower temperature, and for  $p_0$  the extrapolated vapor pressure of the liquid was used rather than the vapor pressure of the solid. From the success of the calculations it seems evident that the adsorbed argon is in the liquid state 6.6 degrees below the normal melting point.

Demougin<sup>65</sup> obtained indications that the adsorbate behaves like a liquid even 100 degrees below the bulk melting point. He investigated the saturation adsorption of iodine on various charcoals and on silica gel at temperatures above and below the melting point ( $114^\circ\text{C}$ .) and found that the amounts adsorbed were the same at 128, 100, 60 and  $17^\circ\text{C}$ . This is shown in Table LXX. At saturation the entire pore space is filled with the adsorbate. If at some temperature solidification had taken place it would have shown up in widely differing weights of iodine adsorbed, since the density of liquid iodine is 3.95 while that of the solid is 4.9. Furthermore, Demougin found that the ratio of the weight of iodine to the weight of ether adsorbed at saturation varied from 5.0 to 5.3 for the seven adsorbents. The ratio of the densities of liquid iodine and ether is 5.4, whereas the ratio of solid iodine and liquid ether is 6.7. It seems therefore that adsorbed iodine is in the liquid state even 97 degrees below the normal melting point.

Coolidge<sup>37</sup> determined eight adsorption isotherms of benzene on coconut charcoal between  $-33.5$  and  $303.7^\circ\text{C}$ . The two isotherms obtained below the melting point of benzene,  $5.5^\circ\text{C}$ ., had exactly the

<sup>64</sup> P. H. Emmett and S. Brunauer, *J. Am. Chem. Soc.*, **57**, 2732 (1935).

<sup>65</sup> P. Demougin, *Compt. rend.*, **200**, 662 (1935).

same shapes as the six isotherms taken above the melting point. Thus Coolidge found no evidence of solidification down to 39 degrees below the melting point of benzene. Likewise, Patrick and Land<sup>66</sup> measured the adsorption of iodine on silica gel and found no evidence of a melting point down to 70° C., 44 degrees below the bulk melting point. The adsorption isobar at 17 mm. pressure was a continuous smooth curve from 137.5 to 85° C.

The experiments so far discussed showed no sign of phase change from liquid to solid. Evidence of phase transition was first noted by

TABLE LXX  
SATURATION ADSORPTION OF IODINE

Adsorbent	Amount Adsorbed (mg./g.)			
	Below the Melting Point			Above the Melting Point
	17°	60°	100°	128°
1. ZnCl <sub>2</sub> activated charcoal	2850	2830	2810	2810
2. Charcoal from rubber	2640	2615	2600	2640
3. Gas activated charcoal	2530	2500	2480	2480
4. Steam activated charcoal	1890	1860	1860	1880
5. Slightly activated charcoal	1320	1330	1315	1350
6. Unactivated charcoal	920	930	945	935
7. Silica gel	1085	1180	1130	1125

Jones and Gortner,<sup>67</sup> who measured by means of a dilatometer the freezing temperature of water adsorbed on silica gel. The gel and water were covered with toluene and the change in volume on cooling was observed. The thermal contractions of water, ice and the gel were negligible; that of toluene was known and was subtracted from the observed contraction. The rest was ascribed to the contraction due to the freezing of water, and from its value the amount of water frozen was calculated. Since Jones and Gortner started with an excess of water freezing began close to the normal melting point, i.e., between - 1 and - 2° C. The water which froze at the initial temperature was considered the "free water," the rest was considered "capillary water." The freezing of the free water occurred at a constant temperature, but the capillary water (or bound water) froze at a continuously decreasing temperature. As the temperature decreased more water solidified, but at - 48° C. the gel still contained

<sup>66</sup> W. A. Patrick and W. E. Land, *J. Phys. Chem.*, **38**, 1201 (1934).

<sup>67</sup> I. D. Jones and R. A. Gortner, *J. Phys. Chem.*, **36**, 387 (1932).

33% unfrozen water. Extrapolation indicated that a temperature of about  $-80^{\circ}\text{C}$ . would have been necessary to freeze all the capillary water. Thus the melting of the adsorbate is very much like that of a glass and not like that of a crystal.

Patrick and Kemper<sup>68</sup> came to a similar conclusion on the basis of specific heat measurements. They used the Andrews calibrated heat conduction method<sup>69</sup> to measure the specific heats of water, naphtha-

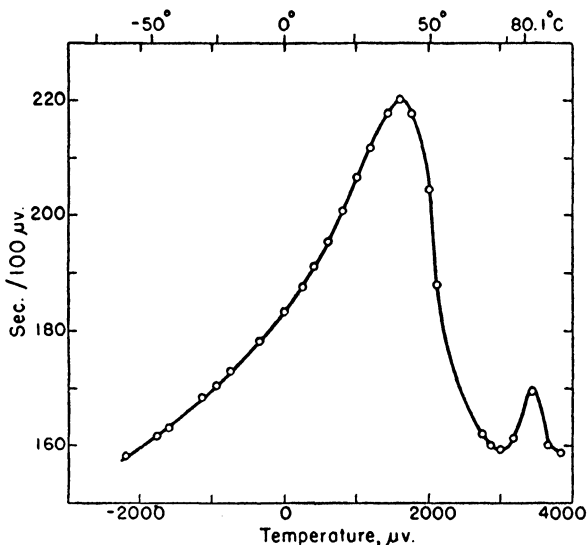


FIG. 150.—The melting point of naphthalene adsorbed on silica gel.

lene, benzene and *p*-nitrotoluene adsorbed on silica gel. The type of result obtained is illustrated in Fig. 150. The ordinates are proportional to the heat capacity of the silica gel-naphthalene system, the abscissae are proportional to the temperature. The small hump in the curve is due to the melting of the excess free naphthalene; at the start of the experiment there was always a slight excess adsorbate present over that necessary to saturate the gel. The large hump was attributed by Patrick and Kemper to the melting of the adsorbed naphthalene. Melting begins at very low temperatures, perhaps 150 degrees below the normal melting point, but the melting temperature

<sup>68</sup> W. A. Patrick and W. A. Kemper, *J. Phys. Chem.*, **42**, 369 (1938).

<sup>69</sup> R. H. Smith and D. H. Andrews, *J. Am. Chem. Soc.*, **53**, 3644 (1931).



risers as more and more of the adsorbate melts. The maximum melting occurs at about 40 degrees below the normal melting point. (With water it occurs 12 degrees below the melting point.)

Patrick and Kemper point out that the lowering of the melting point of the adsorbate can be readily explained on the basis of the capillary condensation theory. One can prove by a simple thermodynamic argument that a liquid under tension should melt at a lower temperature than the normal liquid, provided it is in equilibrium with the normal solid. However, it is difficult to see how the solid, if it forms at all in capillaries of molecular dimensions, can avoid being under stress from the surface forces.<sup>70</sup>

From the foregoing discussion it is clear that so far only the bare beginnings have been made toward establishing the condensation point, the critical point and the melting point of the adsorbate. The need for a great deal of further research is obvious.

<sup>70</sup> W. A. Patrick and W. A. Kemper (*J. Phys. Chem.*, 42, 381, 1938) combining thermodynamic arguments with the Patrick equation (Chapter V), calculated the melting point lowering of their four adsorbates on silica gel and found a rough semiquantitative agreement.

## CHAPTER XIII

### THE KINETICS OF PHYSICAL ADSORPTION

The study of adsorption, like all physico-chemical studies, can be divided into two parts: kinetics and thermodynamics. The former deals with rate processes, the latter with equilibria. In Chapters IV to XII we discussed the adsorption equilibrium, in the present chapter we take up the time dependent processes in physical adsorption. The disproportionate space devoted to the two phases is due to the fact that by far the most work has been done on equilibria. Perhaps the main reason for this is that adsorption processes are very rapid. McBain<sup>1</sup> stated in 1919: "True adsorption is nearly instantaneous. Any lag at present can be accounted for by the time required for the dissipation of the heat evolved, or the comparative inaccessibility of a portion of the surface of a porous adsorbing agent." If in the place of "true adsorption" we substitute "physical adsorption," this statement still expresses our views.

In 1931 Taylor<sup>2</sup> pointed out that some adsorption processes—and interestingly, those occurring at high temperatures—do not take place instantaneously but proceed at a finite rate. Unless too high temperatures are used these rates are conveniently measurable. The kinetics of activated adsorption will be discussed in Volume II; at present we take up only the rate processes in physical adsorption.

According to Langmuir's<sup>3</sup> ideas, now generally adopted, the adsorption process consists of three steps: the motion of the gas molecules to the surface, the sojourn of the molecules on the surface, and the motion of the molecules away from the surface, back to the gas phase. We now know that the second step also involves motion; the adsorbed molecules migrate over the surface. The study of the rates of these three processes (adsorption, surface migration and desorption) constitutes the subject of this chapter.

#### THE MOTION OF THE MOLECULES OVER THE SURFACE

For convenience we start with the period the molecule spends on the surface. Two questions come up in this connection: (1) How long

<sup>1</sup> J. W. McBain, *Trans. Far. Soc.*, 14, 202 (1919).

<sup>2</sup> H. S. Taylor, *J. Am. Chem. Soc.*, 53, 578 (1931).

<sup>3</sup> I. Langmuir, *J. Am. Chem. Soc.*, 40, 1361 (1918).

does the molecule stay on the surface, and (2) what sort of motions is it capable of executing while on the surface? Is the molecule rigidly fixed to the position where it has been adsorbed or is it able to move over the surface? On the basis of the evidence presented in previous chapters about the similarity between the adsorbate and a compressed gas or a liquid we may safely conclude that the molecule can move over the surface, except possibly at very low temperatures. However convincing, this evidence is indirect; the first direct proof of the mobility of adsorbed molecules was supplied by the experiments of Volmer and his collaborators.

In the first experiments Volmer and Estermann<sup>4</sup> proved that the molecules in the top layer of a crystal possess a high degree of mobility during the process of crystallization. They evaporated liquid mercury from a bath held at  $-10^{\circ}\text{C.}$  to a glass surface at  $-63^{\circ}\text{C.}$ , where it condensed to tiny crystals. The crystals were very thin hexagonal plates, the thickness amounting to only about  $1/10,000$  of the diameter.

The rate at which molecules coming from the liquid condense on the crystal surface is given by the Knudsen equation

$$(1) \quad G = \alpha p \sqrt{\frac{M}{2\pi RT}}$$

where  $G$  is the increase in the weight of the crystal per sq. cm. surface per second,  $\alpha$  is the condensation coefficient,  $p$  is the vapor pressure of the liquid and  $M$  is its molecular weight. (This equation is the same as equation 11 in Chapter IV.) The condensation coefficient  $\alpha$  was shown by Volmer and Estermann<sup>5</sup> to be close to unity. The rate of evaporation under the conditions of the experiment was negligible.

The increase in the size of the crystal in the direction of the *normal* to the surface is given by

$$(2) \quad V = G/\delta$$

where  $\delta$  is the specific gravity of the crystal. Assuming that  $\alpha = 1$  and that  $p$  is equal to the vapor pressure of mercury at  $-10^{\circ}\text{C.}$ , the value of  $V$  is  $2.5 \times 10^{-7}$  cm./sec. Accordingly, the plates should reach in one minute a maximum dimension of  $2 \times 60 \times 2.5 \times 10^{-7} = 3 \times 10^{-5}$  cm. Actually the plates reached a dimension of  $3 \times 10^{-2}$  cm. Thus the narrow side of the crystal grew about a thousand times as fast as it received molecules from the vapor phase, while the large hexagonal side grew more slowly than the calculated rate of increase.

<sup>4</sup> M. Volmer and I. Estermann, *Z. Physik*, 7, 13 (1921).

<sup>5</sup> M. Volmer and I. Estermann, *Z. Physik*, 7, 1 (1921).

Volmer and Estermann concluded therefore that the molecules arriving from the gas phase are free to move over the hexagonal side of the crystal until they reach the edge and there become firmly fixed. This is true at least for the initial growth of the crystal. After the plate reaches the size of about 0.3 mm. the increase in size in that

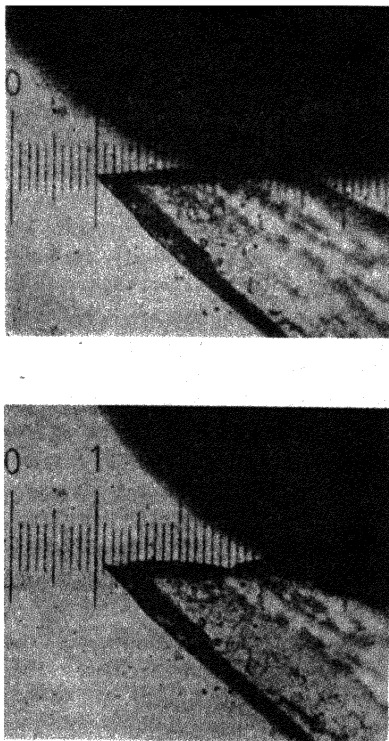


FIG. 151.—Demonstration of the migration of molecules in the surface layer of a benzophenone crystal.

direction goes on more slowly and the thickness begins to increase more rapidly.

Next Volmer and Adhikari<sup>6</sup> proved by two experiments that the molecules in the surface layer of benzophenone crystals also possess mobility. In the first experiment they showed that the crystal needles growing out of a melt pass through the surface of the liquid

<sup>6</sup> M. Volmer and G. Adhikari, *Z. Physik*, 35, 170 (1925).

and keep on growing to a distance of 0.1 mm. above the surface. This can be explained by assuming that the tip of the needle projecting out of the melt is surrounded by an invisible mobile layer in which the molecules can migrate from the melt to the tip, where they remain fixed. In the second experiment droplets of mercury were made to brush against the side of a crystal needle of benzophenone. Great care was taken that the drops should not touch the tip of the needle, and microphotographs showed that the drops never came closer to the tip than within 2 to 13 scale divisions. Nevertheless, within 10 minutes part of the tip wasted away. The decrease amounted to 1-3 scale divisions, depending on the distance from the tip to the place where the mercury touched the needle. Two of the microphotographs are shown in Fig. 151. The lower picture was taken 12 minutes after the upper one. It is easy to see from certain characteristics of the crystal that the needle as a whole did not shift with respect to the eyepiece scale. To show that the effect was not due to evaporation of the fine tip Volmer and Adhikari made blank experiments in which the mercury drops were not allowed quite to touch the needles. There was no noticeable decrease in the tip even after an hour.

Moll<sup>7</sup> confirmed the results of Volmer and Adhikari by using phthalic anhydride, coumarin and diphenylmethane. Paraffin and cetyl alcohol gave negative results because these substances do not spread on the surface of mercury. Moll also devised another experiment to show the mobility in the top layer of a crystal. By watching between crossed Nicols the interference colors from a thin crystal of benzophenone he found that the color changed not only at the places where the mercury touched the crystal, but even at some distance away from those places. The change in color is due to a decrease in the thickness of the layer, which in turn means that molecules of the top layer are free to leave their positions.

The experiments described so far prove conclusively that the surface of a crystal possesses a mobile layer of molecules, at least above the temperatures where recrystallization phenomena begin. Most important for the understanding of adsorption are those experiments of Volmer and Adhikari<sup>8</sup> in which they proved that benzophenone adsorbed on glass possesses mobility. Benzophenone was crystallized on a glass plate at a distance of about 0.02 to 0.09 mm. from the edge of the plate. Drops of mercury were then made to brush against the edge, great care being taken that the mercury should not come in

<sup>7</sup> F. Moll, *Z. phys. Chem.*, **136**, 183 (1928).

<sup>8</sup> M. Volmer and G. Adhikari, *Z. phys. Chem.*, **119**, 46 (1926).

contact with the crystals. After 1 to 5 hours the glass plate with the crystals was weighed on a micro-balance. The amount of benzophenone lost was about five times as large as the loss due to evaporation. Volmer and Adhikari concluded therefore that the benzophenone molecules adsorbed on the glass plate were able to move from the crystal to the edge of the plate, where they were picked up by mercury. A rather idealized calculation showed that the frictional resistance offered to the motion over the surface was only 1/100 as large as that offered to the diffusion of molecules of about the same size in water solution.

Since the molecule in physical adsorption is not held by strong forces, migration over the surface may take place readily even at low temperatures. Nevertheless, the migration is not entirely free. We have seen in Chapter VII that the heat of adsorption of a molecule over different points of a crystal lattice is different. Orr<sup>9</sup> calculated that the heat of adsorption of an argon atom located above the center of a lattice cell of the (100) plane in potassium chloride is about 1600 calories per mole, but the heat of adsorption above the mid-point of a lattice edge is only about 1300 calories per mole. If an argon atom is to move from one potential minimum to another over the surface of potassium chloride it has to pass on its way over the place of higher potential. This requires an activation energy of about 300 calories. Barrer<sup>10</sup> calculated the heats of adsorption of nitrogen, argon and hydrogen on graphite, and found that the value over the center of the carbon hexagon was higher than over an apex by about 400 calories for nitrogen and argon and by about 180 calories for hydrogen. When the thermal energy  $RT$  is approximately equal to these energies of activation the molecules should be able to move freely over the surface. Thus Barrer concluded that free surface mobility should be possible for hydrogen at 90° K. and for nitrogen and argon at about 200° K.

Beebe and Dowden<sup>11</sup> noted that the adsorption of nitrogen, carbon monoxide and oxygen on chromic oxide at  $-183^{\circ}\text{C}$ . was accompanied by a slow process that possessed activation energies ranging from 180 to 690 calories per mole. These values are of the same order of magnitude as the energy differences calculated by Orr and Barrer, and may actually represent the energies of activation of the surface migration of molecules adsorbed by van der Waals forces.<sup>12</sup>

<sup>9</sup> W. J. C. Orr, *Trans. Far. Soc.*, **35**, 1247 (1939).

<sup>10</sup> R. M. Barrer, *Proc. Roy. Soc.*, **A161**, 476 (1937).

<sup>11</sup> R. A. Beebe and D. A. Dowden, *J. Am. Chem. Soc.*, **60**, 2912 (1938).

<sup>12</sup> The experiments of Beebe and Dowden will be further discussed in Volume II.

Tiselius<sup>13,14</sup> investigated the surface migration of adsorbed water and ammonia over the zeolite crystals heulandite and analcite. The adsorption of strong permanent dipole molecules by ionic crystals constitutes the borderline between physical and chemical adsorption, and the above adsorbent-adsorbate systems belong to this group. The heat of adsorption of water on heulandite is 14,100 cal./mole, and that of ammonia on analcite is 16,600 cal./mole. Since the adsorbed molecules are held by strong forces the rate of surface diffusion is slow, and the process necessitates a considerable activation energy.

Due to certain optical characteristics of the zeolites Tiselius succeeded in accomplishing rate measurements on single crystals. Analcite and heulandite remain transparent after dehydration and during the subsequent adsorption experiments, provided that the operations are performed slowly and too high temperatures are avoided.<sup>15</sup> When the empty or partly saturated crystals are investigated under the polarizing microscope they show certain changes in optical properties which can be ascribed to a continuous variation of the double refraction and the angle of extinction with the amount of water or ammonia adsorbed. Measurements of these quantities enabled Tiselius to determine accurately the concentration of the adsorbate in any part of the single crystal. He found that the diffusion of water into the monoclinic crystal heulandite showed strong anisotropy.<sup>13</sup> The energy of activation of diffusion perpendicular to the (201) face was 5400 cal./mole, that perpendicular to the (001) face was 9140 cal./mole. The former represents 40%, the latter 65% of the heat of adsorption. The diffusion of ammonia into the cubic crystal analcite was isotropic.<sup>14</sup> The energy of activation of the surface migration was 14,500 cal./mole, or almost 90% of the heat of adsorption. Tiselius suggests that in heulandite the adsorption centers, or potential minima, are much closer to each other than in analcite. In heulandite the force fields of two neighboring centers overlap, and so only half as much energy is required for an adsorbed molecule to hop from one center to another as to hop away from the lattice completely. In analcite the adsorbing centers are quite far apart; therefore the energy of activation of migration is almost as large as the heat of adsorption. This explanation is

<sup>13</sup> A. Tiselius, *J. Phys. Chem.*, **40**, 223 (1936).

<sup>14</sup> A. Tiselius, *Z. phys. Chem.*, **A174**, 401 (1935).

<sup>15</sup> To obtain conveniently measurable rates Tiselius had to use temperatures over 300° C.

supported by the fact that analcite contains only 8.6% water at saturation, whereas heulandite contains 16.2%.<sup>16</sup>

#### THE AVERAGE LIFE OF THE ADSORBED MOLECULE

The time spent by a molecule on the surface can be evaluated with the help of Langmuir's<sup>8</sup> theory. From equations (11), (17) and (18) in Chapter IV the value of  $\nu_1$ , the rate of evaporation from a completely covered surface, can be calculated if  $\alpha_0$ , the condensation coefficient, is assumed to be unity. Langmuir called the reciprocal of  $\nu_1$  the "relative life"; for the adsorption of nitrogen by mica at 90° K. (Fig. 35) it is  $1.78 \times 10^8$  seconds per sq. cm. surface. This means that it would take about 50 hours for 1 mole of nitrogen to desorb from 1 sq. cm. surface of mica if the surface were kept constantly saturated with nitrogen.

The "average life" spent by a molecule on the surface is defined by

$$(3) \quad \tau = s_1/\nu_1$$

where  $s_1$  is the surface concentration at complete covering. The value of  $s_1$  can be calculated if the surface of the adsorbent is known. If we assume with Langmuir that the true surface of the mica used by him was equal to its geometrical surface, we obtain from his isotherms  $\tau$  values of  $10^{-4}$  to  $10^{-5}$  seconds.

Holst and Clausing<sup>17</sup> attempted to measure  $\tau$  experimentally. They directed a vertical molecular stream against a rapidly rotating horizontal plate. The molecules were adsorbed by the plate; they were carried along in the direction of the motion of the plate during the adsorption time and were finally emitted to a strongly cooled surface. The distance between the deposit and the place where the stream first hit the plate was measured, and the adsorption time was calculated from the known rotational velocity of the plate. Due to great experimental difficulties the investigators could ascertain only that for the adsorption of cadmium vapor on surfaces of glass, picein, mica or copper at 200° K. the upper limit of the mean adsorption time was  $10^{-6}$  seconds.

A more successful determination of  $\tau$  was carried out by Clausing,<sup>18</sup>

<sup>16</sup> The channels in heulandite and analcite are so narrow that all molecules within them are under the influence of surface forces. The diffusion into the channels is therefore surface diffusion and not gas-phase diffusion.

<sup>17</sup> G. Holst and P. Clausing, *Physica*, 6, 48 (1926).

<sup>18</sup> P. Clausing, *Ann. der Phys.*, (5), 7, 489, 521 (1930).



using a different experimental approach.<sup>19</sup> He passed a stream of molecules at low pressure through a capillary tube into an evacuated container and measured the time necessary for the passage. The pressure of the stream was so low that the molecules did not collide with each other, so that all collisions were with the walls of the capillary. The longer the time spent by a molecule on the wall, the longer is the time required for its passage through the capillary. Clausing derived the relationship

$$(4) \quad \tau = 2 \left( \frac{2r}{L} \right)^2 \bar{t} - \frac{2r}{u}$$

where  $r$  and  $L$  are the radius and the length of the capillary,  $u$  is the mean velocity of the molecules, and  $\bar{t}$  is the average time of passage through the capillary. Using a glass capillary he determined  $\tau$  for argon, nitrogen and neon at low temperatures. The value of  $\tau$  for argon at 78° K. was  $75 \times 10^{-5}$ , at 90° K.  $3.1 \times 10^{-6}$  seconds. The values for nitrogen were about the same, but the mean adsorption time of neon on glass was less than  $2 \times 10^{-7}$  seconds at liquid air temperatures.

Clausing found that the temperature dependence of the adsorption time of argon could be expressed by the equation

$$(5) \quad \tau = 1.7 \times 10^{-14} e^{3800/RT}$$

From statistical considerations Frenkel<sup>20</sup> derived the equation

$$(6) \quad \tau = \tau_0 e^{q/RT}$$

where  $\tau_0$  is the period of vibration of a molecule attached to the surface, and  $q$  is the heat of adsorption. Comparison of equations (5) and (6) shows that Clausing's experiments confirm Frenkel's theory.

### THE RATE OF PHYSICAL ADSORPTION

In the derivation of his isotherm equation Langmuir assumed that the rate of adsorption is equal to the rate at which molecules coming from the gas phase strike the surface multiplied by  $\alpha$ , the condensation coefficient. Volmer and Estermann<sup>5</sup> measured  $\alpha$  for the condensation of mercury vapor on surfaces of liquid and solid mercury, and found that its value was 1.0 for the liquid and only slightly less than 1 for

<sup>19</sup> Actually not  $\tau$ , the mean life of the adsorbed molecule on the surface, is measured but  $\alpha\tau$ , the mean adsorption time of all molecules that strike the surface. If the condensation coefficient  $\alpha$  is unity, the two quantities are equal.

<sup>20</sup> J. Frenkel, *Z. Physik*, 26, 117 (1924).

the solid. (At  $-45^{\circ}\text{C}$ .  $\alpha$  was 0.93, at  $-64^{\circ}\text{C}$ ., 0.85.) Since only a small fraction of the impinging gas molecules is reflected back elastically by the solid the rate of adsorption on a free surface is very fast. If, however, the adsorbent contains long and very narrow pores and the gas molecules must diffuse into them, the adsorption will take measurable time. If the incoming molecules must displace other previously adsorbed impurities, or if they must diffuse into the pores against foreign molecules already there, the rate of adsorption may become very slow. Investigators have reported adsorption times measured not merely in hours but in days, and even in months. It is probable that the very long continued uptake of a gas is due to solution in the solid rather than to adsorption, nevertheless equilibration times of many hours are by no means uncommon in physical adsorption.

The theory of adsorption rates was first investigated by McBain.<sup>21</sup> He observed that the adsorption of hydrogen on charcoal consisted of two distinct phenomena. He called one of these adsorption and assumed that its rate was instantaneous; he believed that the other process was solid solution and derived an expression for its rate from Fick's diffusion law. The equation is

$$(7) \quad Q = \frac{4cL}{\pi^2} \left\{ \frac{\pi^2}{8} - \left( e^{-(D\pi^2/L^2)t} + \frac{1}{9} e^{-(9D\pi^2/L^2)t} + \frac{1}{25} e^{-(25D\pi^2/L^2)t} + \dots \right) \right\}$$

where  $Q$  is the amount of gas that has diffused through unit surface at time  $t$ ,  $c$  is the concentration in the gas phase (assumed to remain constant),  $L$  is the total thickness of the solid, and  $D$  is the diffusion constant. If a considerable fraction of the final amount is already dissolved in the solid, all terms but the first in the parenthesis can be neglected to a very good approximation. One obtains then

$$(8) \quad v = A \left( \frac{\pi^2}{8} - e^{-k't} \right)$$

where  $v$  is the volume dissolved at time  $t$ , and  $A$  and  $k'$  are constants. Neglecting the second and higher terms in the expansion causes an error of less than 0.1% when  $v$  is 50% of the final amount dissolved, and less than 1% when  $v$  is 40% of the final value.

McBain did not test equations (7) and (8), nor did any other investigator of adsorption rates in the thirty-three years that elapsed since they were proposed. Nevertheless, the realization that the rate determining step in physical adsorption is a diffusion process finally led back to the adoption of equations identical in form with McBain's

<sup>21</sup> J. W. McBain, *Z. phys. Chem.*, 68, 471 (1909).

equation (7). To be sure, the diffusion is into the pores of the adsorbent and not into its body, but this necessitates only the reinterpretation of some of the terms, as we shall see later.

Bergter<sup>22</sup> was one of the first investigators to carry out systematic adsorption rate experiments. Of greatest interest among these are his measurements of the rate of nitrogen adsorption on charcoal at 18° C. and at pressures between 0.36 and 6.75 mm. The initial rate was always very rapid; about 96% of the final adsorption value was taken up in the first 2 minutes. Since equilibrium was attained even at these low pressures in half an hour there is no doubt that Bergter dealt with pure physical adsorption. To express his results he used the empirical equation

$$(9) \quad v = v_0(1 - 0.95e^{-3.5t} - 0.05e^{-0.15t})$$

Table LXXI shows the agreement between the observed and calculated volumes adsorbed at pressures of 0.94 and 1.34 mm. (The pres-

TABLE LXXI  
RATE OF ADSORPTION OF NITROGEN ON COCONUT CHARCOAL

Pressure = 0.939 mm.			Pressure = 1.344 mm.		
Time	$V_{\text{obs.}}$	$V_{\text{calc.}}$	Time	$V_{\text{obs.}}$	$V_{\text{calc.}}$
0 min. 0 sec.	0	0	0 min. 0 sec.	0	0
1 min. 0 sec.	0.0153	0.0152	1 min. 20 sec.	0.0226	0.0229
1 min. 45 sec.	0.0157	0.0157	2 min. 10 sec.	0.0228	0.0231
6 min. 0 sec.	0.0161	0.0162	3 min. 20 sec.	0.0232	0.0233
10 min. 0 sec.	0.0162	0.0162	8 min. 15 sec.	0.0236	0.0237
30 min. 0 sec.	0.0165	0.0164	10 min. 30 sec.	0.0238	0.0238
70 min. 0 sec.	0.0167	0.0164	21 min. 0 sec.	0.0240	0.0240
			33 min. 0 sec.	0.0240	0.0241

sure determines the value of the constant  $v_0$ .) It should be noted that the empirical equation (9) has some formal resemblance to equation (7).

The theory of the rate of adsorption on a free surface was first derived by Langmuir.<sup>3</sup> The experimentally measured rate is the difference between the rate at which the molecules condense on the surface and the rate at which they leave the surface. If the rate is determined at constant pressure it is given by

$$(10) \quad \frac{d\theta}{dt} = k_1(1 - \theta) - k_2\theta$$

where  $\theta$  is the fraction of the surface covered with adsorbed gas, and  $k_1$

<sup>22</sup> F. Bergter, *Ann. der Phys.*, (5), 37, 472 (1912).

and  $k_2$  are constants. (The constant  $k_1$  includes the pressure.) Integrating with the boundary condition that  $\theta = 0$  when  $t = 0$ , we obtain

$$(11) \quad \theta = \frac{k_1}{k_1 + k_2} [1 - e^{-(k_1 + k_2)t}]$$

When  $t = \infty$ ,  $\theta = \theta_e$ , where  $\theta_e$  is the fraction of the surface covered when equilibrium is reached. This gives the relation

$$(12) \quad \theta_e = \frac{k_1}{k_1 + k_2}$$

from which it follows that

$$(13) \quad \theta = \theta_e(1 - e^{-kt})$$

where  $k = k_1 + k_2$ . Since  $\theta = v/v_m$ , equation (13) can be written in the form

$$(14) \quad v = v_e(1 - e^{-kt})$$

where  $v$  and  $v_e$  are the volumes adsorbed after time  $t$  and at equilibrium respectively.

Harned<sup>23</sup> tested equation (14) for the rate of adsorption of chloropicrin and of carbon tetrachloride on charcoal at low pressures. The equation can be put in the form

$$(15) \quad \ln \frac{v_e}{v_e - v} = kt$$

A plot of the function on the left hand side against  $t$  should give a straight line. Harned found that for charcoals with clean surfaces equation (15) was actually obeyed, as Fig. 152 shows. The temperature of the runs was 20° C., the pressure of chloropicrin 0.61 mm. Prior to these runs the charcoal was evacuated at 700° C. for three hours; the surface was then treated with chloropicrin, and the vapor was removed by evacuation at 700° C. for two hours. Unless adsorbed impurities are removed in some such manner the rate of adsorption becomes very slow. One charcoal, for example, after washing with chloropicrin and evacuation at 700–900° C. reached saturation at 5.9 mm. pressure in 100 seconds. When the surface of this charcoal was not treated with vapor and evacuation was carried out at 350° C. it adsorbed at the same pressure only 60% of the saturation value in 6600 seconds.

<sup>23</sup> H. S. Harned, *J. Am. Chem. Soc.*, **42**, 372 (1920).

If the rate of adsorption is measured at constant volume and variable pressure,  $v_e$  in equation (15) will not be constant but will represent the equilibrium adsorption corresponding to the instantaneous pressure at time  $t$ . Iliin<sup>24</sup> found that with the proper corrections the data of Titoff,<sup>25</sup> obtained for the rates of adsorption of ammonia and carbon dioxide on charcoal at 0° C., conform very well to equation (15).

Berl and Weingaertner<sup>26</sup> tested Langmuir's equation (15) by determining the rates of adsorption of methane, ethane and propane

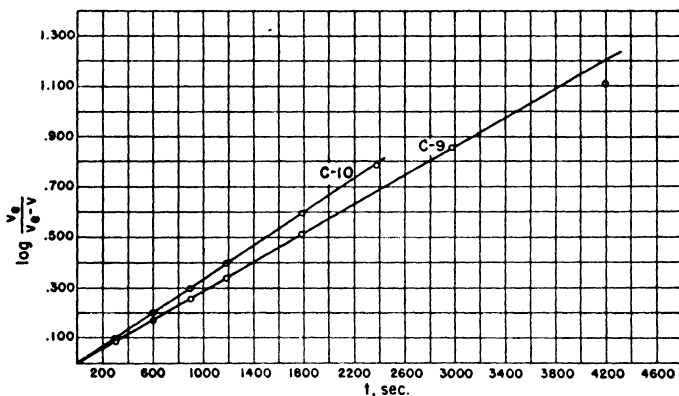


FIG. 152.—The rate of adsorption of chloropicrin on charcoal plotted according to equation (15).

on charcoal at low pressures. They found that the data plotted according to equation (15) gave very good straight lines for the rates measured above the critical temperatures. They attributed the deviations from the straight line below the critical temperature to condensation of the two-dimensional gas to two-dimensional liquid.<sup>27</sup> They also investigated the temperature coefficients of the adsorption rates. Using the Arrhenius equation they calculated that the energy of activation of the adsorption process was 3000 cal./mole for each of the three gases.

<sup>24</sup> B. Iliin, *Z. phys. Chem.*, 107, 145 (1923).

<sup>25</sup> A. Titoff, Dissertation, pp. 268 and 314.

<sup>26</sup> E. Berl and E. Weingaertner, *Z. phys. Chem.*, A173, 35 (1935).

<sup>27</sup> Compare this with the experiments of E. Weingaertner (*Z. Elektrochem.*, 42, 599, 1936), discussed in Chapter XII. T. D. Phillips (*Phys. Rev.*, (2), 45, 215, 1934) also attributes certain peculiarities in the rate of adsorption of hydrogen on charcoal to two-dimensional condensation.

Although the experiments of Harned,<sup>23</sup> Iliin,<sup>24</sup> and Berl and Weingaertner<sup>26</sup> seem to be in complete agreement with the Langmuir rate equation (15), further considerations show that the agreement is only apparent and not real. Here again we have examples of the fact that a good fit between an equation and the experimental data is necessary but not sufficient to prove a theory. One must examine carefully the meaning of the constants evaluated from the data before safe conclusions can be drawn.

If we examine the derivation of the Langmuir equation in Chapter IV we find that the meaning of the constant  $k$  in equations (14) and (15) is given by

$$(16) \quad k = \frac{\alpha\mu + \nu_1}{s_1}$$

where  $\alpha$  is the condensation coefficient,  $\mu$  is the number of moles of gas striking unit surface per second,  $\nu_1$  is the number of moles of gas evaporating from unit surface per second at complete covering, and  $s_1$  is the number of moles of gas adsorbed on unit surface at complete covering. It was pointed out by Langmuir<sup>3</sup> that the time required for the adsorption of half the equilibrium amount,  $t_{1/2}$ , is always less than  $\tau$ , the average life of the molecule on the surface. This follows from equations (15) and (16) because

$$(17) \quad t_{1/2} = \frac{s_1 \ln 2}{\alpha\mu + \nu_1} < \frac{s_1}{\nu_1}$$

As equation (3) shows, the last term is  $\tau$ . The order of magnitude of  $\tau$  at liquid air temperatures is  $10^{-5}$  seconds and at higher temperatures even smaller. According to Damköhler's<sup>28</sup> calculations the value of  $\tau$  for the adsorption of argon on silica gel at  $111^\circ \text{K}$ . is  $2.3 \times 10^{-7}$  seconds, and for oxygen on silica gel at  $373^\circ \text{K}$ . is  $1.2 \times 10^{-10}$  seconds. In contrast with this the  $t_{1/2}$  values measured by Harned<sup>23</sup> and by Berl and Weingaertner<sup>26</sup> were of the order of several minutes. It is clear therefore that these investigators did not deal with adsorption on a free surface according to the Langmuir mechanism. Nor would one expect this, since in adsorbents like charcoal and silica gel the rate determining step should be the diffusion of gases into the narrow pores and not the surface adsorption.

Damköhler<sup>28</sup> pointed out another fact which shows that Berl and Weingaertner did not deal with adsorption on a free surface. In the linear region of the adsorption isotherm, where  $\alpha\mu \ll \nu_1$ , it follows

<sup>28</sup> G. Damköhler, *Z. phys. Chem.*, A174, 222 (1935).

from equation (16) that

$$(18) \quad k \sim \frac{\nu_1}{s_1} = \frac{\nu_0}{s_1} e^{-q/RT}$$

where  $\nu_0$  is a constant, and  $q$  is the heat of adsorption. According to equation (18) the energy of activation of the adsorption process is equal to the heat of adsorption. However, Berl and Weingaertner obtained an energy of activation of 3000 cal./mole for the adsorption of methane, ethane and propane by charcoal, which is much smaller than even the smallest among the three heats of adsorption (about 6000 cal./mole). As we shall see, the smaller energy of activation can be explained too, if we assume that the slow step is the diffusion of the molecules and not the adsorption itself.

The rate equation for the diffusion of molecules in the pores of an adsorbent was derived by Damköhler.<sup>28</sup> Since the molecules can diffuse either through the gas phase or over the surface, the differential equation for the rate of adsorption is

$$(19) \quad \frac{\partial}{\partial t} (N_g + N_a) = D_g \frac{\partial^2 N_g}{\partial x^2} + D_a \frac{\partial^2 N_a}{\partial x^2}$$

where  $N_g$  is the number of molecules in the gas phase per unit length of the pore,  $N_a$  is the number of molecules in the adsorbed phase per unit length of the pore, and  $D_g$  and  $D_a$  are the diffusion coefficients in the gas phase and over the surface. Because the pores have very small cross-sections the problem is considered as a one-dimensional diffusion.

The volume diffusion coefficient for a cylindrical pore is given by

$$(20) \quad D_g = 2r\bar{u}_g/3, \quad \bar{u}_g = (8RT/\pi M)^{1/2}$$

where  $r$  is the radius of the pore, and  $\bar{u}_g$  is the mean molecular velocity in the gas phase. If the pores have any other shape, the equation is

$$(21) \quad D_g = C_g(T/M)^{1/2}$$

where  $C_g$  is a constant. The surface diffusion coefficient is given by

$$(22) \quad D_a = \frac{1}{2} \Lambda_a \bar{u}_a$$

where  $\Lambda_a$  is the mean free path of the molecule over the surface, and  $\bar{u}_a$  is the mean velocity. The latter is also proportional to  $(T/M)^{1/2}$ , therefore

$$(23) \quad D_a = C_a(T/M)^{1/2}$$

The constant  $C_a$  depends strongly on temperature. We have seen

before that when a molecule moves from one position of equilibrium to another over the surface it has to climb over a potential barrier. If the height of this barrier is  $E$ , then

$$(24) \quad C_a = C_0 e^{-E/RT}$$

Thus surface diffusion has an energy of activation even in physical adsorption. The energy of activation must necessarily be smaller than the heat of adsorption, which explains the above discussed results of Berl and Weingartner.<sup>26</sup>

The relation between  $N_a$  and  $N_g$  can be expressed by means of the adsorption isotherm equation. If the rate is measured in the linear region of the isotherm, equation (19) becomes

$$(25) \quad \frac{\partial N_g}{\partial t} = D \frac{\partial^2 N_g}{\partial x^2}$$

with the overall diffusion coefficient given by

$$(26) \quad D = \frac{D_g + AD_a}{1 + A}$$

Here  $A = N_a/N_g$ , which is constant for the linear region of the isotherm. Equation (25) can be solved if the boundary conditions are specified. For adsorption at constant pressure the solution is

$$(27) \quad \vartheta = 1 - \frac{8}{\pi^2} \sum_{m=0}^{\infty} \frac{e^{-\delta(2m+1)^2}}{(2m+1)^2}$$

where  $\vartheta$  is the fraction of the equilibrium amount adsorbed at time  $t$ , and

$$(28) \quad \delta = (2\pi/L)^2 Dt$$

$L$  is the length of the capillary. Damköhler's equation (27) is formally identical with McBain's equation (7); the main difference is in the meaning of the diffusion coefficient  $D$ .

By estimating the values of the constants of his equation Damköhler came to the conclusion that in the region of good adsorption, where  $A$  is about  $10^3$  or greater, the gas-phase diffusion becomes negligible in comparison with the surface diffusion. At small adsorptions  $D_a$  and  $D_g$  are of the same order of magnitude. The rates of diffusion are measurable in minutes, in agreement with the experimentally obtained rates of physical adsorption.

It is easy to see why the results of Harned<sup>23</sup> and of Berl and Weingartner<sup>26</sup> could be fitted so well by the Langmuir rate equation.



There is a strong formal resemblance between that equation and the diffusion equations of Damköhler<sup>28</sup> and McBain.<sup>21</sup> Note, for example, the similarity between equations (8) and (14). Formally the only difference is that in the parenthesis one equation has  $\pi^2/8$ , which is equal to 1.23, the other has 1. Figure 153 gives a comparison between equations (14) and (27), taken from Damköhler. The upper curve gives the rate according to the diffusion equation, the lower

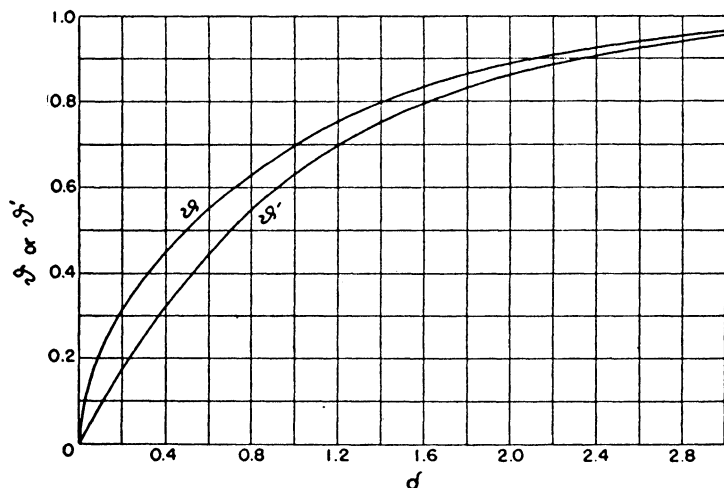


Fig. 153.—The rate of adsorption according to equations (14) and (27).

curve according to the surface adsorption equation. ( $y' = v/v_e$ , and  $\delta = kt$ .) The difference between them is great only at small adsorptions; at  $\delta = 0$  the slope of the  $y$  curve is  $\infty$ , whereas the slope of the  $y'$  curve is unity. It is interesting to note in this connection that although the rate curves of Berl and Weingaertner agreed well with the Langmuir equation (14), the points at the beginning of the adsorption deviated strongly from the theoretical curves, giving larger velocity constants than the later values. This indicates that the  $y$  curve would have given a better fit than the  $y'$  curve.

Damköhler interpreted the rate curves of Giesen<sup>29</sup> for the adsorption of carbon dioxide and ammonia on charcoal in terms of his theory. In Fig. 154 the full curves were calculated on the basis of equation (27), the circles give the experimental points. The four upper curves show

<sup>29</sup> J. Giesen, *Ann. der Phys.*, 10, 830 (1903).

the results for carbon dioxide, the three lower curves for ammonia. Both coordinates are plotted on logarithmic scale. For the first minute the agreement between theory and experiment is not very good, possibly because the temperature equilibration was not complete. From the second to the tenth minute the agreement is very good. According to the theoretical curve adsorption is complete after ten minutes, but actually there is a slight additional adsorption. The

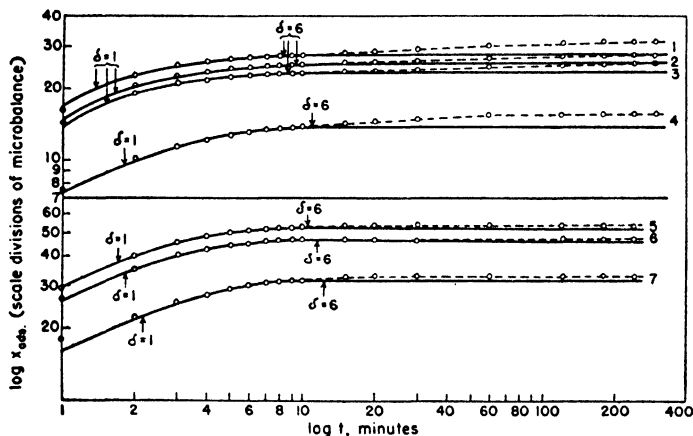


FIG. 154.—The rates of adsorption of carbon dioxide and ammonia on charcoal, calculated on the basis of Damköhler's equation (27).

reason for this is that the theoretical curves were calculated for an average sized capillary, whereas Giesen's charcoal probably had some pores much narrower than the average, into which diffusion continued for several hours.

Barrer and Rideal<sup>30</sup> derived an equation for the rate of physical adsorption which is quite similar to Damköhler's equation (27). They found that the equation was able to express satisfactorily their experimental data for the rates of adsorption of hydrogen, oxygen and nitrogen on sugar carbon at 78 and 195° K. They also found that the data could be represented equally well by an equation formally similar to equation (15). The ratios of the velocity constants  $k$  for the three gases were

$$\text{O}_2 : \text{N}_2 : \text{H}_2 = 1 : 1.1 : 3.2$$

while the rates of diffusion according to the kinetic theory of gases

<sup>30</sup> R. M. Barrer and E. K. Rideal, *Proc. Roy. Soc., A149*, 231 (1935).

would have the ratios

$$\text{O}_2 : \text{N}_2 : \text{H}_2 = 1 : 1.1 : 4$$

Furthermore, the rates had no appreciable temperature coefficients. Barrer and Rideal therefore concluded that the rate determining step was the gas-phase diffusion into the pores. Apparently surface diffusion played a subordinate role in these experiments.

Wicke<sup>31</sup> derived a diffusion equation for the rate of adsorption which is somewhat different from equation (27). He visualizes the adsorbent as being permeated by a system of macropores and micropores, with the micropores surrounding the macropores like fjords. The micropores are assumed to be short but so numerous that their total surface area is 1000 times as large as that of the macropores.<sup>32</sup> Thus the macropores must transport 1000 times as much gas as would be necessary if their walls were smooth. The rate of adsorption according to this picture is determined by the rate of transport of the gases in the macropores; the micropores fill rapidly since they are short and have very small volumes.

Wicke assumed that the adsorbent particles were spherical, and he set up a differential equation for the diffusion of the gas toward the center of a sphere. With certain boundary conditions the solution of the equation is<sup>33</sup>

$$(29) \quad \vartheta = 1 - \frac{6}{\pi^2} \sum_{n=1}^{\infty} \frac{1}{n^2} e^{-\delta n^2}$$

with

$$(30) \quad \delta = (\pi^2/R^2A)Dt$$

Here  $\vartheta$  is the fraction of the equilibrium amount adsorbed at time  $t$ ,  $R$  is the radius of the sphere,  $A$  is a constant, and  $D$  is the diffusion coefficient. The constant  $A$  has a meaning similar to that in equation (26), and  $D$  is identical with  $D_0$  since according to the mechanism suggested by Wicke surface diffusion can not play an important role in the rate process.

Equation (29) is formally not very different from equation (27). The same experimental data can be fitted about equally well by either equation, as Fig. 155 shows. The points represent the rate of adsorption of carbon dioxide on medicinal charcoal at 0° C. and 1 mm. pres-

<sup>31</sup> E. Wicke, *Kolloid Z.*, **86**, 167 (1939).

<sup>32</sup> See the discussion of macropores and micropores in Chapter XI.

<sup>33</sup> The same equation was derived earlier for the solution of hydrogen in copper by A. F. H. Ward (*Proc. Roy. Soc.*, **A133**, 522, 1931).

sure, obtained by Wicke. The full curve represents the rate calculated from the spherical diffusion equation of Wicke, the dotted curve that obtained from the cylindrical diffusion equation of Damköhler.

Figure 155 also shows that the experimentally measured rates of adsorption and desorption are identical. This follows from the diffusion theory if the amount adsorbed in unit time is so small that the adsorbent is not heated up appreciably. At higher pressures the heat

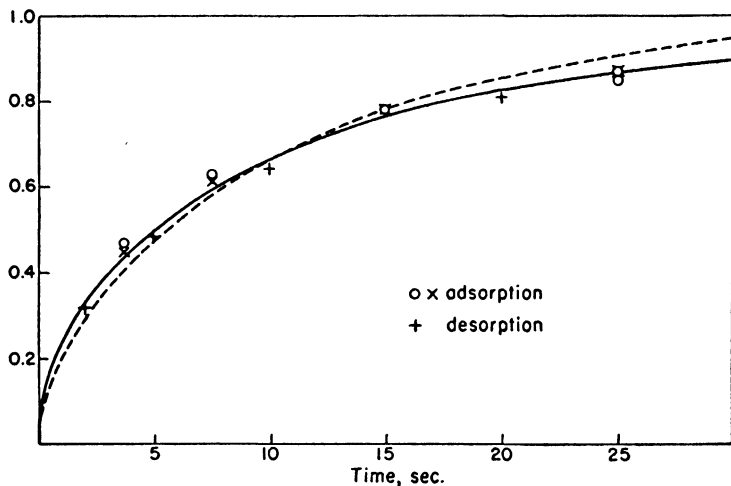


FIG. 155.—The rate of adsorption of carbon dioxide on charcoal, calculated on the basis of Damköhler's equation (27) and Wicke's equation (29). The former is the broken curve, the latter the full curve.

given out in the adsorption process and the heat absorbed in the desorption process make the rates of diffusion different. In addition, in the course of desorption gas is taken out of the pore space with a resulting decrease in heat conductivity. The difference between the rates of adsorption and desorption is particularly great in dynamic processes which play such an important role in the technical application of adsorption.<sup>34</sup>

In the examples discussed so far equilibrium was attained in seconds or minutes. If an adsorbent has long and very narrow pores it may take many hours to reach equilibrium. The extreme example of such

<sup>34</sup> In three papers E. Wicke (*Kolloid Z.*, 86, 295, 1939; 90, 156, 1940; 93, 129, 1940) discusses his theoretical and experimental investigations on the rates of adsorption and desorption in dynamic systems.

an adsorbent is chabasite, which adsorbs molecules as large as nitrogen or ethylene very slowly. Figure 156, taken from Dohse and Mark,<sup>35</sup> shows the rate of adsorption of a number of gases by chabasite. The figure illustrates clearly the great differences between the rates of adsorption of smaller molecules, like ammonia and hydrogen, and somewhat larger molecules, like nitrogen and ethylene. The time of equilibration for the two latter is of the order of 15 to 20 hours.<sup>36</sup>

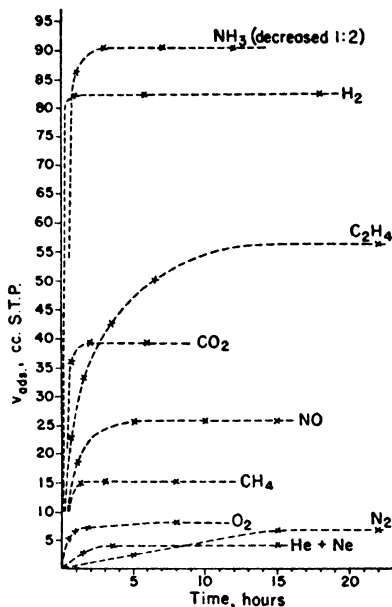


Fig. 156.—The rates of adsorption of gases on chabasite.

If there are impurities present either in the gas phase or in the adsorbed phase the rate of adsorption is cut down very strongly. Patrick and Cohan<sup>37</sup> studied the effect of gaseous impurities on the rate of adsorption of water vapor by silica gel. Their results are shown in Fig. 157 *a* and *b*. Curve 1 in Fig. 157*a* represents the rate of adsorption of water vapor at 4.6 mm. pressure and 25° C. in the presence of small partial pressures of air, ranging from  $2.4 \times 10^{-4}$  mm.

<sup>35</sup> H. Dohse and H. Mark, *Die Adsorption von Gasen und Dämpfen an festen Körpern*, Leipzig, 1935, p. 114.

<sup>36</sup> The authors did not state the temperature and the pressure of these rate runs.

<sup>37</sup> W. A. Patrick and L. H. Cohan, *J. Phys. Chem.*, 41, 437 (1937).

to 0.5 mm. All the experimental points fall on a smooth curve, showing that up to 0.5 mm. pressure there is no inhibition. In Fig. 157b curve 1 is the same as in Fig. 157a, except that the time coordinate is plotted on a different scale. Curve 2 represents the rate in the presence of 1 mm. of air, nitrogen or oxygen, curve 3 in the presence of 3.9 mm. of hydrogen, and curve 4 in the presence of 3.6 mm. of air, nitro-

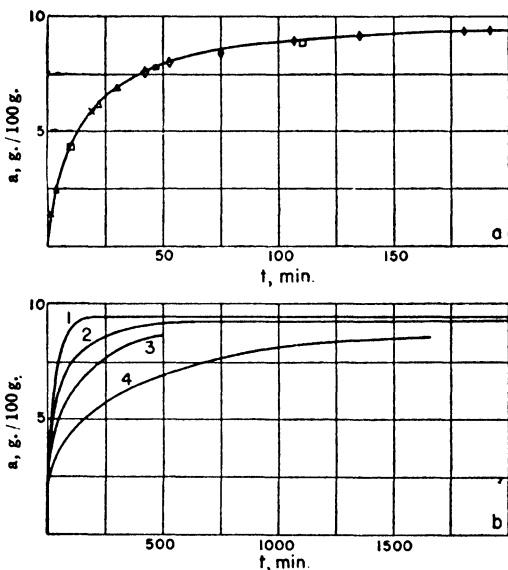


FIG. 157.—The rate of adsorption of water vapor on silica gel in the presence of gaseous impurities.

gen or oxygen. While with air pressures less than 0.5 mm. equilibrium is established in 2 to 3 hours, when the pressure reaches 3.6 mm. equilibrium is not attained even in 25 hours. Hydrogen inhibits the rate less than the heavier molecules. Patrick and Cohan concluded that the rate decreased because the gaseous diffusion of water vapor into the capillaries of silica gel was retarded strongly by the presence of permanent gases inside the capillaries.

A simple calculation shows that small quantities of adsorbed impurities may cause large effects on the rate of adsorption in capillaries. Let us assume that we have a cylindrical capillary of radius  $30\text{\AA}$  and length  $10^{-3}$  cm., and that 1% of the surface of the capillary is covered with adsorbed oxygen. We intend to measure the rate of

adsorption of some organic vapor at 0° C. and 760 mm. pressure. If in the first rush the vapor molecules displace the adsorbed oxygen from the surface there will be enough oxygen molecules in the gas phase to build up a pressure of about 1 atmosphere inside the capillary. It follows from the results of Patrick and Cohan that the rate of diffusion of the vapor into the capillary against this oxygen pressure would be exceedingly slow.

Adsorption on the walls of capillaries reduces the effective diameter of the capillary. The rate of adsorption increases with pressure, but the effect of reducing the capillary diameter usually overbalances the effect of increased pressure on the time of equilibration. Cameron and Reyerson<sup>38</sup> found that in the adsorption of bromine on silica gel equilibration was rapid, except at higher pressures. Deitz and Gleysteen<sup>39</sup> noted that the time of reaching equilibrium in the adsorption of nitrogen on bone chars was longer at higher pressures, and the same was found to be true by the author for a variety of adsorbents and adsorbed gases.

The rate of capillary condensation was investigated by Washburn.<sup>40</sup> For a porous body which behaves like an assemblage of very small cylindrical capillaries he derived the equation

$$(31) \quad v = k(\sigma t/\eta)^{1/2}$$

where  $v$  is the volume of liquid penetrating the capillaries in time  $t$ ,  $k$  is a constant,  $\sigma$  is the surface tension and  $\eta$  is the viscosity of the liquid. He tested this equation with some data obtained by Cude and Hulett<sup>41</sup> for the penetration of water into charcoal. The results are shown in Fig. 158. At first the rate is actually proportional to the square root of the time, but later it becomes much smaller than is demanded by equation (31). Washburn attributed the slower rate to penetration of the liquid into the micropores of the adsorbent.

The rate of adsorption even in adsorbents possessing the narrowest pores is measurable only in hours, as we have seen in Fig. 157. However, some investigators followed the uptake of a gas by an adsorbent for weeks, and even for months. Bangham and Burt<sup>42</sup> investigated the rate of sorption of carbon dioxide by glass and found that their

<sup>38</sup> A. E. Cameron and L. H. Reyerson, *J. Phys. Chem.*, **39**, 169 (1935).

<sup>39</sup> V. R. Deitz and L. F. Gleysteen, To be published in the *Journal of Research* of the National Bureau of Standards.

<sup>40</sup> E. W. Washburn, *Phys. Rev.*, (2), **17**, 374 (1921).

<sup>41</sup> H. E. Cude and G. A. Hulett, *J. Am. Chem. Soc.*, **42**, 391 (1920).

<sup>42</sup> D. H. Bangham and F. P. Burt, *Proc. Roy. Soc.*, **A105**, 481 (1924).

results could be expressed quite accurately by the empirical equation (32)

$$v = kt^{1/m}$$

where  $k$  and  $m$  are empirical constants. The equation has the same form as the Freundlich equation, except that pressure is replaced by time.<sup>43</sup> Further investigations revealed that the sorption of ammonia,

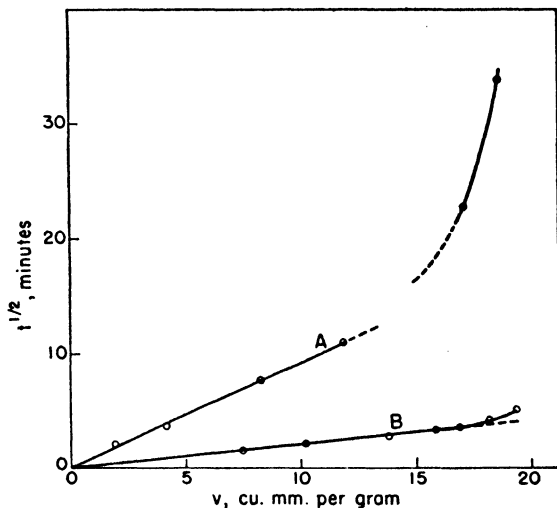


FIG. 158.—The rate of penetration of water into charcoal, calculated on the basis of Washburn's equation (31).

sulfur dioxide and nitrous oxide by glass also obeys this equation. However, it is clear from the form of the equation that it can not be valid close to equilibrium, since it would give infinite sorption for infinite time. For very long runs, reaching into weeks, Bangham and Sever<sup>44</sup> used the equation

$$(33) \quad \log \frac{v_s}{v_s - v} = kt^{1/m}$$

where  $v_s$  is the amount sorbed at equilibrium. It should be noted that for  $m = 1$  equation (33) becomes formally identical with Langmuir's equation (15).

<sup>43</sup> Note the similarity between equations (31) and (32). Since  $\sigma$  and  $\eta$  are constant at constant temperature they can be incorporated into the constant  $k$ . In Washburn's equation  $m = 2$ , but the latter parts of curves A and B in Fig. 158 indicate higher values of  $m$ .

<sup>44</sup> D. H. Bangham and W. Sever, *Phil. Mag.*, (6), 49, 935 (1925).



Bangham and Sever concluded that the long continued sorption of gases by glass in the above experiments was very likely an absorption (or solution) process and not adsorption. They advanced two reasons for this. In the first place the amount of gas taken up was many times greater than that necessary to cover the glass with an adsorbed monolayer. At the temperatures and pressures of the experiments only a fraction of the surface could be covered by physical adsorption, although it is possible that a complete chemisorbed layer was built up by the gases used. Since the true surface area of the glass was not known, this argument is inconclusive. More important is the second point brought up by Bangham and Sever, namely, that the runs continued for very long times, reaching into weeks and even months without attaining complete equilibrium. This sort of behavior is not associated with adsorption processes, and particularly not with adsorption on glass surfaces. It seems probable therefore that the empirical rate equations (32) and (33) refer to solution rather than to adsorption processes. Nevertheless, as we shall see in Chapter XIV, capillary condensation can also go on for weeks. Acetone and benzene can not be soluble in charcoal, and yet Tryhorn and Wyatt<sup>45</sup> found that mixtures of these vapors continued to be adsorbed for weeks. They attributed this slow process to capillary condensation in the intergranular spaces of charcoal.

#### FUNDAMENTAL THEORY OF THE KINETICS OF PHYSICAL ADSORPTION

In a series of twelve papers Lennard-Jones and his collaborators started developing a fundamental theory of adsorption kinetics. The problem was to investigate the detailed mechanism of adsorption on a free surface, based on Langmuir's picture of condensation and evaporation of molecules.

We have seen in Chapter IV, equation (35), that the adsorption constant  $b$  can be derived from statistical considerations. It is proportional to the product  $\alpha\tau$ , where  $\alpha$  is the probability that an atom striking the surface is adsorbed (the condensation coefficient), and  $\tau$  is the average time spent by the molecule in the adsorbed phase. Statistical mechanics permits the evaluation of the product  $\alpha\tau$  but does not enable one to determine  $\alpha$  and  $\tau$  individually. Lennard-Jones and Devonshire,<sup>46</sup> using quantum mechanics, obtained explicit formulas for these constants in terms of the physical properties of the solid and its surface field. To simplify the problem they assumed:

<sup>45</sup> F. G. Tryhorn and W. F. Wyatt, *Trans. Far. Soc.*, **22**, 139 (1926).

<sup>46</sup> J. E. Lennard-Jones and A. F. Devonshire, *Proc. Roy. Soc.*, **A156**, 6, 29 (1936).

(1) that the solid has a simple cubic structure, (2) that the potential of its field of force can be represented by a Morse function, (3) that the heat motion of the surface atoms of the solid is the same as that of the atoms within the solid, and (4) that the heat motion is small compared with the range of the surface forces. Evaporation was supposed to take place by the transfer of a quantum of thermal energy of the solid to the adsorbed molecule.<sup>47</sup> Lennard-Jones and Devonshire worked out the problem for two cases: (1) when the adsorbed

TABLE LXXII  
CONDENSATION COEFFICIENTS OF HYDROGEN

$\Theta$	Temperature, ° K.			
	30	50	100	300
300	0.256	0.279	0.293	0.309
350	0.221	0.226	0.231	0.246
400	0.154	0.163	0.170	0.189
510	0.081	0.085	0.091	0.103

atom can vibrate normally to the surface and migrate freely along it, and (2) when the adsorbed atom can vibrate radially and laterally, but can not migrate over the surface.

We shall not reproduce here the complicated equations for  $\tau$  and  $\alpha$ , but give a few of the numerical results. The condensation coefficient of hydrogen at different temperatures is given in Table LXXII. The value of  $\alpha$  depends on  $\Theta$ , the characteristic temperature of the solid, and calculations were made for four different characteristic temperatures. As the table shows,  $\alpha$  for hydrogen in the temperature interval from 30 to 300° K. is far from being unity. At 30° K. on a solid having  $\Theta = 300^\circ$  the value of  $\alpha$  for deuterium is 66% greater than for hydrogen. It seems likely, therefore, that for heavier molecules  $\alpha$  is close to unity, as was assumed by Langmuir.

The average life of hydrogen on the surface at different temperatures is given in Table LXXIII. Lennard-Jones and Devonshire calculated the average life of  $HD$  and  $D_2$  also on the four different solids. The value of  $\tau$  for deuterium at 300° K. on a solid having  $\Theta = 300^\circ$  is 97% of the hydrogen value, but at 30° K. on a solid having  $\Theta = 510^\circ$  it is 87% higher than the hydrogen value. The

<sup>47</sup> K. F. Herzfeld and Maria Göppert-Mayer (*Z. phys. Chem., Bodenstein Festsband*, 669, 1931) used a similar method to calculate the probability of excitation of the internal degrees of freedom of a molecule by the thermal motion of a solid on which it is adsorbed.

investigators also found that in Frenkel's equation (6)  $\tau_0$  is not independent of the temperature. For hydrogen on a solid with  $\Theta = 510^\circ$ ,  $\tau_0$  decreases by a factor of 5 from 30 to  $300^\circ$  K.

Devonshire<sup>48</sup> worked out the theory of the diffraction and reflection of molecular rays from solid surfaces. He concluded from the diffraction experiments of Frisch and Stern<sup>49</sup> that helium atoms ad-

TABLE LXXIII  
THE AVERAGE LIFE OF HYDROGEN

$\Theta$	Temperature, ° K.			
	30	50	100	300
300	$1.06 \times 10^{-8}$	$2.02 \times 10^{-8}$	$1.73 \times 10^{-10}$	$6.40 \times 10^{-12}$
350	1.23	2.49	2.19	8.06
400	1.77	3.48	3.00	10.5
510	3.37	6.63	5.56	19.3

sorbed on a lithium fluoride crystal have two quantized vibrational levels perpendicular to the surface whose energies are  $-57.5$  and  $-129$  calories per mole. The lower level gives the heat of adsorption. Using these energy levels Lennard-Jones and Devonshire<sup>50</sup> constructed a map of the potential field between the gas atom and the solid, and calculated the lateral velocity of migration of the helium atoms in this field. According to classical mechanics helium atoms would "solidify" on the surface at very low temperatures, i.e., they would remain in one place vibrating about their mean positions, but according to quantum mechanics the atoms can migrate over the surface no matter how low the temperature. There will be an apparent increase of about 8% in the mass of the atom, but otherwise the atoms will move as though the lateral potential barriers did not exist.

<sup>48</sup> A. F. Devonshire, *Proc. Roy. Soc.*, A156, 37 (1936).

<sup>49</sup> R. Frisch and O. Stern, *Z. Physik*, 84, 430 (1933).

<sup>50</sup> J. E. Lennard-Jones and A. F. Devonshire, *Proc. Roy. Soc.*, A158, 242 (1936).

## CHAPTER XIV

### MIXED ADSORPTION

The study of mixed adsorption is of tremendous practical importance. Most of the technical applications of adsorption processes involve gas mixtures rather than one gas alone. Thus in the adsorption of war gases by charcoal the gas is always present in a large excess of air, and in the recovery of solvent vapors like petroleum ether, benzene, alcohol, etc., the organic vapor is removed from air. The phenomenon of mixed adsorption is encountered in the recovery of acetone, ethyl and butyl alcohol from the waste gases produced in fermentation processes; in the recovery of benzene and light oil from illuminating gas; in the purification of air in submarines; in the purification of other gases, such as carbon dioxide (for carbonated water), hydrogen (for hydrogenation processes), ammonia (before catalytic oxidation); and in the refining of helium.<sup>1</sup> These are examples of mixed physical adsorption; mixed chemisorption forms the basis of many important industrial catalytic reactions.

The discussion of mixed adsorption may be divided into three parts. In the first place, one may deal with a single adsorbent and a mixture of gases. This is by far the most important type of mixed physical adsorption. In the second place, one may have only one adsorbate and a mixture of adsorbents. So far very little work has been done in this field. Finally, one may deal with a mixed adsorbent and a mixed adsorbate. This case is by no means uncommon in the practical use of adsorption processes; in fact, many catalytic reactions belong to this group. Promoted, supported, and mixed catalysts are composed of more than one substance, and most catalytic reactions involve more than one gas. However, this case belongs to the subject of mixed chemisorption, while the present chapter deals only with van der Waals adsorption.<sup>2</sup> Most of the chapter discusses the first type of mixed adsorption, although some space is devoted to the second type also.

<sup>1</sup> N. K. Chaney, A. B. Ray, and A. St. John, *Ind. Eng. Chem.*, 15, 1244 (1923).

<sup>2</sup> Gas masks contain soda lime besides charcoal, because charcoal can not handle satisfactorily volatile gases like phosgene or hydrocyanic acid. However, soda lime acts chemically as an *absorbent*, not an adsorbent.

The theoretical handling of mixed adsorption is somewhat more difficult than that of simple adsorption. Nevertheless, some attempts have been made to attack the problem. In the simplest case the adsorption of one of the gases is so much smaller than that of the other that it can be completely neglected. The adsorption of the other gas can then be treated as simple adsorption and, as a matter of fact, we have done this in previous chapters. We may recall as examples the adsorption of carbon tetrachloride from air partly saturated with the vapor <sup>3</sup> (Fig. 140), and the adsorption of benzene from air completely saturated with the vapor <sup>4</sup> (Fig. 139). If the adsorption of the other component is not negligible there are three possibilities: the adsorption is uninfluenced, decreased, or increased by the other component. Examples of all three cases are known and are discussed in this chapter.

Mixed adsorption forms the transition from the adsorption of gases and vapors to adsorption from solutions. Adsorption from solutions always involves at least two adsorbates: the solvent and the solute, competing for place on the surface of the adsorbent. In the simplest case one deals with two liquids that are miscible with each other in all proportions. This case may be approached by investigating the adsorption of the vapors of binary liquid mixtures. Such studies have been made, and their discussion constitutes part of the present chapter.

### THE LANGMUIR EQUATION FOR MIXED ADSORPTION

Due to the complexity of the problem attempts have been made so far only to develop a theory of mixed unimolecular adsorption. Two of the theories of unimolecular adsorption, those of Langmuir and Magnus, have been extended to cover mixed adsorption.

Markham and Benton <sup>5</sup> derived equations for the adsorption of binary mixtures based on the same two assumptions which form the foundation of the Langmuir equation <sup>6</sup> for simple adsorption. The assumptions are: unimolecularity of adsorption and constancy of the heat of adsorption. The latter implies both uniformity of the surface of the adsorbent and absence of interaction between the adsorbed particles. If these two conditions are fulfilled the only effect that one

<sup>3</sup> W. A. Patrick, J. C. W. Frazer, and R. I. Rush, *J. Phys. Chem.*, **31**, 1511 (1927).

<sup>4</sup> H. N. Holmes and A. L. Elder, *J. Phys. Chem.*, **35**, 82 (1931).

<sup>5</sup> E. C. Markham and A. F. Benton, *J. Am. Chem. Soc.*, **53**, 497 (1931).

<sup>6</sup> I. Langmuir, *J. Am. Chem. Soc.*, **40**, 1361 (1918).

adsorbate can have on the adsorption of the other is to cut down the available surface.

Let  $\theta_1$  and  $\theta_2$  be the fractions of the surface covered by Gases 1 and 2, respectively. Since the fraction of the surface which is bare is given by  $1 - \theta_1 - \theta_2$ , the rate of adsorption of Gas 1 will be  $k_1 p_1 (1 - \theta_1 - \theta_2)$ , and that of Gas 2 will be  $k_2 p_2 (1 - \theta_1 - \theta_2)$ . Here  $p_1$  and  $p_2$  are the partial pressures of the two gases, and  $k_1$  and  $k_2$  are constants. The rates of desorption of the two gases will be  $k_1' \theta_1$  and  $k_2' \theta_2$ , where  $k_1'$  and  $k_2'$  are other constants. The equilibrium conditions are expressed by the equations

$$(1) \quad k_1 p_1 (1 - \theta_1 - \theta_2) = k_1' \theta_1$$

$$(2) \quad k_2 p_2 (1 - \theta_1 - \theta_2) = k_2' \theta_2$$

Solving the two equations simultaneously one obtains for  $\theta_1$  and  $\theta_2$  the expressions

$$(3) \quad \theta_1 = \frac{b_1 p_1}{1 + b_1 p_1 + b_2 p_2}$$

$$(4) \quad \theta_2 = \frac{b_2 p_2}{1 + b_1 p_1 + b_2 p_2}$$

where  $b_1 = k_1/k_1'$  and  $b_2 = k_2/k_2'$ . The constants  $b_1$  and  $b_2$  are the individual adsorption coefficients of Gases 1 and 2 respectively.<sup>7</sup> If we set  $p_2 = 0$  in equation (3), it reduces to the simple Langmuir equation (18) of Chapter IV.

The volumes of gas adsorbed are  $v_1 = v_m^{(1)} \theta_1$  and  $v_2 = v_m^{(2)} \theta_2$ , where  $v_m^{(1)}$  is the volume of gas necessary to cover the entire surface with a unimolecular adsorbed layer of Gas 1, and  $v_m^{(2)}$  is defined in the same way for Gas 2. Substitution into (3) and (4) gives

$$(5) \quad v_1 = \frac{v_m^{(1)} b_1 p_1}{1 + b_1 p_1 + b_2 p_2}$$

$$(6) \quad v_2 = \frac{v_m^{(2)} b_2 p_2}{1 + b_1 p_1 + b_2 p_2}$$

The difference between the simple Langmuir equation (21) of Chapter IV and equation (5) of Markham and Benton<sup>8</sup> is the extra term in the denominator,  $b_2 p_2$ . Gas 2 decreases the adsorption of Gas 1 the more, the greater are  $p_2$  and  $b_2$ , i.e., its partial pressure and adsorption coefficient. Similarly, Gas 1 decreases the adsorption of Gas 2 according

<sup>7</sup> Equations (3) and (4) were also derived statistically by G. Damköhler, *Z. phys. Chem.*, B23, 58 (1933), and F. J. Wilkins, *Nature*, 141, 1054 (1938).

to its partial pressure and adsorption coefficient,  $p_1$  and  $b_1$ . It follows from equations (5) and (6) that one gas always decreases the adsorption of the other. Enhancement of the adsorption by another gas can not be explained on the basis of the Langmuir theory.

We shall now consider two limiting cases of equations (5) and (6). If in the denominators both  $b_1p_1$  and  $b_2p_2$  are negligible compared to 1, the equations reduce to

$$(7) \quad v_1 = v_m^{(1)}b_1p_1$$

$$(8) \quad v_2 = v_m^{(2)}b_2p_2$$

In this case each gas is adsorbed as though the other were not present at all. The adsorption isotherm of each gas individually and of the mixture as a whole obeys Henry's law, provided, of course, that  $b_1$  and  $b_2$  are independent of the amount of gas adsorbed.

If the product  $bp$  becomes comparable to 1 for Gas 1 but is still negligible compared to 1 for Gas 2, equations (5) and (6) become

$$(9) \quad v_1 = \frac{v_m^{(1)}b_1p_1}{1 + b_1p_1}$$

$$(10) \quad v_2 = \frac{v_m^{(2)}b_2p_2}{1 + b_1p_1}$$

In this case Gas 1 will be adsorbed as though Gas 2 were not there at all, but the adsorption of Gas 2 will be cut down very strongly by Gas 1. This happens, for example, in the adsorption of organic vapors by charcoal in the presence of air. Air is displaced from the surface of the adsorbent by the organic vapor, while the adsorption of the vapor remains unaffected by the presence of air. This may be true even if the partial pressure of the vapor is much smaller than that of air. The reason is that  $b$  depends exponentially on the heat of adsorption (equation (19), Chapter IV).

Equations (5) to (10) have been tested by a number of investigators. Equations (5) and (6) indicate a mutual decrease in the adsorption of both components of a binary mixture. Some of the earliest work on mixed adsorption showed qualitatively that such mutual decrease actually exists. Thus Dewar<sup>8</sup> found that at  $-185^\circ\text{C}$ . and atmospheric pressure a sample of charcoal adsorbed separately 190 cc. carbon monoxide and 230 cc. oxygen. The adsorption from a mixture of carbon monoxide and oxygen was only 195 cc. Although Dewar did not analyze the adsorbate, it is clear from the total amount ad-

<sup>8</sup> J. Dewar, *Compt. rend.*, 139, 261 (1904).

sorbed that each gas decreased the adsorption of the other. Furthermore, Dewar found that two gases decrease each other's adsorption to a different extent. The adsorption of nitrogen and oxygen on charcoal at  $-185^{\circ}\text{C}$ . and atmospheric pressure is 155 cc. and 230 cc. separately. When air is adsorbed the adsorbate contains 56% oxygen and 44% nitrogen, in spite of the fact that the partial pressure of nitrogen in air is four times as large as that of oxygen. Thus oxygen is more strongly adsorbed than nitrogen. This is evidenced also by some desorption experiments performed by Dewar. He adsorbed 6 liters of air on charcoal at  $-185^{\circ}\text{C}$ ., then warmed up the adsorbent gradually and analyzed the desorbing gas. The first liter contained 18.5% oxygen, the second 30.6, the third 53.0, the fourth 72.0, the fifth 79.0, and the sixth 84.0% oxygen. The oxygen comes off more slowly than the nitrogen, indicating a stronger binding to the surface.

Markham and Benton<sup>5</sup> investigated equations (5) and (6) quantitatively and found that the agreement with experiment was rather poor. They determined first the individual isotherms of oxygen, carbon monoxide, and carbon dioxide on silica at 0 and  $100^{\circ}\text{C}$ ., then measured the adsorption of binary mixtures of these gases. The individual isotherms obeyed the simple Langmuir equation (Fig. 39, Chapter IV). This enabled the investigators to evaluate the constants  $v_m$  and  $b$  for each isotherm.<sup>9</sup> Using these constants they calculated the amounts adsorbed from the binary mixtures by means of equations (5) and (6). The degree of agreement obtained is shown in Table LXXIV. The values in columns 3 and 6 give the amounts which would be adsorbed at the given pressure of the gas if the second gas were not present. These were obtained by interpolation from the individual isotherms. The values given in columns 5 and 8 were calculated by means of equations (5) and (6). The observed and calculated values do not agree very well. In the carbon monoxide-oxygen experiments at  $0^{\circ}\text{C}$ . the observed oxygen adsorptions are higher, the observed carbon monoxide adsorptions lower than the calculated ones. The data for the carbon monoxide-carbon dioxide mixtures at  $100^{\circ}\text{C}$ . are especially interesting. The amounts of carbon monoxide adsorbed in the presence of high partial pressures of carbon dioxide are not only greater than the calculated values, but even greater than the amounts adsorbed in the absence of carbon dioxide. In other words, in this case the adsorption is enhanced

<sup>9</sup> It was pointed out in Chapter IV that the  $v_m$  values obtained from isotherms of different gases, and from isotherms of the same gas at different temperatures, were not concordant.



rather than decreased by another gas. The reason is doubtless that the adsorbed carbon dioxide exerts attractive forces upon the carbon monoxide, thereby increasing its heat of adsorption. (Chapter VII.) The adsorption of carbon dioxide likewise increases in the presence of high partial pressures of carbon monoxide. The effect is smaller

TABLE LXXIV  
ADSORPTION OF BINARY GAS MIXTURES ON SILICA

CO-O <sub>2</sub> Mixtures at 0° C.							
<i>P</i> <sub>O<sub>2</sub></sub>	<i>P</i> <sub>CO</sub>	Volume of O <sub>2</sub> Adsorbed			Volume of CO Adsorbed		
		Isotherm	Observed	Calculated	Isotherm	Observed	Calculated
230.2	529.8	8.98	8.31	7.96	35.90	35.02	35.00
391.1	368.9	15.05	14.10	13.79	25.82	24.69	24.84
585.1	174.9	21.93	21.73	21.12	12.80	11.63	12.06

CO <sub>2</sub> -CO Mixtures at 100° C.							
<i>P</i> <sub>CO</sub>	<i>P</i> <sub>CO<sub>2</sub></sub>	Volume of CO Adsorbed			Volume of CO <sub>2</sub> Adsorbed		
		Isotherm	Observed	Calculated	Isotherm	Observed	Calculated
211.6	548.4	2.34	2.93	1.93	62.10	61.51	60.13
259.5	500.5	2.73	3.21	2.38	57.50	57.30	55.16
377.0	383.0	3.89	3.77	3.50	45.40	45.42	42.75
384.9	375.1	3.97	3.70	3.57	44.50	44.68	41.90
555.0	205.0	5.55	5.53	5.25	25.60	25.93	23.32

in this case because the adsorption of carbon monoxide is smaller than that of carbon dioxide. We shall discuss other instances of enhanced adsorption later.

When both gases in a binary mixture are weakly adsorbed, equations (7) and (8) ought to apply, i.e., the adsorption of the mixture should be equal to the sum of the separate adsorptions of the components. This relation has also been tested and was found to express the experimental results fairly satisfactorily. Richardson and Woodhouse<sup>10</sup> investigated the adsorption of carbon dioxide and nitrous oxide on charcoal individually and in three mixtures: 50% CO<sub>2</sub>-50% N<sub>2</sub>O, 75%-CO<sub>2</sub>-25% N<sub>2</sub>O, and 25% CO<sub>2</sub>-75% N<sub>2</sub>O. If the adsorption of the two gases is additive, the volume of the mixture adsorbed can be calculated from the equation

$$(11) \quad v_{\text{mixt.}} = \frac{a_1 v_{\text{N}_2\text{O}} + a_2 v_{\text{CO}_2}}{100}$$

<sup>10</sup> L. B. Richardson and J. C. Woodhouse, *J. Am. Chem. Soc.*, **45**, 2638 (1923).

where  $v_{N_2O}$  and  $v_{CO_2}$  are the volumes of the gases adsorbed separately at the total pressure of the mixture, and  $a_1$  and  $a_2$  are the percentages of  $N_2O$  and  $CO_2$  in the mixture. The experiments were carried out at  $0^\circ C.$  and at pressures up to 2800 mm. Table LXXV shows the agreement between the calculated and the experimental values. At first sight it seems that the agreement is very good in the entire pressure range and for all three mixtures. Actually, however, the

TABLE LXXV

ADSORPTION OF MIXTURES OF CARBON DIOXIDE AND NITROUS OXIDE BY CHARCOAL

Pressure mm.	50% $CO_2$ - 50% $N_2O$		75% $CO_2$ - 25% $N_2O$		25% $CO_2$ - 75% $N_2O$	
	Calculated	Observed	Calculated	Observed	Calculated	Observed
2800	118.3	117.1	118.4	118.4	118.3	118.5
1600	104.2	102.4	102.2	102.3	106.4	105.8
1000	89.7	88.7	87.3	87.0	92.3	91.9
600	73.4	73.2	70.6	70.2	76.5	75.1
200	44.1	43.7	41.7	41.4	46.7	47.1

agreement is good only at higher pressures, from 800 to 2800 mm. As McBain <sup>11</sup> pointed out, at lower pressures more nitrous oxide and less carbon dioxide is adsorbed than should be on the basis of additivity, but the two deviations approximately balance each other. Here again we have an example of enhanced adsorption: in the presence of carbon dioxide more nitrous oxide is adsorbed than in its absence.

Equation (9) should be obeyed in unimolecular adsorption when the disparity between the adsorption coefficients of the two gases is so great that the adsorption of one gas can be entirely neglected in comparison with the other. Probably this equation is never obeyed at low pressures, i.e., in the adsorption on the most active part of the surface, but it may be obeyed for the more homogeneous part of the surface. Pidgeon and Van Winsen <sup>12</sup> showed that the adsorption of water vapor by asbestos fiber is not influenced by the presence of air. Their results are illustrated in Fig. 159. The adsorption follows a Type II isotherm. The experimental points were determined by two different methods: the points marked with crosses were obtained in the absence of air, those marked with circles were obtained from humidified air. The agreement is good, but the points obtained by the second method start only at 24% humidity. This corresponds already to the building up of the second adsorbed layer.

<sup>11</sup> J. W. McBain, *The Sorption of Gases and Vapours by Solids*, London, 1932, p. 163.

<sup>12</sup> L. M. Pidgeon and A. Van Winsen, *Can. J. Res.*, 9, 153 (1933).

The correctness of equation (10) can be qualitatively inferred from the results of Siebert.<sup>13</sup> He measured the adsorption of radium emanation by silica gel in the presence of various other gases, and found that different gases decreased the adsorption to a different extent. He defined as a measure of the adsorption the coefficient  $\alpha$ , the ratio of the concentration of the adsorbed emanation (per gram of adsorbent) to that of the unadsorbed emanation (per cc. of container). The

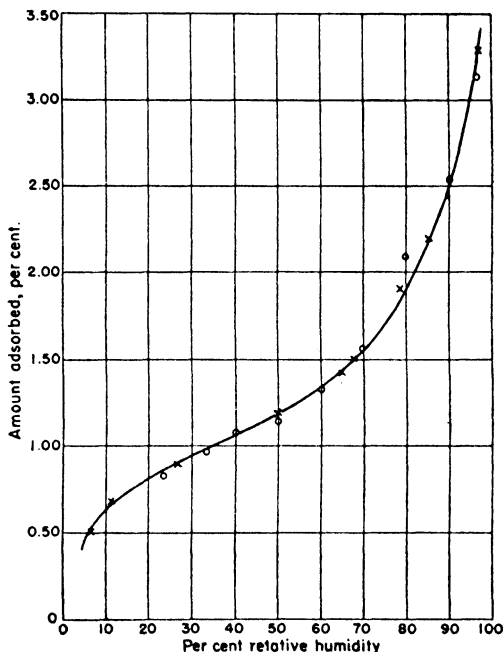


Fig. 159.—Adsorption isotherm of water vapor on asbestos fiber.

results, shown in Table LXXVI, are reported in terms of a more convenient coefficient  $\beta$ , defined by

$$(12) \quad \beta = \alpha m/V$$

where  $m$  is the mass of the adsorbent, and  $V$  is the volume of the vessel. The pressure of the accompanying gas was always 1 atm., and the adsorption was measured at  $-80^{\circ}\text{C}$ . Due to the very low partial pressure of the emanation equation (10) should apply, with  $b_1$  and  $p_1$

<sup>13</sup> W. Siebert, *Z. phys. Chem.*, A180, 169 (1937).

the adsorption coefficient and partial pressure of the accompanying gas. Since  $p_1$  was the same for all of the gases used (1 atm.), the differences in the suppression of the adsorption should be determined by  $b_1$ , which in turn depends primarily on the heat of adsorption. As the table shows, the two gases with the highest heats of adsorption, carbon dioxide and nitrous oxide, suppress the adsorption of the emanation most, krypton and methane come next, argon and air follow, and neon has the least effect.

TABLE LXXVI  
 ADSORPTION OF RADIUM EMANATION FROM MIXTURES

Accompanying Gas	$\beta$
Gel Sample I	
Air	16.94
Ne	23.40
Kr	10.69
CH <sub>4</sub>	10.81
CO <sub>2</sub>	0.39
Gel Sample II	
N <sub>2</sub> O	1.58
Kr	15.28
Ne	32.72
A	21.21
Air	26.13
CO <sub>2</sub>	0.44

A corollary of the above discussed results is that different vapors differ in their abilities to displace impurities from the surfaces of adsorbents. At a given pressure the vapor with the higher heat of adsorption will have the greater power to displace impurities, unless other complicating factors are present. The work of Allmand and his collaborators demonstrates this point. Allmand and Chaplin<sup>14</sup> investigated the displacement of carbon dioxide impurity from charcoal by means of carbon tetrachloride, and Allmand and Lizius<sup>15</sup> studied the displacement by carbon disulfide. The amount of carbon dioxide displaced by carbon disulfide was found to be greater, even though the heat of adsorption of carbon tetrachloride is larger. The reason for this is that the smaller carbon disulfide molecules can penetrate into the finer pores of charcoal, where carbon tetrachloride can not enter. A similar result was obtained by Chaplin,<sup>16</sup> who investigated

<sup>14</sup> A. J. Allmand and R. Chaplin, *Proc. Roy. Soc.*, A129, 252 (1930).

<sup>15</sup> A. J. Allmand and J. L. Lizius, *Proc. Roy. Soc.*, A134, 554 (1932).

<sup>16</sup> R. Chaplin, *Trans. Far. Soc.*, 30, 249 (1934).

the displacement of impurities from the surface of charcoal by means of carbon tetrachloride and hydrogen cyanide. These vapors can not displace all the impurities when used individually, but they can do it together. Carbon tetrachloride has the higher heat of adsorption, and so the greater power to displace impurities, but it can not penetrate into all the pores because of its size. The smaller hydrogen cyanide can enter the narrower pores and clean up the impurities there.<sup>17</sup>

Measurements on the rates of adsorption of binary gas mixtures supply additional qualitative and semi-quantitative confirmation of

TABLE LXXVII  
ADSORPTION OF BINARY VAPOR MIXTURES ON CHARCOAL

Vapor Mixture	Composition of Bulk Equilibrium Mixture (Mole % Alcohol)		Composition of Adsorbed Phase (Mole % Alcohol)		Difference between Observed and Calculated Values
	Liquid	Vapor	Observed	Calculated	
CH <sub>3</sub> OH - C <sub>2</sub> H <sub>6</sub>	4.7	36.0	50.0	46.7	+3.3
	14.7	46.8	60.7	57.9	-2.8
	39.0	48.5	57.0	59.5	-2.5
	53.4	51.7	64.6	64.0	+0.6
	81.75	63.75	68.1	73.2	-5.1
	91.0	73.7	76.1	81.5	-5.4
C <sub>2</sub> H <sub>5</sub> OH - C <sub>2</sub> H <sub>6</sub>	7.9	19.9	29.1	24.45	+4.65
	17.5	26.8	30.2	32.2	-2.0
	29.0	29.9	33.0	35.7	-2.7
	41.1	31.3	33.65	37.2	-3.55
	56.2	34.5	36.3	40.6	-4.3
	72.6	42.0	41.3	48.6	-7.3
	85.2	53.2	50.9	59.7	-8.8
	97.9	87.0	83.9	89.4	-5.5

the Langmuir theory. Tryhorn and Wyatt<sup>18</sup> investigated the adsorption on charcoal from the vapor phase of binary liquid mixtures. For the initial stage of adsorption it may be assumed that the rate is equal to the number of molecules that strike the surface per second

$$(13) \quad \mu = pS/(2\pi MRT)^{1/2}$$

<sup>17</sup> V. R. Deitz and L. F. Gleysteen (*J. Res. Nat. Bureau of Standards*, **28**, 795, 1942) found that charcoal can be brought to constant weight if the sample is exposed to an atmosphere saturated with water vapor for 18 hours and then dried in helium at 105° C. The small water molecules can penetrate readily into the pores of charcoal removing the impurities there; they are themselves then removed with ease because the adsorption of water on charcoal at low relative pressures is very small (Type V isotherm).

<sup>18</sup> F. G. Tryhorn and W. F. Wyatt, *Trans. Far. Soc.*, **24**, 36 (1928).

where  $p$  is the pressure and  $M$  is the molecular weight of the vapor, and  $S$  is the surface of the adsorbent. For a binary mixture the ratio of the two components adsorbed will be

$$(14) \quad \frac{\mu_1}{\mu_2} = \frac{p_1 M_2^{1/2}}{p_2 M_1^{1/2}}$$

if the molecules are adsorbed as rapidly as they reach the surface. If  $x_1$  is the molecular percentage of one of the components in the vapor phase, and  $(100 - x_1)$  is that of the other, we obtain

$$(15) \quad \frac{\mu_1}{\mu_2} = \frac{x_1 M_2^{1/2}}{(100 - x_1) M_1^{1/2}}$$

Equation (15) involves the assumption that the partial pressure of each component is proportional to its mole fraction. This is not

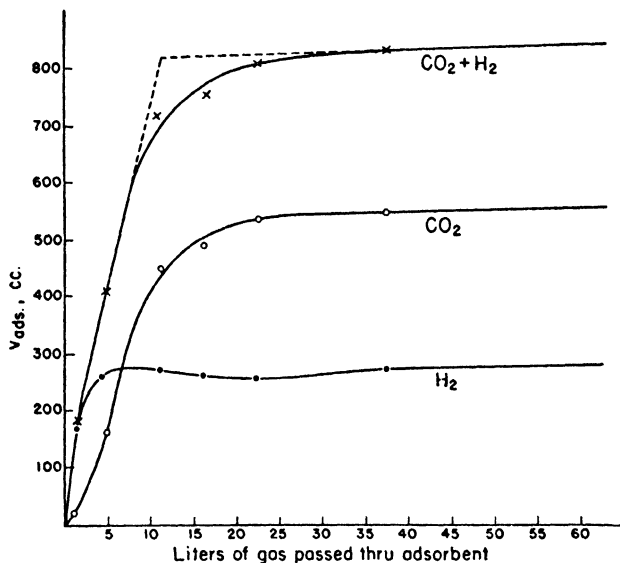


FIG. 160.—The rate of adsorption of carbon dioxide and hydrogen on charcoal from a 95% H<sub>2</sub>—5% CO<sub>2</sub> mixture.

completely true; nevertheless, the calculated and observed compositions of the adsorbed phase show a reasonable agreement. This can be seen in Table LXXVII. The results obtained for the *n*-propyl alcohol-benzene, and the *n*-butyl alcohol-benzene mixtures are not given in the table; they show a somewhat poorer agreement than the

data of the table. Tryhorn and Wyatt point out that the deviations given in the last column approach zero in the vicinity of the composition corresponding to the minimum boiling-point mixtures of the alcohols with benzene. This fact indicates that at least a part of the discrepancy is due to a lack of proportionality between partial pressures and mole fractions.

Lorenz and Wiedbrauck<sup>19</sup> measured the adsorption of carbon dioxide-hydrogen mixtures on charcoal in a dynamic system. Figure 160 shows their rate curves at 18° C. for a 95% H<sub>2</sub>-5% CO<sub>2</sub> mixture. The abscissa represents the amount of gas passed through the adsorbent, which is proportional to the time. (The rate of flow was about 150 cc. per minute.) At first very little carbon dioxide is adsorbed, while hydrogen is picked up with great speed. The reason is that hydrogen diffuses rapidly into the pores of the charcoal, and so its partial pressure near the surface of the adsorbent is much higher than in the gas mixture. The kink in the hydrogen curve is due to the fact that as the equilibrium conditions begin to be approached some of the hydrogen is displaced from the surface by the carbon dioxide. The final amount of carbon dioxide adsorbed is twice as large as the hydrogen adsorption, in spite of the fact that the partial pressure of hydrogen in these experiments is 19 times as large as that of carbon dioxide. This is natural since carbon dioxide has a much higher heat of adsorption than hydrogen.

#### DEVIATIONS FROM THE LANGMUIR EQUATION

In the previous section some experiments were mentioned that can not be explained on the basis of the Langmuir theory, namely, those in which the adsorption is increased by the presence of another gas. Bergter<sup>20</sup> was the first to notice that a charcoal on which oxygen was adsorbed was capable of adsorbing more nitrogen than an oxygen-free charcoal. Little credence was given to his observation until other investigators found similar results. Magnus and Roth<sup>21</sup> determined the adsorption of hydrogen-carbon dioxide mixtures on charcoal in a dynamic system, and obtained the curves shown in Fig. 161. With increasing mole percentage of hydrogen in the gas phase the adsorption at all temperatures first increases according to Henry's law, then passes through a maximum and begins to decrease. This means that the adsorption of carbon dioxide increases the adsorption of hydrogen.

<sup>19</sup> R. Lorenz and E. Wiedbrauck, *Z. anorg. allgem. Chem.*, **135**, 42 (1924).

<sup>20</sup> F. Bergter, *Ann. Physik*, (4), **37**, 472 (1912).

<sup>21</sup> A. Magnus and H. Roth, *Z. anorg. allgem. Chem.*, **150**, 311 (1926).

The van der Waals attraction between the adsorbed molecules adds to the heat of adsorption. The curves can be explained if we assume that the attraction between a hydrogen and a carbon dioxide molecule is greater than between two hydrogen molecules.

It was pointed out before that some of the results of Richardson and Woodhouse<sup>10</sup> and Markham and Benton<sup>5</sup> indicate increased adsorption due to the presence of other gases. The experiments of

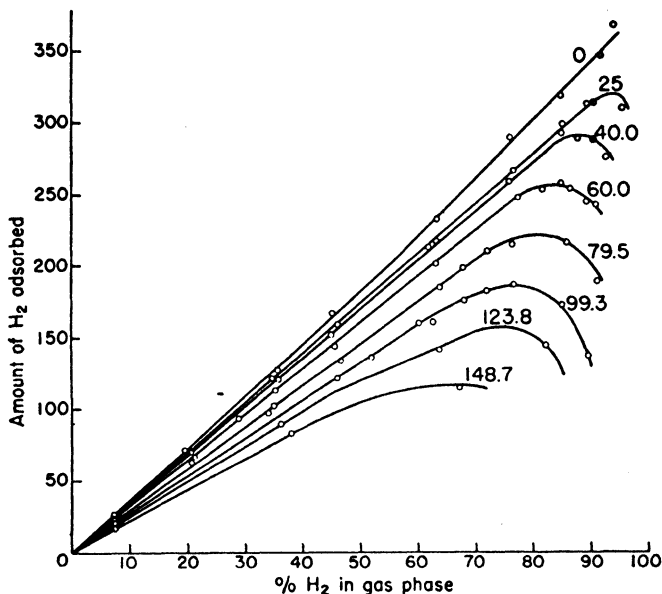


FIG. 161.—Adsorption of hydrogen by charcoal from hydrogen-carbon dioxide mixtures.

Lambert and Peel,<sup>22</sup> shown in Fig. 162, indicate an increase in the adsorption of oxygen on silica gel at 0° C. in the presence of an equal partial pressure of nitrogen, and a simultaneous decrease in the adsorption of nitrogen. This was true for the entire pressure range investigated. These results are truly remarkable if we consider that the maximum adsorption is about 16 cc. of the oxygen-nitrogen mixture on 10 g. of silica gel. In spite of the fact that only about 1% of the surface is covered with adsorbed gas the adsorbate molecules interact with each other, for it is very hard to advance any other ex-

<sup>22</sup> B. Lambert and D. H. P. Peel, *Proc. Roy. Soc., A144*, 205 (1934).



planation for the curves of Fig. 162. Apparently the adsorbed molecules tend to crowd to the places of highest adsorption potential instead of spreading out over the surface. If we assume that the van der Waals attraction between two nitrogen molecules is greater than that between a nitrogen and an oxygen molecule, which in turn is greater than that between two oxygen molecules, the observed increase in the oxygen adsorption by nitrogen and the decrease in the nitrogen adsorption by oxygen is explained.

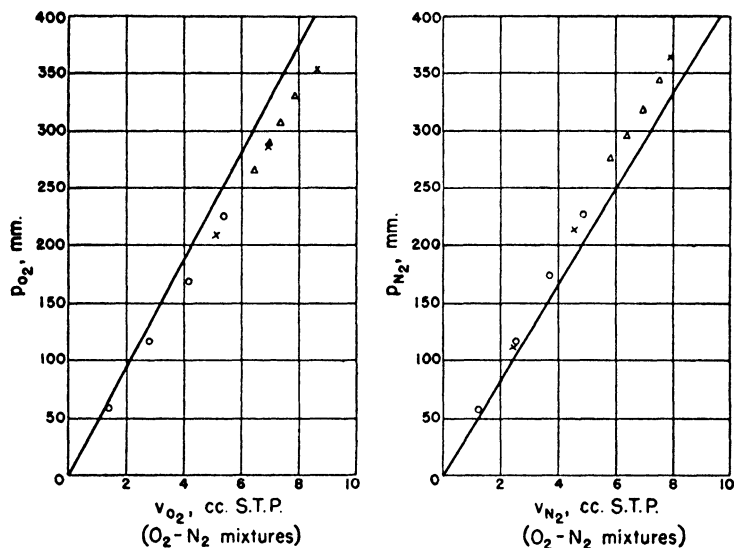


FIG. 162.—Adsorption of oxygen and nitrogen by silica gel in the presence of an equal partial pressure of the other gas.

Lambert and Heaven<sup>23</sup> found that oxygen and argon mutually increase each other's adsorption on silica gel at 0° C. The effect of argon on the oxygen adsorption can be seen by comparing curves *B* and *C* in Fig. 163. Curve *C* represents the adsorption of pure oxygen, curve *B* the adsorption of oxygen in the presence of an equal partial pressure of argon. These results again refer to adsorption on a surface less than 1% covered. The other two curves bring out another puzzling effect. If first oxygen is admitted to the gel and then *separately* an equal partial pressure of argon is added, the oxygen adsorption is represented by curve *A*. If first argon is admitted and then separately an equal

<sup>23</sup> B. Lambert and H. S. Heaven, *Proc. Roy. Soc., A153*, 584 (1936).

partial pressure of oxygen, the adsorption of oxygen is given by curve *D*. If in the course of 24 hours true equilibrium had been established over the gel, curves *B*, *A*, and *D* would coincide. A possible explanation of these results is that the adsorption takes place on the most active part of the silica gel surface, probably in very narrow pores comparable in size to the diameter of an argon atom or an oxygen molecule. The diffusion of oxygen into and out of these pores against

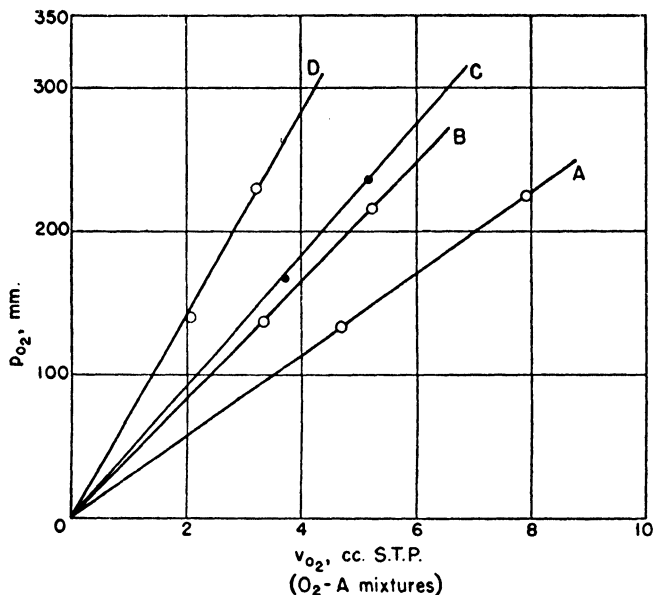


FIG. 163.—Adsorption of oxygen by silica gel from oxygen-argon mixtures.

an equal partial pressure of argon may take much longer than 24 hours. Richardson and Woodhouse<sup>10</sup> also determined the adsorption of carbon dioxide-nitrous oxide mixtures on charcoal in this manner by adding first one gas and then the other. They found that the replacement on the surface went on rapidly at the start but then slowed down, and it was so slow after 39 hours that they doubted whether equilibrium would ever be reached.

The Langmuir theory demands that the adsorption of one gas should always be diminished by the presence of another. If the temperature and pressure are kept constant and the composition of the gas phase is varied, then a plot of the concentration of Component 1

in the adsorbed phase against its concentration in the gas phase should give either curve 1 or 2 in Fig. 164. The figure was taken from Damköhler.<sup>24</sup> If Component 1 has a higher adsorption coefficient than Component 2, curve 1 is obtained; if Component 2 has the higher adsorption coefficient, curve 2 is obtained. Curve 3 can not be obtained on the basis of the Langmuir theory. It indicates variable heats of adsorption or possibly multimolecular adsorption. Dam-

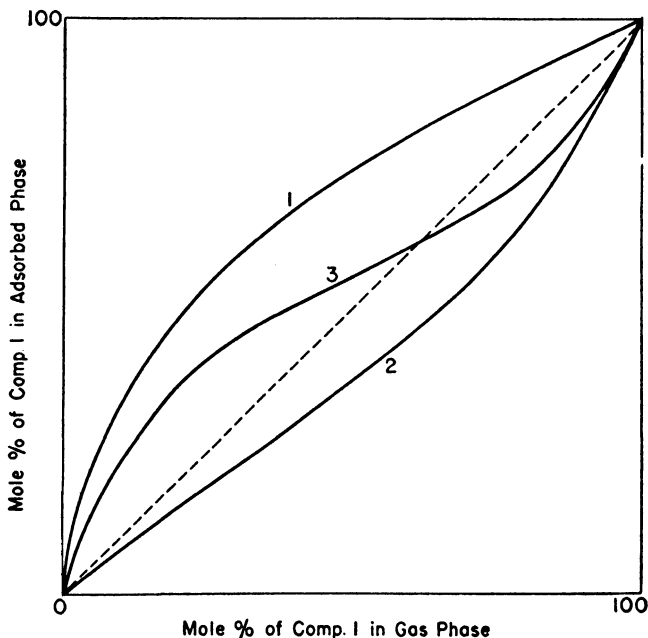


Fig. 164.—Adsorption of one of the components from a binary mixture.

köhler found that mixtures of nitrogen and argon on both silica gel and norite gave in certain temperature and pressure ranges curves that were similar to curve 3. At low concentrations of nitrogen in the gas phase the adsorbed phase was richer in nitrogen than in argon, whereas at high concentrations of nitrogen the reverse was true. Damköhler explained this on the basis of multimolecular adsorption; he assumed that the transition occurs when the first adsorbed layer is approximately complete and the second layer begins to form. On the basis of the theory of multimolecular adsorption Damköhler's ex-

<sup>24</sup> G. Damköhler, *Z. phys. Chem.*, B23, 58, 69 (1933).

planation is very plausible. The measured heats of adsorption of nitrogen are usually slightly higher than those of argon when the gases are in contact with the surface. The heats of adsorption in the second layer, however, are equal to the heats of liquefaction, and the heat of liquefaction of argon is slightly higher than that of nitrogen.

#### THE MAGNUS THEORY FOR MIXED ADSORPTION

The Magnus equation for simple adsorption was discussed in Chapter IV. Magnus<sup>25</sup> also derived equations for the adsorption of gases from binary mixtures. For molecules not possessing dipoles these equations are

$$(16) \quad p_1 = v_1 \left[ \left( \frac{p}{v} \right)_0 \right]_1 \left[ \frac{1}{1 - \frac{\beta_1}{A} v_1 - \frac{\beta_2}{A} v_2} + \frac{\alpha_1}{ART} v_1 + \frac{\alpha_{12}}{ART} v_2 \right]$$

$$(17) \quad p_2 = v_2 \left[ \left( \frac{p}{v} \right)_0 \right]_2 \left[ \frac{1}{1 - \frac{\beta_1}{A} v_1 - \frac{\beta_2}{A} v_2} + \frac{\alpha_2}{ART} v_2 + \frac{\alpha_{12}}{ART} v_1 \right]$$

The terms of these two equations have the same meanings as in equation (62), Chapter IV. All of the constants can be evaluated from the isotherms of the individual gases except the constant  $\alpha_{12}$ , which represents the interaction forces between the two different types of molecules. While  $\alpha_1$  and  $\alpha_2$  are always supposed to be positive, representing repulsion,  $\alpha_{12}$  may be either positive or negative, depending on whether the mutually induced dipoles repel or attract each other. Equation (16) reduces to the simple Magnus equation (62) of Chapter IV if one sets  $v_2 = 0$ . The relation between equations (16) and (17) of Magnus on the one hand and equations (5) and (6) of Markham and Benton<sup>5</sup> on the other is the same as between the simple Magnus equation and the Langmuir equation. If the interaction forces between the adsorbed molecules are neglected, i.e., if  $\alpha_1$ ,  $\alpha_2$ , and  $\alpha_{12}$  are set equal to zero, equations (16) and (17) reduce to equations (5) and (6).

Magnus and Krauss<sup>26</sup> measured the adsorption of mixtures of acetylene and methyl ether on charcoal, using an interferometric method for the analysis of the gases. Although in an earlier paper<sup>25</sup> Magnus states that the adsorption of these mixtures obeys equations (16) and (17), in the paper of Magnus and Krauss no attempt is made to show that the experimental data actually obey the equations.

<sup>25</sup> A. Magnus, *Trans. Far. Soc.*, **28**, 386 (1932).

<sup>26</sup> A. Magnus and A. Krauss, *Z. phys. Chem.*, **A158**, 161 (1932).

### ADSORPTION FROM MIXTURES OF SATURATED VAPORS

The adsorption of binary mixtures of saturated vapors on charcoal was investigated by Tryhorn and Wyatt.<sup>27</sup> They noted three distinct stages in the adsorption process, which are illustrated in Fig. 165. In the curves the number of moles of one component adsorbed are plotted against the total number of moles adsorbed. The initial stage is represented by the two straight lines starting from the origin; in

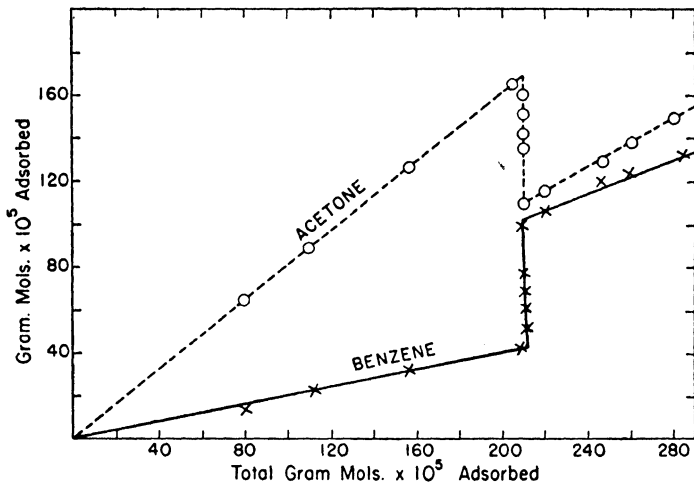


FIG. 165.—Adsorption of saturated vapor mixtures of acetone and benzene on charcoal.

this stage acetone and benzene are adsorbed in a constant ratio. This process lasts for 2 to 6 hours, then an abrupt break occurs. In the second stage, which lasts for 2 to 3 days, there is either no increase at all in the total number of moles adsorbed or only a slow increase. Instead, there is an adjustment in the composition of the adsorbed phase during this time. As the figure shows, the adsorption of acetone decreases, that of benzene increases quite strongly. At the end of this stage there is a second sharp break in the curves, and the adsorption of both components continues to increase slowly. The ratio of the adsorptions is again constant, and so again two straight lines are obtained which, however, are not parallel with the original straight lines.

<sup>27</sup> F. G. Tryhorn and W. F. Wyatt, *Trans. Far. Soc.*, **22**, 139 (1926).

Tryhorn and Wyatt interpreted the first stage as being due to the adsorption of both components in the form of vapors. The ratio of the amounts adsorbed is equal to the ratio in which the molecules reach the surface, as was shown in Table LXXVII. Since this ratio is constant the first stage is represented by two straight lines. The second stage is due to the condensation of the adsorbed vapor to liquid. When this liquid begins to condense it has the same composition as the adsorbed vapor, but in order to remain in equilibrium with the vapor phase and the bulk liquid it must adjust its composition.

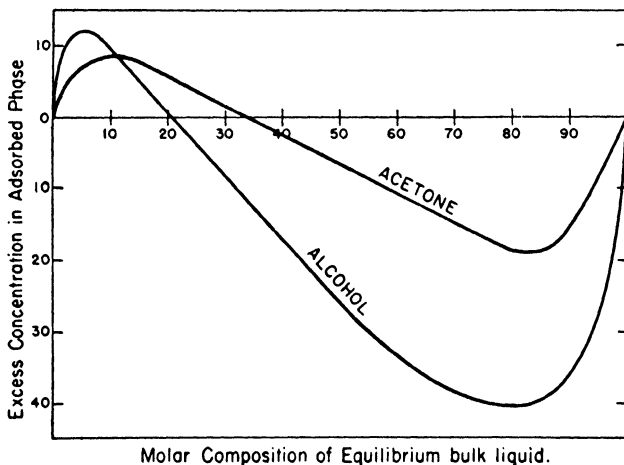


Fig. 166.—Negative adsorption from binary saturated vapor mixtures on charcoal.

If the interaction between the surface and the adsorbed liquid were negligible this adjustment would proceed until the adsorbed liquid had the same composition as the bulk liquid. However, due to the fact that one of the liquids is more strongly adsorbed than the other the compositions of the adsorbed liquid and the bulk liquid will not be the same. This "selectivity" of the adsorption process is illustrated in Fig. 166. In these curves the difference between the compositions of the adsorbed liquid and the equilibrium liquid is plotted against the composition of the equilibrium liquid. The composition of the adsorbed phase is that corresponding to the second break-point in Fig. 165. Alcohol-benzene and acetone-benzene mixtures were used. The curves of Fig. 166 illustrate the phenomenon of "negative" adsorption. Positive adsorption of acetone and alcohol occurs from

liquid mixtures up to 33.3 mole per cent acetone and 20.5 mole per cent alcohol. From mixtures containing more acetone or alcohol the adsorption of benzene is greater than that of the other component; thus the adsorption of acetone or alcohol appears to be negative.

Tryhorn and Wyatt attribute the third stage to capillary condensation in the intergranular spaces of charcoal. This is a slow process which goes on for weeks. The liquid first condensing in the spaces between the grains differs in composition from the bulk liquid. This is probably because the liquid forming at the contact points of the charcoal granules has a marked concave curvature, and consequently a somewhat different vapor pressure than the bulk liquid. As the spaces fill up gradually the curvature becomes smaller and smaller, and the condensing liquid approaches the bulk liquid in composition. This process usually takes two to three weeks.

The above explanation of the three stages of the adsorption process may be regarded as a working hypothesis; it accounts semi-quantitatively for the first stage and qualitatively for the second and third. However, even though it explains the observed facts there is not sufficient evidence cited to give it a firm foundation. There exists another effect that should be kept in mind in experiments with binary mixtures, mentioned already in connection with the experiments of Lorenz and Wiedbrauck.<sup>19</sup> The lighter molecules always move faster and diffuse into the pores more rapidly than the heavier ones. On the other hand, the heavier molecules usually have the higher heat of adsorption, and so a larger amount adsorbed at equilibrium. In the beginning therefore more of the lighter and less of the heavier molecules are adsorbed than at the end. When one deals with fairly large molecules and not too low pressures the diffusion into and out of very narrow pores will take a long time, which may account at least in part for the results of Tryhorn and Wyatt.

Rao<sup>28</sup> investigated the adsorption of four different binary mixtures of saturated vapors on silica gel. He expressed his results by plotting "selectivity" against the composition of the bulk liquid. He defined selectivity by the equation

$$(18) \quad s = \frac{x(c_g - c_l)}{100m}$$

where  $x$  is the weight of the adsorbed liquid held by  $m$  grams of gel,  $c_g$  is the percentage by weight of one of the components adsorbed on the gel, and  $c_l$  is the percentage of the same component in the bulk

<sup>28</sup> B. S. Rao, *J. Phys. Chem.*, **36**, 616 (1932).

liquid. The selectivity-composition curves for benzene-carbon tetrachloride mixtures on two gel samples are given in Fig. 167. The three types of points represent three different methods used for the determination of the amounts adsorbed. It will be seen that benzene is selectively adsorbed at all concentrations. Similarly, Rao found that alcohol is selectively adsorbed over benzene at all concentrations. On the other hand, the alcohol-water and acetone-water curves he

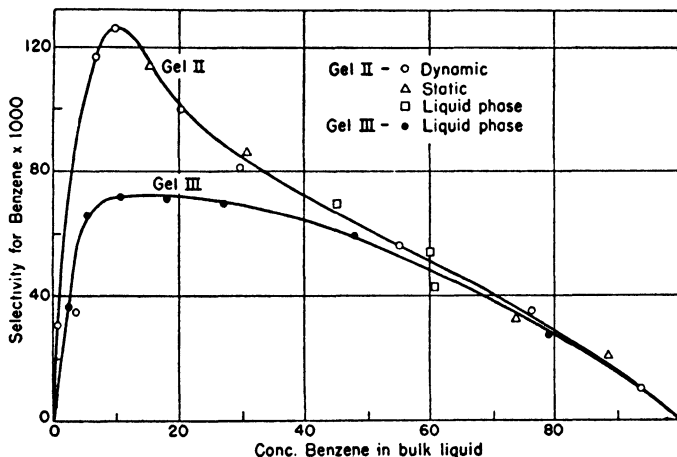


Fig. 167.—Selectivity-composition curves of benzene-carbon tetrachloride mixtures adsorbed on silica gel.

obtained were similar to those shown in Fig. 166, giving positive adsorption of alcohol or acetone over water at small concentrations but negative adsorption at large concentrations.

Rao interpreted the above data by assuming that the silica gel surface is covered with a tightly bound layer of water. When benzene is adsorbed by silica gel the free surface energy is reduced, since a water-air interface with an energy of 73 ergs per sq. cm. is replaced by a benzene-water interface having an energy of only 35 ergs per sq. cm. If a gel saturated with benzene is dropped into water the benzene is replaced by water, with a disappearance of the benzene-water interface and a further decrease in free surface energy. From a benzene-carbon tetrachloride mixture benzene is adsorbed selectively, since the energy of the water-benzene interface (35 ergs per sq. cm.) is less than that of the water-carbon tetrachloride interface (43.3 ergs



per sq. cm.).<sup>29</sup> From a benzene-alcohol mixture alcohol is adsorbed selectively, since alcohol is miscible with water while benzene is not. Liquid mixtures miscible with water give the negative adsorption type of curve on silica gel.

The adsorption of mixtures of saturated vapors constitutes the borderline between the adsorption of vapors and adsorption from solutions. Further investigations would doubtless prove fruitful in throwing light on both phenomena.<sup>30</sup>

### MIXED ADSORBENTS

If two adsorbents are mechanically mixed, the adsorption by the mixture should be equal to the sum of the adsorptions by the individual components. This is certainly true if the mixture is coarse, but if the

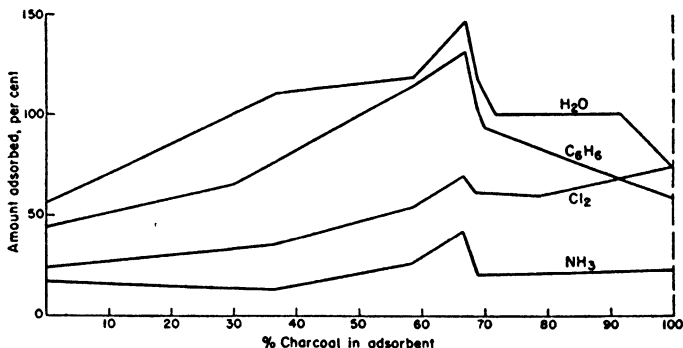


Fig. 168.—Adsorption of vapors on mixed charcoal-silica gel adsorbents.

mixing is intimate, approaching colloidal or molecular dimensions, the resulting adsorbent may have very different properties from the individual components. For example, the effect of promoters on some of the adsorptive properties of catalysts has been pointed out in previous chapters. Although such effects are more marked in chemisorption, they occasionally play an important role even in the physical adsorption of gases.

Schilow, Dubinin, and Toropow<sup>31</sup> prepared very intimate mixtures

<sup>29</sup> The free surface energy values were taken from W. D. Harkins, F. E. Brown, and E. C. H. Davies, *J. Am. Chem. Soc.*, **59**, 354 (1927).

<sup>30</sup> An interesting comparison between adsorption of liquid mixtures and their saturated vapors is found in a paper by D. C. Jones and L. Outridge (*J. Chem. Soc.*, 1930, 1574). The system investigated was silica gel—butyl alcohol—benzene.

<sup>31</sup> N. Schilow, M. Dubinin, and S. Toropow, *Kolloid Z.*, **49**, 120 (1929).

of charcoal and silica gel and measured the adsorption of benzene, water, chlorine, and ammonia on these adsorbents. Their results are shown in Fig. 168. The amount adsorbed, in per cent of the weight of the adsorbent, is plotted against the composition of the adsorbent. The adsorption of chlorine and ammonia was determined by passing the vapor over the adsorbent until a constant weight was reached; the adsorption of benzene and water was obtained by keeping the adsorbent over the liquid in a desiccator until the weight became constant. As the figure shows, the optimum composition is reached

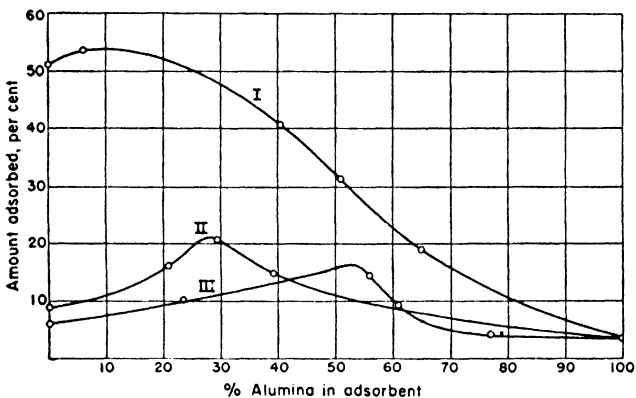


FIG. 169.—Adsorption of benzene on mixed adsorbents.

somewhere between 60 and 70% charcoal in the mixture. For three of the four vapors this mixture gives much higher adsorption than either charcoal or silica gel. Obviously, in this case the two adsorbents strongly influence each other. Since the investigators determined no isotherms for any of the vapors, it is impossible to say whether this influence manifests itself in changing the surfaces or the pore structures of the component adsorbents, or both.

Chowdhury and Pal<sup>32</sup> investigated the adsorption of benzene vapor by a number of mixed adsorbents. Their results for three of these are shown in Fig. 169. Curve I represents the adsorption on charcoal-alumina mixtures, curve II on silica gel-alumina mixtures, and curve III on ferric oxide gel-alumina mixtures. Individually charcoal is by far the best among the four adsorbents. Addition of 6.7% alumina to charcoal increases its activity slightly, but further addition causes

<sup>32</sup> J. K. Chowdhury and H. N. Pal, *J. Indian Chem. Soc.*, 7, 451 (1930).

a strong decrease. For the two other mixtures, however, compositions exist which are considerably more active than the individual adsorbents. The investigators also tried mixing bauxite (69%  $\text{Al}_2\text{O}_3$  and 23%  $\text{Fe}_2\text{O}_3$ ) with silica gel, and they found that some of these ternary mixtures were not only more active than the individual adsorbents, but even more active than the optimum binary mixtures. A mixture containing 40.8%  $\text{SiO}_2$ , 39.7%  $\text{Al}_2\text{O}_3$ , and 13.6%  $\text{Fe}_2\text{O}_3$  adsorbed 37.9% benzene by weight, approaching the activity of charcoal. In the experiments of Chowdhury and Pal actually a mixed adsorbate was used, since the benzene was adsorbed out of an air stream at 26° C. However, the adsorption coefficient of benzene is so much higher than that of air that the influence of air on the adsorption of benzene is negligible.

The case of mixed adsorbents and mixed adsorbates is of vital importance in chemisorption, but nothing of significance has been published on it as yet in the field of physical adsorption. The discussion of this subject therefore is reserved for Volume II.



## AUTHOR INDEX

- Adam, N. K. 303  
 Adhikari, G. 205, 450-2  
 Alexander, L. T. 355, 357, 412  
 Allmand, A. J. 346-8, 350, 352-3, 482  
 Almy, E. G. 414  
 Anderson, J. S. 386, 396, 407-8  
 Andreasen, A. H. M. 305  
 Andress, K. 238-9, 350  
 Andrews, D. H. 446  
 Antropoff, A. 82, 114  
 Armbruster, M. H. 298, 320, 432  
 Arrhenius, S. 12, 459  
 Ashby, C. T. 243  
 Austin, J. B. 298, 320, 432  
  
 Baba, T. 368  
 Bachmann, W. 376, 378  
 Bakr, A. M. 37-9, 41, 345  
 Balandin, A. A. 342  
 Baly, E. C. C. 83, 151  
 Band, W. 66  
 Bangham, D. H. 295, 320, 411, 432-6, 469-71  
 Bardeen, J. 211, 213  
 Barker, M. E. 362, 416  
 Barrer, R. M. 214-6, 247-8, 255, 264, 335, 341-2, 371-2, 452, 464-5  
 Barrett, H. M. 41, 273-4, 295  
 Bartell, F. E. 238-9, 306-9, 364, 414  
 Bartoszewicz, E. 265  
 Beebe, R. A. 36, 47, 49-50, 228-31, 244, 452  
 Beeck, O. 342, 357  
 van Bemmelen, J. M. 408, 418  
 Bemmels, C. 166  
 Benton, A. F. 22, 30, 33, 36-7, 76, 230, 244, 285-6, 346-8, 475-6, 478, 486, 490  
 Berenyi, L. 101-4, 107-10, 119  
 Bergter, F. 457, 485  
 Berl, E. 238-9, 350, 459-63  
 Berthelot, D. 110  
 Birnie, A. W. 41, 273-4, 295  
 Blench, E. A. 47, 227  
 Blinoff, H. 414  
 Blodgett, K. B. 44  
 Bloomquist, C. R. 295  
 de Boer, J. H. 140-2, 147, 206, 233, 341, 371, 423-4  
 du Bois-Reymond, E. 3  
  
 Born, M. 195, 208, 214  
 Bowden, F. P. 282-4, 360-1  
 Boyd, G. E. 158, 296  
 Bradley, H. 82  
 Bradley, R. S. 140, 142-5, 147, 162  
 Bramston-Cook, H. E. 45, 227  
 Braner, M. 47  
 Bray, R. I. 294, 297, 306, 319  
 Bray, W. C. 147  
 Brenecke, W. 47  
 Bridgeman, P. W. 235  
 Briggs, H. 339  
 Brill, R. 311, 358  
 Britton, G. T. 39-40, 81, 115, 339  
 Brown, F. E. 495  
 Brunauer, S. 7, 9, 13, 16, 19, 30-1, 36, 79, 92, 113, 119, 140, 144-5, 162-3, 170, 180, 229, 232, 258-9, 264, 286, 291, 293, 297, 309, 318-9, 340, 349, 351, 353, 357-9, 361, 372, 388, 420, 444  
 Bull, H. I. 47-8  
 Burk, R. E. 342  
 Burrage, L. J. 42, 346, 348, 408  
 Burt, F. P. 469  
  
 Cameron, A. E. 19, 125, 163-4, 233, 243, 293, 351, 469  
 Cameron, G. H. 314  
 Cameron, H. K. 241  
 Carman, P. C. 303-4, 306  
 Cassel, H. 260, 289, 320, 422, 433  
 Chambers, H. H. 42, 346  
 Chaney, N. K. 6, 7, 332, 345, 361, 474  
 Chaplin, R. 71, 346, 348, 350, 352, 482  
 Chapman, P. F. 119  
 Chappuis, P. 109, 245-6, 250, 252  
 Chariton, J. 438  
 Chlopin, V. 277  
 Chowdhury, J. K. 496-7  
 Clark, A. 295  
 Clark, A. M. 17, 136-7, 172, 351, 388, 396  
 Clark, R. E. D. 148, 302-3  
 Clausing, P. 454-5  
 Coelingh, M. B. 43, 404-5, 407-8  
 Cohan, L. H. 8, 126, 137, 395, 400, 405-7, 467-9  
 Cohen, M. 41, 273-4, 295  
 Constable, F. H. 309-10

- Coolidge, A. S. 19, 31, 33, 35, 40, 45, 95,  
 114, 118-9, 123-4, 130-4, 136, 175, 177,  
 224-5, 232-6, 239, 241, 249-52, 260,  
 263, 265, 357, 378, 411, 433-4, 444-5  
 Cooper, W. 339  
 Crittenden, E. D. 358  
 Cude, H. E. 469  
 Culbertson, J. L. 238-9, 383-5  
 Cunningham, G. E. 338  
 Custers, J. F. H. 206, 341, 371, 423-4  
 Cuthbertson, C. 188  
 Cuthbertson, M. 188  
  
 Damköhler, G. 460-4, 466-7, 489  
 Danforth, J. D. 420  
 Davidhesier, L. Y. 124  
 Davidson, G. F. 385  
 Davies, E. C. H. 495  
 Debye, P. 182-5, 202  
 Deitz, V. R. 314, 331, 387-9, 469, 483  
 Deming, L. S. 62, 140, 163, 170, 180, 232,  
 291, 319, 388  
 Deming, W. E. 62, 140, 163, 170, 180,  
 232, 291, 319, 388  
 Demougin, P. 444  
 De Vries, T. 419-20  
 Devonshire, A. F. 441, 471-3  
 Dewar, J. 44, 227-8, 234, 244, 477-8  
 De Witt, T. 293-4, 296-7, 319, 332  
 van Dingenen, W. 248, 264-7  
 Dixon, J. K. 260  
 Dohse, H. 467  
 Dowden, D. A. 229, 231, 452  
 Draper, H. D. 147  
 Driver, J. 363  
 Drude, P. 43  
 Dubinin, M. 495  
 Dunbar, A. 383  
 Durau, F. 300, 337  
  
 Edwards, J. 337, 442  
 Egerton, A. 37  
 Eggertsen, F. T. 275  
 Elder, A. L. 414, 418  
 Emmett, P. H. 7, 9, 13, 16, 19, 24, 30-1,  
 36, 62, 79, 92, 113, 119, 140, 144-5,  
 162-3, 166, 174, 180, 229-30, 244, 259,  
 264, 286, 291, 293-7, 299, 309, 318, 322,  
 332, 340, 349, 351, 353, 357-9, 361, 368,  
 372, 388, 407, 420, 444  
 Estermann, I. 438, 449-50, 455  
 Eucken, A. 96, 196-9, 203  
 Evans, M. G. 72-3, 246, 413  
 Eversole, J. F. 243  
 Ewing, D. T. 112, 126, 235  
  
 Ewing, W. W. 296, 381-4, 419  
 Eyring, H. 11, 67, 257, 342-3  
  
 Fakhoury, N. 411, 432, 434  
 Falckenhagen, H. 185  
 Favre, P. A. 44, 241, 245  
 Felsing, W. A. 243  
 Fermi, E. 67, 208  
 Fieldner, A. C. 36  
 Firth, J. B. 363  
 Flösdorf, E. W. 46-7  
 Fontana, F. 3  
 Fornwalt, H. J. 40, 114  
 Fortunatow, N. 376-7  
 Foster, A. G. 43, 137-8, 346, 378, 396,  
 401-5, 408  
 Fowler, R. H. 60, 66-7, 257  
 Frank, H. S. 323  
 Frankenburg, W. 21  
 Frazer, J. C. W. 9, 166, 233, 320, 322,  
 324, 326, 328, 360, 363, 417, 475  
 Frazer, J. H. 43, 326-7  
 Frenkel, J. 455, 473  
 Freundlich, H. 7, 15, 55, 82, 89, 427  
 Frisch, R. 473  
 Frost, A. A. 426  
 Fu, Y. 238-9, 306-9  
  
 Galitzin, Prince B. 110  
 Ganguli, A. 66  
 Garner, W. E. 47-9, 227, 231  
 Gehman, S. C. 293  
 Giauque, W. F. 234  
 Giebenhain, H. 50  
 Giesen, J. 42, 463-4  
 Glasstone, S. 67, 257  
 Gleysteen, L. F. 314, 331, 387-9, 469, 483  
 Goldmann, F. 15, 34, 80, 95, 111-2,  
 117-8, 126, 130, 132-3, 167, 236-8,  
 258-9, 268, 346, 378, 423, 439  
 Goldwasser, S. 36, 49  
 Gooden, E. L. 305  
 Gorbatschew, A. 89  
 Gortner, R. A. 445  
 Graham, J. I. 339  
 Gregg, S. J. 46, 88, 124-5, 225, 241,  
 244-5, 251-2  
 Greider, C. G. 238, 250  
 Greiff, F. 346  
 Griffin, C. W. 349  
 Grimm, F. V. 238  
 Gustaver, B. 201  
  
 Hall, M. H. 47-8  
 Hand, P. G. T. 352-3

- Hanson, A. C. 243  
 Harbard, E. H. 355-6, 409  
 Haring, M. M. 357  
 Harkins, W. D. 112, 126, 158, 235, 381-4, 495  
 Harkness, R. W. 24, 230, 244  
 Harned, H. S. 8, 30, 458, 460, 462  
 von Hartel, H. 11  
 Heard, L. 9  
 Heaven, H. S. 487  
 Hendricks, S. B. 274, 280, 282, 355, 357, 412  
 Hene, W. 11  
 Henry, D. C. 84-5, 95, 410  
 Hertel, K. L. 306  
 Herzfeld, K. F. 43, 61, 268, 472  
 Heywood, H. 272-3  
 Higuti, I. 407  
 Hillier, J. 294  
 Hodler, A. 21  
 Hofmann, U. 311-4, 411-2  
 Holmes, H. N. 414, 418  
 Holst, G. 454  
 Homfray, I. F. 32-3, 55, 57, 75, 83, 86-7, 108-9, 197-8, 204, 224, 267, 285, 436  
 Howard, H. C. 359, 382-3, 417  
 Howard, J. 31, 33, 353-4  
 Hückel, E. 185, 204, 219, 222  
 Hüttig, G. F. 142  
 Hulet, G. A. 359, 382-3, 417, 469  
 Hurka, V. R. 426  
  
 Iliin, B. 202-4, 459-60  
 Innes, W. B. 427-8, 437-8, 440  
 Iredale, T. 319  
 Isselstein, M. T. 30, 301  
 van Itterbeek, A. 248, 264-7, 320  
  
 Jackman, D. N. 345  
 Jacquet, E. 200-4  
 Johnstone, H. F. 225  
 Jones, D. C. 495  
 Jones, I. D. 445  
 Juza, R. 142  
  
 Kälberer, W. 50, 68, 70, 91, 244-5, 260, 263, 285, 336, 349  
 Kar, S. C. 66  
 Kautsky, H. 346, 414  
 Kayser, H. 3  
 Keenan, R. G. 258  
 Keeson, W. H. 167, 182-4, 198  
 Kelvin, Lord 90, 198-9  
 Kemper, W. A. 446-7  
  
 Kenrick, F. B. 273, 316  
 Keyes, F. G. 45, 177, 195, 225, 227-8, 232, 235, 239, 245, 251, 260  
 King, A. 42, 346, 355-6, 409, 416  
 Kirkwood, J. G. 194-5, 214-5  
 Kistiakowsky, G. B. 46-7, 230  
 Kistler, S. S. 315-6  
 Klar, R. 92  
 Knudsen, M. 437  
 Kolthoff, I. M. 275, 296  
 Kozeny, J. 303  
 Kraemer, E. O. 295, 322, 368, 398, 407  
 Krauss, A. 37, 490  
 Kratz, H. 91  
 Krieger, K. A. 360  
 Kruyt, H. R. 223, 239, 245, 251, 264, 266-7, 269, 335  
 Kubelka, P. 127-31, 133, 373-4, 376, 379, 389-93, 401-2  
 Kusnetzowa, W. 277  
  
 Laidler, K. J. 67, 257  
 Lamb, A. B. 7, 45, 224, 234-5, 239, 241, 249-52, 265, 369-72, 417  
 Lambert, B. 17, 136-7, 172, 351, 388, 396, 401, 407-8, 418, 486-7  
 Land, W. E. 233, 445  
 Landé, A. 198-200, 202  
 Langmuir, I. 6, 16, 22, 31, 44, 60, 62-4, 66-7, 71, 73-4, 76-7, 82, 89, 95, 150-1, 154, 166, 233, 285, 318, 427-9, 448, 454-5, 457, 459-60, 470-2, 475  
 Latham, G. H. 329  
 von Laue, M. 311, 313  
 Lawrence, J. N. 36  
 Lea, F. M. 305  
 Lemecke, W. 411  
 Lenel, F. V. 207, 209, 215-6, 341-2  
 Lenher, S. 148, 166, 233, 320-4, 326, 329  
 Lennard-Jones, J. E. 191, 210-1, 213, 215, 471-3  
 Lewis, G. N. 5, 65, 97, 122, 220  
 Lindau, G. 129-33  
 Lizius, J. L. 482  
 Lloyd, L. E. 364  
 London, F. 135, 141, 182, 186-90, 192-3  
 Long, J. S. 124  
 Lorenz, R. 198-200, 202, 485, 493  
 Love, K. S. 258, 357  
 Low, G. W. 49  
 Lowitz, T. 3  
 Lowry, H. H. 100, 109-10, 119, 363, 420, 426  
 Lucas, H. S. 119

- Maass, O. 39, 40, 337, 442-4  
 McBain, J. W. 3, 8, 15, 37-41, 71, 81-2, 112, 115, 119, 129, 226, 239, 308, 322, 339, 345, 350, 365, 367, 380, 398, 410-1, 413, 448, 456, 462-3, 480  
 McGavack, J. 95, 104, 121-2, 124, 134, 161, 201, 264, 308, 359-60  
 McHaffie, I. R. 148, 166, 233, 320-4, 326, 329  
 McKinley, L. 251-2, 265  
 McKinney, P. V. 36  
 Magnus, A. 37, 47, 50, 89-95, 198, 244-5, 260, 263, 336, 349, 430, 475, 485, 490  
 Makower, B. 357  
 Manegold, E. 373, 418  
 Manning, J. E. 353  
 Marc, R. 277  
 Margenau, H. 191, 211-3  
 Mark, H. 68, 285, 467  
 Markham, E. C. 36-7, 76, 285, 475-6, 478, 486, 490  
 Marshall, M. 45, 177, 225, 227-8, 232, 235, 239, 245, 251, 260  
 Maxted, E. B. 49  
 Mayer, J. E. 195, 207, 214, 337, 443  
 Mayer, M. G. 337, 443, 472  
 Meehan, F. T. 410  
 Meer, N. 11  
 Meyer, G. E. 126  
 Miller, A. R. 257  
 Modderman, J. G. 223, 239, 245, 251, 264, 266-7, 269, 335  
 Moelwyn-Hughes, E. A. 181  
 Mohamed, A. F. 411, 432, 434  
 Moll, F. 451  
 Monroe, C. E. 382  
 Moon, C. H. 49  
 Morgan, S. O. 109, 363  
 Morris, H. E. 39, 40, 337, 442  
 Morris, T. C. 293  
 Mosallam, S. 295, 320  
 Müller, A. 92  
 Müller, M. 379, 391  
  
 Nelson, R. A. 282, 355, 357, 361, 412  
 Nurse, R. V. 305  
  
 Oberfell, G. G. 36  
 O'Connor, E. A. 283  
 Ogden, G. 231  
 Ohl, E. N. 371-2  
 Oliphant, M. L. 319  
 Olmstead, P. S. 100, 109-10, 119, 420, 426  
 Opdycke, L. H. 124  
  
 Orfield, H. M. 49, 50  
 Orr, W. J. 215-6, 254, 256-8, 341-2, 452  
 Osterhof, H. J. 307  
 Ouellet, C. 425-6  
 Outridge, L. 495  
 Owens, A. E. 125, 441  
  
 Pal, H. N. 496-7  
 Palmer, W. G. 148-9, 260-1, 302-3, 430-2, 436  
 Paneth, F. 274-80, 300  
 Patrick, W. A. 8, 95, 104, 120-2, 124-6, 134, 161, 166, 201, 233, 238, 250, 264, 308, 322, 324, 326, 328, 351, 360, 363, 395-6, 414-5, 417, 441, 445-7, 467-9, 475  
 Pearce, J. N. 225-6, 241, 243, 251-2, 265, 333  
 Pease, R. N. 32, 35  
 Peel, D. H. P. 486  
 Peierls, R. 257  
 Pelzer, H. 311  
 Peters, K. 57-9  
 Peters, P. E. 243  
 Phillips, T. D. 459  
 Pidgeon, L. M. 174, 396, 416, 480  
 Pietsch, E. 342  
 Piper, G. H. 348  
 Polanyi, M. 11, 15, 34, 60, 71, 76, 80, 95-7, 99, 101, 107, 110-2, 117-8, 126, 130-4, 167, 236-8, 253, 255-6, 258-9, 269, 346, 378, 423, 437, 439  
 Pollard, W. G. 211-3  
 Porter, E. E. 420  
 Porter, J. L. 281, 410-1, 413  
 Preston, W. C. 125, 441  
 Prosen, E. J. R. 213, 268  
 Pyzhev, V. 257  
  
 Rabinowitsch, E. 368  
 Rabinowitsch, M. 376-7  
 Radu, A. 280  
 Radulescu, D. 408  
 Radulescu, F. 408  
 Randall, M. 5, 65, 97, 122, 220  
 Rao, B. S. 493-4  
 Rao, K. S. 396-8, 400, 407, 409  
 Ratner, A. 277  
 Ray, A. B. 6, 332, 345, 474  
 Rayleigh, Lord 43  
 Razouk, R. I. 411, 433-5  
 Reed, G. H. 225-6, 241, 265  
 Reyerson, L. H. 19, 78, 125, 163-6, 233, 243, 293, 351, 469  
 Rice, M. J. 333



- Rice, O. K. 181  
Richardson, L. B. 32, 75-6, 89, 108-9, 426, 479, 486, 488  
Rideal, E. K. 82, 282-4, 360-1, 425-6, 430, 464-5  
Roberts, J. K. 9, 30, 44, 50, 60, 254-7  
Rogers, W. 57  
Rosenblum, C. 275  
Roth, H. 485  
Rowley, H. H. 427-8, 437-8, 440  
Rush, R. I. 360, 363, 417, 475  
  
Sachs, R. G. 213, 268  
Sachse, H. 46  
St. John, A. 6, 332, 345, 474  
Salditt, F. 433  
de Saussure, T. 3, 11, 96, 196  
Scheele, C. W. 3  
Schelte, F. 301-2  
Scherrer, P. 310-1  
Schilow, N. 495  
Schlüter, H. 174  
Schmidt, G. 167  
Schmidt, G. C. 300  
Schmidt, O. 12, 231, 367  
Schofield, R. K. 430  
Schuchowitski, A. A. 134-6, 393  
Schuster, C. 68, 70, 91, 244, 263  
Schwab, G. M. 47, 342  
Schweyer, H. E. 310  
Sclar, M. 57  
Seborg, R. M. 385  
Seliger, R. 42  
Semenoff, N. 90, 430, 437-9  
Sessions, R. F. 410-1  
Sever, W. 470-1  
Sextl, T. 66  
Shah, M. S. 7  
Shaw, T. M. 357  
Shereshefsky, J. L. 71, 126, 440  
Sherman, A. 342-3  
Shiels, D. O. 352-3  
Sickman, D. V. 10, 230  
Siebert, W. 481  
Silverman, S. 327  
Simon, F. 421  
Slater, J. C. 181, 194  
Smith, A. E. 342, 357  
Smith, C. M. 305  
Smith, H. E. 166, 233, 320, 322, 324, 326, 328  
Smith, H. G. 345  
Smith, J. W. 329  
Smith, R. H. 446  
Smith, W. R. 294, 297, 306, 319  
  
Smyth, C. P. 201, 243, 268  
Soller, T. 36  
Speakman, J. B. 413  
Spurway, C. H. 419  
Stamm, A. J. 385  
Steacie, E. W. R. 443  
Steinhof, E. 367  
Stern, O. 473  
Stevens, N. P. 228-9  
Stout, J. W. 233-4  
Stranski, I. N. 342  
Strother, C. O. 24, 35  
Sullivan, R. R. 306  
Swain, R. C. 420-2  
Swietoslowski, W. 265  
  
Tanner, H. G. 41  
Tapp, J. S. 443  
Taylor, A. L. 225-6  
Taylor, H. S. 4, 9, 10, 24, 26, 33, 35, 46-9, 230-1, 244, 343, 398, 448  
Teague, M. C. 36  
Teller, E. 62, 140, 163, 170, 180, 208, 213, 232, 264, 291, 318-9, 388, 420  
Temkin, M. 66, 257  
Thimann, W. 276, 278  
Thomas, S. B. 420  
Thomson, W. 120  
Thornhill, F. S. 294, 297, 306, 319  
Tilenschi, S. 408  
Tiselius, A. 453  
Titoff, A. 14, 21, 24, 32, 45, 53, 57, 75, 87, 99, 108-9, 201, 204, 219, 223, 235, 245, 252, 436, 459  
Tonks, L. 429  
Toropow, S. 495  
Traube, J. 427  
Trouton, F. T. 328  
Tryhorn, F. G. 471, 483, 485, 491-3  
  
Ubbelohde, A. R. 37  
Urquhart, A. R. 396  
Urry, W. D. 83, 441  
  
Van Winsen, A. 480  
Veal, F. J. 49, 231  
Vereycken, W. 320  
Volmer, M. 60, 64-6, 90-1, 205, 428, 449-52, 455  
Vorwerk, W. 274-6, 278  
  
Wang, J. S. 257  
Ward, A. F. H. 49, 436, 465  
Washburn, E. W. 469-70  
Weber, M. K. 384

- Weigel, O. 367  
Weil, K. 57-9  
Weingartner, E. 439-41, 459-63  
Weir, C. E. 71, 440  
Weiser, H. B. 281, 289  
Welke, K. 71, 253, 255, 437  
West, C. D. 371  
Wheeler, A. 342, 357  
White, T. A. 22, 30, 285, 346-8  
Whitehouse, A. G. R. 241  
Wicke, E. 375-6, 380, 465-6  
Wiedbrauck, E. 485, 493  
Wildner, E. L. 49  
Wilkins, F. J. 85, 89, 226, 257, 348, 436, 476  
Williams, A. M. 84, 86-9, 95, 252, 255-6, 285, 410  
Williams, E. C. 42  
Williamson, A. J. 9, 231  
Wilm, D. 311-4  
Wilson, R. E. 7  
Windeck, H. 92  
Winter, L. L. 238-9  
Wishart, A. W. 78, 165, 243  
Wolff, H. 299-301  
Wood, R. W. 437  
Wood, W. C. 368  
Woodhouse, J. C. 369-70, 417, 479, 486, 488  
Work, L. T. 310  
Wyatt, W. F. 471, 483, 485, 491-3  
Wyckoff, R. W. G. 358  
Zeise, H. 75-6  
Zeldowitsch, J. 82-3, 442  
Zsigmondy, R. 95-6, 120-1, 386, 394-5, 413  
Zwicker, C. 140-2, 147

## SUBJECT INDEX

- absorption, 3, 53
- absolute reaction rates, theory of 67
- accommodation coefficient 44
- activated adsorption 4, 8-11, 389
  - migration 11, 452-4
- activation 360-4, 414-7
  - and pore structure 414-7
  - and surface composition 363-4
  - and surface structure 363
  - by alternate oxidation and reduction 361
  - by chemical agents 361
  - by dehydration 361-3
  - by heat 360-1, 363
  - by increasing pore size 362
  - by removal of other molecules than water 361, 363
  - by removing impurities 361
- active centers 79, 158, 336-46
- adiabatic calorimeter 47-50
- adlineation 342
- adsorbate (*see also* adsorbed phase) 3, 419-47
  - coefficient of thermal expansion of 423
  - compressibility of 102
  - condensation point of 254, 437-40
  - critical temperature of 440-4
  - definition of 3
  - density (*see also* adsorbed phase, density distribution in) 419-20
  - effect of photoelectric emission 424-6
  - effect on surface electrical potential 426
  - equation of state of 98, 119, 426-37
  - light absorption of 423-4
  - melting point of 444-7
  - phase changes in 437-47
  - phase rule for 438-9
  - physical properties of 419-26
  - specific heat of 420-2
  - supersaturation in 440
- adsorbed atoms 5, 8
- adsorbed phase (*see also* adsorbate)
  - compression in 102, 112-6, 126, 235-8, 379-85
  - cross section of 97-8
  - density distribution in (*see also* adsorbate, density of) 100, 106, 112
  - tension in 122, 126
  - thermal expansion of 102-3, 112-4, 423
  - thickness of 96, 320-9
  - volume of (*see also* pores of adsorbent, total volume of) 112
- adsorbent, definition of 3
  - density of 377, 380-5
  - efficiency of 36
  - evacuation of 29
  - expansion of 410-3, 432-6
  - mixed 495-7
  - pores of, *see* pores of adsorbent
  - surface of, *see* surface of adsorbent
  - swelling of 410-3, 432-6
- adsorption (*see also* chemisorption, physical adsorption)
  - above the critical temperature 104-7, 336-8
  - applications of 6, 474
  - at high pressures 68, 81, 114-6, 338-9
  - at low pressures 68-71, 134
  - coefficient 64, 67
  - definition of 3
  - early history of 3
  - entropy increase in 5
  - equilibrium 7, 11
  - heat content decrease in 5
  - heat of, *see* heat of adsorption
  - in second layer 62
- adsorption isobar 21-4, 28
  - definition of 13
- adsorption isostere 24-5, 28, 85-9
  - and vapor pressure curve 24-5
  - definition of 13
- adsorption isotherm (*see also* isotherm) 14-21, 53-179
  - definition of 13
  - discontinuous 62, 346-9
  - five different types 14-21, 149-50
  - stepwise 346-9
- adsorption, kinetics of (*see also* rate of adsorption) 448-73
  - mixed (*see also* mixed adsorption) 474-97
  - multimolecular 6, 62, 83, 92, 95-6, 117, 138, 140-79
  - negative 492-3
  - on heterogeneous surfaces 94, 119, 329-55

- adsorption potential 97, 135, 237  
variation with temperature 99
- adsorption, primary 4  
rate of 61, 455-71  
reversibility in 28  
secondary 4  
specificity in 12, 27, 329-35  
unimolecular 6, 63, 67, 82, 85, 89, 92,  
95-6, 117, 177
- affinity curve 111-4, 258-9
- ageing 418
- alteration of pore structure 408-18  
by activation 414-7  
by ageing 418  
by chemical agents 414, 416-7  
by dehydration 369-71, 409  
by heat 417  
by removal of other molecules than  
water 414-6  
by sintering 369-71  
by the adsorbate 409-13  
by water treatment 409, 413, 418  
irreversible 409  
reversible 410-8
- alteration of surface of adsorbent *see*  
activation, sintering, surface of ad-  
sorbent
- amorphous patches 343
- amount adsorbed, definition of 40, 114  
determination of 32-50  
units of 13
- apparatus (*see also* determination of  
amount adsorbed) 32-50
- apparatus, gravimetric, beam balance 41  
dynamic 42  
floating balance 42  
spring balance 37-40  
torsion balance 42  
high pressure 39-41
- apparatus, heat of adsorption, adiabatic  
calorimeter 47-50  
isothermal calorimeter 44-6
- apparatus, volumetric, constant pressure  
35  
constant volume 32-7  
dynamic 36
- average life of adsorbed molecule 61,  
454-5, 471-3
- boiling point and physical adsorption 12
- breaks in adsorption isotherms 346-9,  
404, 408
- buoyancy correction 40-41
- calorimeter 44-50
- calorimetric heat of adsorption 71, 177,  
218-20
- capillaries, *see* pores of adsorbent
- capillary condensation, hysteresis in 18,  
136, 394-408  
rate of 469  
theory 95-6, 120-39, 178
- capillary space, *see* pores of adsorbent
- characteristic curve 99, 101-11
- characteristic energy 188-9
- chemical adsorption, *see* chemisorption
- chemisorption, comparison with physical  
adsorption 27-8  
definition of 4  
energy of activation of 10, 27  
isobars 22-4  
isotherms 19  
rate of 7-11, 27  
two different types 24
- Clapeyron-Clausius equation 24, 223
- cleaning of surface 29-31
- composite surface (*see also* surface of ad-  
sorbent, heterogeneous fraction of)  
74, 77
- compressed film (*see also* potential the-  
ory) 96
- compressibility of adsorbate 102
- compression, heat of 235-40, 259-60
- compression in the adsorbed phase 102,  
112-6, 126, 235-8, 379-85
- condensation, capillary, *see* capillary con-  
densation
- condensation coefficient, definition of 61  
experimental determination of 455-6  
fundamental theory of 471-3
- condensation in adsorbed phase 254, 437-  
40
- Coulomb forces 5
- cracks, surface located in 345-6
- critical temperature and physical adsorp-  
tion 12  
of adsorbate 440-4
- cross section of adsorbed phase 97-8
- dead space correction 33
- density of adsorbent 377, 380-5
- determination of amount adsorbed (*see*  
*also* apparatus) 32-44  
direct 32-43  
indirect 43-4  
method of accommodation coefficients  
44  
optical methods 43  
surface tension methods 289, 319-20

- determination of heat of adsorption (*see also* apparatus) 44-50
- determination of particle size, distribution of sizes 272, 304
- gas adsorption method 293-5
  - microscopic methods 272-4
  - permeability method 303-6
  - x-ray diffraction method 310-4
- determination of surface area, adsorption from solutions 274-85
- adsorption methods 277-99
  - dye adsorption methods, 277-82
  - electrolytic method 282-5
  - gas adsorption methods 285-99
  - heat conductivity method 315-6
  - heat of wetting method 306-9
  - interference method 309-10
  - microscopic methods 272-4
  - optical methods 309-10
  - permeability methods 303-6
  - radioactive indicator method 274-7
  - rate of solution method 299-303
  - turbidimetric analysis method 310
  - visual methods 272-4
  - x-ray diffraction method 310-4
- differentiated structure curve 392-3, 402-3
- diffusion against gas phase impurities 467-9
- in dynamic systems 466
  - inhibition of 467-9
  - into a solid 461-71
  - into cylindrical pores 461-5
  - into very narrow pores 466-7
  - over surface (*see also* migration) 461-2, 472-3
  - rate of 461-71
  - toward the center of a sphere 465-6
- dipole, fluctuating 186-7
- induced 90, 140-2, 184-5
  - permanent 90, 147, 182
  - polarizable 141-2, 184-5
  - rigid 182-4
- discontinuities in adsorption isotherms 346-9, 404, 408
- dispersion energy 186-90, 204-7, 254-7
- distribution of pores 131, 368, 385-93
- dye adsorption method 277-82
- dynamic retentivity method 42
- edges of the adsorbent 340-42
- efficiency of adsorbent 36
- electrolytic method 282-5
- electrostatic image forces 90
- energy constants 180
- energy of activation of chemisorption 10, 27
- of migration 452-4
- entropy increase in adsorption 5
- equation of state of adsorbate 98, 119, 426-37
- and adsorption isotherm 64-6, 90-1
  - and expansion of adsorbent 432-6
  - and Langmuir equation 428
  - and van der Waals equation 89, 430
  - for hard, elastic spheres 429
  - for imperfect gas 64, 428-32
  - for perfect gas 427
  - testing of 432-7
- equivalent pressure curves 128-36
- evacuation of adsorbent 29
- exponential formula, *see* Freundlich isotherm equation
- floating balance 42
- fluctuating dipole 186-7
- quadrupole 191
- forces (*see also* Coulomb forces, valence forces, etc.) 27, 63, 89
- range of 61, 95, 140
- free energy of adsorption 5, 64
- Freundlich isotherm equation 15, 54-9, 121, 125
- derivation of 82-4
- f-value 194
- gas adsorption method 285-99
- gas-phase diffusion (*see* diffusion)
- gas-solid interface 4
- Gibbs equation 289, 319, 433
- heat conductivity method 315-6
- heat content decrease in adsorption 5
- heat of adsorption 5, 25-7 61, 87-8, 92, 151, 180-270, 371
- borderline cases between physical and chemical adsorption 334-5
  - calorimetric 71, 177, 218-20
  - comparison between calorimetric and isosteric 223-6
  - comparison between differential and integral 219-20
  - comparison between heats of physical adsorption and liquefaction 231-4
  - comparison between heats of physical and chemical adsorption 27, 226-31
  - determination of 44-50
  - differential, definition of 26, 219
  - in first layer 61, 151, 156-8, 180
  - in last layer 168, 180

- in second layer 61, 151-2
- integral 27, 218, 249-51
- isosteric 25, 177, 220-6
- isosteric, difficulties in calculation 226
- isosteric, thermodynamics of 220-3
- isothermal 219
- maxima and minima 251-8, 269
- net 235-40
- of different gases on the same adsorbent 240-3
- of the same gas on different adsorbents 243-5
- variation due to interaction of adsorbed particles 26, 69
- variation over the adsorbent surface 26, 68, 70, 78, 120, 246-7
- variation with amount adsorbed 26, 246-62
- variation with pressure 265-6
- variation with temperature 262-70
- heat of compression 235-40, 259-60
- heat of sublimation 193
- heat of vaporization and physical adsorption 12
- heat of wetting, differential 237-8
- integral 238-40
- method 306-9
- heat treatment of adsorbent, *see* sintering
- Henry's law in adsorption 15, 68-71, 91
- heterogeneous surface (*see also* surface of adsorbent, heterogeneous fraction) 26, 82
- high pressure adsorption 68, 81, 114-6, 338-9
- apparatus 39-41
- high temperature adsorption 4
- homogeneous surface 77, 335-9
- hysteresis 18, 136, 394-408
- and pore structure 394-408
- branches of loop 137-8, 399-408
- discontinuities in desorption branch 404, 408
- incomplete wetting theory 394-6
- ink bottle theory 398-400
- irreversible 394-6
- open pore theory 401-8
- point of inflection of desorption branch 403
- reversible 397-408
- scanning the loop 398-400
- impurities, effect on amount adsorbed 30, 349-55
- effect on hysteresis 351-3
- effect on rate of adsorption 8, 458, 467-9
- removal of 29-31
- incompletely crystallized atom groups 343
- incomplete wetting (*see also* hysteresis, incomplete wetting theory) 127-9
- indirect methods of adsorption measurements 43-4
- induction energy 183-5
- influence energy 208-9, 256-7
- inhibition by impurities (*see* impurities)
- ink bottle theory 398-400
- integral heat of adsorption 27, 218, 249-51
- heat of wetting 238-40
- interaction energy between molecule and surface 196-217
- dispersion 204-7
- ionic surface—induced dipole (influence) 208-9
- ionic surface—quadrupole 210
- metal—non-polar gas 203-4, 210-3
- metal—polarizable dipole 200-1
- metal—polarizable quadrupole 202
- metal—rigid dipole 198-200
- metal—rigid quadrupole 201-2
- semi-conductor—non-polar gas 214
- interaction energy between molecules, dipole-dipole (orientation) 182-3, 254-6
- dipole—induced dipole (induction) 183-5
- dispersion 186-90, 254-7
- ion—dipole 334-5
- ion—induced dipole (influence) 208-9, 256-7
- quadrupole—dipole 185-6
- quadrupole—induced dipole 191
- quadrupole—quadrupole 191
- repulsion 191-2
- interface, solid-gas 4
- interference method 309-10
- in capillary condensation 404-5
- internal surface 3-4, 145
- isobar 21-4, 28
- isostere 24-5, 28, 85-9
- isosteric heat of adsorption 25, 177, 220-6
- isotherm (*see also* absorption isotherm, adsorption isotherm)
- Langmuir type 16, 114, 150, 155, 166-8
- of chemical reaction 54
- S-shaped 17, 114, 141-5, 150, 155-62
- Type I, *see* isotherm, Langmuir type

- Type II, *see* isotherm, S-shaped  
Type III 155, 162-6  
Type IV 172-7  
Type V 172-7  
isothermal calorimeter 44-6
- Kelvin equation 120, 123-4, 126-7, 131-2, 137-9, 170  
kinetics of adsorption 448-73
- Langmuir equation 60-82, 84, 89, 119, 125, 178  
  and the equation of state 428  
  derivations of 60-7  
  for composite surface 74  
  for mixed adsorption 475-90  
  testing of 67-82  
Langmuir type isotherm 16, 114, 150, 155, 166-8  
light absorption of adsorbate 423-4  
low pressure adsorption 68-71, 134  
low temperature adsorption 4
- macropores 374-7  
magnetic susceptibility and adsorption 210-1, 214-5  
melting point of adsorbate 444-7  
metal-gas interaction, *see* interaction energy  
micropores 374-77  
microscopic methods 272-4  
migration, activated 11, 452-4  
  energy of activation of 452-4  
  fundamental theory 472-3  
  of adsorbed molecules 448-54  
  of molecules in surface layer of a crystal 449-51  
mixed adsorbent 495-7  
mixed adsorption 474-97  
  of saturated vapors 483-4, 491-5  
  rate of 483-5  
  technical importance of 474  
  types of 474  
molecular sieve 366-73  
monolayer, *see* adsorption, unimolecular  
multimolecular adsorption 6, 62, 83, 92, 95-6, 117, 138, 140-79  
multimolecular adsorption theory 140-1, 149-79  
  applications 155-68, 172-7  
  comparison with capillary condensation theory 170-2  
  criticism of 177-9  
  derivations of 151-5, 168-70  
  multiple adsorption theory 342  
  mutual polarization 423-6  
  negative adsorption 492-3  
    hydrostatic pressure 122-3  
  net heat of adsorption 235-40  
    and Polanyi potential 237-8  
    differential (*see also* heat of wetting, differential) 237, 259  
    negative 235  
    positive 235  
    variation with amount adsorbed, 258-9, 290  
  open pore theory 401-8  
  optical methods 43, 309-10  
  orientation energy 182-3, 254-6
- packing of adsorbed molecules 74, 79-81, 159  
particle size, determination of, *see* determination of particle size  
permeability method 303-6  
persorption 366-73  
phase changes in adsorbate 437-47  
phase rule for adsorbate 438-9  
photoelectric emission and adsorption 424-6  
physical adsorption (*see also* adsorption)  
  and boiling point 12  
  and critical temperature 12  
  and heat of vaporization 12  
  and van der Waals constants a 12  
  definition of 4  
  effect of chemisorption on 353-5  
  effect of physical adsorption on 349-53  
  on plane surfaces 317-29, 457-61  
  rate of 7-8, 27, 455-71  
  physical properties of adsorbate 419-26  
  plane surface, adsorption on 317-29  
  rate of adsorption on 457-61  
  polarizability 146-7, 184, 194  
  polarization during electrolysis 282-5  
  mutual, of adsorbent and adsorbate 423-6  
  polarization theory 140-9  
    criticism of 143-7  
    derivation of 141-2  
    testing of 142-9  
  polar molecules, *see* dipoles, quadrupoles  
  polishing, effect on adsorption 283-4  
  pores of adsorbent, alteration of 408-18  
    and hysteresis 394-408  
    average radius 386

- destruction of 417-8
- diameters of 386-408
- differentiated structure curve 392-3, 402-3
- diffusion into 461-7
- increase in size of 414-7
- macropores 374-7
- micropores 374-7
- penetration into the 80, 381-5
- shapes 398-400
- size distribution of 131, 368, 385-93
- structure curve 390-3, 401-3
- structure of 365-418
- total volume of 121, 373-80
- potential, adsorption 97, 135, 237
- potential theory 60, 95-120, 131-6, 138
  - applications of 101-15, 131-6
  - criticism of 115-20
  - modification of 115-20
  - testing of 101-20, 131-6
- pressure, effect on amount adsorbed 13-6
  - effect on heat of adsorption 265-6
- primary adsorption 4
- promoters, effect of 358-9
- purification of surface 29-31
  - by chemical means 30
  - by evacuation 29
  - by heating 29-31
  - by treatment with the adsorbate 30
  - from stopcock grease 31
- quadrupole, rod-shaped 185
  - three-dimensional 185
- radioactive indicator method 274-7
- range of forces 61, 95, 140
- rate of adsorption 61, 455-71
  - capillary condensation 469
  - chemical adsorption (*see also* activated adsorption) 7-11, 27
  - mixed adsorption 483-5
- rate of physical adsorption 7-8, 27, 455-71
  - and desorption 61, 466
  - and solution 456, 470-1
  - fundamental theory 471-3
  - inhibition by impurities 8, 458, 467-9
  - in porous bodies 8, 461-9
  - on plane surfaces 457-61
- rate of solution method 299-303
- reflection of incident molecules 60, 63
- repulsive forces 181, 191-2
- retentivity 345-6
- saturated vapors, adsorption from 483-4, 491-5
- saturation adsorption 79-82, 112, 117-19, 121, 124
- saturation of surface 79-82
- secondary adsorption 4
- second virial coefficient, *see* virial coefficients
- selective adsorption 492-5
- selectivity 493
- shape factor 272
- shapes of pores 398-408
- sigmoid isotherm, *see* isotherm, S-shaped
- sintering (*see also* alteration of pore structure, alteration of surface) 357-60
  - by cold-rolling 283-4, 360
  - by crystal growth 357-60
  - by plugging of pores 359
  - mechanism of 357-60
- size analysis 272-4, 304-5
  - constants 180
  - distribution 131, 368, 385-93
- solid-gas interface 4
- solution of gas in solid 4, 54
  - rate of 456, 470-1
- isorption 3
  - balance 37-40
- specific heat of adsorbate 420-2
- specificity in adsorption 12, 27, 329-35
- spreading force 65, 427-37
- spring balance 37-40
- S-shaped isotherm 17, 114, 141-5, 150, 155-62
- stepwise isotherms 346-9
- structure curve 390-3, 401-3
  - differentiated 392-3, 402-3
- structure of pores 365-418
  - of surface 341, 359
- supersaturation in adsorbed phase 440
- surface area 79, 87, 144, 158, 298, 308, 313
  - covered by a molecule 276, 278, 287
  - determination of, *see* determination of surface area
- surface diffusion 461-2, 472-3
- migration 448-54
- surface of adsorbent 271-364
  - active lines 340-2
  - active points 79, 158, 336-46
  - adsorption on plane surfaces 317-29
  - alteration of, *see* activation, sintering, etc.
  - chemical nature of 340, 359
  - cleaning of 29-31



- composition of 340
- different geometrical configurations on 341
- effect of adsorbate 355-7
- effect of alternate oxidation-reduction 283-4
- effect of annealing 283-4
- effect of cold-rolling 283-4
- effect of polishing 283-4
- effect of repeated flushings 355-6
- effect of solidification of liquid 283-4
- electrical potential of 426
- external 3, 144
- heterogeneous fraction of 77, 335-46
- homogeneous fraction of 77, 335-9
- internal 3, 4, 145
- located in cracks 345-6
- packing of molecules on 74, 79-81, 159
- purification of 29-31
- sintering of, *see* sintering
- structure of 341, 359
- surface pressure 65, 427-37
- surface tension in capillaries 126
  - methods 289, 319-20
  - of solid 5
- swelling of adsorbent 410-3, 432-6
- thermal expansion of adsorbate 102-3, 112-4, 423
- thickness of adsorbed film 96, 320-9
- torsion balance 42
- turbidimetric analysis 310
- unimolecular adsorption 6, 63, 67, 82, 85, 89, 92, 95-6, 117, 177
  - layer 74, 76
- valence forces 5
- van der Waals adsorption, *see* adsorption, physical adsorption
  - definition of 4
- van der Waals constant *a* 90, 110-1, 131, 182, 192
  - constant *b* 65, 90, 181
- van der Waals equation 90, 106, 181
  - for the adsorbate 90, 430
- van der Waals forces 5
  - attractive 182
  - repulsive 181
- van Laar's equation 109
- vapor pressure lowering 120
- virial coefficients 85, 89, 195
- volumetric apparatus 32-7
- water treatment 409, 413, 418
- wetting angle (*see also* incomplete wetting) 127-9
  - heat of 237-40
- x-ray diffraction method 310-4









